

A new species of the paper wasp genus *Ropalidia* Guérin-Méneville, *plebeja* group (Hymenoptera, Vespidae, Polistinae), from Vietnam

Hoa Thi Quynh Bui^{1,2}, Thai Van Mai³, Lien Thi Phuong Nguyen^{1,4}

1 Graduate University of Science and Technology, Vietnam Academy of Science and Technology, 18 Hoang Quoc Viet Road, Nghia Do, Cau Giay, Hanoi, Vietnam **2** Department of Natural Science and Technology, Tay Nguyen University, Buon Ma Thuot 6300, Dak Lak, Vietnam **3** Vietnam National Museum of Nature, Vietnam Academy of Science and Technology, 18 Hoang Quoc Viet Road, Nghia Do, Cau Giay, Hanoi, Vietnam **4** Institute of Ecology and Biological Resources, Vietnam Academy of Science and Technology, 18 Hoang Quoc Viet Road, Nghia Do, Cau Giay, Hanoi, Vietnam

Corresponding author: Lien Thi Phuong Nguyen (phuonglientit@gmail.com)

Academic editor: Volker Lohrmann | Received 15 March 2023 | Accepted 2 June 2023 | Published 26 June 2023

<https://zoobank.org/A4790089-F94A-42BC-89F4-3F990802EB4B>

Citation: Bui HTQ, Mai TV, Nguyen LTP (2023) A new species of the paper wasp genus *Ropalidia* Guérin-Méneville, *plebeja* group (Hymenoptera, Vespidae, Polistinae), from Vietnam. Journal of Hymenoptera Research 96: 543–553. <https://doi.org/10.3897/jhr.96.103533>

Abstract

A new species, *Ropalidia daklak* Bui, Mai & Nguyen, **sp. nov.**, belonging to the *plebeja*-group of the genus *Ropalidia* Guérin-Méneville, 1831 is described and figured based on females and males from Vietnam. The nest structure of the new species is described, and an updated key is provided to all known species of the group.

Keywords

Nest, new species, Polistinae, *R. plebeja* group, Vespidae, Vietnam

Introduction

The social wasp genus *Ropalidia* Guérin-Méneville, 1831, is one of the largest genera among the social wasps, consisting of about 180 extant species (Kojima and Carpenter 1997). Given the considerable diversity, several publications have organized the species within the genus, either as formal subgenera or informal species-groups (Richards 1978; Kojima 1997, 2001). Currently, several species-groups have been proposed (Kojima 2001), with

the *R. plebeja* group being a notable one. The *R. plebeja* group has hitherto contained six species: *Ropalidia andamanensis* Das & Gupta, 1989, *R. celebensis* van der Vecht, 1941, *R. cristata* Kojima, 1989, *R. plebeja* (de Saussure, 1862), *R. rufoplagiata* (Cameron, 1905), and *R. turneri* Richards, 1978 (Kojima et al. 2002). The defining character for this species group is the morphology of first metasomal tergum: barely petiolate basally and abruptly swollen dorsally at the posterior end of the basal slit (Kojima 2001; Kojima et al. 2002). The most recent publication on the *R. plebeja* group by Kojima et al. (2002), described the males, larvae, and nests of some species in this group, such as *R. plebeja*, *R. celebensis*, and *R. rufoplagiata*, along with a key to all of the species. In Vietnam, only one species in this species group, *R. rufoplagiata*, has been recorded previously (Nguyen et al. 2006).

In present work, based on specimens deposited in the Institute of Ecology and Biological Resources, Hanoi, Vietnam (**IEBR**), one species of the *R. plebeja* species group is described as new to science. In addition, an updated key is provided to all known species in the group.

Material and methods

The material examined in the present study is deposited in the collections of the Institute of Ecology and Biological Resources (IEBR), Hanoi, Vietnam. Adult morphological and color characters were observed on pinned specimens with the aid of a stereomicroscope. The male terminal sterna and genitalia were dissected out, cleared in KOH, and mounted on hand-washing gel for observation and taking photos with the stereomicroscope. Terminology for male genitalia follows that of Kojima (1999). Measurements of body parts were made with an ocular micrometer attached to the stereomicroscope, with accuracy to 0.1 mm. Nest characters were examined after the nest had been air-dried (see Figs 18, 19), and the terminology of Wenzel (1998) was used for nest characters. Photographs of the nest were taken in the field (Fig. 10) and after further development of the offspring in the lab (Figs 18, 19; note the difference in the number of cells with cocoon caps). Photographic images of the wasps were obtained using a Nikon SMZ 800N Digital StereoMicroscope with ILCE-5000L/WAP2 digital camera attached, using Helicon Focus 7 software for stacking; the plates were edited with Photoshop CS6. The abbreviations F, S, and T (I, II, III, ...) refer to numbered flagellomeres, metasomal sterna, and metasomal terga, respectively.

Systematics

Ropalidia daklak Bui, Mai & Nguyen, sp. nov.

<https://zoobank.org/F9F11C23-ED67-44BB-AB4A-C612F458F581>

Figs 1–19

Material examined. *Holotype* (deposited in IEBR): VIETNAM: • ♀; Dak Lak province, Krong Ana, Dray Sap; 12°32'53.5"N, 107°58'27.9"E; 19 Jun. 2020; Bui TQH leg.;

Nest#VN-TN-2020-R-01; QHoa-A11-12. **Paratype** (deposited in IEBR): VIETNAM: • 3 ♂♂, 8 ♀♀, same data as holotype.

Diagnosis. This species can be distinguished from other species in the *R. plebeja* group by the following combination of characters: pronotal carina raised into thin lamella but somewhat weaker at dorsal part; vertex weakly sloping down to occipital carina behind posterior ocelli; epicnemial carina absent, border between punctured posterodorsal and unpunctured anteroventral areas of mesepisternum well-defined; disc of mesoscutellum flat, in lateral view mesoscutellum smoothly passing into mesoscutum; median concavity of propodeum deep and wide, with distinct lateral edges; TI with posterior lamella depressed, wide and flat; TII dorsally with lateral margins abruptly diverging in basal third, then almost parallel to near apical margin. In female, head in frontal view 1.2 times as wide as high; distance between posterior ocelli about 2.2 times as long as their diameter. In male, antennal scape about 2.45 times as long as wide; digitus gradually widened from base to near apex, then abruptly curved to a sharp point at apex; penis valves short, slightly more than half as long as basal apodeme.

Description. Female (Fig. 10). Body length (head + mesosoma + first two metasomal segments) 8.14–10.62 mm (holotype: 9.22 mm); forewing length 6.8–8.5 mm (holotype: 8.08 mm).

Head black; clypeus yellow to orange, dorsal margins black, with two black spots medially; spot at inner orbit close to clypeus and spot between antennal toruli (usually separated into paired smaller spots) brown; ill-defined spot above yellow spot at inner orbit, central spot behind posterior ocelli (usually absent), and most of gena (sometimes reduced to posterior band narrowing ventrally) reddish-brown; mandible brown in apical half, ivory white basally. Antenna brown to dark brown, but yellowish beneath. Mesosoma black; pronotum reddish-brown, except black pronotal collar and yellow band along carina. Tegula brown; mesoscutum black with two triangular orange spots at anterior margin; disc of mesoscutellum dull orange with black anterior margin and yellow to light brown posterior margin, metanotum yellow, propodeum black, propodeal teeth and propodeal valvula brown. First metasomal segment reddish-brown, with wide, pre-apical yellow band on tergum (sometimes interrupted medially on tergum); second metasomal segment black, thin lamella brown; third to sixth metasomal segments black. Legs reddish-brown; coxae black with a yellow spot; trochanters black basally; femora black basally. Wings hyaline, with subapical blackish cloud; pterostigma yellowish-orange; veins brown.

Body covered with appressed tomentum and dense, suberect, silvery setae; setae longer on apical part of clypeus and apical margin of propodeum than on other body parts. Clypeus with sparse, shallow punctures; frons with dense, deep punctures, interspaces between punctures much narrower than their diameters; vertex less densely punctured, interspaces between punctures narrower than their diameters; punctures on gena large, sparse, shallow, interspaces between punctures wider than their diameters. Pronotum, mesoscutum, metapleuron, and lateral surfaces of propodeum with dense punctures as on frons; punctures on mesoscutellum and metanotum slightly larger, with interspaces slightly wider than those on mesoscutum; posterior margin of metanotum impunctate and polished; median concavity of propodeum with fine, transverse



Figures 1–11. *Ropalidia daklak* sp. nov. 1–10 female 1 head, frontal view 2 head, dorsal view 3 antenna 4 gena 5 mesosoma, dorsal view 6 mesosoma, lateral view 7 propodeum 8 metasoma, dorsal view 9 metasoma, lateral view 10 habitus 11 nest (photo was taken on 19 June 2020). Scale bars: 1 mm.



Figures 12–19. *Ropalidia daklak* sp. nov. **12–17** male **18, 19** nest (photos were taken on 12 March 2023) **12** head, frontal view **13** antenna **14** inner aspect of paramere with digitus and volsella **15** digitus **16, 17** aedeagus (**16** ventral view **17** lateral view) **18** nest, view from cell opening **19** nest, beneath. Scale bars: 1 mm (**12–14, 18**); 0.5 mm (**15–17**).

striae; dorsolateral surface of propodeum with distinct and oblique striae. First metasomal tergum impunctate on anterior surface, with ill-defined punctures preapically; punctures on second metasomal tergum relatively large, their interspaces smaller than their diameters; punctures on second sternum similar to those on second tergum.

Head: In frontal view (Fig. 1) about 1.13 times as wide as high; in dorsal view (Fig. 2) about 2.5 times as wide as long, with gena slightly convex and distinctly narrowing posteriorly. Distance between posterior ocelli 2.25 times as long as their diameter, about 0.59 times as long as distance between posterior ocellus and inner compound eye margin; area between ocelli slightly raised. Vertex (Fig. 2) weakly sloping down to occipital carina. Inner compound eye margins converging ventrally; distance between them at vertex nearly 1.25 times as wide as at clypeus. Clypeus weakly convex, pointed below, transverse, nearly 1.53 times as wide (excluding lateral lobes) as high (measured from bottom of dorsal emargination to apex). Mandible normal, not twisted. Gena (Fig. 4) in profile weakly widening ventrally to level of compound eye mid-height, then slightly narrowing further ventrally, about 1.26 times as wide as compound eye; occipital carina complete, fine, smoothly and weakly curved. Malar space short, about 0.70 times as wide as diameter of antennal torulus. Antenna as in Fig. 3; scape slightly curved, slightly more than 3.60 times as long as wide; flagellum weakly thickened apically to FIX; FI about 2.71 times as long as its own apical width, about 1.41 times as long as FII and FIII combined; each of FII to FIX wider than long; FIX slightly more than 1.46 times as wide as FI; FX nearly bullet-shaped, about 1.1 times as wide as long.

Mesosoma: Rather thick, about as long as thorax, and as wide as mesoscutum between tegulae. Pronotum (Fig. 5) in dorsal view with anterior margin weakly rounded; lateral sides slightly concave and weakly diverging posteriorly; pronotal carina complete, raised into low lamella, barely sinuate at humeral angles. Mesoscutum strongly convex, about as long as wide (Fig. 5). Disc of mesoscutellum trapezoidal, nearly flat, with lateral margins truncate. Disc of metanotum weakly produced posteromedially, nearly on same level of mesoscutellum (Fig. 6), with fine lateral marginal carinae. Concavity on posterior surface of propodeum (Fig. 7) deep and wide, its margins marked laterally by ridges; posterior surface broadly angled at two-thirds anteriorly of propodeum; propodeal orifice rounded above, about 1.65 times as long as wide; propodeal valvula small (most of propodeal tooth visible in lateral view), with broadly rounded triangular outline and marginal carina at base.

Metasoma: First metasomal segment short, T1 in dorsal view (Fig. 8) strongly widened after short, basal, parallel-sided part, then almost not constricted near apical margin; maximum width of posterior widened part nearly 3.27 times as wide as width of basal, parallel-sided part; in profile (Fig. 9) abruptly swollen dorsally at posterior end of basal slit, then dorsal margin weakly and broadly convex and broadly curved down to posterior lamella near apical margin, posterior lamella depressed, wide and flat, in dorsal view barely narrowing posteriorly near posterior margin; sternum emarginate posteriorly. Second metasomal segment about 1.06 times as long as wide, about 2.06 times as wide as maximum width of first tergum; suture between TII and SII barely visible; posterior lamella narrow, weakly depressed.

Male. Similar to female except as follows: Body length (head+mesosoma+first two metasomal segments) 8.32–9.22 mm; forewing length 6.84–8.04 mm.

Coloration generally as in female, but markings partly reduced or absent: head black, clypeus entirely black, spot at inner orbit and spot between antennal sockets light-brown, mandible dark brown with a large yellow mark in the middle, mesosoma entirely black, propodeum black with short narrow yellow band, tegulae pale yellow, first metasomal segment (Fig. 13) orange with wide, yellow band on pre-apical tergum (sometimes interrupted medially on tergum).

Head: In frontal view relatively wider than in female (Fig. 12), about 1.26 times as wide as high; compound eye slightly more swollen laterally; inner compound eye margins more strongly converging ventrally than in female, their distance at vertex about 1.43 times as long as that at clypeus; clypeus less produced below, about 1.54 times as wide as high; gena in profile proportionally slightly wider than in female, about 1.27 times as wide as compound eye; posterior ocelli more widely separated from each other, distance between them about 0.58 times as long as distance from posterior ocellus to inner compound eye margin, area around ocellus strongly elevated. Mandible with deep and wide emargination between dorsal first and second teeth. Antennal (Fig. 13) scape short, thick, swollen medially, about 2.45 times as long as wide; flagellum much less strongly swollen apically, widest at FVII, then weakly narrowed apically; FXI rounded apically, nearly 0.67 times as long as its own basal width; apical third of FI, FII to FX, and basal half of FXI with longitudinal ridge-like tyloids.

Genitalia: As in Figs 14–17. Parameral spine lacking setae. Volsella flattened, strongly spatulate, and wide in inner aspect (Fig. 14). Digitus gradually widened from base to near apex, then abruptly curved to a sharp point at apex (Fig. 15). Penis valves short, slightly more than half as long as basal apodeme (about 0.51 times as long as basal apodeme); in ventral view proximal part strongly produced laterally into fin-like shape (Fig. 16); apical part curved ventrally in profile (Fig. 17); proximal margin without teeth.

Nest (Figs 11, 18, 19; note that the photos of the nest were taken on different dates). One nest (Nest#VN-TN-2020-R-01, QHoa-A11-12) together with nine females and three males was collected in Dray Sap, Krong Ana, Dak Lak Province, at 12°32'53.5"N, 107°58'27.9"E on 19 June 2020. The nest was found in a pepper (*Piper nigrum* L.) and coffee (*Coffea robusta* Chev.) tree garden, with 5 to 6 year old pepper and 15 year old coffee plants. The nest was constructed on the leaf of a pepper tree about 1 m from the ground, which was under the shade of a large coffee tree. It was horizontally attached to the dorsal surface of the dried pepper leaf. It had one main terminal and seven smaller pedicels (Figs 18, 19). The length of the main pedicel was 5.2 mm, the width was 12.16 mm. The lengths of seven smaller pedicels ranged from 4.0 mm to 6.88 mm and the widths from 2.06 mm to 7.36 mm. The color of the nest was light brown with dark brown and white bands interleaved, indicating that the nest was made from different material sources. The nest carton was brittle, made from small chips of plant fiber mixed with a small amount of oral secretion. The nest was under construction with 86 completed cells and eight unfinished cells. Among 86 cells, 20 cells had larvae, there were no egg cells, and 32 cells had cocoon caps. The outer cells

were elliptical or rounded, with an average depth and diameter of 8.1 mm ($n = 12$, range 6.12–11.48 mm) and 4.1 mm ($n = 12$, range 3.38–4.82 mm), respectively. The cells inside were hexagonal in section, average depth and diameter of cell with cocoon caps were 10.43 mm ($n = 19$, range 9.02–12.78 mm) and 4.55 mm ($n = 12$, range 4.2–4.88), respectively; non-cocoon cap cells were usually shorter than cells with cocoon caps, with depths ranging from 8.54 to 11.18 mm, and side to side diameters from 3.92 to 4.78 mm. The cocoon cap was light brown, and became dark brown with time, and was strongly convex.

Distribution. Vietnam (Tay Nguyen highland).

Etymology. The specific epithet refers to the name of the province where the holotype was collected.

Remarks. The new species is compared with *R. rufoplagiata* based on the description of Kojima et al. (2002) and the one specimen of this species from Vietnam. The new species comes close to *R. rufoplagiata* in the following characters: medial concavity of propodeum deep and wide, with distinct lateral edges; metanotum slightly produced medioposteriorly; penis valves short, slightly more than half as long as basal apodeme; first metasomal tergum in profile relatively weakly swollen dorsally in posterior half with posterior lamella depressed and flattened. It is differentiated by: mesoscutellum in lateral view smoothly passing to mesoscutum (strongly convex at the anterior margin in *R. rufoplagiata*); gena of female in profile wider than compound eye, about 1.26 times as wide as the compound eye (about 0.9 times as wide as the compound eye in *R. rufoplagiata*), distance between posterior ocelli 2.2 times as long as their diameter (slightly more than twice in *R. rufoplagiata*); clypeus of male about 1.54 times as wide as high (1.4 times as wide as high in *R. rufoplagiata*), distance between posterior ocelli about 0.58 times as long as distance from posterior ocellus to inner compound eye margin (0.85 times in *R. rufoplagiata*), antennal scape about 2.45 times as long as wide (slightly less than 3 times as long as wide in *R. rufoplagiata*), digitus gradually widened from base to near apex, then abruptly curved to a sharp apex (digitus gradually narrowed from midlength to apex, with a bluntly pointed apex in *R. rufoplagiata*) [the characters of the male of *R. rufoplagiata* were taken from Kojima et al. (2002)].

Ropalidia rufoplagiata (Cameron, 1905)

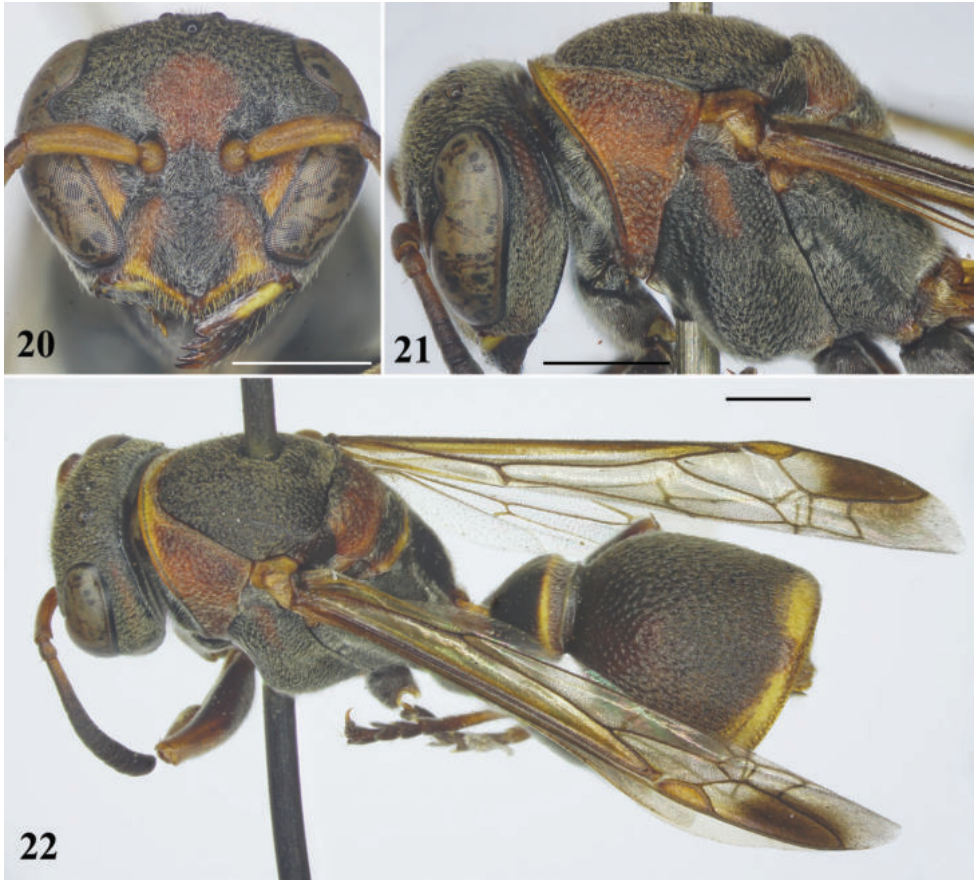
Figs 20–22

Icaria rufoplagiata Cameron, 1905: 71, ♂, ♀, “Tjandi near Semarang”; van der Vecht 1941: 167 [designation of lectotype].

Ropalidia rufoplagiata (Cameron): van der Vecht 1941: 111, 165.

Material examined. VIETNAM: • ♀; Hai Phong, Cat Ba national park; 18.Jul.2003, Nguyen TPL leg.

Distribution. India; China; Myanmar; Thailand; Malaysia; Vietnam; Taiwan.



Figures 20–22. *Ropalidia rufoplagiata*, female. 20. Head, frontal view. 21. Mesosoma, lateral view. 22. Habitus. Scale bars: 1 mm.

Key to species of the *Ropalidia plebeja* group

This key is based on the one by Kojima et al. (2002) (unless the sexes are specified, the characters given in the key can be applied to both sexes). From couplet 1 to couplet 4, follow the key by Kojima et al. (2002), and then use the following modified couplets:

- 5 Median concavity of propodeum deep and wide, with distinct lateral edges; metanotum slightly produced medioposteriorly **6**
- Median concavity of propodeum shallow and narrow, without distinct lateral edges; metanotum not produced medioposteriorly *R. andamanensis*
- 6 Gena of female in profile about 0.9 times as wide as compound eye; distance between posterior ocelli slightly more than twice as long as their diameter; clypeus of male about 1.4 times as wide as high; antennal scape slightly less

- than 3 times as long as wide; digitus gradually narrowed from midlength to apex, with a bluntly pointed apex.....*R. rufoplagiata*
- Gena of female wider than compound eye; distance between posterior ocelli about 2.2 times as long as their diameter; clypeus of male greater than 1.5 times as wide as high; antennal scape about 2.45 times as long as wide; digitus gradually widened from base to near apex, then abruptly curved to a sharp-pointed apex *R. daklak* sp. nov.

Acknowledgements

We thank Michael S. Engel for providing English proofreading of the manuscript. The present study was supported by the grant from Tay Nguyen University to the first author (T2021- 53CBTĐ).

References

Cameron P (1905) On the Malay fossorial Hymenoptera and Vespidae of the Museum of the R. Zool. Soc. “Natura Artis Magistra” at Amsterdam. Tijdschrift voor Entomologie 48: 48–78.

Das BP, Gupta VK (1989) The social wasps of India and the adjacent countries (Hymenoptera: Vespidae). Oriental Insects Monograph 11: 176–189.

de Saussure H (1862) Sur divers Vespides asiatiques et africains du Musee de Leyden. Stettiner Entomologische Zeitung 23: 129–141.

Kojima J (1989) A new polistine species of *Ropalidia* (Hymenoptera, Vespidae) from Papua New Guinea. Japanese Journal of Entomology 57: 143–147.

Kojima J (1997) Abandonment of the subgeneric concept in the Old World polistine genus *Ropalidia* Guérin-Ménéville, IB31 (Insecta: Hymenoptera: Vespidae). Natural History Bulletin of Ibaraki University 1: 93–106.

Kojima J (1999) Male genitalia and antennae in an Old World paper wasp genus *Ropalidia* Guérin-Ménéville, 1831 (Insecta: Hymenoptera; Vespidae, Polistinae). Natural History Bulletin of Ibaraki University 3: 51–68.

Kojima J (2001) *Ropalidia* wasps (Insecta: Hymenoptera; Vespidae, Polistinae) in New Guinea and its adjacent islands (first part), Natural History Bulletin of Ibaraki University 5: 31–60.

Kojima J, Carpenter JM (1997) Catalog of species in the polistine tribe Ropalidiini (Insecta: Hymenoptera: Vespidae). American Museum Novitates 3199: 1–96.

Kojima J, Hartini S, Kahono S, Fujiyama N, Katakura H (2002) Males, mature larvae, and nests of *Ropalidia plebeja*, a nearly solitary paper wasp endemic to Sulawesi (Insecta: Hymenoptera: Vespidae), with taxonomic notes on the *R. plebeja* group. Species Diversity 7: 1–28. <https://doi.org/10.12782/specdiv.7.1>

Nguyen LTP, Saito F, Kojima J, Carpenter JM (2006) Vespidae (Hymenoptera) of Viet Nam 3. Synoptic key to Vietnamese species of the polistine genus *Ropalidia*, with notes on

- taxonomy and distribution. *Entomological Science* 9: 93–107. <https://doi.org/10.1111/j.1479-8298.2006.00157.x>
- Richards OW (1978) The Australian social wasps (Hymenoptera: Vespidae). *Australian Journal of Zoology, Supplementary Series* 61: 1–132. <https://doi.org/10.1071/AJZS061>
- van der Vecht J (1941) The Indo-Australian species of the genus *Ropalidia* (= *Icaria*) (Hymenoptera, Vespidae) (first part). *Treubia* 18: 103–190.
- Wenzel JW (1998) A generic key to the nests of hornets, yellowjackets, and paper wasps worldwide (Vespidae: Vespinae, Polistinae). *American Museum Novitates* 3224: 1–39.

Inquiline insects of the honey bee *Apis mellifera* in Western Siberia (Hymenoptera, Apidae)

Victoria V. Stolbova¹, Vitaly A. Stolbov²

1 All-Russian Scientific Research Institute of Veterinary Entomology and Arachnology – a Branch of the Federal State Budgetary Institution of Science of the Federal Research Center of the Tyumen Scientific Center of the Siberian Branch of the Russian Academy of Sciences, Tumen, Russia **2** Tyumen State University, Tyumen, Russia

Corresponding author: Victoria V. Stolbova (victorysva@mail.ru)

Academic editor: Christopher K. Starr | Received 8 April 2023 | Accepted 21 June 2023 | Published 6 July 2023

<https://zoobank.org/037D5900-5303-432E-912B-631A669C8DB1>

Citation: Stolbova VV, Stolbov VA (2023) Inquiline insects of the honey bee *Apis mellifera* in Western Siberia (Hymenoptera, Apidae). Journal of Hymenoptera Research 96: 555–568. <https://doi.org/10.3897/jhr.96.104720>

Abstract

The multi-species associations of insects (symbiocenosis) in honey bee hives currently include more than 15 orders of Insecta. We present the results of studying the inquilines of bee hives in the south of Western Siberia. In the honeybee hives of this region 37 insect species from 8 orders (Dermaptera, Thysanoptera, Psocoptera, Hemiptera, Coleoptera, Hymenoptera, Lepidoptera, Diptera) were identified. Inquiline insects were observed in 77% of hives in 81.5% of the studied apiaries. Coleoptera prevailed among the orders, accounting for 94% of observations. The overall eudominant was *Cryptophagus scanicus* (Linnaeus, 1758) (87.8%); the subdominants were *Dermestes lardarius* Linnaeus, 1758 and *Contacyphon variabilis* (Thunberg, 1787). The smallest number of insect species can be attributed to specific groups. These are *C. scanicus*, a detritophage that primarily feeds on mold fungi hyphae, but can also consume bee supplies; and *Galleria melonella* (Linnaeus, 1758), a widespread pest of bee colonies, that feeds on bee bread, honey, wax and bee brood. The facultative group includes detritophages, pollen- and honey-feeding species, that find suitable conditions for feeding and developing in beehives (Vespidae, Formicidae, etc.). Representatives of accidental group were the most diverse in species composition and type of nutrition but they were always individually found in hives. In total, 42 species of insects are currently recorded in the beehives of Western Siberia.

Keywords

Bee hives, beekeeping, Coleoptera, *Galleria melonella*, honey bee hives, Insecta

Introduction

The honey bee nest is an apiophilic symbiocenosis of the nidicolous (nest) type (Sidorov 1968). A honeybee hive can be considered an artificial nidicolous ecotope – a community habitat with sufficient ventilation and a relatively stable microclimate that provide favorable conditions for symbionts – consortium members (Bakalova 2011a).

Arthropods are an integral part of bee hive biocenosis. Mites and insects are the main symbionts of bees, predominant in quantity and taxonomic diversity (Stolbova 2022).

Insects (Insecta) show the most diversity in apiophilic symbiocenoses, to date representatives of the Collembola and 14 orders insects have been noted: Zygentoma, Blattodea, Dermaptera, Psocodea, Thysanoptera, Heteroptera, Coleoptera, Hymenoptera, Neuroptera, Raphidioidea, Lepidoptera, Mecoptera, Diptera, Siphonaptera (Orösi Pal 1939; Sidorov 1968; Banaszak 1980; Bakalova 2011a; Semmar et al. 2014). The total number of insects found in honeybee hives amounts to several hundred species (Bakalova 2011a).

The most numerous insect symbionts of bees are Coleoptera (Sidorov 1968). According to the latest data, the list of beetles in honeybee hives includes 155 species from 30 families (Bakalova 2011a).

Among insects, there are both specific species whose entire life cycle is tied to bees, and numerous facultative species that visit hives periodically, or enter them accidentally, for example, in search of shelter for wintering.

A range of insect species is serious pests of beekeeping, primarily the greater wax moth *Galleria mellonella* (Linnaeus, 1758) and the lesser wax moth *Achroea grisella* (Fabricius, 1794). Some Coleoptera are also serious pests, in particular, *Aethina tumida* Murray, 1867, which has been actively settling in different countries in recent years (Neumann et al. 2016).

A number of researchers believe that wasps occupy the first place among the pests of honey bees from the insect class, in terms of damage caused. To date, there are 26 species and subspecies of honey bee pest wasps from 6 genera and 2 families (Pusceddu et al. 2017; Konovalova 2018). There are over 50 species of Diptera associated with bees, most of them are parasitoids (Zimina 1973; Bakalova 2011a).

In addition to the direct harm caused to bees, many insects can be carriers of fungal spores and viruses that cause diseases of bees, such as nosematosis, ascospherosis, etc. Beetles transfer mold spores and *Nosema apis* (Zander, 1909) microsporidia from the bottom of the hive to the honeycomb of the brood nest or from one hive another. It was found that single adult individuals of *Tribolium madens* (Charpentier, 1825) and *Dermestes lardarius* Linnaeus, 1758 can carry about 150 and 285 thousand spores of *Ascosphaera apis* (Maasen ex Claussen) Olive & Spiltoir, 1955 – the causative agent of ascospherosis of bees on the surface of their bodies (Measures to control beetles 1998).

However, most of the insects found in hives are commensals, which often not only do not harm beekeeping but on the contrary, are useful. First of all, these are detritophages, which dispose of garbage, mold fungi and dead bees from the bottom of hives. These include beetles, earwigs, cockroaches. These species feed on the waste

of bee colonies (wax crumbs, contaminated bee bread, feces and corpses of bees) and thus, contribute to the cleaning of the honey bee nest.

No less important for bee symbiogenesis are predatory insect species that regulate the number of other arthropods in the hive. This group includes beetles (Carabidae, Staphilinidae, Coccinellidae, etc.), Hymenoptera (Vespidae, Formicidae), Raphidioptera, Chrysopidae, etc. (Bakalova 2011a). Permanent predatory species of hive symbionts, as a rule, are mutualists in relation to bees but facultative species ones can be harmful (Measures to control beetles 1998).

There are quite a large number of papers on bee symbionts, however, most of them cover individual practically significant species, such as *Varroa destructor* ticks Anderson & Trueman, 2000, wax moth, small hive beetle and other bee parasites and pests. The most complete reports on the entomofauna of bee hives were obtained quite a long time ago, and mainly cover Europe (Orösi Pal 1939; Banaszak 1980). These papers describe the composition of symbionts give general data on their ecology.

A number of works are available on the European part of Russia and the Caucasus (Sidorov 1968; Atakishiev 1969; Pushkin 2009; Bakalova 2011a). At the same time, in all the above works, the emphasis was placed either on individual groups of symbionts (according to the degree of harmfulness to bees), or on specific conditions of detention (bee-trees, wild hive).

In Siberia, there are papers on specific groups of symbiont insects (Coleoptera, earwigs) (Zbanatsky 1997b; Domatsky and Domatskaya 2020). At the same time, considering the symbiogenesis of the nidicolous type, all members of which are important for its full functioning, it is necessary to study all bee symbionts in the complex.

Earlier, we studied in detail the composition of the acarofauna of honey bee hives in Western Siberia (Stolbova 2022). This paper considers entomofauna.

Material and method

The topic was studied in 2020–2022 in the south of Western Siberia, within the southern taiga and forest-steppe zones. The short summer period in this region is characterized by high temperatures, the winter period is long and severe (5–6 months), with frequent frosts. The main breed of bees in the region is *Apis m. mellifera* Linnaeus, 1758, but beekeepers also contain other breeds, such as the *Apis m. carpathica* Avetisyan, Gubin & Davidenco, 1966, *Apis m. carnica* Pollmann, 1879, and *Apis m. buckfast*, thus most of the bees in Western Siberia are mixed (Pashayan and Endovitsky 2018).

A total of 193 bee colonies from 27 apiaries from 20 settlements in the south of the Sverdlovsk Oblast, Tyumen Oblast and Altai Krai were studied. Collection from the south of the Tyumen Oblast prevailed. A detailed description of the collection points is to be found in (Suppl. material 1).

For the study, dead bees, wax and bee bread crumbs, and waste from the bottom of hives were collected in paper bags, labelled and delivered to the laboratory. Part of the material was selected and provided to the laboratory by apiaries owners.

To study the qualitative and quantitative composition of the bee hive fauna, the same amount of dead bees was taken from the selected or received material in the laboratory, the quantity was a standard completely full Falcon-type test tube (volume 50 ml). The sample was filled with water and kept for 1–2 hours, periodically turning the tube over to mix the contents. After that, the sample was carefully examined under a stereomicroscope against a dark background.

Some of the samples were pre-treated in Berlese funnel for 2 weeks until the substrate was completely dry. After that, the dry residue was examined under a stereomicroscope.

Thysanoptera, Psocoptera, Hemiptera, Hymenoptera (Formicidae, Parasitica), Diptera insects and all insect larvae were fixed in 70% alcohol, the rest were placed on entomological mattresses. Coleoptera and Hemiptera were subsequently mounted on entomological plates. Psocoptera were mounted on slides using Hoyer's medium. Taxonomic identification of symbionts was made using identification guides, scientific articles and Internet resources (Bey-Bienko 1965; Ler 1992; Lyubarsky 2002; Ellis et al. 2013; Opit G et al. 2022).

Statistical data processing was carried out in the Microsoft Excel 2016 program. In this paper, the following terms are used: abundance – the number of insects per infected sample (min–max, average, ex.); occurrence – the number of samples (bee colonies) with insects, as a percentage of the number of samples studied; dominance index – the number of individuals of this species to the total number of individuals of all detected species (%).

Results

A total of 37 insect species were identified (Table 1). Some of the insects were identified only to genus or family, since many specimens lacked diagnostic features. Identification of larvae was often especially difficult.

Nine insect species were found in bee hives for the first time: *Cryptophagus hauseri*, *Sciodreporides watsoni*, *Phyllobius contemptus*, *Epuraea biguttata*, *E. boreella*, *Brachypterus fulvipes*, *Litargus connexus* (Coleoptera), *Scolopostethus pictus* and *Rhyparochromus pini* (Heteroptera).

In addition to these species, *Forficula tomis*, *Formica rufibarbis* and *Liposcelis bostrychophila* were recorded in bee brood nests in Western Siberia for the first time.

Other insect species were regularly observed in honey bee hives, including in Western Siberia.

In numbers of species, the Coleoptera predominated, which accounted for half (18) of all identified insect species. Hymenoptera were also quite numerous, at the same time the particular species of Parasitica representatives were not identified. The remaining orders were represented by just one or two species.

Symbiont insects were observed in 81.5% of the studied apiaries (Table 2). The occurrence in the studied bee hives was 77%.

Both in terms of occurrence, and especially in number, representatives of Coleoptera prevailed among the orders, which accounted for 94% of all insects detected.

Table 1. Species composition, occurrence and abundance of insects in the studied bee hives of Western Siberia.

Taxon	Total number	Abundance, min-max (median)	Occurrence, %	Dominance index, %
Dermaptera				
Family Forficulidae				
<i>Forficula tomis</i> Kolenati, 1846	5	1–2 (1)	2.072	0.204
Thysanoptera				
Thysanoptera indet.	5	1–3 (2)	1.554	0.204
Psocoptera				
Family Liposcelididae				
<i>Liposcelis bostrychophila</i> Badonnel, 1931	9	1–3 (1)	3.108	0.367
Psocoptera indet.	1	1–1 (1)	0.518	0.040
Hemiptera				
Cicadoidea				
Cicadellidae gen. sp.	11	1–9 (1)	1.554	0.449
Aphidoidea				
Aphidoidea indet.	1	1–1 (1)	0.518	0.040
Heteroptera				
Family Anthocoridae				
<i>Orius</i> sp.	2	2–2 (2)	0.518	0.081
Family Rhyparochromidae				
<i>Rhyparochromus pini</i> (Linnaeus, 1758)	1	1–1 (1)	0.518	0.040
<i>Scolopostethus pictus</i> (Schilling, 1829)	1	1–1 (1)	0.518	0.040
Heteroptera fam. sp. Larva	1	1–1 (1)	0.518	0.040
Coleoptera				
Family Leiodidae				
<i>Sciodrepsoides watsoni</i> (Spense, 1813)	2	2–2 (2)	0.518	0.081
Family Staphylinidae				
Aleocharinae gen. sp.	4	1–3 (2)	1.036	0.163
Family Scirtidae				
<i>Contactyphon variabilis</i> (Thunberg, 1787)	69	1–10 (3)	9.844	2.817
<i>Contactyphon padi</i> (Linnaeus, 1758)	1	1–1 (1)	0.518	0.040
<i>Contactyphon pubescens</i> (Fabricius, 1792)	2	2–2 (2)	0.518	0.081
Family Dermestidae				
<i>Dermestes lardarius</i> Linnaeus, 1758	6	1–2 (1)	2.590	0.244
<i>Trogoderma</i> sp.	1	1–1 (1)	0.518	0.040
Dermestidae Larvae	46	1–19 (4)	4.145	1.878
Family Kateretidae				
<i>Brachypterus fulvipes</i> Erichson, 1843	3	1–2 (1)	1.036	0.122
Family Nitidulidae				
<i>Epuraea biguttata</i> (Thunberg, 1784)	5	5–5 (5)	0.518	0.204
<i>Epuraea borrella</i> (Zetterstedt, 1828)	1	1–1 (1)	0.518	0.040
Family Cryptophagidae				
<i>Cryptophagus scanicus</i> (Linnaeus, 1758)	2150	1–150 (12)	52.332	87.791
<i>Cryptophagus hauseri</i> Reitter, 1890	7	1–2 (1)	3.108	0.285
Family Laemphloeidae				
<i>Cryptolestes ferrugineus</i> (Stephens, 1831)	5	2–3 (2.5)	1.036	0.204
Family Mycetophagidae				
<i>Litargus connexus</i> (Fourcroy, 1785)	1	1–1 (1)	0.518	0.040
Family Latridiidae				
<i>Latridius</i> sp.	1	1–1 (1)	0.518	0.040

Taxon	Total number	Abundance, min-max (median)	Occurrence, %	Dominance index, %
<i>Corticicara gibbosa</i> (Herbst, 1793)	1	1–1 (1)	0.518	0.040
Family Curculionidae				
<i>Phyllobius contemptus</i> Schoenherr, 1832	1	1–1 (1)	0.518	0.040
<i>Apion</i> sp.	1	1–1 (1)	0.518	0.040
Hymenoptera				
Family Vespidae				
<i>Vespula germanica</i> (Fabricius, 1793)	17	1–5 (1)	3.626	0.694
Family Apidae				
<i>Bombus lucorum</i> Linnaeus, 1761	1	1–1 (1)	0.518	0.040
Family Formicidae				
<i>Lasius niger</i> (Linnaeus, 1758)	10	1–5 (1)	3.108	0.408
<i>Formica rufibarbis</i> Fabricius, 1793	1	1 (1)	0.518	0.040
Parasitica indet.	32	1–4 (1)	12.435	1.306
Lepidoptera				
Family Galleriidae				
<i>Galleria mellonella</i> (Linnaeus, 1758)	16	1–11 (1)	3.108	0.653
Diptera				
Family Drosophilidae				
<i>Drosophila</i> sp.	18	3–8 (7)	1.554	0.734
Family Phoridae				
Phoridae gen. sp.	4	1–2 (1)	1.554	0.163
Diptera indet.	6	6–6 (6)	0.518	0.244
Total	2449	1–151 (9)	76.683	100

Table 2. The occurrence of dominant symbiont species in colonies and apiaries.

Taxon	Occurrence in the studied colonies, %	Occurrence in the studied apiaries, %
<i>Cryptophagus scanicus</i>	52.3	54.5
<i>Contacyphon variabilis</i>	9.8	22.2
Dermestidae larvae	4.1	22.2
<i>Vespula germanica</i>	3.6	22.2
<i>Liposcelis bostrychophila</i>	3.1	18.5
<i>Dermestes lardarius</i>	2.6	14.8
Parasitica indet.	12.4	11.1
Phoridae gen. sp.	3.6	11.1
<i>Cryptophagus hauseri</i>	3.1	11.1
<i>Galleria mellonella</i>	3.1	11.1
Thysanoptera indet.	1.5	11.1
Cicadellidae gen. sp.	1.5	11.1
<i>Lasius niger</i>	3.6	7.4
<i>Forficula tomis</i>	2.1	7.4
<i>Cryptolestes ferrugineus</i>	1.0	7.4
Aleocharinae gen. sp.	1.0	7.4

The absolute dominant species was *Cryptophagus scanicus*, which, the preimaginal stages included, accounted for 93.2% of all beetles and 87.8% of all insects.

Two other species of Coleoptera, *Dermestes lardarius* and *Contacyphon variabilis*, also had a fairly high number: *D. lardarius*, larval stages included accounted for 2.1%

of all insects, and the second species took 2.8%. It is characteristic that in the most numerous symbionts – *C. scanicus* and *D. lardarius*, larval stages prevailed in the studied hives (88.4% and 88.5%, respectively).

Vespa germanica wasps, Parasitica and a greater wax moth also had a relatively high occurrence and abundance. The rest of the insect representatives were observed singly.

The occurrence of symbionts in different apiaries varied. Of the 37 insect species found, less than half (16) were recorded in two or more apiaries (44.4%).

The occurrence of symbionts among the studied bee colonies was not very high (Table 2), with the exception of *C. scanicus*, all species had an occurrence below 20%. However, the occurrence in the studied apiaries was significantly higher, while in the dominant species it almost did not change. This shows that the dominant species had a consistently stable high occurrence both in different apiaries and in bee colonies in the same apiary, while other insect species associated with bees were also regularly found in different apiaries of the studied region, although they had a lower number.

Discussion

The insects found in hives can be divided into several ecological groups that play different roles in hives (Fig. 1).

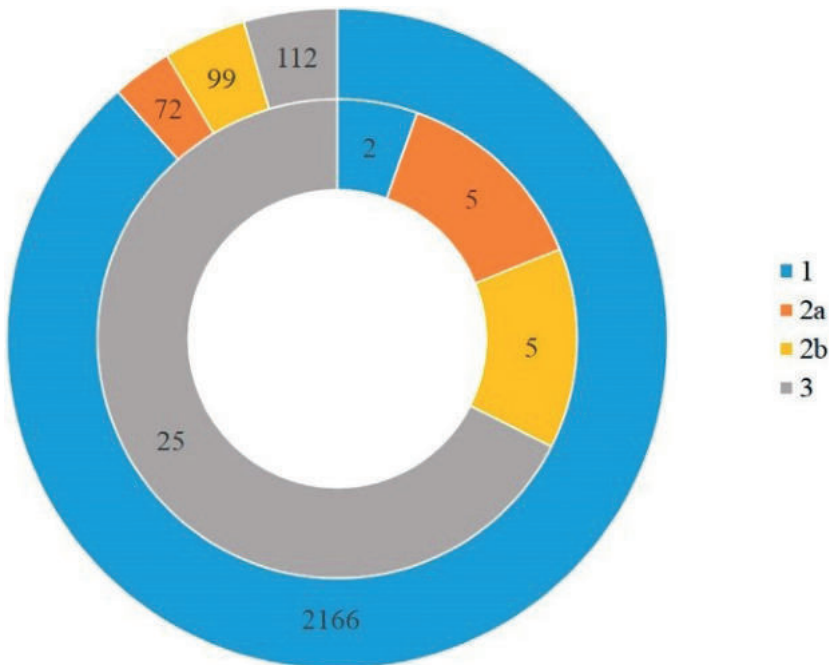


Figure 1. Proportion of ecological groups of insects by abundance (outer circle) and number of species (inner circle): 1 – specific species, 2a, 2b – facultative species (a – Detritophages; b – species feeding on pollen and honey), 3 – accidental species.

Obligate inquilines

Species whose entire life cycle is tied with bees were represented by only two species. However, they had the greatest abundance.

The greater wax moth *Galleria melonella* is a widespread pest of bee colonies, registered in 60 countries but potentially living wherever beekeeping is practiced (Kwadha et al. 2017).

In the hive, *G. mellonella* larvae feed on bee bread, honey, wax and bee brood. In the process of life, the larvae damage the honeycomb, and honey flows out of the cells through the holes. The silk threads produced by the larvae entangle the hatched young bees, which can not to move and may die of hunger. A similar phenomenon is described as galleriosis. In addition, transmission of honeybee viruses (IAPV, BQCV) and participation in the spread of foul brood diseases has been proven for *G. mellonella* (Stolbov et al. 1990; Traiyasut et al. 2016). The destructive effect of the pest is explained by its high reproductive potential and short development time (Kwadha et al. 2017).

In general, this species had a low occurrence (3.1%) in our study. This is probably due to the fact that we have studied dead bees, wax and bee bread crumb, in which *G. mellonella* larvae are found relatively rarely. Females of *G. mellonella* lay eggs in crevices and cracks inside the hive, which prevents their detection, and after leaving the egg, the larvae move to the honeycomb, where they subsequently pupate (Kwadha et al. 2017). Thus, only isolated individuals can be found in the dead bees at the bottom of the hive.

The second specific species, the *Cryptophagus scanicus* beetle, is a typical inhabitant of bee hives, and predominates in numbers among symbionts in most apiaries (Sidorov 1968; Banaszak 1980; Zbanatsky 1997a; Bakalova 2011b; Skulachev 2017).

A high percentage of *C. scanicus* larval stages found in the dead bees' bed (88.4%) indicates active reproduction of this species in honey bee hives. The annual life cycle of *C. scanicus* is adapted to the inactive stages of bee colonies' life, the maximum abundance index of the species is noted in September in preparation for wintering and in April when hives are taken out (Sidorov 1968). All stages of *C. scanicus* develop in the hive (Skulachev 2017). Imago and larvae of *C. scanicus* primarily feed on hyphae of mold fungi, they can also consume bee bread, bee feces and the entrails of dead bees. Despite the fact that *C. scanicus* larvae can develop on products of non-hive origin, in this case the percentage of their death is significantly higher than when developing on honey and bee bread (Measures to control beetles 1998).

This species was the eudominant both in number and occurrence vs. all insects. It was found in 54.5% of the studied apiaries, and in these apiaries it was widespread, occupying about 70% of the hives. Based on the distribution, biology and nature of the connection with honey bees, it is possible to establish the similarity of *C. scanicus* with a small beehive beetle, *Aethina tumida*. *C. scanicus* is a species of northern origin (Sidorov 1967), and is adapted to the conditions of Western Siberia, unlike *A. tumida*, a southern species, for which the climate factor in this case is a deterrent (Schäfer et al. 2010).

Facultative inquilines

Species that are able to exist outside of hives but are regularly found in them and can develop in a hive were listed in facultative group. The species in this group mainly develop in organic-rich substrates and are often synanthropic. They probably get into hives from a human house, and find suitable conditions there, which gives them the opportunity to develop all stages in hives.

In the trophic structure, the facultative species include detritophages, and pollen- and honey-feeding species:

1. Detritophages. Among the representatives of this group, it is worth noting first of all the larder beetle *Dermestes lardarius*. This is a typical synanthropic species that live in human homes. Also, the larder beetle is regularly found in bee hives, including in Western Siberia. Beetles are able to survive the Siberian winter in honeycombs stored in unheated rooms, therefore *D. lardarius* can be considered the most cold-resistant species of beetles found in honeybee hives (Measures to control beetles 1998). We identified both adult beetles and larvae in the hives, and the latter predominated (88.5%), were among the subdominants in number and had a fairly high occurrence. In hives, *D. lardarius* feeds on dead bees and can be considered a useful scavenger species. *Cryptolestes ferrugineus* was also noted among other representatives of synanthropic Coleoptera.

Earwigs often find refuge in hives, while the most common is *Forficula auricularia*, which is classified as an apiophilic species (Sidorov 1968; Domatsky and Domatskaya 2020). We have found individual larvae of *Forficula tomis*, which was previously recorded in hives on the territory of Russia and the countries of the former USSR (Sidorov 1968; Atakishiev 1969; Bakalova 2011a). Earwigs are considered pests of beekeeping, since when high in number they plunder a noticeable amount of honey. However, there are cases of earwigs eating wax moth larvae and eggs of other harmful insects in the hive (Atakishiev 1968).

Two species of Liposcelididae family were found, of which *Liposcelis bostrychophila* had a fairly high frequency. Synanthropic species of Liposcelididae family are regularly observed everywhere in bee hives, and sometimes in significant numbers (Rolnik and Szmids 1959).

2. Species feeding on pollen and honey. These species purposefully get into bee hives for additional nutrition with pollen and honey, as well as dead (and sometimes live) bees.

These include representatives of Hymenoptera – *Lasius niger* ants and *Vespula germanica* wasps. These insects had a high occurrence and were found in hives from different regions. They are also regularly found in hives around the world (Clapperton et al. 1989; Pusceddu et al. 2017; Pusceddu et al. 2018; Buteler et al. 2021). These insects are certainly pests, stealing food supplies from bees, however, due to their small number in hives of strong colonies, they do not cause any noticeable damage. The predatory activity of *V. germanica* is observed most often at ground level, under beehives, where

they target weak single bees falling from the hive entrance (Pusceddu et al. 2017). The relationship between bees and wasps is very interesting and requires a separate study. It is known that bees calmly react to *Vespula* wasps penetrating into the hive and do not attack them, unlike hornets, which hunt bees themselves and cause aggression among the latter. It has been noted that wasps can build their nests in functioning bee hives (T.F. Domatskaya, Tyumen, pers. comm.).

We conditionally include beetles of the Scirtidae family in this group. In our collections, three species of marsh beetles were found in hives – *C. padi*, *C. pubescens* and *C. variabilis* (Sazhnev et al. 2022), the latter prevailed, in terms of number and occurrence ranked the second of all insects following the eudominant *C. scanicus*.

Marsh beetle larvae develop in water and heavily moistened substrates. Adult beetles can enter hives for wintering. It is believed that adult marsh beetles do not feed, however, some species of Scirtidae (*Contacyphon coarctatus* (Paykull, 1799), *C. padi*, *Elodes minuta* (Linnaeus, 1767), *Scirtes* spp.) were found on flowering vegetation, therefore, it is possible that these beetles eat plant pollen (Sazhnev et al. 2022). Previously, *C. variabilis* was also observed in bee hives in Western Siberia (Zbanatsky 1997a). Taking into account the fact that marsh beetles were numerous in hives in our study, and were found in hives with an interval of more than 20 years, we assume that they can penetrate into hives not only for wintering but also possibly find additional food there.

Accidentals

These insects are not normally beehive-associated and enter hives accidentally, mainly in autumn, in search of shelter for wintering. Also, accidental intake into hives by beekeepers or by bees themselves from flowers can not be excluded. Representatives of this group were the most diverse in species composition and type of nutrition but they were always individually found in hives.

Most of the beetles and bugs from this group were recorded in early spring, after wintering and in late autumn. Probably, these species found themselves in hives in search of places for wintering.

Some species probably end up in hives attracted by the smell of honey. So, bumblebees were previously found in brood nests of bees (Sidorov 1968; Banaszak 1980; Bakalova 2011a). However, unlike the German wasp, bumblebees do not occur regularly in hives, so we refer them to accidental species. It is possible that *Brachypterus* beetles, which feed on the pollen of plants, also got into hives attracted by the smell of honey (Ler 1992).

Finally, aphids, larvae of cicadas of younger ages and thrips were recorded in hives. These insects feed on the sap of plants, and probably get into hives accidentally. Perhaps the latter is brought by bees when feeding on flowers (Orösi Pal 1939; Kulikov 1966).

A number of groups (Latriidiidae, Staphylinidae) include species that theoretically can be obligate or facultative apiophiles due to their type of nutrition and biology features, however, due to their rarity in hives and insufficient knowledge, we tentatively assign them to a group of accidental species.

The Parasitica found in hives we tentatively also refer to this group. However, a sufficiently high number and occurrence of Parasitica makes it worth to be paid attention to. These insects can be both parasites of bees and parasites of other symbionts (in particular, *C. scanicus*). Thus, Sidorov (1968) also found a large number of Parasitica in hives in the Volga-Kama region. He considered them parasites of beetles of the *Cryptophagus* genus; however, this issue requires further study.

Conclusions

Earlier, one paper on beetles in hives of Western Siberia in the region lists 22 species of Coleoptera – symbionts of bees (Zbanatsky 1997a). Our research complements the list of 20 species of Coleoptera and other insects. Thus, at the moment, 42 species of insects have been recorded in bee hives in Western Siberia.

At the turn of the 20th and 21st centuries, the same species prevailed in the bee hives of Western Siberia – the specific commensal *C. scanicus*, the marsh beetles *C. variabilis* were numerous. These results match the results of our study. Facultative and accidental species were diverse but not numerous. At the same time, in our study did not occur *Tribolium madens*, indicated as numerous in previously study, which can be a serious pest of hives (Zbanatsky 1997a).

The species composition and structure of bee symbionts in Western Siberia are very similar to the symbiocenoses of hives in the regions of the European part of Russia and other countries (Kazakhstan, Poland) (Rolnik and Szmidt 1959; Banaszak 1980; Semmar et al. 2014; Skulachev 2017). In most studies, a few specific species had the greatest number and occurrence. *Cryptophagus scanicus* is a typical commensal of bees, which dominates in number and occurrence in many regions. Such facultative species as ants, earwigs and the German wasp are regularly and in large numbers recorded in hives of Russia, Europe and other countries (links). The latter, which has become cosmopolitan thanks to human activities, is noted in most countries of the world, is numerous in hives and is considered one of the most dangerous pests of beekeeping.

The study of the fauna of insects living in honeybee hives should be continued, paying special attention to the role of marsh beetles and Parasitica in the structure of the symbiocenosis of bee colonies.

Acknowledgements

The authors expresses deep gratitude for help in identifying some doubtful species of insects to A.G. Kirejtshuk (Nitidulidae, Kateretidae), A.V. Kovalev (Latridiidae), A.A. Legalov (Curculionidae), G.Yu. Lyubarsky (Cryptophagidae), S.A. Ivanov (Heteroptera), A.S. Sazhnev (Scirtidae). Authors also wish to thank Stephen J. Martin (University of Salford, Manchester, United Kingdom) and Michał Woyciechowski (Jagiellonian University, Kraków, Poland) for valuable comments when reviewing the article. The

paper has been prepared with the financial support from the Ministry of Education and Science within the framework of the project 121042000066-6 “Study and analysis of the epizootic state of diseases of invasive etiology of agricultural and unproductive animals, bees and birds, changes in the species composition and bioecological patterns of the development cycle of parasites in conditions of displacement of their habitats”.

References

- Atakishiev TA (1968) Earwigs control. *Pchelovodstvo* 12: 1–33. [In Russian]
- Atakishiev TA (1969) Ecology and distribution of honeybee pests in the Azerbaijan SSR. PhD Thesis, Kazan Veterinary Institute, Kazan, USSR. [In Russian]
- Bakalova MV (2011a) Apiophilic nidicoloceneses of the honey bee *Apis mellifera mellifera* in the Shulgan-Tash Nature Reserve. PhD Thesis, Bashkir State University, Tolyatti, Russia. [In Russian]
- Bakalova MV (2011b) Coleoptera from log houses and beehives of the Shulgan-Tash Nature Reserve in Bashkortostan, Russia. *Euroasian Entomological Journal* 10 (1): 45–52. [In Russian]
- Banaszak J (1980) Badania nad fauną towarzyszącą w zasiedlonych ulach pszczelich. *Fragmenta Faunistica*, 25(10): 127–178. <https://doi.org/10.3161/00159301FF1980.25.10.127> [In Polish]
- Bey-Bienko GYa [Ed.] (1965) Keys to the Insects of the European Part of the USSR. V. II. Beetles and Twisted-Wing Insects. Science, Moscow, Leningrad, 668 pp. [In Russian]
- Buteler M, Yossen MB, Alma AM, Lozada M (2021) Interaction between *Vespula germanica* and *Apis mellifera* in Patagonia Argentina apiaries. *Apidologie* 52: 848–859. <https://doi.org/10.1007/s13592-021-00871-9>
- Clapperton BK, Alspach PA, Moller H, Matheson AG (1989) The impact of common and *German wasps* (Hymenoptera: Vespidae) on the New Zealand beekeeping industry. *New Zealand Journal of Zoology* 16(3): 325–332. <https://doi.org/10.1080/03014223.1989.10422897>
- Domatsky AN, Domatskaya TF (2020) Earwigs – pests of honey bees *Apis mellifera*. *Ukrainian Journal of Ecology* 10(6): 103–107. https://doi.org/10.15421/2020_266
- Ellis JD, Graham JR, Mortensen A (2013) Standard methods for wax moth research. *Journal of Apicultural Research* 52(1): 1–17. <https://doi.org/10.3896/IBRA.1.52.1.10>
- Konovalova TV (2018) Species composition of wasp pests of the honey bee *Apis mellifera*. *Veterinary and Nutrition* 1: 28–31. <https://doi.org/10.30917/ATT-VK-1814-9588-2018-1-8> [In Russian]
- Kulikov NS (1966) Various insects that are harmful to bees. *Pchelovodstvo* 9: 45–48. [In Russian]
- Kwadha CA, Ong’amo GO, Ndegwa PN, Raina SK, Fombong AT (2017) The biology and control of the Greater Wax Moth, *Galleria mellonella*. *Insects* 8(2): 1–17. <https://doi.org/10.3390/insects8020061>
- Ler PA (1992) Key to insects of the Far East of the USSR (Vol. 3). Coleoptera, or beetles. Part 2. Nauka, Saint Petersburg, 704 pp. [In Russian]
- Lyubarsky GYu (2002) Cryptophaginae (Coleoptera: Cucujoidea: Cryptophagidae): Diagnostics, Arealogy, Ecology. Moscow University Publisher, Moscow, 421 pp. [In Russian]

- Measures to control beetles (1998) Measures to control beetles (Coleoptera) that are harmful to honey bees in Western Siberia (recommendations): approved by the Department of Veterinary Medicine of the Tyumen Region 10.19.1998. Tyumen, 32 pp. [In Russian]
- Neumann P, Pettis JS, Schäfer MO (2016) Quo vadis *Aethina tumida*? Biology and control of small hive beetles. *Apidologie* 47: 427–466. <https://doi.org/10.1007/s13592-016-0426-x>
- Orösi Pal Z (1939) Méhellenségek A köpü Állatvilága. Budapest, 258 pp. [In Hungarian]
- Pashayan SA, Endovitsky RV (2018) Beekeeping of Tyumen region. In: Modern scientific and practical solutions in AIC. II All-Russian (National) Scientific and Practical Conference, Tyumen, Russia, October 2018. Northern Trans-Ural State Agricultural University Publishers, Tyumen, 178–181. [In Russian]
- Opit G, Throne J, Friesen K (2022) Psocid ID: Stored-Product Psocid Identification Website. Agricultural Research Service. <https://www.ars.usda.gov/plains-area/mhk/cgahr/spieru/docs/psocid-id-introduction/>
- Pusceddu M, Floris I, Buffa F, Salaris E, Satta A (2017) Agonistic interactions between the honeybee (*Apis mellifera ligustica*) and the European wasp (*Vespula germanica*) reveal context-dependent defense strategies. *PLoS ONE* 12(7): e0180278. <https://doi.org/10.1371/journal.pone.0180278>
- Pusceddu M, Mura A, Floris I, Satta A (2018) Feeding strategies and intraspecific competition in German yellowjacket (*Vespula germanica*). *PLoS ONE* 13(10): e0206301. <https://doi.org/10.1371/journal.pone.0206301>
- Pushkin SV (2009) Beetles are symbionts of honey bee nests. *Pchelovodstvo* 6: 1–23. [In Russian]
- Rolnik S, Szmidt A (1959) Z badan nad entomofauna pasieki doswiadczalnej w nadlesnictwie zielonka. *Pszczelnicze Zeszyty Naukowe* 3(2): 61–76. [In Polish]
- Sazhnev AS, Stolbov VA, Sergeeva EV (2022) Notes on the Fauna of Marsh Beetles (Coleoptera: Scirtidae) of Western Siberia. *Field Biologist Journal* 4(1): 5–14. <https://doi.org/10.52575/2712-9047-2022-4-1-5-14> [In Russian]
- Schäfer MO, Ritter W, Pettis JS, Neumann P (2010) Winter losses of honeybee colonies (Hymenoptera: Apidae): the role of infestations with *Aethina tumida* (Coleoptera: Nitidulidae) and *Varroa destructor* (Parasitiformes: Varroidae). *Journal of Economic Entomology* 103(1): 10–16. <https://doi.org/10.1603/EC09233>
- Semmar S, Daoudi-Hacini S, Doumandji S (2014) Some species of Arthropods in hives of *Apis mellifera intermissa* (Von Buttel-Reepen, 1906) (Hymenoptera, Apidae) in the Mitidja (Algeria). *International Journal of Zoology Research* 4(3): 15–22.
- Sidorov NG (1967) Symbionts of wintering bees. *Pchelovodstvo* 12: 20–23. [In Russian]
- Sidorov NG (1968) Honey bee symbionts. PhD Thesis, Kazan State Veterinary Institute, Kazan, USSR. [In Russian]
- Skulachev IL (2017) Symbionts of honey bees. In: Solovyov VB (Ed.) *Advances in Science and Technology. VIII International Scientific-Practical conference, Moscow (Russia), April, 2017. Actualnots. RF, Moscow, 19–20.* [In Russian]
- Stolbov NM, Kashina GV, Zerova MD (1990) Against wax moths – *Dibrachis*. *Pchelovodstvo* 12: 12–13. [In Russian]
- Stolbova VV (2022) New Data on the distribution of mites in honey bee hives in the south of Western Siberia. *Parazitologiya* 56(3): 209–225. <https://doi.org/10.31857/S0031184722030048> [In Russian]

- Traiyasut P, Mookhploy W, Kimura K, Yoshiyama M, Khongphinitbunjong K, Chantawannakul P, Buawangpong N, Saraithong P, Burgett M, Chukeatirote E (2016) First detection of honey bee viruses in wax moth. *Chiang Mai University Journal of Natural Sciences* 43(4): 695–698.
- Zbanatsky OV (1997a) Beetles (Coleoptera), harmful to honey bees in Western Siberia, and their control measures. PhD Thesis, All-Russian Scientific Research Institute of Veterinary Entomology and Arachnology, Tyumen, Russia. [In Russian]
- Zbanatsky OV (1997b) Species composition of Coleoptera of Western Siberia, harmful in the hive of honey bees. *Agrarian science and education in the conditions of agrarian reform in the Tyumen region. Materials of scientific-methodical and practical conference, Tyumen (Russia), March 1997.* [In Russian]
- Zimina LV (1973) *Physocephala truncata* (Diptera, Conopidae) – parasite of honey bees in Tuva. *Zoological journal LII* (11): 1732–1733. [In Russian]

Supplementary material I

Studied apiaries in Western Siberia

Authors: Victoria V. Stolbova, Vitaly A. Stolbov

Data type: table (excel document)

Copyright notice: This dataset is made available under the Open Database License (<http://opendatacommons.org/licenses/odbl/1.0/>). The Open Database License (ODbL) is a license agreement intended to allow users to freely share, modify, and use this Dataset while maintaining this same freedom for others, provided that the original source and author(s) are credited.

Link: <https://doi.org/10.3897/jhr.96.104720.suppl1>

Neomegadicylus, a new genus of Pteromalidae (Hymenoptera, Chalcidoidea) from the Palearctic region

Ekaterina V. Tselikh¹, Jean-Yves Rasplus², Jaehyeon Lee³, Deok-Seo Ku³

1 Zoological Institute, Russian Academy of Sciences, St. Petersburg, Russia **2** CBGP, INRAE, CIRAD, IRD, Montpellier SupAgro, University of Montpellier, Montpellier, France **3** The Science Museum of Natural Enemies, Geochang 50147, Republic of Korea

Corresponding author: Ekaterina V. Tselikh (tselikhk@gmail.com)

Academic editor: Petr Janšta | Received 6 April 2023 | Accepted 16 June 2023 | Published 7 July 2023

<https://zoobank.org/0DEA4F80-F4AD-4FAF-A770-82C205FD75DA>

Citation: Tselikh EV, Rasplus J-Y, Lee J, Ku D-S (2023) *Neomegadicylus*, a new genus of Pteromalidae (Hymenoptera, Chalcidoidea) from the Palearctic region. Journal of Hymenoptera Research 96: 569–577. <https://doi.org/10.3897/jhr.96.104628>

Abstract

A new genus of Pteromalidae *Neomegadicylus* **gen. nov.**, along with its type species *Neomegadicylus gracileus* **sp. nov.**, is described from the Republic of Korea and Japan, and *N. klarissae* **sp. nov.**, is described from the Republic of Korea. This genus can be distinguished from its putatively close relative *Megadicylus* Girault, 1929 by the following combination of characters – antennal clava with large micropilosity area, F1–F6 much longer than broad; clypeus smooth and shiny; notauli deep and incomplete and anterior part of propodeum strongly sloping in lateral view. An identification key to species of *Neomegadicylus* is provided, based on females.

Keywords

Key, new species, Pteromalinae, taxonomy

Introduction

With an estimated diversity of about 500,000 species, Chalcidoidea (Hymenoptera) has undergone a spectacular radiation (Cruaud et al., submitted). Although phytophagous species are known, most species are parasitoids. Because chalcidoid wasps attack all life stages from eggs to adults in virtually all insect orders, they represent one of the most important group of insects for biological control in both natural and agricultural ecosystems (Noyes 2019). With 33 subfamilies and about 640 genera, Pteromalidae was the largest family in Chalcidoidea. It has been recently revised to include 8 subfamilies and 424 genera (Burks et al. 2022). Like other chalcidoid families, Pteromalidae is poorly known and many species remained to be described. During our study of the family in the Eastern Palaearctic region, several specimens were collected in forested areas of South Korea and Japan that appeared to belong to a new genus.

Herein, the new genus *Neomegadicylus* gen. nov., and two new species *Neomegadicylus gracileus* sp. nov., and *N. klarissae* sp. nov., are described. Unfortunately, males and biology are not known but females exhibit morphological characters diagnostic of Pteromalinae in which the new genus is placed. An identification key to females of Palaearctic species of *Neomegadicylus* is also provided.

Materials and methods

The material used in this study is deposited in the Hymenoptera collections of the Science Museum of Natural Enemies, Geochang, Republic of Korea (**SMNE**), the National Institute of Biological Resources, Incheon, Republic of Korea (**NIBR**), the Korea National Arboretum, Pocheon, Republic of Korea (**KNA**), Zoological Institute of the Russian Academy of Sciences, St. Petersburg, Russia (**ZISP**) and the Centre for Population Biology and Management, Montpellier, France (**CBGP**).

Morphological terminology, including sculpture and wing venation nomenclature, follows Bouček and Rasplus (1991) and Gibson (1997). The flagellum consists of two anelli, the funicle composed of six funicular segments and the clava. The following abbreviations are used: **POL** – posterior ocellar line, the minimum distance between the posterior ocelli; **OOL** – ocello–ocular line, the minimum distance between a posterior ocellus and compound eye; **C1–C3** – claval segments; **PST** – parastigma; **M** – marginal vein; **S** – stigmal vein; **PM** – postmarginal vein; **F1–F6** – funicular segments; **Mt2–Mt8** – metasomal tergites (**Mt1** – petiole). The scape is measured without the radicle; the pedicel is measured in lateral view. The distance between the clypeal lower margin and the toruli is measured from the lower margins of the toruli. Eye height is measured as maximum diameter, eye length as minimum diameter. The mesosoma and metasoma are measured in lateral view, the latter including the ovipositor sheaths.

Observations were made using Micromed MC-2 ZOOM and Leica MZ16 stereomicroscopes, and images were acquired using a Keyence VHX-5000 multiple-focus imaging system.

Taxonomy

Neomegadicylus Tselikh, Rasplus & Ku, gen. nov.

<https://zoobank.org/A308ABA4-1A09-44D9-9120-8D8A56747E81>

Figs 1–16

Type species. *Neomegadicylus gracileus* Tselikh, Rasplus & Ku, sp. nov., by present designation.

Description. Clypeus smooth and shiny, with lower margin slightly emarginated medially, tentorial pits indistinct (Figs 3, 10); antennal formula 11263, toruli slightly above lower ocular line; F1–F6 longer than broad, antennal clava with large micropilosity area on C1–C3 (Fig. 2); gena conspicuously carinate (Fig. 7); right mandible with 4 teeth, left with 3 teeth; occiput with carina. Pronotum almost as wide as mesoscutum, with collar margin weakly carinate (Figs 7, 15); prepectus as long as tegula; notauli deep, long but incomplete (Figs 2, 11); scutellum convex and with distinct reticulate frenal area, but without frenal groove (Figs 2, 11, 16); upper mesepimeron alutaceous or with lower part smooth, upper part alutaceous; metapleuron strongly reticulate; part of propodeum before nucha strongly sloping in lateral view (Fig. 15), dorsally with poorly defined converging plicae and large convex nucha (Figs 8, 16). Fore wing hyaline with distinct speculum (Figs 4, 12). Hind coxa dorsally bare. Metasoma lanceolate, on distinct but short smooth cylindrical petiole, Mt2 longer than broad (Figs 6, 14); cerci with setae subequal in length; ovipositor not much protruding.

Remarks. The new genus is similar to the Australian genus *Megadicylus* Girault, 1929 (Bouček, 1988) in having the clypeal lower margin slightly emarginated (Figs 3, 18); antennal formula 11263 (Figs 5, 13, 19); propodeum in lateral view sloping (Figs 9, 13, 17), dorsally with converging plicae and large nucha (Figs 8, 16, 20); cylindrical petiole.

However, *Megadicylus* Girault (based on observation of non-type female of *Megadicylus dubius* Girault, 1917, only known species of the genus, collected in Australia and deposited in CBGP) and *Neomegadicylus*, gen. nov., can be distinguished as follows:

Neomegadicylus – antennal clava with large micropilosity area extending over C1–C3 (Fig. 2), F5–F6 much longer than broad (Figs 5, 13); clypeus smooth and shiny medially (Figs 3, 10); notauli deep but incomplete (Figs 2, 11); anterior part of propodeum strongly sloping in lateral view (Fig. 15);

Megadicylus – antennal clava with small micropilosity area only on C3 (Fig. 19), F5–F6 shorter than broad (Fig. 19); clypeus radially striate (Fig. 18); notauli shallow but complete (Fig. 20); propodeum in lateral view not that strongly sloping (Fig. 17).

Key to females of *Neomegadicylus* gen. nov.

- 1 Propodeum without costula (Fig. 8). Mt2 posteriorly emarginate (Fig. 6). Antenna with F1 3.25–3.65 times as long as broad (Fig. 5). Scape 1.27–1.33

times as long as eye length. Combined length of pedicel and flagellum 1.57–1.75 times breadth of head. Notauli straight (Fig. 2). Fore wing with basal cell bare, M 1.94–2.10 times as long as S (Fig. 4).....

.....*N. gracileus* Tselikh, Rasplus & Ku, sp. nov.

- Propodeum with costula (Fig. 16). Mt2 posteriorly curved (Fig. 14). Antenna with F1 2.45–2.60 times as long as broad (Fig. 13). Scape 1.05–1.09 times as long as eye length. Combined length of pedicel and flagellum 1.24–1.30 times breadth of head. Notauli curved (Fig. 11). Fore wing with basal cell pilose apically, M 2.60–2.80 times as long as S (Fig. 12).....

.....*N. klarissae* Tselikh, Rasplus & Ku, sp. nov.

***Neomegadicylus gracileus* Tselikh, Rasplus & Ku, sp. nov.**

<https://zoobank.org/D47451C7-960E-4995-A0F3-E6F40F91BB89>

Figs 1–8

Description. Female. Body length 2.60–2.80 mm. Fore wing length 1.90–2.10 mm.

Head and mesosoma dark metallic green with diffuse coppery lustre; metasoma brown, partly with metallic green and coppery lustre. Antenna with scape and pedicel yellowish-brown, F1–F4 dorsally yellowish-brown, ventrally yellowish-brown or yellow, F5 dorsally yellowish-brown, ventrally yellow, F6 and clava brown. All coxae dark metallic blue-green with diffuse coppery lustre; all femora yellowish-brown; tibiae and tarsi yellow. Fore wing hyaline, venation yellowish-brown.

Head in dorsal view 2.14–2.26 times as broad as long and 1.24–1.25 times as broad as mesoscutum; in frontal view 1.17–1.18 times as broad as high. POL 1.30–1.44 times OOL. Eye height 1.40 times eye length and 1.75–1.82 times as long as malar space. Distance between antennal toruli and lower margin of clypeus 0.84–0.88 times distance between antennal toruli and median ocellus. Antenna with scape 0.90–0.95 times as long as eye height and 1.27–1.33 times as long as eye length; pedicel 2.25–2.35 times as long as broad and 0.63–0.71 times as long as F1; combined length of pedicel and flagellum 1.57–1.75 times breadth of head; F1 3.25–3.65 times as long as broad, F2–F6 longer than broad; clava 3.40–3.60 times as long as broad.

Mesosoma 1.60–1.68 times as long as broad, notauli straight. Scutellum finely reticulate, 0.90–0.95 times as long as broad. Propodeum 0.66–0.80 times as long as scutellum; costula absent, median carina not complete or absent; nucha large and reticulate. Fore wing 2.40–2.50 times as long as maximum width; basal cell bare; basal vein pilose; speculum open; M 1.07–1.19 times as long as P and 1.94–2.10 times as long as S.

Metasoma 3.30–4.30 times as long as broad, 1.04–1.15 times as long as mesosoma and head; Mt2 posteriorly emarginate. Ovipositor sheath projecting beyond apex of metasoma.

Etymology. The name is a noun in apposition derived from the Latin word “*gracilis*”.

Material examined. Holotype: SOUTH KOREA • ♀; **Gyeonggi-do**, Pocheon-si, Soheul-eup, 37°45'29.2"N, 127°10'0.4"E, 15.X–30.X.2015, coll. Park, Choi,



Figures 1–8. *Neomegadicylus gracileus* Tselikh, Rasplus & Ku, sp. nov., holotype female (**1, 2, 5, 7, 8**), paratype female (**3, 4, 6**) **1** body, lateral view **2** head, dorso-lateral view and mesosoma, dorsal view **3** clypeus, frontal view **4** wings **5** antenna **6** metasoma, dorsal view **7** head and mesosoma, lateral view **8** propodeum, dorsal view.

Nam, Shin, Kim; deposited in NIBR. **Paratypes:** SOUTH KOREA • 2 ♀♀; **Gyeongsangbuk-do**, Bonghwa-gun, Myeongho-myeon, Gwanchang-ri, Mt. Cheongryangsan, 14.VII.2015, coll. E. Tselikh; ZISP • 1 ♀, **Gyeongsangbuk-do**, Gyeongju-si, Hyeongok-myeon, Namsa-ri, 15–29.IX.2005, coll. J.O. Lim; SMNE • 5 ♀♀; **Gyeonggi-do**, Pocheon-si, Soheul-eup, 37°45'29.2"N, 127°10'0.4"E, 15.V.2015, coll. Park, Choi, Nam, Shin, Kim; ZISP • 6 ♀♀; same locality, 30.IX–15.X.2015, 15.X–30.X.2015, coll. Park, Choi, Nam, Shin, Kim; SMNE • 1 ♀; same locality, 37°45'08.7"N, 127°09'07.2"E, 4.V–15.V.2018, coll. Kim, Kim, Gi, Jo; KNA • 1 ♀; **Gyeongsangnam-do**, Geochang-gun, Namsang-myeon, Muchan-ri, Malaise Trap, 8.IX–23.IX.2021, coll. J. Lee, H. Jeong; SMNE. JAPAN • 1 ♀; **Honshu**, Hyogo Pref, Kobe, Rokko Mts., Maya Mt., forest, 4.IX.2005, coll. S. Belokobylskij; (ZISP).

Distribution. South Korea, Japan.

***Neomegadicylus klarissae* Tselikh, Rasplus & Ku, sp. nov.**

<https://zoobank.org/6C8E6728-4492-4A1C-838D-EB6A1C43D36E>

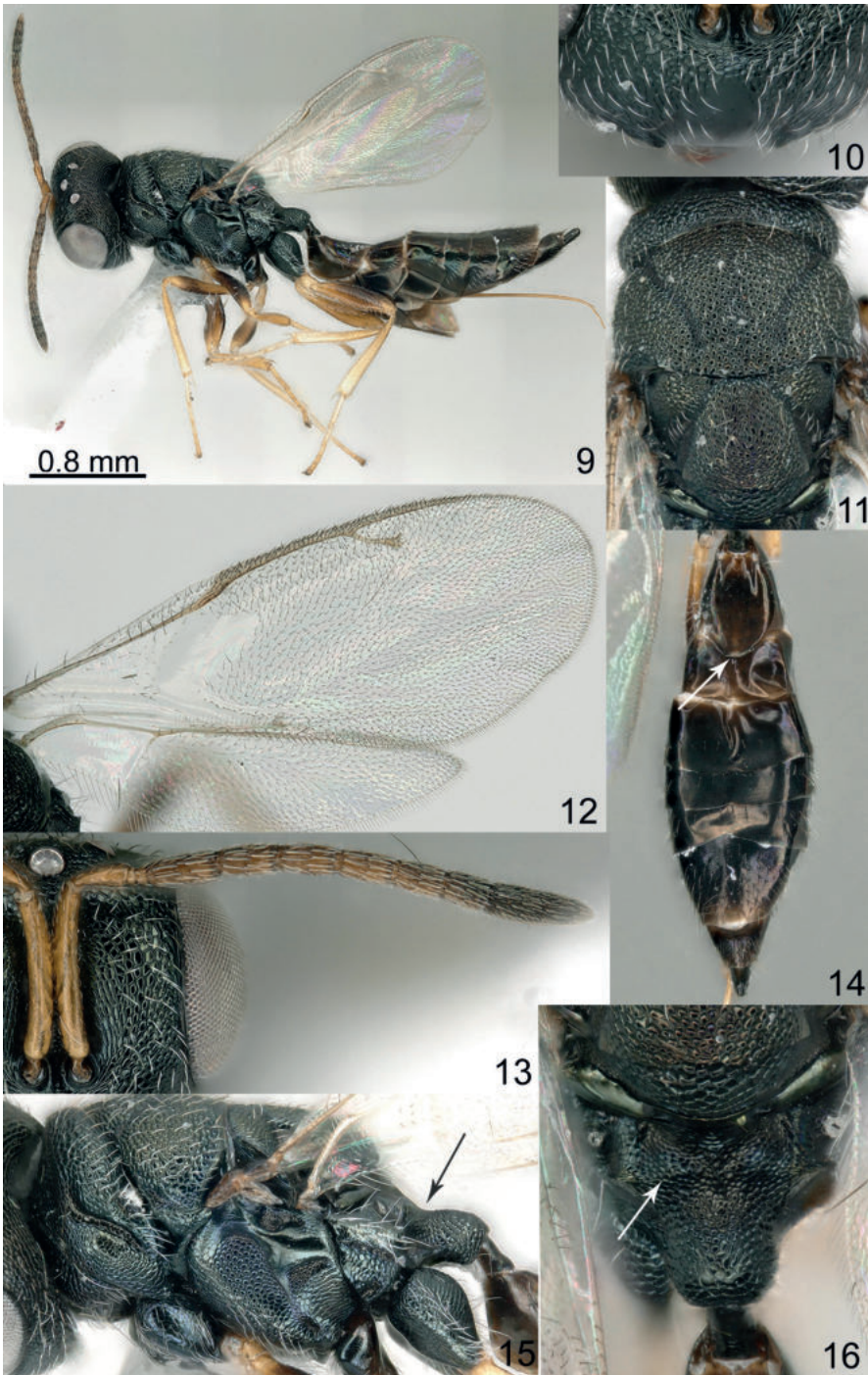
Figs 9–16

Description. Female. Body length 3.20–3.50 mm. Fore wing length 2.00–2.10 mm.

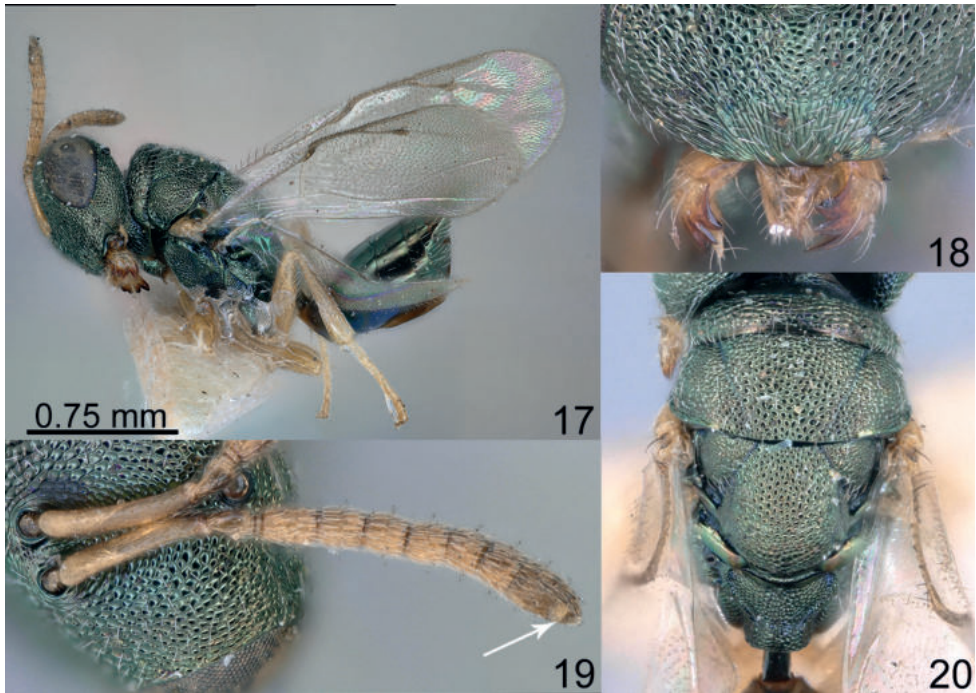
Head and mesosoma black with weak dark metallic blue and coppery lustre; metasoma dark brown, laterally M2–M8 with metallic blue green and coppery lustre, dorsally Mt3, Mt4, Mt7 and Mt8 partly with metallic violet and coppery lustre. Antenna with scape, pedicel and F1–F5 yellowish-brown, F6 dorsally brown, ventrally yellowish-brown, clava brown. All coxae black with dark metallic blue lustre; all femora brown; tibiae and tarsi yellow. Fore wing hyaline, venation yellowish-brown.

Head in dorsal view 1.93–1.95 times as broad as long and 1.28–1.32 times as broad as mesoscutum; in frontal view 1.20–1.22 times as broad as high. POL 1.45–1.55 times OOL. Eye height 1.33–1.35 times eye length and 2.00–2.09 times as long as malar space. Distance between antennal toruli and lower margin of clypeus 0.91–0.94 times distance between antennal toruli and median ocellus. Antenna with scape 0.78–0.81 times as long as eye height and 1.05–1.09 times as long as eye length; pedicel 2.22–2.40 times as long as broad and 0.76–0.81 times as long as F1; combined length of pedicel and flagellum 1.24–1.30 times breadth of head; F1 2.45–2.60 times as long as broad, F2–F6 longer than broad; clava 3.10–3.28 times as long as broad.

Mesosoma 2.00 times as long as broad, notauli curved. Scutellum finely reticulate, 1.05 times as long as broad. Propodeum 0.75–0.76 times as long as scutellum; costula distinct, median carina weak; nucha large and reticulate. Fore wing 2.40–2.56 times as long as maximum width; basal cell pilose on upper part; basal vein pilose; speculum open; M 1.16–1.26 times as long as P and 2.60–2.80 times as long as S.



Figures 9–16. *Neomegadicylus klarissae* Tselikh, Rasplus & Ku, sp. nov., holotype female **9** body, lateral view **10** clypeus, frontal view **11** mesosoma, dorsal view **12** wings **13** antenna **14** metasoma, dorsal view **15** mesosoma, lateral view **16** propodeum, dorsal view.



Figures 17–20. *Megadicylus dubius* Girault, 1917, not type female **17** body, lateral view **18** clypeus, frontal view **19** antenna **20** mesosoma, dorsal view.

Metasoma 3.28–3.30 times as long as broad, 1.01–1.06 times as long as mesosoma and head; Mt2 posteriorly curved. Ovipositor sheath projecting beyond apex of metasoma.

Etymology. The species is named in honour of the prominent entomologist, Dr. Klarissa Alekseevna Dzhankmen, an expert on Pteromalidae (Hymenoptera).

Material examined. *Holotype*: SOUTH KOREA • ♀; **Gyeongsangnam-do**, Geochang-gun, Mari-myeon, Daedong-ri, Malaise Trap, 28.VII–15.VIII.2021, coll. J. Lee, H. Jeong; deposited in NIBR. *Paratype*: SOUTH KOREA • 1 ♀; same data as holotype; ZISP.

Distribution. South Korea.

Conclusion

The pteromalid genus *Neomegadicylus* gen. nov. (type species *Neomegadicylus gracileus* sp. nov.) belongs to the family Pteromalidae, subfamily Pteromalinae and comprises only two species, *N. gracileus* sp. nov. and *N. klarissae* sp. nov. Both species are found in the eastern Palearctic. Unfortunately, the biology of the species of this genus is unknown, but all specimens were collected in the deciduous broadleaved forests.

Acknowledgements

This work was supported by funding of the Russian state (research project No. AAAA-A19-122031100272-3 to E. Tselikh), a grant from the National Institute of Biological Resources (NIBR) funded by the Ministry of Environment (MOE) of the Republic of Korea (NIBR 202002205, 202304203 to Deok-Seo Ku).

References

- Bouček Z (1988) Australasian Chalcidoidea Hymenoptera). A biosystematic revision of genera of fourteen families, with a reclassification of species. CAB International, Wallingford, UK, 832 pp.
- Bouček Z, Rasplus J-Y (1991) Illustrated key to West-Palaearctic genera of Pteromalidae (Hymenoptera: Chalcidoidea). Institut National de la Recherche Agronomique, Paris, 140 pp.
- Burks R, Mitroiu M-D, Fusu L, Heraty JM, Janšta P, Heydon S, Papilloud ND-S, Peters RS, Tselikh EV, Woolley JB, van Noort S, Baur H, Cruaud A, Darling C, Haas M, Hanson P, Krogmann L, Rasplus J-Y (2022) From hell's heart I stab at thee! A determined approach towards a monophyletic Pteromalidae and reclassification of Chalcidoidea (Hymenoptera). *Journal of Hymenoptera Research* 94: 13–88. <https://doi.org/10.3897/jhr.94.94263>
- Gibson G (1997) Morphology and Terminology. In: Gibson GAP, Huber JT, Woolley JB (Eds) *Annotated Keys to the Genera of Nearctic Chalcidoidea (Hymenoptera)*. NRC Research Press, Ottawa, 16–44.
- Girault AA (1929) *New pests from Australia*. VI private publication. Brisbane, 4 pp.
- Noyes JS (2019) *Universal Chalcidoidea Database – World Wide Web Electronic Publication*. <https://www.nhm.ac.uk/our-science/data/chalcidoids/database/> [Accessed on 10.05.2021]

A new species of *Typhlomyrmex* from Colombia, re-description of the worker of *T. clavicornis* Emery, description of the worker of *T. prolatus* Brown, and key of known species (Hymenoptera, Formicidae)

Fernando Fernández¹, Gianpiero Fiorentino², Daniel Castro³

1 Instituto de Ciencias Naturales, Universidad Nacional de Colombia, Bogotá D.C., Colombia **2** Federated Department of Biological Sciences, New Jersey Institute of Technology – Rutgers-Newark University, Rutgers, NJ, USA **3** Instituto Amazónico de Investigaciones Científicas SINCHI, Avenida Vásquez Cobo Calles 15 y 16, Leticia, Amazonas, Colombia

Corresponding author: Fernando Fernández (ffernandezca@unal.edu.co)

Academic editor: Francisco Hita García | Received 10 March 2023 | Accepted 29 June 2023 | Published 10 July 2023

<https://zoobank.org/52041BF8-8EDE-4E6B-A2B4-CAF6B87B074A>

Citation: Fernández F, Fiorentino G, Castro D (2023) A new species of *Typhlomyrmex* from Colombia, re-description of the worker of *T. clavicornis* Emery, description of the worker of *T. prolatus* Brown, and key of known species (Hymenoptera, Formicidae). Journal of Hymenoptera Research 96: 579–597. <https://doi.org/10.3897/jhr.96.103219>

Abstract

Typhlomyrmex Mayr is a genus of small and cryptic ants of the subfamily Ectatomminae. Here, we provide taxonomic notes on the ants of the genus *Typhlomyrmex* Mayr from Colombia, along with the description of *Typhlomyrmex encanto* sp. nov. based on the worker caste, and the re-description / description of the worker caste of *T. clavicornis* Emery and *T. prolatus* Brown. Finally, we offer a key for the known species of *Typhlomyrmex*, and distribution maps for the three species this study focuses on.

Keywords

Ectatomminae, Neotropics, Subterranean ants, TSBF method, Wallacean Shortfall

Introduction

The relatively small genus *Typhlomyrmex* Mayr, belongs to the subfamily Ectatomminae, consists of 10 strictly Neotropical extant species. Camacho et al. (2022) explored the internal phylogeny of the Ectaheteromorph clade, sensu (Bolton 2003), and offered a new

classification of this group with a single subfamily (Ectatomminae) consisting of two tribes, Ectatommini and Heteroponerini. Within the Ectatommini tribe, *Typhlomyrmex* is redefined to contain the species *T. clavicornis*, *T. foreli*, *T. major*, *T. meire*, *T. prolatus*, *T. pusillus*, and *T. rogenhoferi* (Brown 1965; Lacau et al. 2004); in addition, the species *T. lavra*, *T. lenis*, and *T. reichenspergeri* are transferred to the genus from *Gnamptogenys* Roger (Camacho et al. 2022). In the new sense, Camacho et al. (2022) define *Typhlomyrmex* as ants with the following characteristics: a sometimes-well-defined antennal club, consisting of 3 or 4 segments; cephalic vertex mostly smooth and shining; eyes absent or reduced, promesonotal suture well marked, totally interrupting dorsal mesosomal sculpture; metacoxal dorsum unarmed or with small lobe or denticle and petiole pedunculate, sometimes with a prominent anteroventral process, among other traits.

Typhlomyrmex species are cataloged as ants with poorly known ecology and biology, owing to them nesting in decomposed wood and soil (Lacau et al. 2008), substrates that are usually under-sampled in traditional samplings while surveys more focused on subterranean and soil nesting ants have proven to be more effective in capturing numerous species (Castro et al. 2018b). Therefore, though *Typhlomyrmex* presents a wide distribution (Mexico to Argentina), this genus does not present high abundances and species richness in robust inventories (Wilkie et al. 2010; Franco et al. 2019; Dáttilo et al. 2020; Meurgey and Ramage 2020; Albuquerque et al. 2021).

Of the 10 known *Typhlomyrmex* species, the worker caste of *T. clavicornis*, *T. foreli* and *T. prolatus*, are not known or briefly described. In this publication, the worker of *T. clavicornis* are re-described and the worker of *T. prolatus* described, along with *Typhlomyrmex encanto* sp. nov. from Colombia, likely the smallest species known of Ectatomminae. A key to all species known based on the worker caste is offered, as well as distribution maps for the three species reviewed in this manuscript.

Materials and methods

The material examined is deposited at Instituto Humboldt, Claustro San Agustín, Villa de Leyva, Boyacá, Colombia (**IAvH**); Instituto de Ciencias Naturales, Universidad Nacional de Colombia, Bogotá D.C., Colombia (**ICN**); Laboratorio de Entomología of the Universidad de la Amazonia, Florencia, Caquetá, Colombia (**LEUA**) and Colección de artrópodos terrestres de la Amazonia Colombiana, Instituto SINCHI, Leticia, Amazonas, Colombia (**CATAC**).

Imaging

Observations, descriptions, measurements, and photographic images of the pin-pointed specimens were obtained with a Nikon SMZ25 stereomicroscope and DS-Ri2 camera with NIS Elements software at the New Jersey Institute of Technology. All images are digitally stacked photomicrographic composites of several individual focal planes, which were obtained using Nikon Elements software. The distribution maps were created using ArcGIS desktop ver. 10.8 (ESRI, Redlands, CA).

Measurements and indices

All measurements were taken using an ocular micrometer at 80× magnification on a Nikon SMZ25 microscope and corroborating with measurements using the NIS Elements software. Morphometric sampling included linear measurements of 8 morphological traits: three cephalic, two mesosomal and three petiolar (Table 1). All measurements are given in millimeters. Measurement protocols follow those commonly used in ant systematics and in previous taxonomic reviews of *Typhlomyrmex* (Lacau et al. 2004).

Table 1. Morphological variables used in morphometric analyses.

HL	Head length. In full-face view, maximum distance from the posterior margin of head to the anterior margin of clypeus (Suppl. material 1: fig. S1A).
HW	Head width. In full-face view, maximum width of head, excluding the eyes (Suppl. material 1: fig. S1A).
SL	Scape length. In frontal view, maximum length of scape excluding basal condyle and neck (Suppl. material 1: fig. S1A).
PrW	Pronotum width. In dorsal view, maximum width of pronotum (Suppl. material 1: fig. S1B).
WL	Weber's length. In lateral view, distance between the anterior margin of the pronotum, excluding collar, to the posteroventral margin of metapleuron (Suppl. material 1: fig. S1C).
PeW	Petiolar width. In dorsal view, maximum width of petiole (Suppl. material 1: fig. S1B).
PeH	Petiolar height. In lateral view, perpendicular distance from the posteroventral lobe of petiolar tergite to its maximum dorsal margin (Suppl. material 1: fig. S1C).
PeL	Petiolar length. In lateral view, distance between the anterior margin of petiole, including its anterolateral projection, to its posterior margin, excluding the posteroventral folded ridge that embraces the helcium (Suppl. material 1: fig. S1C).
TL	Total length: Sum of HL + WL + abdominal segments A2 through A7. Segments A2 – A7 measured as PL and gaster length.
CI	Cephalic index: HW/HL
SI	Scape index: SL/HW

Taxonomy

Typhlomyrmex encanto sp. nov.

<https://zoobank.org/E805A0DA-2284-4133-B69B-EA78487D11D6>

Figs 1, 6A

Typhlomyrmex sp. A Lacau et al. 2008.

Holotype worker. COLOMBIA, Amazonas, El Encanto, 01°44'3.48"S, 73°11'57.7"W, 156 m, 14–17.iv.2022, leg. L. Pérez & R. Nova (ICN 103630).

Paratype. 1 worker, same data as holotype (ICN 103631).

Non-type material examined. COLOMBIA, Vaupés, Pacoa. Río Causuarí, Cerro Morroco, 00°08'19.2"N, 73°11'57.7"W, 195 m, 26.ii.2018, leg. D. Luna & W. Gómez, 2 workers (ICN 103632).

Worker description. *Head.* Rectangular, longer than wide. Vertex slightly concave in the middle, occipital corners rounded. Sides of head slightly convex, its greatest width towards the middle of the head. Head narrowed anteriorly. Anterior margin of the

clypeus slightly convex, with a short and prominent truncated lobe. Eyes reduced to an ommatidium towards the position of the apical third of the head; antennal sockets fully concealed by the frontal lobes; frontal lobes short and subquadrate; toruli circular, antennae 12-segmented with a well-defined 3-segmented club; scape conspicuously curved ventrally at half of its apical length in frontal view, the maximal width nearly equal to pedicel length; when folded backward, scape does not reach the vertexal margin; pedicel about as long as wide, and about as long as the 3 following segments together; segments A3 to A9 very short; segment 10 to 12 forming antennal club; mandible shape elongated-subtriangular, the apical margin joining basal margin at a strongly rounded angle; masticatory margin with a series of small teeth followed by a larger apical tooth.

Mesosoma. Lightly curved and irregular in lateral view, pronotum anteriorly rounded in dorsal view, longer than wide and strongly sloping anteriorly in lateral view, its posterior part curved, mesonotum slightly convex, promesonotal suture well marked, propodeal sutures feebly marked. Propodeal spiracle small, circular, equidistant from the dorsal and lateral margins of the propodeum, its diameter (0.012 mm) roughly equal to the length of the 8th antennomere; dorsal face of the propodeum weakly inclined and convex, gradually rounding beyond the spiracle towards the sloping posterior face; propodeal spiracle opened laterally, its large orifice bordered by a thin cuticular ring; propodeal lobes lacking.

Metasoma. Petiole in lateral view higher than long, with short and stout peduncle; its front face flat, delimited by a poorly defined carinae; dorsum strongly rounded and short. Petiole spiracle distant from the leading edge by a length greater than its diameter. Sub-petiolar process elongate and forward facing, lobe-shaped tapering to a downward point. First tergum with prora marked.

Sculpture. Body generally opaque with restricted smooth shiny areas on the mesopleura; front of head with a sculpture that is a mixture of points and uniform longitudinal striation short, faint longitudinal striation limited to the pronotum and the lower part of the sides of the propodeum, below the propodeal spiracle and partly on the propodeal bulla.

Pilosity and color. The whole body with a dense and very short pubescence. Erect hairs absent. Light brown color. Outer surface of the mid tibiae without a series of hard, spiniform hairs.

Measurements. HW 0.339, HL 0.413, SL 0.211, PrW 0.204, PeW 0.129, PeL 0.186, PeH 0.154, WL 0.488, CI 82, SI 62, TL 1.57.

Diagnosis and comments. A unique feature in *Typhlomyrmex encanto* sp. nov. is the median projection of the clypeal lamella, not known in any other described *Typhlomyrmex*. This species is also the smallest of the genus, and probably the smallest Ectatomminae in the World. In their treatment of the *Typhlomyrmex* from Colombia, Lacau et al. (2008) include one unnamed species, referred to as “sp. A” which matches the description of *Typhlomyrmex encanto* sp. nov. In the key to the species, the following characterization of species A can be obtained, translated from French: “Head capsule whose maximum width is located at half its length, with lateral surfaces clearly converging anteriorly; occipital carina absent; clypeus in dorsal view, with the anterior



Figure 1. Photomicrographs of *Typhlomyrmex encanto* sp. nov. (ICN 103630) **A** head in frontal view **B** body in dorsal view **C** body in lateral view. Scale bars: 0.2 mm (**A**); 0.5 mm (**B, C**).

edge forming a distinct constricted convexity; clypeal lamella bearing a short and narrow median process (its maximum width clearly less than that of the scape), protruding and clearly truncated at the apex; scape in dorsal view greatly enlarged posteriorly at its basal third; indistinct metanotal groove". The authors refer to material of this species from Brazil, Colombia and Peru and mention that the description is "in progress". However, this description was not published and there are no known plans to do so (Jacques Delabie, pers. comm.). Lacau et al. (2008) also mention material from Leticia, Amazonas, Colombia, was deposited in the Museum of Comparative Zoology at Harvard University (MCZ).

Distribution. This species is recorded for the Colombian Amazon and, as mentioned above, Lacau et al. (2008) reports this species also for Brazil and Peru without coordinates or collection vouchers, with the available information this species seems to be restricted to the Amazon region of South America.

Biological notes. This species was collected in leaf litter with the Winkler method, in primary rain forests with a high degree of conservation.

Etymology. This species is named in honor of the “El Encanto”, locality where the type-material was collected; Also, *encanto* is a Spanish word that means “charm”, and refers to the Disney movie *Encanto* (2021) based on Colombian culture.

Typhlomyrmex clavicornis Emery

Figs 2, 6B

Typhlomyrmex clavicornis Emery, 1906: 112. Alate queen, Bolivia.

Typhlomyrmex clavicornis var. *divergens* Forel, 1906: 248. Queen and male, Paraguay, synonymy in Brown 1965: 71.

Typhlomyrmex richardsi Donisthorpe 1939: 161. Male, Guiana. Synonymy in Brown 1965: 71.

Material examined. COLOMBIA: Caquetá, Albania, Vda. Samaria, Fca. Buenavista, 01°18'12"N, 75°52'23"W, 266 m, 26.iii.2019, leg. E. Durán, 1 worker and 1 female alate (LEUA 00000050569); Sebastopol, 01°43'00.12"N, 75°36'49.3"W, 527 m, 29.iii.2016, leg. D. Castro, 2 workers (CATAC-02562; 02563); Palmichar, 01°42'52.2"N, 75°36'53.6"W, 241 m, 23.iii.2016, leg. Y. Virguez, 1 worker (CATAC-00292); Tarquí, 01°50'36.4"N, 75°40'18.3"W, 1247 m, 5.iv.2016, leg. Y. Virguez, 5 workers (CATAC-01025); Vda. La Viciosa, CIMAZ Macagual, 01°30'23"N, 73°30'43"W, 250m, 16.vi.2019, leg. E. Durán, 1 worker and 1 female alate (LEUA 00000043623; 00000043633); Belén de los Andaquíes, 01°42'6.8"N, 75°53'57.5"W, 1500 m, 23.i.2017, leg. D. Castro, 3 workers (CATAC-00893); Morelia, Vda. Campoalegre, Fca. Buenavista, 01°19'21"N, 75°43'12"W, 257 m, 11.vi.2022, leg D. Coy, 2 workers (LEUA 00000050566; 00000050567); San José del Fragua, Bellavista, 1°19'16.21"N, 76°00'21.30"W, 504 m, 4.xii.2018, leg- M. Perez, 1 worker (CATAC-04222); Putumayo, Puerto Leguizamo, La Tagua, 00°05'14.9"S, 74°36'38.4"W 182 m, 14.vii.2016, leg. D. Castro, 1 worker (CATAC-00242).

Worker description. Head. Quadrated, as wide as long. Vertex very slightly concave, occipital corners rounded. Sides of head slightly convex, its greatest width towards one third of the vertex. Anterior margin of the clypeus slightly convex, without any type of projection or prolongation. Eyes reduced to one ommatidia situated in anterior third of the capsule sides; antennal sockets totally concealed by the frontal lobes; frontal lobes elongate and rounded; toruli circular and separated, visible by transparency through the frontal groove integument. Antennae 12-segmented with a well-defined 3-segmented club. Scapes short, and stout, their distal end at rest distant from

the vertexal margin; pedicel about twice as long as wide, and about as long as the 3 following segments together, segments A3–A9 short, much wider than long; segments 10 to 12 forming antennal club; mandibles short and subtriangular; mandibles closed do not fit completely with anterior clypeal margin, masticatory margin with a series of small teeth followed by a large long apical tooth.

Mesosoma. Subrectangular in lateral view; pronotum anteriorly rounded in dorsal view, much wider than long, strongly sloping and without a pronotal carinae; promesonotal suture well defined dorsally; mesonotum flat dorsally; metanotal groove marked distinct and marked by small carinae in profile view; anterior face of propodeum expanded, forming a rounded corner; posterior face of propodeum straight and steep; propodeal spiracle large, circular, equidistant from the dorsal and lateral margins of the propodeum, its diameter (0.062 mm) roughly equal to the length of the penultimate antennomere.

Metasoma. Petiole in lateral view higher than long, its front face flat, delimited from the lateral faces by a sharp corner. Node dorsum slightly convex and short. Petiole spiracle distant from the leading edge by a length greater than its diameter; sub-petiolar process prominent and lobe-shaped, tapering to a downward point.

Sculpture. Body generally opaque with restricted smooth shiny areas, like areas of mesopleura. Front of head with a sculpture that is a mixture of points and faint striations. Oblique longitudinal striation better marked towards the sides of the head and more visible in oblique lateral view. Short longitudinal striation limited to the lower part of the sides of the propodeal, below the propodeal spiracle and partly on the propodeal bulla.

Pilosity and color. The whole body with a dense and short pubescence. A few erect, longer hairs (length about penultimate antennomere) on dome of clypeus and back of petiole. Light brown color, whitish hairs. Outer surface of the mid tibiae with a series of hard, spiniform, erect, dark hairs, which contrast and mix with the soft, light, and ordinary hairs.

Measurements. HW 0.723, HL 0.709, SL 0.450, PrW 0.487, PeW 0.360, PeL 0.395, PeH 0.319, WL 1.01, CI 102, SI 62, TL 3.31.

Diagnosis and comments. According to Brown (1965: 71) the queens and workers of this species are distinguished by a prominent antennal club and mandibles with a long apical tooth (see Brown 1965, Fig. 4). Lacau et al. (2004) also add the presence of spiniform hairs on the mesotibiae (a feature shared with *T. meire*). Two workers examined in the CATAC collection were identified as *T. meire* (CATAC-02562; 02563), although the mesotibia have spiniform hairs and the antennae have 12 segments and not 10 (as in *T. meire*) so we do consider these workers were misidentified. *T. meire* was reported from Colombia in a previous checklist (Castro et al. 2018b) and recorded in Ant Maps, but here we identify these records as *T. clavicornis*. Brown (1965) does not mention the possession of spiniform hairs for *T. clavicornis*, a feature that he would surely have noticed, so the question remains as to what the limits of this species are. Until now, there are no valid records of *T. meire* from Colombia.

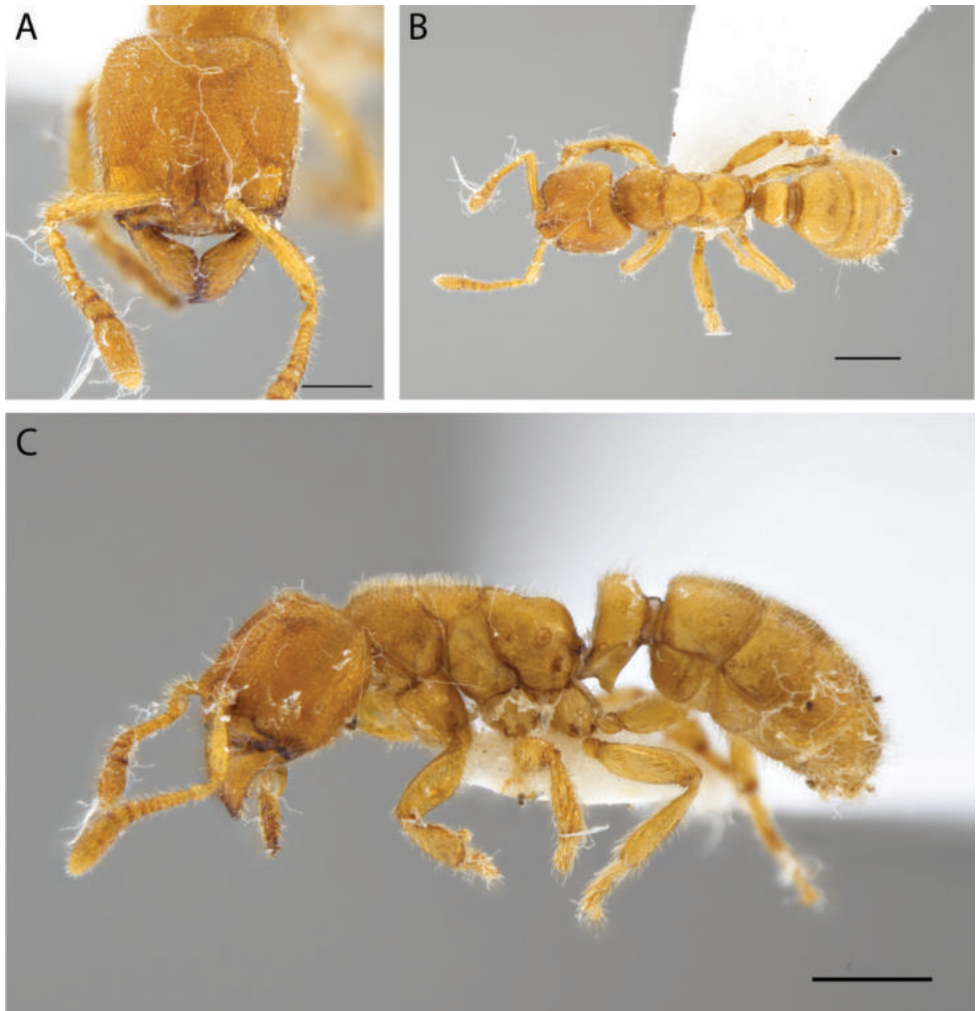


Figure 2. Photomicrographs of *Typhlomyrmex clavicornis* (CATAC-02562) **A** head in frontal view **B** body in dorsal view **C** body in lateral view. Scale bars: 0.2 mm (**A**); 0.5 mm (**B, C**).

There is little variation in the material examined, especially in the teeth of the mandibles, which can be small and uniform, of various sizes, or almost invisible (worn), but the apical tooth is always prominent. In females, the spiniform hairs of the mesotibiae are more noticeable. The metafemur appears more enlarged in the anterior view, which would explain why a specimen from LEUA (00000050566) is identified as *T. major*. However, in *T. major* this widening is abrupt after a short margin (see fig. 4C in Lacau et al. 2008), which does not occur in the LEUA specimen. On the other hand, in *T. major* the scape is slightly longer, the propodeal spiracle is smaller, the mesotibia presumably do not have spiniform hairs, and the petiole has a more visible peduncle.

Distribution. Species widely distributed in South America, with valid records in Colombia, Bolivia (type-locality), Paraguay, Guyana, and Brazil with only one record worth for the state of Rio de Janeiro (see discussion). In the literature it is also recorded for French Guyana and Surinam (Fernández and Sendoya 2004), however, no coordinates or valid records were found for this information. However, it is evident that it is a species of wide distribution, with records in the Amazon, Chaco, Cerrado and the Atlantic Forest.

Biological notes. The analyzed material was collected in soil and litter, though the species was predominantly found in deep soil strata (< 20–30 cm). The soil specimens were found at 10 cm to 30 cm depth, while they were absent in the 0–10 cm stratum; more than half of the specimens were found in the 10–20 cm stratum, and the largest number of individuals from the same sample were collected in the depth of 20–30 cm (8 individuals), while in litter only one individual per sample was found. Likewise, this species was found in different coverages, both natural and intervened, although it stands out that most occurrences were in pastures. *Typhlomyrmex clavicornis* was also collected in secondary and primary forests.

Typhlomyrmex prolatus Brown

Figs 3, 6C

Typhlomyrmex prolatus Brown, 1965: 72, fig. 6 (queen.) Costa Rica.

Typhlomyrmex prolatus: Kempf, 1972: 256; Bolton, 1995: 422; Camacho et al. 2022: 12.

Material examined. COLOMBIA: Caquetá, Belén de los Andaquíes, 01°37'40.0"N, 75°54'16.8"W, 750 m, 28.i.2017, leg. D. Castro, 2 workers (CATAC-00879); Florencia, Vereda La Viciosa, CIMAZ Macagual, 01°28'46"N, 75°36'16"W, 260 m, 26.x.2019, leg. J. Perdomo, 1 worker (LEUA 00000050568).

Worker description. Head. Elongated; vertexal margin weakly concave; posterolateral corners narrowly rounded; sides of head weakly convex; clypeus medially dome-shaped, the dome conspicuously protruding from the lateral clypeal margins and with a vertical anterior face; clypeal margin medially convex; anterior clypeal lamella narrow, without a medial lobe; eyes reduced to one ommatidia situated near the middle of the capsule sides; antennal sockets partially concealed by the frontal lobes frontal carinae; frontal lobes short and subquadrate; toruli circular and definitely separated, visible by transparency through the frontal groove integument; antenna 12-segmented with a 3 segmented club; scape conspicuously bent ventrally at one third of its apical length in frontal view, the maximal width being nearly equal to the pedicel length; when folded backward, its apex reach the vertexal margin; pedicel about twice as long as wide, and about as long as the 2 following segments together; segments A3–A9 quadrate to wider than long; segment 10 to 12 forming antennal club; mandible shape elongated-subtriangular, the apical margin joining basal margin at a round angle; masticatory margin with 7–9 small teeth from base to apex before the bigger apical tooth.

Mesosoma. Sub-rectangular in lateral view; pronotum anteriorly rounded in dorsal view, a little wider than long and strongly sloping anteriorly in lateral view, its posterior part horizontal; promesonotal suture underlined by a weak furrow, forming an arch, widely concave posteriorly; promesonotal suture well marked in dorsal view; mesonotum almost flat dorsally; metanotal groove distinct but weak; sides of the propodeum weakly concave medially in dorsal view; metapleural gland orifice in profile as a short oblique slit, bounded below by a convex rim of cuticle that directs the orifice posterodorsally; the swollen bulla of the gland is visible through the integument, its anterior margin in touch with the propodeal spiracle; dorsal face of the propodeum weakly inclined and almost flat, gradually rounding beyond the spiracle towards the sloping posterior face; propodeal spiracle opened laterally and slightly downward, its large orifice bordered by a thin cuticular ring, its diameter (0.041 mm); propodeal lobes lacking.

Metasoma. Petiole short, higher than wide, shortly pedunculate and broadly constricted between abdominal pre- and postsegment; petiolar node broad, anterior face slightly concave in lateral view, the anterior apex sharp followed by a evenly curved posterior face; in dorsal face node trapezoidal, wider than long, posterior face strongly concave; spiracles on lateral protuberances near anterolateral base of node, their orifices circular, opening laterally and slightly posteriorly; sternite with a short medial carina lengthened anteriorly by a medium sized; subpetiolar process elongated triangular with a sharp point directed forward; gaster elongated, its maximal width at the level of abdominal segment IV; abdominal tergite III with a median short anterior carena strongly produced and seen in lateral view.

Sculpture. Cephalic capsule wholly sculptured with rugosities and punctuations; frons and vertex medially impressed by a narrow longitudinal band striae, from frontal lobes diffusely diverging just before the vertexal margin; the lateral margins of genae with weakly sinuous striae, almost all the dorsum of capsule is covered by scattered piliferous punctuations nearly aligned except on genae at the level of the antennal sockets, on the medial part of the frons and the vertex; punctuations denser dorsally than ventrally, conspicuously more impressed on the posterior two third of the capsule and especially dense at the transition between vertex and genae; mandibles smooth and shiny; pronotum and mesonotum with a dense piliferous punctuation except on a narrow median band and on anterolateral margins of the pronotum which are smooth and shiny; pronotum with narrow longitudinal smooth band; propodeum with a broad smooth and shining area widening toward the propodeal declivity; mesopleura with central area smooth and shining, nearly circular; propodeum finely striated and punctuated laterally but medially smooth and shining; petiole node dull with fine punctuations denser anteriorly and laterally, in lateral view mostly smooth and shining; gaster and femora entirely covered by sparse piliferous punctuation, weaker than on head and thorax.

Pilosity and color. Short and abundant on head and body. Erect hairs (longer than antennal segment 11) on clypeal dome, petiolar dorsum and gaster. Shorter erect hairs on most metasomal sterna; appressed pubescence formed by dense short setae, distributed on most of the body. Color: body reddish brown, antennae, and legs lighter.

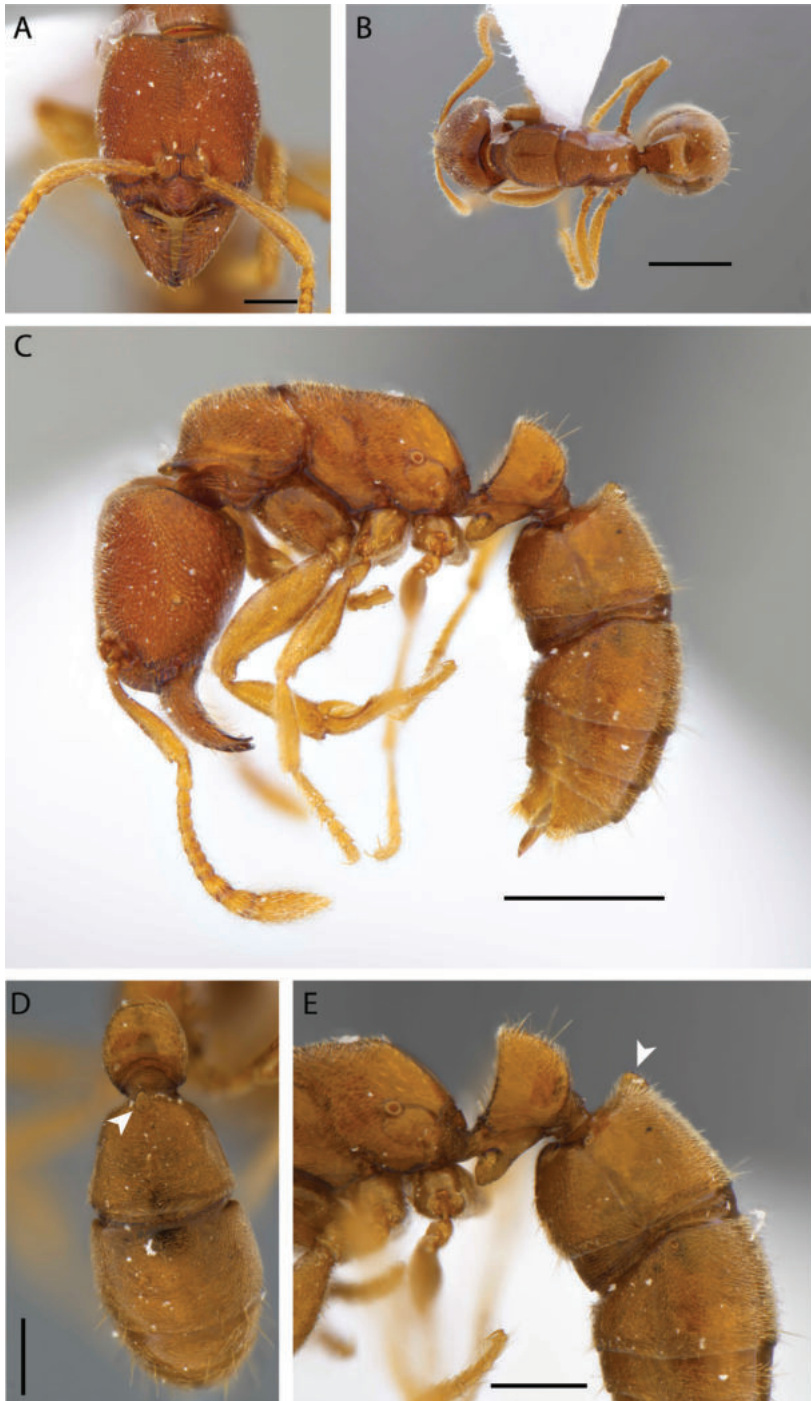


Figure 3. Photomicrographs of *Typhlomyrmex prolatius* (CATAC-00879) **A** head in frontal view **B** body in dorsal view **C** body in lateral view **D** postpetiolar carinae in dorsal view and **E** lateral view. Arrows pointing out the petiolar carinae. Scale bars: 0.25 mm (**A, D, E**); 0.5 mm (**B, C**).

Measurements. HW 0.578, HL 0.528, SL 0.464, PrW 0.307, PeW 0.239, PeL 0.314, PeH 0.305, WL 0.913, CI 109, SI 80, TL 1.85.

Diagnosis and comments. This species is easily separated from any other *Typhlomyrmex* by the possession of the short protruding carina on the anterior dorsum of the first metasomal tergum. This trait is described in the female of the species in Brown (1965) where they posit that it may be present in the worker. All workers examined in this work share this characteristic, so the possibility that it is a pointing error or a mutation in the first specimen observed by Brown is clearly ruled out. The function of this structure, if it exists, is unknown. As far as we know, this structure is unknown in other ants within this genus.

Distribution. Until this present work, the only confirmed localities of this species were in Central America (Brown 1965; Mackay et al. 2004; Dáttilo et al. 2020); however, records for Brazil and Venezuela were mentioned by Lacau et al. (2008) without pointing out the records; our records and the literature records establish an altitudinal distribution from 50 m to 1,200. m for *T. prolatus*. With these records, along with our own presented herein, we confirm the presence of this species in South America. Confirmed records range from Mexico to Colombia, with the possibility of having a broader distribution (see discussion).

Biological notes. *Typhlomyrmex prolatus* specimens examined in this study were collected exclusively in the soil at 0–10 cm depth; the collection substrate in previous records is unknown. This species has been found in fragmented rain forests in piedmont area. The individuals of CATAC-00879 were collected sharing the soil galleries with a colony of *Anoplotermes meridianus*.

Key to known *Typhlomyrmex* based on worker caste (modified from Lacau et al. 2004 and Camacho et al. 2020)

Worker of *T. foreli* unknown.

- 1 At least head frons with longitudinal striation or costulation..... 2
- Head never with conspicuous costulation, striation, if present, faint and limited to lateral sides 5
- 2(1) In dorsal view, mesosomal dorsum totally sculptured, usually costulate or rugulose 3
- In dorsal view, mesosomal dorsum with large smooth and shiny areas..... 4
- 3(2) In frontal view, scape not reaching the vertex margin; metacoxal dorsum with a lobe or denticle; in dorsal view, segments I and II of gaster (abdominal segments III and IV) covered by small ridges or striae, extending from the base of the hairs. Brazil *T. lavra* (Lattke)
- In frontal view, scape slightly surpassing the vertex margin; metacoxal dorsum unarmed; in dorsal view, segments I and II of gaster (abdominal segments III and IV) completely smooth and shiny. Brazil *T. lenis* (Camacho et al.)

- 4(2) Pronotum densely punctate, mesosoma lacking any striations; color generally yellow to light brown. Brazil *T. meire* **Lacau et al.**
 – Pronotum densely costulate and striate, mesosoma with deep striations; color generally dark brown. Colombia and Venezuela *T. reichenspergeri* (**Santschi**)
- 5(1) Antennae 10 segmented, postpetiole (first metasomal tergum) with a distinct, sharp median carinae on the anterior third of its dorsal surface *T. prolatus* **Brown**
 – Antennae with more than 10 segments, postpetiole without dorsal median tubercle or carena **6**
- 6(5) Anterior face of mesotibia with about 10 denticuliform erect setae (Fig. 4B); mandible shape elongated-subtriangular, their basal margins weakly convex, not reaching the anterior clypeal margin at full closure. Bolivia, Brazil, Colombia, Guiana *T. clavicornis* **Emery**
 – Anterior face of mesotibia without denticuliform setae (Fig. 4A, C); mandible shape triangular, their basal margins rectilinear or weakly concave, fitting tightly against clypeus at full closure **7**
- 7(6) Petiole well pedunculate in lateral view; node poorly developed, longer than high, subconvex at its top and without a distinct posterior face; abdominal tergite III without obvious anterior face; size polymorphism marked. Neotropics *T. rogenhoferi* **Mayr**
 – Petiole weakly pedunculate in lateral view; node well developed, higher than long, well rounded at its top and with a distinct posterior face; abdominal tergite III with a distinct anterior face; monomorphic **8**
- 8(7) Metafemora base (posterior view) sharply swollen ventrally, so that it forms a short vertical face at the base, joining the ventral face by an obtuse and rounded angle; head width >0.55 mm *T. major* **Santschi**
 – Metafemora base (posterior view) poorly swollen ventrally, so that it does not form an angle at its base; head width <0.55 mm **9**
- 9(8) Clypeal lamella bearing a short and narrow median process, protruding, and clearly truncated at the apex (Fig. 5A). Colombia *T. encanto* **sp. nov.**
 – Clypeal lamella not bearing a short and narrow median process (Fig. 5B, C). Widespread *T. pusillus* **Emery**



Figure 4. Photomicrographs comparing the mesofemur and mesotibia of **A** *T. encanto* sp. nov. **B** *T. clavicornis* **C** *T. prolatus*. Arrow pointing out the highly modified spiniform setae found only in the mesotibia of *T. clavicornis*. Scale bars: 0.2 mm (**A, C**); 0.1 mm (**B**).

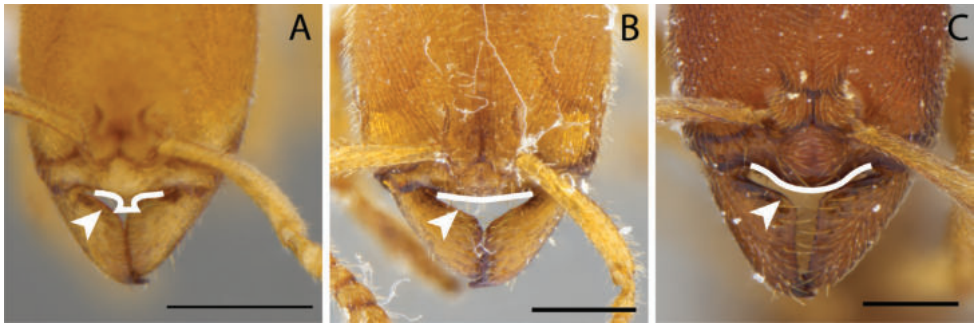


Figure 5. Photomicrographs comparing the clypeus of **A** *T. encanto* sp. nov. **B** *T. clavicornis* **C** *T. prolatus*. Arrow pointing out the highly modified clypeal projection found only in *T. encanto* sp. nov. Scale bars: 0.2 mm.

Discussion

Soil and subterranean ants tend to be under-studied and under-sampled, and thus less represented in biological inventories compared to other ants (Wong and Guénard 2021). *Typhlomyrmex* is a cryptic genus both in its taxonomy and its ecology (Lacau et al. 2008); Its current state seems to compare with that of other subterranean ant genera such as *Leptanilloides* Mann, which has many species still waiting to be described and a largely unknown ecology (Delsinne et al. 2015).

Most of the records reported in this work were collected in soil macrofauna sampling protocols, using the Tropical Soil Biology and Fertility (TSBF) monolith method (Anderson and Ingram 1993, ISO 2011). With the TSBF monolith method, *T. clavicornis* and *T. prolatus* were found even at a depth of 30 cm. Additionally, other species of *Typhlomyrmex* are also abundant at these depths, including *T. pusillus* (Castro et al. 2018b, Castro et al. 2023). This method, which focuses on soil fauna, seems to be useful for collecting cryptic organisms that are usually under-sampled with other methods such as *Winkler* sacs and *Berlese* traps (Castro et al. 2018a).

Based on our results, it can be inferred that *Typhlomyrmex* is a genus affected by the Wallacean shortfall (Bini et al. 2006; Meurgey and Ramage 2020). This premise had already been addressed by Lacau et al. (2004, 2008), where they state that *Typhlomyrmex* species, such as *T. pusillus* and *T. rogenhoferi*, are the most recorded species in the literature, likely due to their wide distribution that ranges from the southern South America to southern North America (Longino et al. 2002; Fernández and Sandoya 2004; Vittar 2008; Basset et al. 2012; Dáttilo et al. 2020; Camacho et al. 2022). Meanwhile, the greater diversity within this genus is largely unknown. Therefore, the presence of *T. prolatus* in South America further indicates that the information for the other *Typhlomyrmex* species is still very limited, and although the species richness may be higher than currently known, so too is the distribution of less abundant or taxonomically more cryptic *Typhlomyrmex* species. Another case of the Wallace shortfall in *Typhlomyrmex* is observed in *T. clavicornis* (Fig. 6B), although this species has records in five South American countries, including Brazil but only in the state of Rio de

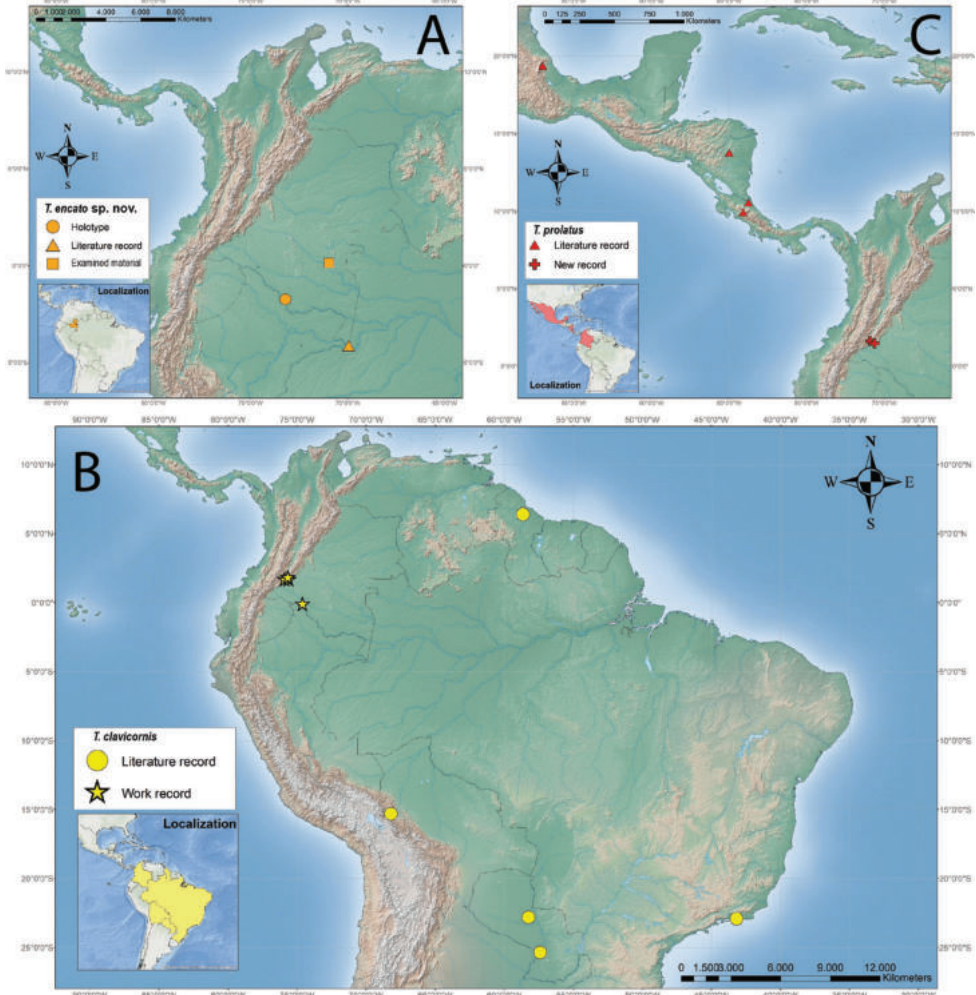


Figure 6. Distribution maps **A** *Typhlomyrmex encanto* sp. nov. **B** *Typhlomyrmex clavicornis* **C** *Typhlomyrmex prolatus*. Note: Literature record refers to records in the literature with coordinates available, records in literature without coordinates are not indicated in maps, but are mentioned in the distribution section of each species.

Janeiro in the southeast. The lack of records in the Brazilian Amazon basin and Cerrado, where it would be presumed to be present by the other valid records in countries with those biomes present; this study is intended to facilitate the identification of these widely distributed species and would help to reduce this biogeographical gap.

Although we described *Typhlomyrmex encanto* sp. nov., this species may have been reported in the literature as *Typhlomyrmex* sp. A (Lacau et al. 2008), however those specimens were not available for study. Given the difficulty in accessibility to the specimens described by Lacau et al. (2008), here we describe specimens from recent collections from

Colombia. In their treatment of the *Typhlomyrmex* from Colombia, Lacau et al. (2008) mention another unnamed species, *Typhlomyrmex* sp. B, which could potentially also be a new species. In the key provided by Lacau et al. (2008), they characterized *T.* sp. B with the following, translated from French: “Head capsule whose maximum width is located at two-thirds of its length, with weakly converging side faces anteriorly; occipital carina visible laterally; clypeus in dorsal view forming a wide, very flared convexity; clypeal lamella bearing a large well-advanced, convex median lobe but clearly truncated at the apex; scape in dorsal view, greatly enlarged towards the back in its distal half; wide and superficial metanotal furrow, little marked but distinct”. The authors refer to 6 workers with vouchers (SL#184, SL#185, SL#186, SL#529, SL#531 and SL#568) and labeled COLOMBIA, Caquetá PNN, Los Picachos, 1775m, 02°48'N, 74°40'W, Manual 3, 3. xi. 1997, F. Escobar, leg. in the IAvH collection. However, in a recent visit to the IAvH collection it was impossible to locate these workers with these voucher specimens, or any other material that could be associated with *Typhlomyrmex* sp. B. As is the case of *Typhlomyrmex* sp. A, the *Typhlomyrmex* sp. B description has not been published nor are there any plans to do so (Jacques Delabie, pers. comm.). Taxonomic work on cryptic groups such as this one is necessary to increase the knowledge of ant groups that, although currently under-studied and poorly understood, may be abundant and widely distributed.

Acknowledgements

This study was partially funded through a SoilBON and GBIF grant for the SoilBON Archive Data Mobilization. The authors thank the Ministerio de Ciencia, Tecnología e Innovación and Instituto Amazónico de Investigaciones Científicas SINCHI for partially financial support through the “Expedición BIO Binacional a la Biodiversidad de la Cuenca del río Putumayo”. We are grateful for the logistical and financial support of Dr. Clara Peña-Venegas. Thanks to Lina Pérez for allowing us to study the workers of the new species, also to Prof. Jean Gamboa and assistant Yennifer Andrea Carreño for loan of specimens from LEUN and Stepfania Sánchez for sorting ants of this genus. Thanks also to three anonymous reviewers who made important comments on the initial manuscript, most of which were considered. This is the 19th contribution in the series Ants of Colombia.

References

- Albuquerque E De, Pires Prado L Do, Andrade-silva J, Laiara Silva Siqueira E De, Liane Silva Sampaio K Da, Lemos Alves D, Brandão CRF, Andrade PL, Machado Feitosa R, Borges Azevedo Koch E De, Hubert Charles Delabie J, Fernandes I, Beggiato Baccaro F, Luiz Pereira Souza J, Peterson Santos Almeida R, Silva RR (2021) Ants of the State of Pará, Brazil: a historical and comprehensive dataset of a key biodiversity hotspot in the Amazon Basin. *Zootaxa* 5001: 1–83. <https://doi.org/10.11646/zootaxa.5001.1.1>

- Anderson J, Ingram J (1993) Tropical soil Biology an fertility a handbook of methods. 2nd edn. Cab International, Oxford University Press, 240 pp. [ISBN 0851988210]
- Basset Y, Cizek L, Cuénoud P, Didham RK, Guilhaumon F, Missa O, Novotny V, Ødegaard F, Roslin T, Schmid J, Tishechkin AK, Winchester NN, Roubik DW, Aberlenc HP, Bail J, Barrios H, Bridle JR, Castaño-Meneses G, Corbara B, Curletti G, Da Rocha WD, De Bakker D, Delabie JHC, Dejean A, Fagan LL, Floren A, Kitching RL, Medianero E, Miller SE, De Oliveira EG, Orivel J, Pollet M, Rapp M, Ribeiro SP, Roisin Y, Schmidt JB, Sørensen L, Leponce M (2012) Arthropod diversity in a tropical forest. *Science* 338: 1481–1484. <https://doi.org/10.1126/science.1226727>
- Bini LM, Diniz-Filho JAF, Rangel TFLVB, Bastos RP, Pinto MP (2006) Challenging Wallacean and Linnean shortfalls: Knowledge gradients and conservation planning in a biodiversity hotspot. *Diversity and Distributions* 12: 475–482. <https://doi.org/10.1111/j.1366-9516.2006.00286.x>
- Bolton B (1995) A new general catalogue of the ants of the world. Cambridge, Mass.: Harvard University Press, 504 pp.
- Bolton B (2003) Synopsis and classification of Formicidae. *Memoirs of the American Entomological Institute* 71: 1–369.
- Brown WL (1965) Contributions to a Reclassification of the Formicidae. IV. Tribe Typhlomyrmecini (Hymenoptera). *Psyche: A Journal of Entomology* 72: 65–78. <https://doi.org/10.1155/1965/36792>
- Camacho GP, Franco W, Feitosa RM (2020) Additions to the taxonomy of *Gnamptogenys* Roger (Hymenoptera: Formicidae: Ectatomminae) with an updated key to the New World species. *Zootaxa* 4747: 450–476. <https://doi.org/10.11646/zootaxa.4747.3.2>
- Camacho GP, Franco W, Branstetter MG, Pie MR, Longino JT, Schultz TR, Feitosa RM (2022) UCE phylogenomics resolves major relationships among ectaheteromorph ants (Hymenoptera: Formicidae: Ectatomminae, Heteroponerinae): A new classification for the subfamilies and the description of a new genus. *Insect Systematics and Diversity* 6: 1–20. <https://doi.org/10.1093/isd/ixab026>
- Castro D, Scheffrahn RH, Carrijo TF (2018a) *Echinotermes biriba*, a new genus and species of soldierless termite from the Colombian and Peruvian Amazon (Termitidae, Apicotermittinae). *ZooKeys* 748: 21–30. <https://doi.org/10.3897/zookeys.748.24253>
- Castro D, Fernández F, Meneses AD, Tocora MC, Sanchez S, Peña-Venegas CP (2018b) A preliminary checklist of soil ants (Hymenoptera: Formicidae) of Colombian Amazon. *Biodiversity Data Journal* 6: e29278. <https://doi.org/10.3897/BDJ.6.e29278>
- Castro D, Fernández F, Peña-Venegas CP (2023) Registros de hormigas y termitas de suelo colectadas en la Amazonia colombiana. Version 2.1. Instituto Amazónico de Investigaciones Científicas - SINCHI. <https://doi.org/10.15472/qxpoz> [Sampling event dataset accessed via GBIF.org on 2023-02-30]
- Dáttilo W, Vásquez-Bolaños M, Ahuatzin DA, Antoniazzi R, Chávez-González E, Corro E, Luna P, Guevara R, Villalobos F, Madrigal-Chavero R, Falcão JC de F, Bonilla-Ramírez A, Romero ARG, Mora A, Ramírez-Hernández A, Escalante-Jiménez AL, Martínez-Falcón AP, Villarreal AI, Sandoval AGC, Aponte B, Juárez-Juárez B, Castillo-Guevara C, Moreno CE, Albor C, Martínez-Tlapa DL, Huber-Sannwald E, Escobar F,

- Montiel-Reyes FJ, Varela-Hernández F, Castaño-Meneses G, Pérez-Lachaud G, Pérez-Toledo GR, Alcalá-Martínez I, Rivera-Salinas IS, Chairez-Hernández I, Chamorro-Florescano IA, Hernández-Flores J, Toledo JM, Lachaud J, Reyes-Muñoz JL, Valenzuela-González JE, Horta-Vega JV, Cruz-Labana JD, Reynoso-Campos JJ, Navarrete-Heredia JL, Rodríguez-Garza JA, Pérez-Domínguez JF, Benítez-Malvido J, Ennis KK, Sáenz L, Díaz-Montiel LA, Tarango-Arámbula LA, Quiroz-Robedo LN, Rosas-Mejía M, Villalvazo-Palacios M, Gómez-Lazaga M, Cuautle M, Aguilar-Méndez MJ, Baena ML, Madora-Astudillo M, Rocha-Ortega M, Pale M, García-Martínez MA, Soto-Cárdenas MA, Correa-Ramírez MM, Janda M, Rojas P, Torres-Ricario R, Jones RW, Coates R, Gómez-Acevedo SL, Ugalde-Lezama S, Philpott SM, Joaqui T, Marques T, Zamora-Gutierrez V, Martínez Mandujano V, Hajian-Forooshani Z, MacGregor-Fors I (2020) Mexico ants: incidence and abundance along the Nearctic–Neotropical interface. *Ecology* 101: e02944. <https://doi.org/10.1002/ecy.2944>
- Delsinne T, Sonet G, Donoso DA (2015) Two new species of *Leptanilloides* Mann, 1823 (Formicidae: Dorylinae) from the Andes of southern Ecuador. *European Journal of Taxonomy* 143: 1–35. <https://doi.org/10.5852/ejt.2015.143>
- Donisthorpe H (1939) *Typhlomyrmex richardsi* (Hym., Formicidae), a new species of ponerine ant from British Guiana. *Entomologist's Monthly Magazine* 75: 161–162
- Emery C (1906) Studi sulle formiche della fauna Neotropica. XXXVII. *Bullettino della Società Entomologica Italiana* 37: 107–194.
- Fernández F, Sandoya S (2004) Lista sinonímica de las hormigas neotropicales (Hymenoptera: Formicidae). *Biota Colombiana*. *Biota Colombiana* 5: 3–105.
- Forel A (1906) Fourmis néotropiques nouvelles ou peu connues. *Annales de la Société Entomologique de Belgique* 50: 225–249.
- Franco W, Ladino N, C Delabie JH, Dejean A, Orivel J, Fichaux M, Groc S, Leponce M, Feitosa RM, Heráclito dos Santos F (2019) First checklist of the ants (Hymenoptera: Formicidae) of French Guiana. *Zootaxa* 4674: 509–543. <https://doi.org/10.11646/zootaxa.4674.5.2>
- ISO I (2011) ISO 23611–5. Soil quality-sampling of soil invertebrates-Part 5. Sampling and extraction of soil macro-invertebrates.
- Kempf WW (1972) Catálogo abreviado das formigas da região Neotropical. *Studia Entomologica* 15: 3–344.
- Lacau S, Villemant C, Delabie JHC (2004) *Typhlomyrmex meire*, a remarkable new species endemic to Southern Bahia, Brazil (Formicidae: Ectatomminae). *Zootaxa* 678: 1–23. <https://doi.org/10.11646/zootaxa678.1.1>
- Lacau S, Villemant C, Jahyny B, Delabie J (2008) *Typhlomyrmex* Mayr, 1862: un genre méconnu de petites fourmis cryptiques et predatrices (Ectatomminae: Typhlomyrmecini). In: Jiménez E, Fernández F, Arias-Penna TM, Lozano-Zambrano FH (Eds) *Sistemática, biogeografía y conservación de las hormigas cazadoras de Colombia*. Instituto de Investigación de Recursos Biológicos Alexander von Humboldt, Bogotá D.C., 241–283.
- Longino JT, Coddington J, Colwell RK (2002) The ant fauna of a tropical rain forest: estimating species richness three different ways. *Ecology* 83: 689–702. <https://doi.org/10.2307/3071874>

- Mackay WP, Maes JM, Fernández PR, Luna G (2004) The ants of North and Central America: the genus *Mycocepurus* (Hymenoptera: Formicidae). *Journal of Insect Science* 4(27): 1–7. <https://doi.org/10.1093/jis/4.1.27>
- Meurgey F, Ramage T (2020) Challenging the Wallacean shortfall: A total assessment of insect diversity on Guadeloupe (French West Indies), a checklist and bibliography. *Insecta Mundi* 0786: 1–183.
- Vittar F (2008) Hormigas (Hymenoptera: Formicidae) de la Mesopotamia Argentina. *INSUGEO Miscelania* 17: 447–466.
- Wilkie KTR, Merl AL, Traniello JFA (2010) Species diversity and distribution patterns of the ants of amazonian Ecuador. *PLoS ONE* 5(10): e13146. <https://doi.org/10.1371/journal.pone.0013146>
- Wong MKL, Guénard B (2021) Subterranean Ants. In: Starr CK (Ed.) *Encyclopedia of Social Insects*. Springer International Publishing, Cham, 901–906. https://doi.org/10.1007/978-3-030-28102-1_180

Supplementary material I

Measurements taken from pin mounted specimens

Authors: Fernando Fernández, Gianpiero Fiorentino, Daniel Castro

Data type: figure (.docx file)

Copyright notice: This dataset is made available under the Open Database License (<http://opendatacommons.org/licenses/odbl/1.0/>). The Open Database License (ODbL) is a license agreement intended to allow users to freely share, modify, and use this Dataset while maintaining this same freedom for others, provided that the original source and author(s) are credited.

Link: <https://doi.org/10.3897/jhr.96.103219.suppl1>

European cuckoo bees of the tribe Dioxyini (Hymenoptera, Megachilidae): distribution, annotated checklist and identification key

Petr Bogusch¹

¹ Department of Biology, Faculty of Science, University of Hradec Králové, Rokitanského 62, CZ-500 03 Hradec Králové, Czech Republic

Corresponding author: Petr Bogusch (bogusch.petr@gmail.com)

Academic editor: Jack Neff | Received 14 April 2023 | Accepted 27 June 2023 | Published 25 July 2023

<https://zoobank.org/16A4A165-5185-4C89-960D-614A74E6D394>

Citation: Bogusch P (2023) European cuckoo bees of the tribe Dioxyini (Hymenoptera, Megachilidae): distribution, annotated checklist and identification key. Journal of Hymenoptera Research 96: 599–628. <https://doi.org/10.3897/jhr.96.104957>

Abstract

Altogether, ten species of cuckoo bees of the tribe Dioxyini have been recorded from Europe, with two species distributed widely in the continent while others are restricted in distribution to only one or several countries in southern Europe. These ten representatives are classified into five genera: *Aglaoapis*, *Dioxyis*, *Ensliniana*, *Metadioxys* and *Paradioxys*. *Dioxyis atlanticus* is reclassified from a subspecies to a valid species, and new occurrence records of this species are reported. New synonymy is established for *Dioxyis cinctus* = *D. montana* **syn. nov.** The distribution, morphology, ecology and hosts of all species were reviewed from both published and unpublished sources. New red-list categories for each species were created according to the new records of occurrence. An identification key including all ten species and photographs of their whole bodies and main identification characteristics was prepared, and distribution maps for all species were created.

Keywords

Europe, *Aglaoapis*, *Dioxyis*, *Ensliniana*, *Metadioxys*, *Paradioxys*, maps, ecology, hosts, conservation

Introduction

Bees (Anthophila) form a group of seven families within the monophylum Aculeata inside the highly diversified order Hymenoptera. This group coevolved with flowering plants, whose pollen, nectar and oils serve as the main food sources for both adults

and their brood (Grimaldi and Engel 2005; Michener 2007). There are many nesting strategies for bees that vary according to the placement of the nest, the care of the brood, the level of social behaviour, and the specialisation of the pollen (Klein et al. 2007; Michener 2007; Bogusch et al. 2020a). While the majority of bees create their own nests, there is a group of interspecific nest kleptoparasites known as cuckoo bees, which is distributed across all regions of the world and comprises approximately 15% of all bee species (Batra 1984; Michener 2007; Sless et al. 2022). Cuckoo bees are not a taxonomical group, but rather are ecological groups of phylogenetically unrelated genera across multiple families, whose females lay their eggs into the nests of other bee species. They utilize a variety of strategies for invading host nests and destroying host broods (Michener 2007; Habermannová et al. 2013; Westrich 2018).

Interspecific cuckoo behaviour is known in four families: Colletidae, Halictidae, Megachilidae and Apidae, including the species-rich subfamily Nomadinae of the family Apidae which is comprised of many genera and species (Sless et al. 2022). Within the Megachilidae, several genera with kleptoparasitic behaviour are distributed across more groups of this family, while the tribe Dioxyini represents the least species-rich group of cuckoo bees within Megachilidae (Gonzalez et al. 2012; Westrich 2018). This group of cuckoo bees comprises eight genera of usually rare cuckoo bees, which are distributed in the Old World and in North America (Popov 1936; Michener 2007). Currently, 36 species are known worldwide (Michener 2007). Of this number, ten species in five genera have been recorded from Europe (Warncke 1977; Tkalcu 2001), most of which are very rare and restricted in their distribution to a small area in the south of the continent. Many of these species have their main distribution area in North Africa and/or the Middle East, and their occurrence in Europe represents only the very small, northernmost part of their distribution (Warncke 1977; Baldock et al. 2018; Lhomme et al. 2020; Varnava et al. 2020; Ghisbain et al. 2023).

Warncke (1977) summarised the taxonomy of all species of the western part of the Palearctic region. However, this study is somewhat outdated and does not contain all known species (i.e., *Dioxys lanzarotensis* Tkalcu, 2001, described after the publication of Warncke's (1977) study). The identification key is useful, especially because of the quite simple identification of this group based on very specific differences among the species, but is very different from modern keys that include photographs. Additionally, current surveys in several countries in southern Europe have improved the knowledge of the distribution and ecology of this group.

The goal of this study is to review the taxonomy, distribution, ecology and conservation of all species of tribe Dioxyini recorded from Europe. An identification key for all species is included.

Materials and methods

The specimens for the study were collected by the author from the field or obtained from other collections. A large part of the material studied included pinned specimens from both private and museum collections. Additionally, material from the following

museums and institutions was studied: Národní muzeum, Praha (Czech Republic, curator Jan Macek), Moravské zemské muzeum, Brno (Czech Republic, curator Igor Malenovský), Natural History Museum, London (United Kingdom, curator Joseph Monks), Naturhistorisches Museum, Wien (Austria, curator Manuela Vizek), Biologiezentrum Linz (Austria, curator Esther Öckermüller), Naturhistorisches Museum Berlin (Germany, curator Stefanie Krause), and Naturkundemuseum Bayern Munich (Germany, curator Stefan Schmidt). Several records were obtained from internet sources, especially from photos on Flickr (<https://www.flickr.com/>) and iNaturalist (<https://www.inaturalist.com/>). In this case, only records from specialists or photos enabling identification to the species level were included. However, the goal of this study was not to create detailed maps of distribution, because this work will be done in several European bee projects in the near future and occurrence records from local authorities, taxonomic specialists and museums are still not completely collected and validated.

The author examined only a part of the type material of both valid species and synonyms and all the original descriptions of all species and their synonyms. The type material was not studied in most cases because the description of the species is comprehensive and clear, and/or there was rich material available in private or museum collections for study, so the examination of the original types was not necessary. All of the type material studied by the author is indicated in the taxonomic treatment sections of species.

Morphology was studied using a digital Keyence VHX-700 photographing microscope with measuring tools. Only specimens clearly exhibiting diagnostic features were imaged. The identification keys for females and males are dichotomous, using the following standard abbreviations before the corresponding number: S – metasomal sternum, T – metasomal tergum, and F – flagellomere. Figure abbreviations in brackets (Fig. 1A, Figs 2–4) are used in the text. Head measurements were performed from the labrum base to the occipital ridge at the end of the head. If the same character applied to both females and males, it was photographed only once (in the female). If the species has a restricted range, it is also mentioned in the key in parentheses.

Species distributions were determined using studied material and literary sources on Dioxyini of Europe. Distribution maps were created in QGIS 3.6. The red-list categories from Nieto et al. (2014) are indicated, and updates to conservation status are proposed for several species.

Results

Identification key for the females of European Dioxyini

- 1 Scutellum without lateral projections (Fig. 15C); S6 and T5 elongated, more than three times longer than wide (Fig. 15D) *Ensliniana bidentata* (Spain and Portugal)
- Scutellum with lateral toothlike projections (Fig. 1C), often with medial tooth; S6 usually shorter (Fig. 1D)..... 2

- 2 Head and thorax with dense reddish-brown hair; metasoma without apical bands of whitish hair; metasoma and legs completely reddish (Fig. 3A) ***Dioxys ardens* (Spain and Portugal)**
- Head and thorax hairy or only sparsely haired, colour of hairs whitish or brownish; metasoma and legs usually completely or partly black; metasomal terga usually with narrow but well-developed apical bands of whitish hair (Fig. 7A) **3**
- 3 Forecoxa with a toothlike carina anteriorly (Fig. 1E) **4**
- Forecoxa rounded anteriorly (Fig. 7C) **5**
- 4 Postscutellum with a medial toothlike projection, which is narrow and elongated (Fig. 1C); T6 rounded and flattened medially; S6 slightly emarginate (Fig. 1D); body completely black with whitish hair (Fig. 1A) ***Aglaopis tridentata***
- Postscutellum with a medial toothlike process, which is not elongated (Fig. 17C); T6 not flattened medially; S6 without an emargination (Fig. 17D); legs, metasoma and antennae usually partly reddish (Fig. 17A) ***Metadioxys graeca* (Greece)**
- 5 S6 and T6 sharp and elongated (Fig. 19C); metasomal bands often not well defined; metasoma and legs partly reddish (Fig. 19A) ***Paradioxys pannonicus***
- S6 and T6 not elongated (Fig. 7D); metasomal bands well or ill-visible; body often completely black **6**
- 6 Apex of T6 truncate; S6 very slightly emarginate apically (Fig. 7D); black with whitish hairs and often basal terga of metasoma reddish (Fig. 7A) ***Dioxys cinctus***
- Apex of T6 convex (Fig. 11C); S6 with or without emargination; body completely black or partly reddish; legs can be also partly or completely reddish **7**
- 7 Metasoma completely black (Fig. 5A); small species (5–7 mm) ***Dioxys atlanticus***
- Metasoma partly reddish (Fig. 13A); legs partly reddish or dark; small to larger species **8**
- 8 Legs at least partly reddish (Fig. 13A, D); T6 coarsely, contiguously punctate (Fig. 13C); S2 with medial part slightly protruded (Fig. 13D); head and mesosoma in part with appressed, squamose pubescence ***Dioxys pumilus***
- Legs black (Fig. 11A); T6 finely, densely, but not contiguously, punctate (Fig. 11C); S2 without protruded medial part (Fig. 11E); head and mesosoma with pubescence semi-erect, not squamose ***Dioxys moestus***

Identification key for the males of European Dioxyini

- 1 Scutellum without lateral projections; postscutellum without apical tooth-like process in the middle (Fig. 15C); S7 and T7 with tooth-like processes laterally (Fig. 15E) ***Ensliniana bidentata* (Spain and Portugal)**
- Scutellum with lateral toothlike projections, often with medial tooth-like process (Fig. 1D); S7 and T7 usually without tooth-like processes **2**

- 2 Head and thorax with dense reddish-brown hair; metasoma without apical bands of whitish hair, metasoma and legs completely reddish (Fig. 3B).....
..... ***Dioxys ardens* (Spain and Portugal)**
- Head and thorax hirsute or only sparsely haired, colour of hairs whitish or brownish; metasoma and legs usually completely or partly black; metasomal terga usually with narrow but well-developed apical bands of whitish hair (Fig. 7B) **3**
- 3 Forecoxa with a toothlike carina anteriorly (Fig. 1E)..... **4**
- Forecoxa rounded anteriorly (Fig. 7C) **5**
- 4 Postscutellum with a medial toothlike projection, which is narrow and elongate (Fig. 1C); T7 emarginated (Fig. 1F); body completely black with whitish hair (Fig. 1B) ***Aglaoapis tridentata***
- Postscutellum with a medial toothlike process, which is not elongated (Fig. 17C); T7 not flattened medially; last tergum not emarginated (Fig. 17E); legs, metasoma and antennae usually partly reddish (Fig. 17B)
..... ***Metadioxys graeca* (Greece)**
- 5 Metasoma completely reddish with semi-transparent apical parts of terga, without well-visible apical bands (Fig. 19B); apex of S4 with two toothlike processes medially (Fig. 19D, E); T7 with straight apex (Fig. 19F); S7 with lateral teeth (Fig. 19E) ***Paradioxys pannonicus***
- Metasoma black or partly reddish (Fig. 7B); rarely completely reddish but then with well-visible apical bands of whitish or yellowish hair, apex of S4 straight or emarginated but without so prominent toothlike processes, S7 without lateral teeth..... **6**
- 6 Apex of S4 medially swollen, bidentate (Fig. 11F); matt and roughly punctate; T7 shiny with coarse but sparse punctures (Fig. 11G) ***Dioxys moestus***
- Apex of S4 straight (Fig. 13E), emarginated or with small toothlike processes (not as prominent as those of *P. pannonicus*); T7 more densely punctate **7**
- 7 Legs and metasoma partly or completely reddish (Fig. 13B, D); T7 triangular with acute apex (Fig. 13F); apex of S4 waved (Fig. 13E) ***Dioxys pumilus***
- Legs dark, metasoma dark or partly reddish; T7 broad (Fig. 7F); with straight or slightly curved apex; apex of S4 different **8**
- 8 Larger species (7–10 mm); at least part of T1 reddish (Fig. 7B); apex of S4 slightly emarginated (Fig. 7E); T7 coarsely and densely punctate (Fig. 7F) ...
..... ***Dioxys cinctus***
- Smaller species (5–7 mm); completely black (Fig. 5B); apex of S4 with two toothlike processes (Fig. 5E); T7 with shiny interspaces **9**
- 9 Mesonotum, scutellum and T1–T3 densely and deeply punctate, punctures larger; mesosternum medially finely rugose (Fig. 5B, C); emargination between toothlike processes on apex of S4 narrow (Fig. 5E)..... ***Dioxys atlanticus***
- Mesonotum, scutellum and T1–T3 more sparsely and finely punctate, punctures smaller and shallow; mesosternum shiny (Fig. 9B, C); emargination between toothlike processes on apex of S4 wider (Fig. 9D)
..... ***Dioxys lanzarotensis* (Canary Islands: Lanzarote)**

Extralimital species

Altogether, 10 species of five genera of tribe Dioxyini are known to occur in Europe. These are representatives of the genera *Aglaopis* Cameron, *Ensliniana* Alfken, *Metadioxys* Popov and *Paradioxys* Mocsáry (one species of each genus) and six species of the genus *Dioxys* Lepeletier & Serville.

In the neighbouring regions, representatives of the genera *Allodioxys* Popov, *Eudioxys* Mavromoustakis and *Prodioxys* Friese are recorded, but no species of these genera has ever been recorded from Europe. Representatives of these genera differ from European species by the following characteristics (adopted from Warncke (1977)).

Both sexes of *Allodioxys* have the mesonotum with elongated projections on both sides and postscutellum with a spine-like process medially. Four species occur in the Middle East and/or North Africa (Libya, Algeria, Israel, Syria): *Allodioxys ammobius* (Mavromoustakis), *A. limbifera* Pérez, *A. moricei* (Friese) and *A. schulthessi* Popov (Warncke 1977; Lhomme et al. 2020).

Two species of *Eudioxys* occur in neighbouring regions: *Eudioxys quadridentata* (Friese) in North Africa (Egypt) and *E. schwarzi* Mavromoustakis in the Middle East (Iran) (Warncke 1977; Lhomme et al. 2020). Both sexes of this genus have axillae with two spines laterally and the scutellum with one spine on both sides.

Three species of *Prodioxys* occur in North Africa: *Prodioxys carneus* Gribodo, *P. longiventris* Pérez and *P. rufiventris* Lepeletier (Warncke 1977; Lhomme et al. 2020). All species are generally similar to *Dioxys ardens* with a completely reddish metasoma and legs and brownish hirsute head and mesosoma, females differ by the very long and narrow last tergum and sternum, males have last sternum of different shape than *D. ardens*.

Accounts of European species

Genus *Aglaopis* Cameron

Aglaopis Cameron, 1901: 262. Type species: *Aglaopis brevipennis* Cameron, 1901, monobasic.

Dioxoides Popov, 1947: 89. Type species: *Coelioxys tridentata* Nylander, 1848, by original designation.

Notes. The genus *Aglaopis* is distributed in Europe, the Middle East, India and South Africa. Three species are known worldwide (Michener 2007), and only one species occurs in Europe (Ghisbain et al. 2023).

Aglaopis tridentata (Nylander)

Coelioxys tridentata Nylander, 1848 (nec *Apis tridentata* Fabricius, 1775): 254.

Dioxys fasciata Schenck, 1861: 383.

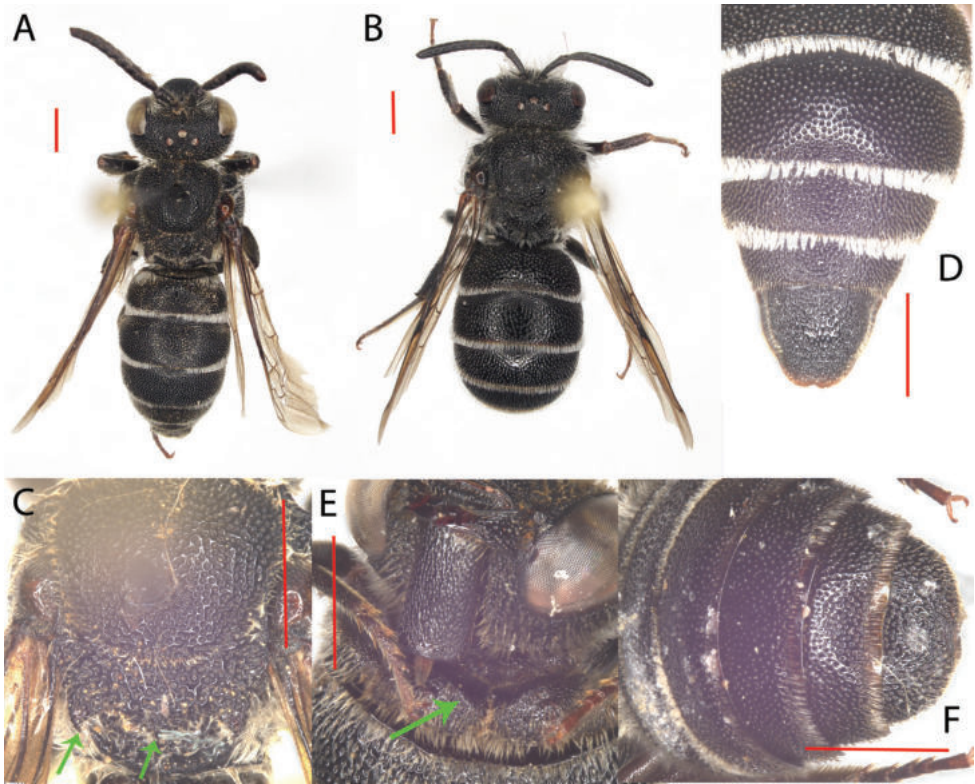


Figure 1. *Aglaoapis tridentata* **A** female, dorsal view **B** male, dorsal view **C** female, mesosoma dorsal view **D** female, metasoma, dorsal view **E** female, fore coxa **F** male, T7, dorsal view. Red scale bars represent the length of 1 mm.

Dioxys kuntzei Noskiewicz, 1940: 99.

Dioxoides tridentata ssp. *limassolica* Mavromoustakis, 1949: 587.

Diagnosis. Larger species (9–12 mm), both sexes are black with well-developed white bands of short hair on metasomal terga (Fig. 1A, B). Both sexes have the fore coxa with a carina anteriorly (Fig. 1E) and a short projection and the scutellum with a medial toothlike projection (Fig. 1C). Females have a longer last tergum than females of the genus *Dioxys* and an emarginated last sternum (Fig. 1D). The last tergum is emarginated for males (Fig. 1F).

Distribution. *Aglaoapis tridentata* is a Palearctic species that occurs in Europe, from Spain in the west to Russia in the east (Fig. 2), and in Asia from the Caucasus, Kyrgyzstan and China, Kazakhstan, Siberia and Russian Far East. This species reaches the farthest north of any species of the tribe, with records from Finland and Sweden (Ornosa et al. 2008; Madsen and Calabuig 2010; Ascher and Pickering 2023).

Biology and hosts: Species recorded especially in steppic formations, sunny slopes, forest steppes and other open or semiopen habitats. Occurs also in abandoned sandpits, spoil

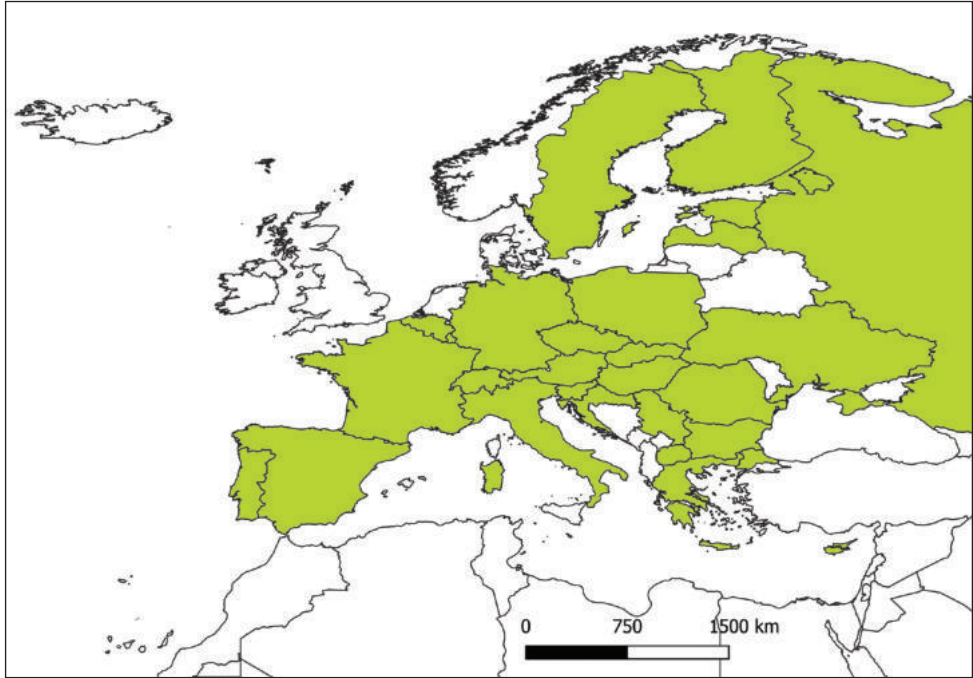


Figure 2. *Aglaopis tridentata*, distribution in Europe.

heaps and other habitats of anthropogenic origin. This species attacks nests of bees of the family Megachilidae, especially those nesting underground or making their own nests near the ground surface. *Hoplitis anthocopoides* (Schenck), *Hoplitis ravouxi* (Pérez), probably also *Hoplitis adunca* (Panzer) and *Megachile pilidens* Alfken, in southern parts of Europe, and also *Chalicodoma parietina* (Geoffroy) were confirmed as hosts of this species (Westrich 2018). Scheuchl and Willner (2016) also listed *Megachile leachella* Curtis as a likely host.

Conservation status. Nieto et al. (2014) classified this species as LC – data deficient. This species is relatively rare throughout its range. Its distribution in Europe is the largest of any species, and it is still being recorded in most countries – it was reported to be regionally extinct only in Belgium and Finland (Ghisbain et al. 2023). It should therefore be classified as LC.

***Dioxys* Lepeletier & Serville**

Dioxys Lepeletier & Serville, 1825: 109, type species: *Trachusa cincta* Jurine, 1807, monobasic.

Hoplospasites Ashmead, 1898: 284, type species: *Phileremus productus* Cresson, 1879, by original designation.

Chrysopheon Titus, 1901: 256, type species: *Chrysopheon aurifuscus* Titus, 1901, monobasic.

Notes. *Dioxys* is a Holarctic genus distributed in most of Europe and North Africa to central Asia in the east and the southwestern USA and adjacent Mexico in the western hemisphere (Hurd 1958; Michener 2007). Five species occur in North America, and approximately 13 occur in the Palaearctic region (Warncke 1977; Ghisbain et al. 2023). Six species occur in Europe.

Dioxys ardens Gerstaecker

Dioxys ardens Gerstaecker, 1869: 161.

Dioxys rufispina Pérez, 1895:26.

Diagnosis. Larger species, body length 8–10 mm. In both sexes, typical in its colouration, the metasoma is completely reddish without terminal or basal bands, and the legs and flagellum are reddish (Fig. 3A, B). T6 of females is elongated and narrowed posteriorly, with a rounded apex. The mesosoma is ferruginously hirsute. Axillae with teeth and postscutellum with short but sharp tooth in the middle. The same characteristics are also typical for males.

Distribution. Spain, Portugal (Fig. 4) and North Africa (Morocco to Libya).

Biology and hosts. Species recorded from semideserts and other arid open habitats. Hosts unknown.

Conservation status. This species is known only from several records from southern parts of Spain and one record from Portugal. Nieto et al. (2014) listed this species as DD – data deficient. According to the distribution records, it can be VU-vulnerable because of its long-lasting rarity. However, we know only a little about the populations and occurrence of this species in recent years.

Note. In general, a similar species, *Dioxys chalicoda* Lucas, was recorded from North Africa (Algeria and Libya). One very old record is from Gibraltar, but this specimen was erroneously identified and belongs to *D. ardens* (coll. Biologiezentrum Linz, Austria). This species differs in the colouration of the metasoma, which has black colouration of at least the last three segments. Females have mandibles with lateral tubercles, and males have ends of S4 with an emargination and S5 and S6 convex.

Dioxys atlanticus Saunders, 1904, stat. nov.

Dioxys atlanticus Saunders, 1904: 232.

Diagnosis. This species is small (5–7 mm in total length) and completely black with well-developed apical bands on metasomal terga (Fig. 5A, B). It is generally similar to *Dioxys lanzarotensis*, from which it can be identified by denser punctation on metasomal terga (Fig. 5C) and clypeus. It is morphologically similar to *D. moestus*, which is probably its near relative, rather than to *D. cinctus*, into which it was previously classified as a subspecies (Warncke 1977). The dark colouration of tibial spurs reported

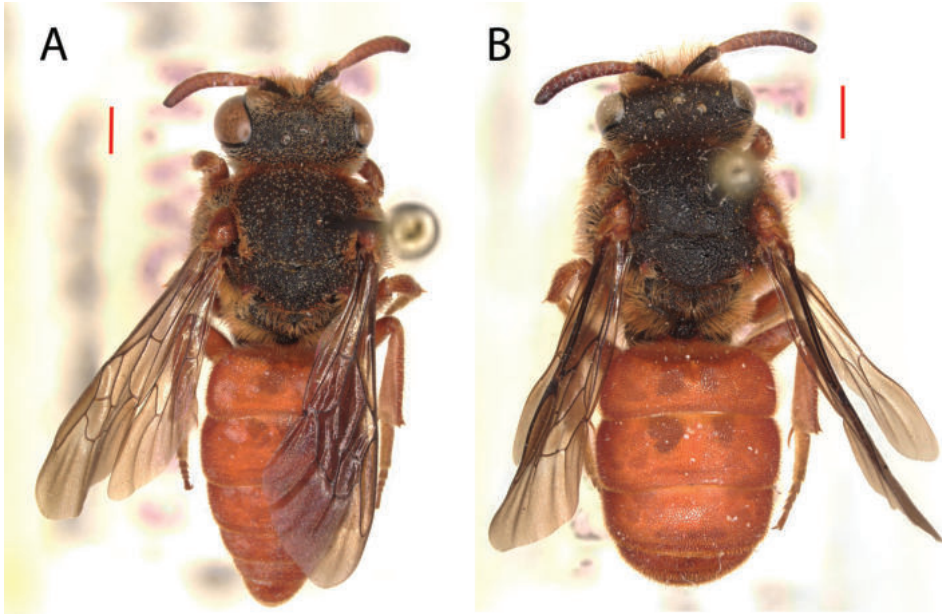


Figure 3. *Dioxys ardens* **A** female, dorsal view **B** male, dorsal view.



Figure 4. *Dioxys ardens*, distribution in Europe.

by Warncke (1977) was not observed in any specimen I have studied (Fig. 5D). Based on the morphology and distribution, it is clearly a separate species. Syntypes (a male and a female from Santa Cruz, Tenerife) from the Natural History Museum London were studied.

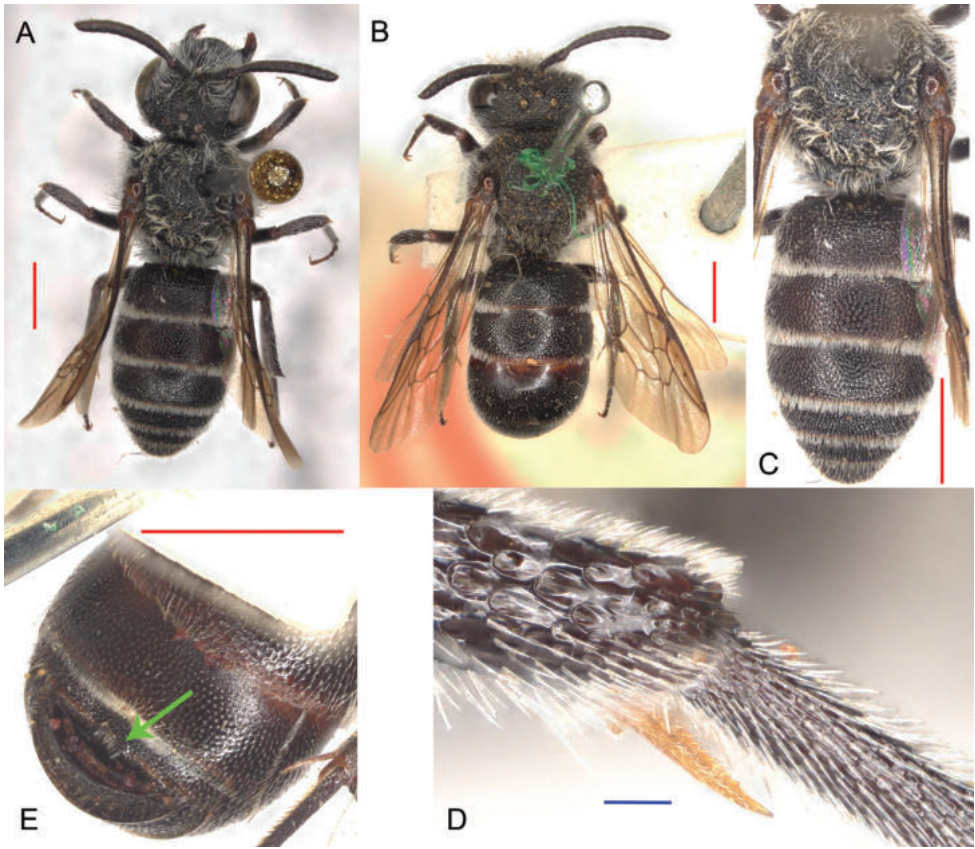


Figure 5. *Dioxys atlanticus* **A** female, dorsal view **B** male, dorsal view **C** female, mesosoma dorsal view **D** female, tibial spur on fore leg **E** male, last metasomal segments, ventral view. Red scale bars represent the length of 1 mm, blue scale bars 100 μm .

Distribution. This species was described from a male and a female from the Canary Islands (Tenerife), where it was also recorded on two other islands – Lanzarote and Gran Canaria (Hohmann et al. 1993) (Fig. 6). It was also recorded in Egypt (Warncke 1977) and currently in Sardinia (Orroli, 02.vi.2011, 6 ♀♀, G. Pagliano lgt., P. Bogusch det., coll. Biologiezentrum Linz, Austria). Based on the records, the species occurs in the Canary Islands and several parts of North Africa, South Europe and perhaps the Middle East, but it is very rare and hard to find. Specimens from Sardinia correspond in size, morphology and colouration with those of the Canary Islands and with both syntypes.

Biology and hosts. The species occurs in open habitats – steppes, semideserts, in rocky areas with shrubby vegetation. Little is known about its biology. Hosts unknown.

Conservation status: Nieto et al. (2014) listed this species as DD – data deficient. There are quite recent records from the Canary Islands and new records from Sardinia (Italy). In my opinion, it should be VU – vulnerable because of its restricted distribution area.

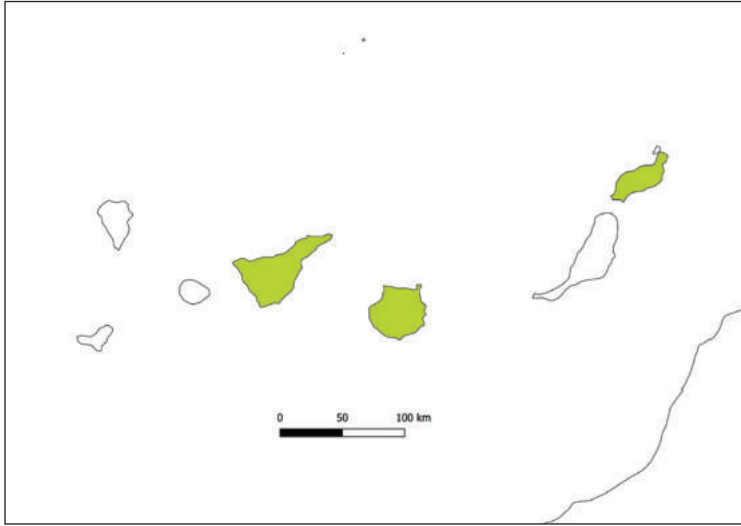


Figure 6. *Dioxys atlanticus*, distribution in Canary Islands.

Dioxys cinctus (Jurine)

Trachusa cincta Jurine, 1807: 253.

Dioxys pyrenaica Lepeletier, 1841: 515.

Dioxys maura Lepeletier, 1841: 516.

Dioxys cruenta Gerstaecker, 1869: 166.

Dioxys spinigera Pérez, 1884: 299.

Dioxys cincta var. *jucunda* Mocsáry, 1894: 36.

Dioxys cincta ab. *friederikae* Mader, 1933: 125.

Dioxys montana Heinrich 1977: 11–12, syn. nov.

Notes. Type specimens of this species and the description were studied in Biologiezentrum Linz, Austria. Both type specimens (a male and a female from the Sertavul Pass in Turkey) do not morphologically differ from typical specimens of *D. cinctus*.

Diagnosis. Larger species, body length variable between 5–12 mm, probably depending on the host. In both sexes, the body is black with the first two metasomal terga entirely or partly reddish and narrow apical bands of whitish short appressed hair (Fig. 7A, B). In several cases, red colouration is present on T3–T4. Mesosoma bears long whitish hair, apex of T6 of females straight and only shortly elongated, shorter than in similar species (Fig. 7D). The legs and antennae are black. This species has a very large distribution area and is connected with many host species. It causes variability in size (5–12 mm), while populations from southern Europe and North Africa are often smaller. The colouration is very variable, too – normally both sexes have first metasomal terga entirely reddish but usually populations from the north of the distribution area are darker and sometimes are entirely black with no reddish pattern.

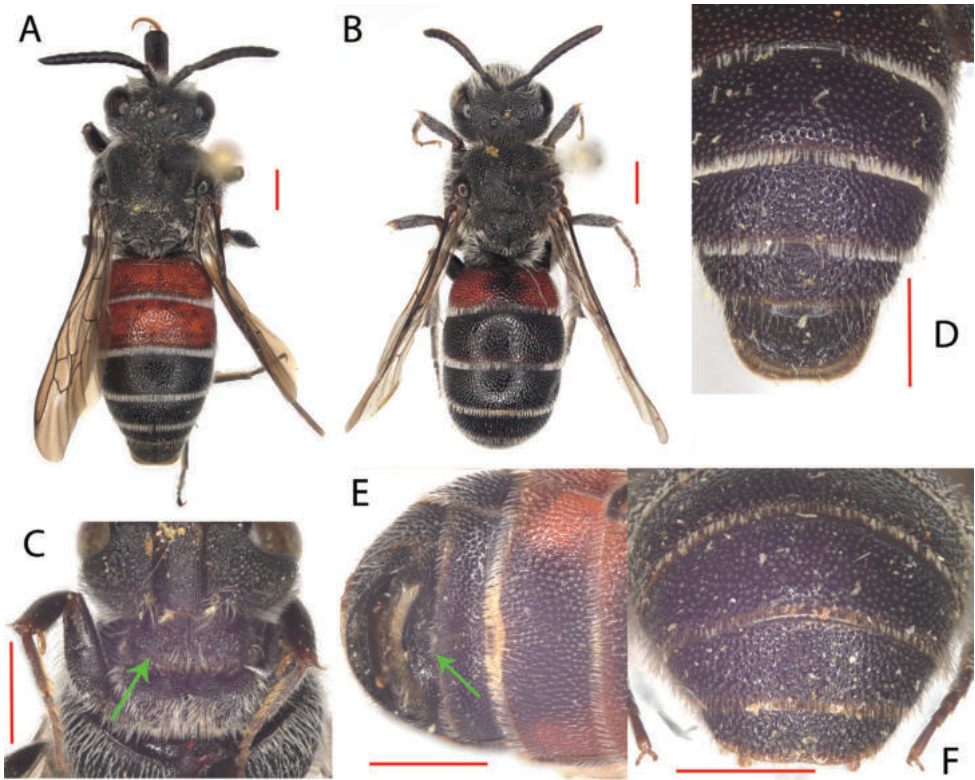


Figure 7. *Dioxyx cinctus* **A** female, dorsal view **B** male, dorsal view **C** female, fore coxa **D** female, mesosoma dorsal view **E** male, last metasomal segments, ventral view **F** male, T4–T6, dorsal view. Red scale bars represent the length of 1 mm.

Distribution. A species with a western Palaearctic distribution known from central and southern Europe from Portugal to Greece and Romania (Fig. 8). Outside of Europe, it is found in North Africa, Israel and as far east as the Caucasus (Dusmet 1921; Popov 1936; Warncke 1977; Standfuss et al. 2003; Ornos et al. 2008; Ascher and Pickering 2023).

Biology and hosts. Species occurring in a variety of open and semi-open habitats: steppe, semideserts, forest steppes and many others. It was also recorded in sites of anthropogenic origin – former sandpits, quarries, spoil heaps and military exercising areas. This species has more host species in its large distribution area: *Chalicodoma parietina*, *Chalicodoma pyrenaica* Lepeletier, *Hoplitis adunca* and *Hoplitis anthocopoides* were confirmed (Scheuchl and Willner 2016). Its hosts nest underground, create nests of mud or resin, or nest in various types of cavities above the ground. Parasitising females of this species were often recorded around bee hotels associated with nests of *H. adunca* in the Czech Republic (P. Bogusch, unpublished records). The actual number of hosts is certainly higher, and the preferred host species differ among the localities within the large distribution area.

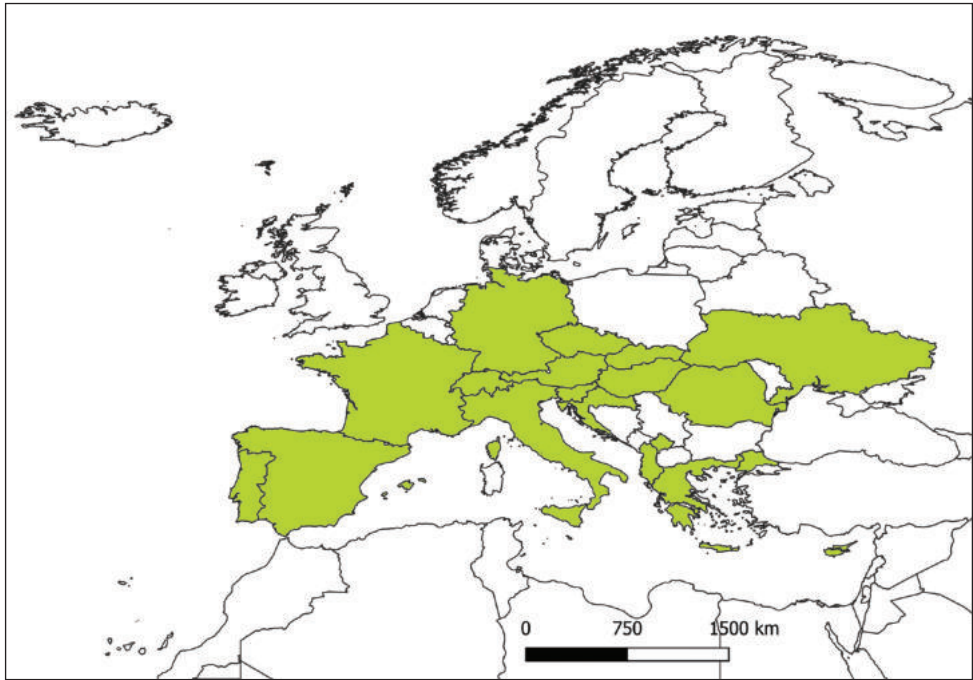


Figure 8. *Dioxys cinctus*, distribution in Europe.

Conservation status. Nieto et al. (2014) classified this species as LC – least concern. It is distributed in most of southern and central Europe, with the northern distribution border in France, Germany, the Czech Republic and Ukraine. In many countries, it is not rare, and the numbers of recorded individuals are even higher than those of *A. tridentata*. In the Czech Republic, the species has spread in the last 20 years (Straka and Bogusch 2017). Thus, it should stay in the category LC.

Dioxys lanzarotensis Tkalcu

Dioxys lanzarotensis Tkalcu, 2001: 49–50.

Diagnosis. Small species very similar in morphology to *D. atlanticus* (Fig. 9A) but differs by sparser punctures on metasomal terga (Fig. 9B) and on clypeus. Only a single male (holotype) was recorded from the island Lanzarote of the Canary Islands (Spain) (Tkalcu 2001). The holotype should be deposited in Übersee-Museum Bremen, Germany, but was discovered in the collection of Francisco La Roche in San Cristóbal de La Laguna, Tenerife, Spain. According to the studies of the holotype, this species is very similar to males of *D. atlanticus* but differs by the above reported characteristics, as well as several others (length and position of toothlike processes on S4 (Fig. 9D), shape of head). It is certainly a separate species; however, its distribution area is restricted to one island.

Distribution. Lanzarote, Canary Islands, Spain (Fig. 10) (Tkalcu 2001).

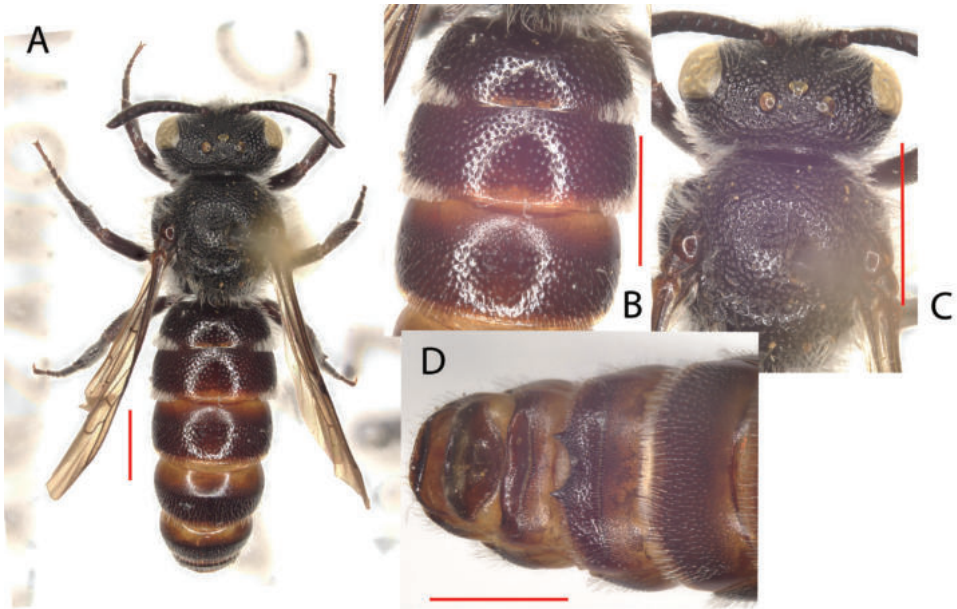


Figure 9. *Dioxys lanzarotensis* **A** male, dorsal view **B** male, metasoma, dorsal view **C** male, mesosoma dorsal view **D** male, last metasomal segments, ventral view. Red scale bars represent the length of 1 mm.

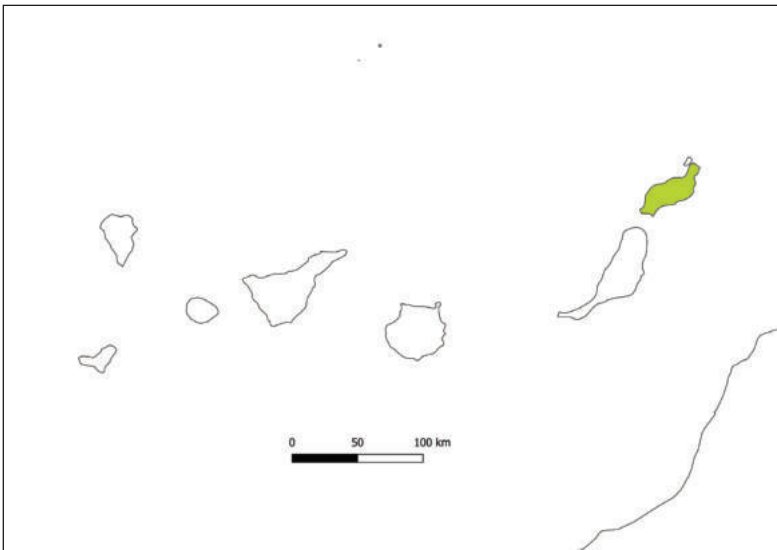


Figure 10. *Dioxys lanzarotensis*, distribution in Canary Islands.

Biology and hosts. Unknown.

Conservation status. Nieto et al. (2014) classified this species as DD – data deficient. It is the only category in which this species can be classified because we know only one specimen, the type.

Dioxys moestus Costa*Dioxys moesta* Costa, 1883: 96.*Dioxys rotundata* Pérez, 1883: 300.

Diagnosis. Middle-sized species, body length 5–8 mm. Species with typical general appearance for this genus, black with first 2–3 metasomal terga entirely or partly reddish, with narrow apical bands of whitish short appressed hair (Fig. 11A, B). Mesosoma with long whitish hair, apex of metasomal T6 rounded (Fig. 11C). The legs and antennae are black. The last metasomal terga in males was not as narrow as that in *D. cinctus*. In general, similar to *D. cinctus* but differs by several characteristics: it is usually smaller and the reddish colouration is more distributed (usually on T1–3, in *D. cinctus* on T1–T2). Females of *D. cinctus* have a straight apex of T6, while females of *D. moestus* have a round apex of T6. Males of *D. moestus* have two

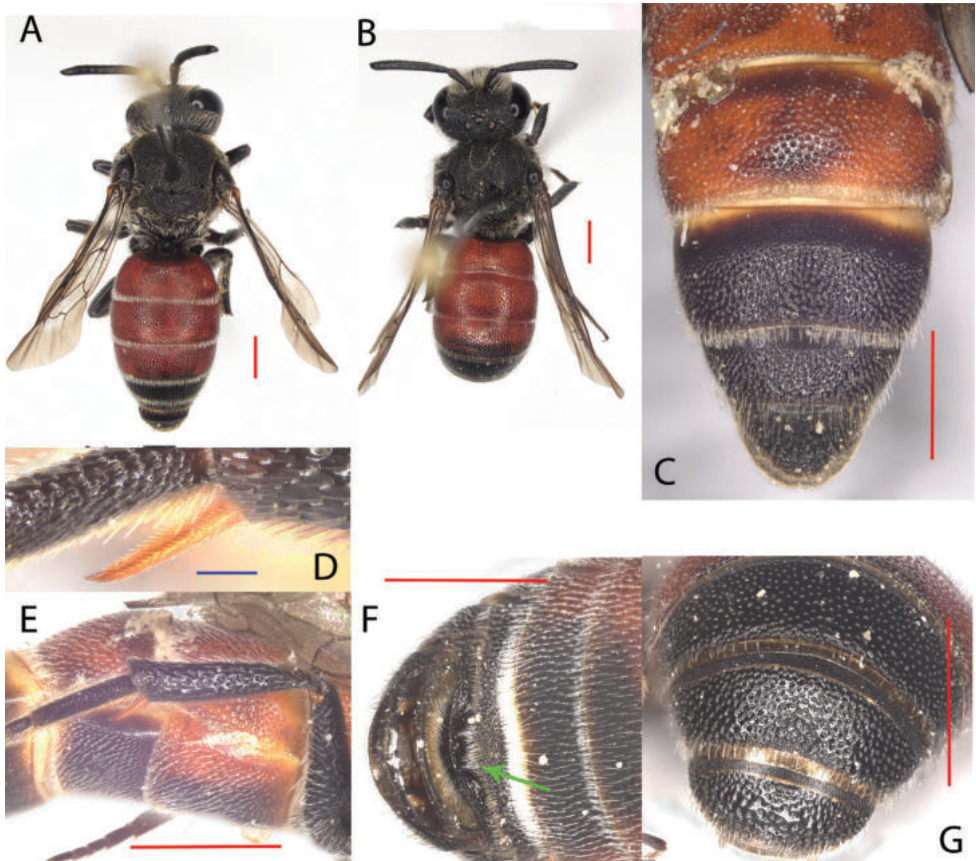


Figure 11. *Dioxys moestus* **A** female, dorsal view **B** male, dorsal view **C** female, mesosoma dorsal view **D** female, metasoma, dorsal view **E** female, metasoma lateral **F** male, last metasomal segments, ventral view **G** male, T4–T6, dorsal view. Red scale bars represent the length of 1 mm, blue scale bars 100 μm .



Figure 12. *Dioxyys moestus*, distribution in Europe.

tooth-like processes on S4 medio-posteriorly (Fig. 11F), and males of *D. cinctus* lack this characteristic. Punctuation of T2–T3 of *D. moestus* is finer and sparser than in *D. cinctus*.

Distribution. Mediterranean species described from Sardinia. Recorded from Portugal to Greece (Fig. 12). Outside of Europe, it is recorded in North Africa, from Morocco to Tunisia, and Israel (Warncke 1977; Ornos et al. 2008).

Biology and hosts. This species occurs in open habitats. It was collected in open habitats with shrubby vegetation, steppic formations or rocky landscapes with almond orchards. Hosts are *Hoplitis benoisti* (Alfken), *Hoplitis fertoni* (Pérez) and *Hoplitis zandeni* (Teunissen & van Achterberg) (Bogusch et al. 2020b), probably also *Hoplitis ochraceicornis* (Ferton) (I. Cross, unpublished record). Several specimens were reared from nests of *H. fertoni* placed inside snail shells (Bogusch et al. 2020b).

Conservation status. Nieto et al. (2014) classified this species as DD – data deficient. This species occurs in most of southern Europe, where it is rare but still frequently recorded. It can be classified as LC – least concern.

Note. *Dioxyys heinrichi* Warncke occurs in North Africa (Morocco and Algeria) and is similar to *D. moestus*. Female *D. heinrichi* have a longer F2 and more convex clypeus, and males do not have a swollen end of S4 and lack the two small teeth. The end of S5 is slightly emarginated.

Dioxys pumilus* GerstaeckerDioxys pumilus* Gerstaecker, 1869: 167.*Dioxys varipes* De Stefani, 1887: 113.*Dioxys maroccana* Popov, 1936: 16.*Dioxys cypriaca* Popov, 1944: 121.

Diagnosis. Smaller species, total body length 4–6 mm. Species with typical general appearance for this genus, black with first 2–4 metasomal terga entirely or partly reddish, with narrow apical bands of whitish short appressed hair (Fig. 13A, B). Mesosoma with long whitish hair, apex of metasomal T6 rounded (Fig. 13C). The legs and antennae are at least partly reddish. Last metasomal terga in males not as narrowed as in *D. cinctus*, last tergum more curved than in *D. moestus* and *D. cinctus*. Species in general similar to smaller individuals of *D. moestus* and *D. cinctus* differ by reddish legs and flagellum. Females have a T6 that is longer than it is wide (distinctly longer than the T6 of both

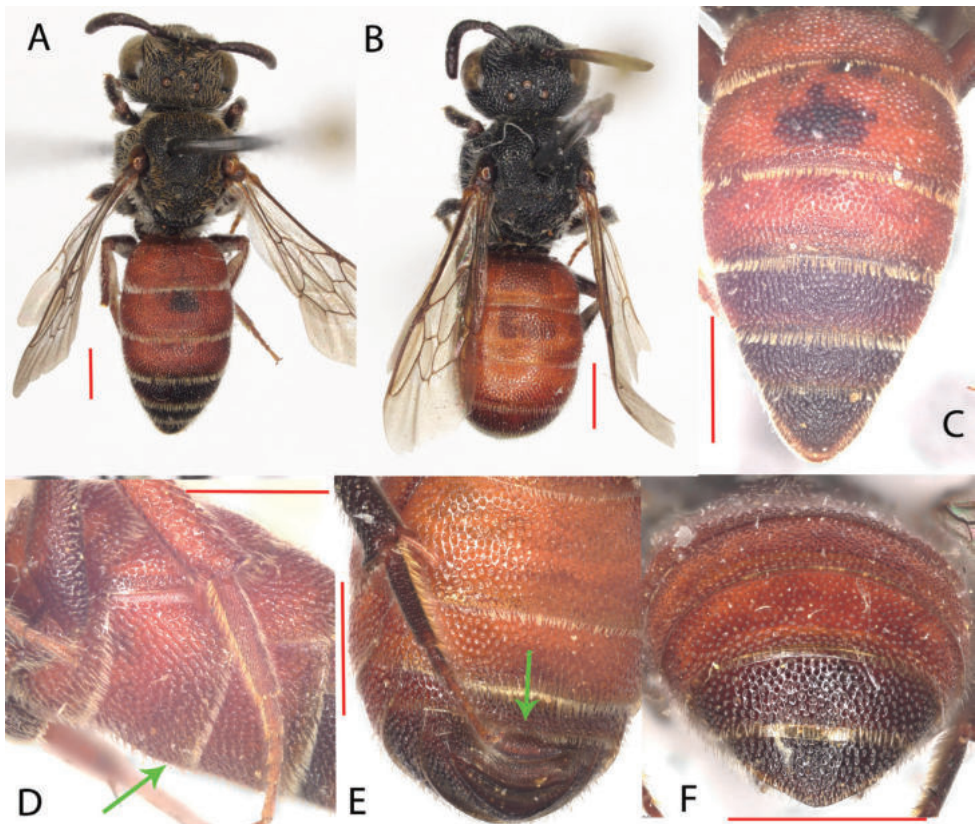


Figure 13. *Dioxys pumilus* **A** female, dorsal view **B** male, dorsal view **C** female, metasoma, dorsal view **D** female, metasoma lateral **E** male, last metasomal segments, ventral view **F** male, last metasomal segments, dorsal view. Red scale bars represent the length of 1 mm.



Figure 14. *Dioxys pumilus*, distribution in Europe.

similar species), males do not have a sharp medio-posterior projection on S4 (present in *D. moestus*) but the apex of S4 is waved, not straight as in *D. cinctus* (Fig. 13E). Punctuation of T2–T3 is coarser and denser than in *D. moestus* and *D. cinctus*. Specimens from Cyprus (described by Popov, 1944 as a separate species) look more colourful at first view but do not differ in their morphology, and the diagnostic characteristics of *D. cypriaca* are variable and form a continuous line to *D. pumilus*. Thus, *D. cypriaca* is currently supposed to be a synonym of *D. pumilus*.

Distribution. This is a western Palearctic species. The nominate subspecies occurs in the eastern Mediterranean basin (Greece, Cyprus, Turkey) (Fig. 14) and spreads towards Asia Minor (Israel, Syria) and Iran. The subspecies *D. p. varipes* occurs in the western Mediterranean basin (Sicily, Spain, Morocco, Algeria, Tunisia). The taxonomic statuses of these subspecies are unclear, but they do not differ in morphology, other than the specimens from western parts of the distribution area often being darker than those from the east.

Biology and hosts. This species was recorded in a variety of open and semi-open habitats – steppes, forest steppes, semideserts, open landscapes with shrubby vegetation and many others. *Heriades crenulatus* Nylander was reported as a likely host of this species in Cyprus (Mavromoustakis 1959). In Portugal, it was recorded in association with *Hoplitis annulata* Latreille (Baldock et al. 2018). Small species of *Osmiini* are also supposed to be host species of *D. pumilus*.

Conservation status. Nieto et al. (2014) classified this species as DD – data deficient. This species occurs in many countries in southern Europe, while in several localities, it has been recorded in large series. It is more local than *D. moestus* but probably more numerous at the localities. It can be classified as LC – least concern.

Ensliniana Alfken

Ensliniana Alfken, 1938: 431, type species: *Ensliniana cuspidata* Alfken, 1938 = *Stelis bidentata* Friese, 1899, by original designation.

Dioxoides Popov, 1947: 89. Type species: *Coelioxys tridentata* Nylander, 1848, by original designation.

Notes. This genus is distributed in North Africa and the Middle East, from Morocco in the west to Turkmenistan in the east. Three species were described, one of which was reported from Europe – Portugal and Spain (Popov 1936, 1953; Michener 2007).

Ensliniana bidentata (Friese)

Stelis bidentata Friese, 1899: 285.

Paradoxys pannonica var. *rufipes* Friese, 1899: 285.

Dioxys richaensis Friese, 1911: 139.

Dioxys bidentata Friese in Schulthess, 1924: 319.

Ensliniana cuspidata Alfken, 1938: 431.

Diagnosis. Larger species, body length 7–10 mm. The only species of the genus recorded from Europe. It is typical by the characteristics of the genus; both sexes are generally similar to *Dioxys* species (Fig. 15A, B) but lack axillar teeth (Fig. 15C). T5 of females is shiny, and T6 and S6 are elongated with two lateral teeth, similar to *Paradoxys pannonica* (Fig. 15D). *P. pannonica* differs in the black or dark brown colour of the entire body, with a reddish pattern only on the first three metasomal terga and distinct apical bands of whitish short appressed hair on the metasomal terga.

Distribution. In Europe, only several specimens are known from Spain and Portugal (Ornosa and Ortiz-Sánchez 2014; Torres 2020; Ascher and Pickering 2023) (Fig. 16). It was described from Israel (Jericho and Oran). Outside of Europe, it is known from Morocco, Algeria, Tunisia, Turkey, Syria, Israel and Jordan (Grace 2010).

Biology and hosts. This species probably occurs in open habitats – steppic grasslands, rocky slopes, semideserts and other habitats. Baldock et al. (2018) listed *Hoplitis zaianorum* (Benoist) as a likely host of this species.

Conservation status. Nieto et al. (2014) classified this species as DD – data deficient. This species is known in Europe only from Spain and Portugal, where it was recorded both in the past and in recent years. It can be classified as VU – vulnerable because of its restricted distribution area in Europe.

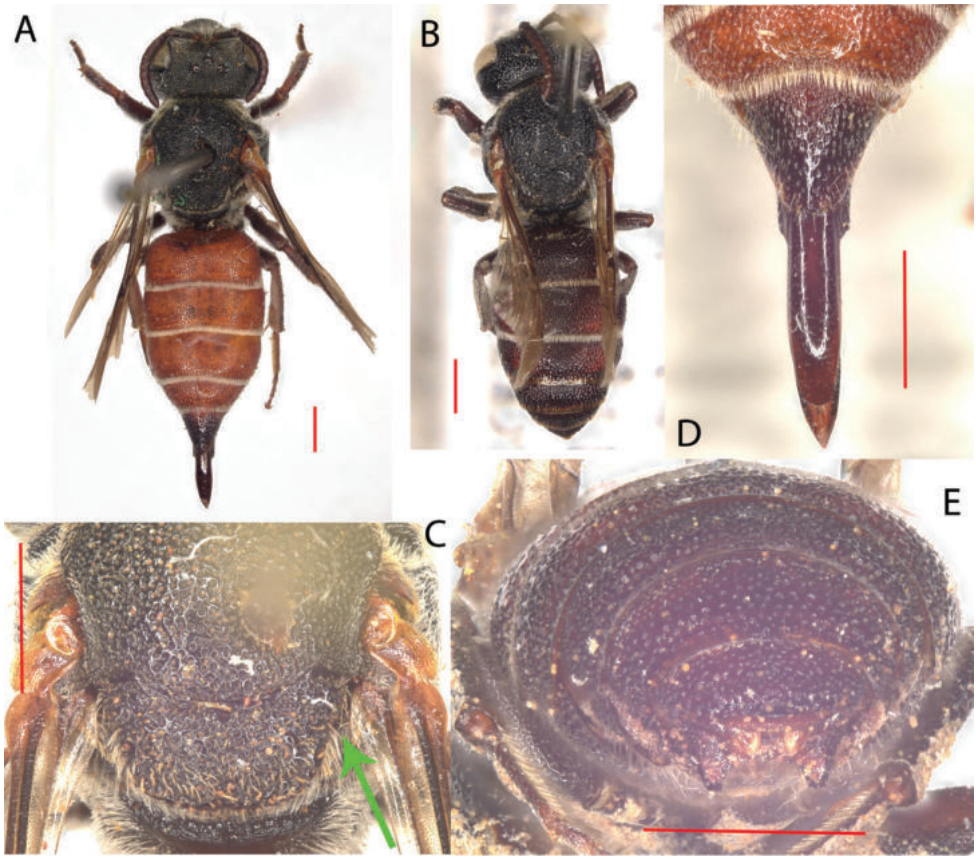


Figure 15. *Ensliniana bidentata* **A** female, dorsal view **B** male, dorsal view **C** female, last metasomal segments, dorsal view **D** female, mesosoma, dorsal view **E** male, last metasomal segments, dorsal view. Red scale bars represent the length of 1 mm.



Figure 16. *Ensliniana bidentata*, distribution in Europe.

Metadioxys Popov

Metadioxys Popov, 1947: 88, type species: *Dioxys formosa* Morawitz, 1875, by original designation.

Notes. This genus has a similar distribution to the previous genera in North Africa and the Middle East, from Morocco in the west to Uzbekistan in the east. Three species were described, one of which was reported from Europe – Greece (Popov 1936, 1953; Michener 2007).

Metadioxys graeca (Mavromoustakis)

Dioxys formosa graeca Mavromoustakis, 1963: 696.

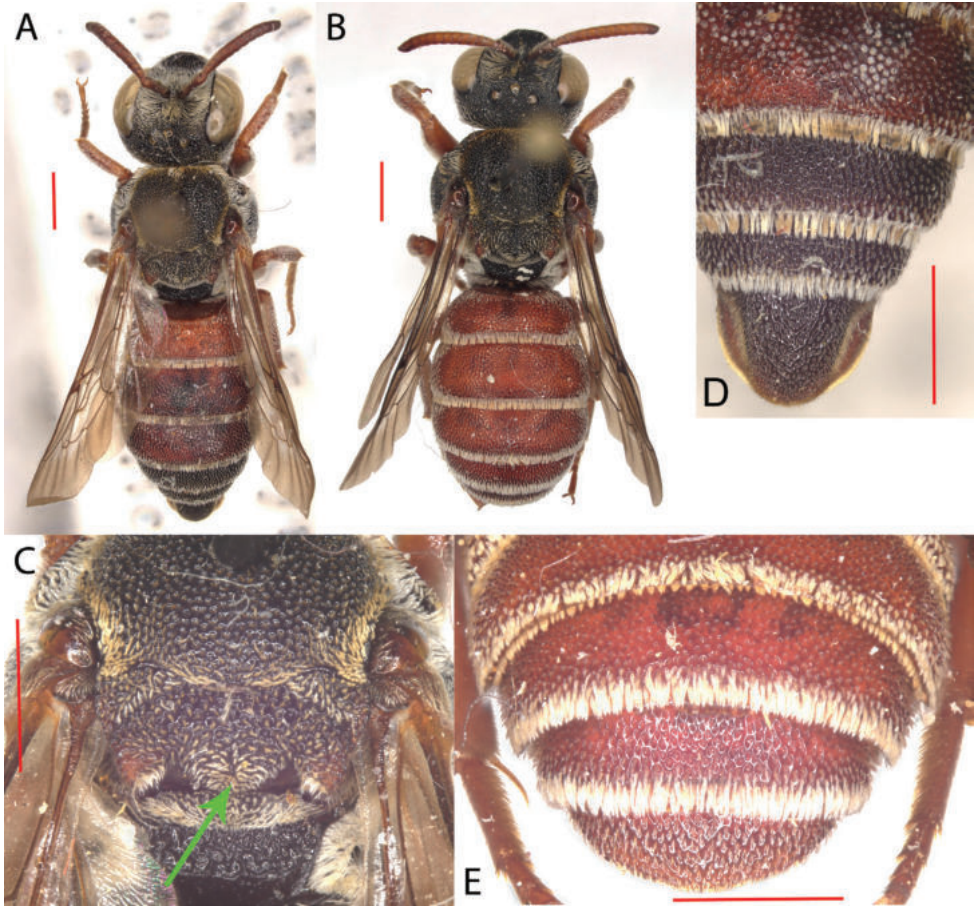


Figure 17. *Metadioxys graeca* **A** female, dorsal view **B** male, dorsal view **C** female, mesosoma dorsal view **D** female, metasoma, dorsal view **E** male, last metasomal segments, dorsal view. Red scale bars represent the length of 1 mm.

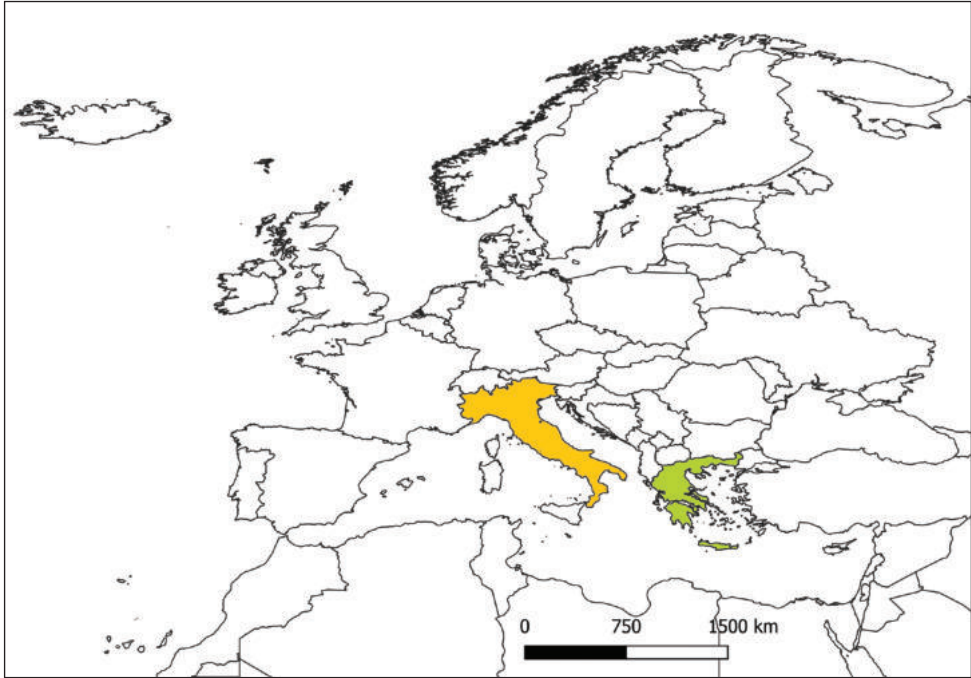


Figure 18. *Metadioxys graeca*, distribution in Europe. Doubtful record from Italy in orange.

Diagnosis. Larger species, body length 8–10 mm. Species generally very similar to those of the genus *Dioxys*, black with first 2–4 metasomal terga entirely or partly reddish (rarely whole metasoma reddish and other body parts reddish), with narrow apical bands of whitish short appressed hair (Fig. 17A, B). Whole body with scale-like whitish short appressed hair, similar to those of *Epeolus* species. Apex of metasomal T6 more elongated than in *Dioxys* and *Aglaopis*, rounded (Fig. 17D). The legs and antennae are at least partly reddish. Typical with sharp carina on coxa of front leg laterally, postscutellum without teeth medioapically, only with an ill-visible tubercle (Fig. 17C). In both sexes, T6 was without emargination (Fig. 17D, E).

Distribution. In the European region, this species is known from Greece (Thessaly and Crete) (Fig. 18). Its range extends out of the European region to Asiatic Turkey, Morocco and Israel (Warncke 1977; Grace 2010; Ascher and Pickering 2023; Kuhlmann et al. 2023).

Biology and hosts. This species probably occurs in open habitats – steppic grasslands, rocky slopes, semideserts and other habitats. Hosts unknown.

Conservation status. Nieto et al. (2014) classified this species as DD – data deficient. There are only old records from Greece and one doubtful record from Italy (certainly this species but probably wrongly labelled), and no recent finds are known. Because of its unknown population trend, we must leave this species in category DD – data deficient.

Note. *Metadioxys formosa* Morawitz occurs in North Africa (Morocco) and the Middle East (Israel and Turkmenistan). It is smaller than *M. graeca* (6–8 mm), and

both sexes have scale-like whitish short appressed hair distributed on more parts of the body than *M. graeca*. Female has last tergum broadened laterally; male has deeply emarginated last sternite.

Paradioxys Mocsáry

Paradioxys Mocsáry, 1894: 35, type species: *Dioxys pannonica* Mocsáry, 1877, monobasic.

Notes. This genus is reported from southeastern Europe and the Middle East. Its occurrence ranges from Austria in the west to Iran in the east. Two species are known, one of which occurs in Europe (Popov 1936; Michener 2007).

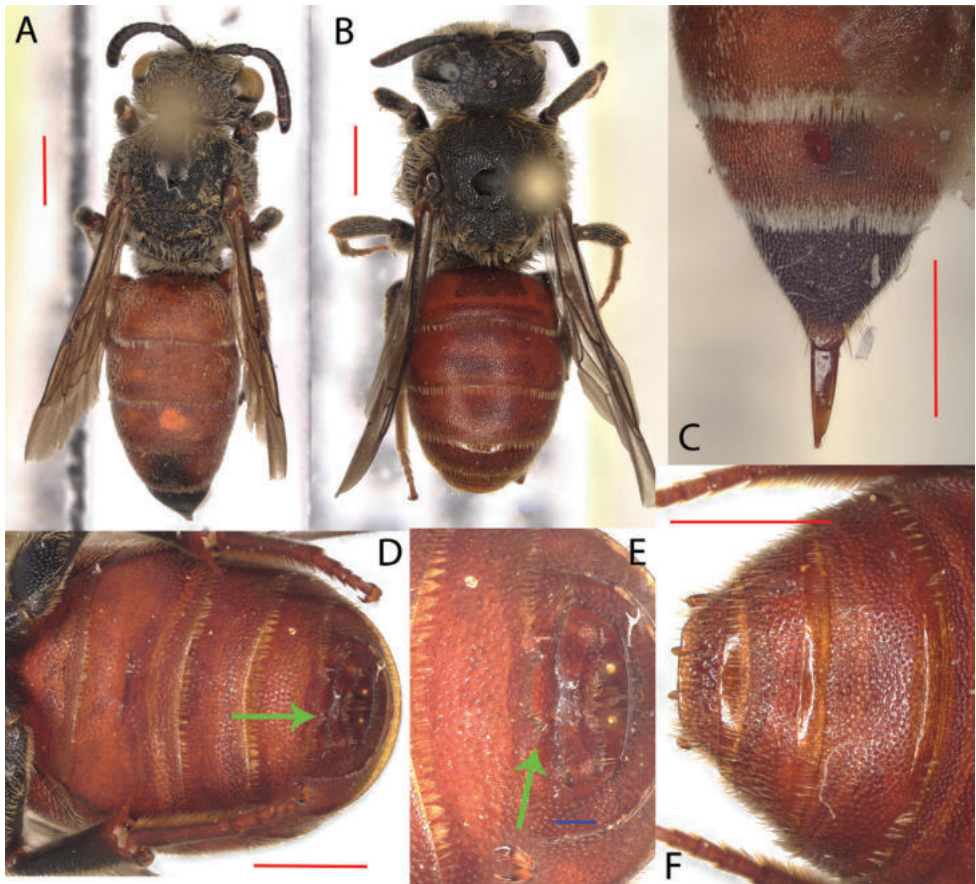


Figure 19. *Paradioxys pannonicus* **A** female, dorsal view **B** male, dorsal view **C** female, last metasomal segments, dorsal view **D** male, metasoma, ventral view **E** male, last metasomal segments, ventral view **F** male, last metasomal segments, dorsal view. Red scale bars represent the length of 1 mm, blue scale bars 100 μ m.

Paradioxys pannonicus (Mocsáry)

Paradioxys pannonica Mocsáry, 1894: 35.

Diagnosis. Middle-sized species, body length 7–10 mm. The only species of the genus within Europe. Typical by the characteristics of the genus, similar to species of the genus *Dioxys*. It is uniform in appearance, females black with first four metasomal terga entirely reddish and males' whole metasoma reddish. Legs are also reddish (Fig. 19A, B). Metasoma of females have narrow apical bands of whitish short appressed hair; similar hairs are also distributed on the first metasomal terga laterally. The metasoma of males have bands of whitish short appressed hair that are sparse and barely visible. The male body has a tomentum-like light brown or yellowish hair. Females have a narrowed T6 and a very long and sharp S6, projecting behind the T6 (Fig. 19C). In males, the end of the metasoma is straight, not curved (Fig. 19F), and the apex of S4 has two prominent toothlike projections, which are larger than in males of *Dioxys* (Fig. 19D, E).

Distribution. This species was described from Hungary and is a Euro-Asiatic species that occurs from central Europe to the north-eastern Mediterranean (Fig. 20) and outside of Europe towards the Middle East and Iran (Popov 1936; Warncke 1977; Bogusch et al. 2007; Gusenleitner et al. 2012; Ascher and Pickering 2023).

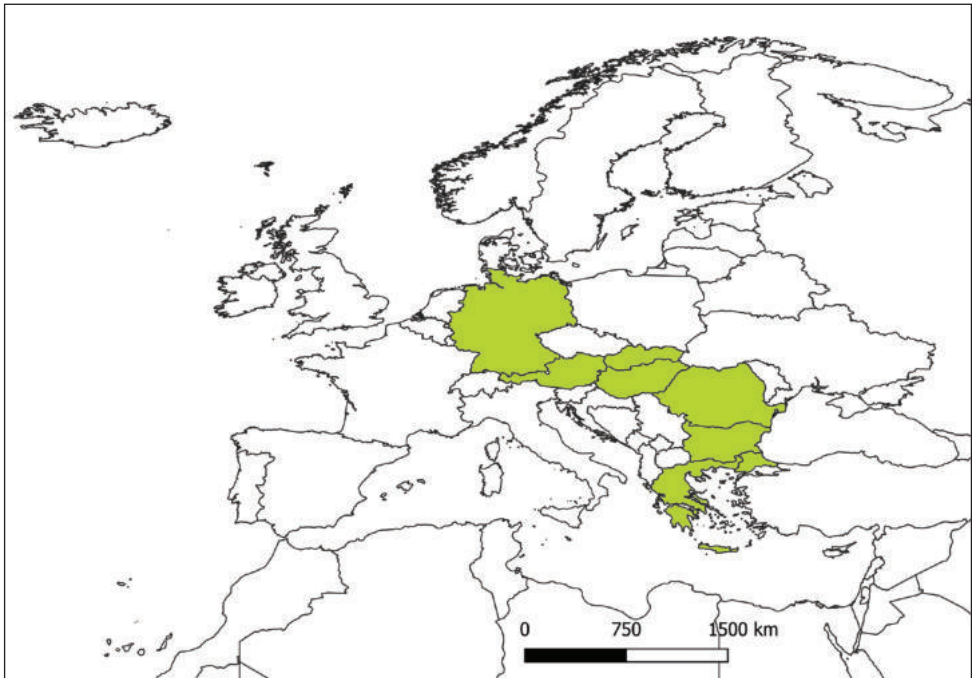


Figure 20. *Paradioxys pannonicus*, distribution in Europe.

Biology and hosts. This species attacks nests of species of the family Megachilidae. Scheuchl and Willner (2016) reported *Chalicodoma hungarica* (Mocsáry) as its main host, and Gusenleitner et al. (2012) included *C. parietina* as its host.

Conservation status. Nieto et al. (2014) classified this species as DD – data deficient. This is a typical Pannonian species occurring in the Pannonian basin. However, there is a lack of records from recent years, and the most recent finds are from the 1970s and 1980s. We suppose this species is CR – critically endangered in Europe.

Discussion

Cuckoo bees of the tribe Dioxyini are represented by ten species in Europe. These cuckoo bees are usually rare, and sightings are not common. Only two species occur in a large part of the continent. *Aglaopis tridentata* is a relatively rare species of steppic habitats whose distribution covers large parts of Europe, including Scandinavia (Sweden and Finland) and Russia. *Dioxys cinctus* occurs in most of southern and central Europe, where it spreads towards the north – the first record from the northwestern part of the Czech Republic (Bohemia) comes from 2012 (Straka et al. 2015) and from Germany from 2019 (Saure and Petrischak 2020). Other species occur only in southern Europe, while two of them were recorded from a larger part of this region. *Dioxys moestus* has a larger distribution but is usually recorded in small numbers of individuals, in contrast to *D. pumilus*, which has a smaller distribution but numerous series of individuals from multiple localities. *Paradioxys pannonicus* is known from central and southeastern Europe historically but there are no recent records on the occurrence of this species in Europe (the latest record I have revised is from Bulgaria from 1983). Two species occur in North Africa and reach their distribution area to Spain and Portugal. *Ensliniana bidentata* was recorded and observed several times after 2000 (Baldock et al. 2018), but for *Dioxys ardens* the latest record from Spain dates back to 1976. A similar case is seen in *Metadioxys graeca*, which occurs in the Middle East and in Greece in Europe, where it was recently recorded only in Crete. *Dioxys atlanticus* and *D. lanzarotensis* were thought to be endemic to the Canary Islands. *Dioxys lanzarotensis* is known only from a single male from Lanzarote, in contrast, *D. atlanticus* was collected on Lanzarote, Gran Canaria and Tenerife, while several specimens were collected on Gran Canaria around the year 2020 (P. Bogusch, own observations). But *D. atlanticus* was also recorded from Egypt (Warncke 1977) and recently from Sardinia.

Several other species were recorded in North Africa or the Middle East. All these species are rare, and their occurrence in Europe is unlikely. The record of *Dioxys chalicoda* from Gibraltar belongs to *D. ardens* (P. Bogusch revised). Thus, in future, studies on the distribution of *D. atlanticus* in southern Europe (if the species will be discovered elsewhere than in Sardinia and Egypt) and attempts to find specimens or populations of *P. pannonica* would be interesting. Although this species has not recorded for a long time, it is likely to occur in Slovakia, Hungary, Bulgaria, Greece or Romania.

Dioxyini are cuckoo bees. This means that discovering these bees is more complicated than discovering nesting bee species. Their hosts are bees of the family Megachilidae, which usually do not nest in aggregations, and thus their nests are harder to find. However, several species have quite visible nests made of mud (genus *Chalicodoma*) or can be recorded in bee hotels (hosts of *D. cinctus* as well as this cuckoo bee species). Furthermore, nests of *Hoplitis fertoni* parasitised by *D. moestus* were reported from empty snail shells in Spain (Bogusch et al. 2020b).

To preserve the fauna of this tribe of cuckoo bees, it is necessary to take care of their habitats. Most species were recorded mainly in open habitats of steppic or semi-desert characteristic. Conservation of these habitats across Europe can go hand in hand with the conservation of the hosts and be helpful for these rare, beautiful and interesting cuckoo bees.

Acknowledgements

I would like to thank to all curators and collection owners for helping with the material. The study was supported by the Excellence Research Project of University of Hradec Kralove Nr. 2202/2023.

References

- Ascher JS, Pickering J (2023) Discover Life bee species guide and world checklist (Hymenoptera: Apoidea: Anthophila). <http://www.discoverlife.org/> [Accessed 29 March, 2023]
- Baldock D, Wood TJ, Cross I, Smit J (2018) The Bees of Portugal (Hymenoptera: Apoidea: Anthophila). *Entomofauna, Supplement 22*: 1–164.
- Batra SWT (1984) Solitary bees. *Scientific American* 250: 86–93. <https://doi.org/10.1038/scientificamerican0284-120>
- Bogusch P, Bláhová E, Horák J (2020a) Pollen specialists are more endangered than non-specialised bees even though they collect pollen on flowers of non-endangered plants. *Arthropod-Plant Interactions* 14: 759–769. <https://doi.org/10.1007/s11829-020-09789-y>
- Bogusch P, Hlaváčková L, Petr L, Bosch J (2020b) Nest structure, pollen utilization and parasites associated with two west-Mediterranean bees (Hymenoptera, Apiformes, Megachilidae) nesting in empty snail shells. *Journal of Hymenoptera Research* 76: 113–125. <https://doi.org/10.3897/jhr.76.49579>
- Bogusch P, Straka J, Kment P (2007) Annotated checklist of the Aculeata (Hymenoptera) of the Czech Republic and Slovakia. *Komentovaný seznam žahadlových blanokřídlých (Hymenoptera: Aculeata) České republiky a Slovenska. Acta Entomologica Musei Nationalis Pragae, Supplementum 11*: 1–300.
- Dusmet JM (1921) Los Ápidos de España. V. Géneros *Stelis* Panz., *Dyoxis* Lep., *Ammobates* Latr., *Phiarus* Gerst., *Pasites* Jur. y *Biastes* Panz. *Memorias de la Real Sociedad española de Historia Natural, Tomo del Cincuentenario 1921*: 177–212.

- Ghisbain G, Rosa P, Bogusch P, Flaminio S, LeDivelec R, Dorchin A, Kasperek M, Litman J, Mignot M, Müller A, Praz C, Radchenko V, Rasmont P, Smit J, Wood TJ, Michez D, Reverté S (2023) The new annotated checklist of the wild bees of Europe (Hymenoptera: Anthophila). *Zootaxa*, accepted.
- Gonzalez VH, Griswold T, Praz CJ, Danforth BN (2012) Phylogeny of the bee family Megachilidae (Hymenoptera: Apoidea) based on adult morphology. *Systematic Entomology* 37: 261–286. <https://doi.org/10.1111/j.1365-3113.2012.00620.x>
- Grace A (2010) *Introductory Biogeography to Bees of the East Mediterranean and Near East*. Bexhill Museum, Sussex, 284 pp.
- Grimaldi D, Engel MS (2005) *Evolution of the Insects*. Cambridge University Press, Cambridge, New York, Melbourne, [xv +] 755 pp.
- Gusenleitner F, Schwarz M, Mazzucco K (2012) Apidae (Insecta: Hymenoptera). In: Schuster R (Ed.) *Checklisten der Fauna Österreichs*, No. 6. Österreichische Akademie der Wissenschaften, Wien, 9–126. [In German]
- Habermannová J, Bogusch P, Straka J (2013) Flexible host choice and common host switches in the evolution of generalist and specialist cuckoo bees (Anthophila: Sphecodes). *PLoS ONE* 8(5): e64537. <https://doi.org/10.1371/journal.pone.0064537>
- Heinrich J (1977) Beitrag zur Kenntnis der türkischen Schmarotzerbienen. *Nachrichten des Naturwissenschaftlichen Museums der Stadt Aschaffenburg* 85: 7–41.
- Hohmann H, La Roche F, Ortega G, Barquín J (1993) *Bienen, Wespen und Ameisen der Kanarischen Inseln*. Band I. Veröffentlichungen aus dem Übersee-Museum Bremen 12: 1–465.
- Hurd Jr PD (1958) American bees of the genus *Dioxys* Lepeletier and Serville. (Hymenoptera: Megachilidae). *University of California Publications in Entomology* 14: 275–302.
- Klein AM, Vaissiere BE, Cane JH, Steffan-Dewenter I, Cunningham SA, Kremen C, Tscharnkte T (2007) Importance of pollinators in changing landscapes for world crops. *Proceedings of the Royal Society in London, Series B* 274: 303–313. <https://doi.org/10.1098/rspb.2006.3721>
- Kuhlmann M, Dathe HH, Ebmer AW, Hartmann P, Michez D, Müller A, Patiny S, Pauly A, Praz C, Rasmont P, Risch S, Scheuchl E, Schwarz M, Terzo M, Williams PH, Amiet F, Baldock D, Berg Ø, Bogusch P, Calabuig I, Cederberg B, Gogala A, Gusenleitner F, Jozan Z, Madsen HB, Nilsson A, Ødegaard F, Ortiz-Sanchez FJ, Paukkunen J, Pawlikowski T, Quaranta M, Roberts SPM, Sáropataki M, Schwenninger HR, Smit J, Söderman G, Tomozei B (2023) Checklist of the Western Palaearctic Bees (Hymenoptera: Apoidea: Anthophila). <https://westpalbees.myspecies.info> [Accessed 12 August 2021]
- Lhomme P, Michez D, Christmann S, Scheuchl E, El Abdouni I, Hamroud L, Ihsane O, Sentil A, Smaili MC, Schwarz M, Dathe HH, Straka J, Pauly A, Schmid-Egger C, Patiny S, Terzo M, Müller A, Praz C, Risch S, Kasperek M, Kuhlmann M, Wood TJ, Bogusch P, Ascher JS, Rasmont P (2020) The wild bees (Hymenoptera: Apoidea) of Morocco. *Zootaxa* 4892: 1–159. <https://doi.org/10.11646/zootaxa.4892.1.1>
- Madsen HB, Calabuig I (2010) Kommenteret checkliste over Danmarks bier – Del 3: Melittidae & Megachilidae (Hymenoptera, Apoidea). *Entomologiske Meddelelser* 78(2): 73–99.

- Mavromoustakis GA (1959) A contribution to our knowledge of the bees (Hymenoptera, Apoidea) of the Island of Rhodos (Greece). Part I. *Annals and Magazine of Natural History* 2(17): 281–302. <https://doi.org/10.1080/00222935908650867>
- Michener CD (2007) *The bees of the world*. Johns Hopkins University Press, Ithaca and New York, 992 pp.
- Nieto A, Roberts SPM, Kemp J, Rasmont P, Kuhlmann M, García Criado M, Biesmeijer JC, Bogusch P, Dathe HH, De la Rúa P, De Meulemeester T, Dehon M, Dewulf A, Ortiz-Sánchez FJ, Lhomme P, Pauly A, Potts SG, Praz C, Quaranta M, Radchenko VG, Scheuchl E, Smit J, Straka J, Terzo M, Tomozei B, Window J, Michez D (2014) *European Red List of Bees*. Publication Office of the European Union, Brussels, Belgium, 96 pp.
- Ornosa C, Ortiz-Sánchez FJ, Torres F (2008) Catálogo de los Megachilidae del Mediterraneo occidental (Hymenoptera, Apoidea). III. Anthidiini y Dioxyini. *Graellsia* 64: 61–86. <https://doi.org/10.3989/graellsia.2008.v64.i1.55>
- Popov VB (1936) To the knowledge of the genus *Dioxys* Lep. (Hymenoptera, Apoidea). *Trudy Zoologicheskogo instituta Akademii nauk SSSR* 3: 3–32. [In Russian]
- Popov VB (1944) Some parasitic bees from Cyprus (Hymenoptera, Apoidea). *Proceedings of the Royal Entomological Society of London (B)* 13(9/10): 120–124. <https://doi.org/10.1111/j.1365-3113.1944.tb00801.x>
- Popov VB (1953) On the reduction of the sting apparatus of Dioxyinae, a subfamily of parasitic bees (Hymenoptera, Megachilidae). *Trudy Zoologicheskogo instituta Akademii nauk SSSR* 13: 337–351. [In Russian]
- Saunders E (1904) Aculeate Hymenoptera collected in Tenerife by the Rev. A. E. Eaton, M.A., in the spring of 1904, with descriptions of new species. *Entomologist's Monthly Magazine* 15(2): 200–208; 229–234.
- Saure C, Petrischak H (2020) *Dioxys cincta* (Jurine 1807), eine für Deutschland neue Bienenart (Hymenoptera, Apiformes). *Eucera* 15: 1–7.
- Scheuchl E, Willner M (2016) *Taschenlexikon der Wildbienen Mitteleuropas: Alle Arten im Porträt*. Quelle & Meyer, Leipzig, 917 pp.
- Sless TJJ, Branstetter MG, Gillung JP, Krichilsky EA, Tobin KB, Straka J, Rozen Jr JG, Freitas FV, Martins AC, Bossert S, Searle JB, Danforth BN (2022) Phylogenetic relationships and the evolution of host preferences in the largest clade of brood parasitic bees (Apidae: Nomadinae). *Molecular Phylogenetics and Evolution* 166: 107326. <https://doi.org/10.1016/j.ympev.2021.107326>
- Standfuss K, Standfuss L, Schwarz M (2003) Zur aktuellen Bienenfauna der Ölbaumzone in SO Thessalien/Griechenland (Hymenoptera: Apoidea: Apiformes). 1. Megachilidae. *Entomofauna* 24(20): 293–304.
- Straka J, Bogusch P (2017) Apiformes (včely). In: Hejda R, Farkač J, Chobot K (Eds) *Červený seznam ohrožených druhů České republiky. Bezobratlí*. Red List of Invertebrates of the Czech Republic. *Příroda* 36: 236–249.
- Straka J, Bogusch P, Tyrner P, Říha M, Benda D, Čížek O, Halada M, Macháčková L, Marhoul P, Tropek R (2015) Faunistic records from the Czech Republic – 380. Hymenoptera: Aculeata. *Klapalekiana* 51: 77–91.

- Tkalcu B (2001) Une nouvelle espece du genre *Dioxys* des Iles Canaries (Hymenoptera, Apoidea, Megachilidae). Bulletin de la Société Entomologique de Mulhouse 57(3): 49–50.
- Torres F (2020) Confirmación de la presencia de *Ensliniana bidentata* (Friese, 1899) (Hymenoptera, Megachilidae) en la fauna de España. Boletín de la Asociación Española de Entomología 44: 223–225.
- Varnava AI, Roberts SPM, Michez D, Ascher JS, Petanidou T, Dimitriou S, Devalez J, Pittara M, Stavriniades MC (2020) The wild bees (Hymenoptera, Apoidea) of the island of Cyprus. ZooKeys 924: 1–114. <https://doi.org/10.3897/zookeys.924.38328>
- Warncke K (1977) Beitrag zur Systematik der westpaUarktischen Bienengattung *Dioxys* LEP. & SERV. (Hymenoptera, Apoidea). Reichenbachia 16: 265–282.
- Westrich P (2018) Die Wildbienen Deutschlands. Eugen Ulmer, Stuttgart, 824 pp.

An alternative host searching strategy found in the subfamily Hybrizontinae (Hymenoptera, Ichneumonidae)

Yu Hisasue^{1,2}, Kazuhiko Konishi³, Kenji Takashino^{4,5}

1 Entomological Laboratory, Graduate School of Bioresource and Bioenvironmental Sciences, Kyushu University, 744, Motoooka, Nishi-ku, Fukuoka, Fukuoka, 819-0395, Japan **2** Present address: Ogasawara Division of Japan Wildlife Research Center, Okumura, Chichijima, Ogasawara, Tokyo 100–2101, Japan **3** Entomological Laboratory, Faculty of Agriculture, Ehime University, Tarumi 3-5-7, Matsuyama, Ehime 790-8566, Japan **4** Hokkaido Agricultural Research Center, NARO, 1 Hitsujigaoka, Toyohira, Sapporo, Hokkaido 062-8555, Japan **5** Present address: Institute for Plant Protection, NARO, 2-1-18 Kannondai, Tsukuba, Ibaraki 305-8666, Japan

Corresponding author: Yu Hisasue (hybrizonist@gmail.com)

Academic editor: Tamara Spasojevic | Received 24 May 2023 | Accepted 16 July 2023 | Published 26 July 2023

<https://zoobank.org/D6F89C9F-66A6-4ADE-BF3D-A5022D67B5EB>

Citation: Hisasue Y, Konishi K, Takashino K (2023) An alternative host searching strategy found in the subfamily Hybrizontinae (Hymenoptera, Ichneumonidae). Journal of Hymenoptera Research 96: 629–639. <https://doi.org/10.3897/jhr.96.106836>

Abstract

The present study reports the oviposition behavior of the ant parasitoid wasp, *Ghilaromma orientalis*, on an undescribed ant species from *Lasius fuliginosus* species group in Japan, illustrated by clear photographs. Previously, the oviposition behavior in the subfamily Hybrizontinae had been limited to species hovering on an ant trail and attacking larvae carried by worker ants. In contrast, in *G. orientalis*, whose oviposition behavior had not been reported to date, the wasp hung on the grass growing along the ants' trail by its hind legs with its head down, and when workers with larvae pass by, directed its abdomen toward the larvae with its hind legs remaining on the grass. Our findings suggest that the subfamily Hybrizontinae employs two host-searching strategies—an active strategy previously known and the ambush-type host-searching strategy employed by *G. orientalis*. The ambush-type strategy affords *G. orientalis* the advantage of laying eggs in a narrow environment where wasps cannot fly without being noticed by ants. Moreover, by avoiding detection through ambush tactics, wasps are increasing their chance for attack, as ants continue to transport their larvae. However, the search range of wasps is reduced, which may limit the opportunities for parasitization. Additionally, while *Lasius nipponensis* has been observed as the sole known host of *G. orientalis*, the oviposition behavior has now been observed in an undescribed species of *L. fuliginosus* group, suggesting that *G. orientalis* may have a subgenus-specific host range.

Keywords

Ghilaromma orientalis, host ant, host-searching behavior, oviposition behavior, parasitoid

Introduction

Parasitoid wasps have developed behaviors to adapt to the ecology of various hosts and overcome the means of avoiding parasitism (Harvey 2005; Fatouros et al. 2008; Johnson 2013). Host searching behavior is a crucial stage for parasitoids, not only for efficient host search, but also for competing with other parasitoids that exploit the same host as a resource. A variety of such behaviors have been reported, including those utilizing chemical or sonic cues (Vet 2001). Parasitoid wasps select their strategies from these options based on their own morphology, the host, and the host's habitat (Tschopp et al. 2013; Yamamoto et al. 2020). In Hymenoptera, various parasitic behaviors have developed, and the host range extends to 19 orders, making it the second most diverse after the one found in Diptera (Eggleton and Belshaw 1992).

Numerous species of hymenopterans are associated with ants, which possess the largest biomass of insects in the world (Schultheiss et al. 2022), through predation, parasitism on the brood and/or adults, cleptoparasitism, parabiosis, mimetism, true symphily, or indirect parasitism through trophobionts and/or social parasites (Kistner 1982; Lachaud et al. 2013). On the other hand, the number of species that parasitize ants is limited, except within the family Eucharitidae, which are ant specialists. This is believed to be due to the social system of ants, which greatly inhibits parasitism by parasitoids (Lachaud and Pérez-Lachaud 2012). Myrmecophilous insects, which share a life history with ants, have evolved unique strategies to exploit sociality (Kistner 1982; Hölldobler and Wilson 1990; Maruyama and Parker 2017). Rove beetles and clown beetles avoid attacks by ants by producing compounds that both appease their hosts and stimulate adoption, and can live in ant nests (Parker 2016; Hölldobler and Kwapich 2019). Ant crickets and the butterfly family Lycaenidae prevent ants from attacking them by altering the components of cuticular hydrocarbons on their body surfaces (Komatsu et al. 2009; Omura et al. 2012).

Parasitoid wasps that challenge ant society are known to have highly specialized morphologies and behaviors that are not deducible from their sister group and their higher classification (Kistner 1982; Lachaud and Pérez-Lachaud 2012). For example, females from the family Eucharitidae oviposit several eggs at random between the spicules on the underside of a leaf (Clausen 1923; Das 1963; Heraty 1994). Once the eggs hatch, the planidial first-instar larvae gain access to the host ant nest by phoretic attachment to foraging ant workers (Das 1963; Heraty 1994; Heraty et al. 2018). Members of the tribe Neoneurini (Braconidae, Euphorinae) are also capable of rapid parasitism of the adults of *Formica* ants because of their high-flying ability and specialized ovipositor that allows them to quickly lay eggs on ant abdomens (Pierre 1893; Donisthorpe 1927; Gómez Durán and van Achterberg 2011). Furthermore, *Smicromorpha* spp. (Chalcididae) approach the nests of weaver ants (*Oecophylla smaragdina* (Fabricius, 1775)) and lay eggs directly on the larvae (Darling 2009).

The subfamily Hybrizontinae of Ichneumonidae (=Darwin wasp) represents the third most diverse group of ant parasitoids after Eucharitidae and Neoneurini (Yu et al. 2016). This subfamily is distributed throughout the Holarctic Region and includes 16 extant species of four genera, namely *Ghilaromma*, *Hybrizon*, *Neohybrizon*, and *Ogkosoma* (Yu et al. 2016; Broad et al. 2018; Hisasue and Konishi 2019; Liu et al. 2019). Among these, the oviposition behavior has been reported for three species belonging to three different genera, *Ogkosoma cremieri* (Romand, 1838) and *Neohybrizon mutus* Hisasue & Konishi, 2019 by Komatsu and Konishi (2010), and *Hybrizon buccatus* (de Brébisson, 1825) by Gómez Durán and van Achterberg (2011). In these species, the females hover over an ant trail, and when they come across ant larvae carried by workers, they attack and lay eggs on the ant larvae. However, the oviposition behavior has not been reported for *Ghilaromma*. The host of this genus is suggested to be the *Lasius fuliginosus* species group based on a few observations (Donisthorpe and Wilkinson 1930; Maruyama et al. 2013). In Japan, females of *Ghilaromma orientalis* Tobias, 1988 were observed hovering over the trail of *Lasius nipponensis* Forel, 1912 and hanging on a branch near the trail (Maruyama et al. 2013). Herein, we present our observations on the oviposition behavior of *G. orientalis*, which are reported for the first time. Additionally, we undertake a comparison of host-searching strategies between those previously known and observed in *G. orientalis*, while also discussing their respective advantages and disadvantages. Furthermore, host-range of *G. orientalis* is also discussed.

Material and method

Study site

Observations were carried out in the vicinity of a Japanese red pine, *Pinus densiflora* Sieb. & Zucc., in the Hitsujigaoka area of Sapporo, Hokkaido, Japan (43.005222°N, 141.416495°E; Fig. 1), where a nest and trails of *Lasius* ants were discovered.

Observation

The observed nest featured an entrance situated at the base of the Japanese red pine, with several trails extending to several meters on the trunk of the tree and several tens of meters on the ground. Though the second and third authors visited and observed this nest every September and October from 2008 to 2021, larval transportation was observed only in 2015. On 18 October 2015, we discovered larvae being transported in one of the ant trails on the ground, and several individuals of *G. orientalis* were flying and *O. cremieri* were hovering around the ant trail, and the second author took the photo of hovering *O. cremieri* using a camera and lens, LUMIX DMC-GX7 (Panasonic, Tokyo, Japan) with Panasonic Leica DG Macro-Elmarit 45 mm f/2.8 lens (Panasonic, Tokyo, Japan). The first author observed more than 10 females of *G. orientalis* flying randomly 50–100 cm above the nest and near the trail without hovering at 11:00 a.m. on 18 October, 2015.



Figure 1. Observation site in the study area (Hitsujigaoka, Sapporo City, Hokkaido, Japan).

On 19 October 2015, we visited this nest again and continued to observe the behavior of *G. orientalis* around the nest and along the ant trail. On 20 October 2015, the third author observed and captured photos of oviposition using a smartphone, iPhone 4S (Apple, California, U.S.A.). To compare host searching and attacking behaviors, we observed *O. cremieri* at the same nest and at a nest of *L. nipponensis* in the same area.

Results

Unlike previously known host-searching behavior in Hybrizontinae, the females of *G. orientalis* did not hover over the ant trail. Instead, they were observed hanging upside down from the grass covering the ant trail with their heads and antennae directed towards the trail (Fig. 2). The ambush behavior before the attack sometimes lasted for up to an hour. When a worker ant with ant larvae passed beneath, the female touched the larva with its front legs and stretched its legs and directed its abdomen toward the larva while gripping the grass with its hind legs (Fig. 3). The ants then continued to advance. However, the female *G. orientalis* did not release the grip with its hind legs from the grass but instead moved for some time while maintaining its position (Fig. 4). During this period, the worker ant was not observed to be bothered by the parasitoid wasp. Unfortunately, it is not confirmed whether the eggs were laid or not.

Females of *O. cremieri* were observed to stop hovering when the wind blew and to rest on a tree trunk nearby. In addition, worker ants were observed to rise their body and open their mandibles wide toward the hovering *O. cremieri* (Fig. 5); some individuals were even caught by ant workers.



Figure 2. Female of *Ghilaromma orientalis* Tobias, 1988 hanging from the grass above the ant trail with her head facing the trail.



Figure 3. Female *Ghilaromma orientalis* Tobias, 1988 using her front legs to contact an ant larva and directing her abdomen towards it, while maintaining a firm grip on the grass with her hind legs.



Figure 4. Female *Ghilaromma orientalis* Tobias, 1988 maintaining a firm grip on the grass with her hind legs while adjusting her body position to oviposition onto a larva being carried away by an ant.



Figure 5. Workers of *Lasius nipponensis* Forel, 1912 with their mandibles open, alerted to the hovering *Ogkosoma cremieri* (Romand, 1838).

The ants that were collected and identified as being parasitized by *G. orientalis* were not *L. nipponensis*, which was previously thought to be the only host species. They were an undescribed species close to *Lasius fuji* (*Lasius* sp. B in the study of Terayama et al. 2014). This species is distributed only in Hokkaido and is larger than *L. nipponensis* (Terayama et al. 2014).

Discussion

The reported oviposition behavior of the ant parasitoid wasp, *Ghilaromma orientalis*, on an ant species from the *Lasius fuliginosus* species group in Japan, provides valuable insights into the host-searching strategies of the subfamily Hybrizontinae. Previous studies have shown that the three species of Hybrizontinae employ an “active type” host-searching strategy by hovering over ant trails (Kawai 1972; Komatsu and Konishi 2010; Gómez Durán and van Achterberg 2011). This strategy has the advantage of covering a wider search area and enable the movement of parasitoid to areas where the ants carrying larvae are located. However, this strategy has the drawback that hovering of parasitoid wasps over an ant trail alerts the ants and prevents larva-carrying ants from exiting the nest entrance or covered area. Similar observations have been made for *Hybrizon buccatus*, suggesting that hovering species may lose parasitism opportunities because they alarm ants (K. Takasuka pers. comm.). During our observations, the ants opened their mandibles to threaten hovering *Ogkosoma cremieri*, which then occasionally failed to fly or were captured by worker ants. These findings suggest that the parasitism efficiency of *O. cremieri* is declining when the workers detect the wasps. Additionally, *O. cremieri* became stationary on a nearby trunk when the wind blew, indicating that wind can disrupt the host-searching behavior of parasitoids while hovering. On the other hand, the host-searching strategy observed in *G. orientalis* can be described as “ambush type”. The advantage of this strategy is considered to lie not only in conserving the energy expended in sustaining hovering but also in avoiding alerting ants. The flight behavior observed in this species suggests that *G. orientalis* flies over the ant colony without hovering not to lay eggs on the larvae but to search for suitable sites to ambush the worker ants transporting larvae. Consequently, the “ambush type” is less likely to attract physical attention from ants than the “active type” and can successfully parasitize in grassy environments. Nevertheless, the “ambush type” has a limitation of a narrow search area. As ant larvae are not always conveniently transported by workers close to the wasp, narrowing the search area directly leads to a decrease in parasitic opportunities.

Parasitoid wasps that utilize hosts with similar biology, but employ different host-searching strategies, are also observed in some Darwin wasps from the *Poly-sphincta* genus-group (Pimplinae: Ephialtini), which are parasitoids of adult and subadult spiders. *Hymenoepimecis argyraphaga* Gauld, 2000 hovers to approach and attack its host (Eberhard 2000). On the other hand, non-hovering parasitoid wasps,

such as *Zatypota albicoxa* (Walker, 1874) and *Brachyzapus nikkoensis* (Uchida, 1928) hide from their web-spinning spider hosts until they have the opportunity to parasitize (Iwata 1942; Takasuka et al. 2009). Furthermore, parasitoid wasps such as *Hymenoepimecis veranii* Loffredo & Penteado-Dias, 2009 have also been observed to ambush host spiders from hidden locations (Gonzaga and Sobczak 2007; Kloss et al. 2022). In the case of the *Polysphincta*-group, the exploratory strategy of hovering is generally restricted to parasitizing spiders that form vertical circular webs. However, the ambush strategy allows them to attack a more diverse range of environmental hosts, and if they fail to do so, they can hide from spiders that will fight back. Taking into account these behaviors, the ambush type without hovering that *G. orientalis* engages in may have the advantage of increasing the wasp's probability of survival and allowing it to take advantage of environments that the active type cannot invade.

According to Komatsu and Konishi (2010), *N. mutus* and *O. cremieri* occur intensively in August and October, and females of *G. orientalis* are collected from July to October. The timing of occurrences for *N. mutus* and *O. cremieri* corresponded with the time when oviposition behavior was observed, while for *G. orientalis*, oviposition behavior was observed only in October within their occurrence period. Further investigation is required to comprehend the activities of female *G. orientalis* before October, when they commence oviposition behavior. It is possible that the ambush strategy employed by *G. orientalis*, which does not entail hovering, is linked to the prolonged seasonal occurrence of this species, unlike other species.

The host of *Ghilaromma* is suggested to be the *Lasius fuliginosus* species group. A European species, *G. fuliginosi* (Donisthorpe & Wilkinson, 1930), has been observed hovering over *Lasius fuliginosus* (Latreille, 1798) ants (Donisthorpe and Wilkinson 1930). Another species, *G. orientalis*, has been suggested to be a parasitoid of *L. fuji* Radchenko, 2005 *sensu lato* (Watanabe 1984). Later, Maruyama et al. (2013) suggested that this species is a specialist parasitoid of *L. nipponensis*, because it was only observed around the nests of *L. nipponensis*. However, the present observations confirm that this species is also a parasitoid of other species of the *Lasius fuliginosus* species group (*Lasius* sp. B of Terayama et al. 2014). Some members of this species group are known to transport their larvae outside the nest (Komatsu and Konishi 2010; Holý et al. 2017). Therefore, it is plausible that *G. orientalis* may use not only a single ant species, but multiple *L. fuliginosus*-group species that have a habit of transporting larvae outside the nest.

Acknowledgements

We thank Dr. Keizo Takasuka for the information on *Hybrizon buccatus*. Thanks to Dr. Tamara Spasojevic for kindly reading and providing useful editorial comments. This study was partially supported by the Grant-in-Aid for JSPS KAKENHI Grant number 19H00942 for KK, JST SPRING (Grant Number: JPMJSP2136) for YH and a Sasakawa Scientific Research Grant from the Japan Science Society for YH (Grant Number: 2020-5031).

References

- Broad GR, Shaw MR, Fitton MG (2018) Ichneumonid wasps (Hymenoptera: Ichneumonidae): their classification and biology. *Handbooks for the Identification of British Insects* 7(12): 1–418.
- Clausen CP (1923) The biology of *Schizaspidia tenuicornis* Ashm., a eucharid parasite of *Camponotus*. *Annals of the Entomological Society of America* 16: 195–217. <https://doi.org/10.1093/aesa/16.3.195>
- Darling DC (2009) A new species of *Smicromorpha* (Hymenoptera, Chalcididae) from Vietnam, with notes on the host association of the genus. *ZooKeys* 20: 155–163. <https://doi.org/10.3897/zookeys.20.195>
- Das GM (1963) Preliminary studies on the biology of *Orasema assectator* Kerrich (Hymenoptera: Eucharitidae) parasitic on *Pheidole* and causing damage to leaves of tea in Assam. *Bulletin of Entomological Research* 54: 393–398. <https://doi.org/10.1017/S0007485300048884>
- Donisthorpe HSJK (1927) The guests of British ants. Their habits and life-histories. George Routledge & Sons, Ltd., London, 244 pp.
- Donisthorpe HSJK, Wilkinson DS (1930) Notes on the genus *Paxylomma* (Hymenoptera, Braconidae) with the description of a new species taken in Britain. *Transactions of the Royal Entomological Society of London* 78: 87–93. <https://doi.org/10.1111/j.1365-2311.1930.tb01203.x>
- Eberhard WG (2000) The natural history and behavior of *Hymenoepimecis argyraphaga* (Hymenoptera: Ichneumonidae) a parasitoid of *Plesiometa argyra* (Araneae: Tetragnathidae). *Journal of Hymenoptera Research* 9: 220–240.
- Eggleton P, Belshaw R (1992) Insect parasitoids: an evolutionary overview. *Philosophical Transactions of the Royal Society B, Biological Sciences* 337(1279): 1–20. <https://doi.org/10.1098/rstb.1992.0079>
- Fatouros NE, Dicke M, Mumm R, Meiners T, Hilker M (2008) Foraging behavior of egg parasitoids exploiting chemical information. *Behavioral Ecology* 19: 677–689. <https://doi.org/10.1093/beheco/arn011>
- Gómez Durán JM, van Achterberg C (2011) Oviposition behaviour of four ant parasitoids (Hymenoptera, Braconidae, Euphorinae, Neoneurini and Ichneumonidae, Hybrizontinae), with the description of three new European species. *ZooKeys* 125: 59–106. <https://doi.org/10.3897/zookeys.125.1754>
- Gonzaga MO, Sobczak JF (2007) Parasitoid-induced mortality of *Araneus omnicolor* (Araneae, Araneidae) by *Hymenoepimecis* sp. (Hymenoptera, Ichneumonidae) in southeastern Brazil. *Naturwissenschaften* 94: 223–227. <https://doi.org/10.1007/s00114-006-0177-z>
- Harvey JA (2005) Factors affecting the evolution of development strategies in parasitoid wasps: the importance of functional constraints and incorporating complexity. *Entomologia Experimentalis et Applicata* 117: 1–13. <https://doi.org/10.1111/j.1570-7458.2005.00348.x>
- Heraty JM (1994) Classification and evolution of the Oraseminae in the Old World, with revisions of two closely related genera of Eucharitinae (Hymenoptera: Eucharitidae). *Life Sciences Contributions, Royal Ontario Museum* 157: 1–174. <https://doi.org/10.5962/bhl.title.53489>

- Heraty JM, Burks RA, Mbanyana N, van Noort S (2018) Morphology and life history of an ant parasitoid, *Psilocharis afra* (Hymenoptera: Eucharitidae). *Zootaxa* 4482(3): 491–510. <https://doi.org/10.11646/zootaxa.4482.3.3>
- Hölldobler B, Kwapich CL (2019) Behavior and exocrine glands in the myrmecophilous beetle *Dinarda dentata* (Gravenhorst, 1806) (Coleoptera: Staphylinidae: Aleocharinae). *PloS ONE* 14(1): e0210524. <https://doi.org/10.1371/journal.pone.0210524>
- Hölldobler B, Wilson EO (1990) *The ants*. Harvard University Press, Cambridge, Massachusetts, xii + 732 pp. <https://doi.org/10.1007/978-3-662-10306-7>
- Hisasue Y, Konishi K (2019) A new genus of the subfamily Hybrizontinae (Hymenoptera: Ichneumonidae) from Japan. *Zootaxa* 4664(2): 241–250. <https://doi.org/10.11646/zootaxa.4664.2.6>
- Holý K, Bezděčková K, Bezděčka P (2017) Occurrence of *Ogkosoma cremieri* Romand (Ichneumonidae: Hybrizontinae) in the Czech Republic with notes on adult behavior. *Acta Musei Moraviae, Scientiae biologicae (Brno)* 102(2): 139–143.
- Iwata K (1942) Biology of some Japanese *Polysphincta*. *Mushi* 14(2): 98–102.
- Johnson NF (2013) Hymenoptera. In: Levin SA (Ed.) *Encyclopedia of Biodiversity*, 2nd edn. Academic Press, Waltham, MA, 177–184. <https://doi.org/10.1016/B978-0-12-384719-5.00163-5>
- Kawai M (1972) Observations of oviposition behavior in *Paxylomma buccatum*. *Kontyû*, Tokyo 40(1): 53–54. [In Japanese]
- Kistner DH (1982) The social insects' bestiary. In: Hermann HR (Ed.) *Social Insects*. Vol. 3. Academic Press, New York, 1–244. <https://doi.org/10.1016/B978-0-12-342203-3.50008-4>
- Kloss TG, de Pádua DG, de Almeida SDS, Pentead-Dias AM, Mendes-Pereira T, Sobczak JF, Lacerda FG, Gonzaga MO (2022) A new Darwin wasp (Hymenoptera: Ichneumonidae) and new records of behavioral manipulation of the host spider *Leucauge volupis* (Araneae: Tetragnathidae). *Neotropical Entomology* 51(6): 821–829. <https://doi.org/10.1007/s13744-022-00991-6>
- Komatsu T, Maruyama M, Itino T (2009) Behavioral differences between two ant cricket species in Nansei Islands: host-specialist versus host-generalist. *Insectes Sociaux* 56: 389–396. <https://doi.org/10.1007/s00040-009-0036-y>
- Komatsu T, Konishi K (2010) Parasitic behaviors of two ant parasitoid wasps (Ichneumonidae: Hybrizontinae). *Sociobiology* 56(3): 575–584.
- Lachaud J-P, Pérez-Lachaud G (2012) Diversity of species and behavior of hymenopteran parasitoids of ants: a review. *Psyche* 2012: 134746. [24 pp.] <https://doi.org/10.1155/2012/134746>
- Lachaud J-P, Lenoir A, Hughes DP [Eds] (2013) *Ants and Their Parasites 2013*. *Psyche Special Issue*. Hindawi Publishing Corporation, New York. <https://doi.org/10.1155/2013/264279>
- Liu J-X, van Achterberg C, Zheng B-Y, Yang Q-M (2019) *Hybrizon* Fallén (Hymenoptera, Ichneumonidae, Hybrizontinae) in China. *Journal of Hymenoptera Research* 72: 11–26. <https://doi.org/10.3897/jhr.72.39333>
- Maruyama M, Komatsu T, Kudo S, Shimada T, Kinomura K (2013) *The guests of Japanese ants*. Tokai University Press, Minamiyana, 208 pp.
- Maruyama M, Parker J (2017) Deep-time convergence in rove beetle symbionts of army ants. *Current Biology* 27(6): 920–926. <https://doi.org/10.1016/j.cub.2017.02.030>

- Omura H, Watanabe M, Honda K (2012) Cuticular hydrocarbon profiles of *Lycaeides subso-lanus* larvae and their attendant ants. *Lepidoptera Science* 63(4): 186–190. https://doi.org/10.18984/lepid.63.4_186
- Parker J (2016) Myrmecophily in beetles (Coleoptera): evolutionary patterns and biological mechanisms. *Myrmecological News* 22: 65–108. https://doi.org/10.25849/myrmecol.news_022:065
- Pierre A (1893) Un parasite des Fourmis *Elasmosoma berolinense* Ruthe. *Revue scientifique du Bourbonnais et du centre de la France* 6: 112–114.
- Schmid-Hempel P (1998) Parasites in Social Insects. *Monographs in Behavior and Ecology*. Princeton University Press, Princeton, New Jersey, 392 pp.
- Schultheiss P, Nooten SS, Wang R, Wong MK, Brassard F, Guénard B (2022) The abundance, biomass, and distribution of ants on Earth. *Proceedings of the National Academy of Sciences* 119(40): e2201550119. <https://doi.org/10.1073/pnas.2201550119>
- Takasuka K, Matsumoto R, Ohbayashi N (2009) Oviposition behavior of *Zatypota albicoxa* (Hymenoptera, Ichneumonidae), an ectoparasitoid of *Achaearanea tepidariorum* (Araneae, Theridiidae). *Entomological Science* 12: 232–237. <https://doi.org/10.1111/j.1479-8298.2009.00338.x>
- Terayama M, Kubota S, Eguchi K (2014) *Encyclopedia of Japanese Ants*. Tokyo, Asakura-shoten, 278 pp. [In Japanese]
- Tschopp A, Riedel M, Kropf C, Nentwig W, Klopstein S (2013) The evolution of host associations in the parasitic wasp genus *Ichneumon* (Hymenoptera: Ichneumonidae): convergent adaptations to host pupation sites. *BMC Evolutionary Biology* 13: 74. <https://doi.org/10.1186/1471-2148-13-74>
- Vet LEM (2001) Parasitoid searching efficiency links behaviour to population processes. *Applied Entomology and Zoology* 36(4): 399–408. <https://doi.org/10.1303/aez.2001.399>
- Watanabe C (1984) Notes on Paxyloommatinae, with review of Japanese species (Hymenoptera, Braconidae). *Kontyû, Tokyo* 52(4): 553–556.
- Yamamoto T, Hasegawa H, Nakase Y, Komatsu T, Itino T (2020) Cryptic diversity in the aphid-parasitizing wasp *Protaphidius nawaii* (Hymenoptera: Braconidae): discovery of two attendant-ant-specific mtDNA lineages. *Zoological Science* 37: 117–121. <https://doi.org/10.2108/zs190093>
- Yu DS, van Achterberg C, Horstmann K (2016) Taxapad 2016, Ichneumonoidea 2015. Database on flash-drive, Nepean, Ontario, Canada. <http://www.taxapad.com> [accessed 3 September 2017]

Two new *Hoplitis* species of the subgenus *Hoplitis* Klug, 1807 (Hymenoptera, Megachilidae) and the nesting biology of *H. astragali* sp. nov. in Dagestan

Alexander V. Fateryga¹, Andreas Müller^{2,3}, Maxim Yu. Proshchalykin⁴

1 T.I. Vjazemsky Karadag Scientific Station, Nature Reserve of RAS, Branch of A.O. Kovalevsky Institute of Biology of the Southern Seas of RAS, Nauki Str. 24, Kurortnoye, 298188 Feodosiya, Russia **2** ETH Zurich, Institute of Agricultural Sciences, Biocommunication and Entomology, Schmelzbergstrasse 9/LFO, 8092 Zurich, Switzerland **3** Natural History Museum Bern, Department of Invertebrates, Bernastrasse 15, 3005 Bern, Switzerland **4** Federal Scientific Center of the East Asia Terrestrial Biodiversity, Far Eastern Branch of the Russian Academy of Sciences, 100-let Vladivostoku Ave. 159, 690022 Vladivostok, Russia

Corresponding author: Alexander V. Fateryga (fater_84@list.ru)

Academic editor: Jack Neff | Received 9 July 2023 | Accepted 8 August 2023 | Published 15 August 2023

<https://zoobank.org/FB63186E-9043-4571-A1FE-EE27E3FA9D1D>

Citation: Fateryga AV, Müller A, Proshchalykin MYu (2023) Two new *Hoplitis* species of the subgenus *Hoplitis* Klug, 1807 (Hymenoptera, Megachilidae) and the nesting biology of *H. astragali* sp. nov. in Dagestan. Journal of Hymenoptera Research 96: 641–656. <https://doi.org/10.3897/jhr.96.109255>

Abstract

Hoplitis astragali sp. nov., a member of the *H. monstrabilis* species group, and *H. dagestanica* sp. nov., a member of the *H. adunca* species group, are described. The former species is known from Dagestan in Russia, Azerbaijan, and Turkmenistan, the latter only from Dagestan. Nests of *H. astragali* are described. Females of this species excavated burrows in a vertical clay cliff, but sometimes chose a horizontal surface for nest excavation, particularly at the entrance of old burrows of *Xylocopa olivieri* (Apidae). The nest burrows of *H. astragali* were either sub-vertical or sub-horizontal. The nests were composed of one to three brood cells, an empty vestibule in front of the outermost cell, and a closing plug at the nest entrance made of moistened mud. The inner surface of the cells was covered with a thin wall composed of compact soil, most probably built by the female bee after cell excavation. The pollen loaf was very liquid and had a spherical shape. The egg was deposited on its top. The cocoon consisted of a single thin layer, which uniformly covered the whole inner surface of the cell. There was one generation per year. The prepupae hibernated. *Sapyga caucasica* (Sapygidae) was recorded in the nests as a kleptoparasite. Both females and males of *H. astragali* exclusively visited flowers of two species of the genus *Astragalus* (Fabaceae).

Keywords

Bionomics, Caucasus, megachilid bees, osmiine bees, Palaearctic region, taxonomy

Introduction

Hoplitis Klug, 1807 is the largest genus of the osmiine bees (Hymenoptera, Megachilidae, Osmiini) with 387 species described so far (Müller 2023). It is distributed in the Palaearctic, the Nearctic, and the Afrotropical region; a few species also occur in the Oriental region (Michener 2007). The genus *Hoplitis* is especially diverse in the Palaearctic region, where 14 subgenera and 311 species occur (Praz et al. 2008; Ungricht et al. 2008; Sedivy et al. 2012a; Müller 2023). The largest subgenus of the genus *Hoplitis* is *Hoplitis* s. str., which is confined to the Palaearctic region. It contains 91 species described so far and a large number of still undescribed species amounting to more than 50. The subgenus comprises several species groups. Among them, the *Hoplitis adunca* species group is the largest and one of the taxonomically most challenging osmiine bee taxa due to the high morphological uniformity among its species, especially in the female sex (Müller 2016, 2023). Members of this species group nest either in various pre-existing cavities (such as rock and stone crevices, hollow stems, abandoned nests of other bees and wasps, insect burrows in wood, rarely empty snail shells) or construct cells freely on the surface of rocks or stones, usually in depressions (Sedivy et al. 2013). The building material used for nest construction is always mud, often combined with small pebbles or gravel. Members of the *Hoplitis annulata* and the *H. monstrabilis* species groups nest in self-excavated burrows in the ground and the *H. erythrogastra* species group contains kleptoparasites, which develop in nests of members of the *H. annulata* species group (Michener 2007; Sedivy et al. 2013; Müller 2023).

The megachilid bee fauna of the Republic of Dagestan (Russia) is very poorly known. A list of just 30 species, including one species later synonymized, was published 150 years ago (Morawitz 1873); six of them were described as new, of which four are currently recognized as valid species. Some recently published papers (Fateryga 2017; Fateryga et al. 2019; Fateryga and Proshchalykin 2020; Litman et al. 2021) added 46 species increasing the total species number to 75, which is expected to be still very far from the true number of megachilid bee species occurring in Dagestan. The present contribution is a part of the currently ongoing study of the megachilid bees of Dagestan. Several field expeditions were made to various districts of this republic in 2015–2022, which resulted in about 2000 newly collected specimens of Megachilidae. The complete list of species will be published in a separate paper, while the purpose of the present contribution is to describe two new *Hoplitis* species of the subgenus *Hoplitis*. Since nests of one of these species were discovered, its bionomics is briefly described in the present paper.

Material and method

The material for the present study was collected in Dagestan in 2018–2022 and deposited in the collections of the Zoological Institute of the Russian Academy of Sciences, Saint Petersburg, Russia [ZISP], the Federal Scientific Center of the East

Asia Terrestrial Biodiversity of the Far Eastern Branch of the Russian Academy of Sciences, Vladivostok, Russia [FSCV], the Entomological Collection of ETH Zurich, Switzerland [ETHZ], and the research collection of A.V. Fateryga, Feodosiya, Russia [CAFK].

Morphological terminology and definitions for body measurements follow Michener (2007) with the following specifications: i) the distance between lateral ocellus and preoccipital margin was measured in top view rather than in lateral view; ii) the diameter of an ocellus includes the ocellar border, which is often of the same colour as the surrounding cuticle thereby differing from the usually light colour of the central part of the ocellus; iii) the length of a segment of the labial palpus was measured from its sclerotized base to the sclerotized base of the subsequent segment; iv) the length of an antennal article was measured along its lower margin, while its width corresponds to the maximal width of the article; v) numbering of antennal articles starts from the scapus, which is antennal article 1, and ends with the last flagellomere, which is antennal article 12 (females) or 13 (males); vi) the number of a segment belonging to a segmented body part is put into parentheses if a character of that segment is not developed in all individuals; thus, “terga (2)3–6 strongly shagreened” means that tergum 2 is strongly shagreened as terga 3–6 in some but not all specimens. Measurements to the nearest 0.1 mm or 0.5 mm (for body length) were taken using an ocular micrometer on an Olympus VNT stereomicroscope. Photomicrographs were taken with a Keyence VHX-2000 digital microscope.

The nesting biology of *Hoplitis astragali* sp. nov. was investigated 6 km northwest of Chirkey in the Buynaksky district (43°00'10"N, 46°53'51"E) in 2022. Six nesting females were recorded on 27 May at a clay cliff. One of them was sealing her nest with soil; this nest was dissected immediately after the female had finished the closing plug. The other five nests were marked with two triangular pieces of red plastic each; the markers were inserted in an equal distance of about 10 cm from the nest entrance, so that the latter lay in the middle between them. The second visit to this place on 31 May revealed that four of the five nests still open on 27 May were sealed with soil plugs and that an additional nest was built and sealed near one of them. All five sealed nests were extracted from the cliff together with the surrounding earth excavated with the help of a shovel. The earth lumps were transferred to the laboratory and the nests were dissected in October 2022 by removing the surrounding earth layer by layer with a knife. In total, six nests were studied, including the freshly sealed one. Plans of the nest structure were drawn on paper and the direction of the nesting burrows and brood cells determined with a compass. Contents of nest cells from the dissected nests were placed into glass tubes sealed with cotton plugs and then kept under outdoor conditions. Photographs of the nests were taken with a Canon EOS RP digital camera, a Sigma AF 105 mm f/2.8 and a Canon RF 35 mm f/1.8 macro lens, and a Yongnuo YN-14EX macro flash. Additional observations on flower visits by both new species of *Hoplitis* were made in Tsudakhar in the Levashi district (42°19'40"N, 47°09'48"E) in 2018–2022.

Taxonomy

Hoplitis (Hoplitis) astragali Fateryga, Müller & Proshchalykin, sp. nov.

<https://zoobank.org/69FC78C0-D4DA-473E-9538-FFCF4E52C810>

Fig. 1A–H

Type material. *Holotype*. RUSSIA. **Dagestan, Levashi district:** Tsudakhar, 42°19'40"N, 47°09'48"E, 10.6.2019, ♂ (leg. A. Fateryga). Deposited in ZISP.

Paratypes. RUSSIA. **Dagestan, Buynaksky district:** 6 km NW Chirkey, 43°00'10"N, 46°53'51"E, 26–27.5.2022, 1 ♀, 7 ♂ (leg. A. Fateryga), 7 ♀, 2 ♂ (leg. M. Proshchalykin); **Dagestan, Kumtorkalinsky district:** Sarykum sand dune, 43°00'08"N, 47°14'15"E, 28–29.5.2019, 8 ♀, 1 ♂ (leg. M. Proshchalykin, V. Loktionov); *ibid.*, 30.5.2019, 2 ♀ (leg. M. Mokrousov); **Dagestan, Levashi district:** Tsudakhar, 42°19'40"N, 47°09'48"E, 23.6.2018, 1 ♂ (leg. A. Fateryga); *ibid.*, 1.6.2019, 2 ♀ (leg. M. Proshchalykin, V. Loktionov), 5 ♂ (leg. A. Fateryga); *ibid.*, 10–11.6.2019, 12 ♀, 4 ♂ (leg. A. Fateryga); *ibid.*, 16.6.2021, 1 ♂ (leg. A. Fateryga); *ibid.*, 28–29.5.2022, 1 ♀, 2 ♂ (leg. A. Fateryga), 5 ♀, 15 ♂ (leg. M. Proshchalykin); **Dagestan, Laksky district:** vicinity of Turtsi, 42°11'34"N, 47°09'33"E, 22.5.2021, 4 ♀ (leg. A. Fateryga). AZERBAIJAN. **Nakhchivan Autonomous Republic:** Babek, Sirab, 1.6.2020, 1 ♀ (leg. M. Maharramov). TURKMENISTAN: Ashgabat environs, 15.5.1993, 3 ♀, 1 ♂ (leg. M. Halada). Deposited in ZISP, FSCV, ETHZ, and CAFK.

Diagnosis. Among the western Palaearctic *Hoplitis* species of the subgenus *Hoplitis* s. str., the female of *H. astragali* (Fig. 1A) is unequivocally characterised by the following combination of characters: i) apical margin of sternum 6 without submarginal carina; ii) tibial spurs of hind leg apically blunt with very short tip oriented at right angles to the longitudinal axis of the spur (Fig. 1G); iii) clypeus medially with impunctate longitudinal zone, which is usually continuous, well delimited, about 2–5× as wide as diameter of adjacent punctures and roughly parallel-sided (Fig. 1C); iv) declivous lateral side of apical part of labrum about as high as length of last antennal article (Fig. 1E); v) marginal zones of terga 1–5 with long, dense and uninterrupted band of cream-coloured hairs, which turn to white in worn specimens. The male of *H. astragali* (Fig. 1B) is easily diagnosed by the following combination of characters: i) apical margin of tergum 7 medially truncate to slightly rounded (Fig. 1H); ii) gonoforceps apically with finger-like projection directed inwards at right angles to its longitudinal axis (Fig. 1H); iii) sterna (2)3–4 medially with inconspicuous, very narrow and little raised longitudinal keel; iv) antennal articles 4–13 longer than wide and ventrally weakly keeled (Fig. 1D); v) marginal zone of sterna 2–4 with rather dense white hair band (Fig. 1F); vi) lobes of bilobed membranous appendage at apical margin of sternum 6 roughly quadrangular in shape and separated from each other by narrow longitudinal zone beset with reddish-brown spines (Fig. 1F).

Assignment to species group. The *Hoplitis monstrabilis* species group of *Hoplitis* (*Hoplitis*) includes several species that are morphologically and biologically intermediate between the members of the *H. adunca* species group and the *H. annulata* species

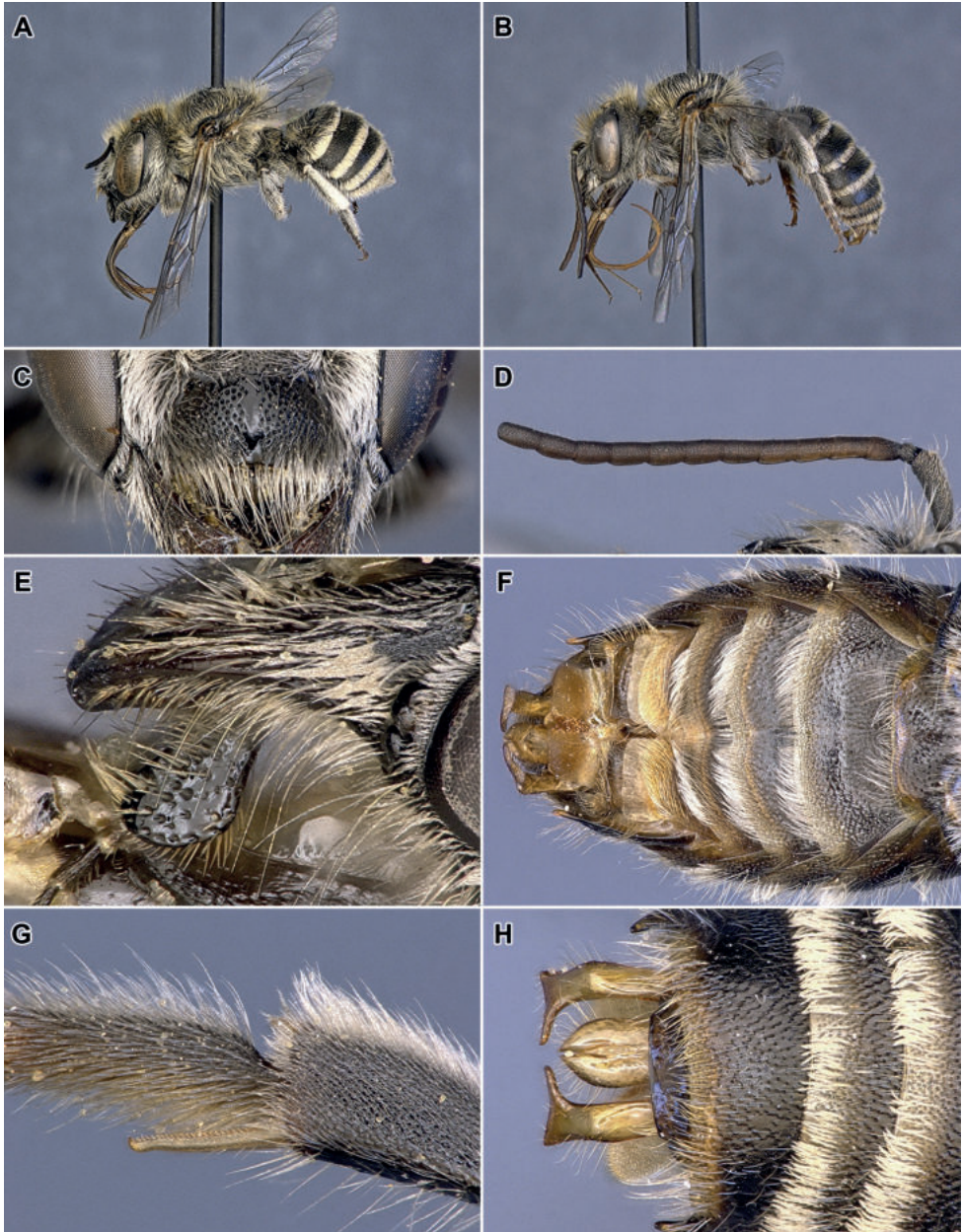


Figure 1. *Hoplitis astragali* sp. nov. **A, C, E, G** female **B, D, F, H** male **A, B** habitus in lateral view **C** clypeus in front view **D** antenna in front view **E** mandible and labrum in lateral view **F** sterna 1–6 in ventral view **G** part of hind leg with inner tibial spur **H** terga 4–7 and genitalia in dorsal view.

group (Sedivy et al. 2012b, 2013; Müller 2023). The representatives of the *H. monstrabilis* species group differ from those of the *H. adunca* species group by the absence of a submarginal carina on female sternum 6 and their habit of nesting in self-excavated

burrows in the ground rather than in pre-existing cavities or stone irregularities above ground. They differ from the *H. annulata* species group by the shape of male tergum 7, which is apically truncate to rounded rather than bidentate. In accordance with these differences, *H. astragali* is assigned here to the *H. monstrabilis* species group.

Description. Due to the uniform morphology of the numerous species of *Hoplitis* (*Hoplitis*), the following description is restricted to characters, which are relevant for the recognition of the new species.

Female. Body length 7–9 mm. **Head:** Head 0.85–0.9× as long as wide. Distance between lateral ocellus and preoccipital margin 2.3–2.4× as long as ocellar diameter. Second segment of labial palpus 1.6–1.7× as long as first segment and 0.8–0.9× as long as compound eye. Proboscis reaching coxa of fore leg when folded. Mandible three-toothed, its preapical zone reddish. Clypeus densely punctate except for median impunctate longitudinal zone, which is usually continuous, well delimited, maximally 4–5× as wide as diameter of adjacent punctures and roughly parallel-sided (Fig. 1C). Apical margin of clypeus medially straight to very shallowly emarginate and weakly crenulate. Yellowish-white pilosity at apical margin of clypeus long, its longest hairs almost as long as maximal length of clypeus (Fig. 1C). Punctuation of supraclypeal area and frons very dense and finer than that of clypeus. Labrum basally impunctate, its lateral sides apically strongly declivous (Fig. 1E) and about as high as length of last antennal article. Antennal article 3 about 1.5× as long as apically wide and 1.4–1.6× as long as article 4. Anterior side of antennal articles (4)5–10(11) partly reddish-brown. **Mesosoma:** Tegula predominantly yellowish-red. Scutum and scutellum densely punctured with interspaces not reaching the diameter of one puncture except medially and laterally, where interspaces may exceed the diameter of one puncture. Basal area of propodeum shagreened except for more or less extended polished zone along lower lateral borders. Posterior surface of propodeum polished with scattered punctures. Propodeal pit polished. Tibial spur of fore leg elongated into tip, which is slightly longer than basally wide and connected to more basal part of spur by straight to weakly concave margin. Tibial spurs of hind leg yellowish, almost parallel-sided and apically blunt with very short tip oriented at right angles to longitudinal axis of spur; inner spur slightly longer than outer spur and roughly 10× as long as maximally wide (Fig. 1G). **Metasoma:** Punctuation of tergal discs dense with interspaces reaching the diameter of one to two punctures. Marginal zone of terga 1–5 reddish to yellowish and covered with long, dense and uninterrupted band of cream-coloured hairs (Fig. 1A), which are medially slightly longer than last antennal article. When seen from behind, longest erect hairs on median half of tergum 1 more than half to almost as long as maximal length of lateral hair tuft. Declivous lateral part of tergum 1 and marginal zone of sterna 2–5 yellowish. Apical margin of sternum 6 without submarginal carina. Scopa white.

Male. Body length 7.5–10 mm. **Head:** Head 0.84–0.87× as long as wide. Distance between lateral ocellus and preoccipital margin 1.7–2× as long as ocellar diameter. Second segment of labial palpus 1.6–1.7× as long as first segment and 0.8–0.9× as long as compound eye. Proboscis reaching coxa of fore leg when folded. Mandible two-toothed, its preapical zone black to more or less reddish. Clypeus rather strongly

convex in profile, its punctation dense except sometimes for its median part, where interspaces between punctures may be larger forming a small polished area or a non-continuous midline. Apical margin of clypeus medially straight to very shallowly emarginate and weakly crenulate. Antennal article 3 about 1.3× as long as apically wide and articles 4–13 1.5–2× as long as wide. Ventral side of antennal articles 4–13 with weakly delimited and rounded longitudinal keel. Ventral and anterior side of antennal articles 3–13 more or less light brown to yellowish-brown (Fig. 1D). **Mesosoma:** Tegula predominantly yellowish-red. Scutum and scutellum densely punctured with interspaces hardly reaching the diameter of one puncture except medially and laterally, where interspaces may exceed the diameter of one puncture. Basal area of propodeum shagreened except for more or less extended polished zone along lower lateral borders. Posterior surface of propodeum polished with scattered punctures. Propodeal pit polished. Tibial spur of fore leg elongated into tip, which is about as long as basally wide and connected to more basal part of spur by straight to weakly concave margin. Tibial spurs of hind leg yellowish and almost parallel-sided except for apex, which is slightly curved. **Metasoma:** Punctuation of tergal discs rather dense with interspaces reaching the diameter of two to three, rarely more punctures. Marginal zone of terga 1–5 reddish to yellowish and covered with long, dense and usually uninterrupted whitish hair band (Fig. 1B). Tergum 6 laterally toothed, its marginal zone yellowish and ciliated with yellowish hairs. Apical margin of tergum 7 medially truncate to slightly rounded (Fig. 1H). Declivous lateral part of tergum 1 and marginal zone of sterna (1)2–5 yellowish. Apical margin of sternum 1 straight, of 2–4 medially shallowly emarginate and of 5 distinctly emarginate (Fig. 1F). Marginal zone of sterna 2–4 with rather dense white hair band (Fig. 1F). Sterna (2)3–4 medially with inconspicuous, very narrow and little raised longitudinal keel. Sternum 5 medially with very narrow longitudinal row of yellowish hairs directed backwards. Sternum 6 basally with pair of membranous flaps. Lobes of bilobed membranous appendage at apical margin of sternum 6 roughly quadrangular in shape (Fig. 1F) and separated from each other by narrow longitudinal zone beset with reddish-brown spines. Gonoforceps slightly wider than penis valve and apically with finger-like projection, which is directed inwards at right angles to its longitudinal axis and about 3× as long as maximally wide (Fig. 1H).

Distribution. Mountainous Dagestan in Russia (from 75 to 1350 m a.s.l.), Nakhchivan Autonomous Republic of Azerbaijan, and southernmost Turkmenistan.

Etymology. The species epithet refers to the flowers of *Astragalus* L. (Fabaceae) exploited by the species for pollen and nectar (see below).

***Hoplitis (Hoplitis) dagestanica* Fateryga, Müller & Proshchalykin, sp. nov.**

<https://zoobank.org/33893507-BAC4-4602-9B50-EFB4869722AF>

Fig. 2A–H

Type material. Holotype. RUSSIA, Dagestan, Levashi district: Tsudakhar, 42°19'40"N, 47°09'48"E, 11.6.2019, ♂ (leg. A. Fateryga). Deposited in ZISP.

Paratypes. RUSSIA. **Dagestan, Levashi district:** Tsudakhar, 42°19'40"N, 47°09'48"E, 1.6.2019, 2 ♂ (leg. A. Fateryga), 3 ♂ (leg. M. Proshchalykin, V. Loktionov); *ibid.*, 10.6.2019, 2 ♂ (leg. A. Fateryga); *ibid.*, 28–29.5.2022, 1 ♀, 1 ♂ (leg. A. Fateryga), 2 ♀, 13 ♂ (leg. M. Proshchalykin); **Dagestan, Rutul district:** near Kufa village, 6 km NW Rutul, 41.565178°N, 47.362029°E, 1500 m, 1.7.2018, 1 ♂ (leg. M. Proshchalykin, V. Loktionov, M. Mokrousov). Deposited in ZISP, FSCV, ETHZ, and CAFK.

Diagnosis. Among the western Palaearctic *Hoplitis* species of the subgenus *Hoplitis* s. str., the female of *H. dagestanica* (Fig. 2A) is unequivocally characterised by the following combination of characters: i) sternum 6 lateroapically with distinct submarginal carina and medioapically not elongated into distinct and well delimited tooth of narrowly triangular to linear shape; ii) proboscis not reaching till trochanter of hind leg in repose and second segment of labial palpus distinctly shorter than maximal length of mesosoma measured in lateral view (Fig. 2A); iii) clypeus and galea of proboscis normally haired, without apically curved or wavy pollen-collecting bristles; iv) lateral lobes of pronotum not inflated; v) apex of inner tibial spur of hind leg strongly curved at an angle of 60 to 80 degrees (Fig. 2G); vi) clypeus medially without uninterrupted sharp and narrow longitudinal carina; vii) disc of tergum 5 covered with rather dense and appressed cream-coloured to yellowish-white pilosity (Fig. 2C); viii) when seen from behind, longest erect hairs on median half of tergum 1 only about 1/7 to 1/8 as long as maximal length of lateral hair tuft (Fig. 2E); ix) punctation of lateroapical part of scutum with interspaces reaching the diameter of one puncture; x) metasomal scopa yellowish (Fig. 2A); xi) anterior side of antennal articles (5)6–11 partly dark reddish-brown. The male of *H. dagestanica* (Fig. 2B) is easily diagnosed by the following combination of characters: i) apical margin of tergum 7 medially rounded (Fig. 2H); ii) second segment of labial palpus shorter than compound eye (Fig. 2B); iii) last article of antenna almost twice as long as basally wide and tapering towards apex with ventral margin slightly concave (Fig. 2D, F); iv) posterior side of antenna with roundish bump near distal end of articles (4)5–6 and small pointed tubercle near distal end of articles 7–11(12) (Fig. 2F); iv) ventral margin of antennal articles (4)5–10(11) distally slightly widened (Fig. 2D); v) antennal article 3 1.4–1.5× as long as apically wide and longer than article 4 (Fig. 2D); vi) lateral lobes of bilobed membranous appendage at apical margin of sternum 6 densely haired, distinctly wider than long, laterally elongated into a distinct and more or less acute tip and separated from each other by only a rather shallow median emargination (Fig. 2H); vii) marginal zone of sterna 4–5 reddish and very densely punctured with interspaces much narrower than the diameter of one puncture (Fig. 2H).

Assignment to species group. Due to the presence of a submarginal carina on female sternum 6 and the apically rounded male tergum 7, *H. dagestanica* is clearly a member of the *H. adunca* species group.

Description. Due to the uniform morphology of the numerous species of *Hoplitis* (*Hoplitis*), the following description is restricted to characters, which are relevant for the recognition of the new species.



Figure 2. *Hoplitis dagestanica* sp. nov. **A, C, E, G** female **B, D, F, H** male **A, B** habitus in lateral view **C** terga 4–6 in dorsal view **D** antenna in front view **E** terga 1–2 from behind **F** antenna in top view **G** part of hind leg with inner tibial spur **H** sterna 5–6 and tergum 7 in ventral view.

Female. Body length 7–8 mm. **Head:** Head about 0.95× as long as wide. Distance between lateral ocellus and preoccipital margin about 1.75× as long as ocellar diameter. Second segment of labial palpus about 1.35× as long as first segment and about 0.75× as long as compound eye. Proboscis reaching coxa of fore leg when folded. Mandible three-toothed, its preapical zone weakly reddish. Clypeus densely punctured with interspaces rarely surpassing the diameter of half a puncture and without distinct polished midline. Antennal article 3 almost 2× as long as apically wide and about 2× as

long as article 4. Anterior side of antennal articles (5)6–11 partly dark reddish-brown.

Mesosoma: Tegula yellowish-brown except for black anterior third and black inner margin. Scutum and scutellum densely punctured with interspaces rarely surpassing the diameter of one and a half punctures except lateroapically on scutum and medially on scutum and scutellum, where interspaces may reach the diameter of one puncture. Basal area of propodeum shagreened throughout. Posterior surface of propodeum shagreened with scattered punctures. Propodeal pit polished. Tibial spur of fore leg elongated into tip, which is slightly longer than basally wide and angularly stepped from more basal part of spur. Tibial spurs of hind leg yellowish; inner spur slightly tapering towards apex, which is strongly curved at an angle of 60 to 80 degrees (Fig. 2G); outer spur slightly shorter than inner spur, its apex curved at an angle of about 45 degrees.

Metasoma: Punctuation of tergal discs moderately dense with interspaces reaching the diameter of two to three punctures on discs 1–3 (Fig. 2E). Marginal zone of terga 1–5 covered with uninterrupted band of cream-coloured to yellowish-white hairs (Fig. 2A), which may be interrupted on tergum 1 in worn specimens (Fig. 2E). Tergal discs 1–4 with short erect pilosity of yellowish hairs, which are shorter than antennal article 2. When seen from behind, longest erect hairs on median half of tergum 1 only about 1/7 to 1/8 as long as maximal length of lateral hair tuft (Fig. 2E). Disc of terga 5–6 covered with rather dense and appressed cream-coloured to yellowish-white pilosity. Sternum 6 lateroapically with distinct submarginal carina and medioapically without well delimited tooth (Fig. 2C). Scopa yellowish.

Male. Body length 7.5–9.5 mm. **Head:** Head about 0.85× as long as wide. Distance between lateral ocellus and preoccipital margin about 1.75× as long as ocellar diameter. Second segment of labial palpus about 1.35× as long as first segment and 0.75× as long as compound eye. Proboscis reaching coxa of fore leg when folded. Mandible two-toothed and predominantly black, sometimes with dark reddish-brown preapical zone. Clypeus rather strongly convex in profile, its punctuation very fine and dense without polished interspaces. Apical margin of clypeus medially straight and crenulate. Antennal article 1 about 2× as long as maximally wide (Fig. 2D). Antennal article 3 1.4–1.5× as long as apically wide and almost 1.5× as long as article 4 (Fig. 2D). Posterior side of antenna with roundish bump near distal end of articles (4)5–6 and small pointed tubercle near distal end of articles 7–11(12) (Fig. 2F). Ventral margin of antennal articles (4)5–10(11) distally slightly widened (Fig. 2D). Last article of antenna almost twice as long as basally wide and tapering towards apex with ventral margin slightly concave (Fig. 2D). Antenna predominantly yellowish-red; black to dark brown are articles 1, 2, base of 3, apex of 13, and sometimes dorsal side of articles 3–7 (Fig. 2F).

Mesosoma: Tegula predominantly yellowish-red. Scutum and scutellum densely punctured with interspaces hardly surpassing the diameter of one puncture. Basal area of propodeum shagreened throughout. Posterior surface of propodeum shagreened with scattered punctures. Propodeal pit polished. Tibial spur of fore leg elongated into tip, which is slightly longer than basally wide and angularly stepped from more basal part of spur. Tibial spur of hind legs yellowish, tapering towards apex and apically curved.

Metasoma: Punctuation of tergal discs moderately dense with interspaces reaching the

diameter of three to four punctures on discs 1–4. Marginal zone of terga 1–5 covered with uninterrupted band of yellowish-white hairs (Fig. 2B). Tergum 6 laterally toothed, its marginal zone reddish, ciliated with yellowish hairs, apically crenulate and medially usually slightly emarginate. Apical margin of tergum 7 medially rounded (Fig. 2H). Marginal zone of sterna 2–5 reddish and very densely punctured with interspaces much narrower than the diameter of one puncture. Apical margin of sterna 1–4 almost straight and of 5 weakly rounded and medially shallowly emarginate. Marginal zone of sterna 2–4 with loose whitish hair band. Sterna 2–5 with preapical transverse swelling, which is sparsely punctured and medioapically emarginate on sterna 3–5. Sternum 6 basally with pair of membranous flaps (Fig. 2H). Lobes of bilobed membranous appendage at apical margin of sternum 6 densely haired, distinctly wider than long, laterally elongated into a distinct and more or less acute tip and separated from each other by only a rather shallow median emargination (Fig. 2H). Gonoforceps very narrow, slightly bent inwards and downwards in its apical third and apically with dense and short tuft of white hairs. Outer margin of penis valve ciliated with white bristles, of which the longest are slightly longer than the maximal valve width.

Distribution. Mountain Dagestan in Russia (from 1120 to 1450 m a.s.l.).

Etymology. The species epithet refers to the occurrence of the species in Dagestan.

Nesting biology

Six nests of *Hoplitis astragali* were studied 6 km northwest of Chirkey at a clay cliff along a dry riverbed (Fig. 3A). All six nests were burrows in the ground. Two nests were located on strongly inclined surface (Fig. 4A), while four nests were located on almost horizontal surface at the entrance of old burrows of *Xylocopa olivieri* Lepeletier, 1841 (Hymenoptera: Apidae) (Fig. 4B). Thus, the main shaft of the former two nests was sub-horizontal (Fig. 4C), while it was sub-vertical in the latter four nests (Fig. 4E,

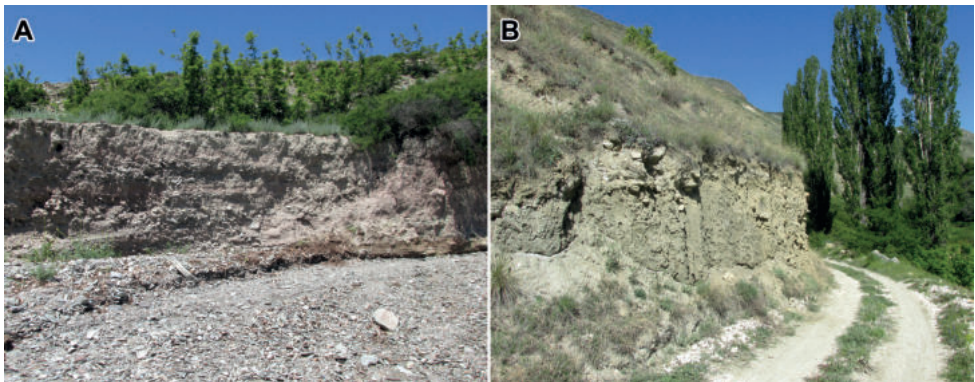


Figure 3. Habitats of the two new species of the genus *Hoplitis* Klug, 1807 in Dagestan **A** clay cliff along dry riverbed 6 km northwest of Chirkey, a nesting site of *H. astragali* sp. nov. **B** clay cliff along unpaved road in Tsudakhar, the type locality of both *H. astragali* and *H. dagestanica* sp. nov.

F). The excavation process was not observed, but it was evident from the following observation that the burrows were self-excavated by the females: two closing plugs were observed on 31 May (Fig. 4D) at the same old *X. olivieri* nest entrance, where there was just one burrow on 27 May (Fig. 4B). Thus, the second burrow was excavated by the female bee, since there was no pre-existing hole available to her. It is noteworthy that the nest entrances were not always circular but sometimes of irregular shape (Fig. 4B).

The nests were composed of one to three brood cells, an empty vestibule, and the closing plug. Of the six nests studied, two had one cell, three were two-celled, and one was three-celled (median two cells per nest). The lengths of the nest burrows were 16–32 mm (median 26 mm). The cells in two- and three-celled nests were linearly arranged in a straight burrow ($n = 3$, Fig. 4F) or lay in an angled burrow with the longitudinal axis of the brood cells diverging at nearly right angles ($n = 1$, Fig. 4E). When measured on the inside, the cells were 6.5–9.5 mm long (median 8.0 mm) and maximally 5.5–7 mm wide (median 6.0 mm). The inner surface of the cells was smooth, dull and not covered with any substance other than mud. Although the cell construction process was not observed, the presence of an about 0.4 mm thin and more or less distinct inner cell wall (Fig. 4C, F) suggests that the female covered the inner surface of the cell with an extra layer of mud. As this extra layer was of the same colour as the surrounding substrate, the material for its construction was probably taken from inside the nest. The material used for the construction of the cell plug was apparently also taken from inside the nest as suggested by the irregular shape of the vestibule, indicating that soil material had been harvested from its walls (Fig. 4C, E, F). In contrast, the closing plug was made from soil taken from outside the nest as evidenced by the plug colour, which usually differed from the surrounding substrate (Fig. 4D). One female was observed to harvest dry clay from the cliff surface at a distance of about 0.5 m from the nest, mixed this material with regurgitated liquid, and transported the moistened mud to the nest entrance to build the sealing plug (Fig. A). The space in front of the outermost brood cell was not filled with soil resulting in an empty vestibule of 5–14 mm in length (median 7.0 mm).

The freshly sealed nest contained a single brood cell with an egg and a pollen loaf (Fig. 4C). The pollen loaf was of orange colour and spherical shape, taking about half of the inner volume of the cell. It was very liquid and probably kept its shape due to surface tension and a significant amount of pollen covering it as suggested by the fact that it immediately lost its shape during an attempt to extract it from the cell. The egg was deposited on the top of the pollen loaf and directed with its free end towards the cell plug; its size was about 2.7×0.8 mm. Other cells, dissected in autumn, contained prepupae hibernating in their self-spun cocoons (Fig. 4E, F). The cocoon consisted of a single thin layer; it was whitish and had a slightly shining inner surface. There was no distinct area for air-exchange as known for many other osmiine bees with more complex cocoon structure (Rozen and Praz 2016). Instead, the cocoon of *H. astragali* uniformly covered the whole inner surface of the cell including the inner side of the cell plug. The larval feces were deposited between the cell wall and the cocoon, where they were spread uniformly and sparsely. The prepupae were of deep yellow colour. There

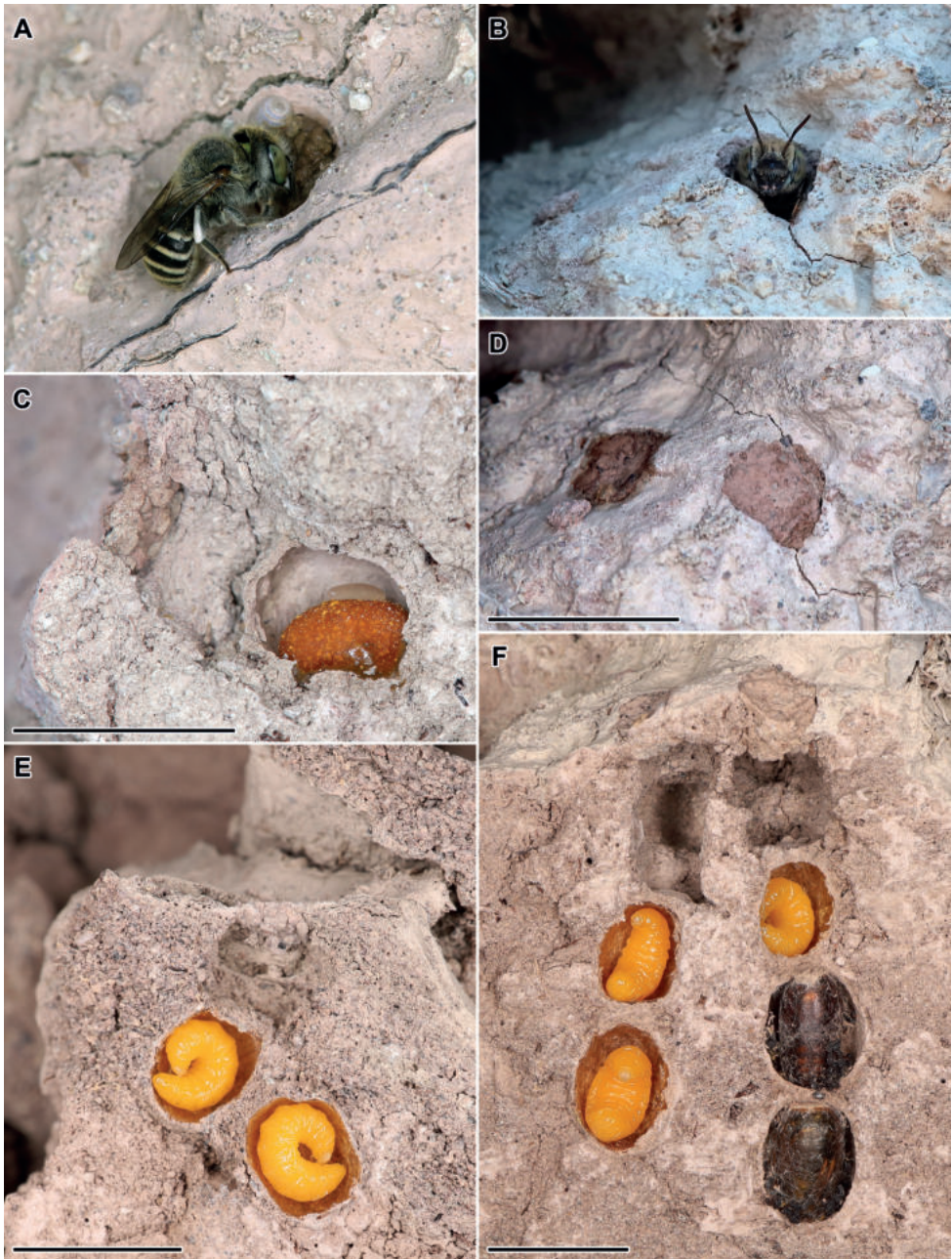


Figure 4. Nesting biology of *Hoplitis astragali* sp. nov. **A** female closing her nest with a plug of mud **B** female inside her nest burrow **C** freshly sealed one-celled nest in lateral view showing a cell with pollen loaf and egg **D** closing plugs of two nests (the right one the same as shown in **B**) **E** two-celled nest in lateral view with hibernating prepupae **F** two nests (the same as in **D**) in lateral view with hibernating prepupae and cocoons of *Sapyga caucasica* Radoszkowski, 1880. Scale bars: 1 cm.

was a single generation, i.e., the progeny of the females nesting in May hibernated. Six prepupae were obtained in 2022 and observed. Two females and two males emerged in 2023, while two prepupae remained alive but did not pupate; they obviously continued hibernation for a second winter.

Cocoons of the kleptoparasitic wasp *Sapyga caucasica* Radoszkowski, 1880 (Hymenoptera: Sapygidae) (Fig. 4F) were found in three of the 11 cells (27%). This wasp hibernates as an imago allowing for its immediate identification to the species level. Several individuals of *S. caucasica* were also observed in May inspecting the surface of the clay cliff where *H. astragali* was nesting.

Flower associations

In Tsudakhar, both new species were observed in the vicinity of a clay cliff along an unpaved road (Fig. 3B). Here, flower-visiting imagines were exclusively recorded on flowers of *Astragalus* (Fabaceae). Two species of this genus were abundant and in flower during the observation period: *Astragalus haesitabundus* Lipsky and *A. onobrychioides* M. Bieb. Females and males of *Hoplitis astragali* as well as a single male of *H. dagestanica* were observed only on the flowers of the former species, whereas no visits to the flowers of the latter species were recorded. In the vicinity of Chirkey *A. haesitabundus* was also abundant and in flower, but here most females and males of *H. astragali* visited the flowers of another *Astragalus* species, *A. bungeanus* Boiss.

Discussion

Hoplitis astragali is the sixth described species of the *H. monstrabilis* species group, while *H. dagestanica* is the 51st described species of the *H. adunca* species group (Müller 2023). Among the members of the *H. monstrabilis* species group, nests were already known for *H. monstrabilis* Tkalců, 2000 and *H. tenuiserrata* (Benoist, 1950) (Rozen et al. 2009; Sedivy et al. 2013; Le Goff 2017). The present contribution supplements those data with the information on the nests of *H. astragali*. All three species excavate their nests in the ground. The nests of *H. monstrabilis* and *H. tenuiserrata*, however, were recorded in horizontal ground and their burrows were sub-vertical. *Hoplitis astragali* nested in vertical cliffs but most of its nests had sub-vertical burrows due to their location at the entrance of horizontal old burrows of *Xylocopa olivieri*. The nests of *H. astragali* have a vestibule, i.e., the burrow between the last brood cell and the sealing plug is not filled with soil. Whether such an empty vestibule is also present in the nests of other members of the *H. monstrabilis* species group is unknown, since all discovered nests of *H. monstrabilis* (n = 2) and *H. tenuiserrata* (n = 1) were incomplete (Rozen et al. 2009; Le Goff 2017). As in *H. astragali*, the cells of *H. monstrabilis* and *H. tenuiserrata* were also found to have a thin wall of compact soil covering the inner cell surface. In the latter two species, it was not clear whether this wall was applied by the female or whether it merely resulted from the smoothing of the inner surface of the

newly excavated cell (Rozen et al. 2009; Le Goff in Müller 2023). Our observations on *H. astragali* suggest that *H. monstrabilis* and *H. tenuiserrata* also cover the inner surface of the cell with an extra layer of mud. Lining the brood cells with an extra layer of mud is also known from members of the *Hoplitis adunca* species group, such as *H. adunca* (Panzer, 1798) and *H. manicata* (Morice, 1901) (Müller 2023 and references therein).

Trophic relationships of *H. astragali* appear to be typical of the *H. monstrabilis* species group. Both *H. monstrabilis* and *H. tenuiserrata* are oligolectic on Fabaceae (Rozen et al. 2009; Sedivy et al. 2012b; Müller 2023). We observed *H. astragali* exclusively visiting flowers of two species of *Astragalus* (Fabaceae), which might indicate narrow oligolecty on a single plant genus (Müller and Kuhlmann 2008). However, more flower visiting data including microscopical analysis of pollen contained in the female scopae are needed to clarify the species' degree of host plant specialization. One male of *H. dagestanica* was also observed on flowers of *Astragalus*. However, as this was the only flower visiting record for this species, any assumption on its pollen host preference is premature, although many members of the *H. adunca* species group exclusively or predominantly exploit Fabaceae for pollen (Müller 2016, 2023; Sedivy et al. 2012b).

Acknowledgements

Mikhail Mokrousov (Nizhny Novgorod, Russia) kindly identified the species of *Sapyga* from the nests of *Hoplitis astragali*. Max Kasperek (Heidelberg, Germany) and one anonymous reviewer carefully reviewed the manuscript and provided helpful suggestions to improve it. John Neff kindly improved our English.

The research was carried out within the state assignments of the Ministry of Science and Higher Education of the Russian Federation, No. 121032300023-7 (for A.F.) and No. 121031000151-3 (for M.P.).

References

- Fateryga AV (2017) New data on megachilid bees (Hymenoptera: Megachilidae) of the European part of Russia. *Proceedings of the Russian Entomological Society* 88(2): 86–90. https://doi.org/10.47640/1605-7678_2017_88_2_86
- Fateryga AV, Proshchalykin MYu (2020) New records of megachilid bees (Hymenoptera: Megachilidae) from the North Caucasus and the South of European Russia. *Caucasian Entomological Bulletin* 16(2): 225–231. <https://doi.org/10.23885/181433262020162-225331>
- Fateryga AV, Proshchalykin MYu, Astafurova YuV, Popov IB (2019 [“2018”]) New records of megachilid bees (Hymenoptera, Megachilidae) from the North Caucasus and neighboring regions of Russia. *Entomological Review* 98(9): 1165–1174. <https://doi.org/10.1134/S0013873818090026>
- Le Goff G (2017 [“2016”]) Note sur la nidification dans le sol de deux *Hoplitis* du Maroc: *Hoplitis* (*Anthocopa*) *zaianorum* Benoist 1927 et *Hoplitis* (*Hoplitis*) *tenuiserrata* Benoist

- 1950 (Apoidea – Megachilidae – Osmiini). *Osmia* 6: 9–11. <https://doi.org/10.47446/OSMIA6.3>
- Litman JR, Fateryga AV, Griswold TL, Aubert M, Proshchalykin MYu, Le Divelec R, Burrows S, Praz CJ (2021) Paraphyly and low levels of genetic divergence in morphologically distinct taxa: revision of the *Pseudoanthidium scapulare* (Latreille, 1809) complex of carder bees (Apoidea, Megachilidae, Anthidiini). *Zoological Journal of the Linnean Society* 195(4): 1287–1337. <https://doi.org/10.1093/zoolinnean/zlab062>
- Michener CD (2007) *The Bees of the World* (2nd edn.). Johns Hopkins University Press, Baltimore, [xvi +] 953 pp. [+ 20 pls]
- Morawitz F (1873 [“1874”]) *Die Bienen Daghestans*. *Horae Societatis Entomologicae Rossicae* 10(2–4): 129–189.
- Müller A (2016) *Hoplitis (Hoplitis) galichicae* spec. nov., a new osmiine bee species from Macedonia with key to the European representatives of the *Hoplitis adunca* species group (Megachilidae, Osmiini). *Zootaxa* 4111(2): 167–176. <https://doi.org/10.11646/zootaxa.4111.2.5>
- Müller A (2023) Palaeartic Osmiine Bees, ETH Zürich. <http://blogs.ethz.ch/osmiini> [Accessed 12 July 2023]
- Müller A, Kuhlmann M (2008) Pollen hosts of western palaeartic bees of the genus *Colletes* (Hymenoptera: Colletidae): the Asteraceae paradox. *Biological Journal of the Linnean Society* 95(4): 719–733. <https://doi.org/10.1111/j.1095-8312.2008.01113.x>
- Praz CJ, Müller A, Danforth BN, Griswold TL, Widmer A, Dorn S (2008) Phylogeny and biogeography of bees of the tribe Osmiini (Hymenoptera: Megachilidae). *Molecular Phylogenetics and Evolution* 49(1): 185–197. <https://doi.org/10.1016/j.ympev.2008.07.005>
- Rozen Jr JG, Özbek H, Ascher JS, Rightmyer MG (2009) Biology of the bee *Hoplitis (Hoplitis) monstrabilis* Tkalcü and descriptions of its egg and larva (Megachilidae: Megachilinae: Osmiini). *American Museum Novitates* 3645: 1–12. <https://doi.org/10.1206/646.1>
- Rozen Jr JG, Praz CJ (2016) Mature larvae and nesting biologies of bees currently assigned to the Osmiini (Apoidea: Megachilidae). *American Museum Novitates* 3864: 1–46. <https://doi.org/10.1206/3864.1>
- Sedivy C, Dorn S, Müller A (2012a) Molecular phylogeny of the bee genus *Hoplitis* (Megachilidae: Osmiini) – how does nesting biology affect biogeography? *Zoological Journal of the Linnean Society* 167(1): 28–42. <https://doi.org/10.1111/j.1096-3642.2012.00876.x>
- Sedivy C, Dorn S, Müller A (2013) Evolution of nesting behaviour and kleptoparasitism in a selected group of osmiine bees (Hymenoptera: Megachilidae). *Biological Journal of the Linnean Society* 108(2): 349–360. <https://doi.org/10.1111/j.1095-8312.2012.02024.x>
- Sedivy C, Dorn S, Widmer A, Müller A (2012b) Host range evolution in a selected group of osmiine bees (Hymenoptera: Megachilidae): the Boraginaceae-Fabaceae paradox. *Biological Journal of the Linnean Society* 108(1): 35–54. <https://doi.org/10.1111/j.1095-8312.2012.02013.x>
- Ungricht S, Müller A, Dorn S (2008) A taxonomic catalogue of the Palaeartic bees of the tribe Osmiini (Hymenoptera: Apoidea: Megachilidae). *Zootaxa* 1865: 1–253. <https://doi.org/10.11646/zootaxa.1865.1.1>

A new compression fossil, *Eotriadomeroides abjunctus* Huber, gen. & sp. nov. (Hymenoptera, Mymaridae), in Eocene shale from the Kishenehn Formation, USA

John T. Huber¹, Dale E. Greenwalt²

1 Natural Resources Canada c/o Canadian National Collection of Insects, Arachnids and Nematodes, K.W. Neatby Building, 960 Carling Ave., Ottawa, ON, K1A 0C6, Canada **2** Department of Paleobiology, National Museum of Natural History, MRC 121, Smithsonian Institution, 10th & Constitution Ave. NW, Washington, D.C., 20013-7012, USA

Corresponding author: John T. Huber (john.huber2@agr.gc.ca)

Academic editor: Petr Janšta | Received 1 June 2023 | Accepted 31 July 2023 | Published 15 August 2023

<https://zoobank.org/D3EF3F05-9185-41B9-A524-1CAC7B9C2D6B>

Citation: Huber JT, Greenwalt DE (2023) A new compression fossil, *Eotriadomeroides abjunctus* Huber, gen. & sp. nov. (Hymenoptera, Mymaridae), in Eocene shale from the Kishenehn Formation, USA. Journal of Hymenoptera Research 96: 657–666. <https://doi.org/10.3897/jhr.96.107379>

Abstract

A new fossil genus and species of fairyfly, *Eotriadomeroides abjunctus* Huber & Greenwalt, **gen. and sp. nov.** (Hymenoptera: Chalcidoidea: Mymaridae), is described and illustrated from a female preserved as a compression fossil in middle Eocene shale from the Kishenehn Formation, Montana, USA. It is compared to extant species of *Neotriadomerus* Huber, known only from Australia, and *Triadomerus* Yoshimoto, a Cretaceous amber fossil from Canada. It is suggested that these three genera, classified together in Triadomerini, likely the most ancestral lineage of Mymaridae, are evidence of the Middle or perhaps Late Jurassic origin of the family.

Keywords

Chalcidoidea, Eocene compression fossil, Mymaridae

Introduction

Parasitoid wasps of the family Mymaridae (Hymenoptera), almost all parasitic in eggs of other insects, are common and widespread, occurring on all continents except Antarctica, from 81°49'N (Hazen Camp, Canada) to 54°57'S (Bahía Aguirre, Tierra del Fuego, Argentina). They also occur on most islands, even those farthest

from continents, e.g., the Hawaiian Islands, St. Helena, and French Polynesia, or those with harsh climates, e.g., Greenland, Iceland, Auckland Islands, Campbell Island and South Georgia; the latter three more than 50°S. Mymaridae are also one of the two best represented families of Chalcidoidea in the fossil record (the other is Baeomorphiidae), represented almost entirely by inclusions in amber (Yoshimoto 1975; Poinar and Huber 2011; Engel et al. 2013). Very few Mymaridae are described from compression fossils (Huber and Greenwalt 2011). The fossil records for the family are from the Cretaceous to the Pleistocene, a duration of at least 100 my, though with a large time gap of about 40 my between the Cretaceous and Tertiary fossils records. A compression fossil specimen from the Kishenehn Formation in Montana, USA, representing a new genus and species, is described here.

Methods

Huber and Greenwalt (2011) described the methods of collecting and photographing insect compression fossils from the Kishenehn Formation. The fossil described below was collected in accordance with the United States Forest Service Special Use Permit HUN465. Greenwalt et al. (2015) described the taphonomy of the Kishenehn Formation.

Measurements, in millimeters, were taken from the photographs as accurately as possible and converted into micrometers (μm). Given that the end points of a structure were not always clear, their measurements were rounded to the nearest 5 μm and should be treated as approximate only. Length/width ratios of the antennal segments were calculated from the millimeter measurements, not from the rounded-off micrometer measurements.

Abbreviations used

fu = funicle segment, **mps** = multiporous plate sensilla. The specimen is deposited in:

NMNH Department of Paleobiology, National Museum of Natural History, Washington, DC, USA.

Results

Eotriadomeroides Huber, gen. nov.

<https://zoobank.org/3A127582-2F52-40DF-BDA3-ECDB8FBA27A3>

Figs 1–8

Type species. *Eotriadomeroides abjunctus* Huber, here designated.

Diagnosis. Female. Antenna with funicle 8-segmented and clava 1-segmented (Figs 2–5); fore wing with venation extending almost to wing apex, with postmarginal

vein as wide as marginal vein or parastigma and $\sim 2.7\times$ as long as parastigma + marginal + stigmal veins (Fig. 7); tarsi 5-segmented (Fig. 8); fore wing microtrichia apparently extending to base of parastigma; hind wing relatively narrow, with acute apex; ovipositor extending ventral to mesosoma almost to level of head and not exerted posterior to apex of gaster (Fig. 1). Other details are apparently the same as for *Neotriadomerus* Huber, morphologically the genus most similar to *Eotriadomeroides*.

Male. Unknown.

Derivation of genus name. From the Greek, *eos*, meaning early + *Triadomerus* (a compound word derived from Greek, *tries*, meaning three, and *meros*, meaning part, referring to the 3-segmented clava) + the suffix *-oides*, meaning like, resembling. *Eotriadomeroides* (gender masculine) is therefore an “early *Triadomerus*-like” genus, referring to its geological age (the Eocene) and morphological similarity to the two other, evidently related genera: *Neotriadomerus* (with all its species extant) and *Triadomerus* (with its single species extinct).

Relationships. Genera of Mymaridae are usually divided formally into subgenera if females of different species within a given genus have either a 1- or 2-segmented clava, or either a 2- or 3-segmented clava, and the other morphological features are essentially identical. So far, no genus is known to have its included species with either a 1-segmented or a 3-segmented clava but none with a 2-segmented clava. Only one genus (*Anaphes* Haliday) possibly has its included species with a 1-, 2-, or 3-segmented clava but so far *Anaphes* species with 3-segmented clava have yet been described and named. Examination of the clava of *Eotriadomeroides* does not suggest it is 2- or 3-segmented but rather that it is clearly 1-segmented, i.e., entire (Fig. 5). For comparison, the species of *Eoanaphes* Huber and *Eoestochus* Huber from the same formation and apparently with the same quality of preservation, are clearly 3-segmented whereas those of *Gonatocerus* Nees are just as clearly 1-segmented (Huber and Greenwalt 2011). If the clava of *E. abjunctus* were 2- or 3-segmented then it could be classified as a subgenus of *Neotriadomerus*, given that all other features, except relative lengths of postmarginal vein to the rest of the venation, are almost the same in both taxa. *Eotriadomeroides* would then key to *Neotriadomerus* in the key to Cretaceous genera of Mymaridae (Poinar and Huber 2011). Another possibility would be to treat *E. abjunctus* as a subgenus within *Triadomerus* Yoshimoto, described from amber from Cedar Lake, Manitoba (Yoshimoto 1975), which is only about 1000 km away from the type locality (the Kishenehn Basin, Montana) of *E. abjunctus*. According to McAlpine and Martin (1969) the actual source of the Cedar Lake amber is more likely to be upstream, along the Saskatoon River either near Saskatoon, Saskatchewan, or Medicine Hat, Alberta, respectively about 650 km and ~ 280 km from the type locality of *E. abjunctus* as determined from the present day configuration of the localities (essentially unchanged from 46 my years ago). *Triadomerus* does not have the ovipositor extending anteriorly ventral to the mesosoma and it has a relatively short postmarginal vein compared to length of stigma + marginal + parastigmal veins, so we treat *E. abjunctus* as belonging to a new genus, different from both *Neotriadomerus* and *Triadomerus*, both of which have a 3-segmented female clava and are known, respectively, from seven extant and one extinct species. *Eotriadomeroides* is best classified in *Triadomerini* (Huber 2017) but exact relationships among the genera still need resolution.

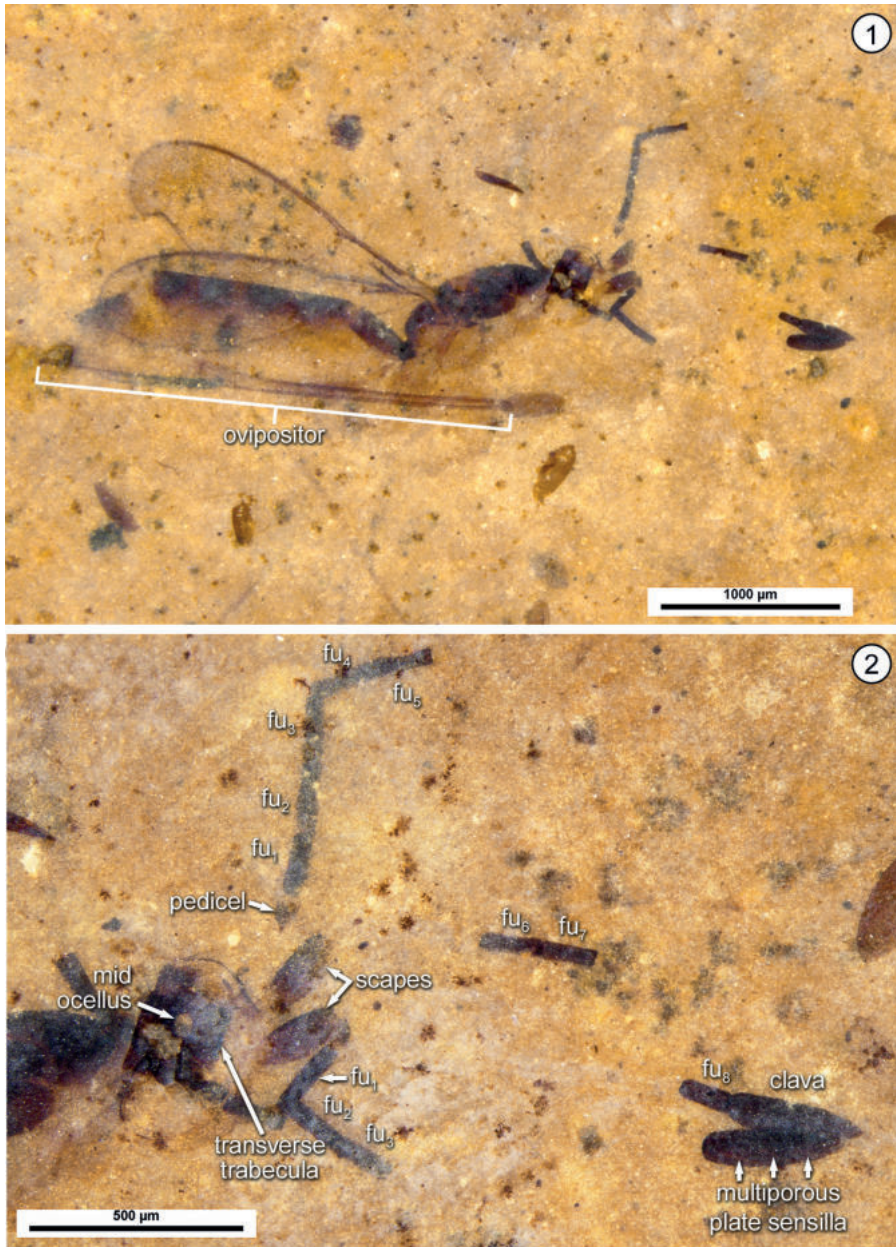
***Eotriadomeroides abjunctus* Huber, sp. nov.**<https://zoobank.org/F0BF8666-43A7-4DFA-A7F9-5ED916490407>

Figs 1–8

Material examined. *Holotype* female (NMNH), on 18 × 14 × 0.15 cm piece of oil shale (Fig. 9), labelled “Holotype *Eotriadomeroides abjunctus* Huber. USNM # PAL 620738”. The circle/square scratched onto the surface of the shale indicates the holotype location. The specimen was collected in 2012 at locality #43946, Park site, Kishenehn Formation, Montana, USA.

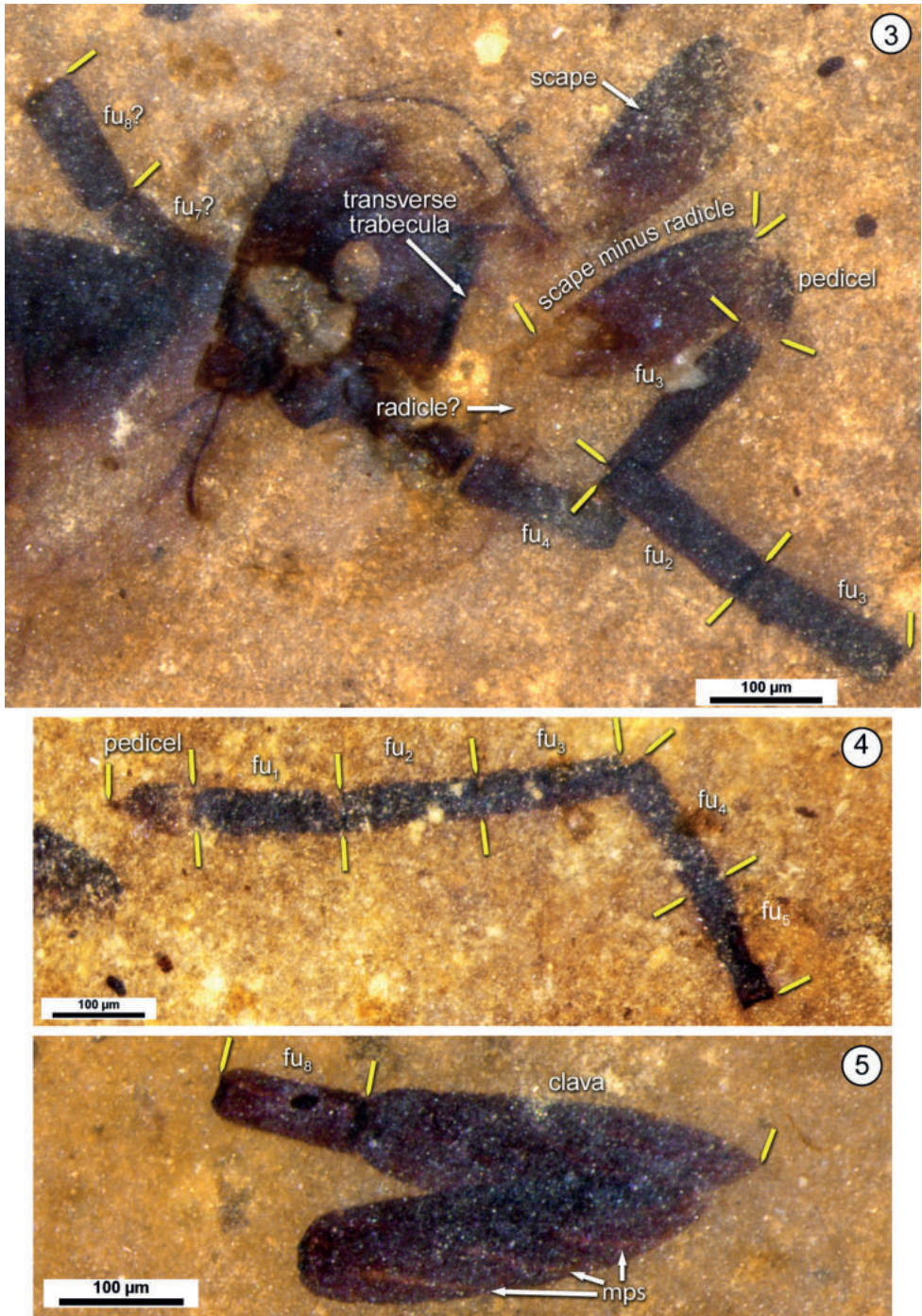
Diagnosis. *Eotriadomeroides abjunctus* is the only described species in the genus. Its diagnosis is therefore the same as for the generic description. Comparing it with species of morphologically similar genera, it differs from all the described species of *Neotriadomerus* (Huber 2017) as follows: clava 1-segmented (clava 3-segmented in *Neotriadomerus* species); postmarginal vein ~2.7× as long as parastigma + marginal vein + stigmal veins (postmarginal vein at most 0.90× as long in *Neotriadomerus* species); hind wing narrow and apically acute (hind wing wide and apically blunt in *Neotriadomerus* species). The apparent absence of a straight setal line extending from apical margin of fore wing about halfway towards the parastigma + marginal veins (Fig. 7) is an additional feature that may separate *E. abjunctus* from *Neotriadomerus* but the wing surface of *E. abjunctus* is not clear enough to be sure if the setal line is absent. *Eotriadomeroides abjunctus* differs from *Triadomerus bulbosus* Yoshimoto by the clava 1-segmented (3-segmented in *T. bulbosus*), ovipositor extending ventral to mesosoma as far as head (ovipositor not extending anteriorly ventral to mesosoma in *T. bulbosus*), and relatively longer postmarginal vein (relatively shorter in *T. bulbosus*).

Description. Female. Color. Vertex, antenna except radicle, dorsum of body, except for scutellum, and ovipositor sheaths dark brown or almost black; face, radicle, scutellum, and mesosoma and metasoma ventrally apparently lighter brown (Fig. 1). **Total body length** ~2850. **Head.** Head length ~205, head width ~600; mid ocellus diameter ~35. **Antenna** (Figs 2–5). Three (possibly 4) mps are visible on the right clava and one on fu₈ of the left antenna (Fig. 5); the mps that most likely should occur on the remaining funicle segments are not visible. Length/width measurements: range (ratios) of antennal segments: radicle? ~85/~12 (2.08), scape excluding radicle ~230/~90 (2.53), pedicel ~75/~50 (1.47), fu₁ ~170/~45 (3.85), fu₂ ~160/~40 (3.83), fu₃ ~150/~40 (3.67), fu₄ ~150/~45 (3.33), fu₅ ~140/~40 (3.08), fu₆ ~150/~40 (3.60), fu₇ ~135/~40 (4.00), fu₈ ~125/~150 (2.57), clava ~325/~85 (3.76). **Mesosoma.** Mesosoma length ~900, metanotum with dorsellum almost certainly triangular (Fig. 6). **Wings.** Fore wing (Fig. 7) with microtrichia uniformly covering entire surface, apparently to base of parastigma and apparently with one row of a few microtrichia posterior to apex of submarginal vein; fore wing length/width ~1930/~560, length/width 3.50, longest marginal setae ~80; hind wing length ~1150, width ~45, longest marginal setae ~115, with wing apex acute. **Legs.** Tarsi 5-segmented, the tarsomeres becoming shorter towards apex of tarsus (legs segments mostly unrecognizable except two tibiae in part and two tarsi visible, with the end points of basal tarsomeres unclear). **Metasoma.** Petiole (Fig. 6) evidently short; gaster with terga apparently about equal in length. Metasoma length ~1875; ovipositor length ~2640, with sheaths extending anteriorly ventral to mesosoma to level of pronotum.

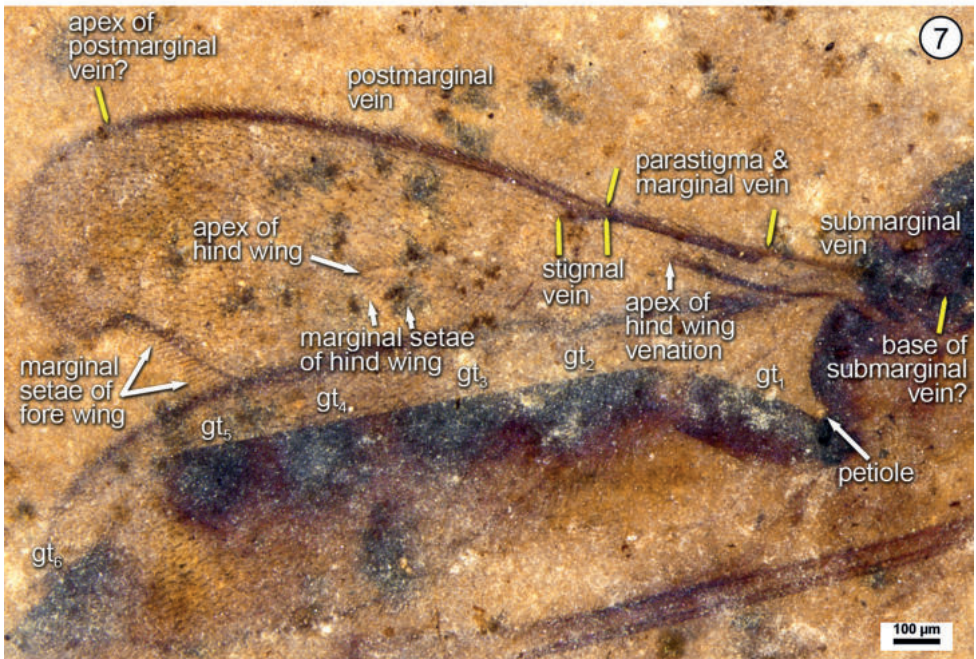
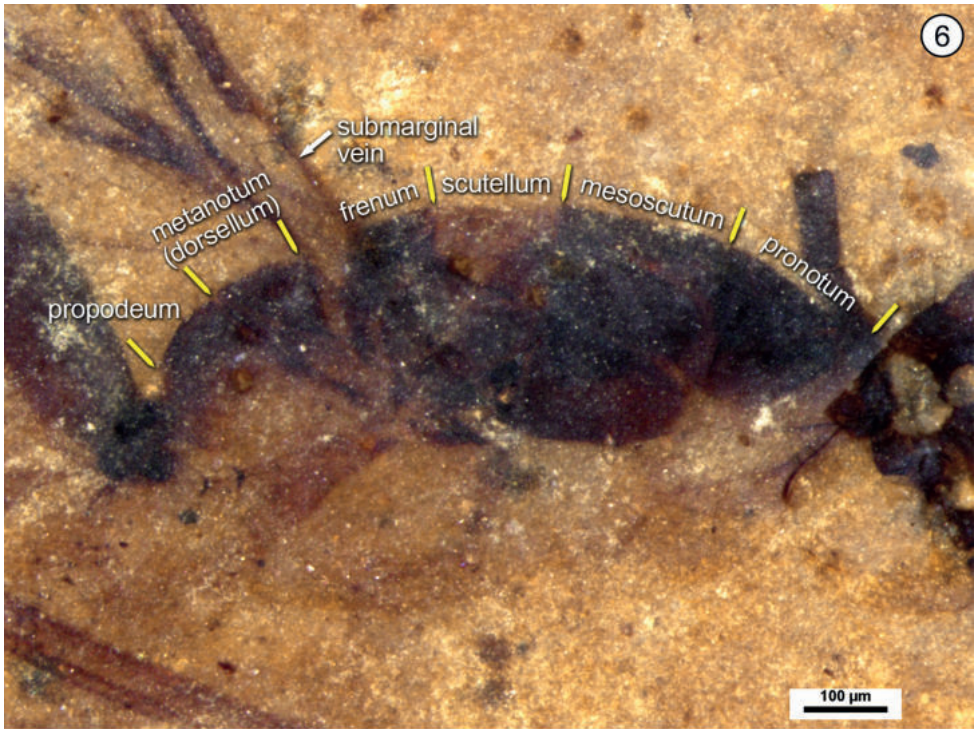


Figures 1, 2. *Eotriadomeroides abjunctus* Huber, holotype female **1** habitus (except most legs not visible) **2** pronotum + head + partly disarticulated antennae.

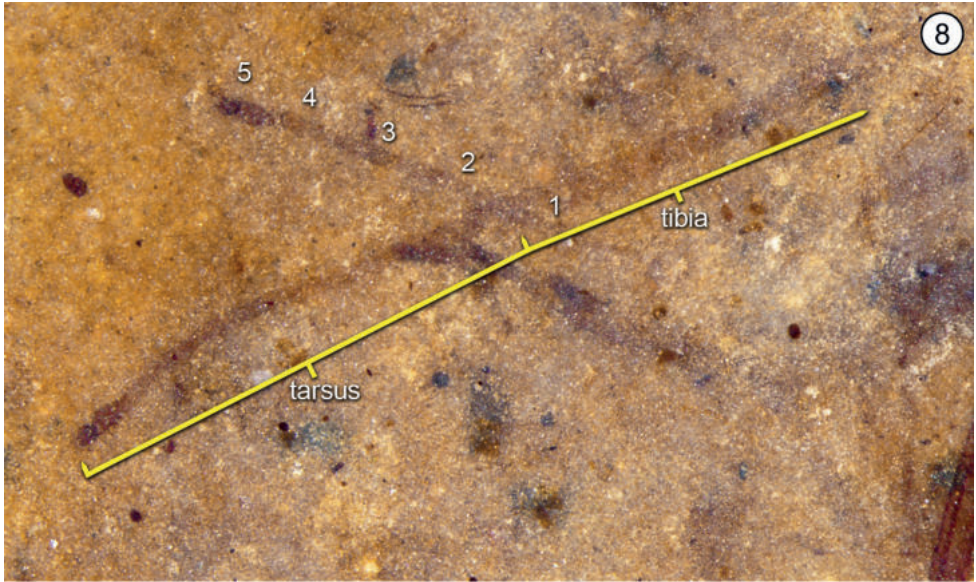
Derivation of species name. From the Latin *abjunctus*, meaning disunited or separated, refers both to the strongly disjunct geographic distribution of this 40 my old fossil from extant members of *Neotriadomerus*, the most similar looking genus, and to the fact that some of the fossil's appendages are broken into parts (the antennae) or are separated from the body (the legs).



Figures 3–5. *Eotriadomeroides abjunctus* Huber, holotype female **3** head + part of antennae **4** left antenna (pedicel– fu_3) **5** fu_8 + clava of both antennae.



Figures 6, 7. *Eotriadomeroides abjunctus* Huber, holotype female **6** mesosoma **7** wings + metasoma.



Figures 8, 9. *Eotriadomeroides abjunctus* Huber, holotype female **8** tibiae and tarsi of one? pair of legs **9** shale piece containing holotype (circled) of *Eotriadomeroides abjunctus* Huber.

Discussion

Amorim and Greenwalt (2020) described *Synneuron* (Diptera: Canthylosceldidae) from the wings of two fossil specimens, one from the Kishenehn Formation and one from the Koonwarra Fossil Bed in Australia. Given their strongly disjunct (perhaps worldwide) distribution, they suggested the Cretaceous as the minimum age for *Synneuron*, but, more likely, based on their phylogenetic analysis of the tribe it is classified in, they proposed the Middle Jurassic as the minimum age of the genus. *Synneuron* has two extant species, one Palearctic and the other Nearctic. The case of *Eotriadomeroides* and *Neotriadomerus* may be similar. Although they are classified in different genera, they, together with the Cretaceous genus *Triadomerus*, are best classified in the same lineage, the Triadomerini (Huber 2017), with only the species of *Neotriadomerus* extant. This tribe is likely the most ancestral lineage within Mymaridae, based on its morphology, and its included genera were possibly worldwide in distribution early in the existence of Mymaridae as a recognizable taxon, just as the present day Mymaridae are worldwide. And, as with *Synneuron* and its relatives, the Triadomerini may also have originated as a Pangaeian clade. More likely, however, Triadomerini originated more recently, in the middle Jurassic, as estimated by Peters et al. (2018). Regardless of the actual age of origin, Mymaridae are small wasps easily capable of being dispersed aerially for long distances, as evidenced by their current existence on remote islands. So, if they did originate well after the breakup of Pangaea, dispersal worldwide from one or other of those putative centres of origin, either Laurasia or, much more likely, Gondwana would certainly have been possible.

Chronologically, *Eotriadomeroides* (43–46 my), falls almost midway between *Triadomerus* (70–90 my) and *Neotriadomerus* (present day). Evidently, Triadomerini is an ancient lineage that occurs continuously throughout much of the geological history of Mymaridae as currently understood. A related lineage within Triadomerinae, the Aresconini, contains extant species in three genera (Huber 2017), and one extinct species in one genus, *Myanmymar*, from 100 my Burmese amber (Poinar and Huber 2011). One hopes that the large time gaps will eventually be filled as more fossils deposits containing Mymaridae are discovered and better evidence for the age of origin of the family will be found.

The middle Jurassic and early Cretaceous had gymnosperm-dominant environments worldwide, which changed to angiosperm-dominant environments in the later Cretaceous (Wing 2000). This change in flora, presumably accompanied by a similar change in fauna (including perhaps the hosts of Mymaridae), may partly explain why two of the genera (*Eotriadomeroides* and *Triadomerus*) of Triadomerini are extinct and only one genus (*Neotriadomerus*) is extant and found only in the southern Hemisphere, which is where many of the archaic taxa of extant Hymenoptera seem to occur.

The piece of shale that contained *Eotriadomeroides* also contained other synimpressions, as follows: 2 Aphididae and 22 Corixidae (Hemiptera), 16 Chaoboridae, 1 Culicidae and 3 other flies (Diptera), 1 Chalcididae, 1 Chalcidoidea, 1 Formicidae and 1 other wasps (Hymenoptera), 1 Thysanoptera, and 1 plant (Cupressoideae). These insects together suggest they occurred in moist habitat near water.

Acknowledgements

We thank the United States Forest Service for allowing D. Greenwalt to collect compression fossils from the Kishenehn Formation under the auspices of United States Forest Service Special Use Permit HUN465. We gratefully acknowledge the help of Jennifer Read (Canadian National Collection of Insects, Arachnids and Nematodes, Ottawa, Canada) for labelling the figures and compiling them into plates.

References

- Amorim DS, Greenwalt DE (2020) Cretaceous and Eocene fossils of the rare extant genus *Syneuron* Lundstrom (Diptera: Canthyloscedidae): evidence of a true Pangean clade. *Cladistics* 36(4): 413–423. <https://doi.org/10.1111/cla.12413>
- Engel JT, McKellar RC, Huber JT (2013) A fossil species of the primitive mymarid genus *Borneomymar* (Hymenoptera: Mymaridae) in Eocene Baltic amber. *Novitates Paleontologicae* 5: 1–8. <https://doi.org/10.17161/np.v0i5.4651>
- Greenwalt DE, Rose TR, Siljestrom SM, Goreva YS, Constenius KN, Wingerath JG (2015) Taphonomy of the fossil insects of the middle Eocene Kishenehn Formation. *Acta Palaeontologica Polonica* 60(4): 931–947. <https://doi.org/10.4202/app.00071.2014>
- Huber JT (2017) *Eustochomorpha* Girault, *Neotriadomerus*, gen. n., and *Proarescon*, gen. n. (Hymenoptera: Mymaridae), early extant lineages in evolution of the family. *Journal of Hymenoptera Research* 57: 1–87. <https://doi.org/10.3897/jhr.57.12892>
- Huber JT, Greenwalt D (2011) Compression fossil Mymaridae (Hymenoptera) from Kishenehn oil shales, with description of two new genera and review of Tertiary amber genera. *ZooKeys* 130: 473–494. <https://doi.org/10.3897/zookeys.130.1717>
- McAlpine JF, Martin JEH (1969) Canadian amber – a paleontological treasure chest. *The Canadian Entomologist* 101: e819833. <https://doi.org/10.4039/Ent101819-8>
- Peters RS, Niehuis O, Gunkel S, Bläser M, Mayer C, Podsiadlowski L, Kozlov A, Donath A, van Noort S, Liu S, Zhou X, Misof B, Heraty B, Krogmann L (2018) Transcriptome sequence-based phylogeny of chalcidoid wasps (Hymenoptera: Chalcidoidea) reveals a history of rapid radiations, convergence, and evolutionary success. *Molecular Phylogeny and Evolution* 120: 286–296. <https://doi.org/10.1016/j.ympev.2017.12.005>
- Poinar Jr G, Huber JT (2011) A new genus of fossil Mymaridae (Hymenoptera) from Cretaceous amber and key to Cretaceous mymarid genera. *ZooKeys* 130: 461–472. <https://doi.org/10.3897/zookeys.130.1241>
- Wing SL (2000) Evolution and expansion of flowering plants. 209–232. In: Gastaldo RA, DiMichele WA (Eds) *Phanerozoic Terrestrial Ecosystems*. Paleontological Society, Pittsburgh, 308 pp. <https://doi.org/10.1017/S1089332600000772>
- Yoshimoto CM (1975) Cretaceous chalcidoid fossils from Canadian amber. *The Canadian Entomologist* 107: 499–528. <https://doi.org/10.4039/Ent107499-5>

Two new species of the genus *Cryptopimpla* Taschenberg (Hymenoptera, Ichneumonidae, Banchinae) with an updated key to African species

Terry Reynolds¹, Simon van Noort^{1,2}

1 *Research and Exhibitions Department, South African Museum, Iziko Museums of South Africa, P.O. Box 61, Cape Town, 8000, South Africa* **2** *Department of Biological Sciences, University of Cape Town, Private Bag, Rondebosch, 7701, South Africa*

Corresponding author: Simon van Noort (svannoort@iziko.org.za)

Academic editor: T. Spasojevic | Received 24 March 2023 | Accepted 15 August 2023 | Published 24 August 2023

<https://zoobank.org/12C02F38-A9F6-4BCA-AEEB-A7155829867C>

Citation: Reynolds T, van Noort S (2023) Two new species of the genus *Cryptopimpla* Taschenberg (Hymenoptera, Ichneumonidae, Banchinae) with an updated key to African species. *Journal of Hymenoptera Research* 96: 667–696. <https://doi.org/10.3897/jhr.96.104038>

Abstract

A revised illustrated key to Afrotropical species of the genus *Cryptopimpla* Taschenberg is provided, with the inclusion of two new South African species, *C. orenji* Reynolds & van Noort, **sp. nov.** and *C. horikwagga* Reynolds & van Noort, **sp. nov.**, which are described and illustrated. The recovery of the first female specimens of *Cryptopimpla goci* Reynolds & van Noort in samples from Fernkloof and Grootbos nature reserves, and subsequent morphological reassessment of generic affinity based on female characters, no longer supports the placement of this species in *Cryptopimpla*. The transfer of *C. goci* to *Lissonota* Gravenhorst is proposed here: *Lissonota goci* (Reynolds & van Noort), **comb. nov.**, and the female is described. New Afrotropical distributional records for the previously described *Cryptopimpla* species are presented and notes on the distribution and diversification of the species are also provided. Online interactive Lucid keys to the 11 Afrotropical *Cryptopimpla* species are available at: <http://www.wasweb.org>.

Keywords

Afrotropical region, Atrophini, distribution, Ichneumonoidea, Lucid identification keys, South Africa, species diversity, taxonomy

Introduction

Afrotropical *Cryptopimpla* Taschenberg, 1863 represent 17% of the world's *Cryptopimpla* species (Reynolds Berry and van Noort 2016; Yu et al. 2016; Kang et al. 2019) and are restricted to three of the nine provinces of South Africa, namely Northern, Eastern and Western Cape. This narrow distribution is largely concordant with the Fynbos biome of the Greater Cape Floristic Region (CFR) encompassing the south-western part of South Africa (Reynolds Berry and van Noort 2016). No species are known from elsewhere in Africa despite recent intensive sampling effort having been conducted in other parts of southern Africa and in the tropical areas of central and eastern Africa.

The hosts of *Cryptopimpla* species that occur in the Afrotropical region remain unknown. Members of the tribe Atrophini generally attack semi-concealed hosts such as lepidopteran leaf rollers (Momi et al. 1975; Quicke 2015). A couple of Atrophini genera including *Cryptopimpla* and *Spilopimpla* have short ovipositors and utilize exposed hosts (Townes 1969; Gauld et al. 2002). There is some evidence to suggest British species of *Cryptopimpla* are parasitoids of Geometridae larvae feeding in low vegetation, a habitat association appearing to be typical for the genus (Townes and Townes 1978; Brock 2017; Broad et al. 2018).

Although *Cryptopimpla* has a worldwide distribution, its species richness in the temperate regions of South Africa (and elsewhere) support relative affinities of the genus to specific biogeographic areas defined by habitat and climate (Sheng and Zheng 2005; Kuslitzky 2007; Reynolds Berry and van Noort 2016; Yu et al. 2016). African *Cryptopimpla* species are predominately distributionally centred in the fynbos biome, a temperate shrubland vegetation that is fire-adapted, occurring in the southwestern region of South Africa. Ten of the species are fynbos associates but several of these extend into the neighbouring Succulent Karoo and Grassland biomes, or into relict forest patches within fynbos. Only one species occurs in Albany thicket.

In this paper, we update the species key to African *Cryptopimpla*, reassess the generic affinities of *Cryptopimpla goci* Reynolds & van Noort, 2016, describe two new species, and provide links to the revised online interactive Lucid pathway and Lucid matrix keys available on WaspWeb at <http://www.waspweb.org> (van Noort 2023a).

Materials and methods

Photographs

Images were acquired at the Iziko South African Museum (**SAMC**) with a Leica LAS 4.9 imaging system, comprising a Leica Z16 microscope with a Leica DFC450 Camera and 0.63× video objective attached. The imaging process, using an automated Z-stepper, was managed using the Leica Application Suite V 4.9 software installed on a desktop computer. Diffused lighting was achieved using a Leica LED 5000 Dome. All images presented in this paper as well as images of all the African *Cryptopimpla* species are available on WaspWeb (van Noort 2023a).

Mapping

The distribution maps for the African *Cryptopimpla* species were produced using SimpleMappr (Shorthouse 2010).

Specimen acquisition

Specimens were extracted from bulk inventory survey samples preserved in 96% ethanol and housed in the Iziko South African Museum entomology wet collection that had been sorted to family level. These samples emanate from continuous inventory surveys using a range of collecting methods including Malaise traps, yellow pan traps, yellow funnel traps, pitfall traps, sweeping, Winkler bag extraction of leaf litter and UV light trapping conducted in Africa over the last 31 years by the second author (van Noort 2019, 2022, 2023b). By June 2019; Malaise trapping effort equated to 73 000 trap days (van Noort 2019), increasing to 87 147 trap days as at June 2022 (van Noort 2022), but the surveys are ongoing and the current effort at February 2023 sits at 94 000 Malaise trap days (= 257 Malaise trap years) (van Noort 2023b).

Digitization

All specimen data has been digitized into the Iziko South African Museum Specify 6 database.

Depositories

SAMC Iziko South African Museum, Cape Town, South Africa (Curator: Simon vanNoort).

Nomenclature and abbreviations

The morphological terminology follows Wahl and Sharkey (1993), but the wing venation nomenclature follows Gauld (1991). Most morphological terms are also defined on the HAO website (<http://portal.hymao.org/projects/32/public/ontology/>). The following morphometric abbreviations are used (in order of appearance in the descriptions):

B	body length, from toruli to metasomal apex (mm);
A	antenna length, from base of scape to flagellar apex (mm);
F	fore wing length, from tegula to wing apex (mm);
CT (clypeus transversality index)	maximum width of clypeus: median height;
ML (malar space length index)	malar space (shortest distance between mandible base and compound eye): basal mandibular width;
IO (inter-ocellar index)	shortest distance between posterior ocelli: ocellus diameter;

OO (oculo-ocellar index)	shortest distance between eye and posterior ocellus: ocellus diameter;
Fl_n (length index of flagellomere n)	length: width of flagellomere n;
OT (ovipositor sheath-tibia index)	length of ovipositor sheath: length of hind tibia.

The first three measurements (absolute measures) were measured on all specimens in the type series, with measurements from the primary type reported separately in brackets if necessary.

Identification keys

Lucid pathway and Lucid matrix keys were developed using Lucid Builder version 4.0.37. Character matrices were generated and edited using Microsoft Excel; matrices were then used as input into Lucid matrix key production (Penev et al. 2009). The online interactive keys were produced using Lucid, meeting the requirements of publishing both static and dynamic interactive keys under an open access model (Penev et al. 2009). All keys were illustrated using high quality annotated images, highlighting diagnostic characters. The images are integrated into the key below each couplet resulting in a user-friendly output. This key format reduces the requirement of familiarity with morphological terminology associated with a particular taxonomic group, because the characters are visually illustrated, making the keys usable by a wide range of end-users including ecologists and conservationists. Online identification keys are presented in two different formats on WaspWeb: traditional static dichotomous keys where a choice needs to be made at each key couplet to continue, which are also presented as an interactive Lucid pathway (dichotomous) key; and Lucid matrix keys where relevant states from multiple character features can be selected independently until identification is achieved. For more information concerning Lucid keys visit <http://www.lucidcentral.org>.

Results

Specimen acquisition and distribution maps

Historically there were two *Cryptopimpla* specimens in the Iziko South African Museum collection: the holotype of *C. rubrithorax* Morley, 1916 (collected in 1914) and a specimen of the recently described species *C. zwarti* Reynolds Berry & van Noort, 2016 (collected in 1990). The remaining 60 specimens were collected by the second author over the last thirty years from many diverse vegetational localities. The majority of the resultant bulk samples have yet to be sorted and we expect that numerous further specimens reside in the unsorted samples, probably at least tripling the number of known specimens. Most of the mobilized specimens were collected in Malaise traps, with a single specimen collected by sweeping and two specimens recovered from yellow pan trap samples. A summary of the abundance and distribution of the species treated here is provided in Table 1.

Distribution maps are provided depicting the overall distribution of the genus in South Africa (Fig. 1), the individual species distributions plotted on a topographical map (Fig. 2), and species distributions plotted on a biome vegetation map (Fig. 3).

Digitization

The output of specimen data digitized into the Iziko South African Museum Specify 6 database is included as a supplementary excel file (Suppl. material 1).

Table 1. Number of known specimens, the known provincial distribution and vegetation biome association of African *Cryptopimpla* species.

<i>Cryptopimpla</i> species	Known specimens	Recorded distribution	Biome association
<i>C. elongatus</i>	1	Northern Cape	Fynbos
<i>C. fernkloofensis</i>	1	Western Cape	Fynbos
<i>C. hantami</i>	2	Western Cape	Fynbos
<i>C. hoerikwagga</i>	1	Western Cape	Fynbos
<i>C. kogelbergensis</i>	6	Northern & Western Cape	Fynbos; Succulent Karoo
<i>C. neili</i>	1	Western Cape	Fynbos
<i>C. onyxi</i>	13	Eastern & Western Cape	Fynbos; Grassland
<i>C. orenji</i>	1	Western Cape	Fynbos
<i>C. parslactis</i>	1	Northern Cape	Fynbos
<i>C. rubrithorax</i>	34	Northern & Western Cape	Forest; Fynbos
<i>C. zwarti</i>	1	Eastern Cape	Albany Thicket
Total	62		



Figure 1. Distribution map depicting the known African *Cryptopimpla* locality records. In the Afrotropical region *Cryptopimpla* species are currently only known from South Africa.

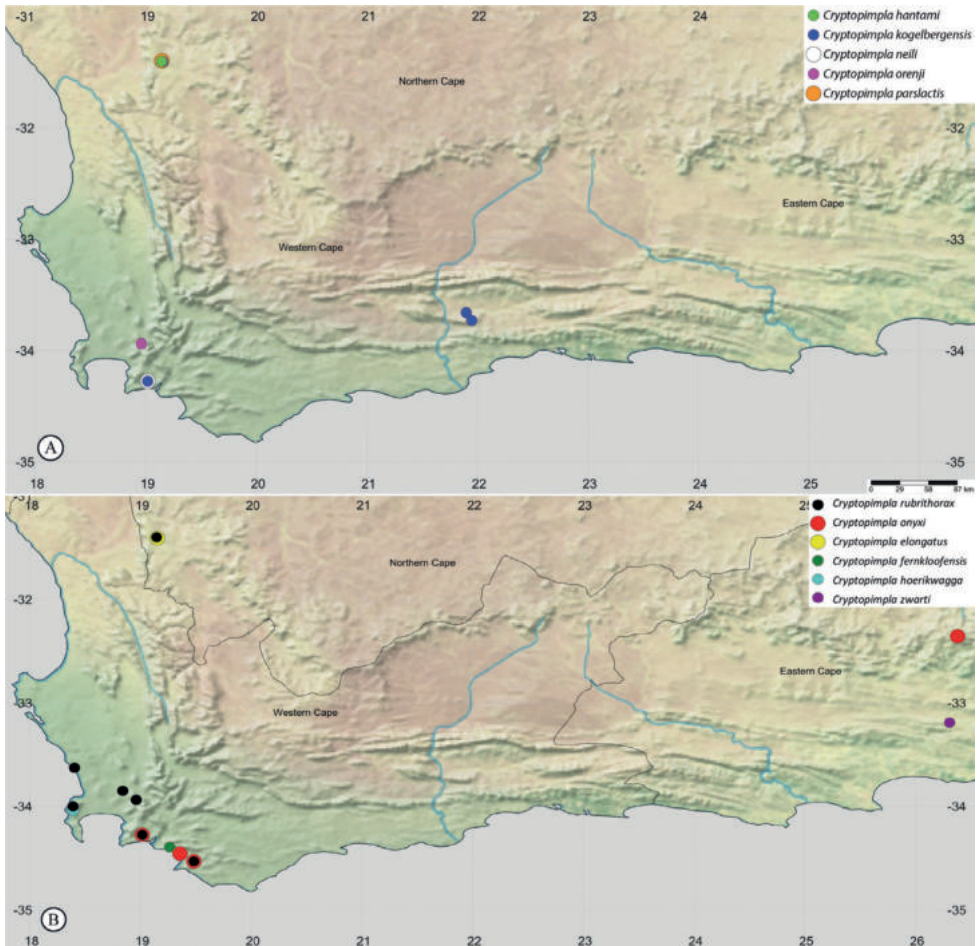


Figure 2. Recorded distribution for each *Cryptopimpla* species plotted on topographical maps. The genus is currently only recorded from the Eastern, Northern and Western Cape provinces within South Africa. Note that when two species are present in a single locality one of the species icons is larger, but centrally covered by the second species icon **A** *C. hantami*, *C. kogelbergensis*, *C. neili*, *C. orenji*, and *C. parslactis* **B** *C. elongatus*, *C. fernkloofensis*, *C. hoerikwagga*, *C. onyxi*, *C. rubrithorax* and *C. zwarti*.

Identification keys

A standard dichotomous key to the African species of *Cryptopimpla* is presented below. Online interactive Lucid pathway and Lucid matrix keys are available on WaspWeb (van Noort 2023a). The LIF3 file for the online Lucid matrix key to the African species is provided as Supplementary Material (Suppl. material 2). Lucid Interchange Format v. 3 (LIF3) files are XML based files that store all the Lucid3 key data, allowing exchange of the key with other key developers such as Intkey (DELTA), or MX. The provision of this LIF3 data set allows future workers to edit the key and to add newly described taxa. The data file for the published key that is stored on the publisher’s

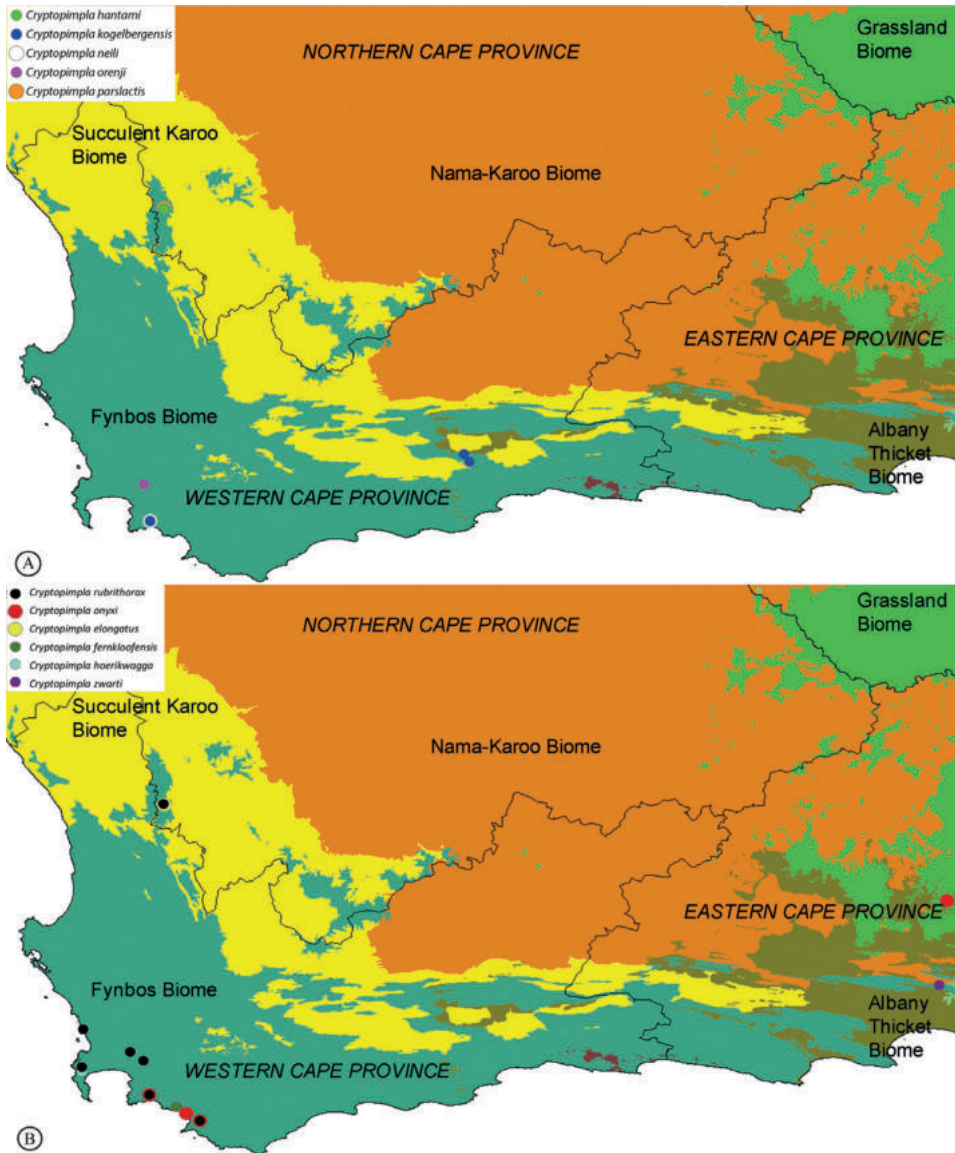
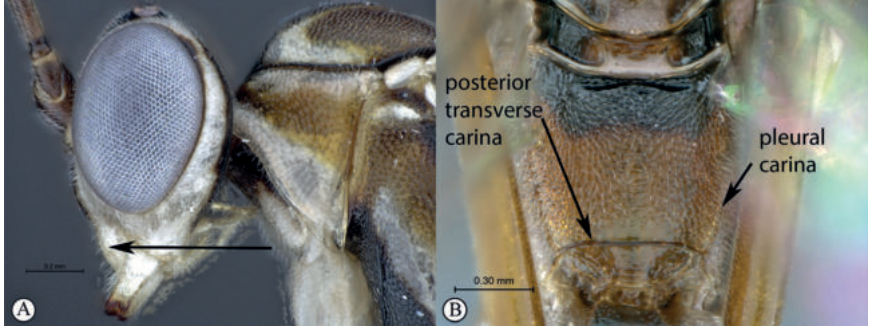


Figure 3. Recorded distribution for each *Cryptopimpla* species plotted on biome maps. Note that when two species are present in a single locality one of the species icons is larger, but centrally covered by the second species icon **A** *C. hantami*, *C. kogelbergensis*, *C. neili*, *C. orenji*, and *C. parslactis* **B** *C. elongatus*, *C. fernkloofensis*, *C. hoerikwagga*, *C. onyxi*, *C. rubrithorax* and *C. zwarti*.

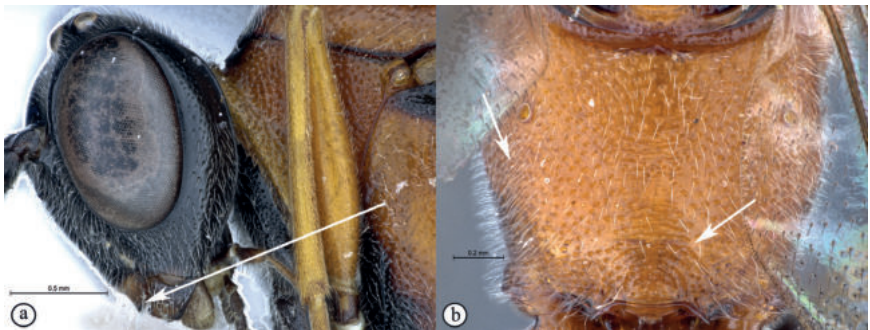
website and in e-archives has the rights of “first publication” identified by its bibliography data, location, and citation (Sharkey et al. 2009). The concept of publication, citation, preservation, and re-use of data files to interactive keys under the open access model is detailed in Penev et al. (2009).

Key to African species of the genus *Cryptopimpla* Taschenberg, 1863

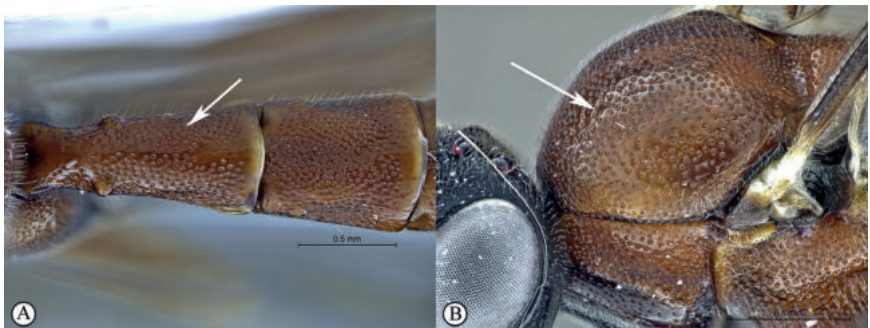
- 1 Clypeal profile distinctly convex and bulbous (A). Pleural carinae of propodeum present, but may be weak; posterior transverse carina present and well-defined (B).....*C. kogelbergensis*



- Clypeal profile weakly convex with a curved lip on ventral margin (a). Pleural carinae absent and posterior transverse carina of propodeum, if present, weak or reduced to a wrinkle (b)..... 2 (*rubrithorax* species-group)



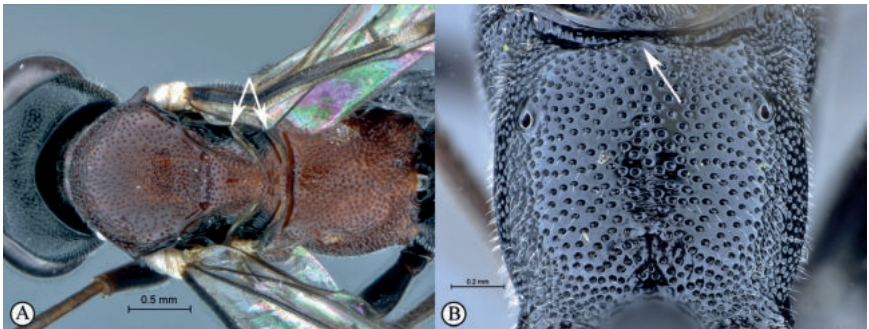
- 2 Metasomal tergite I punctate over most of surface (A). Median lobe of the mesocutum not raised above lateral lobes (B)..... 3



- Metasomal tergite I punctate posteriorly, strigate over anterior three-quarters (a). Median lobe of the mesoscutum distinctly raised (b) *C. orenji* sp. nov.



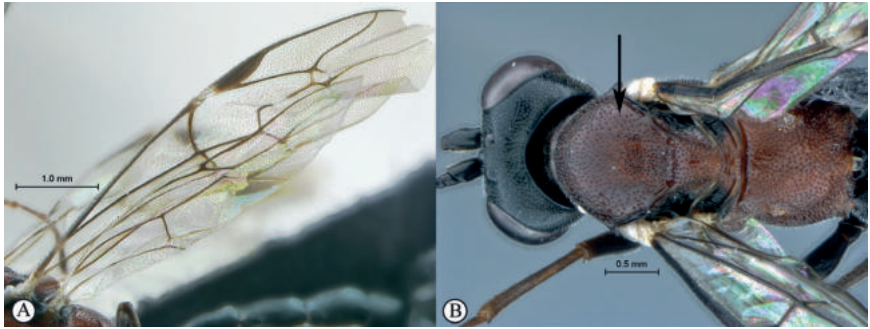
- 3 Mesosoma with axillar and metanotal struts subparallel, not strongly converging towards medial area (A). Propodeal anterior margin without defined medial tooth, but may have a blunt medial projection (B) 4



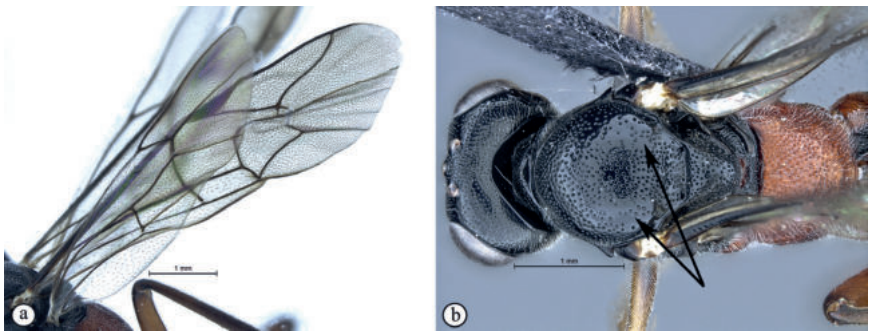
- Metanotum with axillar and metonotal struts converging towards medial area (a). Propodeal anterior margin with medial tooth (b)..... *C. fernkloofensis*



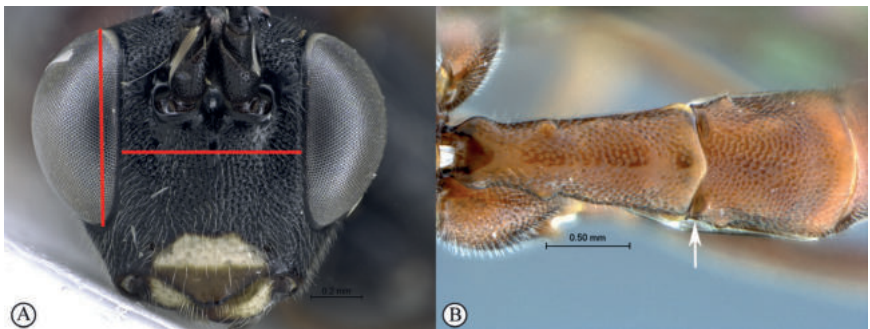
4 Wings with pale microtrichia (A). Mesoscutum evenly punctate (B)..... 5



– Wings with dark microtrichia, venation darker (a). Mesoscutum with fewer punctures inward of wing bases, resulting in polished areas (b) *C. parslactis*



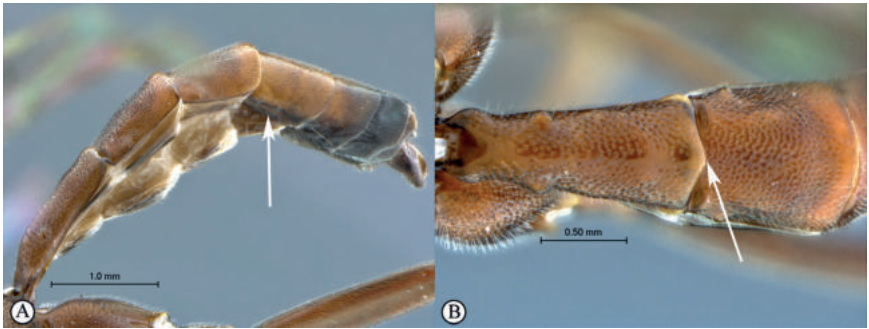
5 Inter-ocular distance broad, equivalent to eye height in anterior view (A). Thyridia small and indistinct (B) 6



- Inter-ocular distance narrow, shorter than eye height in anterior view (a). Thyridia moderately large and distinct, elongate to circular (b) **8**



- 6 Male tergite IV dorso-laterally compressed (A). Posterior margin of tergite I medially projected as a blunt angle (B)..... *C. neili*



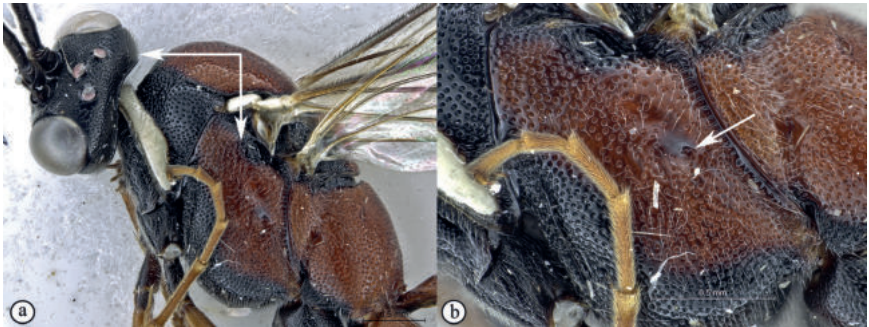
- Male tergite IV dorso-ventrally depressed (a). Posterior margin of tergite I weakly convex to straight (b)..... **7**



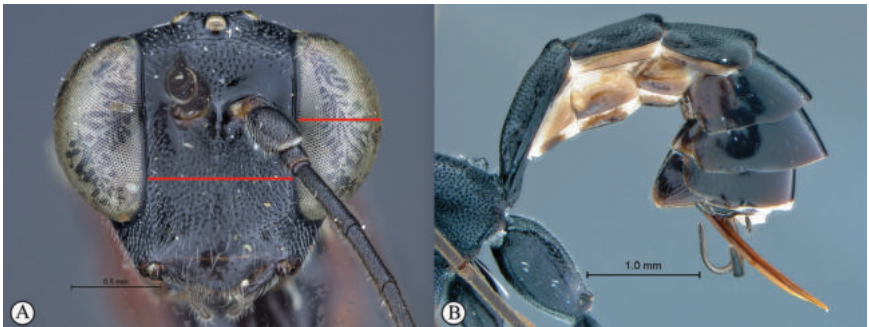
- 7 Mesosoma uniformly brownish orange (A). Head and mesosoma matt, moderately covered in short setae (A). Mesopleural pit shallow with surrounding area punctate (B) *C. hantami*



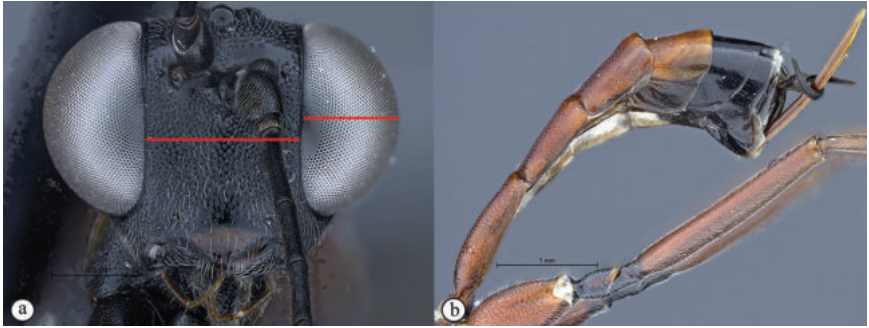
- Mesosoma tricoloured with a distinct white pronotal collar; pronotum, propleuron, posterior mesoscutal border, ventral parts of mesopleuron and lateral areas of scutellum and metanotum black, with remaining mesosoma dark reddish brown (a). Head and mesosoma subpolished, sparsely covered in short setae (a). Mesopleural pit distinct with surrounding polished area (b)
 *C. hoerikwagga* sp. nov.



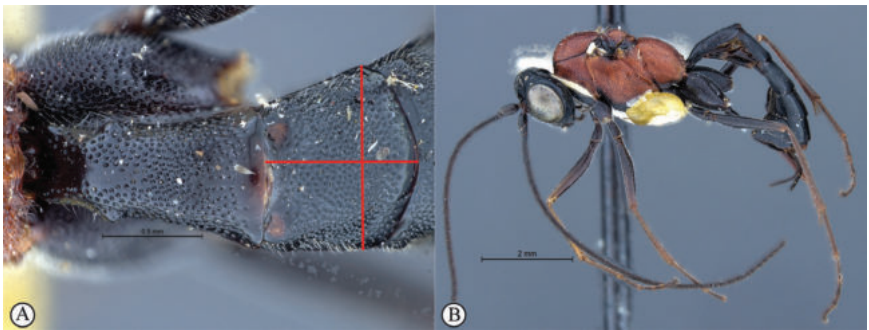
- 8 Eye in anterior view narrow to moderately-sized: eye maximum width in anterior view 0.4–0.66× shortest inter-ocular distance (A). Female metasomal tergites IV–VIII slightly compressed; metasoma black (B), legs brown to black 9



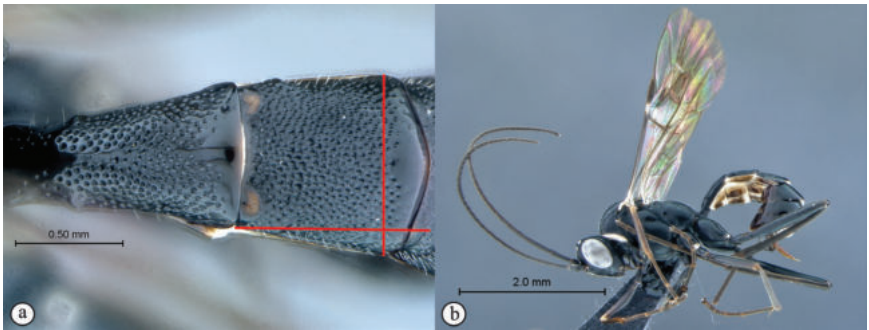
- Eye in anterior view larger, bulbous: eye maximum width in anterior view 0.73× shortest inter-ocular distance (a). Female metasoma elongated, depressed; metasoma and legs mostly rufescent (b) *C. elongatus*



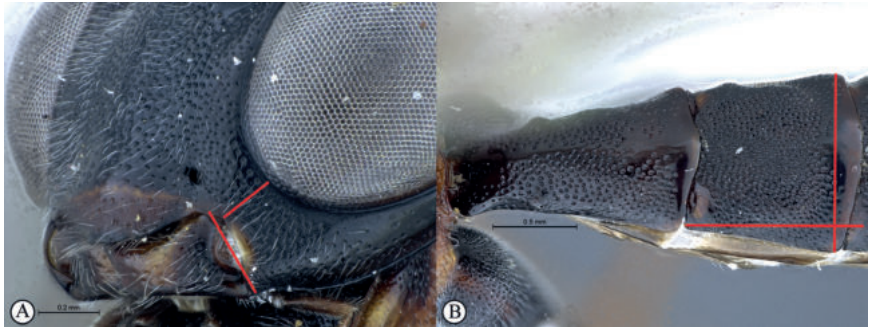
- 9 Metasomal tergite II 1.1–1.25× wider than long (A). Mesosoma predominantly rufous with some small black markings, with or without white pronotal collar (B) 10



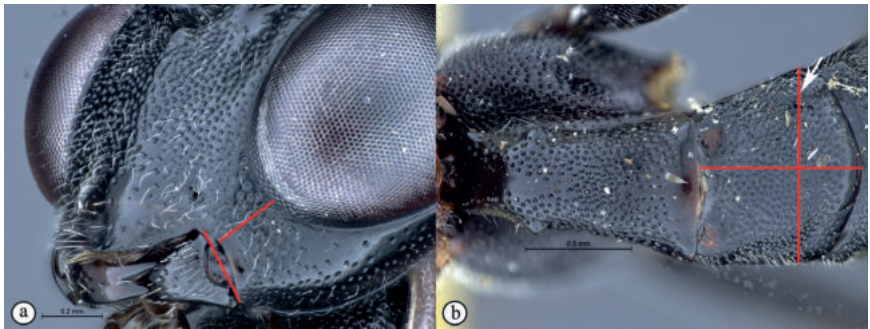
- Metasomal tergite II 1.09–1.25× longer than wide (a). Mesosoma black with white pronotal collar (b) *C. onyxi*



- 10 Malar space $0.6\times$ as long as basal mandibular width (A). Second tergite posteriorly $1.25\times$ wider than long (B) *C. zwarti*



- Malar space $0.9\text{--}1.3\times$ as long as basal mandibular width (a). Tergite II posteriorly no more than $1.1\times$ wider than long (b)..... *C. rubrithorax*



Cryptopimpla Taschenberg, 1863

Cryptopimpla Taschenberg, 1863. Zeitschrift für die Gesamten Naturwissenschaften, 21: 292. Type-species *Phytodietus blandus* Gravenhorst, 1914.

Complete diagnosis. Provided in Reynolds Berry and van Noort (2016).

Summary diagnosis. Afrotropical representatives of the genus can be distinguished by a combination of traits: a flagellum that tapers to a slender apex; a complete occipital carina, that joins the hypostomal carina distant from the base of the mandible; a longer upper mandibular tooth than lower tooth; absence of the epomia; a truncate-shaped fore wing areolet; the hind wing with Cu1 longer than cu-a; presence of a glymma; a strongly anteriorly narrowed first tergite, and an ovipositor that is $0.5\text{--}0.7\times$ as long as the hind tibia (Reynolds Berry and van Noort 2020).

Species-groups

The Afrotropical species cluster in two morphological species-groups:

- *rubrithorax* species-group (*C. elongatus*, *C. fernkloofensis*, *C. hantami*, *C. hoerikwagga* sp. nov., *C. neili*, *C. onyxi*, *C. orenji* sp. nov., *C. parslactis*, *C. rubrithorax*, and *C. zwarti*) is defined by the presence of a weakly convex clypeus with a curved lip on the ventral margin, small tentorial pits, absence of the pleural carinae, and absence of the posterior transverse carina on the propodeum.

- *kogelbergensis* species-group (*C. kogelbergensis*) is defined by the presence of a convex and bulbous clypeus with large tentorial pits, pleural carinae, and a distinct and well-defined posterior transverse carina on the propodeum. This species group was referred to as the *goci* species-group in Reynolds Berry and van Noort (2016), but with the current transfer of *C. goci* to *Lissonota* Gravenhorst, 1829 in this paper the name has had to be changed to that of the single species remaining in this species-group.

***Cryptopimpla hoerikwagga* Reynolds & van Noort, sp. nov.**

<https://zoobank.org/7E25DED0-03D1-4457-8901-593D15688BD8>

Fig. 4

Type material. *Holotype* ♂: SOUTH AFRICA, W. Cape, Constantiaberge, 640 m, 34°02.5'S, 18°23.5'E, above road to mast overlooking Hout Bay, 23 Feb–2 March 1994, S. van Noort, Mesic Mountain Fynbos, Malaise trap, SAM-HYM-P00591 (SAMC).

Description. Body overall subpolished. Colour. Body mostly fulvous. Head black, clypeus and mandibles white to brown. Propleuron, fore and mid coxae, dorso-posterior margin of mesoscutum, axillary troughs of mesonotum and metanotum, submeta-pleural carina black. Pronotum black, pronotal collar and tegula white. Trochanters, trochantellus and tergite V brown to fulvous. Remainder of metasoma brown with tergites VII and VIII white at posterior margins. Head densely punctate. Frons unarmed. Clypeus profile weakly convex with curved lip on ventral margin. Clypeus edge convex. Upper tooth of mandible longer than lower. Setae on head and clypeus short and sparse. Tentorial pits small and indistinct. Flagellum tapered to a slender apex. Eye in lateral view 1.03 times as long as wide, maximum width in anterior view 0.55 times shortest inter-ocular distance. Mesosoma not compressed. Scuto-scutellar sulcus broad with dorso-lateral indentations. Mesoscutum evenly punctate. Epicnemial carinae present ventrally and dorsally, dorsally converging toward anterior edge of mesopleuron; mesopleural pit distinct, surrounding area polished. Propodeum without carinae, its anterior margin straight. Wings hyaline. Fore wing with two bullae close together appearing as one; vein 2m-cu sinuate; areolet truncate-shaped. Hind wing with two basal hamuli and seven distal hamuli. Metasomal tergite I with dorso-lateral wrinkles, densely punctate, with posterior margin weakly convex; tergite II 1.2 times as long as wide posteriorly, spiracle situated at anterior 0.28 of tergite (measured in lateral view), thyridia small.

CT 2.5; ML 0.9; IO 1.9; OO 1.3; Fl₁ 3.3; body length 9.7 mm; flagella length 9.5 mm; fore wing length 7.5 mm.

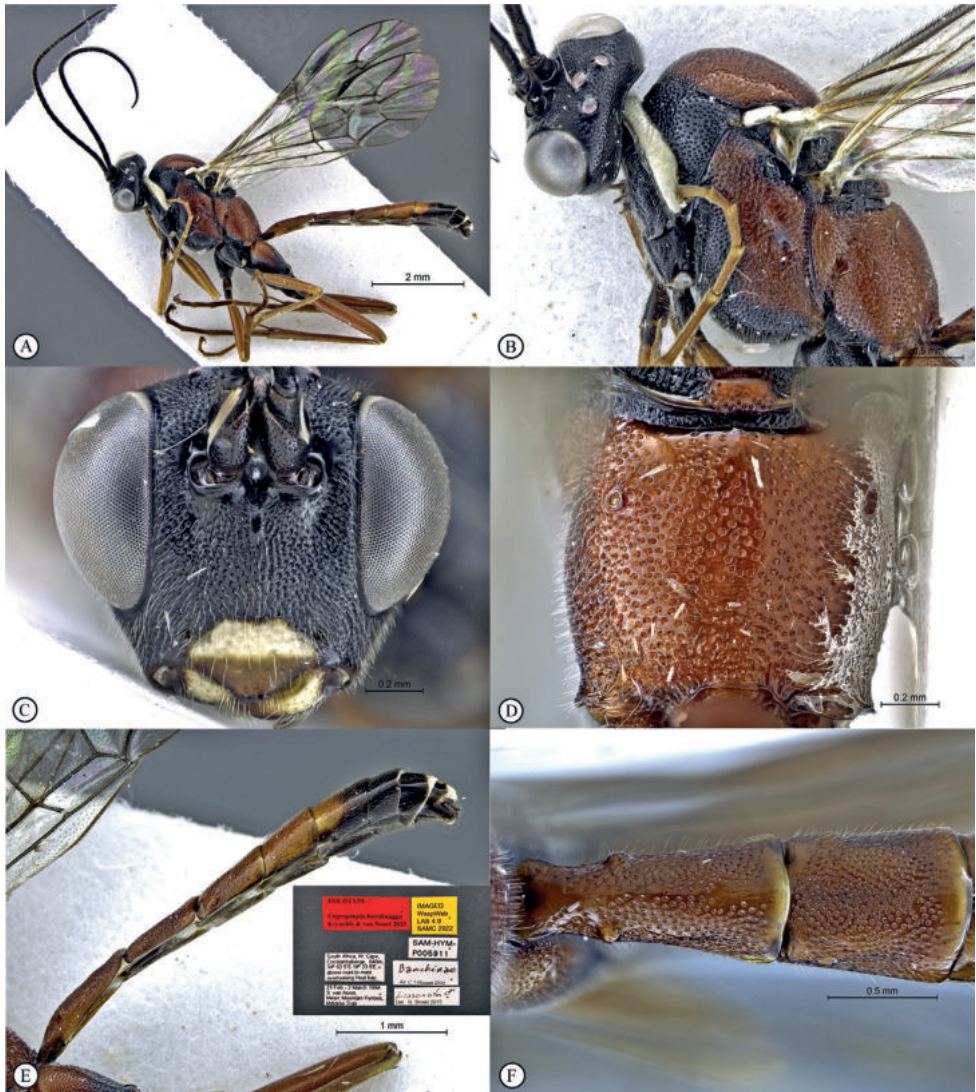


Figure 4. *Cryptopimpla hoerikwagga* Holotype **A** habitus, lateral view **B** head and mesosoma, lateral view **C** head, anterior view **D** propodeum, dorsal view **E** metasoma, lateral view (inset: data labels) **F** metasomal terga 1 and 2, dorsal view.

Diagnosis. This species belongs to the *rubrithorax* species-group and is the most strikingly coloured species of African *Cryptopimpla*. The mesosoma is tricoloured with a distinct white pronotal collar; a black pronotum, propleuron, posterior mesoscutal border, ventral parts of mesopleuron and lateral areas of scutellum and metanotum, with remaining mesosoma dark reddish brown. The head and mesosoma is subpolished, sparsely covered in short setae; the mesopleural pit is distinct with a surrounding polished area; axillar and metanotal struts are subparallel, not strongly converging towards the medial area; the propodeal anterior margin lacks a defined medial tooth;

the metasomal tergite I is punctate over most of the surface, posterior margin weakly convex; and the thyridia are small and distinct.

Differential diagnoses. The propodeal anterior margin is straight, distinguishing the species from several members of the *rubrithorax* species-group (except for *C. rubrithorax*, *C. parslactis* and *C. orenji*) where the margin may have a blunt medial projection or medial tooth. A broad scuto-scutellar sulcus with deep lateral indentations separates the species from *C. fernkloofensis*, *C. neili*, *C. hantami*, *C. kogelbergensis*, *C. parslactis*, and *C. orenji* where the dorso-lateral indentations and/or sulcus is absent. The densely punctate tergite I distinguish this species from *C. kogelbergensis* and *C. orenji* where punctation is reduced to absent. Dorso-lateral carinae of the metasomal tergite I substituted with wrinkling separates *C. hoerikwagga* from *C. fernkloofensis* and *C. neili* where one or no carinae are present. Small thyridia on tergite II distinguishes this species from all other members of the *rubrithorax* species-group, (except for *C. neili* and *C. hantami*), where the thyridia can be elongate or moderately large and circular.

Etymology. Named after the Khoisan word for Table Mountain “hoerikwagga” which directly translates to “mountain of the sea”. Noun in apposition.

Distribution. South Africa (Western Cape) (Fig. 2).

Comments. A rare species known only from one specimen. Intensive sampling in the type locality as well as other areas of the Cape region have so far produced no further specimens, there is, however, a major backlog of unsorted samples (van Noort 2023b), which may produce further specimens.

***Cryptopimpla orenji* Reynolds & van Noort, sp. nov.**

<https://zoobank.org/C43A1AE4-1774-4B3D-8A2F-FD70A2407943>

Fig. 5

Type material. *Holotype* ♀: SOUTH AFRICA, Western Cape, Banghoek Valley, Dwar-sriviershoek Farm, 33°56.232'S, 18°57.711'E, 410 m, 25 April–16 May 2013, S. van Noort, Malaise trap, BH12-FYN3-M08, Burnt Mesic Mountain Fynbos, SAM-HYM-P063260 (SAMC).

Description. Body subpolished, covered in short setae. Colour. Body mostly fulvous. Epicnecium, submetapleural carinae and dorso-lateral corners of axillary troughs of meso- and metanotum black. Paraocular area of eyes, malar space, clypeus and mandibles yellow. Head densely punctate. Frons unarmed. Clypeus profile weakly convex with a curved lip on the ventral margin. Clypeus edge convex. Upper tooth of mandible longer than lower. Setae on head and clypeus short and sparse. Tentorial pits small and indistinct. Flagellum tapered to a slender apex. Eye in lateral view 1.3 times as long as wide, maximum width in anterior view 0.75 times shortest inter-ocular distance. Mesosoma not compressed. Scuto-scutellar sulcus without dorso-lateral indentations. Mesoscutum densely punctate, median lobe distinctly raised. Epicnemial carinae present ventrally and dorsally, dorsally converging toward anterior edge of mesopleuron; area surrounding mesopleural pit punctate. Propodeum with posterior transverse carinae present but weak, its anterior margin straight, spiracle elongate. Wings hyaline.

CT 2.2; ML 0.8; IO 1.6; OO 1.6; Fl₁ 5; OT 0.5; body length 6.5 mm; flagella length 9.4 mm; fore wing length 6.9 mm.

Diagnosis. *Cryptopimpla orenji* is immediately distinguishable from all other Afro-tropical *Cryptopimpla* by possessing a distinctly raised median lobe on the mesoscutum, and by having tergite I distinctly strigate in anterior three-quarters and only punctate posteriorly. The head coloration is fulvous; and the paraocular area of the eyes, malar space, clypeus and mandibles are yellow, a colour pattern that is unique to this species.

Differential diagnoses. The area surrounding the mesopleural pit is punctate distinguishing *C. orenji* from *C. hoerikwagga* and *C. fernkloofensis* where the area surrounding the pit is polished. The propodeal anterior margin is straight distinguishing the species from several members of the *rubrithorax* species-group (excluding *C. rubrithorax*, *C. parslactis* and *C. orenji*) where the margin may have a blunt medial projection or medial tooth. A scuto-scutellar sulcus without dorso-lateral indentations separates *C. orenji* from several closely related species (excluding *C. fernkloofensis*, *C. parslactis* and *C. hoerikwagga*) where the dorso-lateral indentations are present and/or the sulcus is absent. Indistinct thyridia on tergite II distinguishes the species from several members of the *rubrithorax* species-group (excluding *C. neili*, *C. hantami* and *C. hoerikwagga*) where the thyridia can be elongate to moderately large and circular.

Etymology. So named owing to the colour of this species. Orenji is the Xhosa name for orange. Noun in apposition.

Distribution. South Africa (Western Cape) (Fig. 2).

Comments. A rare species known only from one specimen. Intensive sampling in the type locality and in other areas of the Cape region have so far produced no further specimens, there is, however, a major backlog of unsorted samples (van Noort 2023b), which may produce further specimens.

***Lissonota goci* (Reynolds Berry & van Noort, 2016), comb. nov.**

Fig. 6

= *Cryptopimpla goci* Reynolds Berry & van Noort, 2016.

Type material examined. *Holotype* ♂: SOUTH AFRICA, Western Cape, Koeberg Nature Reserve, 33°37.622'S, 18°24.259'E, 741 m, 3–31 October 1997, S. van Noort, KO97-M12, Malaise trap, West Coast Strandveld, SAM-HYM-P0474345 (SAMC).

Additional material examined for description of female. 5♀: SOUTH AFRICA, Western Cape, Grootbos Private Nature Reserve, site LEU, 305 m, 34.531500°S, 19.482723°E, 6 Dec 2018–1 Feb 2019, S. van Noort, Malaise trap, Agulhas Limestone Fynbos, GPNR18-LEU-M09, SAM-HYM-P096893, SAM-HYM-P096967, SAM-HYM-P097347, SAM-HYM-P099594, SAM-HYM-P099621 (SAMC). 1♀: SOUTH AFRICA, Western Cape, Fernkloof Nature Reserve, Mosselberg, 60 m, south slope, 14 May–16 June 1995, S. van Noort, Malaise trap, Mesic Mountain Fynbos, SAM-HYM-P006315.

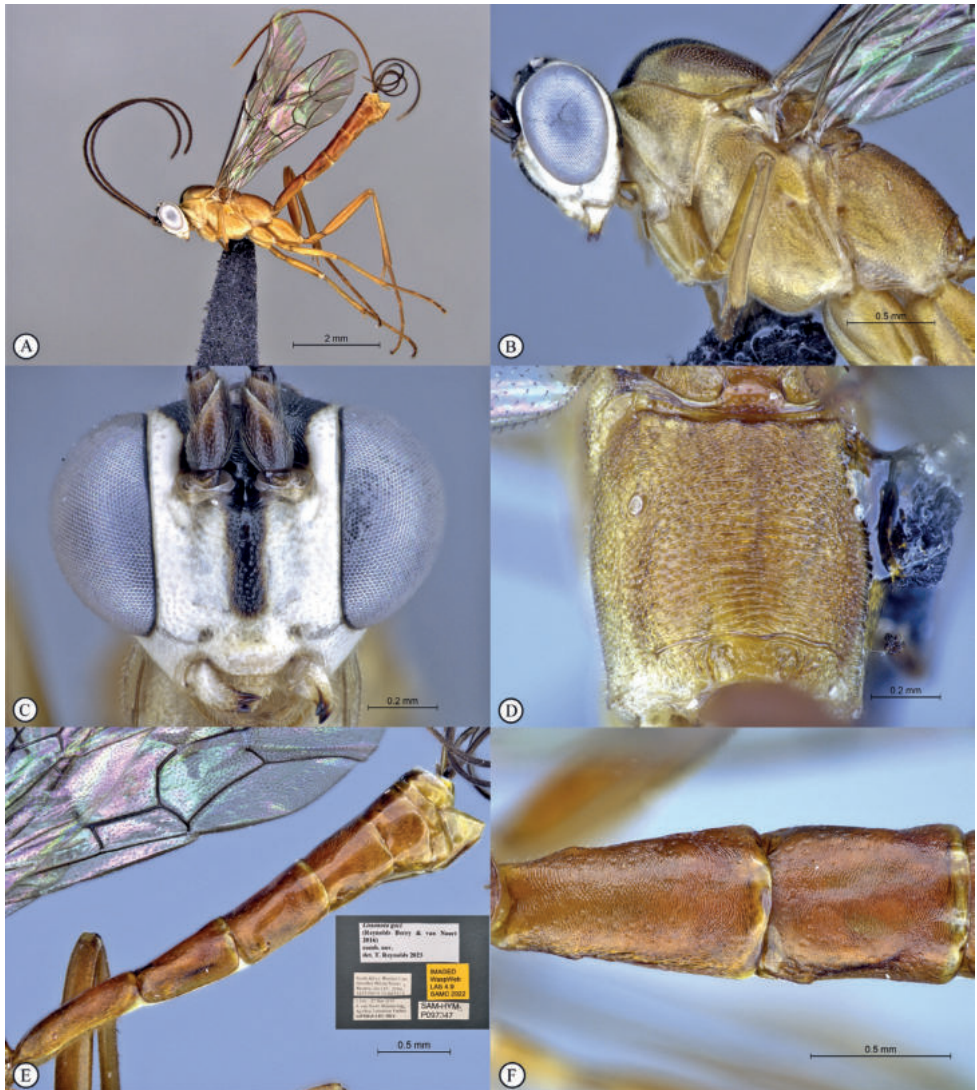


Figure 6. *Lissonota goci* (Reynolds Berry & van Noort, 2016) comb. nov. non-type female **A** habitus, lateral view **B** head and mesosoma, lateral view **C** head, anterior view **D** propodeum, dorsal view **E** metasoma, lateral view (inset: data labels) **F** metasomal terga 1 and 2, dorsal view.

Additional material of males newly recorded. 3♂: SOUTH AFRICA, W. Cape, Hermanus, Fernkloof Nature Reserve, Mosselberg, 60 m, south slope, 34°24.46'S, 19°18.00'E, 14 May–16 June 1995, S. van Noort, Malaise trap, Mesic Mountain Fynbos, SAM-HYM-P006415a-c (SAMC). 36♂: South Africa, Western Cape, Grootbos Private Nature Reserve, site LEU, 305 m, 34.531500°S, 19.482723°E, 6 Dec 2018–1 Feb 2019, S. van Noort, Malaise trap, Agulhas Limestone Fynbos, GPNR18-LEU-M09, SAM-HYM-P096887, SAM-HYM-P096888, SAM-HYM-P096892, SAM-

HYM-P096895–P096899, SAM-HYM-P096901, SAM-HYM-P097300, SAM-HYM-P097305, SAM-HYM-P097307, SAM-HYM-P097335, SAM-HYM-P097336, SAM-HYM-P097340, SAM-HYM-P097341, SAM-HYM-P097346–P097348, SAM-HYM-P097351, SAM-HYM-P097353, SAM-HYM-P097394, SAM-HYM-P099598, SAM-HYM-P099617–P099620, SAM-HYM-P099622–P099624, SAM-HYM-P099626–P099631 (SAMC). 21♂: SOUTH AFRICA, Western Cape, Grootbos Private Nature Reserve, site LEU, 305 m, 34.531500°S, 19.482723°E, 6 Dec 2018–1 Feb 2019, S. van Noort, Malaise trap, Agulhas Limestone Fynbos, GPNR18-LEU-M14, SAM-HYM-P098708, SAM-HYM-P098715, SAM-HYM-P099730, SAM-HYM-P099734–P099737, SAM-HYM-P099741–P099744, SAM-HYM-P099745–P099747, SAM-HYM-P099749–P099751, SAM-HYM-P099753, SAM-HYM-P099754–P099756 (SAMC). 1♂: SOUTH AFRICA, Western Cape, Grootbos Private Nature Reserve, site FOR, 340 m, 34.54133°S, 19.43876°E, 25 Mar–31 May 2019, S. van Noort, Malaise trap, Afromontane Forest, GPNR18-FOR-M17, SAM-HYM-P099498 (SAMC). 1♂: SOUTH AFRICA, Western Cape, Grootbos Private Nature Reserve, site MILK, 240 m, 34.52831°S, 19.48496°E, 25 Mar–1 June 2019, S. van Noort, Malaise trap, Milkwood Scrub Forest, GPNR18-MILK-M20, SAM-HYM-P099485 (SAMC).

Description of female. Colour, sculpture and proportions as in male with the following exceptions: head with flagellum not tapered. Eye in lateral view 0.69–0.74 times as long as wide; in anterior view with maximum width slightly broader, 0.48–0.56 times shortest inter-ocular distance. Hind wing with one-two basal hamuli and seven-eight distal hamuli. Metasoma with tergite I impunctate, wrinkles or a single carina present dorso-laterally with no secondary carina leading from the single carina to the spiracle; second tergite 0.98–1.39 times longer than broad, spiracle situated more anteriorly at 0.27–0.3 of tergite (measured in lateral view), ovipositor 2.31–2.36 times longer than hind tibia.

Body length 7.1–8.7 mm; antenna length 7.1–8.1 mm; fore wing length 5.3–6.1 mm.

Distribution. South Africa (Western Cape) (Fig. 2).

Cryptopimpla elongatus Reynolds Berry & van Noort, 2016

Type material examined. *Holotype* ♀: SOUTH AFRICA, Northern Cape, Hantam National Botanical Garden, 31°24.274'S, 19°09.164'E, 755 m, 22 May–12 June 2008, S. van Noort, GL07-DOL1-M39, Malaise trap, Nieuwoudtville-Roggeveld Dolerite Renosterveld, SAM-HYM-P047468 (SAMC).

Cryptopimpla fernkloofensis Reynolds Berry & van Noort, 2016

Type material examined. *Holotype* ♂: SOUTH AFRICA, Western Cape, Fernkloof Nature Reserve, 33°39.941'S, 21°53.505'E, 300–340 m, 13 May 1995, S. van Noort, Sweep, Mesic Mountain Fynbos, SAM-HYM-P008237 (SAMC).

***Cryptopimpla hantami* Reynolds Berry & van Noort, 2016**

Type material examined. *Holotype* ♀: SOUTH AFRICA, Northern Cape, Hantam National Botanical Garden, 31°24.182'S, 19°08.587'E, 741 m, 17 March–21 April 2008, S. van Noort, GL07-REN3-M24, Malaise trap, Nieuwoudtville Shale Renosterveld, SAM-HYM-P047467 (SAMC).

***Cryptopimpla kogelbergensis* Reynolds Berry & van Noort, 2016**

Type material examined. *Holotype* ♀: SOUTH AFRICA, Western Cape, Kogelberg Nature Reserve, 34°16.481'S, 19°01.033'E, 118 m, 16 May–16 June 1999, S. van Noort, KO98-M23, Malaise trap, Mesic Mountain Fynbos, last burnt c. 1988, SAM-HYM-P047475 (SAMC).

Additional material newly recorded. 1♀: SOUTH AFRICA, Northern Cape, Hantam National Botanical Garden, 31°24.274'S, 19°09.164'E, 23 March–06 May 2008, S. van Noort, GL07-REN3-M38, 741 m, Malaise trap, Nieuwoudtville-Roggeveld Dolerite Renosterveld, SAM-HYM-P064320 (SAMC).

***Cryptopimpla neili* Reynolds Berry & van Noort, 2016**

Type material examined. *Holotype* ♂: SOUTH AFRICA, Western Cape, Kogelberg Nature Reserve, 34°16.481'S, 19°01.033'E, 118 m, 16 March 1999–16 April 1999, S. van Noort, KO98-M18, Malaise trap, Mesic Mountain Fynbos, last burnt c. 1988, SAM-HYM-P047436 (SAMC).

***Cryptopimpla onyxi* Reynolds Berry & van Noort, 2016**

Type material examined. *Holotype* ♀: SOUTH AFRICA, Western Cape, Walker Bay Nature Reserve, 34°27.414'S, 19°21.393'E, 57 m, 14 May–14 June 1997, S. van Noort, WB97-M01, Malaise trap, South coast Strandveld, SAM-HYM-P047460 (SAMC).

Additional material newly recorded. 1♂: SOUTH AFRICA, Western Cape, Grootbos Private Nature Reserve, site LEU, 305 m, 34.531500°S, 19.482723°E, 25 March–31 May 2019, S. van Noort, Malaise trap, Agulhas Limestone Fynbos, GPNR18-LEU-M19, SAM-HYM-P098730 (SAMC). 1♂: SOUTH AFRICA, Western Cape, Grootbos Private Nature Reserve, site MILK, 240 m, 34.52831°S, 19.48496°E, 1 June–7 Aug 2019, S. van Noort, Malaise trap, Milkwood Scrub Forest, GPNR18-LEU-M24, SAM-HYM-P101469 (SAMC). 1♀: SOUTH AFRICA, Eastern Cape, Winterberg, The Hoek farm, 31°21.260'S, 26°23.001'E, 1879 m, 6.x.2010–18.i.2011, S. van Noort, Malaise trap, Amathole Mistbelt Grassland, WTB09-GRA1-M05, SAM-HYM-P062421 (SAMC).

***Cryptopimpla parslactis* Reynolds Berry & van Noort, 2016**

Type material examined. Holotype ♂: SOUTH AFRICA, Northern Cape, Hantam National Botanical Garden, 31°23.802'S, 19°08.799'E, 752 m, 23 July–23 Aug 2008, S. van Noort, GL07-REN1-M43, Malaise trap, Nieuwoudtville Shale Renosterveld, SAM-HYM-P044547 (SAMC).

***Cryptopimpla rubrithorax* Morley, 1916**

Type material examined. Holotype ♀: SOUTH AFRICA, Western Cape, Elsenerberg, 11 October 1914, Mally and Petty, SAM-HYM-P000874 (SAMC).

Additional material newly recorded. 3♂: SOUTH AFRICA, Western Cape, Banghoek Valley, Dwarsriviershoek Farm, 33°56.232'S, 18°57.711'E, 410 m, 28 Aug–28 Sept 2012, S. van Noort, Malaise trap, Mesic Mountain Fynbos, BH12-FYN3-M02, SAM-HYM-P063982, SAM-HYM-P064071, SAM-HYM-P097386 (SAMC). 4♀, 3♂: SOUTH AFRICA, Western Cape, Banghoek Valley, Dwarsriviershoek Farm, 33°56.232'S, 18°57.711'E, 410 m, 3–25 April 2013, S. van Noort, Malaise trap, Burnt Mesic Mountain Fynbos, BH12-FYN3-M03, SAM-HYM-P063159, SAM-HYM-P063497, SAM-HYM-P093877–P093878, SAM-HYM-P093879–P093881 (SAMC). 3♂: SOUTH AFRICA, Western Cape, Banghoek Valley, Dwarsriviershoek Farm, 33°56.232'S, 18°57.711'E, 410 m, 28 Sept–24 Oct 2012, S. van Noort, Malaise trap, Mesic Mountain Fynbos, BH12-FYN3-M07, SAM-HYM-P063492, SAM-HYM-P063537 (SAMC). 3♂: SOUTH AFRICA, Western Cape, Banghoek Valley, Dwarsriviershoek Farm, 33°56.232'S, 18°57.711'E, 410 m, 8 Aug–2 Oct 2013, S. van Noort, Malaise trap, Burnt Mesic Mountain Fynbos, BH12-FYN3-M12, SAM-HYM-P063516, SAM-HYM-P063704, SAM-HYM-P063716 (SAMC). 3♀, 1♂: SOUTH AFRICA, Western Cape, Banghoek Valley, Dwarsriviershoek Farm, 33°56.232'S, 18°57.711'E, 410 m, 25 April–16 May 2013, S. van Noort, Malaise trap, Burnt Mesic Mountain Fynbos, BH12-FYN3-M08, SAM-HYM-P063076, SAM-HYM-P063278, SAM-HYM-P093875–P093876 (SAMC). 2♀: SOUTH AFRICA, W. Cape, Koeberg Nature Reserve, 33°37.622'S, 18°24.259'E, 8 Aug–5 Sept 1997, S. van Noort, Malaise trap, KO97-M07, West Coast Strandveld, SAM-HYM-P047476 (SAMC). 1♀: SOUTH AFRICA, Western Cape, Banghoek Valley, Dwarsriviershoek Farm, 33°56.232'S, 18°57.711'E, 410 m, 2–22 October 2013, S. van Noort, Malaise trap, Mesic Mountain Fynbos, BH12-FYN3-M13, SAM-HYM-P064020 (SAMC). 1♀, 1♂: SOUTH AFRICA, Western Cape, Banghoek Valley, Grootbos Private Nature Reserve, site LEU, 305 m, 34.531500°S, 19.482723°E, 25 March–31 May 2019, S. van Noort, Malaise trap, Agulhas Limestone Fynbos, GPNR18-LEU-M19, SAM-HYM-P098731, SAM-HYM-P098765 (SAMC). 1♀: SOUTH AFRICA, Western Cape, Banghoek Valley, Dwarsriviershoek Farm, 33°56.232'S, 18°57.711'E, 410 m, 24 Oct–10 Dec 2012, S. van Noort, Malaise trap, Mesic Mountain Fynbos, BH12-FYN3-M04, SAM-HYM-P064919 (SAMC). 1♀: SOUTH AFRICA, Western Cape, Table Mountain National Park, Orangetkloof, Disa River, 34°0.035'S, 18°23.492'E, 136 m, 11 Nov–11 Dec 2014, S. van Noort, Malaise trap, Afromontane Forest, ODK13-FOR1-M27, SAM-HYM-P062973 (SAMC).

***Cryptopimpla zwarti* Reynolds Berry & van Noort, 2016**

Type material examined. *Holotype* ♀: SOUTH AFRICA, Eastern Cape, Grahamstown, Faraway Farm 33.19'S, 19°26.31'E, April 1990, I. Crampton, Malaise trap, SAM-HYM-P005220 (SAMC).

Discussion**Species-groups**

The two newly described species (*C. orenji* sp. nov. and *C. hoerikwagga* sp. nov.) both belong to the *rubrithorax* species-group. In addition to possessing the morphological characters that distinguish members of the *rubrithorax* species-group, these two new species also have larger fore wings (length = 5.8–7.5 mm) compared to the *kogelbergensis* species-group where the fore wing lengths are smaller (length = 4.6–5.1 mm). *Cryptopimpla hoerikwagga* sp. nov. is the largest African *Cryptopimpla* species (body length 9.7 mm; fore wing length 7.5 mm) and *C. kogelbergensis* is the smallest African *Cryptopimpla* species (body length 4.2–5.6 mm; fore wing length 4.6–5.1 mm). The remaining species have sizes ranging between these two extremes (body length 6.5–9.4 mm; fore wing length 5.8–7.2 mm).

The maximum length of the ovipositor sheath relative to the hind tibia for the genus ranges from 0.7× for Afrotropical species (Reynolds Berry and van Noort 2016) to 1.0× (Townes 1969; Sheng 2011; Takasuka et al. 2011; Kang et al. 2019) for world species. However, the newly discovered female specimens of *Lissonota goci* comb. nov. possess an ovipositor sheath relative to the hind tibia that is up to 2.4× as long. *Cryptopimpla* has morphological affinities with the banchine genus *Lissonota* (Broad 2022) and without females to confirm the presence of the diagnostic generic character of a shortened ovipositor sheath, male *Cryptopimpla* may be incorrectly determined as the cosmopolitan banchine genus *Lissonota* (e.g. Holmgren 1860; Fig. 4), corroborated by the fact that the type species for *Cryptopimpla* was originally described as *Lissonota caligata* Gravenhorst, 1829. Within a global context both genera appear to be paraphyletic (Reynolds Berry 2019) and may warrant splitting up.

The discovery of the female of *Lissonota goci* comb. nov. has allowed us to reassess generic affinities of this species and based on female characters this species is better placed within *Lissonota*. The apical 0.3–0.4 portion of the flagellum is tapered to a slender apex in *Cryptopimpla* whereas the female flagellum in this species, as typical for *Lissonota*, is only weakly tapered at the apex (Townes 1969; Takasuka et al. 2011; Reynolds Berry and van Noort 2020). Besides the ovipositor length, which is more than 1.4× as long as the hind tibia confirming placement in *Lissonota* (Reynolds Berry and van Noort 2020), the general habitus is also typical of *Lissonota*, and tergite I is very flat in profile (Fig. 6, A, E), lacking the anteriorly “humped” appearance of *Cryptopimpla* (as shown in identification key image 8B and 8b). In addition, the areolet is barely truncate anteriorly, i.e. veins 2rs-m and 3rs-m are barely separated. we have here proposed that this species is transferred to the genus *Lissonota* as *Lissonota goci* comb. nov. (Fig. 6) and

the *goci* species-group (Reynolds Berry and van Noort 2016) will by resultant default be referred to as the *kogelbergensis* species-group. Phylogenetic analyses, using both morphological and genetic data, of Afrotropical Banchinae separates *C. kogelbergensis* from *C. onyxi* and *C. rubrithorax* with robust support, reinforcing the morphological distinction of these two species-groups (Reynolds Berry 2019). Unfortunately, attempts to extract DNA from specimens of *Lissonota goci* comb. nov. to provide additional support for the revised placement of this species in *Lissonota* were unsuccessful.

Distribution and diversity

Cryptopimpla hoerikwagga sp. nov. and *C. orenji* sp. nov. are described based on single specimens that were collected from the western slopes of the Constantiaberg mountain, and Banghoek Valley adjacent to the Helshoogte mountain, of Western Cape South Africa, respectively. These are areas with no previous records for *Cryptopimpla*. Both have been collected in Mesic Mountain Fynbos, a vegetation type that is a habitat association for most of the previously described species (i.e. *C. fernkloofensis*, *C. neili*, *C. onyxi*, *C. rubrithorax* and *C. kogelbergensis*). Approximately 55% of Afrotropical *Cryptopimpla* species have been described based on a single specimen, and 90% of the overall Afrotropical *Cryptopimpla* species diversity is currently recorded from fynbos (Fig. 3), suggesting that the Fynbos biome may be the centre of species richness for African *Cryptopimpla* species. The remarkable floristic richness, endemism (fauna and flora) and major climatic features of the Fynbos biome has identified it as a global biodiversity hot-spot (Myers et al. 2000). It is likely that the fynbos associated species specialise on host Lepidoptera species that are specific to hostplants also endemic to the Fynbos biome. A relatively recent (5–3 million years before present) rapid radiation of the flora of the CFR has been proposed (Linder 2003). Although originally hypothesized that banchine species occurring in the Cape region would be more derived because of their association with the climatically and environmentally unique and much younger CFR compared to forest-associated species, this hypothesis was subsequently refuted with the phylogenetic dating of the origin of the African *Cryptopimpla* clade to the early Eocene (56 million to 47.8 mya, Reynolds Berry 2019). *Cryptopimpla* has a much broader worldwide temperate distribution (Yu et al. 2016), suggesting that *Cryptopimpla* species may have been more widespread in Africa during temperate epochs and that their distribution has subsequently retracted to the CFR. Interestingly, species of *Lissonota* occurring within the Afrotropical region are also largely restricted to the temperate regions of South Africa (Reynolds Berry 2019). Future evolutionary assessments of *Cryptopimpla* should be considered in relation to this genus, to which it is morphologically similar, with both genera showing paraphyly at a global scale (Broad et al. 2018; Reynolds Berry 2019).

Due to the relatively limited availability of specimens for several species within *Cryptopimpla*, any assessments of the distribution and diversification of the different species are still likely to be biased. This is corroborated by unique locality records for the newly described species presented in this paper. While sustained continuous inventory surveys over the last three decades has revealed the genus to be increasingly species rich, it is still rare in terms of abundance with more than half of the Afrotropical spe-

cies represented by a single specimen. Further specimens will no doubt be recovered from the backlog of unsorted samples resulting from 31 years of continuous inventory surveys run by Simon van Noort, using a range of collecting methods (Malaise traps, yellow pan traps, yellow funnel traps, pitfall traps, sweeping, Winkler bag extraction of leaf litter and UV light trapping) (van Noort 2019, 2022, 2023b). The large backlog of unsorted samples (94 000 Malaise trap days = 257 Malaise trap years as at February 2023) housed in the Iziko South African Museum entomology collection is a function of capacity constraints – we simply do not have the human and financial resources to process the backlog of the estimated 39 million specimens in the Malaise trap samples alone, which requires R7,5 billion to achieve (van Noort 2023b).

Cryptopimpla rubrithorax is the most common Afrotropical species, occurring across various vegetation types within the Cape Floristic Region, including Strandveld, Mesic Mountain Fynbos, Agulhas Limestone Fynbos, Renosterveld, and Afromontane forest (Reynolds Berry and van Noort 2016). *Cryptopimpla rubrithorax* may have adapted to a wider range of lepidopteran hosts by shifting to related host species that are more polyphagous, and hence potentially associated with host plant species that are only present in the neighbouring biomes; alternatively, *C. rubrithorax* is historically polyphagous, and the *Cryptopimpla* species with narrower distributional ranges that are associated with the Cape Floristic Region have evolved higher levels of host specialisation, as hypothesized for *Aloeides* species where host specialisation appears to have driven species evolution (Shaw 2022). Parasitoids require several basic habitat needs, such as a stable host population with sufficient host foodplant presence, shelter and mating sites etc., but parasitoids don't always occur across their entire host insect range due to functional refugia and divisions of space (Shaw 2006), suggesting that the rare *Cryptopimpla* species may either be specialists on hosts with narrow distributional ranges, or alternatively constrained by lack of suitable habitat needs. Nevertheless, the hypothesised potential host polyphagy of *C. rubrithorax* may possibly account for the species' wider distribution, broader habitat association and higher abundance. *Cryptopimpla kogelbergensis* is the only other species to occur in three different vegetation types and is the only species to have been collected from Gamka Thicket, a vegetation type very different to both Fynbos and to Renosterveld in which the species also occurs. Five of the eleven species (*C. rubrithorax*, *C. parslactis*, *C. kogelbergensis*, *C. hantami* and *C. elongatus*) have been collected in the Hantam National Botanical Garden (NBG) in Nieuwoudtville Shale Renosterveld and Nieuwoudtville-Roggeveld Dolerite Renosterveld vegetation (Fig. 2), where sampling effort by Simon van Noort has been high (258 trap months) with many of the Hantam samples processed, suggesting that with further processing of the backlog of the other South African samples present in SAMC a better assessment of distribution will be attained. Hantam NBG, however, is florally extremely rich, particularly with respect to geophytes (Snijman and Perry 1987, van Wyk and Smith 2011), and the high local *Cryptopimpla* species richness at this locality may suggest a host correlation with Lepidoptera species associated with geophytes as their hostplants. Of concern is the fact that Renosterveld is a highly endangered habitat with only 10% left (von Hase et al. 2003; Topp and Loos 2019), threatening the continued survival

of taxa such as the African clade of *Cryptopimpla*. Loss or degradation of Renosterveld and the resultant demise of the host lepidopteran species which are likely to be specific to host plants only occurring in this vegetation type will result in the potential extinction of the associated parasitoids, not to mention the plethora of other invertebrate taxa dependent on this vegetation type. Habitat transformation or even minor degradation of habitat quality (Habel et al. 2023) can have major ramifications for biodiversity conservation (Cardoso et al. 2011, 2019, 2022; Ceballos 2015). Given that only 10% of Renosterveld remains it is likely that we have already lost *Cryptopimpla* species to extinction before we have been able to discover and describe them.

Acknowledgements

Cape Nature, the Eastern Cape Department of Environmental Affairs, and the Northern Cape Department of Nature and Environmental Conservation provided collecting permits. SANParks provided a research permit. SvN was funded by South African NRF (National Research Foundation) grants: GUN 2068865; GUN 61497; GUN 79004; GUN 79211; GUN 81139. Part of the South African field work conducted by SvN was funded by the National Science Foundation under PlatyPBI grant No. DEB-0614764 to N.F. Johnson and A.D. Austin. Thanks to Gavin Broad and Niklas Johansson for their valuable reviews of the manuscript.

Project conceptualization (SvN, TR); funding (SvN); field work (SvN); data curation (TR, SvN); taxonomy – species descriptions and species delimitation assessments (TR, SvN); imaging (TR); figure plates and identification key plate production (TR, SvN); production of identification keys (TR, SvN); manuscript production and editing (TR, SvN).

References

- Broad GR, Shaw MR, Fitton MG (2018) Ichneumonid wasps (Hymenoptera: Ichneumonidae): their classification and biology. Handbooks for the Identification of British Insects 7. Royal Entomological Society, 418 pp.
- Broad GR (2022) Presentation: Large-scale species revisions. Darwin wasp Conference, Öland. July 2022.
- Brock JP (2017) The banchine wasps (Ichneumonidae: Banchinae) of the British Isles. Handbooks for the identification of British insects 7. Royal Entomological Society, 150 pp.
- Cardoso P, Erwin T, Borges P, New T (2011) The seven impediments in invertebrate conservation and how to overcome them. *Biological Conservation* 144: 2647–2655. <https://doi.org/10.1016/j.biocon.2011.07.024>
- Cardoso P, Leather SR (2019) Predicting a global insect apocalypse. *Insect Conservation and Diversity* 12: 263–267. <https://doi.org/10.1111/icad.12367>
- Cardoso P, Barton PS, Birkhofer K, Chichorro F, Deacon C, Fartmann T, Fukushima CS, Gaigher R, Habel JC, Hallmann CA, Hill MJ, Hochkirch A, Kwak ML, Mammola S,

- Noriega JA, Orfinger AB, Pedraza F, Pryke JS, Roque FO, Settele J, Samways MJ (2020) Scientists' warning to humanity on insect extinctions. *Biological Conservation* 242: e108426. <https://doi.org/10.1016/j.biocon.2020.108426>
- Ceballos G, Ehrlich PR, Barnosky AD, García A, Pringle RM, Palmer TM (2015) Accelerated modern human-induced species losses: Entering the sixth mass extinction. *Science Advances* 1(5): e1400253. <https://doi.org/10.1126/sciadv.1400253>
- Gauld ID (1991) The Ichneumonidae of Costa Rica 1. *Memoirs of the American Entomological Institute* 47: 1–589.
- Gauld ID, Gomez J, Godoy C (2002) Subfamily Banchinae. In: Gauld ID (Ed.) *The Ichneumonidae of Costa Rica*, 4. *Memoirs of the American Entomological Institute* 66: 263–746.
- Habel J, Schmitt T, Gros P, Ulrich W (2023) Breakpoints in butterfly decline in Central Europe over the last century. *Science of The Total Environment* 851: e158315. <https://doi.org/10.1016/j.scitotenv.2022.158315>
- Holmgren AE (1860) Forsök till uppställning och beskrifning af Sveriges Ichneumonider. Tredje Serien. Fam. Pimplariae. (Monographia Pimpliarum Sueciae). *Kongliga Svenska Vetenskapsakademiens Handlingar* 3: 1–76.
- Kang GW, Kolarov J, Lee JW (2019) *Cryptopimpla* (Hymenoptera, Ichneumonidae, Banchinae) of South Korea, with description of two new species. *ZooKeys* 830: 99–109. <https://doi.org/10.3897/zookeys.830.31974>
- Kuslitzky WS (2007) 12. Subfamily Banchinae. In: Lelej AS (Ed.) *A Key to the Insects of Russian Far East* (Vol. 4). Neuropteroidea, Mecoptera, Hymenoptera. Part 5.: Dal'nauka, Vladivostok 433–472. [in Russian]
- Linder HP (2003) The radiation of the Cape flora, southern Africa. *Biological Reviews* 78: 597–638. <https://doi.org/10.1017/S1464793103006171>
- Myers N, Mittermeier RA, Mittermeier CG, da Fonseca GAB, Kent J (2000) Biodiversity hotspots for conservation priorities. *Nature* 403 (6772): 853–858. <https://doi.org/10.1038/35002501>
- Momoi S, Sugawara H, Honma K (1975) Ichneumonid and Braconid parasites of Lepidopterous leaf-rollers of economic importance in horticulture and teaculture. In: Yasumatsu K, Mori H (Eds) *Approaches to Biological Control* 7: 47–60.
- Penev L, Sharkey M, Erwin T, van Noort S, Buffington M, Seltmann K, Johnson N, Taylor M, Thompson C, Dallwitz M (2009) Data publication and dissemination of interactive keys under the open access model. *ZooKeys* 21: 1–17. <https://doi.org/10.3897/zookeys.21.274>
- Quicke DLJ (2015) *The braconid and ichneumonid parasitoid wasps: Biology, systematics, evolution and ecology*. Wiley Blackwell: 1–704. <https://doi.org/10.1002/9781118907085>
- Reynolds Berry T (2019) Systematics of the parasitoid wasp subfamily Banchinae (Hymenoptera; Ichneumonidae) in the Afrotropical region. PhD thesis. Stellenbosch University (South Africa). <http://hdl.handle.net/10019.1/106917>
- Reynolds Berry T, van Noort S (2016) Review of Afrotropical *Cryptopimpla* Taschenberg (Hymenoptera, Ichneumonidae, Banchinae), with description of nine new species. *Zookeys* 640: 103–137. <https://doi.org/10.3897/zookeys.640.10334>
- Reynolds Berry T, van Noort S (2020) Revision of the endemic Afrotropical genus *Tetractenion* (Hymenoptera, Ichneumonidae) with an identification key to genera of Banchinae for the region. *ZooKeys* 1007: 49–84. <https://doi.org/10.3897/zookeys.1007.55543>

- Sharkey M, Yu D, van Noort S, Seltmann K, Penev L (2009) Revision of the Oriental genera of Agathidinae (Hymenoptera, Braconidae) with an emphasis on Thailand and interactive keys to genera published in three different formats. *ZooKeys* 21: 19–54. <https://doi.org/10.3897/zookeys.21.271>
- Shaw M (2006) Habitat considerations for parasitic wasps (Hymenoptera). *Journal of Insect Conservation* 10: 117–127. <https://doi.org/10.1007/s10841-006-6288-1>
- Shaw MR (2022) Host ranges of *Aleiodes* species (Hymenoptera: Braconidae), and an evolutionary hypothesis. In: Melika G, Thuróczy C (Eds) *Parasitic Wasps: Evolution, Systematics, Biodiversity and Biological Control*. Agroiinform, Budapest, 321–327.
- Sheng ML (2011) Five new species of the genus *Cryptopimpla* Taschenberg (Hymenoptera, Ichneumonidae) with a key to species known from China. *ZooKeys* 117: 9–49. <https://doi.org/10.3897/zookeys.117.1302>
- Sheng ML, Zheng H (2005) The genus *Cryptopimpla* from China (Hymenoptera, Ichneumonidae). *Acta Zootaxonomica Sinica* 30: 415–418.
- Shorthouse DP (2010) SimpleMappr, an online tool to produce publication-quality point maps. <https://www.simplemappr.net> [Accessed 2022/07/28]
- Snijman D, Perry P (1987) A floristic analysis of the Nieuwoudtville Wild Flower Reserve, north-western Cape. *South African Journal of Botany* 53: 445–454. [https://doi.org/10.1016/S0254-6299\(16\)31378-3](https://doi.org/10.1016/S0254-6299(16)31378-3)
- Takasuka K, Watanabe K, Konishi K (2011) Genus *Cryptopimpla* Taschenberg new to Sulawesi, Indonesia, with description of a new species (Hymenoptera, Ichneumonidae, Banchinae). *Journal of Hymenoptera Research* 23: 65–75. <https://doi.org/10.3897/jhr.23.1595>
- Taschenberg EL (1863) Die Schlupfwespenfamilie Pimplariae der deutschen Fauna, mit besonderer Rücksicht auf die Umgegend von Halle. *Zeitschrift für die Gesamten Naturwissenschaften* 21: 245–305.
- Topp EN, Loos J (2019) Fragmented landscape, fragmented knowledge: a synthesis of renostrveld ecology and conservation. *Environmental Conservation* 46: 171–179. <https://doi.org/10.1017/S0376892918000498>
- Townes HK (1969) Genera of Ichneumonidae, Part 3 (Lycorininae, Banchinae, Scolobatinae, Porizontinae). *Memoirs of the American Entomological Institute* 13: 1–307.
- Townes HK, Townes M (1978) Ichneumon-flies of America north of Mexico: 7. Subfamily Banchinae, tribes Lissonotini and Banchini. *Memoirs of the American Entomological Institute* 26: 1–614.
- van Noort S (2019) Assessing the status quo of Afrotropical ichneumonid knowledge. Conference: identifying the next challenges in ichneumonid systematics and evolutionary ecology. Basel, Sweden, 24–29 June 2019. <https://doi.org/10.5281/zenodo.3395821>
- van Noort S (2022) Keynote presentation: Darwin wasps for Africa: Status quo of Afrotropical Ichneumonidae. #HYMATHON2022 A 24-hour virtual symposium from the International Society of Hymenopterists. 31 March–1 April 2022.
- van Noort S (2023a) WaspWeb: Hymenoptera of the Afrotropical region. www.waspweb.org [Accessed on 24 March 2023]
- van Noort S (2023b) Thirty years of sampling effort and status quo of African Darwin wasp diversity (Ichneumonidae, Hymenoptera). 23rd Congress of the Entomological Society of Southern Africa (ESSA), 12–14 July 2023, Stellenbosch University, Stellenbosch, South Africa.

van Wyk AE, Smith GF (2001) Regions of floristic endemism in southern Africa: A review with emphasis on succulents. Umdaus Press (Hatfield, South Africa), 199 pp.

Von Hase A, Rouget M, Maze K, Helme N (2003) A fine-scale conservation plan for Cape lowlands renosterveld: technical report. Report CCU [www document]. <http://bgis.sanbi.org/cfr>

Wahl DB, Sharkey MJ (1993) Chapter 10. Superfamily Ichneumonoidea. In: Goulet H, Huber JT (Eds) Hymenoptera of the World: An Identification Guide to Families. Agriculture Canada: 358–509.

Yu DSK, van Achterberg C, Hortsman K (2016) Taxapad 2016, Ichneumonidae 2011. www.taxapad.com [Accessed on 30/11/2018]

Supplementary material 1

The output of *Cryptopimpla* (Ichneumonidae, Hymenoptera) specimen data digitized into the Iziko South African Museum Specify 6 database provided as a supplementary excel file

Authors: Terry Reynolds, Simon van Noort

Data type: xls

Copyright notice: This dataset is made available under the Open Database License (<http://opendatacommons.org/licenses/odbl/1.0/>). The Open Database License (ODbL) is a license agreement intended to allow users to freely share, modify, and use this Dataset while maintaining this same freedom for others, provided that the original source and author(s) are credited.

Link: <https://doi.org/10.3897/jhr.96.104038.suppl1>

Supplementary material 2

Lucid Interchange Format version 3 (LIF3) files to the WaspWeb online Lucid matrix identification key to Afrotropical species of *Cryptopimpla* (Ichneumonidae, Hymenoptera)

Authors: Terry Reynolds, Simon van Noort

Data type: lif3

Explanation note: The LIF3 file is an XML-based file that stores all the Lucid3 key data, allowing exchange of the key with other key developers.

Copyright notice: This dataset is made available under the Open Database License (<http://opendatacommons.org/licenses/odbl/1.0/>). The Open Database License (ODbL) is a license agreement intended to allow users to freely share, modify, and use this Dataset while maintaining this same freedom for others, provided that the original source and author(s) are credited.

Link: <https://doi.org/10.3897/jhr.96.104038.suppl2>

Additions to the knowledge of the genus *Eumenes* Latreille, 1802 from China (Hymenoptera, Vespidae, Eumeninae)

Jiong Qin¹, Bin Chen¹, Ting-Jing Li¹

¹ Chongqing Key Laboratory of Vector Insects, Institute of Entomology and Molecular Biology, Chongqing Normal University, Chongqing 401331, China

Corresponding author: Ting-Jing Li (ltjing1979@hotmail.com)

Academic editor: Michael Ohl | Received 8 June 2023 | Accepted 21 July 2023 | Published 31 August 2023

<https://zoobank.org/D5020B71-C940-4F41-88CA-31E31D492DC1>

Citation: Qin J, Chen B, Li T-J (2023) Additions to the knowledge of the genus *Eumenes* Latreille, 1802 from China (Hymenoptera, Vespidae, Eumeninae). Journal of Hymenoptera Research 96: 697–714. <https://doi.org/10.3897/jhr.96.107701>

Abstract

In this paper one new species namely *Eumenes ferruapiculus* **sp. nov.**, from Yunnan (China) is described and illustrated in detail. In addition, *E. affinis* de Saussure, 1852, *E. aquilonius* Yamane, 1977, *E. belli* Giordani Soika, 1973, *E. gibbosus* Nguyen, 2015, and *E. rubrofemoratus* Giordani Soika, 1941 are newly recorded from China. An updated key to the Chinese species of the genus *Eumenes* is provided.

Keywords

China, *Eumenes*, Eumeninae, Hymenoptera, new record, new species

Introduction

The genus *Eumenes* Latreille, 1802 with 107 species and 43 subspecies is one of the largest genera of the subfamily Eumeninae, widely distributed in the Palearctic, Oriental, Australian, Ethiopian, Nearctic and Neotropical regions (Girish Kumar et al. 2017). In early studies on the genus *Eumenes*, Giordani Soika (1940, 1941, 1960), Yamane (1977a, b), Kim and Yamane (2001) researched and made some revisions of the genus from Far East Asia. Then, Nguyen (2015) and Girish Kumar et al. (2017) reviewed it from Vietnam and India, respectively. In our study on the genus *Eumenes*

from China, Zhou et al. (2012) described two new species of *Eumenes* and provided a key to ten species in this genus from Southwestern China, but did not include all the known species yet. In our follow-up study of Chinese eumenids, a total of 31 species and 7 subspecies of the genus *Eumenes* were recognized, containing one new species and five new records. In the present paper, the new species is described and illustrated in detail, and the new records are provided with diagnoses and illustrations. Based on the specimens and related literature, a key to all the known Chinese species of *Eumenes* is given.

Material and method

Examined specimens are deposited in the Institute of Entomology and Molecular Biology, Chongqing Normal University, Chongqing, China (CNU). Descriptions and measurements were made under a Nikon SMZ1500 stereomicroscope, and all figures were taken with a Leica EX4HD stereomicroscope attached to a computer using the Leica Application Suite version 2.1.0 software. Body length was measured from the anterior margin of the head to the posterior margin of metasomal tergum 2. For the density description of punctures, “sparsely” means that interspaces are larger than one puncture diameter, “moderately” means equal to the diameter, and “densely” means less than one diameter. The abbreviations used in the text are as follows: A (1, 2, ...) for antennal segments, T (1, 2, ...) for metasomal terga, S (1, 2, ...) for metasomal sterna, OOL for ocellocular distance, and POL for post ocellar distance.

Taxonomy

Genus *Eumenes* Latreille, 1802

Eumenes Latreille, 1802: 360; Giordani Soika 1941: 131; Yamane 1997a: 14; Kim and Yamane 2001: 139; Zhou et al. 2012: 467; Nguyen 2015: 564; Girish Kumar et al. 2017: 469; Tan et al. 2018: 139.

Type species. *Vespa coarctata* Linnaeus, 1758 “*Eumenes coarctata*, Fab.” [= *Vespa coarctata* Linnaeus, 1758], by subsequent designation of Latreille, 1810: 438.

Diagnosis. Cephalic fovea absent (Figs 5, 15, 25, 42, 52) in both sexes; clypeus emarginate both basally and apically (Figs 3, 4, 13, 14, 23, 24, 32, 40, 41, 50, 51); pronotal carina lacking (Figs 5, 15, 25, 36, 42, 52); tegula short, convex and not equalling parategula posteriorly; both pretegular carina and epicnemial carina absent; propodeal orifice with a pair of processes which are easily observed when the first metasomal segment is removed; metasomal segment 1 elongate and petiolate, and bulged apically (Figs 9, 19, 29, 35, 44, 56); T2 with a well-developed lamella at apical margin (Figs 7, 20, 30, 37, 47, 57); fore coxa with a well-developed carina on its outer face; A13 of

male antenna hook-like and apically pointed (Figs 6, 16, 26, 43, 53); parameral spine of male genitalia with a bundle of setae at its mid length (Kim and Yamane 2001).

Distribution. Worldwide.

Key to all the known Chinese species of the genus *Eumenes*

- 1 Metasomal segment 1 more than 4× as long as apical width (Fig. 35) **2**
- Metasomal segment 1 less than 4× as long as apical width (Figs 9, 19, 29, 44, 56)..... **7**
- 2 T1 abruptly swollen at 1/2 or 1/3 from base..... **3**
- T1 gradually widened from base to apex (fig. 7 in Nguyen 2015) **4**
- 3 T1 not pear-shaped, two lateral margins of postpetiole substraight and parallel (Fig. 35) ***E. belli* Giordani Soika, 1973**
- T1 pear-shaped, two lateral margins of postpetiolus not substraight and parallel (fig. 20 in Girish Kumar et al. 2017) ***E. atrophicus* (Fabricius, 1798)**
- 4 Apical lamella of T2 not reflex, with small and sparse punctures at lateral side and apex (figs 10, 18 in Nguyen 2015)..... ***E. multipictus* de Saussure, 1855**
- Apical lamella of T2 reflex, with large and dense punctures at lateral side and apex (figs 7, 9 in Nguyen 2015)..... ***E. quadratus* Smith (5)**
- 5 T2 black at apex ***E. q. obsoletus* Dover, 1926**
- T2 with yellow band at apex..... **6**
- 6 A long band on pronotum (figs 12–14 in Li et al. 2019).....
- ***E. q. quadratus* Smith, 1852**
- A short band on pronotum (in Sonan 1939)..... ***E. q. urainus* Sonan, 1939**
- 7 Setae on postgena and propleuron shorter than those on head (fig. 7 in Kim and Yamane 2001) ***E. transbaicalicus* Kurzenko, 1984**
- Setae on postgena and propleuron equal to or longer than those on head (fig. 10 Kim and Yamane 2001) **8**
- 8 T1 with sparse punctures in the middle, interspaces larger than diameter of punctures (fig. 8 in Nguyen 2015)..... **9**
- T1 with dense punctures in the middle, interspaces smaller than diameter of punctures..... **14**
- 9 Basal angle of metasomal segment 2 acute (fig. 51 in Kim and Yamane 2001)..... ***E. kiangsuensis* Giordani Soika, 1941**
- Basal angle of metasomal segment 2 obtuse..... **10**
- 10 T1 with transverse groove at apex, with preapical bulge (fig. 6 in Giordani Soika 1941) ***E. tosawae* Giordani Soika (11)**
- T1 without transverse groove at apex, without preapical bulge (fig. 8 in Nguyen 2015) ***E. labiatus* Giordani Soika (12)**
- 11 T1 with wide yellow band at apex, without depression in the middle of the band ***E. t. tosawae* Giordani Soika, 1941**
- T1 with narrow yellow band at apex, with two depressions in the middle of the band ***E. t. lofouensis* Giordani Soika, 1973**

12	Body with maculation ferruginous.....	<i>E. l. labiatus</i> Giordani Soika, 1941	
–	Body with maculation bright yellow		13
13	T2 with a pair of small lateral spots	<i>E. l. sinicus</i> Giordani Soika, 1941	
–	T2 without a pair of small lateral spots	<i>E. l. flavoniger</i> Giordani Soika, 1986	
14	T2 bright yellow, with three connected or separated black spots in the middle	<i>E. tripunctatus</i> (Christ, 1791)	
–	T2 black, without three connected or separated black spots in the middle.....		15
15	T2 with sparse punctures		16
–	T2 with dense punctures.....		19
16	Punctures on T2 equal to or larger than those on T1		17
–	Punctures on T2 smaller than those on T1.....		18
17	Metasomal segments almost without setae except for the first two	<i>E. variepunctatus</i> Giordani Soika, 1941	
–	Metasomal segments with white short setae	<i>E. architectus</i> Smith, 1859	
18	T1 stumpy, apical width more than 3× as long as basal one; T2 almost without setae (fig. 16 in Kim and Yamane 2001).....	<i>E. fraterculus</i> Dalla Torre, 1894	
–	T1 slender, apical width less than 3× as long as basal one; T2 with long setae (Fig. 19).....	<i>E. affinissimus</i> de Saussure, 1852	
19	Basal angle of metasomal segment 2 acute.....		20
–	Basal angle of metasomal segment 2 obtuse.....		25
20	Punctures on T2 smaller than those on mesosoma		21
–	Punctures on T2 equal to or larger than those on mesosoma.....		24
21	Lateral margin of T1 constrict at apex (fig. 32 in Kim and Yamane 2001)	<i>E. pedunculatus</i> (Panzer, 1799)	
–	Lateral margin of T1 parallel or expansile at apex.....		22
22	Clypeus with long setae, longer than scape width.....	<i>E. fulvopilosellus</i> Giordani Soika, 1965	
–	Clypeus with short setae, shorter than scape width (Fig. 51)		23
23	Lateral view, T1 swollen upwards near apical margin (fig. 25 in Kim and Yamane 2001).....	<i>E. rubrofemoratus</i> Giordani Soika, 1941	
–	Lateral view, T1 flat near apical margin (fig. 12 in Kim and Yamane 2001).....	<i>E. mediterraneus manchurianus</i> Giordani Soika, 1971	
24	Lateral margin of T1 constrict at apex; metasomal segments 3–6 with yellow bands at apex (figs 31, 35 in Girish Kumar et al. 2017)	<i>E. kangrae</i> Dover, 1925	
–	Lateral margin of T1 parallel at apex; metasomal segments 3–6 ferruginous (Figs 8, 9)	<i>E. ferruapiculus</i> sp. nov.	
25	Punctures on T2 smaller than those on mesosoma		26
–	Punctures on T2 equal to or larger than those on mesosoma.....		29
26	T2 with transverse wrinkles in its preapical part (Fig. 28)	<i>E. aquilonius</i> Yamane, 1977	
–	T2 without transverse wrinkles in its preapical part		27

- 27 Apical width of T1 more than 3× as long as basal one.....
*E. septentrionalis* Giordani Soika, 1940 (28)
- Apical width of T1 less than 3× as long as basal one.....
*E. formosensis* Giordani Soika, 1941
- 28 Tibiae ferruginous.....*E. s. khangmarensis* Giordani Soika, 1966
- Tibiae black, with yellow band.....*E. s. septentrionalis* Giordani Soika, 1940
- 29 Lateral margin of T1 constrict at apex..... 30
- Lateral margin of T1 parallel or expansile at apex..... 34
- 30 Apical width of T1 more than 3× as long as basal one..... 31
- Apical width of T1 less than 3× as long as basal one..... 33
- 31 T2 swollen in the middle, depressed in its preapical part..... 32
- T2 normal in the middle, flat in its preapical part.....
*E. coarctatus coarctatus* (Linnaeus, 1758)
- 32 Apical lamella of T2 not depressed in the middle (fig. 13, in Girish Kumar et al. 2017) *E. assamensis* Meade-Waldo, 1910
- Apical lamella of T2 depressed in the middle*E. rubronotatus* Pérez, 1905
- 33 T2 swollen in the middle, depressed in its preapical part (Fig. 46)
*E. gibbosus* Nguyen, 2015
- T2 normal in the middle, flat in its preapical part.....
*E. ferrugiantennus* Zhou, Chen & Li, 2012
- 34 S2 with setae as long as those on head (fig. a in Smit 2005)
*E. coronatus coronatus* (Panzer, 1799)
- S2 with setae shorter those on head (fig. b in Smit 2005)..... 35
- 35 T2 swollen at apex, with transverse groove in its preapical part (figs 21, 22 in Zhou et al. 2012).....*E. nigriscutatus* Zhou, Chen & Li, 2012
- T2 normal at apex, without transverse groove in its preapical part 36
- 36 T1 abruptly swollen at 1/2 from base..... 37
- T1 abruptly swollen at 1/3 from base..... *E. punctatus* de Saussure, 1852
- 37 Apical lamella of T2 not depressed in the middle.....
*E. pomiformis* (Fabricius, 1781)
- Apical lamella of T2 depressed in the middle*E. buddha* Cameron, 1897

***Eumenes ferruapiculus* Qin, Chen & Li, sp. nov.**

<https://zoobank.org/FB87AB7F-16B7-49C9-AA64-8AB56D2CB9FB>

Figs 1–10

Material examined. *Holotype*, ♀, CHINA, Yunnan Province, Diqing Tibetan Autonomous Prefecture, Deqin County, Benzilan Town, 29°34'08"N, 106°33'28"E, 3400 m, 2011.vii.21, Ting-Jing Li (CNU); *Paratype*, 2♀1♂, same data as holotype.

Diagnosis. This species is similar to *E. labiatus* by the following character combination: T1 with pear-shaped, two lateral margins of postpetiole substraight and parallel from basal third to apex (Fig. 9). It is easily distinguished from the related species and

other members of the genus by the combination of following characters: head and antennal scape with dense setae about as long as scape width (Fig. 3), basal angle of metasomal segment 2 acute, T1 and T2 black, other metasomal segments almost ferruginous (Fig. 7), and apex of penis valves convex in genitalia (Fig. 10) (depressed in *E. labiatus*).

Description. Female (Fig. 1): body length 14.2–15.6 mm. Body black, with dense and short setae, with following parts ferruginous: clypeus (Fig. 3), mandible except base, antenna except small spots of A1 and A2, lower margin of ocular sinus, inter-antennal spot reaching clypeus, a band on upper gena (Fig. 5), pronotum (Fig. 5), tegula, apex of parategula, tibiae and tarsi (Fig. 1), apical thin and interrupted band on T2, and visible parts of metasomal segments 3–6 (Figs 12, 14); wing mostly ferruginous brown.

Head. Head (Fig. 3) wider than long in frontal view, maximum width of head $1.12\times$ its length; clypeus with punctures denser at base than other part, clypeal maximum width $1.10\times$ its length, slightly convex, apex emarginate forming two wide lateral teeth, apical width $1.57\times$ distance between antennal sockets; inter-antennal area with longitudinal carina; scape with dense setae shorter than scape width; frons coarsely punctate and distinctly reticulated, punctures on vertex and gena similar to those of frons; POL $0.91\times$ OOL; distance between anterior and posterior ocelli $1.1\times$ diameter of anterior ocellus (Fig. 5).

Mesosoma. Mesosoma (Fig. 5) with short and dense setae as long as those on head, wholly with coarse and dense punctures similar to or denser than those on vertex, those on mesoscutum and mesopleuron a little denser and reticulate; median length of mesoscutum $1.02\times$ its maximum width; propodeum with median longitudinal groove.

Metasoma. (Figs 7–9). Metasoma with sparse setae shorter than those on mesosoma; T1 densely punctate, punctures similar to those on mesoscutum, length of T1 less than $4\times$ its apical width and abruptly swollen from one-third near base, then lateral margin parallel at apex, and not constrict near apical margin (Fig. 9); T2 densely punctate, punctures obviously smaller than those of T1, apical lamella of T2 not reflex and not depressed in the middle (Fig. 7); basal angle of segment 2 acute in lateral view (Fig. 8); T2 not strongly swollen in the middle, weakly depressed in its preapical part; visible parts of other metasomal segments normal, with sparse short setae (Fig. 8).

Male. Body length 11.1 mm (Fig. 2). Sculpture, setae, and coloration similar to female except as follows: clypeus entirely yellow (Fig. 4), apex of A13 reaching basal fourth of A11 (Fig. 6), apex of penis valves convex in genitalia (Fig. 10).

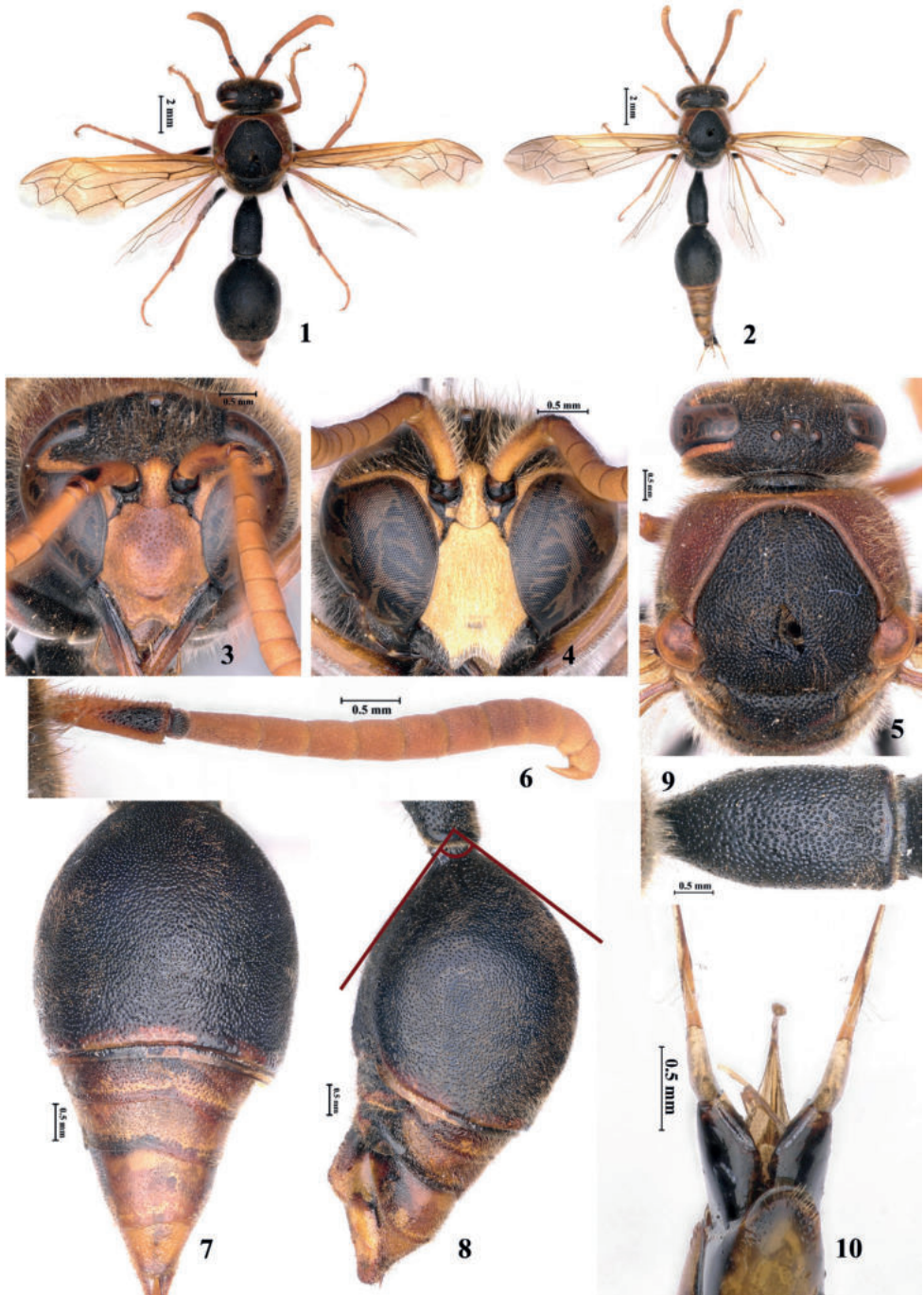
Distribution. China (Yunnan).

Etymology. The specific name *ferruapiculus* is derived from two Latin words: *ferrugineus* (= ferruginous) and *apex*, referring to ferruginous apex of metasoma.

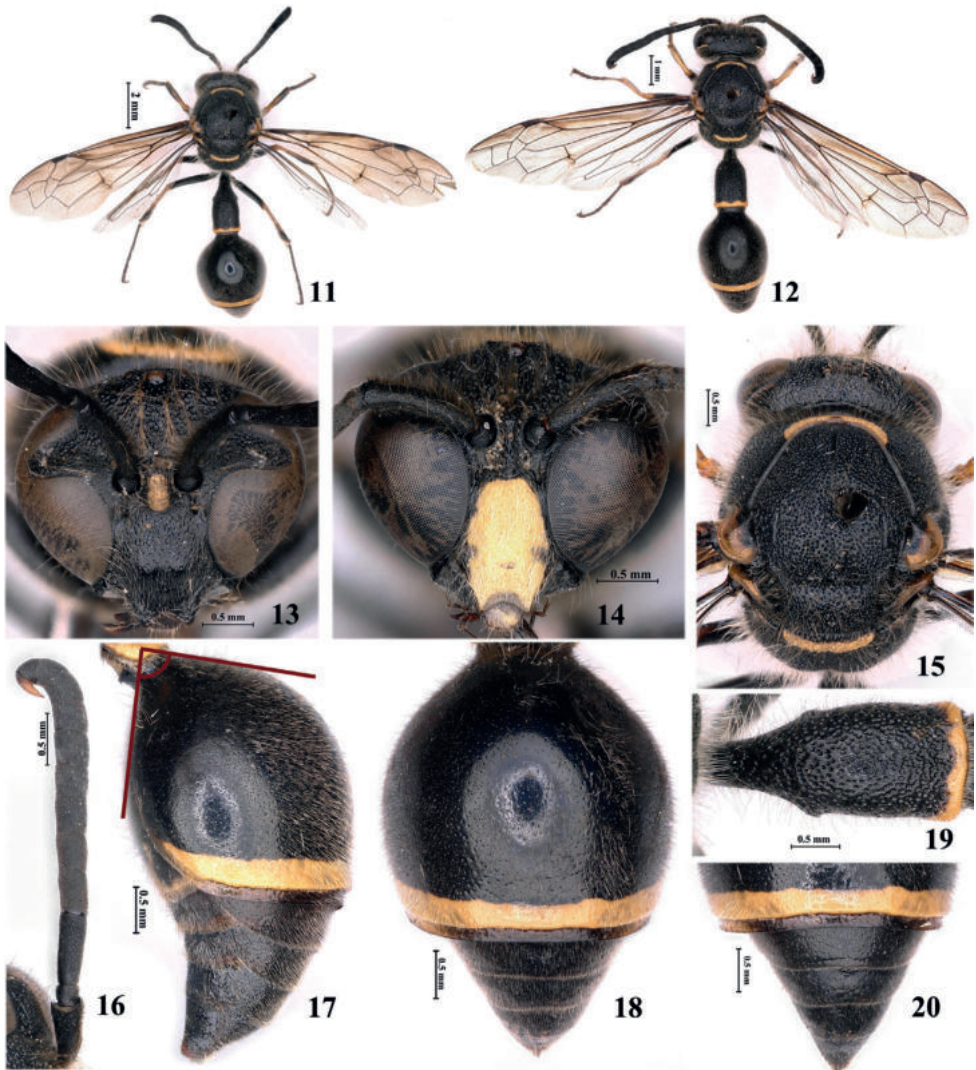
Eumenes affinissimus de Saussure, 1852, new record

Figs 11–20

Eumenes affinissima de Saussure, 1852: 37; Smith 1873: 371; Bingham 1897: 335, 340; Paiva 1907: 15; Dutt 1912: 229; Dover and Rao 1922: 237; Dover 1925



Figures 1–10. *Eumenes ferruapiculus* sp. nov. holotype (♀) (1, 3, 5, 7–9) paratype (♂) (2, 4, 6, 10) 1, 2 habitus (dorsal view) 3, 4 clypeus (frontal view) 5 head and pronotum (dorsal view) 6 antenna 7 T2–T6 (dorsal view) 8 metasomal segments 2–6 (lateral view) 9 T1 (dorsal view) 10 genitalia.



Figures 11–20. *Eumenes affinissimus* de Saussure, 1852. ♀: 11, 13, 15, 17–20 ♂: 12, 14, 16. 11, 12 habitus (dorsal view) 13, 14 clypeus (frontal view) 15 head and pronotum (dorsal view) 16 antenna 17 metasomal segments 2–6 (lateral view) 18 T2 (dorsal view) 19 T1 (dorsal view) 20 lamella of T2 apical margin (dorsal view).

(1924): 292; von Schulthess 1935: 299; Giordani Soika 1960: 159; Gusenleitner 2006: 693; Girish Kumar et al. 2017: 471; Fateryga et al. 2023: 447.

? *Eumenes pomiformis* var. *affinissima*: Maindron, 1882: 268; Dalla Torre 1894: 30; 1904: 24; Dover 1931: 252.

Eumenes coelestimontana Kostylev, 1940: 140; Gusenleitner 1972: 71, 87; van der Vecht and Fischer 1972: 126; Gusenleitner 2006: 693.

Material examined. 1♂, CHINA, Tibet, Linzhi City, Bomi County, Yigong Village, 29°34'08"N, 106°33'28"E, 3300 m, 2014.viii.1, Ting-Jing Li (CNU); 3♀6♂,

CHINA, Gansu Province, Zhangye City, Sunan County, 36°40'40"N, 102°25'19"E, 3200 m, 2019.vii.2, Xue Zhang (CNU); 1♂, CHINA, Ningxia Province, Guyuan City, Jingyuan County, Shan'an Village, 35°26'49"N, 106°25'37"E, 1778 m, 2020.vii.30, Qian Han (CNU).

Diagnosis. Female. Body length 10.3–11.4 mm. Body black, with yellow markings (Fig. 11): interantennal spot reaching clypeus, gena, pronotum anteriorly, band of metanotum, tegula mostly (Fig. 15), fore tibia largely, and apical bands of T1 and T2; body with setae dense and long, those on head longer than scape width; clypeus entirely black, longer than wide, with long setae (Fig. 13); dorsal view (Figs 18, 19), T1 densely punctate, length of T1 less than 4× its apical width and abruptly swollen from one-third near base, then lateral margin parallel at apex, and not constrict near apical margin; T2 sparsely punctate, punctures obviously smaller than those of T1, apical lamella of T2 not reflex, and not depressed in the middle (Fig. 20); basal angle of segment 2 acute in lateral view (Fig. 17), T2 not strongly swollen in the middle, weakly depressed in its preapical part; and wings pale brown.

Male. Body length 8.6–9.7 mm (Fig. 12). Sculpture, setae, and coloration similar to female except as follows: clypeus yellow except lateral margin (Fig. 14); apex of A13 reaching basal fourth of A10 (Fig. 16).

Distribution. China (Tibet, Gansu, Ningxia); Pakistan; Tajikistan; Uzbekistan; Kyrgyzstan; Kazakhstan; Mongolia; India; Bangladesh; Myanmar; Malaysia; Indonesia: Java.

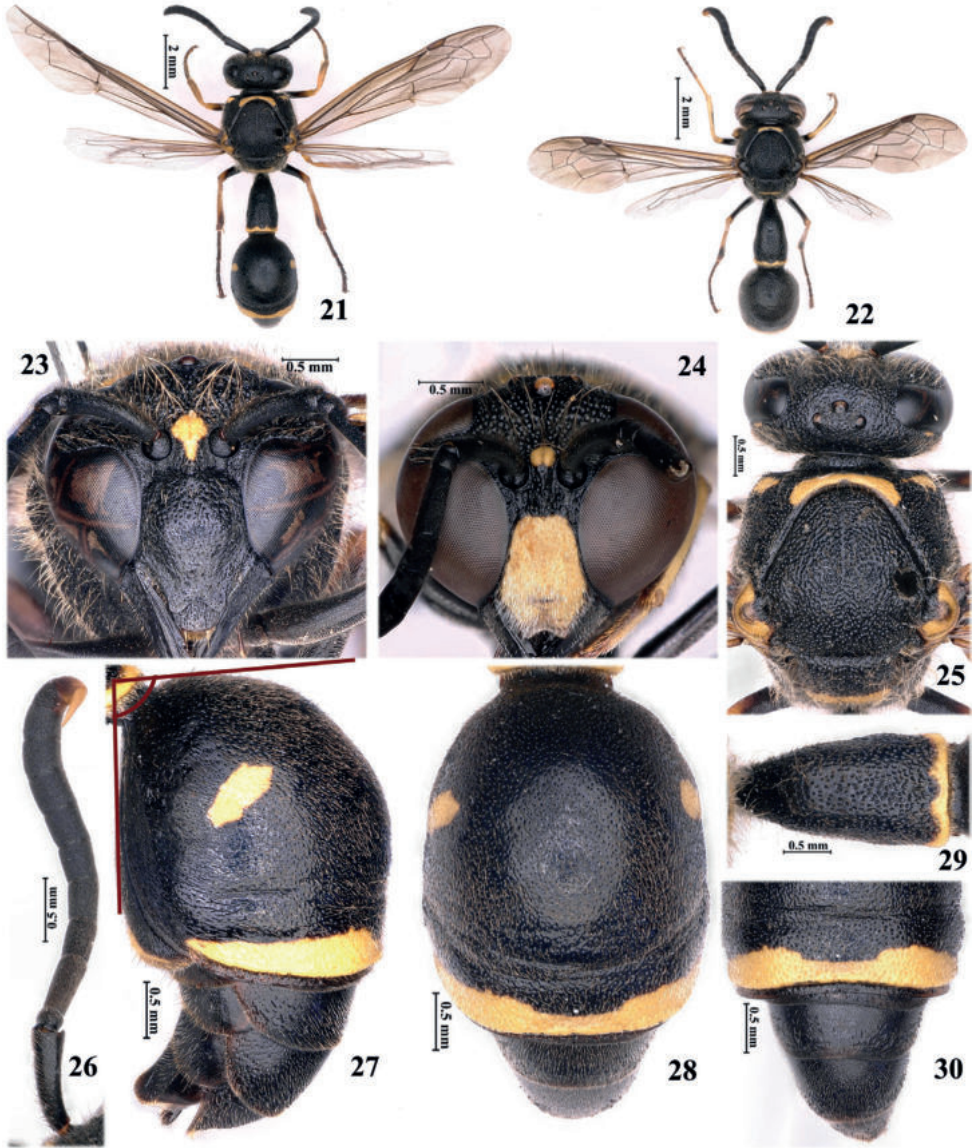
Eumenes aquilonius Yamane, 1977, new record

Figs 21–30

Eumenes rubronotatus aquilonius Yamane, 1977b: 59; 1990: 148; Kurzenko 1995: 321.
Eumenes aquilonius: Kim and Yamane 2001: 139, 143, 153; Yoon and Kim 2014: 234.

Material examined. 2♀, CHINA, Inner Mongolia, Alxa League, Ho-lan Mountains, 38°58'08"N, 105°51'32"E, 2000 m, 2010.vii.29, Fangzhou Ma (CNU); 1♂, CHINA, Jilin Province, Linjiang City, Naozhi Town, 38°12'50"N, 105°24'07"E, 510 m, 2012.vii.8, Xin Zhou (CNU); 2♀, CHINA, Sichuan Province, Guangyuan City, Qingchuan County, Qingxi Town, Pingqiao Village, 32°28'51"N, 104°51'36"E, 1200 m, 22.VII.2018, Xue Zhang (CNU); 1♀1♂, CHINA, Sichuan Province, Langzhong City, Boshu Hui Autonomous County, Qingzhen Village, 31°33'54"N, 106°03'36"E, 608 m, 2020.vii.18, Jie Chen (CNU); 1♀, CHINA, Sichuan Province, Chengdu City, Dayi County, Xieyuan Town, 30°37'12"N, 103°20'49"E, 500 m, 2018.viii.13, Huachan Wang (CNU); 1♂, CHINA, Shanxi Province, Hanzhong City, Nanzhen County, Hongmiao Town Qunfu Village, 32°47'38"N, 106°54'14"E, 484 m, 2017.vii.16, Pan Huang (CNU).

Diagnosis. Female. Body length 9.6–10.4 mm; black, with yellow markings (Fig. 21): interantennal spot, gena, lateral side of pronotum, pronotum anteriorly, band of metanotum, tegula mostly (Fig. 25), fore tibia largely, apical bands of both T1



Figures 21–30. *Eumenes aquilonius* Yamane, 1977. ♀ (21, 23, 25, 27–30) ♂ (22, 24, 26) 21, 22 habitus (dorsal view) 23, 24 clypeus (frontal view) 25 head and pronotum (dorsal view) 26 antenna 27 metasomal segments 2–6 (lateral view) 28 T2 (dorsal view) 29 T1 (dorsal view) 30 lamella of T2 apical margin (dorsal view).

and T2, and lateral spots of T2; body with setae sparse and short, those on head longer than scape width; clypeus entirely black, longer than wide, with short setae (Fig. 23); dorsal view (Figs 28, 29), T1 densely punctate, length of T1 less than 4× its apical width and abruptly swollen before middle; T2 sparsely punctate, punctures obviously

smaller than those of T1, apical lamella of T2 not reflex and weakly depressed in the middle (Fig. 30); lateral view (Fig. 27), basal angle of metasomal segment 2 obtuse, T2 swollen in the middle, with transverse wrinkles and weakly depressed in its preapical part; wings pale brown.

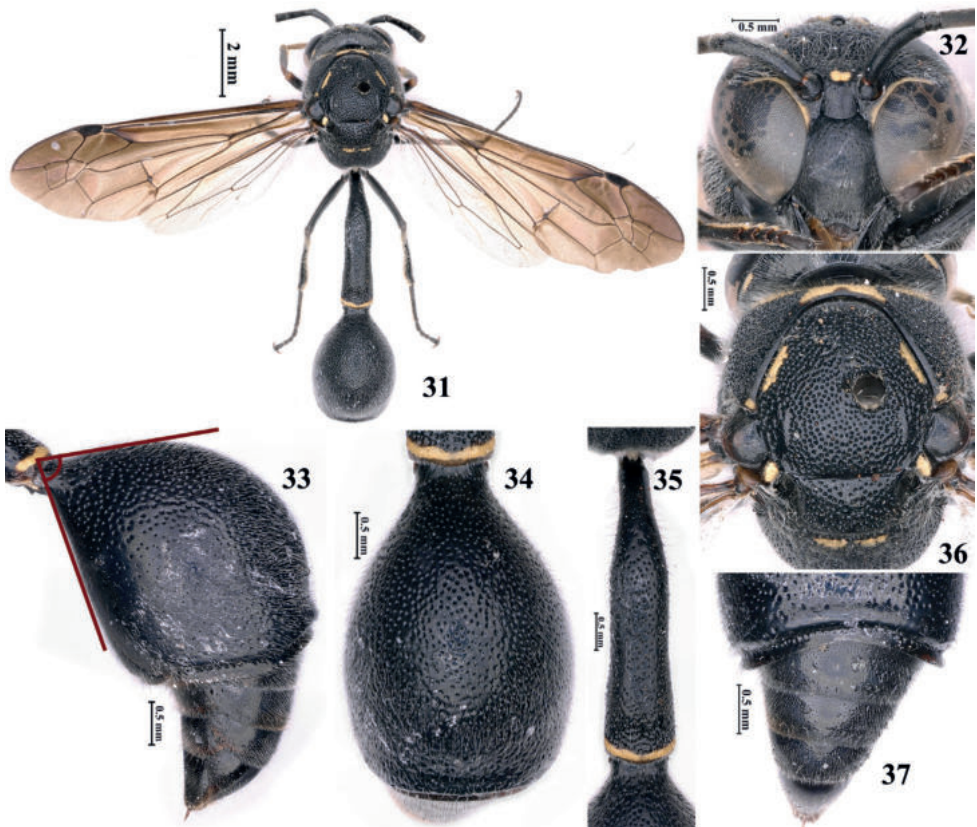
Male. Body length 7.8–8.4 mm (Fig. 22). Sculpture, setae, and coloration similar to female except as follows: clypeus entirely yellow (Fig. 24); apex of A13 reaching basal fourth of A10 (Fig. 26).

Distribution. China (Inner Mongolia, Jilin, Sichuan, Shanxi); Russia; Korea; Japan.

Eumenes belli Giordani Soika, 1973, new record

Figs 31–37

Eumenes belli Giordani Soika, 1973: 125; 1986a: 82; Girish Kumar et al. 2017: 477.



Figures 31–37. *Eumenes belli* Giordani Soika, 1973. ♀ **31** habitus (dorsal view) **32** clypeus (frontal view) **33** metasomal segments 2–6 (lateral view) **34** T2 (dorsal view) **35** T1 (dorsal view) **36** head and pronotum (dorsal view) **37** lamella of T2 apical margin (dorsal view).

Material examined. 1♀, CHINA, Yunnan Province, Lincang City, Shuangjiang County, Mengling Village, Nangong River, 23°23'13"N, 99°47'04"E, 1050 m, 2019.vi.3, Huachuan Wang (CNU).

Diagnosis. Female. Body length 12.1 mm. Body black, with yellow markings (Fig. 31): ocular sinus, interantennal spot, gena, three separated narrow transverse bands on pronotum, mesoscutum spot, metanotum separated spots, parategula (Fig. 36) and apical band of T1; body with setae sparse and short; clypeus entirely black, sparsely punctate, longer than wide, with short setae (Fig. 32); dorsal view (Figs 34, 35), T1 densely punctate, very long, slender, length of T1 longer than 4× its apical width and abruptly swollen before middle, lateral margins of postpetiole substraight and parallel, not swollen in apical part; T2 densely punctate, punctures obviously larger than those of T1, apical lamella of T2 reflex and obviously depressed in the middle (Fig. 37); lateral view (Fig. 33), basal angle of metasomal segment 2 acute, T2 not swollen in the middle, obviously depressed in its preapical part; wings pale brown.

Male. (in Girish Kumar et al. 2017). Body length: 10.5–11.5 mm. Sculpture, punctuation, setae, and coloration similar to female, including clypeus entirely black.

Distribution. China (Yunnan); India.

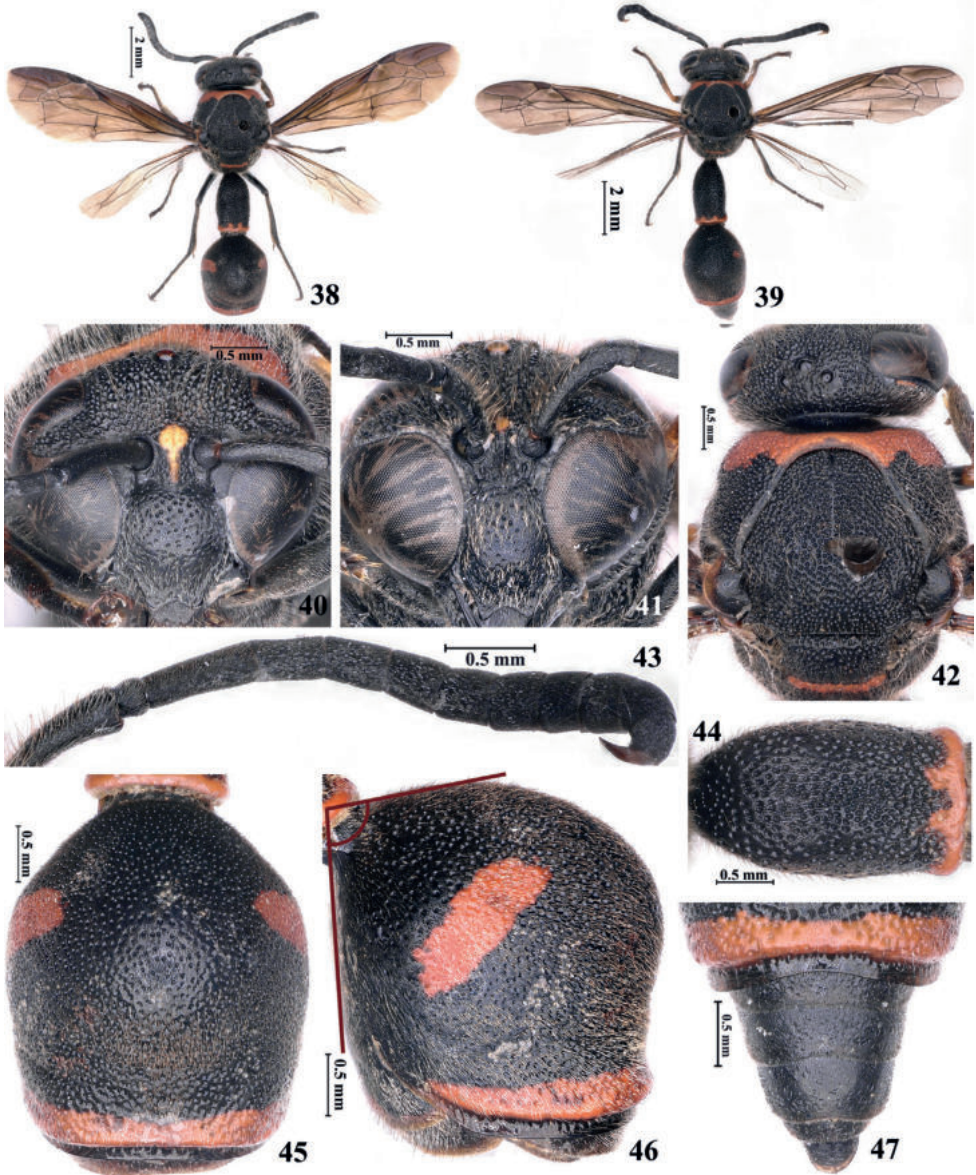
Eumenes gibbosus Nguyen, 2015, new record

Figs 38–47

Eumenes gibbosus Nguyen, 2015: 565.

Material examined. 2♂, CHINA, Sichuan Province, Liangshan Yi Autonomous Prefecture, Dechang County, Ayue Village, 27°30'25"N, 102°10'51"E, 1800 m, 2011.viii.3, Ting-Jing Li (CNU); 3♂, CHINA, Sichuan Province, Liangshan Yi Autonomous Prefecture, Xide County, Hongmo Town, 28°06'10"N, 102°15'32"E, 1800 m, 2011.viii.3, Ting-Jing Li (CNU); 1♂, CHINA, Sichuan Province, Panzhihua City, Miyi County, Baima Twon, 27°30'46"N, 102°10'04"E, 2566 m, 2011.viii.29, Ting-Jing Li (CNU); 3♀6♂, CHINA, Yunnan Province, Lijiang City, Ninglang Yi autonomous County, Daxing Town, 27°17'16"N, 100°51'32"E, 2416 m, 2011.vii.26, Ting-Jing Li (CNU); 2♀3♂, CHINA, Yunnan Province, Lijiang City, Yulong Naxi autonomous County, Shigu Town, 26°52'19"N, 99°58'11"E, 2416 m, 2011.vii.23, Ting-Jing Li (CNU); 1♀1♂, CHINA, Yunnan Province, Baoshan City, Lujiang Dam, Puman Village, 24°56'13"N, 98°47'31"E, 1800 m, 2006.vii.11, Rui Zhang (CNU); 4♀2♂, CHINA, Yunnan Province, Dali City, Yunlong County, Nuodun Town, 25°53'31"N, 99°22'37"E, 2512 m, 2011.vii.10, Ting-Jing Li (CNU).

Diagnosis. Female. Body length 10.8–11.3 mm. Body black, with ferruginous markings (Fig. 38): gena, pronotum anteriorly, band of metanotum (Fig. 42), apical bands of both T1 and T2, and lateral spots of T2; interantennal with yellow spot, tegula and fore tibia mostly black; setae dense and short; clypeus entirely black, longer than wide, with short white setae, with deep and sparse punctures at center



Figures 38–47. *Eumenes gibbosus* Nguyen, 2015. ♀ (38, 40, 42, 44–46) ♂ (39, 41, 43, 47). 38, 39 habitus (dorsal view) 40, 41 clypeus (frontal view) 42 head and pronotum (dorsal view) 43 antenna 44 T1 (dorsal view) 45 T2 (dorsal view) 46 metasomal segments 2 (lateral view) 47 lamella of T2 apical margin (dorsal view).

(Fig. 40); dorsal view (Figs 44, 45), T1 densely punctate, length of T1 less than 4× its apical width and abruptly swollen from one-third near base, then lateral margin parallel at apex, and slightly constrict near apical margin; T2 densely punctate, punctures smaller than those of T1, apical lamella of T2 not reflex and depressed in the

middle (Fig. 47); lateral view (Fig. 46), basal angle of metasomal segment 2 obtuse, T2 obviously swollen in the middle, obviously depressed in its preapical part; wings pale brown.

Male. Body length 9.8–10.2 mm (Fig. 39). Sculpture, setae, and coloration similar to female, including clypeus entirely black (Fig. 41); apex of A13 reaching basal fourth of A10 (Fig. 43).

Distribution. China (Sichuan, Yunnan); Vietnam.

Eumenes rubrofemoratus Giordani Soika, 1941, new record

Figs 48–57

Eumenes rubrofemoratus Giordani Soika, 1941: 135, 145; Iwata 1953: 25–44; Ishikawa 1965: 292; van der Vecht and Fischer 1972: 132; Yamane 1977a: 16; Giordani Soika 1986b: 156; Yamane 1990: 144; Borsato and Ratti 1999: 93; Kim and Yamane 2001: 141, 147.

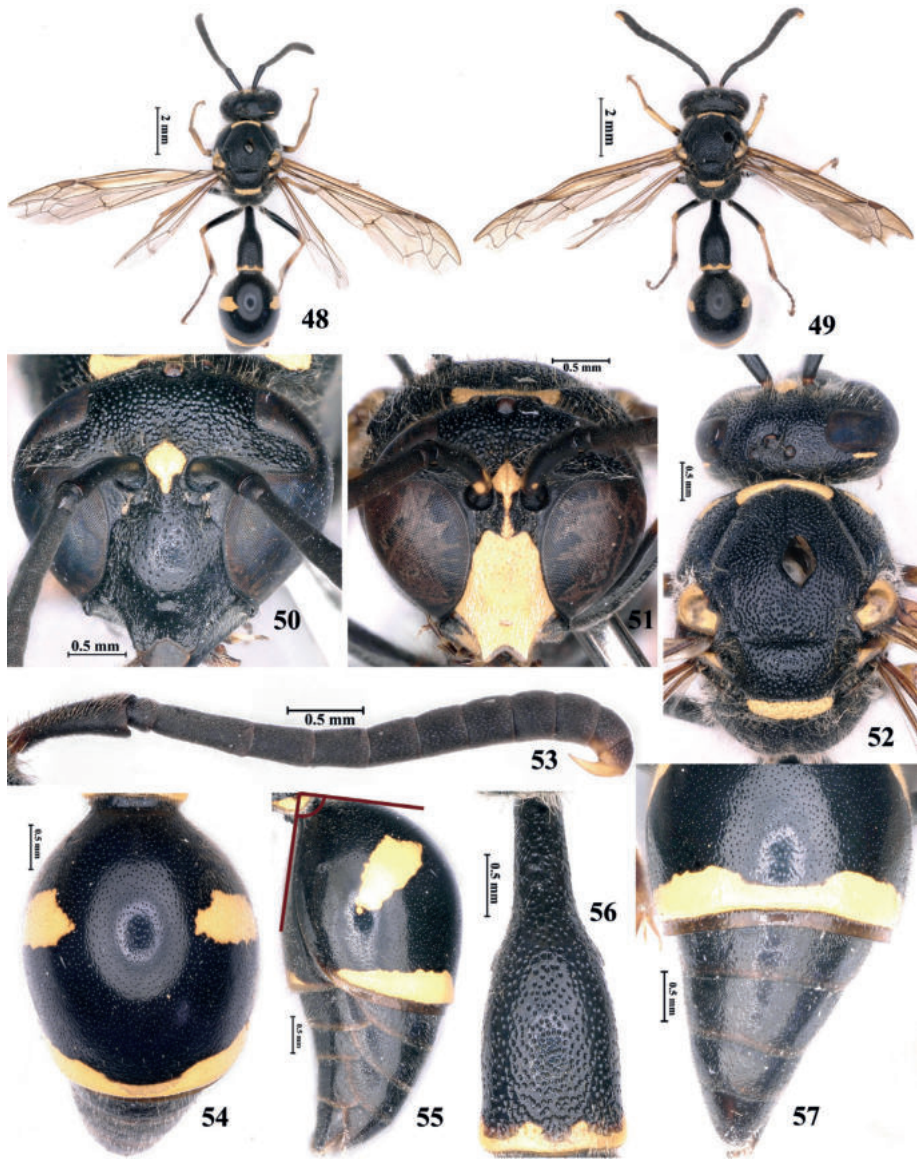
Eumenes coarctatus rubrofemoratus: Kurzenko 1995: 320.

Material examined. 8♀6♂, CHINA, Inner Mongolia Autonomous Region, Alxa League, Ho-lan Mountains, 38°58'08"N, 105°51'32"E, 2000 m, 2010.vii.29, Fangzhou Ma (CNU); 1♂, CHINA, Gansu Province, Longnan City, Liangdang County, Liangdang Village, 33°58'19"N, 106°24'21"E, 1000 m, 2016.vii.15, Zhenxia Ma (CNU); 1♂, CHINA, Gansu Province, Zhangye City, Sunan County, Daba Village, 38°48'54"N, 99°37'37"E, 3633 m, 2019.vii.3, Xue Zhang (CNU); 1♂, CHINA, Shanxi Province, Xian City, Zhuque national forest park 33°47'20"N, 108°35'17"E, 2257 m, 2012.vii.12, Ting-Jing Li (CNU); 3♀1♂, CHINA, Liaoning Province, Liaoyang City, Gongchangling District 41°09'25"N, 123°25'37"E, 569 m, 2012.vii.13, Xin Zhou (CNU).

Diagnosis. Female. Body length 11.3–11.6 mm. Body black, with yellow markings (Fig. 48): interantennal spot, gena, pronotum anteriorly, band of metanotum, tegula mostly (Fig. 52), fore tibia largely, apical bands of both T1 and T2, and lateral spots of T2; body with setae sparse and short; clypeus entirely black, longer than wide, with shallow and sparse punctures at center (Fig. 50); dorsal view (Figs 54, 56), T1 densely punctate, length of T1 less than 4× its apical width and abruptly swollen before middle, then lateral margin expansile at apex, and not constrict near apical margin; T2 sparsely punctate, punctures obviously smaller than those of T1, apical lamella of T2 not reflex and not depressed in the middle (Fig. 57); lateral view (Fig. 55), basal angle of metasomal segment 2 acute, T2 not strongly swollen in the middle, weakly depressed in its preapical part; wings pale brown.

Male. Body length 9.6–10.1 mm (Fig. 49). Sculpture, setae, and coloration similar to female except as follows: clypeus entirely yellow (Fig. 51); apex of A13 reaching basal fourth of A10 (Fig. 53).

Distribution. China (Inner Mongolia, Liaoning, Shanxi, Gansu); Japan.



Figures 48–57. *Eumenes rubrofemoratus* Giordani Soika, 1941. ♀ (48, 50, 52, 54–57) ♂ (49, 51, 53). 48–49 habitus (dorsal view) 50, 51 clypeus (frontal view) 52 head and pronotum (dorsal view) 53 antenna 54 T2 (dorsal view) 55 metasomal segments 2 (lateral view) 56 T1 (dorsal view) 57 lamella of T2 apical margin (dorsal view).

Acknowledgements

This study was funded by Science & Technology Fundamental Resources Investigation Program (Grant No. 2022FY202100) and the National Natural Science Foundation of China (Nos: 31772490, 31372247, 31000976).

References

- Bingham CT (1897) The fauna of British India, including Ceylon and Burma, Hymenoptera, I. wasps and bees. Taylor and Francis, London, [xxix +] 579 pp. <https://doi.org/10.5962/bhl.title.100738>
- Borsato W, Ratti E (1999) Antonio Giordani Soika (1913–1997): la produzione scientifica. *Memorie della Società Entomologica Italiana* 77: 43–103.
- Dalla Torre KW von (1894) *Catalogus Hymenopterorum* (Vol. 9). Vespidae (Diploptera). G. Engelmann, Leipzig, 181 pp.
- Dalla Torre KW von (1904) Hymenoptera, Fam. Vespidae, *Genera Insectorum* 19: 1–108.
- de Saussure H (1852–1853) Études sur la famille des Vespides 1: Monographie des Guêpes solitaires ou de la tribu des Euméniens. J. Cherbuliez, Genève & V. Masson, Paris, [xix +] 286 pp. [22 pls. 1–128, pls. 2–5, 7, 10, 14 (1852); pp. i–xix + 129–286, pls. 1, 6, 8, 9, 11–13, 15–22 (1853), dates of publication after Griffin 1939]
- Dover C (1925) Further notes on the Indian Diplopterous wasps. *The Journal of the Asiatic Society of Bengal, New Series* 20: 289–305.
- Dover C (1926) A contribution to a list of the Aculeate Hymenoptera (excepting ants) of Hongkong. *China Journal of Science and Arts, Shanghai* 4: 233–235.
- Dover C (1931) The Vespidae in the F.M.S. Museums. *Journal of the Federated Malay States Museums* 16: 251–260.
- Dover C, Rao HS (1922) A note on the Diplopterous wasps in the collection of the Indian Museum. *The Journal of the Asiatic Society of Bengal, New Series* 18: 235–249.
- Dutt GR (1912) Life histories of Indian insects (Hymenoptera). *Memoirs of the Department of Agriculture in India, Entomology Series* 4(4): 229–240.
- Fateryga AV, Proshchalykin MY, Mokrousov MV, Akhmedov AG (2023) To the knowledge of the solitary vespid wasps (Hymenoptera: Vespidae: Masarinae and Eumeninae s. l.) of Uzbekistan. *Zootaxa* 5278(3): 439–460. <https://doi.org/10.11646/zootaxa.5278.3.2>
- Giordani Soika A (1940) Diagnosi di nuovi *Eumenes* dell'Asia nordorientale (Hym. Vespidae). Estratto dal Bollettino della Società Veneziana di Storia Naturale 2: 96–98.
- Giordani Soika A (1941) Studi sui Vespidi Solitari. *Bollettino della Società Veneziana di Storia Naturale* 2(3): 130–280.
- Giordani Soika A (1960) Notulae vespidologicae XII. – Sugli *Eumenes* s. str. dell'India continentale. *Bollettino della Società Entomologica Italiana* 90(9–10): 158–161.
- Giordani Soika A (1973) Notulae vespidologicae XXXV. – Descrizione di nuovi Eumenidi. *Bollettino del Museo Civico di Storia Naturale di Venezia* 24: 97–131.
- Giordani Soika A (1986a) Notulae vespidologicae XLVI. – Nuovi Eumenidi indomalesi. *Lavori della Società Veneziana di Scienze Naturali* 11: 77–82.
- Giordani Soika A (1986b) Eumenidi palearctici nuovi o poco noti. *Bollettino del Museo civico di storia naturale di Venezia*: 35: 91–162.
- Girish Kumar P, Carpenter JM, Leopoldo C, Sureshan PM (2017) A taxonomic review of the Indian species of the genus *Eumenes* Latreille (Hymenoptera: Vespidae: Eumeninae). *Zootaxa* 4317(3): 469–498. <https://doi.org/10.11646/zootaxa.4317.3.3>

- Gusenleitner J (1972) Übersicht über die derzeit bekannten westpaläarktischen Arten der Gattung *Eumenes* Latr. (Hym., Vespoidea). Bollettino del Museo civico di storia naturale di Venezia 22/23: 67–117.
- Gusenleitner J (2006) Über Aufsammlungen von Faltenwespen in Indien (Hymenoptera, Vespidae). Linzer biologische Beiträge 38 (1): 677–695.
- Ishikawa R (1965) Vespidae. In Asahina S et al. (Eds) Iconographia Insectorum Japonicorum. Colore Naturali Edita 3: 291–297 [pls. 146–149]. Hokuryu-kan, Tokyo. [In Japanese]
- Iwata K (1953) Biology of *Eumenes* in Japan (Hymenoptera: Vespidae). Mushi 25: 25–44.
- Kim JK, Yamane Sk (2001) A revision of *Eumenes* Latreille (Hymenoptera: Vespidae) from the Far East Asia, with descriptions of one new species and one new subspecies. Entomological Science 4 (2): 139–155.
- Kostylev G (1940) Espèces nouvelles et peu connues de Vespides, d'Euménides et de Masarides paléarctiques (Hymenoptera). Bulletin de la Société des naturalistes de Moscou, Section Biologique 49(3–4): 137–154.
- Kurzenko NV (1995) 65. Family Vespidae. In: Lehr PA (Ed.) Key to the Insects of Russian Far East in Six Volumes. IV. Neuropteroidea, Mecoptera, Hymenoptera. Part 1. Nauka, St. Petersburg, 264–324.
- Latreille PA (1802) Histoire Naturelle, Générale et Particulière des Crustacés et des Insectes (Vol. 3). F. Dufart, Paris, [Xii +] 467 pp. <https://doi.org/10.5962/bhl.title.15764>
- Latreille PA (1810) Considérations Générale sur L'ordre Naturel des Animaux Composant les Classes des Crustacés, des Arachnides, et des Insectes; Avec un Tableau Méthodique de Leurs Genres, Disposés en Familles. Schoell, Paris, [2 +] 444 pp. <https://doi.org/10.5962/bhl.title.39620>
- Linnaeus C (1758) Systema Naturae Per Regna Tria Naturae, Secundum Classes, Ordines, Genera, Species, Cum characteribus, differentiis, synonymis, locis. Tomus I. Editio Decima, Reformata. Laurentii Salvii, Holmiae, 823 pp. <https://doi.org/10.5962/bhl.title.542>
- Li TJ, Barthélémy C, Carpenter JM (2019) The Eumeninae (Hymenoptera, Vespidae) of Hong Kong (China), with description of two new species, two new synonymies and a key to the known taxa. Journal of Hymenoptera Research 72: 127–176. <https://doi.org/10.3897/jhr.72.37691>
- Maindron MM (1882) Histoire des Guêpes Solitaires (Euméniens) de l'Archipel Indien et de la Nouvelle-Guinée. 2e Partie (1). Annales de la Société Entomologique de France 6(2): 267–286.
- Nguyen LTP (2015) Potter wasps of the genus *Eumenes* Latreille, 1802 (Hymenoptera: Vespidae: Eumeninae) from Vietnam, with description of a new species and key to species. Zootaxa 3974 (4): 564–572. <https://doi.org/10.11646/zootaxa.3974.4.7>
- Paiva CA (1907) Records of Hemiptera and Hymenoptera from the Himalayas. Records of the Indian Museum 1: 13–20. <https://doi.org/10.26515/rzsi/v1/i1/1907/163419>
- de Saussure H (1852–1853) Études sur la famille des Vespides 1: Monographie des Guêpes solitaires ou de la tribu des Euméniens. J. Cherbuliez, Genève & V. Masson, Paris, [xix +] 286 pp. [2 pls. 1–128, pls. 2–5, 7, 10, 14 (1852); pp. i–xix + 129–286, pls. 1, 6, 8, 9, 11–13, 15–22 (1853), dates of publication after Griffin 1939]

- Smit J (2005) De urntjeswesp *Eumenes coronatus* zoekt het hogerop (hymenoptera: vespidae) (Hymenoptera: Vespidae). Nederlandse Faunistische Mededelingen 22: 23–26.
- Smith F (1873) A catalogue of the Aculeate Hymenoptera and Ichneumonidae of India and the eastern Archipelago, with Introductory Remarks by A.R. Wallace. Journal of the Linnean Society, Zoology 11: 285–415. <https://doi.org/10.1111/j.1096-3642.1871.tb02225.x>
- Sonan J (1939) Descriptions of eight new species of Eumenidae in Formosa (Hymenoptera). Transactions of the Natural History Society of Formosa 29: 131–140.
- Tan JL, Carpenter JM, van Achterberg C (2018) An illustrated key to the genera of Eumeninae from China, with a checklist of species (Hymenoptera, Vespidae). ZooKeys 740: 109–149. <https://doi.org/10.3897/zookeys.740.22654>
- van der Vecht J, Fischer FCJ (1972) Palaeartic Eumenidae. Hymenopterum Catalogus. New Edition (Vol. 8). Uitg. W. Jung, 's-Gravenhage, [v +] 199 pp.
- von Schulthess RA (1935) Hymenoptera aus des Sundainseln und Nordaustralien. Revue Suisse de Zoologie 42(9): 293–323. <https://doi.org/10.5962/bhl.part.117934>
- Yamane Sk (1977a) Notes on eumenid wasps from Japan and its adjacent regions (Hymenoptera: Vespoidea) (1). New Entomologist 26: 14–18.
- Yamane Sk (1977b) Notes on eumenid wasps from Japan and its adjacent regions (Hymenoptera: Vespoidea) (2). New Entomologist 26: 59–63.
- Yamane Sk (1990) A revision of the Japanese Eumenidae (Hymenoptera, Vespoidea). Insecta Matsumurana. Sapporo 43: 1–189.
- Yoon TJ, Kim JK (2014) Taxonomy of *Eumenes punctatus*-complex (Hymenoptera; Vespidae; Eumeninae) from Korea with DNA barcoding and key to Far Eastern species of the genus *Eumenes* Latreille, 1802. Zootaxa 3893 (2): 232–242. <https://doi.org/10.11646/zootaxa.3893.2.4>
- Zhou X, Chen B, Li TJ (2012) Two new species and a key to species of the genus *Eumenes* Latreille (Hymenoptera: Vespidae: Eumeninae) from southwestern China. Entomotaxonomia 34(2): 467–474.

Extraordinary drilling capabilities of the tiny parasitoid *Eupelmus messene* Walker (Hymenoptera, Eupelmidae)

Matvey I. Nikelshparg¹, Evelina I. Nikelshparg², Vasily V. Anikin¹, Alexey A. Polilov²

1 Faculty of Biology, Saratov State University, 83 Astrakhanskaya Street, Saratov, 410012, Russia **2** Faculty of Biology, Moscow State University, Leninskie gory 1-12, Moscow, 119234, Russia

Corresponding author: Matvey I. Nikelshparg (matveynikel88@gmail.com)

Academic editor: Ankita Gupta | Received 10 June 2023 | Accepted 22 August 2023 | Published 31 August 2023

<https://zoobank.org/54FB55A9-EA35-4B98-99BF-826E5511C520>

Citation: Nikelshparg MI, Nikelshparg EI, Anikin VV, Polilov AA (2023) Extraordinary drilling capabilities of the tiny parasitoid *Eupelmus messene* Walker (Hymenoptera, Eupelmidae). Journal of Hymenoptera Research 96: 715–722. <https://doi.org/10.3897/jhr.96.107786>

Abstract

In the course of evolution, animals and particularly insects, have developed efficient and complex mechanisms for survival. Biomimetics aims to find applications for these features of organisms (or organs) in industry, agriculture, and medicine. One of these features is the thin, flexible, and mobile insect ovipositor, which is also capable of carrying substances and drilling various substrates, usually of plant origin. Despite the well-studied structure of the ovipositor, the principles of its operation and real possibilities remain poorly understood. In our study, we first discovered an unusual behavioral pattern of oviposition of the female parasitoid *Eupelmus messene* Walker (Hymenoptera: Eupelmidae): she drilled with her ovipositor through the wall of a polystyrene Petri dish and laid her egg outside the dish. Due to the transparency of the plastic, we described the technique of ovipositor movement and studied its structure using scanning electron microscopy. Our research may contribute to developing minimally invasive guided probes and various other instruments.

Keywords

Chalcidoidea, gall, oviposition, ovipositor structure, parasitoid

Introduction

Insects inspire researchers to develop new biomimetic substances for industry and biomedicine (Elvin et al. 2005); to improve mobility, strength, and control systems of robots; to develop micro-electro-mechanical devices (MEMS) for supersensitive

sensory systems in medicine, etc. (Gorb 2011); to produce new materials (Scarangella et al. 2020).

One of the examples of structures that may be beneficial for bionics is the ovipositor which in parasitoid wasps is a flexible and thin egg-laying organ used to drill holes in various natural materials, for example, host puparia, plant buds, stems, and galls (Askew 1971; Peters and Abraham 2010; Polidori et al. 2013). Studying the drilling process in nature is challenging due to the dense structure of plant substrates (for ex., fig syconia) (Kundanati and Gundiah 2014). Transparent gel-like substrates on the other hand, allow a detailed investigation of ovipositor insertion and steering (Gouache et al. 2010; Quicke 2014; Cerkvenik et al. 2017; van Meer et al. 2020); however, the mechanisms may differ due to the differences in stiffness of natural and artificial substrates.

Here we present the first observation of drilling and egg laying by the parasitoid wasp *Eupelmus messene* Walker (Hymenoptera: Eupelmidae) in a transparent and solid substrate – wall of a polystyrene Petri dish.

Eupelmus messene, which was recently separated from its synonym *Eupelmus vesicularis* Retzius (Hymenoptera: Eupelmidae) by Fusu (2017), is a 2–3 mm wasp. Among other hosts, it is a parasitoid of the gall wasp *Aulacidea hieracii* Linnaeus (Hymenoptera: Cynipidae). The latter forms a gall on the stems of the hawkweed *Hieracium × robustum* Fr. (Anikin and Nikelshparg 2017). The female of *E. messene* drills the walls of the gall with her ovipositor in search of a gall wasp larva and, upon finding it, lays an egg next to it (Gokhman and Nikelshparg 2021). Study of the drilling the gall is challenging due to its opaque and dense structure, whereas the transparency of the polystyrene made it possible to describe the drilling process and oviposition in detail.

Methods

Insects

We reared 56 females from galls of *H. × robustum* collected in the fields near the city of Saratov, Russia (51°32'00"N, 46°00'00"E) during the years 2017–2023. 18 females were used to observe drilling through plastic in the Petri dishes without galls while 38 were used to observe drilling of their natural host in the Petri dishes with galls. Each female was moved to a separate Petri dish, excluding the first specimen that showed such a behavior. This wasp was transferred to the sterile Petri dish later after drilling 3 perforations. *Eupelmus messene* was kindly identified by Lucian Fusu (Faculty of Biology, Alexandru Ioan Cuza University, Iasi, Romania) and V. E. Gokhman (Botanical Garden, Moscow State University, Moscow, Russia). The voucher specimen of the *E. messene* has been kindly deposited in the Canadian National Collection of Insects, Arachnids, and Nematodes by Gary A. P. Gibson (Ottawa Research and Development Centre, Agriculture and Agri-Food Canada, Ottawa, Ontario, Canada).

Drilling process visualization

To study the drilling process, we placed *E. messene* females into a polystyrene Petri dish (diameter 90 mm, wall thickness 1 mm, manufactured by MiniMed), kept at a temperature of 23–25 °C and relative humidity of 30–40%, and provided with food (diluted sugar syrup) and water. The control lot drilled galls on *H. × robustum*. Photo and video materials were obtained using a Canon S100 camera and a Micromed MC-2-ZOOM stereoscopic microscope. About 1000 video segments were captured (from 1 to 180 minutes each) to analyze *E. messene* behavior. Measurement of ovipositor movements were made from the videos using the software Movavi Video Editor Plus 2021. Fig. 1A–C and Suppl. material 1 contain information about one female whereas the statistical analysis of the movements was made using the video data of all females that drilled the plastic and galls in the period 2017–2023.

Scanning electron microscopy imaging

The insect was studied with the scanning electron microscope (SEM Jeol JSM-6380) after fixation in 70% ethanol, dehydration (rising ethanol series and acetone), critical point drying (Hitachi HCP-2), and gold coating (Giko IB-3).

Results

Out of 18 females that were placed in Petri dishes without host galls, only 5 started drilling the wall of the Petri dish (Fig. 1A). Also, 3 wasps drilled the plastic in the other group of 38 females despite having the host galls inside the Petri dish. Each drilled between one and five holes (mean \pm SE = 1.75 ± 0.5). The process of drilling each perforation in the polystyrene wall took more than two hours. Periodically the process was interrupted by feeding, drinking, or washing, after which the female found the same place in the Petri dish and continued drilling. In the end, the insect managed to complete the perforation in the plastic wall and lay one egg on the outside of the Petri dish (Fig. 1B, See Suppl. material 1). This process was repeated 4 more times, by the same female. After the female drilled 3 holes, it was transferred to a new Petri dish, where she drilled 2 more times. We recorded the drilling of four perforations out of five (See Suppl. material 1).

Several strictly sequential movement patterns for drilling a polystyrene dish can be distinguished:

1. Pushing movements resembling shaking, with a frequency of 5.7 ± 0.5 Hz and small amplitude, 0.21 ± 0.07 mm;
2. Rotational movements – the insect rotates the ovipositor in both directions up to 360 degrees – such movements were often combined with pushing movements;
3. Ejection movements, jerky movements of the ovipositor towards the insect body with a frequency of 0.8 Hz and an amplitude of 0.58 ± 0.07 mm. To move upwards, *E. messene* straightened its legs and partially retracted the ovipositor inside the body but never completely removed it from the drilled perforation.

4. Cementing step, this is the longest uninterrupted step in oviposition, lasting about 6–7 minutes, resulting in dome-shaped insulation at the entrance of the perforation, consisting of the UV fluorescent biological substance (Fig. 1C).

Drilling of natural substance (a plant gall) differs from drilling the polystyrene substrate. We studied in detail the drilling by 9 *E. messene* females out of 38 at six winter galls on *H. × robustum*. The frequency of pushing movements was 4.66 ± 0.34 Hz while the amplitude was 0.24 ± 0.03 mm. Thus, such movements in galls are less frequent than in polystyrene. Rotational movements were also observed, but we never observed ejection movements while the wasp was drilling a gall.



Figure 1. Drilling with the ovipositor through a plastic wall of a Petri dish by *Eupelmus messene* (A), a newly laid egg into the external environment (B), and UV fluorescent biological substance inside the perforations (C). ov – ovipositor, per – perforation, egg – egg.

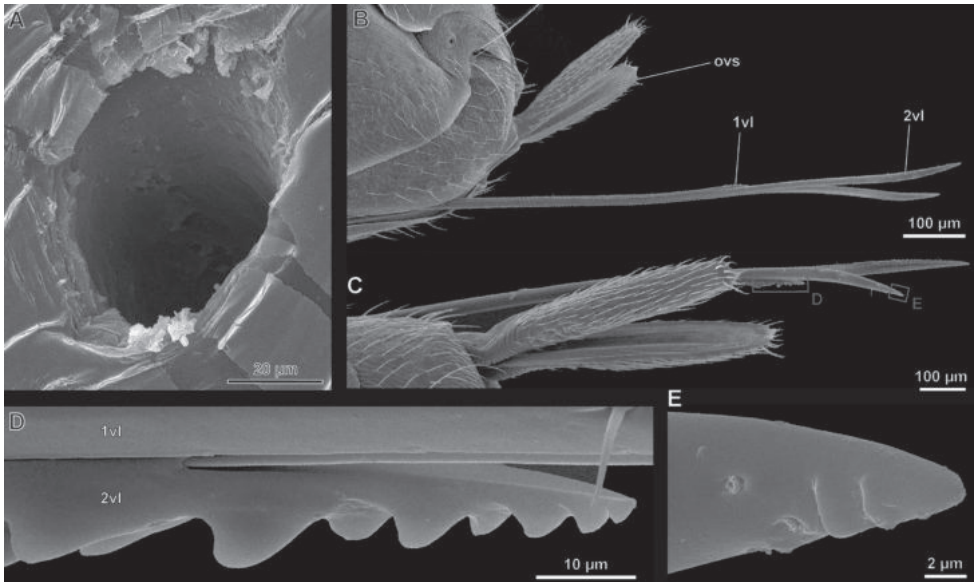


Figure 2. Ovipositor structure of the *Eupelmus messene* and perforation drilled in plastic, SEM **A** perforation in the Petri dish made by *E. messene* **B–E** structure of the *E. messene* ovipositor, lateral view: **B** apex of gaster **C** ovipositor **D** apex of 1st valvifer **E** apex of 2nd valvifer. ovs – ovipositor sheath, 2vl – 2nd valvula, 1vl – 1st valvula.

The structure of the ovipositor and the drilled perforation in the Petri dish was examined using a scanning electron microscope. The diameter of the drilled perforation is about 30 µm (Fig. 2A). As in all apocritans the ovipositor consists of paired ovipositor sheaths (3rd valvulae), paired 2nd valvulae that enclose a pair of 1st valvulae. The 1st and 2nd valvulae form the ovipositor stylets. The exerted part of the stylets in the measured specimen has a total length of 2 mm and diameter of 20 µm (Fig. 2B–E). The apical part of 1st valvula has a sawtooth structure (Fig. 2D). The length of this section is 70 µm, with about 6 teeth in a row; height of each tooth is 1 to 4.5 µm. We assume that with the help of the multiple teeth on the stylet, the *E. messene* not only cuts the perforation but also ejects excess material.

Discussion

We described an interesting case of *E. messene* spontaneous drilling in a polystyrene Petri dish wall for oviposition in the absence of a host stimulus. The reason for such behavior of the parasitoid wasp remains unknown. Since plant gall is opaque, the mechanism of egg-laying behavior has never been described in detail. The unusual behavior of the female allowed us to characterize the drilling patterns. We distinguished four steps of drilling: pushing movements, rotational movements, ejection movements, as well as the cementing step. However, in natural gall, we never observed ejection movements. We suppose that such a type of movement is required to rake out plastic particles, which is unnecessary

for more elastic plant gall substrate. Also, we suggest that pushing movements in galls are less frequent than in plastic as gall has other material properties than polystyrene. Importantly, fresh summer galls are suggested to be less solid than winter ones used here. Thus, we assume that the frequency of pushing movements would be decreased even more. The process of drilling the polystyrene and gall tissue may differ due to the difference in stiffness, however, a more detailed study of the gall and polystyrene material properties should be conducted. To mimic the drilling of wasps, Cerkvenik et al. (2017) applied gel-lan gel. However, we suggest that polystyrene is a more relevant model material to study drilling and oviposition in natural substrates, especially autumn firm galls.

The transparency of the polystyrene allows for describing the features of drilling in a solid substrate invisible in natural materials. Studying in details the drilling behavior of parasitic mycrophymenopterans can be useful in medicine for the creation of minimally invasive guided probes in neurosurgery (Frasson et al. 2010; Ramadi et al. 2019), the development of orthopedic surgical instruments (Nakajima and Schwarz 2014), needle biopsies using functionally graded tools (Kundanati and Gundiah 2014). Due to the flexibility, potential hardness, and effective types of movement, ovipositor structures can be used to develop methods of vertical and directional drilling, whereas ultra-low mass and energy efficiency make it possible to use ovipositor features for studying space structures and celestial bodies, extraterrestrial drilling or sampling (Gouache et al. 2010). Some eupelmid species (such as *Eupelmus vuilleti* Craw (Hymenoptera: Eupelmidae) and *Eupelmus microzonus* Förster (Hymenoptera: Eupelmidae)) provide a protective web-like coating for their eggs (Leveque et al. 1993; Gokhman and Nikelshparg 2021), but *E. messene* has not previously shown any ability to protect its offspring. Due to the transparency of the plastic Petri dish, we found that after laying the egg, the female carefully cements the drilled perforation with a yet unknown biological substance. We suggest that this substance plays a role in isolation from temperature fluctuations, water, microorganisms, etc. It should be noted that it is practically impossible to detect such perforation cementing under natural conditions.

Conclusion

We revealed the phenomenon of *E. messene* drilling the plastic Petri dish using three types of ovipositor movements: pushing, rotational, and ejection. In the natural gall, the ejection movements were absent, and the pushing movements were less frequent in the gall than in plastic. Additionally, we provided the first evidence that *E. messene* isolates the perforation after the oviposition. The structure of the ovipositor was described with SEM. The proposed analysis may contribute to developing minimally invasive guided probes for medicine or methods of vertical and directional drilling of rocks.

Acknowledgements

We acknowledge Lucian Fusu (Faculty of Biology, Alexandru Ioan Cuza University, Iasi, Romania) and V. E. Gokhman (Botanical Garden, Moscow State University, Moscow,

Russia) for the identification of the parasitoid. We would like to express our gratitude to Lucian Fusu and the anonymous reviewer for their meticulous review of the manuscript. We are grateful to Gary A.P. Gibson (Ottawa Research and Development Centre, Agriculture and Agri-Food Canada, Ottawa, Ontario, Canada) for depositing the voucher specimen of the *E. messene* in the Canadian National Collection of Insects, Arachnids, and Nematodes. The work was supported by the Russian Science Foundation (project No. 22–14–00028, <https://rscf.ru/en/project/22-14-00028/> to A.A.P., morphological part of the study). The authors have declared that no competing interests exist.

References

- Anikin VV, Nikelshparg MI (2017) Details of parasitism by *Eupelmus* sp. (Hymenoptera: Eupelmidae) on *Aulacidea hieracii* (Hymenoptera: Cynipidae), a gall-maker of the hawkweed, *Hieracium virosum*. Entomological and parasitological studies in the Volga Region 14: 67–71. [In Russian]
- Askew RR (1971) Parasitic insects. Heinemann Educational Bks., London. [ISBN 978-0435620455]
- Cerkvenik U, van de Straat B, Gussekloo SWS, van Leeuwen JL (2017) Mechanisms of ovipositor insertion and steering of a parasitic wasp. Proceedings of the National Academy of Sciences of the United States of America 114: E7822–E7831. <https://doi.org/10.1073/pnas.1706162114>
- Elvin CM, Carr AG, Huson MG, Maxwell JM, Pearson RD, Vuocolo T, Liyou NE, Wong DCC, Merritt DJ, Dixon NE (2005) Synthesis and properties of crosslinked recombinant pro-resilin. Nature 437: 999–1002. <https://doi.org/10.1038/nature04085>
- Frasson L, Ko SY, Turner A, Parittotokkaporn T, Vincent JF, Rodriguez y Baena F (2010) STING: A soft-tissue intervention and neurosurgical guide to access deep brain lesions through curved trajectories. Proceedings of the Institution of Mechanical Engineers, Part H: Journal of Engineering in Medicine 224(6): 775–788. <https://doi.org/10.1243/09544119JEIM663>
- Fusu L (2017) An integrative taxonomic study of European *Eupelmus* (*Macroneura*) (Hymenoptera: Chalcidoidea: Eupelmidae), with a molecular and cytogenetic analysis of *Eupelmus* (*Macroneura*) *vesicularis*: several species hiding under one name for 240 years. Zoological Journal of the Linnean Society 181(3): 519–603. <https://doi.org/10.1093/zoolinnean/zw021>
- Gokhman VE, Nikelshparg MI (2021) *Eupelmus messene* Walker, 1839 and *E. microzonus* Förster, 1860 as parasitoids of *Aulacidea hieracii* (Bouché, 1834) (Hymenoptera, Eupelmidae, Cynipidae). Journal of Hymenoptera Research 84: 87–102. <https://doi.org/10.3897/jhr.84.68556>
- Gorb SN (2011) Insect-Inspired Technologies: Insects as a Source for Biomimetics. In: Vilcinskas A (Ed.) Insect Biotechnology. Biologically-Inspired Systems, vol 2. Springer, Dordrecht, 241–264. https://doi.org/10.1007/978-90-481-9641-8_13
- Gouache T, Gao Y, Gourinay Y, Coste P (2010) Wood Wasp Inspired Planetary and Earth Drill. In: Mukherjee A (Ed.) Biomimetics Learning from Nature, InTech Open, 467–486. <https://doi.org/10.5772/8775>
- Kundanati L, Gundiah N (2014) Biomechanics of substrate boring by fig wasps. Journal of Experimental Biology 217(11): 1946–1954. <https://doi.org/10.1242/jeb.098228>

- Leveque L, Monge J-P, Rojas-Rousse D, Van Alebeek F, Huignard J (1993) Analysis of multiparasitism by *Eupelmus vuilleti* (Craw) (Eupelmidae) and *Dinarmus basalis* (Rond) (Pteromalidae) in the presence of one of their common hosts, *Bruchidius atrolineatus* (Pic) (Coleoptera Bruchidae). *Oecologia* 94: 272–277. <https://doi.org/10.1007/BF00341327>
- Nakajima K, Schwarz O (2014) How to use the ovipositor drilling mechanism of Hymenoptera for developing a surgical instrument in biomimetic design. *International Journal of Design & Nature and Ecodynamics* 9(3): 177–189. <https://doi.org/10.2495/DNE-V9-N3-177-189>
- Peters RS, Abraham R (2010) The food web of parasitoid wasps and their non-phytophagous fly hosts in birds' nests (Hymenoptera: Chalcidoidea, and Diptera: Cyclorrhapha). *Journal of Natural History* 44: 9–10, 625–638. <https://doi.org/10.1080/00222930903437317>
- Polidori C, García AJ, Nieves-Aldrey JL (2013) Breaking up the wall: Metal-enrichment in ovipositors, but not in mandibles, co-varies with substrate hardness in gall-wasps and their associates. *PLoS ONE* 8: e70529. <https://doi.org/10.1371/journal.pone.0070529>
- Quicke DLJ (2014) The Ovipositor and Ovipositor Sheaths. In: Quicke DLJ (Ed.) *The Bracoonid and Ichneumonid Parasitoid Wasps*. John Wiley & Sons, Ltd, Chichester, UK, 35–55. [ISBN: 978-1-118-90705-4] <https://doi.org/10.1002/9781118907085.ch3>
- Ramadi KB, Cima MJ (2019) Materials and devices for micro-invasive neural interfacing. *MRS Advances* 4: 2805–2816. <https://doi.org/10.1557/adv.2019.424>
- Scarangella A, Soldan V, Mitov M (2020) Biomimetic design of iridescent insect cuticles with tailored, self-organized cholesteric patterns. *Nature Communications* 11: 4108. <https://doi.org/10.1038/s41467-020-17884-0>
- van Meer NMME, Cerkvenik U, Schlepütz CM, van Leeuwen JL, Gussekloo SWS (2020) The ovipositor actuation mechanism of a parasitic wasp and its functional implications. *Journal of Anatomy* 237(4): 689–703. <https://doi.org/10.1111/joa.13216>

Supplementary material I

Eupelmus messene drilling the wall of the polystyrene Petri dish

Authors: Matvey I. Nikelshparg, Evelina I. Nikelshparg, Vasily V. Anikin, Alexey A. Polilov
Data type: mp4

Explanation note: A detailed captioned video recording of *Eupelmus messene* drilling the wall of the polystyrene Petri dish. ×10 and ×1.5 – speed is increased by 10 and 1.5 times, respectively.

Copyright notice: This dataset is made available under the Open Database License (<http://opendatacommons.org/licenses/odbl/1.0/>). The Open Database License (ODbL) is a license agreement intended to allow users to freely share, modify, and use this Dataset while maintaining this same freedom for others, provided that the original source and author(s) are credited.

Link: <https://doi.org/10.3897/jhr.96.107786.suppl1>

A new species and a new record species of *Megischus* Brullé (Hymenoptera, Stephanidae) from Vietnam

Si-Xun Ge¹, Li-Li Ren¹, Jiang-Li Tan²

1 College of Forestry, Beijing Forestry University, Beijing 100083, China **2** Shaanxi Key Laboratory for Animal Conservation / Key Laboratory of Resource Biology and Biotechnology in Western China, College of Life Sciences, Northwest University, 229 North Taibai Road, Xi'an, Shaanxi 710069, China

Corresponding authors: Jiang-Li Tan (tanjl@nwu.edu.cn); Li-Li Ren (lily_ren@bjfu.edu.cn)

Academic editor: Michael Ohl | Received 4 June 2023 | Accepted 1 September 2023 | Published 11 September 2023

<https://zoobank.org/ECF92C76-DDDD-4FBD-B379-139EEC430CDE>

Citation: Ge S-X, Ren L-L, Tan J-L (2023) A new species and a new record species of *Megischus* Brullé (Hymenoptera, Stephanidae) from Vietnam. Journal of Hymenoptera Research 96: 723–734. <https://doi.org/10.3897/jhr.96.107502>

Abstract

A new crown wasp species, *Megischus shixiangi* Ge & Tan, **sp. nov.** from Vietnam (Hymenoptera: Stephanidae), is described and illustrated. In addition, *M. kuafu* Ge & Tan is first recorded in Vietnam. A distribution map of the Vietnamese species is provided.

Keywords

Crown wasps, Oriental, parasitoids, Taxonomy

Introduction

The genus *Megischus* Brullé, 1846, is the second species-rich genus of the crown wasps family Stephanidae Leach, 1815 which is a clade with the superfamily Evanioidea sister to all other groups of the aculeate Hymenoptera (Branstetter et al. 2017; Peters et al. 2017). The genus *Megischus* consists of 89 extant species up to date, with a worldwide distribution but mainly found in the Oriental regions (Aguiar 2004; Hong et al. 2011; Binoy et al. 2020; Ge et al. 2021a, 2021b, 2022). This genus can be easily recognized by the comparatively large body size, the complete venation with subdiscal cell 1 elongated and 2Cub pigmented, as well as the distinct ivory subapical band on the ovipositor sheath.

van Achterberg (2002) made a revision from the Old World *Megischus* recognizing 42 species belonging to 7 groups. In the world catalog of the Stephanidae by Aguiar,

(2004) a total of 73 *Megischus* species were recorded with 34 of them distributed in Oriental regions. Afterward, more Oriental species of *Megischus* were described in China, India and the Ryukyu Islands (van Achterberg and Yang 2004; Hong et al. 2010; Binoy et al. 2020; Ge et al. 2021a, 2022).

However, as a country located in the hot spot area of species diversity of the crown wasp, up to now, only two species of *Megischus* are recorded in Vietnam, *i.e.* *M. ruficeps* de Saussure and *M. tonkinensis* van Achterberg. Here we describe a new species and report a new record species of *Megischus* in Vietnam. A key to the Vietnamese species of the genus is compiled, as well as a distribution map.

Materials and methods

For identification of the genera of Stephanidae, van Achterberg (2002) and Hong et al. (2011) were used.

Observations, descriptions and photographic images were made with a SONY ILCE-7RM4A a7r4a Alpha 7R IVA mirrorless camera attached with LAOWA 90mm F2.8 CA-Dreamer Macro 2X lens. Morphological terminology follows van Achterberg (2002) including the abbreviations for the wing venation. The types are deposited in the College of Forest Protection, Beijing Forestry University (BFU), China.

Key to species of the genus *Megischus* Brullé from Vietnam

- 1 Lateral view of widened part of hind tibia deeply concave ventrally; Ivory part of ovipositor sheath 1.0–1.5 times as long as its dark apical part *M. ruficeps* de Saussure
- Lateral view of the hind tibia below depression nearly parallel-sided or rather weakly concave; Ivory part of ovipositor sheath 2.0 times as long as its dark apical part or longer **2**
- 2 Neck with only interrupted carina before pronotal fold; Forewing with vein 1-M 5.9× as long as vein 1-SR and 0.8× vein m-cu; vein 2-SR 0.9× as long as vein r; vein 1-SR 1.1× as long as parastigmal vein *M. kuafu* Ge & Tan
- Neck with both complete and interrupted carina before pronotal fold; Forewing with vein 1-M 6.5–6.7× as long as vein 1-SR and 1.1–1.3× vein m-cu; vein 2-SR about as long as vein r or longer; vein 1-SR 0.5× as long as parastigmal vein **3**
- 3 Vertex reddish brown (in original description chestnut-brown), not distinct contrast to the temple. Rugosity of the vertex comparatively regular with five strong regularly curved lamelliform carinae behind posterior teeth; Pronotum robust, with less than 1.2× its length than maximum width; Propodeum coarsely and densely foveolate *M. tonkinensis* van Achterberg
- Vertex blackish, distinct contrast to the dark reddish temple. Rugosity of the vertex more irregular with three or four (the last one rather weak and in-

complete) strong regularly curved lamelliform carinae behind posterior teeth; Pronotum relatively slender, with more than 1.3× its length than maximum width; Propodeum with large foveolate sparsely distributed
*M. shixiangi* Ge & Tan, sp. nov.

Genus *Megischus* Brullé, 1846

Megischus Brullé, 1846: 537. Type species (designated by Viereck 1914): *M. annulator* Brullé, 1846 [= *M. furcatus* (Lepeletier & Serville, 1825)].

Megischus Brullé, 1846: van Achterberg 2002: 53–168; Aguiar and Johnson 2003: 469–482.

Bothriocerus Sichel, 1860: 759. Type species: *Bothriocerus europaeus* Sichel, 1860 (by monotypy) (= *Stephanus anomalipes* Foerster, 1855, according to Madl 1991).

Diagnosis. Medium to large size. First subdiscal cell comparatively narrow basally, approximately as wide as the first discal cell or narrower; vein M+CU1 with four short, erect, equidistant spiny setae; veins 1-M and 2-SR straight or nearly so. Dorsal tooth of hind coxa absent; hind femur with two distinct teeth; hind tibia narrowed basally and inner side usually with wide sub-medial depression, without oblique striae or rugae on outer side; hind tarsus of females with three tarsomeres. Ovipositor sheath with distinct ivory subapical band.

Distribution. Cosmopolitan.

Megischus shixiangi Ge & Tan, sp. nov.

<https://zoobank.org/1B52BB7E-EEDF-4193-9B3F-3E52AACF923F>

Figs 1–15

Material examined. *Holotype*, ♀ (BFU), Tuong Duong, Nghe An, Vietnam XI. 2021, leg. Local collector.

Etymology. We named the new species after Prof. Shi-Xiang Zong. To thank him for his kind support for the first author's taxonomy research.

Diagnosis. Head with blackish vertex distinctly contrasting with dark reddish temple; Vertex irregular rugosity, with three or four (the last one rather weak and incomplete) strong regularly curved lamelliform carinae behind posterior teeth. Pronotum comparatively slender, pronotal fold distinct developed; neck at distinct lower level than the middle part of pronotum in lateral view; Forewing with vein 2Cub distinctly shorter than vein cu+a; Hind tibia with its widened part rather weakly concaves basally in lateral view.

Description. Holotype. ♀, length of body 22 mm. Forewing 12 mm long; ovipositor sheath 24.5 mm long.



Figures 1–4. *Megischus shixiangi* Ge & Tan, sp. nov. Holotype ♀ **1** head, frontal view **2** head, dorsal view **3** head, lateral view **4** pronotum, dorsal view.

Head. Antenna incomplete; frons strongly reticulate-rugose (Fig. 3); three anterior coronal teeth large and lobe-shaped, while the posterior two relatively small and wide. Three or four (the last one rather weak and incomplete) regularly curved lamelliform carinae behind posterior teeth. Vertex with a large irregularly rugose area almost reaching occipital carina (Fig. 3); temple moderately bulging, smooth and shiny, except for some fine punctures (Fig. 2).

Mesosoma. Neck robust and with both complete and incomplete carina anteriorly (Fig. 4), at lower level than middle pronotum postero-dorsally. Pronotal fold distinct and with its before area rather shallowly concave; middle part of pronotum transversely rugose (Fig. 4); middle part of pronotum weakly differentiated from posterior part; middle and posterior part of pronotum generally with rather sparse and long setosity, propleuron more or less granular to reticulate-rugose; mesopleuron strongly reticulate-rugose with sparsely long setosity (Fig. 6); mesosternum largely smooth (except some fine punctures); scutellum with its margin large foveolae and smooth medially (Fig. 5); propodeum with sparsely large foveolate (Fig. 5).



Figures 5–7. *Megischus shixiangi* Ge & Tan, sp. nov. Holotype ♀ **5** mesosoma, dorsal view **6** mesosoma, lateral view **7** wings.

Wings. Fore wing: wing membrane subhyaline (Fig. 7), and surface evenly bristly; vein 1-M straight, $6.5\times$ as long as vein 1-SR and $1.2\times$ vein m-cu; vein 2-SR $1.05\times$ as long as vein r; vein r ends $0.5\times$ length of pterostigma behind the level of apex of pterostigma; vein 1-SR $0.52\times$ as long as parastigmal vein; vein 2-CU_b distinctly pigmented and curved apically; vein 2-1A straight, basally sclerotized, distinctly extended beyond Cu-a.



Figures 8–11. *Megischus shixiangi* Ge & Tan, sp. nov. Holotype ♀ **8** hind coxa **9** hind femur **10** hind tibia **11** hind tarsi.



Figures 12–14. *Megischus shixiangi* Ge & Tan, sp. nov. Holotype ♀ **12** tergite I, dorsal view **13** tergite II– VIII, dorsal view **14** distal part of ovipositor and sheath, lateral view.

Legs. Hind coxa strong, annular, sparsely transverse striate, with long whitish setosity (Fig. 8); hind femur robust, largely smooth to coriaceous with long whitish setosity (Fig. 9), hind femur ventrally with two large teeth and six-minute teeth behind large posterior tooth; hind tibia robust, distinctly curved basally (Fig. 10), basal narrow part 0.7× as long as apical widened part; apical widened part of hind tibia rather weakly concave basally in lateral view; hind basitarsus parallel-sided, bristly setose ventrally, ventral length 5.8× its maximum width (Fig. 11).

Metasoma. Tergite I (T1) finely reticulate to transversely-rugose (Fig. 12), ca 14× as long as its maximum width, 2.5× as long as TII; remaining tergites largely coriaceous (Fig. 13); pygidial area coriaceous dorsally, medially moderately convex and distinctly punctate medially; Ovipositor sheath with length of subapical whitish band 2.6× as long as dark apical part (Fig. 14).

Colour. Generally blackish to brownish; frons dark reddish to blackish; vertex blackish (Fig. 3), temple ventrally dark reddish along compound eye, distinctly contrasting with frons and vertex; wing membrane slightly brownish, subhyaline (Fig. 7), wing veins dark brownish to blackish; hind femur, hind tibia and metasoma largely dark brownish to blackish; ovipositor sheath largely black and with whitish subapical band.



Figure 15. Habitus of *Megischus shixiangi* Ge & Tan, sp. nov. Holotype ♀.

Distribution. Vietnam.

Biology. Collected in November. Host is unknown.

Note. The new species resembles the sympatric *M. tonkinensis* van Achterberg, 2002, but differs from the color and sculpture on the vertex (in the new species with vertex blackish, more or less reticulate, while in *M. tonkinensis* reddish and more



Figures 16, 17. Habitus of *Megischus kuafu* Ge & Tan, collected in Vietnam **16** habitus without ovipositor sheath **17** ovipositor sheath.

regular); the pronotum (in the new species slender but in *M. tonkinensis* comparatively strong and short); the venation (the new species with vein 2Cub distinct shorter than vein cu+a, while in *M. tonkinensis* vein 2Cub about as long as vein cu+a); as well as the pronodum (sparsely large foveolate in *M. shixiangi* but coarsely and densely foveolate in *M. tonkinensis*).

New recorded species in Vietnam

Megischus kuafu Ge & Tan, 2021

Figs 16, 17

Material examined. ♀ (BFU), Tuong Duong, Nghe An, Vietnam IX. 2022, leg. Local collector.

Diagnosis. Large size; head dark reddish brown, temples slightly bulging behind eyes; ocellar area transversely rugose; vertex reticulate-rugose medially, followed by weakly transverse rugae posteriorly almost reaching occipital carina; neck robust with incomplete carina before pronotal fold; scutellum almost glabrous; vein 1-M ca 5.9× as long as vein 1-SR; hind tibia comparatively slender; hind basitarsus densely setose and parallel-sided, ventral length 7.4× maximum width.



Figure 18. Distribution map of *Megischus* species of Vietnam (map from: <https://cn.bing.com/maps>).

Distribution. China (Guizhou); Vietnam.

Biology. Collected in November. Host is unknown.

Note. The specimen reported here is the second specimen of this species after the holotype. In terms of body size, specimen collected in Vietnam are smaller than the holotype (this specimen with length of body 36.5 mm, forewing 19 mm and ovipositor sheath 46 mm; while the holotype with length of body 39.1 mm, forewing 21.3 mm and ovipositor sheath 59 mm). In addition, the new specimen was collected in November (holotype in May), thus we speculate the species may be at least bivoltine.

Acknowledgements

We thank Prof. Shi-Xiang Zong and Dr. Tao Li (General Station of Forest and Grassland Pest Management, National Forestry and Grassland Administration, Shenyang) for their great support for this study. The research was supported jointly by the National Natural Science Foundation of China (NSFC, No. 31872263, 31572300, 32370476) and the National Key R & D Program of China (2022YFD1401000).

References

- Aguiar AP (2004) World catalog of the Stephanidae (Hymenoptera: Stephanoidea). *Zootaxa* 753: 1–120. <https://doi.org/10.11646/zootaxa.464.1.1>
- Binoy C, van Achterberg C, Girish Kumar P, Santhoshi S, Sheela S (2020) A review of Stephanidae (Hymenoptera: Stephanoidea) from India, with the description of five new species. *Zootaxa* 4838(1): 1–51. <https://doi.org/10.11646/zootaxa.4838.1.1>
- Branstetter MG, Danforth BN, Pitts JP, Faircloth BC, Ward PS, Buffington ML, Gates MW, Kula RR, Brady SG (2017) Phylogenomic insights into the evolution of stinging wasps and the origins of ants and bees. *Current Biology* 27: 1019–1025. <https://doi.org/10.1016/j.cub.2017.03.027>
- Brullé A (1846) Histoire naturelle des Insectes. Hyménoptères, vol. IV. Paris, [VIII +] 680 pp.
- Chen HY, van Achterberg C, Xu ZF (2016) Description of a new species of *Foenatopus* Smith from China and the male of *Parastephanus brevicoxalis* (Hymenoptera, Stephanidae). *ZooKeys* 612: 113–123. <https://doi.org/10.3897/zookeys.612.9781>
- Ge SX, Shi HL, Ren LL, Tan JL (2021a) Description of a new species of *Megischus* Brullé (Hymenoptera, Stephanidae), with a key to the species from China. *ZooKeys* 1022: 65–77. <https://doi.org/10.3897/zookeys.1022.62833>
- Ge SX, Ren LL, Tan JL (2021b) Description of a new species of *Foenatopus* Smith (Hymenoptera, Stephanidae), with a key to the species from Vietnam. *Journal of Hymenoptera Research* 88: 71–83. <https://doi.org/10.3897/jhr.88.76421>
- Ge SX, Ren LL, Tan JL (2022) First discovery of *Megischus* Brullé (Hymenoptera, Stephanidae) in Ryukyu Islands, with description of a new species. *Journal of Hymenoptera Research* 91: 309–320. <https://doi.org/10.3897/jhr.91.85373>
- Hong CD, van Achterberg C, Xu ZF (2010) A new species of *Megischus* Brullé (Hymenoptera, Stephanidae) from China, with a key to the Chinese species. *ZooKeys* 69: 59–64. <https://doi.org/10.3897/zookeys.69.738>
- Hong CD, van Achterberg C, Xu ZF (2011) A revision of the Chinese Stephanidae (Hymenoptera, Stephanoidea). *ZooKeys* 110: 1–108. <https://doi.org/10.3897/zookeys.110.918>
- Peters RS, Krogmann L, Mayer C, Donath A, Gunkel S, Meusemann K, Kozlov A, Podsiadlowski L, Petersen M, Lanfear R, Diez PA, Heraty J, Kjer KM, Klopstein S, Meier R, Polidori C, Schmitt T, Liu S, Zhou X, Wappler T, Rust J, Misof B, Niehuis O (2017) Evolutionary history of the Hymenoptera. *Current Biology* 27: 1013–1018. <https://doi.org/10.1016/j.cub.2017.01.027>
- de Saussure H (1890) Histoire naturelle les Hyménoptères. In: Grandidier A (Ed.) Histoire physique, naturelle et politique de Madagascar 20. Imprimerie Nationale, Paris, [i–xxi +] 1–176. <https://doi.org/10.5962/bhl.title.9201>
- Tan JL, Fan XL, van Achterberg C, Li T (2015a) A new species of *Pseudomegischus* van Achterberg from China, with a key to the species (Hymenoptera, Stephanidae). *ZooKeys* 537: 103–110. <https://doi.org/10.3897/zookeys.537.6592>
- Tan JL, van Achterberg C, Tan QQ, Zhou T, Li T (2018) *Parastephanellus* Enderlein (Hymenoptera: Stephanidae) revisited, with description of two new species from China. *Zootaxa* 4459(2): 327–349. <https://doi.org/10.11646/zootaxa.4459.2.7>

- Tan QQ, van Achterberg C, Tan JL, Chen XX (2015b) A new species of *Schlettererius* Ashmead from China, with a key to the species (Hymenoptera, Stephanidae). *Journal of Hymenoptera Research* 45: 75–86. <https://doi.org/10.3897/JHR.45.5069>
- van Achterberg C (2002) A revision of the Old World species of *Megischus* Brullé, *Stephanus* Jurine and *Pseudomegischus* gen. nov., with a key to the genera of the family Stephanidae (Hymenoptera: Stephanoidea). *Zoologische Verhandelingen Leiden* 339: 1–206.
- van Achterberg C, Yang ZQ (2004) New species of the genera *Megischus* Brullé and *Stephanus* Jurine from China (Hymenoptera: Stephanoidea: Stephanidae), with a key to world species of the genus *Stephanus*. *Zoologische Mededelingen Leiden* 78(3): 101–117.

Brood cells like conifer cones: the peculiar nesting biology of the osmiine bee *Hoplitis (Alcidamea) curvipes* (Morawitz, 1871) (Hymenoptera, Megachilidae)

Sergey P. Ivanov¹, Alexander V. Fateryga², Andreas Müller³

1 Institute of Biochemical Technology, Ecology and Pharmacy of the V.I. Vernadsky Crimean Federal University, Vernadskogo Ave. 4, 295007 Simferopol, Russia **2** .I. Vyazemsky Karadag Scientific Station – Nature Reserve of RAS – Branch of A.O. Kovalevsky Institute of Biology of the Southern Seas of RAS, Nauki Str. 24, Kurortnoye, 298188 Feodosiya, Russia **3** ETH Zurich, Institute of Agricultural Sciences, Biocommunication and Entomology, Schmelzbergstrasse 9/LFO, 8092 Zurich, Switzerland

Corresponding author: Alexander V. Fateryga (fater_84@list.ru)

Academic editor: C. K. Starr | Received 14 July 2023 | Accepted 16 September 2023 | Published 25 September 2023

<https://zoobank.org/213C2A69-6A60-471F-B438-35FBBB201E71>

Citation: Ivanov SP, Fateryga AV, Müller A (2023) Brood cells like conifer cones: the peculiar nesting biology of the osmiine bee *Hoplitis (Alcidamea) curvipes* (Morawitz, 1871) (Hymenoptera, Megachilidae). Journal of Hymenoptera Research 96: 735–750. <https://doi.org/10.3897/jhr.96.109587>

Abstract

Two nests of *Hoplitis curvipes* are described from Apulia (Italy) and Dagestan (Russia). Both nests consisted of two brood cells placed side by side under a stone. The cells were neither attached to each other nor to the substrate. They were constructed from leaf fragments, which were imbricately arranged, forming a cone-like structure; each leaf fragment consisted of a basal part that was masticated to leaf pulp and an apical part that protruded freely from the cell wall. The cell wall was formed by the fusion of the masticated basal parts of the leaf fragments and thus entirely consisted of leaf pulp. The cell was sealed with a closing plug made of pure leaf pulp; a few leaf fragments were glued to its outer surface. The cocoon consisted of two layers: the outer layer was restricted to the anterior portion of the cell and had several longitudinal air-exchange slits on its lateral surface, while the inner layer had an air-exchange orifice in its most anterior dome-shaped top. Results of measurements of brood cell dimensions and contents are provided. The nesting biology of species of the *H. curvipes* group is discussed.

Keywords

Anthophila, Apiformes, bionomics, Caucasus, Gargano, *Hoplitis mitis*, megachilid bees, Palearctic region

Introduction

The genus *Hoplitis* Klug, 1807 is distributed in the Palaearctic, the Nearctic, and the Afro-tropical region; a few species also occur in the Oriental region (Michener 2007). It is the largest genus of the osmiine bees (Hymenoptera, Megachilidae, Osmiini) with 389 species described so far (Müller 2023). The genus is especially diverse in the Palaearctic region, where 14 subgenera and 313 species occur (Praz et al. 2008; Ungricht et al. 2008; Sedivy et al. 2012; Müller 2023). The nesting biology of *Hoplitis* is extremely diverse and encompasses the whole diversity observed in the osmiine bees (Müller 2023). The 110 species, for which nests have been found so far, build their brood cells in self-excavated burrows in the ground or pithy stems, in various kinds of pre-existing cavities (such as hollow stems, insect burrows in wood or pithy stems, abandoned nests of other bees and wasps, rock and stone crevices, rarely galls or empty snail shells), or construct them freely on the surface of rocks or stones, usually in depressions; a few species are kleptoparasitic. Many species of *Hoplitis* build brood cells with complete constructed lateral walls. Other species only divide the nest cavity into cells with transverse partitions and seal it with a closing plug at or near its opening. The building material used for nest and cell construction is also very diverse; depending on the subgenus or species, mud and pebbles, leaf pulp, leaf fragments, petals or pith are used alone or in diverse combinations (Michener 2007; Sedivy et al. 2012; Müller 2023).

Alcidamea Cresson, 1864 is one of the largest subgenera of *Hoplitis*. It occurs in the Palaearctic and the Nearctic region; there are 81 described species, 64 of which occur in the Palaearctic (Michener 2007; Ungricht et al. 2008; Müller 2023). Most representatives of this subgenus nest above ground, mostly in self-excavated burrows in pithy stems or in pre-existing cavities. They usually use plant material for nest and cell construction, particularly leaf pulp, which is sometimes mixed with pith or sand (Müller 2023). One Nearctic species, *Hoplitis biscutellae* (Cockerell, 1897), is known to collect resin (Rust 1980). The Palaearctic species *Hoplitis tuberculata* (Nylander, 1848) uses significant amounts of small pebbles and soil particles, which are densely packed between partitions made of leaf pulp (Müller 2015). Bees of the subgenus *Alcidamea* usually do not construct lateral cell walls except for some species of the *Hoplitis fulva* group, which make complete cells of plant pulp in either self-excavated or pre-existing cavities in the ground (Marikovskaja 1968; Ivanov and Fateryga 2018).

The most unusual nesting habits are, however, known for *Alcidamea* species of the *Hoplitis curvipes* group, which contains five species. Nests of one of them, *Hoplitis mitis* (Nylander, 1852), have been described so far. This species nests below stones, in rock crevices, in grass tussocks, between dried leaves or in old cells of other bees. The brood cells, which are built singly or in small groups of up to 12, entirely consist of leaf fragments imbricately glued together, forming a cone-like structure. The cell closure is made of leaf pulp, which is occasionally reinforced by sand grains or leaf fragments (Maneval 1925; Koller and Hamann 1950; Bonelli 1967; Müller et al. 1997; Westrich 1989). Trophic relationships are known for four species of the *H. curvipes* group: *H. mitis* is oligolectic on Campanulaceae, particularly *Campanula* L. (Fig. 6G), *H. curvipes* (Morawitz, 1871) is oligolectic on *Allium* L. (Amaryllidaceae) (Fig. 1E), *H. tricolor* (Saunders, 1908) is probably oligolectic on *Reseda* Tourn. ex L. (Resedaceae), and *H. epeoliformis* (Ducke, 1899) is polylectic (Müller 2023).

Hoplitis curvipes is known from Spain, France, Italy (including Sicily), Greece, Bulgaria, Russia (Dagestan), Azerbaijan, Turkey, and Syria (Müller 2023). In spite of its relatively large distribution area, nests of *H. curvipes* have not been described so far. The purpose of the present contribution is to report the nesting biology of this rare species based on two nests found in Italy and Russia.

Material and methods

Field observations were carried out in Apulia (Italy) in the vicinity of San Giovanni Rotondo (Monte Gargano, Province of Foggia, 41°42'44"N, 15°44'11"E, ca. 600 m a.s.l.) on 5 July 1994 and in Dagestan (Russia) in the vicinity of Talgi (foothills of the Greater Caucasus, Makhachkala urban okrug, 42°52'36"N, 47°26'42"E, ca. 270 m a.s.l., Fig. 1A) on 13 and 27 June 2021.

The nest from Dagestan was first recorded on 13 June when it was provisioned by the female bee. During the second visit on 27 June, the nest was completed and consisted of two brood cells, which were transported to the laboratory, where they were kept in outdoor conditions in the shade. In January 2022, the two cells were separated from each other, softened in a humid environment, and dismantled. Leaf fragments were detached from the cell walls, pressed between sheets of paper, and dried. They were measured with an ocular micrometer scale of an MBS-9 stereomicroscope and weighed with a precise torsion balance. The cells with the outer coverage of leaf fragments removed were subjected to longitudinal dissection. The cocoons with fecal pellets were removed from the cells. The thickness and dimensions of cell walls and cocoons were measured. The cell walls, the cocoons with fecal pellets, and the prepupae found inside the cocoons were weighed. The prepupae were placed into glass tubes sealed with cotton plugs and kept under outdoor conditions. An emerged bee specimen was deposited in the collection of the V.I. Vernadsky Crimean Federal University.

To ascertain how much of the initial leaf fragments was masticated to leaf pulp, the following calculation was performed. We supposed that the initial average length of the leaf fragments of a brood cell consisted of the sum of the average length of the basal parts of the fragments, which had been masticated to leaf pulp (l_1), and the average length of the intact ends of the fragments (l_2). The total mass of the building material consisted of the mass of the cell wall consisting of leaf pulp (m_1) and the total mass of the removed intact ends of the leaf fragments (m_2). If all leaf fragments would be parallel-sided, l_1 could be calculated as m_1 multiplied by l_2 and divided by m_2 . However, the leaf fragments were approximately 1.5 times broader at their base than at their apex due to apical narrowing. Therefore, the average length of the masticated basal part of a leaf fragment was calculated according to the following formula:

$$l_1 = \frac{m_1 \times l_2}{1.5m_2}.$$

Photographs of the nest were taken with a Canon EOS RP and a Canon EOS Rebel T2i digital camera, a Sigma AF 105 mm f/2.8 and a Tamron SP AF 90 mm f/2.8 Di macro lens, and a Yongnuo YN-14EX macro flash.

Nest architecture and brood cell structure of *Hoplitis curvipes* were compared with those of *H. mitis* based on literature data (Maneval 1925; Koller and Hamann 1950; Bonelli 1967; Westrich 1989) and four nests discovered in the Swiss and Italian Alps (Zeneggen/Valais, 15 July 1990; Val Piora/Ticino, 30 July 1991; St. Pierre/Aosta Valley, 8 July 1996; Surses/Grisons, 10 July 2021).

Results

Nesting sites and nest architecture

The nesting site of *Hoplitis curvipes* in the Monte Gargano/Apulia was situated on an extensively used stony pasture. The nest was found on the ground under a stone. It consisted of two brood cells, which had been built side by side but did not adhere to each other. The cells were constructed from leaf fragments, which were imbricately glued together, forming a cone-like structure (Fig. 1F).

The nesting site in Dagestan was situated on an abandoned open mine covered with sparse herbaceous vegetation with solitary shrubs. No flower-visiting individuals of *H. curvipes* were observed. However, four males of this species were recorded in inflorescences of *A. rotundum* L. s. l. (= *A. erubescens* sensu Grossh., non K. Koch), where they slept during a thunderstorm (Fig. 1E). This plant taxon may represent a separate undescribed species but additional data are required to confirm this assumption (Seregin 2004).

The nest was found due to the observation of the female bee, which was periodically entering the underside of a medium-sized stone (Fig. 1B). After removing this stone two weeks later, the completed nest was found located between several much smaller stones (Fig. 1C). Similar to the nest from Apulia, this nest also consisted of two sub-vertical brood cells, which had been built side by side. The cell, which had been made by the female bee first (hereafter, cell No. 1), was situated lower than the subsequently constructed cell (hereafter, cell No. 2), so that the closing plug of cell No. 1 was approximately at the same level as the medial part of cell No. 2 (Figs 1D, 2A). The cells were neither attached to each other nor to the surrounding stones and could therefore be easily removed. In external view, they consisted of leaf fragments, which were imbricately glued together, forming a cone-like structure like the nest from Apulia.

Brood cell structure

The examination of the nest from Dagestan revealed that the outer coverage of leaf fragments concealed the cell wall made of leaf pulp (Fig. 2C, D). However, the cell wall was not first made by the bee from leaf pulp and then covered with leaf fragments. Instead, each leaf fragment was added to the growing cell wall with its basal part, which



Figure 1. Bionomics of *Hoplitis curvipes* **A** habitat in Dagestan **B** medium-sized stone, under which a female bee entered (arrow) **C** position of the nest under the stone after its removal **D** extracted nest consisting of two brood cells **E** male sleeping in an inflorescence of *Allium rotundum* s. l. **F** nest from Apulia after removal of covering stone consisting of two brood cells with the female entering a cell. Scale bar: 1 cm (**D**).

had been masticated to leaf pulp. Thus, each intact leaf fragment projecting from the cell wall was a shortened remainder of a longer initial leaf fragment, which had been processed to leaf pulp at its base. Therefore, the outer surface of the cell wall was rough

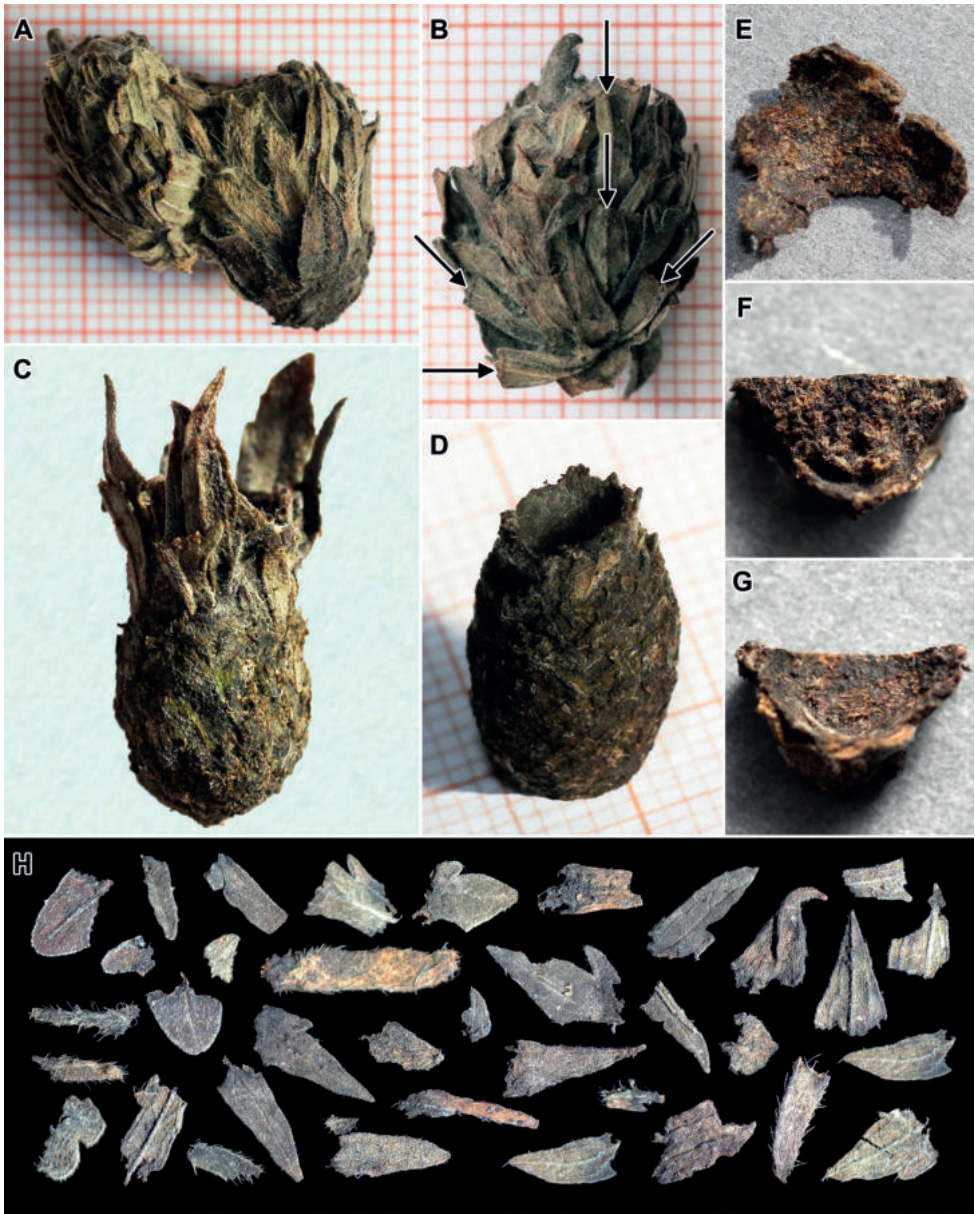


Figure 2. Nest structure of *Hoplitis curvipes* **A** overview of the two-celled nest from Dagestan **B** cell No. 2 (arrows indicate leaf fragments cut from leaves from which other fragments had been previously cut as indicated by their cut apexes) **C** cell after removal of most leaf fragments **D** cell after removal of all leaf fragments **E** part of cell wall from inside **F** part of cell plug from inside **G** part of cell plug from outside **H** intact apical parts of leaf fragments removed from the cell wall.

due to the remnants of the removed intact apical parts of leaf fragments. In contrast, the inner surface of the cell wall was rather smooth (Fig. 2E). The cell was sealed with a closing plug made of pure leaf pulp; its inner surface was irregularly rough (Fig. 2F),

whereas the outer surface was evenly concave and rather smooth (Fig. 2D, G). In both cells, a few leaf fragments were glued to the outer surface of the plug (Fig. 1D).

Cell No. 1 was larger and made from a higher number of leaf fragments than cell No. 2 (Table 1). Both the total mass of the intact apical parts of the leaf fragments and the total mass of the building material comprising both the masticated basal and the intact apical leaf fragment parts were also larger in cell No. 1. However, the total mass of leaf pulp originating from the masticated basal parts was larger in cell No. 2, as was the thickness of the cell wall. Therefore, the leaf fragments used by the female bee were probably masticated at their base to a higher percentage in cell No. 2. This is in line with the finding that the average length of the intact apical parts was larger in cell No. 1, whereas the calculated average length of the initial leaf fragment length was nearly equal (about 9 mm) in both cells (Table 1).

Table 1. Dimensions and contents of the two brood cells of a single nest of *Hoplitis curvipes* from Dagestan.

Parameter	Cell No. 1 (male progeny?)	Cell No. 2 (female progeny)
Cell outer length (without coverage of leaf fragments), mm	13.8	11.6
Cell outer width (without coverage of leaf fragments), mm	10.2	8.8
Cell wall thickness in medial part (without coverage of leaf fragments), mm	0.24	0.29
Total mass of leaf pulp from cell walls and plug, mg	78	100
Number of leaf fragments used for cell walls and plug	92	78
Average length of the intact apical part of the leaf fragments (mean \pm confidence interval, $p = 0.05$), mm	6.79 \pm 0.47	5.43 \pm 0.41
Total mass of the intact apical parts of the leaf fragments, mg	161	100
Estimated average length of the basal part of the leaf fragments, which have been masticated to leaf pulp, mm	2.19	3.62
Estimated average length of the initial leaf fragments, mm	8.98	9.05
Total mass of the building material, mg	239	200
Cocoon outer length, mm	12.9	10.7
Cocoon outer width, mm	8.6	7.2
Cocoon wall thickness (inner layer) in medial part, mm	0.1	0.1
Cocoon mass (with fecal pellets), mg	83	76
Prepupa mass, mg	136	97
Total cell mass (with all contents), mg	458	373

The intact apical parts of the leaf fragments removed from the cell wall had variable lengths ranging from 2.1 to 13.3 mm. They were arranged irregularly so that long fragments imbricately alternated with short ones. However, a general trend was found for both cells, when all intact apical fragments were measured in the order of their application to the cell wall by the female bee: on average, the longest fragments were present in the second quarter, while the shortest fragments were found mainly in the fourth (anterior-most) quarter (Fig. 3). Probably, the female bee cut approximately equally long fragments from the plant source, but then masticated their basal ends to various degrees, so that a longer or shorter apical part remained. If a larger part remained, a smaller amount of leaf pulp was integrated into the growing cell wall, and vice versa. This is consistent with the thickness of the cell wall, which was thinnest in its medial part, where the longest intact leaf fragments were found on average (Fig. 4A).

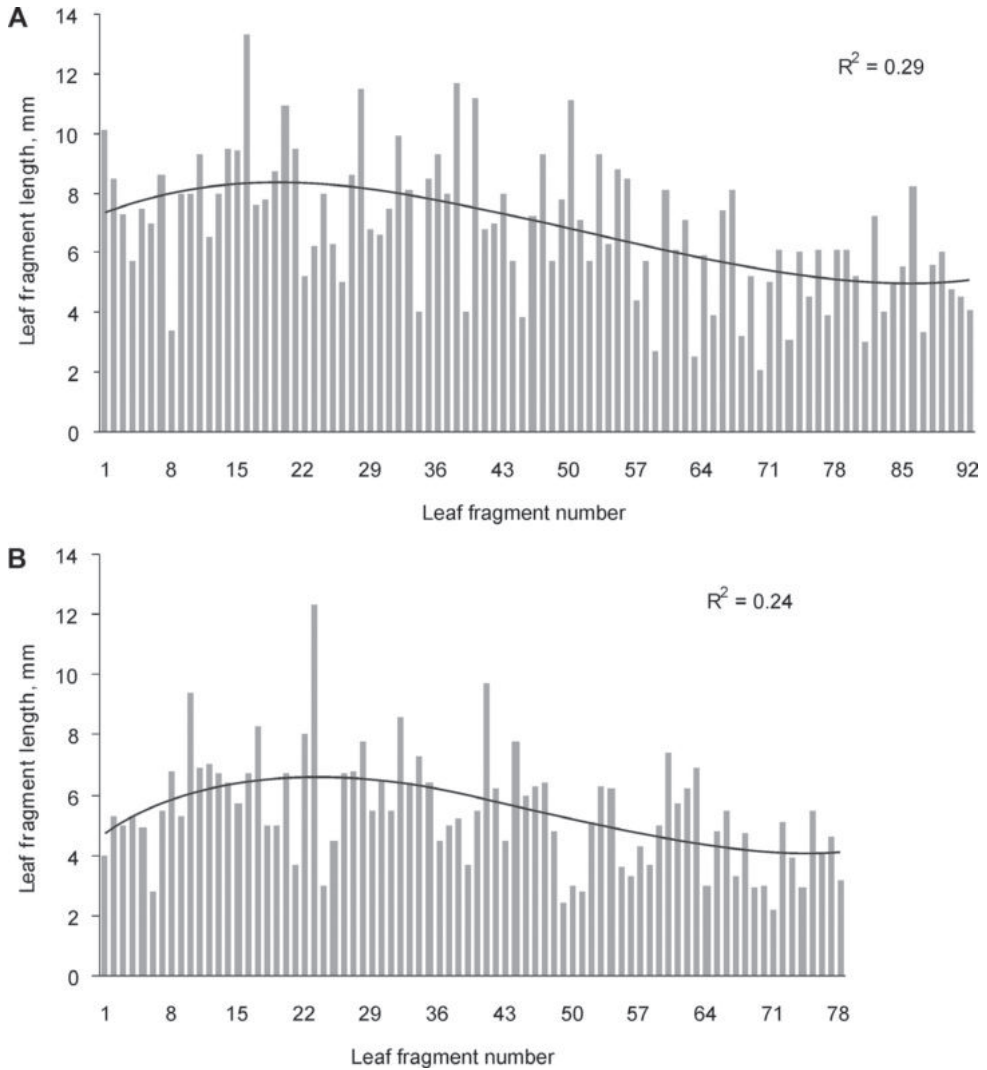


Figure 3. Length of the intact apical parts of the leaf fragments from two cells of *Hoplitis curvipes* from Dagestan, with cubic polynomial approximations **A** cell No. 1 **B** cell No. 2.

The shape of the intact part of the leaf fragments varied (Figs 2H, 4B). It depended mostly on the plant species from which they had been cut. At least five plant species were used by the female bee as the source of the leaf fragments. About 77% of the fragments belonged to an unidentified species with acutely narrowed apex and short trichomes on the underside. About 17% of the fragments were of another unidentified species with a similar leaf shape but with longer trichomes on both upper side and underside. About 4% of the fragments had a rounded apex and also remained unidentified, whereas about 2% of the fragments were of a species of grass (Poaceae) and at least one fragment with a crenated lateral margin originated from *Teucrium* sp. (Lamiaceae).

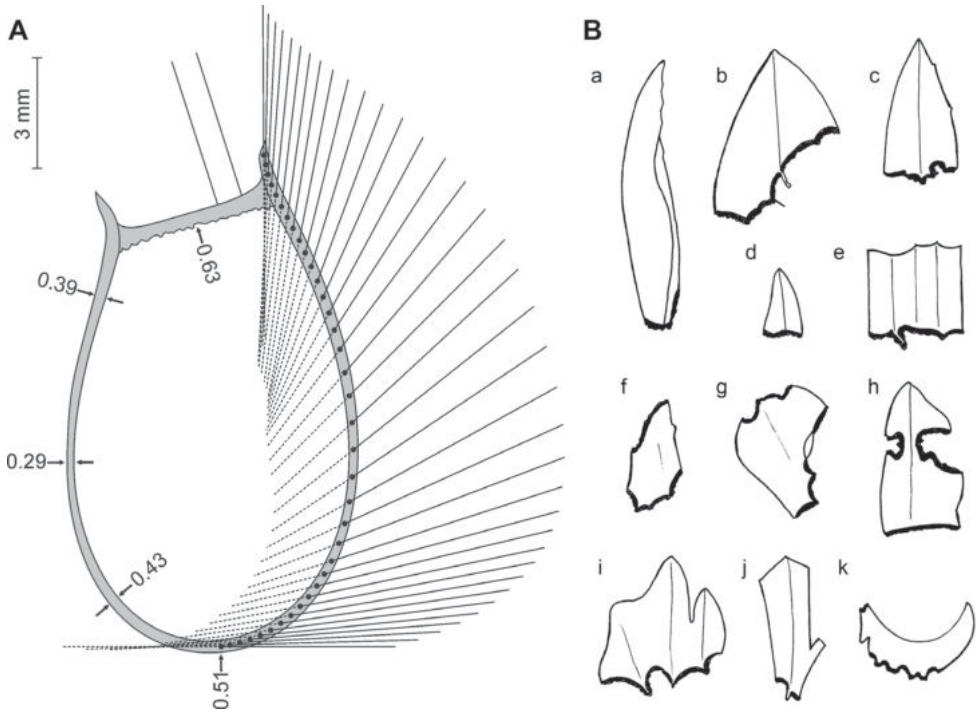


Figure 4. Nest structure of *Hoplitis curvipes* **A** scheme of cell No. 2 of the nest from Dagestan showing the thickness of cell wall and closing plug on the left and the orientation of the leaf fragments incorporated into the cell wall on the right (solid lines correspond to the length of the intact apical parts of the leaf fragments according to the approximation in Fig. 3B, dotted lines represent supposed length of the basal parts of the leaf fragments being masticated to leaf pulp) **B** various examples of intact apical parts of leaf fragments removed from the cell wall.

The base of each intact apical leaf fragment had a chewed margin (Fig. 4B), indicating that the part behind it had been masticated to leaf pulp and incorporated into the growing cell wall. This margin was sometimes straight (Fig. 4B: d, h), but often of irregular shape (Fig. 4B: b, c, i). The irregular margin might be explained by the assumption that the female bee chewed soft parts of the leaf blade but left veins intact. Some leaf fragments had chewed margins not only along the base but also at the apex (Fig. 4B: f, g) or on the lateral sides (Fig. 4B: h). This suggests that the female bee masticated these parts of the leaf fragment only after its base had been incorporated into the cell wall and that she used the resulting leaf pulp to reinforce the cell walls from inside.

The apical margin of some leaf fragments was cut. These fragments were evidently cut from leaves, from which another fragment had been previously cut (Figs 2B, 4B: e, j, k), and suggest that the female bees prefer to collect the nest building material at the very same place. This assumption is supported by the fact that cell No. 2 had more leaf fragments with cut apical margins (20 fragments, 25.6%) than cell No. 1 (six fragments, 6.5%), suggesting that the female bee found a rewarding leaf source during the

construction of cell No. 2. Generally, the shape of the leaf fragments did not seem to be important for the female bee, since even longitudinally folded leaves were applied to the cell walls without unfolding them (Fig. 4B: a).

Cocoon structure and development of prepupae

The cocoon of *Hoplitis curvipes* filled the entire inner surface of the brood cell, neatly corresponding to the cell shape (Fig. 5F–H). It consisted of two layers. The walls of both layers were rather thick, presumably airtight, and largely consisting of a solid brown matrix, which was matt on its outside (Fig. 5A). The outer layer (Fig. 5D: b) covered the inner surface of the closing plug and the most anterior part of the lateral cell walls. This layer had several longitudinal slits on its lateral surface (Fig. 5A), which probably served as air-exchange portals. Below the slits, the outer layer was fused to the inner layer. The inner layer was rather shining on its inside, especially in its posterior half (Fig. 5B, C, H), whereas the anterior half was less shining due to its coverage with free silk strands, which were not incorporated into the matrix (Fig. 5D: e). In its most anterior part, the inner layer had a dome-shaped summit separated from the outer layer by a narrow space. The walls of this “dome” (Fig. 5D: f) gradually became thinner towards the summit, where a small orifice served as air-portal (Fig. 5D: d). The narrow space between the outer and the inner cocoon layer (Fig. 5D: c) was filled with concentric air-permeable “films” woven from silk strands. These “films” covered also the inner side of the air-exchange slits of the outer cocoon layer. The fecal pellets lay densely packed outside the cocoon on its anterior top (Fig. 5E).

Cell No. 1 contained a larger cocoon and a larger prepupa than cell No. 2 (Table 1). The prepupa from cell No. 2 pupated in 2022 and a female bee emerged from it, while the prepupa from cell No. 1 remained hibernating for a second winter. It is known since the original description by Morawitz (1871) that males of *H. curvipes* are larger than females, suggesting that the prepupa from cell No. 1 was a male. Unfortunately, this prepupa died in May 2023 rendering sex determination impossible.

Comparison with *Hoplitis mitis*

The examination of four nests of *Hoplitis mitis* revealed close similarities, but also some differences compared to *H. curvipes*. The structure of the cells, which were 10–12 mm long and 8–9 mm wide, proved to be largely identical as revealed by the following characteristics: i) the cells of *H. mitis* were constructed from imbricately arranged leaf fragments, which formed a cone-like structure (Fig. 6A, B, D, E, F); ii) the leaf fragments consisted of a basal part that was chewed to leaf pulp and an apical part that protruded from the cell; the cell wall was formed by the fusion of the masticated basal parts of the leaf fragments and thus had a smooth inner surface (Fig. 6C); iii) the cells were sealed with a 1 mm thick plug made of leaf pulp, into which a few pieces of leaf

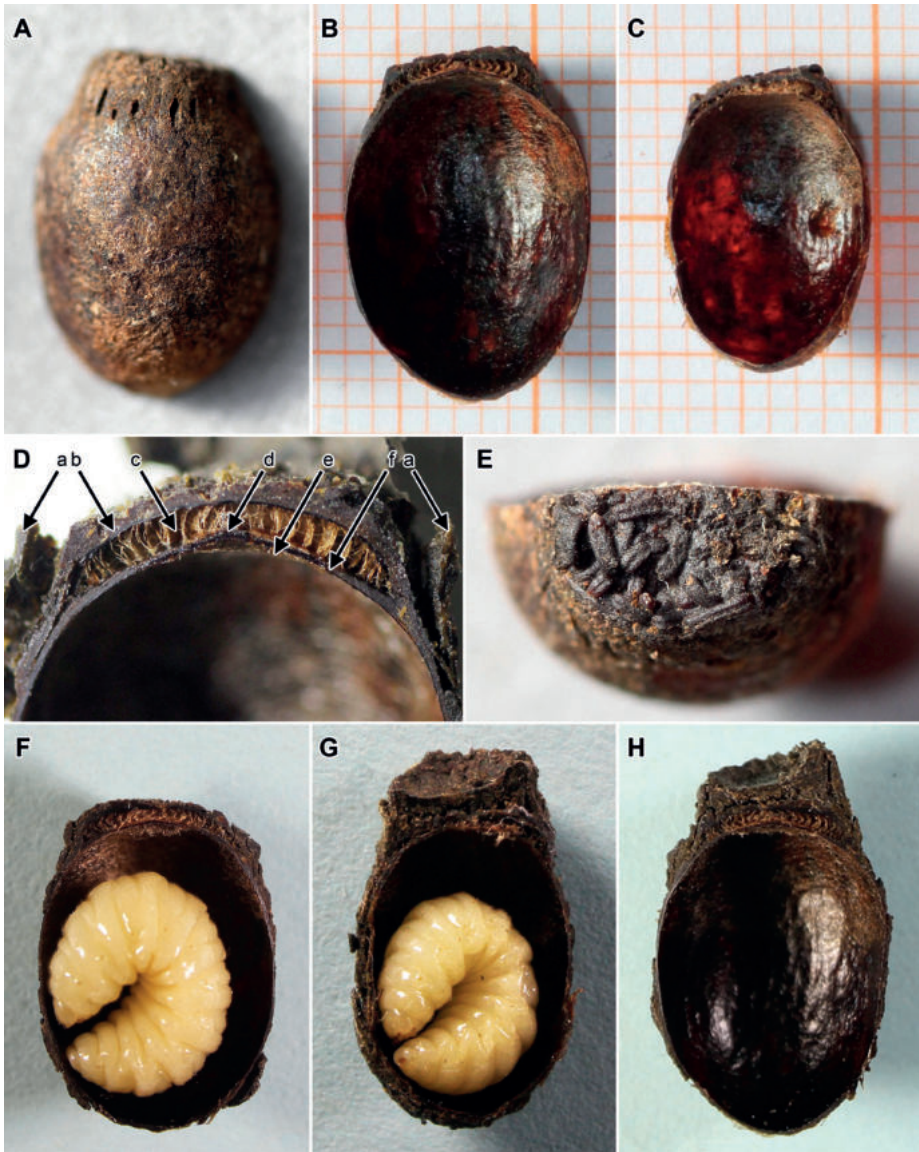


Figure 5. Nest contents of *Hoplitis curvipes* from Dagestan **A** cocoon from cell No. 1 from outside **B** same, from inside **C** cocoon from cell No. 2 from inside **D** anterior part of cocoon in longitudinal section (**a** = cell wall **b** = outer cocoon layer **c** = cavity filled with concentric “films” woven from silk strands **d** = air portal opening **e** = silk strands below the air portal **f** = inner cocoon layer) **E** anterior top of cocoon from above showing amassed fecal pellets **F** dissected cell No. 1 with prepupa hibernating in cocoon **G** same, cell No. 2 **H** dissected cell No. 1 with cocoon after removal of prepupa.

fragments were incorporated by their chewed base; these fragments were directed in longitudinal direction to the cell and slightly curved inwards, so that the nest plug was no longer visible (Fig. 6B, D).



Figure 6. Bionomics of *Hoplitis mitis* **A** nest in dorsal view consisting of three brood cells, which were hidden among dead blades in a grass tussock (Surses, Grisons, Switzerland) **B** same nest as above in frontal view with one brood cell still being provisioned **C** inner surface of brood cell **D** nest consisting of three brood cells, which were hidden under a removed stone (Zeneggen, Valais, Switzerland) **E** single brood cell, which was hidden in dense plant litter (Val Piora, Ticino, Switzerland) **F** single brood cell attached to a stem (St. Pierre, Aosta Valley, Italy) **G** female collecting pollen on *Campanula rotundifolia* (Bräntschu, Valais, Switzerland).

In contrast, some nests of *H. mitis* differed from those of *H. curvipes* in the following characteristics: iv) the brood cells of *H. mitis* may adhere to each other (Fig. 6A, B, D) by smoothed-out leaf pulp from chewed leaf margins, whereas the brood cells

in both discovered nests of *H. curvipes* lay freely side by side; v) while in most nests of *H. mitis* the brood cells did not adhere to the substrate as in *H. curvipes*, one brood cell of *H. mitis* was found attached to a plant stem (Fig. 6F); interestingly, in this cell the leaf fragments were more irregularly arranged and not all aligned longitudinally to the cell axis as is the case for the free-lying cells (Fig. 6A, B, D, E); this more irregular arrangement of the leaf fragments was probably due to the necessity to build part of the cell from the side rather than evenly from the posterior to the anterior end.

Our examination of the four nests of *H. mitis* confirmed the findings of other authors (Westrich 1989 and references therein) except for characteristic ii), which is described here for the first time.

Discussion

In the present study, nest architecture and brood cell structure of *Hoplitis curvipes* are described for the first time. The nesting biology of *H. curvipes* is very similar to that of *H. mitis*, which also belongs to the *H. curvipes* species group of the subgenus *Alcidamea* and whose nesting biology has been described by several authors (Maneval 1925; Koller and Hamann 1950; Bonelli 1967; Müller et al. 1997; Westrich 1989). Both species construct the brood cells from leaf fragments, which are imbricately glued together resulting in a cone-like structure of the cell.

Both nests of *H. curvipes* discovered at two localities 2500 km apart were largely identical: they consisted of two brood cells, which lay freely side by side under a stone and adhered neither to each other nor to the surrounding substrate. Whether these characteristics are universal for *H. curvipes* across the species' entire distribution range is unclear due to the small number of nests discovered so far. It may be possible that the species is more flexible with respect to nesting site or nest architecture as is the case for *H. mitis*, which shows an amazing variability in its nesting behaviour (Maneval 1925; Koller and Hamann 1950; Bonelli 1967; Müller et al. 1997; Westrich 1989; present study): i) *H. mitis* constructs its brood cells either in pre-existing cavities (below stones, rock crevices, abandoned cells of other bees), in vegetation (grass tussocks, plant litter) or attached to plant stems or in angles of pine crotches; ii) the nests contain a varying number of brood cells ranging from 1 to 12, which lie freely side by side or are (partly) attached to each other; iii) the leaf fragments for cell construction are collected on various plant taxa; and iv) the cell closure made from leaf pulp is occasionally reinforced by sand grains.

The nests of *H. curvipes* and *H. mitis* are not only unique among species of the subgenus *Alcidamea*, but also among all other osmiine bees. As reviewed in the Introduction, most other *Alcidamea* species nest in self-excavated or pre-existing cavities and use leaf pulp as building material. Representatives of other taxa of osmiine bees build their nests also from materials other than leaf pulp, such as mud and pebbles or petals. Whole petals or large petal pieces are used by *Hoplitis* species of the subgenus *Anthocopa* Lepeletier & Serville, 1825 and *Osmia* species of the subgenus *Tergosmia* Warncke, 1988 (Rozen et al. 2010; Müller 2020). Although petals are quite similar to leaf fragments, they are applied in a different way for cell construction by *Anthocopa*

and *Tergosmia* species than the leaf fragments in *H. curvipes* and *H. mitis*. Species of *Anthocopa* use the petals to merely line the walls of brood cell cavities and nest burrows, while species of *Tergosmia* construct three-layered cells consisting of two layers of petals that sandwich a thin middle layer of mud (Ivanov and Filatov 2008; Rozen et al. 2010; Müller 2020). The unusual structure of the brood cells of species of the *H. curvipes* group, which do not require the support of the surrounding substrate, enables the construction of nests in cavities of various sizes. One nest of *H. mitis* consisting of six loosely attached cells was even found in the angle of the lowest crotch of a 0.8 m tall pine tree (Koller and Hamann 1950).

Most probably, the ancestors of the *H. curvipes* species group constructed their brood cells from leaf pulp alone, but then evolved to leave the apical parts of the collected leaves unmasticated. This is consistent with the reconstructed phylogeny of the genus *Hoplitis*, which placed *H. curvipes* and *H. mitis* as members of the same clade amidst and not basal to species of *Alcidamea*, which use leaf pulp as nest building material (Sedivy et al. 2012). Within the family Megachilidae, the use of leaf fragments for brood cell construction is most typical for numerous species of the genus *Megachile* Latreille, 1802 (*Megachilini*), which, however, differ from *H. curvipes* and *H. mitis* by their habit to usually cut regularly circular to elliptical leaf pieces (Michener 2007; Ivanov and Zhidkov 2010; Gonzalez et al. 2019). Some *Megachile* species, however, masticate the margins of the cut leaf pieces in order to glue them together (Ivanov and Filatov 2008). As in the *H. curvipes* species group, the leaf-cutting behaviour of *Megachile* probably evolved from ancestors, which used leaf pulp as the main nest building material, but did not completely masticate the cut leaves (Michener 2007; Gonzalez et al. 2019).

Interestingly, the brood cells of species of the *H. curvipes* group are most similar to those of communal wasps of the Indo-Malayan genus *Calligaster* de Saussure, 1852 (Hymenoptera, Vespidae, Zethinae). These wasps construct aerial nests with several brood cells attached together side by side; the cells are cone-shaped and made from leaf fragments, which are imbricately arranged (Nugroho et al. 2016). The difference of these nests from those of the *H. curvipes* species group is that the free apical ends of the leaf fragments are always directed to the posterior end of the cell rather than to the anterior one. Thus, the nests of these wasps look like “inverted” cones, which is an interesting example of convergent evolution of a similar cell structure in solitary bees and vespid wasps.

The cocoon of *H. curvipes* has a structure which corresponds to the generalized scheme of the osmiine bee cocoon with an outer and an inner layer (Rozen and Praz 2016). The outer layer is restricted to the anterior portion of the cell and separated from the inner layer by a narrow space. The inner layer is mostly airtight except for an air-exchange portal at the anterior top. In *H. curvipes*, additional air-exchange slits occur at the lateral sides of the outer layer. In combination, these structures provide humidity control and air exchange and simultaneously serve as a barrier against parasites and predators (Rozen and Praz 2016). A similar structure of the cocoon (“cocoon with an arch”) is found in some chrysidid wasps of the genera *Omalus* Panzer, 1801, *Pseudomalus* Ashmead, 1902, and *Chrysellampus* Semenov, 1932 (Hymenoptera, Chrysididae) (Martynova 2020).

Acknowledgements

Comments by Laurence Packer on the first version of this paper led to improvements. The research was carried out within the state assignment of the Ministry of Science and Higher Education of the Russian Federation, No. 121032300023-7 (for A.F.).

References

- Bonelli B (1967) Osservazioni biologiche sugli Imenotteri melliferi e predatori della Val di Fiemme. XXVI. Bollettino dell'Istituto di Entomologia della Università degli Studi di Bologna 28: 305–317. [+ pls I–III]
- Gonzalez VH, Gustafson GT, Engel MS (2019) Morphological phylogeny of Megachilini and the evolution of leaf-cutter behavior in bees (Hymenoptera: Megachilidae). *Journal of Melittology* 85: 1–123. <https://doi.org/10.17161/jom.v0i85.11541>
- Ivanov SP, Fateryga AV (2018) Nesting biology of the bee *Hoplitis princeps* (Morawitz) (Hymenoptera, Megachilidae) in Crimea. *Entomological Review* 98(8): 995–1005. <https://doi.org/10.1134/S0013873818080067>
- Ivanov SP, Filatov MA (2008) Nest cells construction of wild bees *Megachile albisecta*, *Hoplitis mocsaryi* and *Osmia tergestensis* (Hymenoptera: Apoidea: Megachilidae). *Kharkov Entomological Society Gazette* 15(1–2): 109–116. [In Russian]
- Ivanov SP, Zhidkov VYu (2010) Variety of the forms and sizes of leaf-cuts used by leafcutter-bees (Hymenoptera: Megachilidae, *Megachile* Latreille) when building their nests and theirs functional role. *Proceedings of the Russian Entomological Society* 81(2): 103–111. [In Russian]
- Koller F, Hamann HHF (1950) Nestbau von *Osmia mitis* Nyl. (= *montivaga* Mor.) Hymenopt. (Apidae). *Naturkundliche Mitteilungen aus Oberösterreich* 1: 16–17. [+ pl. II]
- Maneval H (1925) Nidification de l'*Osmia mitis* Nyl. [Hym. Apidae]. *Bulletin de la Société Entomologique de France* 30(12): 199–200. [+ pl. 2] <https://doi.org/10.3406/bsef.1925.27526>
- Marikovskaja TP (1968) New data on the biology of some species of colonial bees (Hymenoptera, Megachilidae) from South-East Kazakhstan. *Entomologicheskoe Obozrenie* 47(4): 796–805. [In Russian]
- Martynova KV (2020) Cocoons of cuckoo wasps (Hymenoptera: Chrysididae): first overview of morphology reveals unexpected traces of taxonomy. *Zoologischer Anzeiger* 285: 122–138. <https://doi.org/10.1016/j.jcz.2020.02.002>
- Michener CD (2007) *The bees of the world* (2nd edn). Johns Hopkins University Press, Baltimore, [xvi +] 953 pp. [+ 20 pls]
- Morawitz F (1871) Neue suedeuropaeische Bienen. *Horae Societatis Entomologicae Rossicae* 8(3): 201–231.
- Müller A (2015) Nest architecture and pollen hosts of the boreoalpine osmiine bee species *Hoplitis (Alcidamea) tuberculata* (Hymenoptera, Megachilidae). *Journal of Hymenoptera Research* 47: 53–64. <https://doi.org/10.3897/JHR.47.7278>

- Müller A (2020) Palaearctic *Osmia* bees of the subgenera *Hemiosmia*, *Tergosmia* and *Erythrosmia* (Megachilidae, Osmiini): biology, taxonomy and key to species. *Zootaxa* 4778(2): 201–236. <https://doi.org/10.11646/zootaxa.4778.2.1>
- Müller A (2023) Palaearctic Osmiine Bees, ETH Zürich. <http://blogs.ethz.ch/osmiini> [accessed 3 September 2023]
- Müller A, Krebs A, Amiet F (1997) Bienen. Mitteleuropäische Gattungen, Lebensweise, Beobachtung. Naturbuch Verlag, Augsburg, 384 pp.
- Nugroho H, Ubaidillah R, Kojima J (2016) Taxonomy of the Indo-Malayan presocial potter wasp genus *Calligaster* de Saussure (Hymenoptera, Vespidae, Eumeninae). *Journal of Hymenoptera Research* 48: 19–32. <https://doi.org/10.3897/JHR.48.7045>
- Praz CJ, Müller A, Danforth BN, Griswold TL, Widmer A, Dorn S (2008) Phylogeny and biogeography of bees of the tribe Osmiini (Hymenoptera: Megachilidae). *Molecular Phylogenetics and Evolution* 49(1): 185–197. <https://doi.org/10.1016/j.ympev.2008.07.005>
- Rozen Jr JG, Özbek H, Ascher JS, Sedivy C, Praz CJ, Monfared A, Müller A (2010) Nests, petal usage, floral preferences, and immatures of *Osmia* (*Ozbekosmia*) *avosetta* (Megachilidae: Megachilinae: Osmiini), including biological comparisons with other osmiine bees. *American Museum Novitates* 3680: 1–22. <https://doi.org/10.1206/701.1>
- Rozen Jr JG, Praz CJ (2016) Mature larvae and nesting biologies of bees currently assigned to the Osmiini (Apoidea: Megachilidae). *American Museum Novitates* 3864: 1–46. <https://doi.org/10.1206/3864.1>
- Rust RW (1980) Nesting biology of *Hoplitis biscutellae* (Cockerell) (Hymenoptera: Megachilidae). *Entomological News* 91(4): 105–109.
- Sedivy C, Dorn S, Müller A (2012) Molecular phylogeny of the bee genus *Hoplitis* (Megachilidae: Osmiini) – how does nesting biology affect biogeography? *Zoological Journal of the Linnean Society* 167(1): 28–42. <https://doi.org/10.1111/j.1096-3642.2012.00876.x>
- Seregin AP (2004) *Allium nathaliae* (Alliaceae), a new species from the Crimea (Ukraine, Europe), and taxonomic notes on the related species *A. erubescens* C. Koch. *Wulfenia* 11: 15–28.
- Ungricht S, Müller A, Dorn S (2008) A taxonomic catalogue of the Palaearctic bees of the tribe Osmiini (Hymenoptera: Apoidea: Megachilidae). *Zootaxa* 1865: 1–253. <https://doi.org/10.11646/zootaxa.1865.1.1>
- Westrich P (1989) Die Wildbienen Baden-Württembergs. Ulmer, Stuttgart, 972 pp.

An updated molecular phylogeny of the stingless bees of the genus *Trigona* (Hymenoptera, Meliponini) of the northern Peruvian forests

Marilena Marconi¹, Daniel Ushiñahua Ramírez², Agustín Cerna Mendoza²,
Carlos Daniel Vecco-Giove², Javier Ormeño Luna², Liliia Baikova³,
Andrea Di Giulio¹, Emiliano Mancini³

1 Department of Science, Roma Tre University, Viale Guglielmo Marconi, 446, 00146 Roma, Italy
2 Universidad Nacional de San Martín, Jr. Maynas, 177, 22200 Tarapoto, Peru **3** Department of Biology and Biotechnology “Charles Darwin”, Sapienza University of Rome, Viale dell’Università, 32, 00185 Roma, Italy

Corresponding author: Marilena Marconi (marilena.marconi@gmail.com)

Academic editor: Jack Neff | Received 21 April 2023 | Accepted 11 August 2023 | Published 11 October 2023

<https://zoobank.org/18173776-109D-4DD4-9BF0-C6E264C7CD07>

Citation: Marconi M, Ushiñahua Ramírez D, Cerna Mendoza A, Vecco-Giove CD, Ormeño Luna J, Baikova L, Di Giulio A, Mancini E (2023) An updated molecular phylogeny of the stingless bees of the genus *Trigona* (Hymenoptera, Meliponini) of the northern Peruvian forests. Journal of Hymenoptera Research 96: 751–760. <https://doi.org/10.3897/jhr.96.105311>

Abstract

Stingless bees (Hymenoptera, Meliponini) are a large and diverse group including 59 extant groups, representing the main pollinators of Amazon forests. Among those, *Trigona* is one of the largest endemic genera of Neotropical Meliponini. In this work, we updated the molecular phylogeny of *Trigona* proposed by Rasmussen and Camargo (2008), including data from 59 new specimens collected in 2020 in the forests of northern Peru, through a multigene phylogenetic approach combining sequences from four gene fragments (16S, ArgK, EF-1a, opsin). Our results confirmed the monophyly of *Trigona* and of all proposed subgenera, except *Aphaneura*. In addition, most *Trigona* species-groups resulted monophyletic but the ‘*spinipes*’ and ‘*pallens*’ groups appeared paraphyletic and polyphyletic, respectively. Moreover, the cohesion of the “*fulviventris*” species group was hindered by the inclusion of *T. williana* (previously included in the “*pallens*” group) within this clade. Finally, we provided further evidence for a subdivision into two (geographically) distinct clades within *T. guianae* in northern Peruvian Amazon, which highlighted the importance of Neotropical biogeographical barriers in Meliponini divergence and evolution. Finally, to avoid misidentifications of *Trigona* specimens, the need for a robust taxonomic revision based on a cladistic approach of the whole genus is discussed.

Keywords

Apoidea, Neotropical biogeography, Peruvian Amazon, Taxonomy

Introduction

Stingless bees (Hymenoptera, Meliponini) are major pollinators in tropical forests (Roubik 1989) with about 623 species belonging to 59 extant and fossil groups (considered as genera, subgenera or synonymized depending on the classification) (Engel et al. 2023). Meliponini are distributed throughout the tropical and subtropical areas of the Afrotropical, Australasian, Indo-Malayan and Neotropical Regions, exhibiting the highest diversity in the New World Amazonian rainforests (Michener 1978; Roubik 1993; Michener 2007). Currently, 26 extant genera are considered endemic to the New World (Engel et al. 2023). Among these, *Trigona* Jurine, 1807 is exclusive to the Neotropics and is one of the largest genera of stingless bees (Michener 2007; Rasmussen and Cameron 2007). Recent molecular phylogenetic data confirmed the monophyly of the New World species of *Trigona*, a genus with 32 currently considered valid species (Camargo et al. 2013; Costa et al. 2003; Rasmussen and Cameron 2007; Rasmussen and Camargo 2008). Nine species-groups have been recognized based on morphological, ecological and distributional data, and largely supported by genetic analyses (Rasmussen and Camargo 2008). More recently, seven of these species-groups were elevated to subgenera of *Trigona* (Engel 2021) [i.e., ‘*cilipes*’ as *Aphaneuropsis* Engel, 2021; ‘*fulviventris*’ as *Koilotrigona* Engel, 2021; ‘*crassipes*’ as *Necrotrigona* Engel, 2021; ‘*pallens*’ as *Aphaneura* Gray, 1832; ‘*dimidiata*’ as *Dichrotrigona* Engel, 2021; ‘*fuscipennis*’ as *Ktinotrofia* Engel, 2021; ‘*recurva*’ as *Nostotrigona* Engel, 2021], with the remaining two groups, ‘*amalthea*’ and ‘*spinipes*’ forming the subgenus *Trigona s. str.* Jurine, 1807.

This group of bees, characterized by small to large workers (5.5–11 mm), shows a variety of defense behaviors and nesting habits (i.e. nests are built on branches of plants or walls, in anthills or underground; Costa et al. 2004), as well as different foraging ecologies, from pollen and nectar gatherers (Fig. 1) to obligated necrophages (i.e., *Trigona crassipes* Fabricius, 1793, *T. hypogea* Silvestri, 1902 and *T. necrophaga* Camargo & Roubik, 1991; Roubik 1982; Camargo and Roubik 1991).

About 22 species of *Trigona* have been reported in Peru (Rasmussen and Gonzalez 2009; Camargo et al. 2013; Sánchez Sandoval et al. 2015; Castillo-Carrillo et al. 2016; Rasmussen and Delgado 2020), but the overall number is likely underestimated because many forested areas of the country remain unexplored.

Recently, several *Trigona* specimens dwelling in humid and seasonally dry forests of northern Peru (in San Martín and Piura regions) were identified through an integrative taxonomy approach, i.e., considering both morphology and COI barcoding (Marconi et al. 2022). As expected, the COI-based reconstructed phylogeny was mostly unresolved at deep nodes. In addition, the newly collected Peruvian specimens ascribed to *T. fulviventris* Guérin-Meneville, 1845 and *T. guianae* Cockerell, 1912 were split into four distinct clades, two for each species (named provisionally as ‘A’ and ‘B’ clades in both cases). The same phylogenetic analysis also detected two lineages that were unrelated to other identified species, which were provisionally attributed to *T. sp. 1* and *T. sp. 2*, respectively (Marconi et al. 2022).



Figure 1. *Trigona* cf. *chanchamayoensis* Schwarz, 1948 sucking nectar from a flower (Photo M. Marconi).

In this work we conducted a multigene phylogenetic analysis of the Neotropical genus *Trigona* by integrating novel molecular data of four genes obtained from northern Peruvian specimens (Marconi et al. 2022) with a previously published dataset (Rasmussen and Camargo 2008). By updating the current phylogeny, we aimed to clarify the taxonomic issues emerged in our previous work (Marconi et al. 2022) and further validate the currently recognized species-groups within *Trigona* (Rasmussen and Camargo 2008) and the recently proposed subgenera (Engel 2021).

Methods

59 specimens of *Trigona* were collected in 2020 in five Northern Peruvian forests, all located east of Andes except Mangamanguilla [Juliampampa (JP) (800–110 m a.s.l. and $-6^{\circ}26'3.5556''\text{N}$, $-76^{\circ}19'47.5896''\text{E}$), Pabloyacu (PY) (950–1200 m a.s.l. and $-6^{\circ}4'6.3984''\text{N}$, $-76^{\circ}56'24.8388''\text{E}$), Pongo de Cainarachy (POA) (150–550 m a.s.l. and $-6^{\circ}21'22.608''\text{N}$, $-76^{\circ}17'3.174''\text{E}$), Utcurarca (UT) (250–550 m a.s.l. and $-6^{\circ}39'43.7616''\text{N}$, $-76^{\circ}17'0.438''\text{E}$) and Mangamanguilla (MA) (140–450 m a.s.l. and $-5^{\circ}18'46.5228''\text{N}$, $-79^{\circ}51'51.084''\text{E}$)] and tentatively assigned through an integrative taxonomic approach (i.e. combining morphology and COI barcoding, after a 'salting-out' DNA extraction from one middle leg) to ten different species (Marconi et al. 2022). PCR was conducted to amplify gene fragments of mitochondrial 16S rRNA (16S), nuclear long-wavelength rhodopsin copy 1 (opsin), elongation factor-1a copy F2 (EF-1a), and arginine kinase (ArgK) using published primers (Rasmussen and Cameron 2007; Rasmussen and Camargo 2008). The total reaction volume (25 μl) contained 0.5 pmol of each primer, 10 mM Tris-Cl, pH 8.3 and 50 mM KCl, 1.5 mM MgCl_2 , 2.5 mM dNTPs, 2 μl of the DNA template and 1 unit of Taq DNA polymerase (Meridian). PCR cycling conditions consisted of an initial denaturation of

3 min. at 94 °C followed by 35 cycles of 30 sec. at 94 °C, 30 sec. at 50 °C and 1 min. at 72 °C, and a final elongation step of 10 min. at 72 °C. Products were visualized on a 1% agarose gel stained using Midori Green Advance dye (Nippongenetics). PCR products were purified using the ExoSAP-IT PCR Product Cleanup Reagent (Applied Biosystem) and sent to the sequencing facility of Microsynth AG (Switzerland).

DNA sequences were edited and aligned with STADEN PACKAGE 2.0.0b11-2016 (<http://staden.sourceforge.net/>). Sequences (including those of outgroup taxa) from Rasmussen and Camargo (2008) were downloaded and aligned with our data using MAFFT v1.4.0 (Kato and Standley 2013) to produce comprehensive datasets. Phylogenetic analyses were conducted with Maximum Likelihood (ML) and Bayesian Inference (BI) on both single gene and combined datasets. For both ML and BI approaches, ModelFinder (Kalyaanamoorthy et al. 2017) implemented in IQ-TREE v 1.6.12 (Nguyen et al. 2015) was used to find the best substitution model for each gene (= partition) according to the BIC criterion. ML analyses were performed with IQ-TREE v 1.6.12 (Nguyen et al. 2015) setting 2000 replicates to estimate node supports with ultrafast bootstrap (UFBboot2; Hoang et al. 2018). MRBAYES v3.2.7a (Ronquist et al. 2012) was used for Bayesian Inferences by running two MCMC and four chains for 10 million generations with a default (25%) burn-in. Trees were sampled every 1000 generations, and convergence assessed with Tracer v1.6 (Rambaut et al. 2014). FIGTREE v1.3.1 (Rambaut and Drummond 2009) was used to inspect the obtained trees. Only clades with UFBoot (UFB) values $\geq 95\%$ (Minh et al. 2013) and posterior probability (PP) values ≥ 0.95 (Erixon et al. 2003) were considered as strongly supported upon analyses. All voucher specimens were deposited in Estudios Amazonicos Biological Material Depository Center (Tarapoto, Peru) (Marconi et al. 2022).

Results

We obtained 58 sequences of 16S (Genbank Acc. n° OR353456–OR353513), 26 of ArgK, 41 of EF-1a and 26 of opsin (Genbank Acc. n° OR393480–OR393571) from a total of 59 northern Peruvian *Trigona* specimens collected in 2020 (Marconi et al. 2022). The combined dataset, including previously generated sequences of *Trigona* and outgroup species (Rasmussen and Camargo 2008), consisted of a total of 88 individuals (including 5 outgroups) with 2329 aligned positions composed by the four gene fragments: 485 base pairs (bp) of 16S, 592 bp of ArgK, 729 bp of EF-1a and 522 bp of opsin gene. ML and BY tree topologies largely overlapped (hence, BY topology only is shown; Fig. 2). The combined ML and BY analysis confirmed the monophyly of the genus *Trigona* (Fig. 2: PP = 1.00/UFB = 100) and the presence of two main distinct clades, one (PP = 1.00/UFB = 98) including members of the ‘*amalthea*’ + ‘*spinipes*’ (= *Trigona s. str.*), ‘*fuscipennis*’, (= *Ktinotrofia*) ‘*recurva*’ (= *Nostotrigona*) and ‘*crassipes*’ (= *Necrotrigona*) species groups (or subgenera) (PP = 1.00/UFB = 100), the other including members of the ‘*cilipes*’ (= *Aphaneuropsis*), ‘*pallens*’ (= *Aphaneura*) and ‘*fulviventris*’ (= *Koilotrigona*) species groups (or subgenera) (Rasmussen and Camargo 2008; Engel

2021) (Fig. 2). Five out of the 8 *Trigona* species groups were recovered as monophyletic: ‘*amalthea*’ (PP = 1.00/UFB = 99), ‘*fuscipennis*’ (PP = 1.00/UFB = 100), ‘*recurva*’ (also including *T. sp. 1*; PP = 1.00/UFB = 98), ‘*crassipes*’ (PP = 1.00/UFB = 98), ‘*cilipes*’ (PP = 1.00/UFB = 100). The ‘*spinipes*’ group appeared paraphyletic since it was split into two distinct, though poorly supported clades (Fig. 2). One included *T. spinipes*, *T. hyalinata*, *T. corvina* and *T. amazonensis* (‘*spinipes*’ 1; PP = 0.80/UFB = 94), whereas the other grouped *T. nigerrima* and *T. dallatorreana* (= *T. sp. 2*) (‘*spinipes*’ 2; PP = 0.93/UFB = 71). However, all ‘*spinipes*’ members clustered with those of ‘*amalthea*’, thus supporting the monophyly (PP = 1.00/UFB = 100) of the subgenus *T.* (*Trigona s. str.*) *sensu* Engel 2021. *T. williana* did not cluster within the ‘*pallens*’ group, but was genetically closer to members of the ‘*fulviventris*’ group (= *Koilotrigona*). However, its placement within the ‘*fulviventris*’ group or *Koilotrigona* subgenus remains doubtful since it received a low Bayesian support (PP = 0.52; Fig. 2). Hence, the ‘*pallens*’ group and the subgenus *Aphaneura* Gray 1832 (Engel 2021) are tenable only if *T. williana* is excluded and placed in a different group/subgenus, still to be defined. Finally, as already reported (Marconi et al. 2022), Peruvian specimens of *T. guianae* were subdivided into two well-supported and distinct clades (A and B) (Fig. 2), whereas those ascribed to *T. fulviventris* were included in the same clade (A+B; see Marconi et al. 2022).

Discussion

We here built upon the molecular phylogeny of the Neotropical genus *Trigona* (Rasmussen and Camargo 2008) by adding genetic data from newly collected specimens in northern Peruvian forests (Marconi et al. 2022).

We confirmed the monophyly of the Neotropical genus *Trigona* and of all proposed subgenera, except for *Aphaneura* Gray, 1832 (Engel 2021). In addition, most *Trigona* species-groups were found to be monophyletic (Fig. 2). However, as already observed (Rasmussen and Camargo 2008), the ‘*spinipes*’ and ‘*pallens*’ species groups were paraphyletic and polyphyletic, respectively (Fig. 2). Our results support combining members of the ‘*amalthea*’ and ‘*spinipes*’ groups into the proposed subgenus *T.* (*Trigona s. str.*). However, the closely related *T.* (*Trigona*) *dallatorreana* (= *T. sp. 2*; Marconi et al. 2022) and *T.* (*Trigona*) *nigerrima* should be ascribed to a different species-group (provisionally named ‘*spinipes*’ 2 in Fig. 2). As previously mentioned, the ‘*pallens*’ group (= *Aphaneura*) as usually recognized is polyphyletic due to the large genetic distance of *T. williana* from all other members of this group/subgenus. In fact, *T. williana* is similar only in coloration to members of the ‘*pallens*’ group and differs in the shape of metasoma and metatibiae (F.F. De Oliveira, pers. comm.). The placement of *T. williana* within the ‘*fulviventris*’ group is also doubtful as it differs in many morphological and biological features from other members of the group. Its true placement will require further investigation. In general, since some taxonomic issues affect the ‘*pallens*’ group (e.g., the types of both *T. muzoensis* Schwarz, 1948 and *T. ferricauda* Cockerell, 1917 should be re-examined to exclude possible synonymies), we cannot rule out that

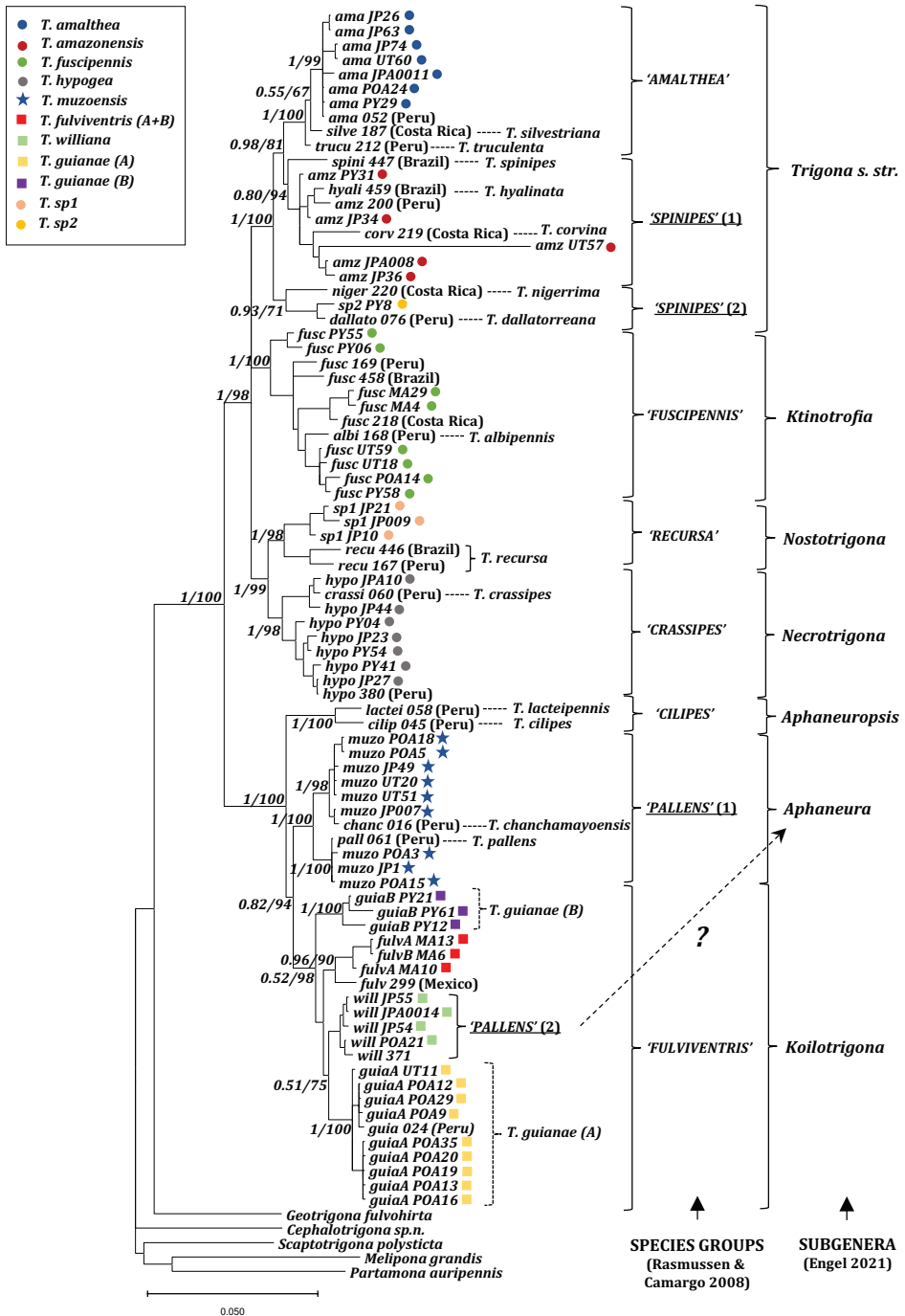


Figure 2. *Trigona* Bayesian phylogenetic tree topology estimated from combined sequence data from four gene fragments (16S, ArgK, EF-1a, opsin). Posterior probability and ultra-fast bootstrap values (BY - PP/ML - UFB) are shown at deepest nodes only. Color marks are assigned to tips leading to the 59 northern Peruvian specimens belonging to *Trigona* species, whose taxonomic identification and geographic origin are reported in detail in table 1 of Marconi et al. 2022.

our specimens, formerly recognized through the integrative taxonomic approach as *T. muzoensis* (Marconi et al. 2022), could be instead ascribed to *T. chanchamayoensis* Schwarz, 1948 - occurring in Peru east of Andes (type locality: San Ramon, Valle de Chanchamayo, Peru) - or to *T. pallens* Fabricius, 1798. In fact, the specimens morphologically identified by Rasmussen and Camargo (2008) as *T. chanchamayoensis* and *T. pallens* (i.e., chanc 016 and pall 061; Fig. 2) are placed in two distinct clades including two separate groups of individuals previously identified as *T. muzoensis* (Marconi et al. 2022), respectively (Fig. 2). When these northern Peruvian specimens were identified in BoldSystems (www.boldsystems.org) (Marconi et al. 2022), they received ID scores ranging 96.43 (POA) - 98.46% (e.g., JP007) for *T. muzoensis*, but did not match with the single *T. chanchamayoensis* available in BoldSystems (from Brazil), nor with *T. pallens*, totally lacking COI data. Unfortunately, taxonomic keys to promptly distinguish morphologically all members of the ‘*pallens*’ group are also lacking. Similarly, doubts could be raised to our previous attribution of northern Peruvian specimens to *T. cf. hypogea* or *T. cf. fuscipennis* (Marconi et al. 2022), because these show a close (although scarcely supported) phylogenetic relatedness to two species identified by Rasmussen and Camargo (2008), i.e., *T. crassipes* (crassi 060) and *T. albipennis* (albi 168), respectively (Fig. 2). However, for these two species as well, data are lacking in BoldSystems, nor valuable keys of distinctive morphological characters are available for ‘*crassipes*’ and ‘*fuscipennis*’ groups. In general, the absence of published dichotomous keys based on reliable diagnostic morphological characters and cladistic approaches integrating extensive genetic (COI or other marker) datasets aimed to define species boundaries, still hinder the correct identification of stingless bee species (see also, Marconi et al. 2022). These data deficiencies are likely to generate conflicts in *Trigona* identification (as, in this case, with those of Rasmussen and Camargo 2008) and favor the description of new species without truthfully considering their morphological and genetic internal cohesion, as well as their distinction from other (sibling) taxa.

We also confirmed a genetic subdivision within *T. guianae* into two putatively distinct taxonomic and/or geographic units, possibly originated by limited gene flow due to biogeographic barriers in the Neotropics (Marconi et al. 2022). Indeed, comparative analysis of metatarsi of *T. guianae* (Clade A) and *T. guianae* (Clade B) revealed morphological differences at the retrodorsal margin and distal angle (unpublished data). Further data will allow establishing if *T. guianae* (Clade B) could be ascribed to a novel species endemic to Pabloyacu, or to one of the approximately 28 novel species awaiting description (Rasmussen and Camargo 2008). On the other hand, the combined molecular dataset did not support the split into two distinct entities in *T. fulviventris*, as previously suggested based on COI marker only (Marconi et al. 2022). However, a recent morphological analysis showed that *T. cf. fulviventris* (Clade A) has a narrow subtriangular metatibia, whereas *T. cf. fulviventris* (Clade B) (MA6) has a broad, “drop-like” shape (unpublished data). Additional specimens will be examined, both genetically and morphologically, to clarify such issues.

Concerning the two previously unidentified *Trigona* species (Marconi et al. 2022), as reported above we confirm that *T. sp. 2* is *T. dallatorreana*, whereas *T. sp. 1* seems to be related to *T. recursa*, although its taxonomic relationships need further examination.

Novel genetic/genomic data from populations sampled across the entire geographic ranges of all of the *Trigona* species groups will shed light on the phylogenetic relationships among members of this large genus of Neotropical stingless bees. Further morphological work is also needed to produce and/or refine taxonomic keys and accurately revise the taxonomy of this speciose genus. Such an effort would not only resolve some taxonomic issues within this large genus of stingless bees, but also enhance our understanding of the role of Neotropical biogeographic barriers in the evolution of this main group of pollinators of the Amazon forests.

Acknowledgements

The authors thank the community of Mangamanguilla, Paolo Villegas Ogoña, Miguel Tapullima and Hitler Panduro Salas for facilitating sampling activities in Northern Peruvian forests; Noemi Centrone and Alessandro Modesti for helping the laboratory work; Leydi Paz Alvarez to assist the field activities; the NGO Estudios Amazónicos to support all research on Meliponini in Peru. This work was supported by the Cooperation Project of Sapienza 2022 (Prot. n° 0001626) “Verso una Meliponicoltura Consapevole e Tutela delle Api senza Pungiglione nella Foresta Amazzonica del Perù”; by the Department of Excellence of the University of Roma Tre; Proyectos de Investigación Básica 2023-01 (PROCIENCIA n° 82163) “Modelo transdisciplinar para la comprensión de la diversidad clave de las abejas peruanas sin aguijón (Hymenoptera: Apidae: Meliponini) con fines de conservación y el desarrollo de una meliponicultura competitiva en la Amazonia”; the Project “Monitoraggio e protezione degli impollinatori del PN Circeo” (University of Roma Tre and PN Circeo).

References

- Camargo JMF, Roubik DW (1991) Systematics and bionomics of the apoid obligate necrophages: the *Trigona hypogea* group (Hymenoptera: Apidae: Meliponinae). *Biological Journal of the Linnean Society* 44: 13–39. <https://doi.org/10.1111/j.1095-8312.1991.tb00604.x>
- Camargo JMF, Pedro SRM, Melo GAR (2013) Meliponini Lepeletier, 1836. In: Moure JS, Urban D, Melo GAR (Eds) *Catalogue of Bees (Hymenoptera, Apoidea) in the Neotropical Region*, online version. <http://www.moure.cria.org.br/catalogue>
- Castillo-Carrillo P, Elizalde R, Rasmussen C (2016) Inventario de las abejas nativas sin aguijón (Hymenoptera: Apidae: Meliponini) en Tumbes-Perú. *Revista Notas Apícolas* 16: 43–50.
- Costa MA, Del Lama MA, Melo GAR, Sheppard WS (2003) Molecular phylogeny of the stingless bees (Apidae, Apinae, Meliponini) inferred from mitochondrial 16S rDNA sequences. *Apidologie* 34: 73–84. <https://doi.org/10.1051/apido:2007051>
- Costa KF, Brito RM, Miyazawa CS (2004) Karyotypic description of four species of *Trigona* (Jurine, 1807) (Hymenoptera, Apidae, Meliponini) from the State of Mato Grosso, Brazil. *Genetics and Molecular Biology* 27(2): 187–190. <https://doi.org/10.1590/S1415-47572004000200010>

- Engel MS (2021) Emendations to the classification of the Meliponini (Apinae): The genera *Axestotrigona*, *Nannotrigona*, *Asperplebeia*, *Plebeia*, *Schwarziana*, and *Trigona*, with keys to the African fauna and *Plebeia*-group genera, 55–83. In: Engel MS, Herhold HW, Davis SR, Wang B, Thomas JC (2021) Stingless bees in Miocene amber of southeastern China (Hymenoptera: Apidae). *Journal of Melittology* 105: 1–83. <https://doi.org/10.17161/jom.i105.15734>
- Engel MS, Rasmussen C, Ayala R, de Oliveira FF (2023) Stingless bee classification and biology (Hymenoptera, Apidae): a review, with an updated key to genera and subgenera. *ZooKeys* 1172: 239–312. <https://doi.org/10.3897/zookeys.1172.104944>
- Erixon P, Svennblad B, Britton T, Oxelman B (2003) Reliability of Bayesian posterior probabilities and bootstrap frequencies in phylogenetics. *Systematic Biology* 52(5): 665–673. <https://doi.org/10.1080/10635150390235485>
- Hoang DT, Chernomor O, Haeseler A, Minh BQ, Vinh LS (2018) UFBoot2: improving the ultrafast bootstrap approximation. *Molecular Biology and Evolution* 35(2): 518–522. <https://doi.org/10.1093/molbev/msx281>
- Kalyaanamoorthy S, Minh BQ, Wong TKF, von Haeseler A, Jermin LS (2017) ModelFinder: fast model selection for accurate phylogenetic estimates. *Nature Methods* 14: 587–589. <https://doi.org/10.1038/nmeth.4285>
- Katoh K, Standley DM (2013) MAFFT multiple sequence alignment software version 7: improvements in performance and usability. *Molecular Biology and Evolution* 30: 772–780. <https://doi.org/10.1093/molbev/mst010>
- Marconi M, Modesti A, Alvarez LP, Ogoña PV, Mendoza AC, Vecco-Giove CD, Ormeño Luna J, Di Giulio A, Mancini E (2022) DNA barcoding of stingless bees (Hymenoptera: Meliponini) in northern Peruvian forests: a plea for integrative taxonomy. *Diversity* 14(8): 632–651. <https://doi.org/10.3390/d14080632>
- Michener CD, Winston ML, Jander R (1978) Pollen manipulation and related activities and structures in bees of the family Apidae. *University of Kansas Science Bulletin* 51(19): 575–601. <https://doi.org/10.5962/bhl.part.17249>
- Michener CD (2007) *The Bees of the World*, 2nd ed. Johns Hopkins University Press, Baltimore, 953 pp.
- Minh BQ, Nguyen MAT, von Haeseler A (2013) Ultrafast approximation for phylogenetic bootstrap. *Molecular Biology and Evolution* 30: 1188–1195. <https://doi.org/10.1093/molbev/mst024>
- Nguyen LT, Schmidt HA, von Haeseler A, Minh BQ (2015) IQ-TREE: a fast and effective stochastic algorithm for estimating maximum likelihood phylogenies. *Molecular Biology and Evolution* 32: 268–274. <https://doi.org/10.1093/molbev/msu300>
- Rambaut A, Drummond AJ (2009) FigTree, version 1.3.1. Institute of Evolutionary Biology, University of Edinburgh, Edinburgh. <http://tree.bio.ed.ac.uk/software/figtree/>
- Rambaut A, Drummond AJ, Suchard M (2014) Tracer v1. 6. <http://beast.bio.ed.ac.uk/Tracer>
- Rasmussen C, Delgado C (2019) Abejas sin aguijón (Apidae: Meliponini) en Loreto, Perú. Instituto de Investigaciones de la Amazonia Peruana (Iquitos), 1–70.
- Rasmussen C, Camargo JMF (2008) A molecular phylogeny and the evolution of nest architecture and behavior in *Trigona* s.s. (Hymenoptera: Apidae: Meliponini). *Apidologie* 39: 102–118. <https://doi.org/10.1051/apido:2007051>

- Rasmussen C, Cameron SA (2007) A molecular phylogeny of the Old World stingless bees (Hymenoptera: Apidae: Meliponini) and the non-monophyly of the large genus *Trigona*. *Systematic Entomology* 32: 26–39. <https://doi.org/10.1111/j.1365-3113.2006.00362.x>
- Rasmussen C, Gonzalez VH (2009) Abejas sin aguijón del Cerro Escalera, San Martín, Perú (Hymenoptera: Apidae: Meliponini). *Sistemas agroeconómicos y modelos biomatemáticos* 2(2): 26–32.
- Ronquist F, Teslenko M, van der Mark P, Ayres DL, Darling A, Höhna S, Larget B, Liu L, Suchard MA, Huelsenbeck JP (2012) MrBayes 3.2: efficient bayesian phylogenetic inference and model choice across a large model space. *Systematic Biology* 61: 539–542. <https://doi.org/10.1093/sysbio/sys029>
- Roubik DW (1982) Obligate necrophagy in a social bee. *Science* 217: 1059–1060. <https://doi.org/10.1126/science.217.4564.1059>
- Roubik DW (1989) *Ecology and natural history of tropical bees*. Cambridge University Press, New York, 528 pp. <https://doi.org/10.1017/CBO9780511574641>
- Roubik DW (1993) Tropical pollinators in the canopy and understory: field data and theory for stratum “preferences”. *Journal of Insect Behavior* 6: 659–673. <https://doi.org/10.1007/BF01201668>
- Sánchez Sandoval EY, Rasmussen C (2015) Estudio de polinizadores en la subcuenca de Alto Mayo, región San Martín, Perú. Simposio Proyecto BioCuencas Recursos Hídricos y Biodiversidad Andino Amazónicos, Moyobamba (Peru), 16 October. *Conservación Internacional Perú*: 1.

New records for the wild bee fauna (Hymenoptera, Anthophila) of Serbia

Sonja Mudri-Stojnić¹, Andrijana Andrić², Zsolt Józán³,
Laura Likov¹, Tamara Tot¹, Ana Grković¹, Ante Vujić¹

1 *University of Novi Sad, Faculty of Sciences, Department of Biology and Ecology, Trg Dositeja Obradovića 2, 21000 Novi Sad, Serbia* **2** *University of Novi Sad, BioSense Institute, Dr Zorana Đinđića 1, 21000 Novi Sad, Serbia* **3** *Rákóczi utca 5, 7453 Mernye, Hungary*

Corresponding author: Sonja Mudri-Stojnić (sonja.mudri-stojnic@dbe.uns.ac.rs)

Academic editor: Jack Neff | Received 6 June 2023 | Accepted 5 September 2023 | Published 11 October 2023

<https://zoobank.org/2ABB47EF-3BDA-4500-A77B-E76E5E7C32E7>

Citation: Mudri-Stojnić S, Andrić A, Józán Z, Likov L, Tot T, Grković A, Vujić A (2023) New records for the wild bee fauna (Hymenoptera, Anthophila) of Serbia. *Journal of Hymenoptera Research* 96: 761–781. <https://doi.org/10.3897/jhr.96.107595>

Abstract

Numerous scientific projects have been initiated with the aim of tackling the decline in insect pollinators, a crucial group for the functioning of terrestrial ecosystems. One of the first steps is to address information gaps on species spatial distribution, diversity, and abundance that prevent effective conservation actions in Europe. Given that Serbia belongs to the understudied areas, efforts are being made to improve knowledge of its bee diversity and abundance. The present study includes the monitoring of bees at 54 sites, surveyed three times during 2022. The conducted protocol combined two methods, transect walks and pan traps, resulting in the discovery of 312 bee species. The main results present the records of 25 species, not previously mentioned in Serbia, while another important finding is the confirmation of the presence of 26 species, without any available records from the 21st century. Moreover, 79 here examined species were known only from literature-based data. Six of the recorded species are considered threatened and 67 (10 newly recorded) have been assessed as Data Deficient in the European Red List of Bees. Therefore, the present study not only contributes to an update and confirms the list of bee species in Serbia, that now counts 731 species, but also provides additional information about European distribution, required for new assessment at the European level. In addition, the results indicate that the combination of complementary sampling methods is an effective way to assess bee diversity and abundance.

Keywords

bees, Data Deficient, monitoring, new data, pan traps, transect walks

Introduction

It has become common knowledge that pollinators play a crucial role in ecosystems by supporting sexual reproduction for most flowering plants (e.g., Ollerton et al. 2011), with bees being the most important pollinator group (Ballantyne et al. 2017; Willmer et al. 2017). It is also widely known that the global entomofauna is declining (Goulson 2019; Sánchez-Bayo and Wyckhuys 2019; Wagner 2020), primarily due to urbanization and agriculture (Uhler et al. 2021). Most pollinators, including wild bees, show negative population trends (Potts et al. 2010, 2015; Goulson et al. 2015; Dicks et al. 2021; but see Ghisbain et al. 2021). Loss of habitat caused by changes in land use and management (e.g., Kremen et al. 2002; Steffan-Dewenter and Westphal 2008; Kennedy et al. 2013), pollution (Gill et al. 2012), diseases (Power and Mitchell 2004; Colla et al. 2006; Purkiss and Lach 2019), exotic species and climate change (González-Varo et al. 2013; Martinet et al. 2021), as well as the interaction of these factors, are the main drivers of change and the decline in pollinator communities (LeBuhn and Vargas Luna 2021). The last decade has seen a considerable increase in interest among the scientific and general public with respect to the conservation of pollinators (Drossart and Gérard 2020). The research on biodiversity has generally expanded, however, the under-representation of insects in published literature, compared to vertebrates, is caused by the fact that working with more diverse taxa is more challenging, particularly in terms of species identification (Tittley et al. 2017). Although there is evidence of changes in bee abundance and species richness, there is still a lack of data on global decline (IPBES 2016; Zattara and Aizen 2021).

Regarding the status and trends of bees (Anthophila) in Europe, the European Red List of Bees (Nieto et al. 2014) indicates that 37% of bee species, excluding Data Deficient, have declining populations, while other national Red Lists in Europe imply that up to 40% of bee species are threatened (IPBES 2016; Drossart et al. 2019). However, available knowledge on the spatial distribution of most bee species is incomplete (Nieto et al. 2014) and uneven between countries (Potts et al. 2021). According to Nieto et al. (2014), more than half (56.7%) out of 1,942 assessed species have been listed as Data Deficient in Europe. Significant work has been conducted under the EU (European Union) Biodiversity Strategy for 2030, with one of its key commitments being the reversal of the decline of pollinators (European Commission 2021). The European Commission established the EU Pollinators Initiative, the first-ever EU framework for tackling the decline of wild pollinators, and set up the EU Pollinator Monitoring Scheme (EU-PoMS) to harmonize the systematic monitoring of the status and trends of pollinators across the EU. It has been emphasized that significant data gaps prevent effective conservation actions, especially in the south-eastern part of Europe (Potts et al. 2021).

Currently, at the European level, numerous scientific projects are being implemented, simultaneously, directed towards gathering information on pollinators, including bees. Apart from the widely recognized need for systematic monitoring, these projects stress the need to strengthen education and communication, through training of taxonomists, engaging the potential of citizen science, creating platforms for facilitating

information sharing and the collaboration between stakeholders. Some projects, such as the PoshBee (2018–2023), address direct threats with the aim of providing the first pan-European assessment of the hazard to managed and wild bees from chemical exposure (Brown et al. 2021). Other projects aim to tackle gaps in pollinators' taxonomy, distribution and extinction risk. Namely, the project Safeguard (2021–2025) provides a comprehensive re-assessment of the status and trends of European wild pollinators, including their diversity and abundance, filling knowledge gaps associated primarily with Data Deficient species. The objective of the project SPRING (2021–2023) is to strengthen taxonomic capacity in EU Member States with regard to pollinating insects, and provide support for the implementation of the EU-PoMS (Potts et al. 2021). The project PULSE (2022–2023) prepares updates for the European Red List of Bees, collecting databases from taxonomists and national champions and digitizing museum collections. The project ORBIT (2021–2024) aims to create a centralized taxonomic facility that lays the groundwork for the identification of European wild bees, supporting all the above mentioned European projects. Furthermore, initiatives at national levels represent a very important contribution to filling information gaps, especially in understudied areas. In Serbia, the project SPAS (2022–2024) has been established as a preparatory phase for the EU-PoMS, with the objective of building a long-term national monitoring strategy for wild insect pollinators compatible with the European one.

Recognizing the above mentioned issues, primarily the lack of publicly available data on national occurrence records, two European studies have been recently published to update the checklist of European bees (Ghisbain et al. 2023) and European bees country records (Reverté et al. 2023). Moreover, focusing on Serbia, Mudri-Stojnić et al. (2021) recently published a preliminary list of 706 bee species. For the first time, all accessible records had been summarized, emphasizing the fact that, undoubtedly, more species are yet to be discovered. The main purpose of the present study is to propose an update, including the most recent observations on wild bee species occurrences in Serbia. The specific goals of the study are: (1) to introduce the first published records from Serbia for 25 species; (2) to confirm the presence of 26 species, for which records referring to the 21st century are lacking; (3) to contribute to the information about distribution, needed for the evaluation of Data Deficient species in Europe; (4) to discuss various monitoring and sampling methods. The results aim to contribute to updating knowledge on wild bee diversity in Serbia, necessary for determining conservation priorities and future endeavors at the national level, but also for improving an understanding of the status of European pollinators.

Materials and methods

Survey methodology

The data for the present study was primarily gathered during the implementation of the national project, Serbian Pollinator Advice Strategy – for the next normal (SPAS

2022–2024), and partially within the EU-funded project, Safeguarding European wild pollinators (Safeguard 2021–2025). Both projects aim to address the diversity of major pollinator taxa with a focus on bees, hoverflies and butterflies as the most species-rich and functionally relevant groups.

In order to monitor the diversity and abundance of insect pollinators in Serbia, 54 sites were selected (Fig. 1) on the basis of expert opinion; the intention was to include as many semi-natural habitats as possible. For the Safeguard project, localities were chosen to represent the open semi-natural habitat type – steppe grasslands. The SPAS project localities included other habitat types as well: forest-steppe, forest meadow, wet meadow, mountain meadow, sub-Mediterranean grassland, and rocky grassland, with a minimum separation distance of 2 km to reduce spatial autocorrelation. The goal was to achieve a representative depiction of geographical regions, while enabling proportional representation of different habitats in the sample. The sites were surveyed three times each, throughout the 2022 season (March–May, June, and August–September), so as to reduce the phenology effects and to increase species richness accumulation, i.e., sampling completeness. The survey period was adapted to the expected weather conditions and flower availability.

The assessment of bee diversity and abundance was conducted in accordance with the methodology and recommendations of the EU-PoMS (Potts et al. 2021). The protocol combined two methods: the passive method (does not rely on attracting insects), i.e., transect walks, conducted at all 54 studied sites, and the active method (relies on attracting insects), i.e., pan traps, conducted as an additional method at a subset of 31 sites.

Pan traps, a lethal sampling technique designed to survey nectar-searching insects, consisted of a cluster of three water-filled bowls (with some soap to break the surface) of three colors (blue, white and yellow per group) and set on stakes at a vegetation height to mimic flowers and attract insects. Based on the EU-PoMS (Potts et al. 2021) the protocol included the placement of 10 pan trap clusters (around 8 a.m.), across the grid square, and the collection of specimens, after approximately 12 hours (around 8 p.m.), which were then transported to the laboratory for further identification.

Transect walks were undertaken ~100 m apart from the pan traps. This method, designed to survey flying insects, included walks along the transect route, at a steady speed, to record every bee individual observed along a transect route of constant width ahead and to the side of the surveyor. The transects were ~500 m in length and 2 m in width (1 m to each side of the surveyor), resulting in ~1000 m² of transect area. The transect time per site was 30 min with 5 min sub-transects (~80 m), not including handling time (i.e., transferring and labelling the specimens), namely only time spent for searching and catching bees. Specimens that could not be identified with certainty to species level in the field, were collected in plastic vials with the aid of drops of acetone on a cotton ball. These specimens were subsequently identified in the laboratory of the Department of Biology and Ecology, Faculty of Sciences, University of Novi Sad, Serbia (FSUNS) and by expert Józsan Zsolt (Mernye, Hungary).

The QGIS Geographic Information System (QGIS Development Team 2022) was used to create the map of 54 examined sites (Fig. 1).

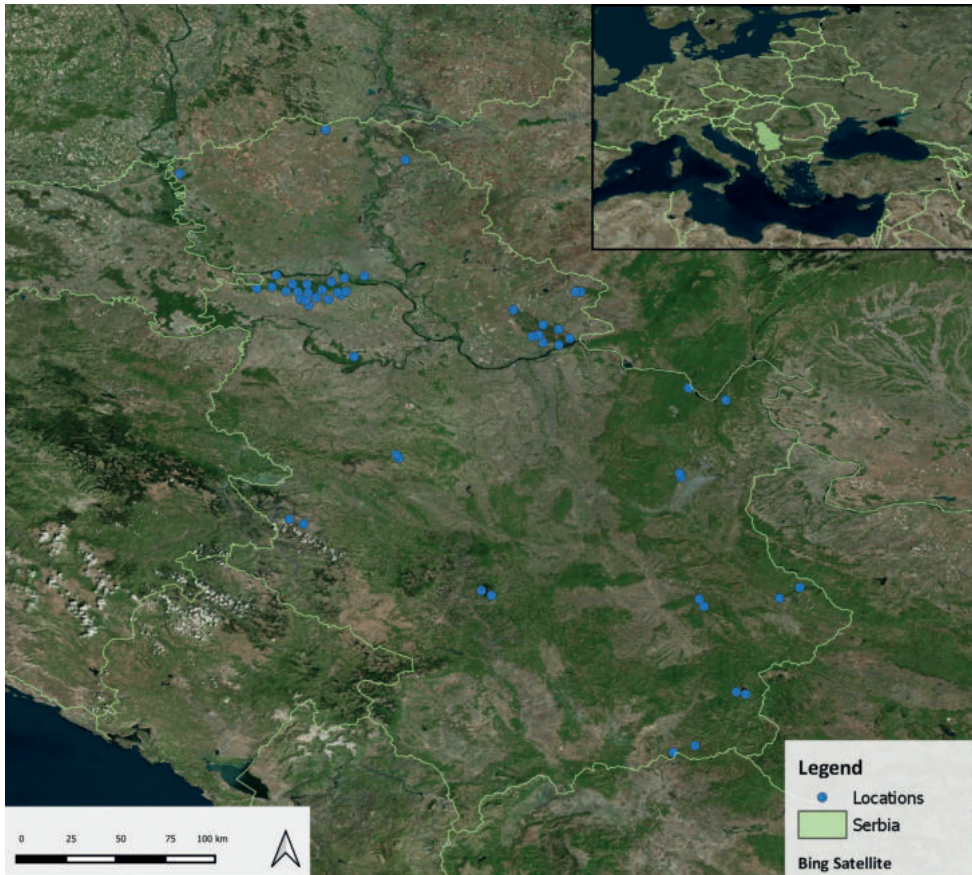


Figure 1. Map of Serbia showing the localities where bee specimens were collected.

Examined material

All of the examined specimens were dry pinned and stored in FSUNS's entomological collection. The list of previously unpublished records of bee species for Serbia has been given in full, as has the list of species considered threatened in Europe according to the European Red List (Nieto et al. 2014), with families, genera and species arranged in alphabetical order. The recently published annotated checklist of the wild bees of Europe (Ghisbain et al. 2023) has been consulted for the nomenclature. Information on examined material has been provided in the following order: number and sex of specimens after a bullet point (indicating the beginning of material citation); locality data; geographical coordinates; collection date; collector followed by "leg." (if specimens were detected during the transect walks) or the color of pan trap, depending on collection methodology; institution code and specimen codes, i.e., unique identifiers ("to" indicates range). If a species was found in multiple localities, the specimens have been listed by increasing latitude (south to north). The IUCN (The International Union for Conservation of Nature) Red List Categories (Europe) (Nieto et al. 2014) were indicated in square brackets for each species (abbreviations: EN – Endangered, VU – Vulnerable,

NT – Near Threatened, LC – Least Concern, DD – Data Deficient). For the records of wild bee species considered threatened in Europe, additional data has been provided, regarding habitat type and the main floral resources. The latter refers to the plant species on whose flowers the insects were caught during transect walks, whereas this information is lacking for the specimens caught on flight, on the ground, or collected from pan traps.

The list of all recorded species can be found in the Suppl. material 1. Additional information has been provided for each species: IUCN categories; collection methodology types; data on the presence of listed species in the online maps of the Checklist of the Western Palaearctic Bees (Kuhlmann et al. 2023); data on the species with occurrences previously available only from sources prior to year 2000. The list of references and collections' abbreviations cited in Suppl. material 1 follows the list of species at the end of the table.

Results

The present study included field research which resulted in the recording of 2,645 bee (Anthophila) specimens, 851 collected from pan traps (334 in blue, 278 in yellow and 239 in white) and 1,794 observed during transect walks. An identification of the material revealed 312 species in total (see Suppl. material 1). These species belong to the following IUCN categories: EN (four species), VU (two species), NT (22 species), LC (216 species), DD (67 species) and *Dasygaster morawitzi* Radchenko still uncategorized. According to sampling methodologies, 166 species were detected during transect walks, 51 were caught in pan traps and 95 species were found both in pan traps and during transect walks (Fig. 2A). Considering only the subset of 31 sites where both sampling methods were conducted, 247 species were detected, i.e., 101 by transect walks, 68 by pan traps and 78 by both methods (Fig. 2B).

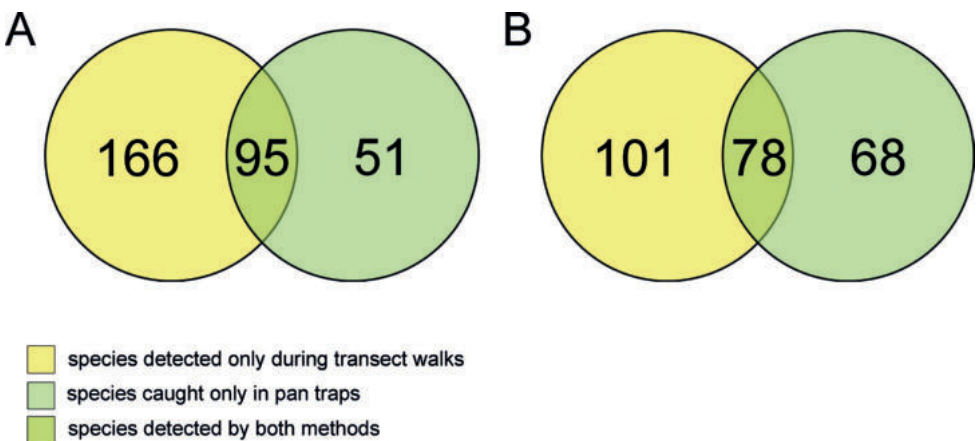


Figure 2. Graphic view of the number of species detected depending on the sampling methods **A** at all studied sites **B** at a subset of sites where both sampling methods were conducted.

Concerning available information on the presence of here listed species in Serbia, 25 are without previous records, 26 have records only from sources prior to year 2000, 15 have data of occurrence only from Kuhlmann et al. (2023), while 52 species are from both older literature sources and Kuhlmann et al. (2023) (see Suppl. material 1). The newly detected species were found in 37 out of 54 studied localities across Serbia. Regarding sampling methodologies, 12 of these 25 species were detected during transect walks, seven were caught in pan traps, and six were found using both methods. The records of species without previously published occurrences in Serbia, as well as of the six species considered threatened in Europe (according to Nieto et al. (2014)), have been presented in the following lists.

New records of wild bee species in Serbia

Family Andrenidae

Andrena Fabricius

Andrena bisulcata Morawitz [LC]

- 1 ♀; Pčinja, Vražji kamen; 42.3838°N, 22.0528°E; 20 Apr. 2022; Laura Likov leg.; FSUNS SPAS10082.

Andrena braunsiana Friese [DD]

- 7 ♀♀; Fruška gora, Stejanovci; 45.0428°N, 19.7199°E; 5 May 2022; Ante Vujić leg.; FSUNS SG0018, SG0021, SG0022, SG0025 to SG0028 • 1 ♂; Fruška gora, Šuljam; 45.0814°N, 19.6717°E; 5 May 2022; Ante Vujić leg.; FSUNS SG0073.

Andrena florivaga Eversmann [LC]

- 1 ♂; 'The great bustard pastures' ['Pašnjaci velike droplje'], Mokrin; 45.9217°N, 20.3033°E; 4 May 2022; Sonja Mudri-Stojnić leg.; FSUNS SPAS00161.

Andrena fulva (Müller) [DD]

- 1 ♀; Zlot, towards Malinik; 44.0055°N, 21.9676°E; 27 Apr. 2022; yellow pan trap; FSUNS SPAS20492.

Andrena fulvata Stöckhert [DD]

- 1 ♀; Zlatibor, Obudovica; 43.7227°N, 19.6881°E; 11 May 2022; yellow pan trap; FSUNS SPAS30391 • 2 ♀♀; Zlatibor, Semegnjevo; 43.7514°N, 19.6037°E; 10 May 2022; white pan trap; FSUNS SPAS30407, SPAS30409.

***Andrena mitis* Schmiedeknecht [DD]**

• 1 ♂; Jelašnica river gorge, Čukljenik; 43.2686°N, 22.0779°E; 22 Apr. 2022; blue pan trap; FSUNS SPAS10396.

***Andrena pallitarsis* Pérez [DD]**

• 1 ♀; Fruška gora, Vrdnik; 45.1372°N, 19.8013°E; 30 Aug. 2022; Ante Vujić leg.; FSUNS SG0885.

***Andrena russula* Lepeletier [DD]**

• 1 ♂; Rajac, Slavkovic; 44.1408°N, 20.2474°E; 9 May 2022; Ana Grković leg.; FSUNS SPAS30072.

***Andrena saxonica* Stöckhert [DD]**

• 2 ♀♀; Zlatibor, Semegnjevo; 43.7514°N, 19.6037°E; 18 Jun. 2022; Ana Grković leg.; FSUNS SPAS30211, SPAS30215 • 1 ♀; Zlot, towards Malinik; 44.0055°N, 21.9676°E; 27 Apr. 2022; white pan trap; FSUNS SPAS20513 • 1 ♀; Đerdap, Ciganski potok; 44.5436°N, 22.0146°E; 26 Apr. 2022; yellow pan trap; FSUNS SPAS20425 • 1 ♀; Fruška gora, Šuljam; 45.0814°N, 19.6717°E; 5 May 2022; Ante Vujić leg.; FSUNS SG0044.

***Andrena tscheki* Morawitz [DD]**

• 1 ♀; Suva planina, Bojanine vode; 43.2260°N, 22.1068°E; 22 Apr. 2022; white pan trap; FSUNS SPAS10337 • 1 ♂; same data as for preceding; yellow pan trap; FSUNS SPAS10339 • 1 ♀; Stara planina, Topli Do; 43.3400°N, 22.6856°E; 30 Apr. 2022; Tamara Tot leg.; FSUNS SPAS20095 • 1 ♀; Zlatibor, Obudovica; 43.7227°N, 19.6881°E; 11 May 2022; Ana Grković leg.; FSUNS SPAS30122 • 1 ♀; Zlot, towards Malinik; 44.0055°N, 21.9676°E; 27 Apr. 2022; white pan trap; FSUNS SPAS20499 • 3 ♀♀; same data as for preceding; Tamara Tot leg.; FSUNS SPAS20069 to SPAS20071 • 1 ♂; same data as for preceding; FSUNS, SPAS20065 • 1 ♀; Lazar's canyon, Lazar's cave; 44.0286°N, 21.9587°E; 28 Apr. 2022; Tamara Tot leg.; FSUNS SPAS20076 • 1 ♀; Đerdap, Ciganski potok; 44.5436°N, 22.0146°E; 26 Apr. 2022; Tamara Tot leg.; FSUNS SPAS20042 • 1 ♀; Vršачki breg, Kula; 45.1245°N, 21.3283°E; 24 Jun. 2022; Sonja Mudri-Stojnić leg.; FSUNS SPAS00083.

Family Apidae***Ceratina* Latreille*****Ceratina gravidula* Gerstaecker [LC]**

- 1 ♀; Lazar's canyon, Lazar's cave; 44.0286°N, 21.9587°E; 27 Aug. 2022; Tamara Tot leg.; FSUNS SPAS20557
- 1 ♀; Fruška gora, Neradin Česma; 45.1061°N, 19.9156°E; 14 Sep. 2022; Sonja Mudri-Stojnić leg.; FSUNS SPAS00740.

Family Colletidae***Hylaeus* Fabricius*****Hylaeus nigrifacies* Bramson [LC]**

- 1 ♀; Deliblato sands, Čardak II; 44.8628°N, 21.1059°E; 27 Aug. 2022; Ante Vujić leg.; FSUNS SG1104
- 1 ♀; Fruška gora, Šuljam; 45.0814°N, 19.6717°E; 18 Jun. 2022; Ante Vujić leg.; FSUNS SG0692.

Family Halictidae***Lasioglossum* Curtis*****Lasioglossum bluethgeni* Ebmer [LC]**

- 6 ♀♀; Suva planina, Bojanine vode; 43.2260°N, 22.1068°E; 15 Jun. 2022; blue pan trap; FSUNS SPAS10510, SPAS10511, SPAS10515 to SPAS10517, SPAS10519
- 3 ♀♀; same data as for preceding; white pan trap; FSUNS SPAS10522 to SPAS10524
- 1 ♀; same data as for preceding; yellow pan trap; FSUNS SPAS10526
- 1 ♀; Jelašnica river gorge, Čukljenik; 43.2686°N, 22.0779°E; 22 Apr. 2022; yellow pan trap; FSUNS SPAS10382
- 4 ♀♀; same data as for preceding; 15 Jun. 2022; blue pan trap; FSUNS SPAS10489 to SPAS10492
- 2 ♀♀; same data as for preceding; white pan trap; FSUNS SPAS10477, SPAS10478
- 2 ♀♀; Lazar's canyon, Lazar's cave; 44.0286°N, 21.9587°E; 9 Jun. 2022; blue pan trap; FSUNS SPAS20324, SPAS20325
- 1 ♀; Rajac, Gornji Banjani; 44.1199°N, 20.2645°E; 16 Jun. 2022; Ana Grković leg.; FSUNS SPAS30188
- 2 ♀♀; Đerdap, Ciganski potok; 44.5436°N, 22.0146°E; 7 Jun. 2022; blue pan trap; FSUNS SPAS20335, SPAS20337
- 1 ♀; Obedska bara, Debela gora; 44.7336°N, 19.9921°E; 2 Jun. 2022; blue pan trap; FSUNS SPAS10332.
- 7 ♀♀; Vršački breg, Kula; 45.1245°N, 21.3283°E; 20 Jun. 2022; blue pan trap; FSUNS SPAS00872, SPAS00877 to SPAS00882
- 1 ♀; same data as for preceding; 25 Aug. 2022; FSUNS SPAS00758
- 1 ♀; Vršački breg, Dom; 45.1253°N, 21.3615°E; 20 Jun. 2022; blue pan trap; FSUNS SPAS00546
- 2 ♀♀; Fruška gora, Grabovo; 45.1717°N, 19.6227°E; 14 Jun. 2022; blue pan trap; FSUNS SPAS20293, SPAS20294.

***Lasioglossum damascenum* (Pérez) [DD]**

- 1 ♀; Deliblato sands, Šušara; 44.9261°N, 21.1353°E; 21 Jun. 2022; blue pan trap; FSUNS SPAS00556.

***Lasioglossum laterale* (Brullé) [DD]**

- 1 ♀; Pčinja, Vogance; 42.3436°N, 21.9215°E; 20 Apr. 2022; white pan trap; FSUNS SPAS10358 • 1 ♀; Bačko podunavlje, Bezdan; 45.8390°N, 18.9400°E; 6 Apr. 2022; blue pan trap; FSUNS SPAS00899.

***Seladonia* Robertson**

***Seladonia confusa* (Smith) [LC]**

- 1 ♀; Pčinja, Vražji kamen; 42.3838°N, 22.0528°E; 16 Jun. 2022; white pan trap; FSUNS SPAS10441.

Family Megachilidae

***Heriades* Spinola**

***Heriades rubicola* Pérez [LC]**

- 1 ♂; Bačko podunavlje, Bezdan; 45.8390°N, 18.9400°E; 6 Sep. 2022; Sonja Mudri-Stojnić leg.; FSUNS SPAS00477 • 1 ♂; Subotica, Ludaš lake; 46.1040°N, 19.8212°E; 15 Jun. 2022; Sonja Mudri-Stojnić leg.; FSUNS SPAS00293.

***Hoplitis* Klug**

***Hoplitis mazzuccoi* (Schwarz & Gusenleitner) [LC]**

- 1 ♂; Fruška gora, Grgurevci; 45.1228°N, 19.6504°E; 19 Jun. 2022; Ante Vujić leg.; FSUNS SG0795.

***Hoplitis papaveris* (Latreille) [LC]**

- 2 ♀♀; Zlatibor, Obudovica; 43.7227°N, 19.6881°E; 18 Jun. 2022; blue pan trap; FSUNS SPAS30454, SPAS30455 • 1 ♂; same data as for preceding; yellow pan trap; FSUNS SPAS30436.

***Hoplitis villosa* (Schenck) [LC]**

- 1 ♂; Kopaonik, Mali Karaman; 43.2910°N, 20.8235°E; 20 Jun. 2022; Ana Grković leg.; FSUNS SPAS30248.

Osmia* Panzer**Osmia bischoffi* Atanassov [LC]**

• 3 ♀♀; Đerdap, Ciganski potok; 44.5436°N, 22.0146°E; 26 Apr. 2022; yellow pan trap; FSUNS SPAS20401, SPAS20457, SPAS20461 • 7 ♀♀; same data as for preceding; white pan trap; FSUNS SPAS20341, SPAS20397, SPAS20402, SPAS20405, SPAS20411, SPAS20413, SPAS20415 • 5 ♀♀; same data as for preceding; blue pan trap; FSUNS SPAS20395, SPAS20435, SPAS20436, SPAS20440, SPAS20443 • 1 ♂; same data as for preceding; FSUNS SPAS20433 • 2 ♀♀; Fruška gora, Vrdnik; 45.1372°N, 19.8013°E; 21 Jun. 2022; Ante Vujić leg.; FSUNS SG0570, SG0573 • 1 ♀; Fruška gora, Sremski Karlovci; 45.2089°N, 19.9358°E; 20 Jun. 2022; Ante Vujić leg.; FSUNS SG0497.

***Osmia scutellaris* Morawitz [LC]**

• 1 ♂; Fruška gora, Vrdnik; 45.1372°N, 19.8013°E; 21 Jun. 2022; Ante Vujić leg.; FSUNS SG0572.

***Osmia xanthomelana* (Kirby) [LC]**

• 1 ♂; Kopaonik, Mali Karaman; 43.2910°N, 20.8235°E; 20 Jun. 2022; Ana Grković leg.; FSUNS SPAS30242.

Pseudoanthidium* Friese**Pseudoanthidium nanum* (Mocsáry) [LC]**

• 1 ♀; Stara planina, Temska; 43.2751°N, 22.5626°E; 28 Aug. 2022; blue pan trap; FSUNS SPAS20665 • 1 ♂; same data as for preceding; Tamara Tot leg.; FSUNS SPAS20595 • 1 ♀; Deliblato sands, Grebenac; 44.8991°N, 21.2286°E; 26 Aug. 2022; Ante Vujić leg.; FSUNS SG0259 • 1 ♀; Deliblato sands, Alibunar; 45.0674°N, 20.9667°E; 26 Aug. 2022; Ante Vujić leg.; FSUNS SG1043 • 1 ♀; Fruška gora, Bešenovo; 45.0718°N, 19.7035°E; 21 Jun. 2022; Ante Vujić leg.; FSUNS SG0656 • 1 ♀; Fruška gora, Jazak; 45.0911°N, 19.7668°E; 21 Jun. 2022; Ante Vujić leg.; FSUNS SG0523 • 1 ♀; Fruška gora, Neradin; 45.1219°N, 19.8940°E; 20 Jun. 2022; Ante Vujić leg.; FSUNS SG0741 • 1 ♀; same data as for preceding; 31 Aug. 2022; FSUNS SG0892 • 1 ♀; Fruška gora, Vrdnik; 45.1372°N, 19.8013°E; 21 Jun. 2022; Ante Vujić leg.; FSUNS SG0576 • 1 ♀; 'The great bustard pastures' ['Pašnjaci velike droplje'], Mokrin; 45.9217°N, 20.3033°E; 14 Jun. 2022; Sonja Mudri-Stojnić leg.; FSUNS SPAS00251 • 1 ♀; same data as for preceding; 29 Aug. 2022; FSUNS SPAS00469.

Family Melittidae

Dasyпода Latreille

Dasyпода morawitzi Radchenko

- 1 ♂; Deliblato sands, Šumarak; 44.8173°N, 21.1346°E; 27 Aug. 2022; Ante Vujić leg.; FSUNS SG1070
- 2 ♂♂; Deliblato sands, Labudovo okno; 44.8440°N, 21.2958°E; 27 Aug. 2022; Ante Vujić leg.; FSUNS SG1109, SG1112
- 1 ♂; Deliblato sands, Čardak I; 44.8550°N, 21.0681°E; 21 Jun. 2022; yellow pan trap; FSUNS SPAS00632
- 1 ♀; Deliblato sands, Šušara; 44.9261°N, 21.1353°E; 26 Aug. 2022; blue pan trap; FSUNS SPAS00838
- 2 ♂♂; same data as for preceding; 28 Aug. 2022; Ante Vujić leg.; FSUNS SG0955, SG0957
- 1 ♀; same data as for preceding; FSUNS SG0970.

Records of wild bee species considered threatened in Europe

Family Colletidae

Colletes Latreille

Colletes anchusae Noskiewicz [EN]

- 1 ♀; Đerdap, Ciganski potok; 44.5436°N, 22.0146°E; 07 Jun. 2022; Tamara Tot leg.; FSUNS SPAS20151.

Habitat type is stream within deciduous forest.

Colletes chengtehensis Yasumatsu [VU]

- 1 ♂; Deliblato sands, Čardak I; 44.8550°N, 21.0681°E; 26 Aug. 2022; Sonja Mudri-Stojnić leg.; FSUNS SPAS00704
- 1 ♂; Deliblato sands, Alibunar; 45.0674°N, 20.9667°E; 14 Jun. 2022; Ante Vujić leg.; FSUNS SG0308.

Habitat type at locality Čardak is a mosaic of steppe grassland on sand with forests and shrubs. Main floral resource of this species at this locality is *Berteroa incana* (L.) DC. (Brassicaceae). At locality Alibunar, habitat type is a mosaic of steppe grassland on loess with forest patches and shrubs.

Colletes nasutus Smith [EN]

- 2 ♀♀; Deliblato sands, Čardak I; 44.8550°N, 21.0681°E; 21 Jun. 2022; Sonja Mudri-Stojnić leg.; FSUNS SPAS00383, SPAS00390.

Habitat type is mosaic of steppe grassland on sand with forests and shrubs. Main floral resource of this species at this locality is *Carduus acanthoides* L. (Asteraceae).

Family Halictidae***Systropha* Illiger*****Systropha planidens* Giraud [VU]**

- 1 ♂; Stara planina, Temska; 43.2751°N, 22.5626°E; 10 Jul. 2022; Tamara Tot leg.; FSUNS SPAS20230
- 2 ♂♂; Fruška gora, Stejanovci; 45.0428°N, 19.7199°E; 18 Jun. 2022; Ante Vujić leg.; FSUNS SG0680, SG0688
- 1 ♂; Fruška gora, Šuljam; 45.0814°N, 19.6717°E; 18 Jun. 2022; Ante Vujić leg.; FSUNS SG0595
- 1 ♀; same data as for preceding; FSUNS SG0608
- 1 ♀; Fruška gora, Krušedol; 45.1279°N, 19.9442°E; 20 Jun. 2022; Ante Vujić leg.; FSUNS SG0538.

At the Fruška gora localities (Stejanovci, Krušedol and Šuljam), habitat type is steppe grassland with shrubs. Main floral resource of this species at these localities is *Convolvulus arvensis* L. (Convolvulaceae). At locality Temska, habitat type is meadow in agricultural mosaic.

Seladonia* Robertson**Seladonia semitecta* (Morawitz) [EN]**

- 3 ♀♀; Fruška gora, Bešenovo; 45.0718°N, 19.7035°E; 21 Jun. 2022; Ante Vujić leg.; FSUNS SG0672.

Habitat type is steppe grassland with shrubs. Main floral resource of this species at this locality is *Teucrium chamaedrys* L. (Lamiaceae).

Family Melittidae***Dasypoda* Latreille*****Dasypoda braccata* Eversmann [EN]**

- 1 ♂; Deliblato sands, Čardak I; 44.8550°N, 21.0681°E; 21 Jun. 2022; blue pan trap; FSUNS SPAS00607.

Habitat type is mosaic of steppe grassland on sand with forests and shrubs.

Discussion

The results of the present study include new records for 25 bee species that have not been previously recorded for Serbia. Most of them are from the family Andrenidae, i.e., 10 species of the genus *Andrena*. They are followed by eight species from Megachilidae (three from genera *Hoplitis* and *Osmia* respectively, and one from *Heriades* and

Pseudoanthidium), four from Halictidae (three *Lasioglossum* and one *Seladonia*), and one from Apidae (*Ceratina*), Colletidae (*Hylaeus*), and Melittidae (*Dasypoda*) respectively. The latest published list of bee species occurring in Serbia, as provided by Mudri-Stojnić et al. (2021), presented 706 species. Therefore, with the current extension, the total number of species is 731. Furthermore, Mudri-Stojnić et al. (2021) included 56% (392) species that were only known from literature data, i.e., those species were not confirmed by material examination. The present study provides confirmation of 79 of those species.

Ten of the newly recorded species have been listed as DD in the European Red List of Bees (Nieto et al. 2014), 14 are in the LC category, while one species is uncategorized (*Dasypoda morawitzi* Radchenko, 2016) as it was described after the publication of the IUCN Red List. The majority (69%) of all bee species (312) recorded within the present study belong to the LC category; however, 7% are classified as NT, two species as VU and four species as EN in Europe. Moreover, 21% of the here listed species were assessed as DD (Nieto et al. 2014), since there was not enough scientific data to evaluate their risk of extinction. Ten of these species were not previously recorded for Serbia. Furthermore, the preparation of an update of the European Red List of Bees is ongoing (PULSE 2022–2023) and many species could be expected to have their IUCN categories revised, primarily the ones previously assessed as DD. Therefore, the results of the present study could act as a contribution to the information about distribution, needed for the threat evaluation of these species in Europe. It is also worth mentioning that the Pannonian steppe grasslands on loess (Fruška gora localities) and on sand (Deliblato sands localities), on which bee species considered threatened in Europe were recorded, belong to the habitat types of conservation priority in Serbia (Official Gazette RS 2010).

Another important finding includes the confirmation of the presence of 26 species without available records for Serbia dating from the 21st century. Mudri-Stojnić et al. (2021) emphasized the fact that further research is needed in order to confirm older data, as the current presence of these species, within the given localities, is not certain. Therefore, the present study gives a relevant contribution towards clarifying such information, especially with several literary records dating back more than a century, i.e., *Melitta dimidiata* Morawitz (NT) in Apfelbeck (1896), *Triepeolus tristis* (Smith) (NT) and *Pseudoanthidium tenellum* Mocsáry (DD) in Mocsáry (1897), and *Eucera caspica* Morawitz (LC) in Vorgin (1918).

According to the available distribution maps of bees (Kuhlmann et al. 2023; Rasmont and Haubruge 2023) and literature sources (e.g., Michez et al. 2019), the new bee species' records for Serbia were not surprising; i.e., they were expected based on the known distributions. The findings of the present study thus indicate the need for additional research in terms of bees' diversity, biology and ecology (including habitat types, floral resources and nesting sites), in order to expand knowledge about them, both locally and at the European level. From 15 bee species recorded in the present study, whose sole previous source of occurrence in Serbia was the Checklist of the Western Palaearctic Bees (Kuhlmann et al. 2023), two of these species are threatened at the European level (one EN and VU respectively), one is NT, eight are LC, and four are DD. Moreover, available data for 52 species came only from Kuhlmann et al. (2023) and from published occurrences prior to

the year 2000. On the other hand, 103 here recorded species are not listed in Kuhlmann et al. (2023), thus they are a potential addition to the distribution maps for the Checklist.

Two different collection methodologies were used in the present study, i.e., the transect walks, a passive method designed to survey flying insects, and the pan traps, an active method designed to survey nectar-searching insects, both recognized as suitable for the monitoring of bees (Nielsen et al. 2011; Potts et al. 2021). The advantage of pan traps is in that they provide data on bee abundance without observer bias (Cane et al. 2000; Roulston et al. 2007; Westphal et al. 2008), whereas the validity of transect walks is dependent on the experience of collectors (Nielsen et al. 2011). Due to bee species with flower color preferences, an exhaustive survey of bee fauna requires the use of multiple pan trap colors (Toler et al. 2005). Moreover, there is evidence suggesting the presence of not only species-specific but also sex-specific color preferences in Aculeata (Heneberg and Bogusch 2014). However, the effectiveness of pan traps is related to surrounding floral resources (Roulston et al. 2007) and the resulting data does not always represent the local community (Cane et al. 2000). Due to their respective limitations, none of the methods for sampling pollinators are ideal, hence a combination of complementary approaches has been suggested as the most effective (Nielsen et al. 2011; Potts et al. 2021; Leclercq et al. 2022). Considering the localities of the present study where both methods were conducted, most of the species (41%) were detected during transect walks, 32% were found using both methods, while 27% were caught in pan traps. Concerning the number of individuals recorded in pan traps, the highest share (39%) was found in blue ones, followed by 33% in yellow traps, while the lowest share (28%) was found in white pan traps. Taking into account new records for the 25 bee species that had not been previously recorded for Serbia, out of the 123 recorded specimens, 54 were detected during transect walks, whereas 69 specimens were caught in pan traps (39 in blue, 19 in white, and 11 in yellow pan traps). Out of these 25 species, 48% were detected during transect walks, 28% were caught in pan traps, and 24% species were detected by both methods. Given the fact that many species were detected by only one of the two used sampling methods, the results of the present study indicate that the use of both is the best way to assess bee diversity and abundance. Identifying the most suitable monitoring and sampling techniques is an important step towards assessing the bee populations' status and trends, a prerequisite for comprehensive knowledge of bee diversity and, consequently, for effective conservation practices.

By presenting new records and confirming some old ones, the results of the present study contribute to updating and reverifying data on bee species occurrences in Serbia. Given the fact that more than half of the European bee species have been assessed as Data Deficient (Nieto et al. 2014), investigations such as this one add to tackling the existing lack of information. Furthermore, the knowledge gaps recognized across certain geographic regions, such as the Mediterranean and Eastern European areas, could be addressed through the implementation of the standardized monitoring activities (Potts et al. 2021). Therefore, by taking part in ongoing scientific projects and applying consistent methodologies, we aim to continue gathering data through the systematic monitoring of pollinators in order to update and revise current evidence.

Acknowledgements

We wish to thank Igor Ivkov Bachelor of Arts (Hons.) in English Language and Literature, certified translator for the English Language, for his English proofreading services. We also thank the reviewers, Dr Denis Michez and Dr Petr Bogusch, whose constructive input helped improve this manuscript. The data for this study was obtained as part of the realization of the following projects: SPAS – Serbian Pollinator Advice Strategy – for the next normal (Science Fund of the Republic of Serbia, Program IDEAS, GA ID: 7737504) and Safeguard – Safeguarding European wild pollinators; this project received funding from the European Union’s Horizon 2020 research and innovation programme under grant agreement No. 101003476 (www.safeguard.biozentrum.uni-wuerzburg.de). We also gratefully acknowledge the financial support of the Ministry of Science, Technological Development and Innovation of the Republic of Serbia (Grant No. 451-03-47/2023-01/200125 and Grant No. 451-03-47/2023-01/200358). The authors declare that no competing interests exist.

References

- Apfelbeck V (1896) Balkanske Apide (pčele). Glasnik zemaljskog muzeja u Bosni i Hercegovini 8: 329–342.
- Ballantyne G, Baldock KCR, Rendell L, Willmer PG (2017) Pollinator importance networks illustrate the crucial value of bees in a highly speciose plant community. *Scientific Reports* 7: e8389. <https://doi.org/10.1038/s41598-017-08798-x>
- Brown M, Breeze T, Bulet P, Chauzat M-P, Demirova I, de Miranda J, Klein A-M, Mand M, Metodiev T, Michez D, Nazzi F, Neumann P, Paxton R, Potts S, Stout J, Turney G, Yañez O (2021) PoshBee: Pan-European Assessment, Monitoring, and Mitigation of Stressors on the Health of Bees. *ARPHA Preprints*: e72231. <https://doi.org/10.3897/arphapreprints.e72231>
- Cane JH, Minckley RL, Kervin LJ (2000) Sampling bees (Hymenoptera: Apiformes) for pollinator community studies: pitfalls of pan-trapping. *Journal of the Kansas Entomological Society* 73: 225–231. <https://www.jstor.org/stable/25085973>
- Colla SR, Otterstatter MC, Gegeer RJ, Thomson JD (2006) Plight of the bumble bee: Pathogen spillover from commercial to wild populations. *Biological Conservation* 129(4): 461–467. <https://doi.org/10.1016/j.biocon.2005.11.013>
- Dicks L, Breeze T, Ngo H, Senapathi D, An J, Aizen M, Basu P, Buchori D, Galetto L, Garibaldi L, Gemmill-Herren B, Howlett B, Imperatriz-Fonseca VL, Johnson S, Kovács-Hostyánszki A, Kwon Y, Lattorff HM, Lungharwo T, Seymour C, Vanbergen A, Potts S (2021) A global expert assessment of drivers and risks associated with pollinator decline. *Nature Ecology & Evolution* 5(10): 1453–1461. <https://doi.org/10.1038/s41559-021-01534-9>
- Drossart M, Rasmont P, Vanormelingen P, Dufrêne M, Folschweiller M, Pauly A, Vereecken NJ, Vray S, Zambra E, D’Haeseleer J, Michez D (2019) Belgian Red List of bees. *Presse universitaire de l’Université de Mons*, 1–140.

- Drossart M, Gérard M (2020) Beyond the decline of wild bees: Optimizing conservation measures and bringing together the actors. *Insects* 11(9): e649. <https://doi.org/10.3390/insects11090649>
- European Commission (2021) EU biodiversity strategy for 2030: Bringing nature back into our lives. European Commission Directorate-General for Environment, Publications Office of the European Union: 1–35. <https://data.europa.eu/doi/10.2779/677548> [Accessed on 08.03.2023]
- Ghisbain G, Gérard M, Wood TJ, Hines HM, Michez D (2021) Expanding insect pollinators in the Anthropocene. *Biological Reviews* 96(6): 2755–2770. <https://doi.org/10.1111/brv.12777>
- Ghisbain G, Rosa P, Bogusch P, Flaminio S, Le Divelec R, Dorchin A, Kasperek M, Kuhlmann M, Litman J, Mignot M, Müller A, Praz C, Radchenko VG, Rasmont P, Risch S, Roberts SPM, Smit J, Wood TJ, Michez D, Reverté S (2023) The new annotated checklist of the wild bees of Europe (Hymenoptera: Anthophila). *Zootaxa* 5327(1): 1–147. <https://doi.org/10.11646/zootaxa.5327.1.1>
- Gill RJ, Ramos-Rodriguez O, Raine NE (2012) Combined pesticide exposure severely affects individual- and colony-level traits in bees. *Nature* 491: 105–108. <https://doi.org/10.1038/nature11585>
- González-Varo JP, Biesmeijer JC, Bommarco R, Potts SG, Schweiger O, Smith HG, Steffan-Dewenter I, Szentgyörgyi H, Woyciechowski M, Vilà M (2013) Combined effects of global change pressures on animal-mediated pollination. *Trends in Ecology & Evolution* 28(9): 524–530. <https://doi.org/10.1016/j.tree.2013.05.008>
- Goulson D (2019) The insect apocalypse, and why it matters. *Current Biology* 29(19): R967–R971. <https://doi.org/10.1016/j.cub.2019.06.069>
- Goulson D, Nicholls E, Botías C, Rotheray EL (2015) Bee declines driven by combined stress from parasites, pesticides, and lack of flowers. *Science* 347(6229): e1255957. <https://doi.org/10.1126/science.1255957>
- Heneberg P, Bogusch P (2014) To enrich or not to enrich? Are there any benefits of using multiple colors of pan traps when sampling aculeate Hymenoptera? *Journal of Insect Conservation* 18: 1123–1136. <https://doi.org/10.1007/s10841-014-9723-8>
- IPBES (2016) The assessment report of the Intergovernmental Science-Policy Platform on Biodiversity and Ecosystem Services on pollinators, pollination and food production. In: Potts SG, Imperatriz-Fonseca VL, Ngo HT (Eds) Secretariat of the Intergovernmental Science-Policy Platform on Biodiversity and Ecosystem Services, 1–552. <https://doi.org/10.5281/zenodo.3402857>
- Kennedy CM, Lonsdorf E, Neel MC, Williams NM, Ricketts TH, Winfree R, Bommarco R, Brittain C, Burley AL, Cariveau D, Carvalho LG, Chacoff NP, Cunningham SA, Danforth BN, Dudenhöffer J-H, Elle E, Gaines HR, Garibaldi LA, Gratton C, Holzschuh A, Isaacs R, Javorek SK, Jha S, Klein AM, Krewenka K, Mandelik Y, Mayfield MM, Morandin L, Neame LA, Otieno M, Park M, Potts SG, Rundlöf M, Saez A, Steffan-Dewenter I, Taki H, Viana BF, Westphal C, Wilson JK, Greenleaf SS, Kremen C (2013) A global quantitative synthesis of local and landscape effects on wild bee pollinators in agroecosystems. *Ecology Letters* 16(5): 584–599. <https://doi.org/10.1111/ele.12082>

- Kremen C, Williams NM, Thorp RW (2002) Crop pollination from native bees at risk from agricultural intensification. *Proceedings of the National Academy of Sciences of the United States of America* 99(26): 16812–16816. <https://doi.org/10.1073/pnas.262413599>
- Kuhlmann M, Ascher JS, Dathe HH, Ebmer AW, Hartmann P, Michez D, Müller A, Patiny S, Pauly A, Praz C, Rasmont P, Risch S, Scheuchl E, Schwarz M, Terzo M, Williams PH, Amiet F, Baldock D, Berg Ø, Bogusch P, Calabuig I, Cederberg B, Gogala A, Gusenleitner F, Josan Z, Madsen HB, Nilsson A, Ødegaard F, Ortiz-Sanchez J, Paukkunen J, Pawlikowski T, Quaranta M, Roberts SPM, Sáropataki M, Schwenninger H-R, Smit J, Söderman G, Tomozei B (2023) Checklist of the Western Palaearctic bees (Hymenoptera: Apoidea: Anthophila). <http://westpalbees.myspecies.info> [Accessed on 28.02.2023]
- LeBuhn G, Vargas Luna J (2021) Pollinator decline: what do we know about the drivers of solitary bee declines? *Current opinion in insect science* 46: 106–111. <https://doi.org/10.1016/j.cois.2021.05.004>
- Leclercq N, Marshall L, Weekers T, Anselmo A, Benda D, Bevk D, Bogusch P, Cejas D, Drepper B, Galloni M, Gérard M, Ghisbain G, Hutchinson L, Martinet B, Michez D, Molenberg J-M, Nikolic P, Smagghe G, Straka J, Vandamme P, Wood T, Vereecken N (2022) A comparative analysis of crop pollinator survey methods along a climatic gradient. *Agriculture, Ecosystems and Environment* 329: e107871. <https://doi.org/10.1016/j.agee.2022.107871>
- Martinet B, Zambra E, Przybyla K, Lecocq T, Anselmo A, Nonclercq D, Rasmont P, Michez D, Hennebert E (2021) Mating under climate change: Impact of simulated heatwaves on the reproduction of model pollinators. *Functional Ecology* 35(3): 739–752. <https://doi.org/10.1111/1365-2435.13738>
- Michez D, Rasmont P, Terzo M, Vereecken NJ (2019) *Bees of Europe*. Hymenoptera of Europe 1. NAP Editions, 1–547.
- Mocsáry S (1897) Hymenoptera. *A Magyar Birodalom Állatvilága. Fauna Regni Hungariae*, 113 pp.
- Mudri-Stojnić S, Andrić A, Markov-Ristić Z, Đukić A, Vujić A (2021) Contribution to the knowledge of the bee fauna (Hymenoptera, Apoidea, Anthophila) in Serbia. *ZooKeys* 1053: 43–105. <https://doi.org/10.3897/zookeys.1053.67288>
- Nielsen A, Steffan-Dewenter I, Westphal C, Messinger O, Potts SG, Roberts SPM, Settele J, Szentgyörgyi H, Vaissière BE, Vaitis M, Woyciechowski M, Bazos I, Biesmeijer JC, Bommarco R, Kunin WE, Tscheulin T, Lamborn E, Petanidou T (2011) Assessing bee species richness in two Mediterranean communities: importance of habitat type and sampling techniques. *Ecological Research* 26(5): 969–983. <https://doi.org/10.1007/s11284-011-0852-1>
- Nieto A, Roberts SPM, Kemp J, Rasmont P, Kuhlmann M, García Criado M, Biesmeijer JC, Bogusch P, Dathe HH, De la Rúa P, De Meulemeester T, Dehon M, Dewulf A, Ortiz-Sánchez FJ, Lhomme P, Pauly A, Potts SG, Praz C, Quaranta M, Radchenko VG, Scheuchl E, Smit J, Straka J, Terzo M, Tomozii B, Window J, Michez D (2014) *European Red List of Bees*. Publication Office of the European Union, 1–84. <https://doi.org/10.2779/77003>
- Official Gazette RS (2010) Regulation on criteria for distinguishing habitat types, on habitat types, on sensitive, endangered, rare and habitat types of conservation priority, and on the conservation measures for their preservation: 35/2010-29. Official Gazette of Republic of Serbia No 35/2010. <http://www.pravno-informacioni-sistem.rs/SlGlasnikPortal/eli/rep/sgrs/ministarstva/pravilnik/2010/35/5/reg/> [Accessed on 23.08.2023]

- Ollerton J, Winfree R, Tarrant S (2011) How many flowering plants are pollinated by animals? *Oikos* 120(3): 321–326. <https://doi.org/10.1111/j.1600-0706.2010.18644.x>
- ORBIT (2021–2024) Taxonomic resources for European bees. European Commission Directorate-General for Environment, project Contract No: 09.029901/2021/848268/SER/ENV.D.2. <https://orbit-project.eu/> [Accessed on 08.03.2023]
- PoshBee (2018–2023) Pan-European assessment, monitoring, and mitigation of stressors on the health of bees. H2020-SFS-2016-2017, GA ID: 773921. <https://poshbee.eu/> [Accessed on 08.03.2023]
- Potts SG, Biesmeijer JC, Kremen C, Neumann P, Schweiger O, Kunin WE (2010) Global pollinator declines: trends, impacts and drivers. *Trends in Ecology & Evolution* 25(6): 345–353. <https://doi.org/10.1016/j.tree.2010.01.007>
- Potts SG, Biesmeijer K, Bommarco R, Breeze T, Carvalheiro L, Franzén M, González-Varo JP, Holzschuh A, Kleijn D, Klein A-M, Kunin B, Lecocq T, Lundin O, Michez D, Neumann P, Nieto A, Penev L, Rasmont P, Ratamáki O, Riedinger V, Roberts SPM, Rundlöf M, Scheper J, Sorensen P, Steffan-Dewenter I, Stoev P, Vila M, Schwieger O (2015) Status and trends of European pollinators: Key findings of the STEP project. Pensoft Publishers, Sofia, 72 pp. <http://step-project.net/img/uplf/STEP%20brochure%20online-1.pdf> [Accessed on 28.02.2023]
- Potts S, Dauber J, Hochkirch A, Oteman B, Roy D, Ahnre K, Biesmeijer JC, Breeze T, Carvell C, Ferreira C, Fitzpatrick Ú, Isaac N, Kuussaari M, Ljubomirov T, Maes J, Ngo H, Pardo A, Polce C, Quaranta M, Settele J, Sorg M, Stefanesco C, Vujčić A (2021) Proposal for an EU pollinator monitoring scheme. Publications Office of the European Union, 1–310. <https://doi.org/10.2760/881843>
- Power AG, Mitchell CE (2004) Pathogen spillover in disease epidemics. *The American Naturalist* 164(S5): S79–S89. <https://doi.org/10.1086/424610>
- PULSE (2022–2023) Providing technical and scientific support in measuring the pulse of European biodiversity using the Red List Index. European Commission Directorate-General for Environment, project Contract No: 07.027755/2020/840209/SER/ENV.D.2.
- Purkiss T, Lach L (2019) Pathogen spillover from *Apis mellifera* to a stingless bee. *Proceedings of the Royal Society B: Biological Sciences* 286: e20191071. <https://doi.org/10.1098/rspb.2019.1071>
- QGIS Development Team (2022) QGIS Geographic Information System. Open Source Geospatial Foundation Project. <http://qgis.osgeo.or> [Accessed on 28.08.2023]
- Radchenko V (2016) A new widespread European bee species of the genus *Dasygoda* Latreille (Hymenoptera, Apoidea). *Zootaxa* 4184(3): 491–504. <https://doi.org/10.11646/zootaxa.4184.3.4>
- Rasmont P, Haubruge E [Eds] (2020) Atlas Hymenoptera. <http://www.atlashymenoptera.net> [Accessed on 23.08.2023]
- Reverté S, Miličić M, Ačanski J, Andrić A, Aracil A, Aubert M, Balzan MV, Bartomeus I, Bogusch P, Bosch J, Budrys E, Cantú-Salazar L, Castro S, Cornalba M, Demeter I, Devalez J, Dorchin A, Dufrêne E, Đorđević A, Físlér L, Fitzpatrick Ú, Flaminio S, Földesi R, Gaspar H, Genoud D, Geslin B, Ghisbain G, Gilbert F, Gogala A, Grković A, Heimbürg H, Herrera-Mesías F, Jacobs M, Milosavljević MJ, Janssen K, Jensen J-K, Ješovnik A, Józsan Z, Karlis G, Kaspárek M, Kovács-Hostyánszki A, Kuhlmann M, Le Divelec R, Leclercq N,

- Likov L, Litman J, Ljubomirov T, Madsen HB, Marshall L, Mazánek L, Milić D, Mignot M, Mudri-Stojnić S, Müller A, Nedeljković Z, Nikolić P, Ødegaard F, Patiny S, Paukkunen J, Pennards G, Pérez-Bañón C, Perrard A, Petanidou T, Pettersson LB, Popov G, Popov S, Praz C, Prokhorov A, Quaranta M, Radchenko VG, Radenković S, Rasmont P, Rasmussen C, Reemer M, Ricarte A, Risch S, Roberts SPM, Rojo S, Ropars L, Rosa P, Ruiz C, Sentil A, Shparyk V, Smit J, Sommaggio D, Soon V, Ssymank A, Ståhls G, Stavrínides M, Straka J, Tarlap P, Terzo M, Tomozii B, Tot T, van der Ent L-J, van Steenis J, van Steenis W, Varnava AI, Vereecken NJ, Veselić S, Vesnić A, Weigand A, Wisniewski B, Wood TJ, Zimmermann D, Michez D, Vujić A (2023) National records of 3000 European bee and hoverfly species: A contribution to pollinator conservation. *Insect Conservation and Diversity*. <https://doi.org/10.1111/icad.12680>
- Roulston TH, Smith SA, Brewster AL (2007) A comparison of pan trap and intensive net sampling techniques for documenting a bee (Hymenoptera: Apiformes) fauna. *Journal of the Kansas Entomological Society* 80(2): 179–181. [https://doi.org/10.2317/0022-8567\(2007\)80\[179:ACOPTA\]2.0.CO;2](https://doi.org/10.2317/0022-8567(2007)80[179:ACOPTA]2.0.CO;2)
- Safeguard (2021–2025) Safeguarding European wild pollinators. H2020-SC5-2018-2019-2020, GA ID: 101003476. <https://www.safeguard.biozentrum.uni-wuerzburg.de/> [Accessed on 08.03.2023]
- Sánchez-Bayo F, Wyckhuys KAG (2019) Worldwide decline of the entomofauna: A review of its drivers. *Biological Conservation* 232: 8–27. <https://doi.org/10.1016/j.biocon.2019.01.020>
- SPAS (2022–2024) Serbian Pollinator Advice Strategy – for the next normal. Science Fund of the Republic of Serbia, Program IDEAS, [GA ID: 7737504]. <https://spas.pmf.uns.ac.rs/en/> [Accessed on 08.03.2023]
- SPRING (2021–2023) Strengthening pollinator recovery through indicators and monitoring. European Commission Directorate-General for Environment, project Contract No: 09.02001/2021/847887/SER/ENV.D.2. <https://www.ufz.de/spring-pollination/> [Accessed on 08.03.2023]
- Steffan-Dewenter I, Westphal C (2008) The interplay of pollinator diversity, pollination services and landscape change. *Journal of Applied Ecology* 45(3): 737–741. <https://doi.org/10.1111/j.1365-2664.2008.01483.x>
- Titley MA, Snaddon JL, Turner EC (2017) Scientific research on animal biodiversity is systematically biased towards vertebrates and temperate regions. *PLoS ONE* 12(12): e0189577. <https://doi.org/10.1371/journal.pone.0189577>
- Toler TR, Evans EW, Tepedino VJ (2005) Pan-trapping for bees (Hymenoptera: Apiformes) in Utah's West Desert: the importance of color diversity. *Pan Pacific Entomologist* 81(3–4): 103–113.
- Uhler J, Redlich S, Zhang J, Hothorn T, Tobisch C, Ewald J, Thorn S, Seibold S, Mitesser O, Morinière J, Bozicevic V, Benjamin CS, Englmeier J, Fricke U, Ganuza C, Haensel M, Riebl R, Rojas-Botero S, Rummler T, Uphus L, Schmidt S, Steffan-Dewente I, Müller J (2021) Relationship of insect biomass and richness with land use along a climate gradient. *Nature Communications* 12(1): e5946. <https://doi.org/10.1038/s41467-021-26181-3>
- Vorgin V (1918) Pregled Apidae hrvatske Slavonije i hrvatskog Primorja s obzirom na faunu Apida Dalmacije. *Glasnik Hrvatskoga prirodoslovnoga društva, Zagreb* 30: 1–4.

- Wagner DL (2020) Insect declines in the Anthropocene. *Annual Review of Entomology* 65: 457–480. <https://doi.org/10.1146/annurev-ento-011019-025151>
- Westphal C, Bommarco R, Carré G, Lamborn E, Morison N, Petanidou T, Potts SG, Roberts SPM, Szentgyörgyi H, Tscheulin T, Vaissière BE, Woyciechowski M, Biesmeijer JC, Kunin WE, Settele J, Steffan-Dewenter I (2008) Measuring bee diversity in different European habitats and biogeographical regions. *Ecological Monographs* 78(4): 653–671. <https://doi.org/10.1890/07-1292.1>
- Willmer PG, Cunnold H, Ballantyne G (2017) Insights from measuring pollen deposition: Quantifying the pre-eminence of bees as flower visitors and effective pollinators. *Arthropod-Plant Interactions* 11(3): 411–425. <https://doi.org/10.1007/s11829-017-9528-2>
- Zattara EE, Aizen MA (2021) Worldwide occurrence records suggest a global decline in bee species richness. *One Earth* 4(1): 114–123. <https://doi.org/10.1016/j.oneear.2020.12.005>

Supplementary material I

The list of all bee species recorded during the surveys of selected sites in 2022

Authors: Sonja Mudri-Stojnić, Andrijana Andrić, Józán Zsolt, Laura Likov, Tamara Tot, Ana Grković, Ante Vujić

Data type: xlsx

Explanation note: The list of all recorded bee species with additional information: IUCN categories; collection methodology types; data on the presence of listed species in the online maps of the Checklist of the Western Palearctic Bees; data on the species with occurrences previously available only from sources prior to year 2000.

Copyright notice: This dataset is made available under the Open Database License (<http://opendatacommons.org/licenses/odbl/1.0/>). The Open Database License (ODbL) is a license agreement intended to allow users to freely share, modify, and use this Dataset while maintaining this same freedom for others, provided that the original source and author(s) are credited.

Link: <https://doi.org/10.3897/jhr.96.107595.suppl1>

First confirmed parasitism of pleasing fungus beetles (Coleoptera, Erotylidae) by a tropical rhyssine ichneumonid, and first record for *Cyrtorhysa moellerii* Bingham (Hymenoptera, Ichneumonidae) from Thailand

Kittipum Chansri^{1,2}, Kanoktip Somsiri³, Donald L. J. Quicke^{2*}, Buntika A. Butcher^{2*}

1 Program in Zoology, Department of Biology, Faculty of Science, Chulalongkorn University, Bangkok 10330, Thailand **2** Integrative Insect Ecology Research Unit, Department of Biology, Faculty of Science, Chulalongkorn University, Phayathai Road, Pathumwan, Bangkok 10330, Thailand **3** Sakaerat Environmental Research Station, Nakhon Ratchasima 30370, Thailand

Corresponding author: Buntika A. Butcher (buntika.a@chula.ac.th)

Academic editor: T. Spasojevic | Received 30 May 2023 | Accepted 1 October 2023 | Published 11 October 2023

<https://zoobank.org/F47B0A1E-DB24-46D2-85A9-C6663A053622>

Citation: Chansri K, Somsiri K, Quicke DLJ, Butcher BA (2023) First confirmed parasitism of pleasing fungus beetles (Coleoptera, Erotylidae) by a tropical rhyssine ichneumonid, and first record for *Cyrtorhysa moellerii* Bingham (Hymenoptera, Ichneumonidae) from Thailand. Journal of Hymenoptera Research 96: 783–804. <https://doi.org/10.3897/jhr.96.107196>

Abstract

The first record of the Darwin wasp, *Cyrtorhysa moellerii* Bingham, 1898 (Hymenoptera, Ichneumonoidea, Rhyssinae) from Thailand is presented. Members of both sexes are fully described and illustrated. The biology of *C. moellerii*, a parasitoid of the pleasing fungus beetle *Encaustes opaca* Crotch, 1876 (Coleoptera, Erotylidae), is reported for the first time. Hosts were associated with standing deadwood of *Anthoshorea henryana* (Pierre ex Laness.) P. S. Ashton & J. Heck (Dipterocarpaceae) in dry evergreen forest, Nakhon Ratchasima province, northeastern Thailand. DNA barcodes (cytochrome c oxidase subunit 1 sequence (COI)) were generated for both host and parasitoid and phylogenetic trees constructed for these and other members of the same family and subfamily respectively. A key is provided to separate the three known species of *Cyrtorhysa*. This is the first confirmed host record for a tropical species of Rhyssinae as well as the first from Erotylidae.

Keywords

Coleoptera, dead wood, *Encaustes*, host record, Rhyssinae

* These authors contributed equally to this work.

Introduction

Rhyssine Darwin wasps (Ichneumonidae) have mostly been recorded as parasitoids of various woodwasps belonging to the families Siricidae, Xiphydriidae and the monotypic Anaxyelidae from northwest America (Hanson 1939; Couturier 1949; Quicke 2015). In India and Pakistan, *Rhyssa persuasoria himalayensis* Wilkinson, 1927 is reported to attack many species of Siricidae (Kamath and Gupta 1972). In Costa Rica, *Epirhyssa mexicana* Cresson, 1874 have been recorded probing dead wood with cerambycid larvae inside (Gauld 1991), and Porter (1978) also suggested that Neotropical *Epirhyssa* Cresson, 1865 species were parasitoids of xylophagous beetles but without any definitive records. In China although most hosts records involve siricid woodwasps (Sheng and Sun 2010), there are also several reports of long horn beetles (Cerambycidae) acting as hosts. *Moechotypa diphysis* (Pascoe, 1871) is reported as being attacked by *E. lurida* Sheng & Sun, 2010, *Rhyssella approximata* (Fabricius, 1793) and *Triancyra galloisi* (Uchida, 1928); *Anoplophora glabripennis* (Motschulsky, 1854) and *Cerambyx cerdo* Linnaeus, 1758 are reported to be hosts of *Megarhyssa praecegens* (Tosquinet, 1889), *M. jezoensis* (Matsumura, 1912) and *R. approximata* (Sheng and Sun 2010). *Massicus raddei* (Blessig & Solsky, 1872) has been recorded as the host of *M. praecegens* (Cao et al. 2020).

Cyrtorhyssa Baltazar, 1961 is an endemic Asian genus known only from the Indo-Chinese region. It comprises three species: *C. moellerii* Bingham, 1898 from India (Sikkim) and Myanmar (Tenasserim), *C. mesopyrrha* Mocsary, 1905 from Indonesia (Sumatra, Java, Kalimantan), Malaysia (Sarawak) and the Philippines (Kamath and Gupta 1972) and *C. xishuangensis* Wang, 1982 from China (Wang 1982). Up until now, no host records have been reported for any members of the genus.

Only one species of rhyssine wasp has previously been recorded from Thailand, viz *Myllenyxis kuchingensis* Kamath & Gupta, 1972 (Kamath and Gupta 1972). The record is more than 50 years old and there is no associated biological information. Thus, this discovery of *C. moellerii* in 2021 is the second officially reported rhyssine wasp from Thailand and the last published information on *C. moellerii* dates from over a century ago. Here we establish the first host record of *C. moellerii* which was reared from a particularly large-bodied, wood-boring erotyloid beetle (*E. opaca*). Moreover, this is also the first confirmed case of an erotyloid as a host for rhyssine ichneumonids.

Methods

Observation were made in the dry evergreen forest at Sakaerat Environmental Research Station, Nakhon Ratchasima Province, northeastern, Thailand (Fig. 1A). The parasitoid wasps and their host were collected from a standing dead *Anthoshorea henryana* (Pierre ex Laness.) P. S. Ashton & J. Heck (Dipterocarpaceae) tree (Fig. 1B) during January and February 2021. Adults male and female *C. moellerii* (Fig. 2A, B) were collected on and around the tree, approximately 0.5–2.0 m above the ground (Fig. 1C, D), and preserved in 95% ethanol. Hosts and their remains were dissected from



Figure 1. Dry evergreen forest, Sakaerat Environmental Research Station, Thailand (A), dead wood of *A. henryana* (B), teneral stage of *Encaustes opaca* inside the deadwood (C), pupa of *C. moellerii* inside the deadwood (D).

the wood using a hammer and chisel. Living immature beetles and wasps were also collected and reared in a clear plastic container at room temperature. Morphological terminology follows Broad et al. (2018) except for wing venation which follows Sharkey and Wharton (1997); see also fig. 2.2 in Quicke (2015). We provide the alternative nomenclature in parentheses in the relevant places below. Specimens were imaged using a Leica M205C, Leica DMC5400, Digital Camera, and LAS X software.

DNA barcodes (cytochrome c oxidase subunit 1 sequence, COI) were generated from the wasps and the beetle host legs by the Center for Biodiversity Genomics, University of Guelph, using standard methods (Hebert et al. 2003). Host and parasitoid barcodes, as well as sequence from all available relatives, and close outgroups from GenBank database (National Center for Biotechnology Information [NCBI] (2023)) were assembled for phylogenetic analysis. Details of the sequences used in the analyses are presented in Tables 1, 2, respectively, together with specimen provenances and Genbank Accession Number. For the Ichneumonidae analysis, DNA sequences were available for an additional 27 species of Rhyssinae representing seven genera. In addition, four spe-

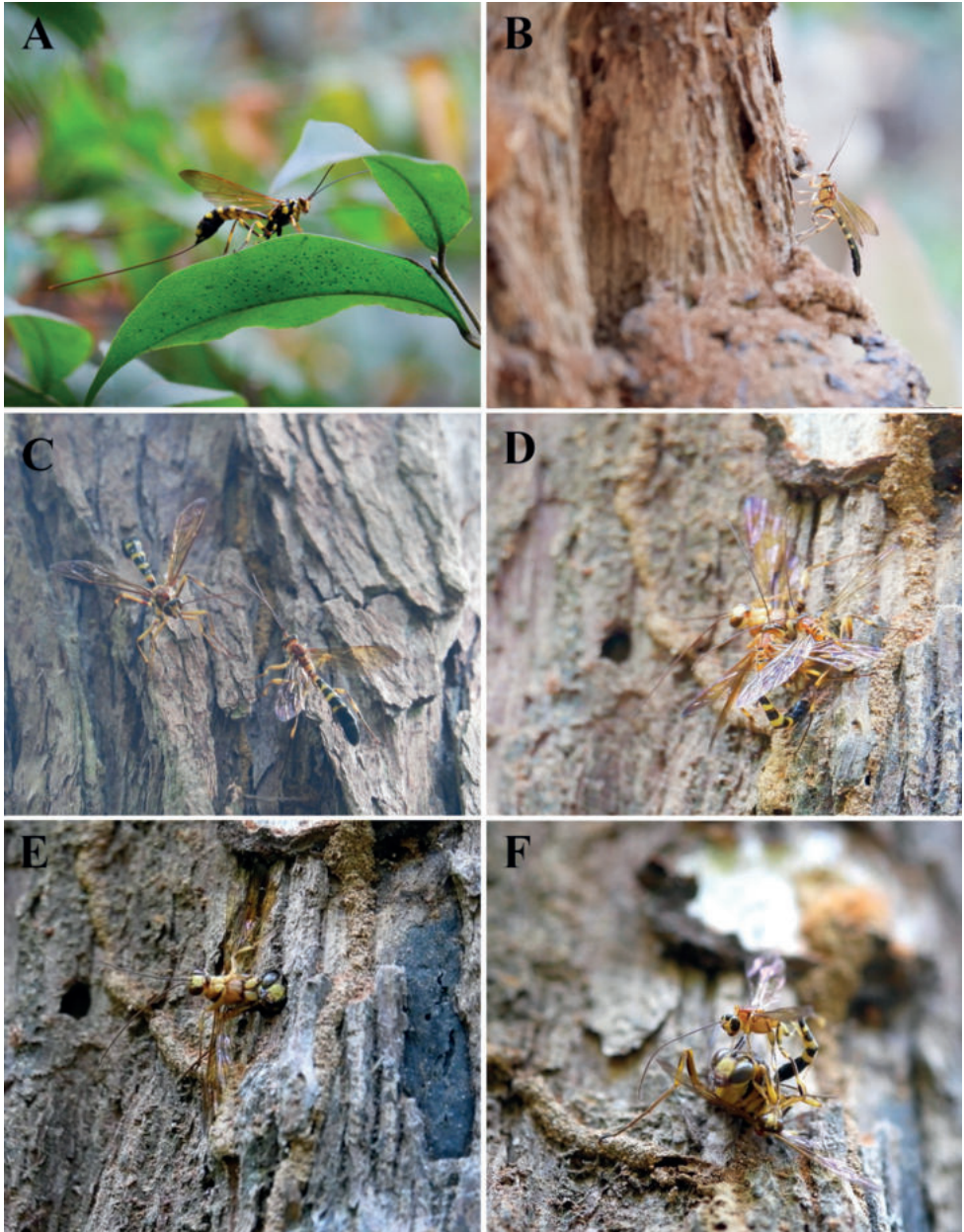


Figure 2. Adult female *C. moellerii* in the natural habitat (A), male of *C. moellerii* during tergal stroke behaviour to marking the location of closely emergence female (B), male aggregation behaviour (C), mating behaviour of female and male *C. moellerii* in natural habitat (D–F).

cies of the closely related subfamily Poemeniinae were included as outgroups (Quicke et al. 2009; Spasojevic et al. 2021). For the analysis of Erotylidae, barcodes from 25 other species were available, representing five subfamilies. Members of two genera of Languriidae were included as outgroups (Bocak et al. 2014). Maximum likelihood phy-

Table 1. List of rhyssine wasp species, including Thai *C. moellerii* and outgroups, with their provenance, GenBank Accession Number, and references.

Subfamily	Species	Provenance	GenBank accession No.	Reference
Poemeniinae	<i>Deuterxorides elevator</i>	Germany	JF963193	Quicke et al. 2012
	<i>Neoxorides caryae</i>	USA	MK959447	Bennett et al. 2019
	<i>Poemenia albipes</i>	Canada	MG355017	Dewaard 2017 unpublished
	<i>Poemenia hectica</i>	Russia	MZ627402	Roslin et al. 2022
Rhyssinae	<i>Cyrtorhyssa moellerii</i>	Thailand	OQ272136	present study
	<i>Cyrtorhyssa moellerii</i>	Thailand	OQ272137	present study
	<i>Epirhyssa latimandibularis</i>	Thailand	OQ272138	present study
	<i>Epirhyssa corralesi</i>	Costa Rica	OQ272125	
	<i>Epirhyssa curtisi</i>	Costa Rica	OQ272126	
	<i>Epirhyssa frobergi</i>	Costa Rica	OQ272135	
	<i>Epirhyssa mexicana</i>	Costa Rica	OQ272133	
	<i>Epirhyssa oranensis</i>	Costa Rica	OQ272132	
	<i>Epirhyssa porteri</i>	Costa Rica	OQ272131	
	<i>Epirhyssa praecincta</i>	Costa Rica	OQ272134	
	<i>Epirhyssa prolasia</i>	Costa Rica	OQ272129	
	<i>Epirhyssa sapporensis</i>	South Korea	KU753248	Suk and Won 2016 unpublished
	<i>Epirhyssa theloides</i>	Costa Rica	OQ272130	
	<i>Megarhyssa atrata</i>	Canada	OQ272127	
	<i>Megarhyssa greenei</i>	USA	HM422919	iBOL 2010 unpublished
	<i>Megarhyssa nortoni</i>	USA	KU496775	Sikes et al. 2017
	<i>Megarhyssa n. nortoni</i>	Canada	KR787310	Hebert et al. 2016
	<i>Megarhyssa macrura</i>	Canada	KR929825	Hebert et al. 2016
	<i>Myllenyxis</i> sp.	Malaysia	JF963636	Quicke et al. 2012
	<i>Rhyssa amoena</i>	Germany	JF963813	Quicke et al. 2012
	<i>Rhyssa crevieri</i>	Canada	KR799965	Hebert et al. 2016
	<i>Rhyssa howdenorum</i>	USA	MN556947	Landry and Landry 2019 unpublished
	<i>Rhyssa persuasoria</i>	Norway	OQ272128	
	<i>Rhyssella humida</i>	Canada	KM997713	Eagalle 2014
	<i>Rhyssella nitida</i>	Canada	KM996159	Eagalle 2014
	<i>Rhyssella furanna</i>	Japan	MW056244	Spasojevic et al. 2021 9
<i>Rhyssella approximata</i>	Finland	MZ625985	Roslin et al. 2022	
<i>Triancyra galloisi</i>	South Korea	KU753388	Suk and Won 2016 unpublished	
<i>Triancyra tricolorata</i>	South Korea	KU753389	Suk and Won 2016 unpublished	

logenic analyses were carried out using RAxML version 8.2.12 (Stamatakis 2006) with a GTRGAMMA substitution model and rapid bootstrap option with 100 randomizations (-f a -# 100). The three-codon position were treated as separated data partitions.

Results

Parasitoid behaviour

As in many rhyssine wasps, males *C. moellerii* emerge before females and they can detect where the female will emerge from. Some males were observed performing a

Table 2. List of erotyliid beetles, including Thai *E. opaca* and outgroups, with their provenance, GenBank Accession Number and references.

Family	Species	Provenance	GenBank accession No.	Reference
Erotylidae	<i>Dacne bipustulata</i>	Germany	HQ954205	iBOL 2011 unpublished
	<i>Dacne picta</i>	NA	KC510126	Cho et al. 2013 unpublished
	<i>Dacne quadrimaculata</i>	Canada	JN288175	iBOL 2011 unpublished
	<i>Dacne ruffrons</i>	France	MN182895	Sire et al. 2019
	<i>Dacne</i> sp.	France	MN182938	Sire et al. 2019
	<i>Aulacochilus quadripustulatus</i>	NA	MN603446	Liu 2019 unpublished
	<i>Aulacochilus xingtaiensis</i>	NA	MN615269	Li 2019 unpublished
	<i>Encaustes cruenta ormosana</i>	NA	MN615271	Li 2019 unpublished
	<i>Encaustes opaca</i>	Thailand	OQ272139	present study
	<i>Iphiclus</i> sp.	NA	KC966646	Cline et al. 2014
	<i>Iphiclus sedecimmaculatus</i>	NA	KP134126	McElrath et al. 2014 unpublished
	<i>Episcapha fortunii</i>	Japan	LC619112	Saito et al. 2021 unpublished
	<i>Megalodacne fasciata</i>	Canada	GU013623	Park et al. 2010
	<i>Ischyryus quadripunctatus</i>	United States	HM433801	iBOL 2010 unpublished
	<i>Triplax aenea</i>	Finland	MZ659828	Roslin et al. 2022
	<i>Triplax dissimulator</i>	Canada	KM843753	Hebert et al. 2014 unpublished
	<i>Triplax frosti</i>	Canada	KR487395	Hebert et al. 2016
	<i>Triplax lacordairei</i>	France	MN182940	Sire et al. 2019
	<i>Triplax lepida</i>	France	KM285906	Rougerie 2014 unpublished
	<i>Triplax rufipes</i>	Belgium	HQ954016	iBOL 2011 unpublished
	<i>Triplax russica</i>	Poland	MH115489	Kolasa et al. 2014 unpublished
	<i>Triplax scutellaris</i>	Finland	MZ631796	Roslin et al. 2022
	<i>Triplax thoracica</i>	Canada	KT706260	Telfer et al. 2015
<i>Tritoma bipustulata</i>	Finland	KJ964373	Pentinsaari et al. 2014	
<i>Tritoma pulchra</i>	Canada	KR489305	Hebert et al. 2016	
Languriidae	<i>Acropteroxys gracilis</i>	Canada	MG059564	Dewaard 2017 unpublished
	<i>Languria mozardi mozardi</i>	Canada	MF635178	deWaard et al. 2019

tergal stroking behaviour (which is thought to be involved in marking the location of a conspecific that was nearing emergence). Male aggregation behaviour (Fig. 2C, Suppl. material 1) was observed, with some individuals showing aggressive guarding behaviour of their marked location. Mating behaviour was also video-recorded (Fig. 2D, Suppl. material 2). Even though the metasoma of male is not extremely slender, larger males inserted their metasomas into the chewed tunnel of female before her completing emergence process (Fig. 2E, Suppl. material 3). The smaller males that did not insert their metasomas into the wood still waited nearby and tried to mate with females when they exited the tree (Fig. 2F, Suppl. material 4).

Host-parasitoid interaction

The adult host beetles were identified as the pleasing fungus beetles, *Encaustes opaca* Crotch, 1876 (Coleoptera, Erotylidae) (Fig. 4A–C) (Crotch 1876; Deelder 1942; Chujo 1968b). Of 12 parasitoid wasp cocoons found, seven were empty and had a

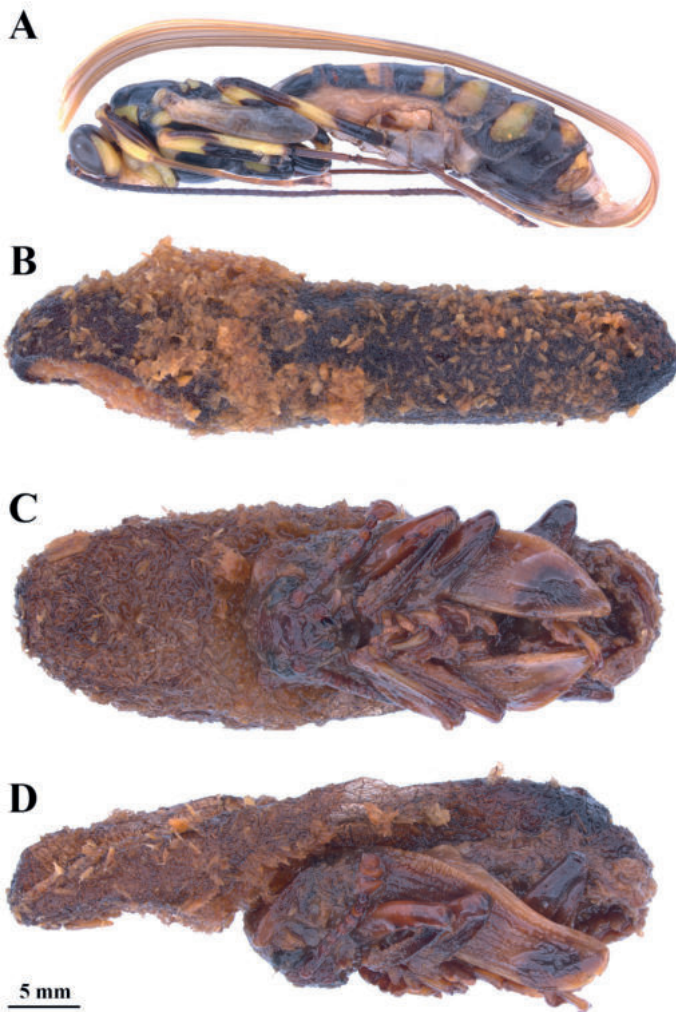


Figure 3. Pupa of female *C. moellerii* (A), empty pupa cocoon of *C. moellerii* with one emergence hole (B), pupa cocoon of *C. moellerii* fused with the teneral stage carcass of *E. opaca*, ventral view (C), lateral view (D).

sub-apical emergence hole (Fig. 3B). The others five cocoons contained living parasitoid pupae. Two of these were opened to allow observation of parasitoid development (Fig. 3A) and three were reared until the wasps (one male and two females) emerged. The captive longevity for the virgin male and two females when fed with 50% honey solution were 14, 16 and 31 days, respectively.

Two *C. moellerii* cocoons were found firmly attached to dried carcasses of a teneral adult of the host beetle (Fig. 3C, D). We concluded that *C. moellerii* is at least facultatively able to develop on teneral adults of *E. opaca*.

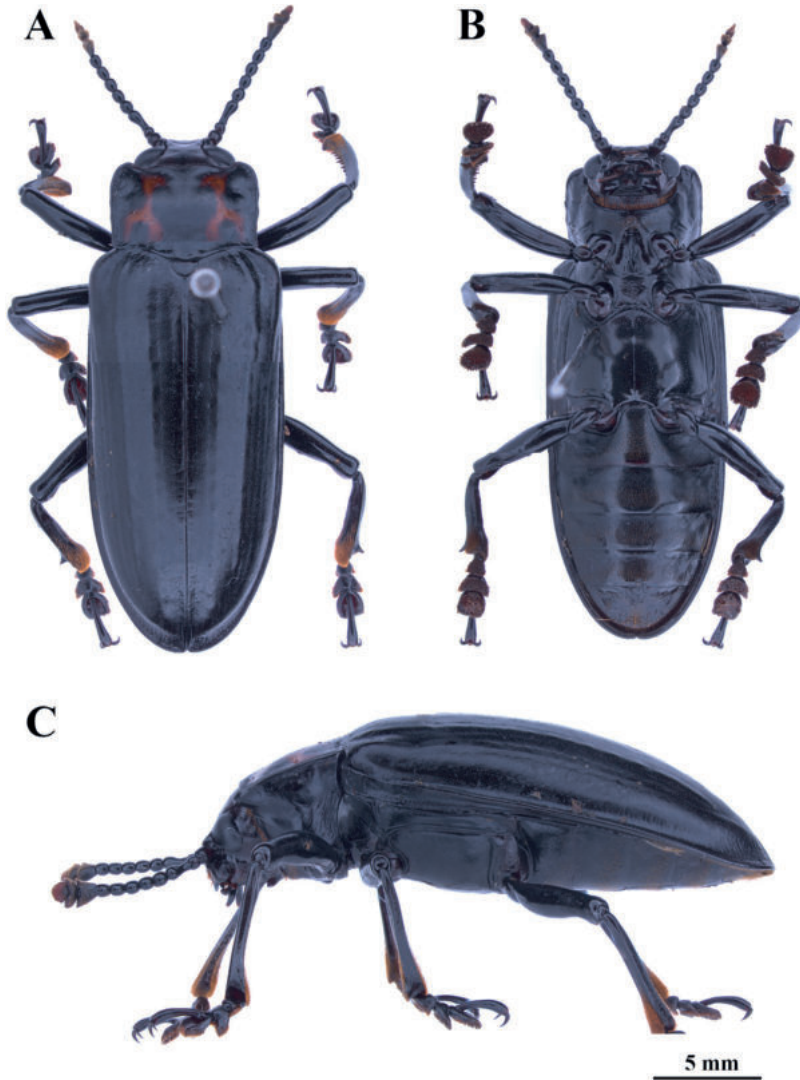


Figure 4. Adult male specimen of *E. opaca* dorsal view(A), ventral view (B), lateral view (C).

Key to species of *Cyrtorhyssa*

- 1 Female 2
- Male 4
- 2 Face yellow with a black longitudinal line; frons with a long tapered ridge that is depressed in the center; fore wing areolet absent; ovipositor sheaths 1.3× length of the body..... ***C. xishuangensis* Wang, 1982**
- Face all yellow; frons with a median carina and with a semicircular groove around ocellar triangle or a shallow furrow on either side; fore wing areolet present; ovipositor sheaths less than 1.3× length of the body..... 3

- 3 Face strongly, transversely striated on its upper 0.6, lower 0.3 coarsely punctate; frons with a median carina and with a semicircular groove around ocellar triangle; clypeus broadly concave at apex; epicnemial carina weakly curved towards anterior edge, about 0.6× height of mesopleuron; propodeum with median longitudinal shallow groove on basal 0.8; fore wing areolet short triangular; abdominal tergites black with broad apical yellow bands; ovipositor sheaths 1.05–1.1× length of the body ***C. moellerii* Bingham, 1898**
- Face strongly transversely striated on its upper 0.3; frons with a shallow furrow on either side; clypeus strongly concave; epicnemial carina less than 0.5 (0.3) × height of mesopleuron, weakly sinuate; propodeum median longitudinal shallow groove present or absent (if present weakly impressed on basal 0.3–0.5); fore wing areolet widely triangular; first to third abdominal tergites reddish, tergite 2 and 3 without any apical yellow bands; ovipositor sheaths 1–1.2× length of the body..... ***C. mesopyrrha* Mocsary, 1905**
- 4 Tubercle on metapleuron well developed; fore wing areolet shortly triangular or absent; fifth tergite without any broad transverse apical yellow band ***C. moellerii* Bingham, 1898**
- Tubercle on metapleuron not so well developed and weak; fore wing areolet present or absent; fifth tergite with a broad transverse apical yellow band ***C. mesopyrrha* Mocsary, 1905**

Redescription of *Cyrtorhyssa moellerii* Bingham, 1898 modified from Kamath and Gupta 1972 (adding male details)

Cyrtorhyssa moellerii

Material examined. Five females, twenty males. THAILAND, Nakhon Ratchasima, Wang Nam Khiao district, Udom Sap subdistrict, Sakaerat Environmental Research Station, dry evergreen forest, 14°29.8'N, 101°54.96'E, 496 m, aerial net, col. K. Chansri (CUMZ) (1♀ 27.i.2021, 1♀ 28.i.2021, 2♀ 15.ii.2021, 1♀ 16.ii.2021, 2♂ 21.i.2021, 2♂ 22.i.2021, 2♂ 23.i.2021, 2♂ 24.i.2021, 1♂ 25.i.2021, 1♂ 27.i.2021, 1♂ 29.i.2021, 5♂ 8.ii.2021, 1♂ 15.ii.2021, 3♂ 25.ii.2021).

Diagnosis. *Cyrtorhyssa moellerii* is clearly different from *C. xishuangensis* in which face with black longitudinal line. In addition, frons of *C. xishuangensis* has a tapered ridge rather than distinct carina, and female fore wing has no areolet. *Cyrtorhyssa moellerii* can be separated from *C. mesopyrrha* because the fore wing areolet of *C. moellerii*, when present, is quite short, whereas the fore wing areolet of female *C. mesopyrrha* is wider (Kamath and Gupta, (1972). The ground colour of tergites 1–3 of female *C. moellerii* is black with yellow bands, while in female *C. mesopyrrha* it is reddish without yellow bands.

Description. Female (Figs 5, 6). Body length, mean = 38.0 mm (range = 36.5–39.0 mm); fore wing length, mean = 27.8 (range = 27.0–28.0 mm); ovipositor sheath length, mean = 40.5 mm (range = 40.0–41.0 mm) (Fig. 5A).

Head. Antenna with 40–41 flagellomeres, terminal flagellomere acuminate; face strongly, transversely striated on its upper 0.6, lower 0.3 coarsely punctate, interspaces 0.5 their diameter, towards orbits punctures finer and sparser; clypeus minutely, finely punctate, broadly concave at apex (Fig. 5B); malar space mat, 0.4× basal width of mandible (Fig. 5C); frons smooth, subpolished with a median carina and with a semi-circular groove around ocellar triangle bordered laterally by fine striations; vertex with a few scattered punctures, smooth and polished; interocellar distance 0.5 ocello-ocular distance; occiput without a median groove dorsally (Fig. 5D). Occipital carina absent medio-dorsally.

Mesosoma. Mesoscutum coarsely transversely scutellum rugose, notauli meeting approximately 0.4 distance from anterior of mesoscutum; scutellum strongly, coarsely punctate; median area of metanotum smooth and polished (Fig. 6A); mesopleuron sparsely punctate, punctures on lower 0.3 separated by 2–3× their diameter, epicnemium with more crowded punctures, interspace 0.5–1.0 their diameter; epicnemial carina weakly curved towards anterior edge, about 0.6 the height of mesopleuron; mesosternum coarsely punctate, punctures sometimes coalescent; metapleuron punctate, interspaces 1–2× their diameter (Fig. 5E); propodeum largely smooth and polished, with very sparse, minute punctures dorsally, dorsolateral corners and lateral sides shallowly punctate, interspace 4–6× their diameter, broadly depressed at extreme base in middle, and medially with a distinct, shallow groove on basal 0.8 (Fig. 6A, C).

Wing. Areolet of fore wing short triangular, lengths of veins 2RS (=2rs-m): 1M: rs-m (= 3rs-m) = 0.6: 0.8: 1.0; vein 2m-cu joining M interstitial with rs-m (= 3rs-m) (Fig. 6B).

Metasoma. First tergite smooth and shiny 2.1× its apical width; second tergite weakly mat at base, with few scattered punctures; third tergite with basal 0.5 distinctly punctate medially, interspace 0.5–1× diameter of punctures, rest smoother (Fig. 6C, E); fourth tergite with basal 0.5 coarsely punctate, elsewhere punctures minute, becoming smoother towards apex with moderately dense, brownish pubescence; basal 0.7 of fifth and following tergites punctate, punctures becoming finer on succeeding segments and with dense brownish pubescence (Fig. 6D, E); ovipositor sheath 2.1× the length of fore wing.

Coloration. Black. Face and clypeus yellow, malar area black; mandibles basally reddish-brown with a yellow macula in middle, teeth black; malar space black; temple yellow; frons with two broad lateral spots touching eye margin, median carina on frons yellow; antenna with scape yellowish in front, flagellum dark brown; occiput largely yellow, dorsally black; pronotum, yellow with black band curving from postero-ventral to anterior margin, and anteriorly pointed mediodorsal mark; mesoscutum black with narrow yellow mark alongside notauli medially; tegula, subtegular tubercle and anterior 0.5 of mesopleuron, and metapleuron with posterior 0.6 including tubercle, yellow; axillae yellow, scutellum, with yellow patch antero-medially; metascutellum black except for small yellow spot medio-dorsally; propodeum yellow except extreme dorsolateral corners, spiracular region and extreme apical margin, black; fore legs yellow ventrally from coxa to tibia, coxa dorsally black; middle leg, coxa black with yellow

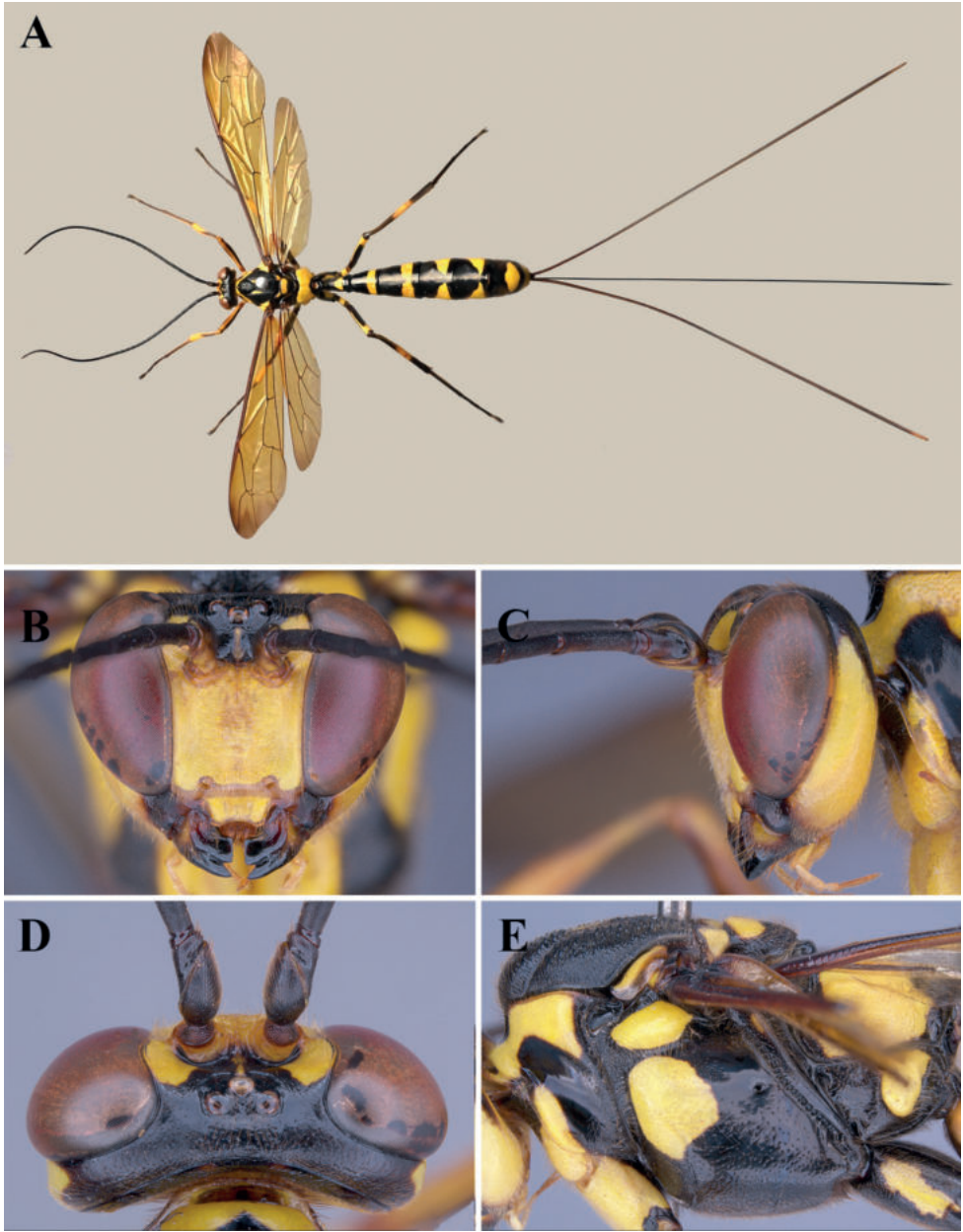


Figure 5. Light micrograph of female *C. moellerii* dorsal view of habitus (A), face (B), lateral view of head (C), dorsal view of head (D), lateral view of mesosoma (E).

low dorsal patch, trochanter black except small dorsal yellow spot, and brownish distal margin, trochantellus black with brownish dorsal part, tibia without apical black, femur black basally, apical 0.3, tibia yellow with dorsal blackish mark on basal 0.5, tarsus black; hind legs as middle leg except trochanter largely yellow, tibia black with medial

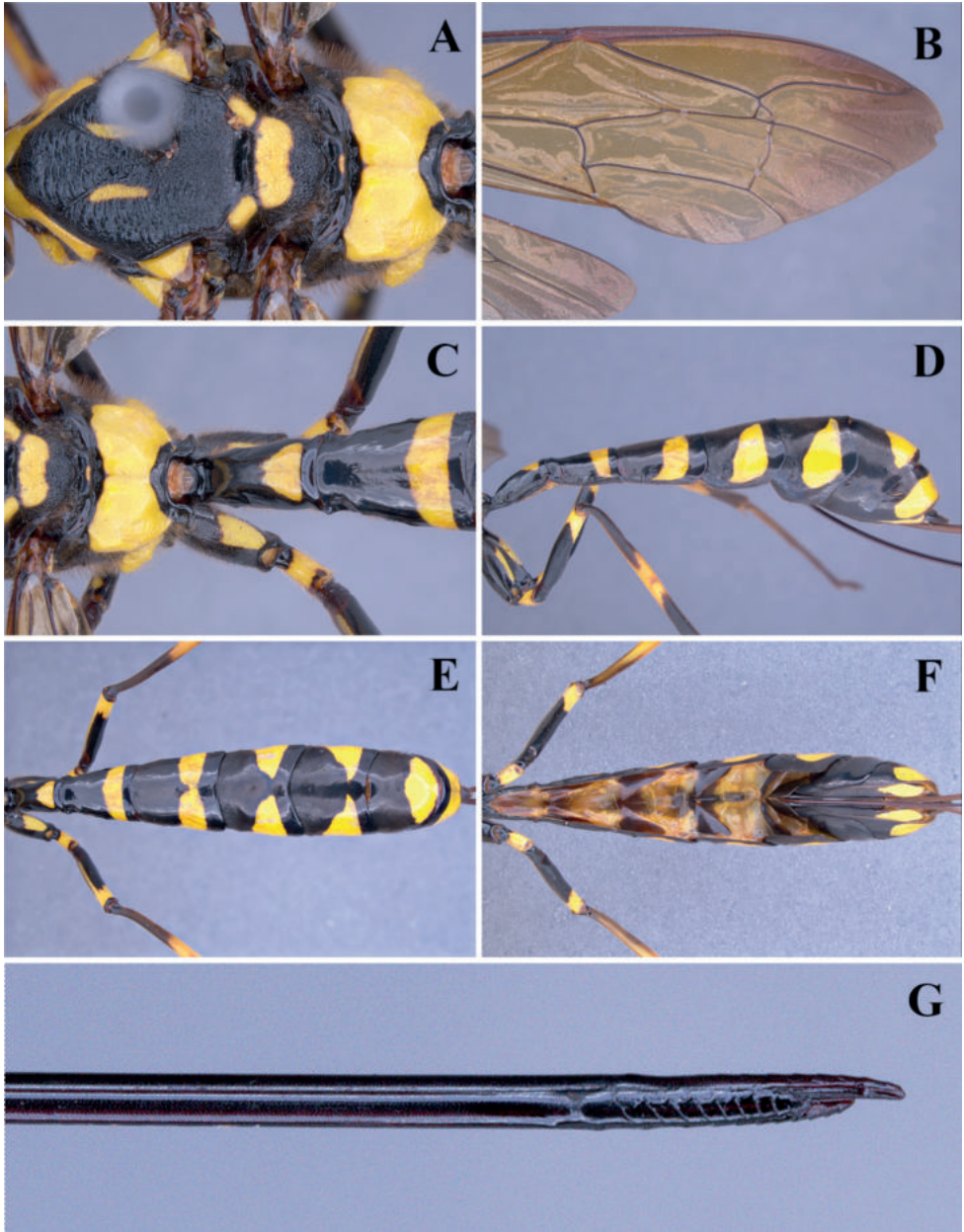


Figure 6. Light micrograph of female *C. moellerii* dorsal view of mesosoma and propodeum (A), fore wing (B), dorsal view of propodeum (C), lateral view of metasoma (D), dorsal view of metasoma (E), ventral view of metasoma (F), lateral view of ovipositor (G).

0.3 brown-yellow around subgenital organ, femur with narrow longitudinal yellow line except basal 0.1; wings yellowish-hyaline with apical margins infuscate; stigma brownish and vein dark brown; metasomal tergites black with the following yellow: tergite

1 subposterior dorsal patch, tergites 2 and three, complete (except laterally) transverse subposterior band, tergites 4 and 5 with large triangular sub posterior patches, tergite 6 large lozenge-shaped postero-dorsal patch, tergite 7 broad yellow posterior transverse band. Ovipositor sheaths black with reddish tinge.

Male (Figs 7, 8). Body length, mean = 23.9 mm (range = 14.0–32.0 mm); fore wing length, mean = 16.8 mm (range = 11.5–24.0 mm) (Fig. 7A).

Head. Antennae with 34–41 flagellomeres, terminal flagellomere acuminate; face strongly transversely striated on its upper 0.8, lower 0.2 coarsely punctate, interspaces 0.5 their diameter, towards orbits punctures finer and sparser; clypeus minutely, finely punctate, broadly concave at apex (Fig. 7B); malar space mat, 0.6× basal width of mandible (Fig. 7D); frons smooth, subpolished with a median carina and with a semi-circular groove around ocellar triangle, vertex with a few scatter punctures, smooth and polished; interocellar distance 0.5× ocello-ocular distance; occiput without a median groove dorsally (Fig. 7C).

Mesosoma. Scutellum strongly, coarsely punctate; median area of metanotum smooth and polished (Fig. 7F); mesopleuron sparsely punctate, punctures on lower 0.3 separated by 2–3× their diameter, epicnemium with more crowded punctures, interspace 0.5–1.0× diameter; epicnemial carina weakly curved towards anterior edge, about 0.5 the height of mesopleuron; mesosternum coarsely punctate, punctures sometime coalescent; metapleuron punctate, interspaces 1–2× their diameter (Fig. 7E); propodeum largely smooth and polished, with very sparse, minute punctures dorsally, dorsolateral corners and lateral sides shallowly punctate, interspace 4–6× their diameter, broadly depressed at extreme base in middle, and medially with a distinct, shallow groove on basal 0.8 (Figs 7E, 8C).

Wing. Areolet of fore wing short triangular, length of veins 2RS (=2rs-m): 1-M: rs-m (=3rs-m) = 0.6: 0.8: 1.0 (Fig. 8A) or absent (Fig. 8B); vein 2m-cu joining M interstitial with rs-m (= 3rs-m).

Metasoma. First tergite smooth and shiny 2.0× its apical width (Fig. 8C); second and third tergites smooth and polished with few scattered punctures; fourth tergite with basal 0.2 coarsely punctate, elsewhere punctures minute, becoming smoother towards apex with moderately dense, brownish pubescence; fifth to seventh third tergites smooth and polished with few scattered punctures with dense brownish pubescence (Fig. 8D, E).

Coloration. Yellow. Mandibles basally with brownish and with a yellow macula in middle, teeth black; malar space brownish-yellow; frons with two broad lateral spots touching eye margin, antenna with scape yellowish in front, flagellum dark brown; occiput dorsally brownish; pronotum, yellow with a curved incomplete black band dorsally and with a reddish-brown stripe in centre; median and lateral lobe of mesoscutum reddish-brown, posterior of merging notauli extending into a black midlongitudinal stripe; scutellum largely dull yellow with posterior 0.2 of piceous; median area of metanotum yellow; tegula, epicnemium, posterior transverse carina of mesosternum, juxtacoxal carina black; propodeum yellow except extreme dorsolateral base, spiracular region and extreme apical margin black; Legs yellow with tarsi gradually infuscate towards apex except: fore femur ventrally brown; fore tibia narrowly brown dorsally on

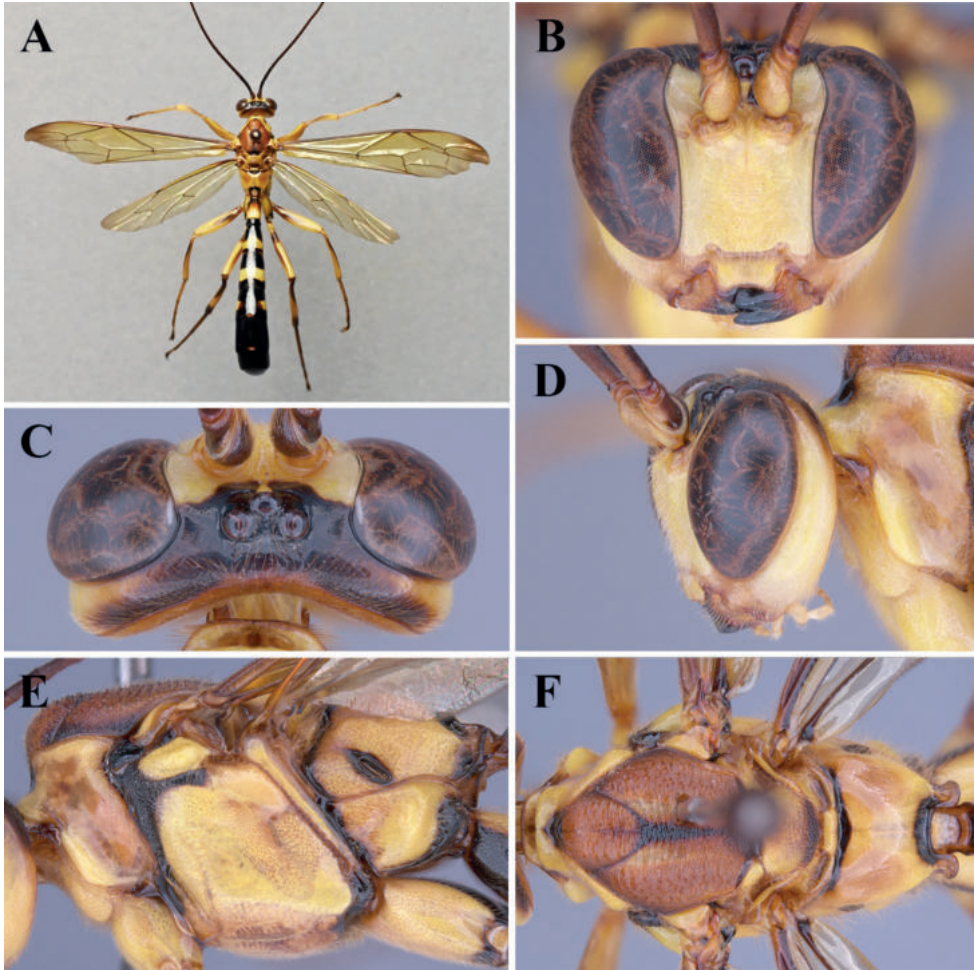


Figure 7. Light micrograph of male *C. moellerii* dorsal view of habitus (A), face (B), dorsal view of head (C), lateral view of head (D), lateral view of mesosoma (E), dorsal view of mesosoma and propodeum (F).

basal 0.7, fore; middle leg similar to fore leg except dark mark on femur on medial side; hind coxa ventrally black, hind femur brown-black basally and medioventrally, hind tibia dorsally with basal 0.5 and distal 0.2 posteriorly dark brown; wing yellowish-hyaline with apical margin infuscate, stigma brownish and vein dark brown; metasomal tergites black with yellow marks as follows: tergite 1 with large, sub-posterior yellow patch, tergites 2 and 3 with broad sub-posterior yellow bands, tergite 4 with yellow patches mediolaterally.

Comment. Male and female of the *C. moellerii* display sexual dimorphism with different colour patterns. Fore wing areolet of female always present according to the keys to species of this genus by Kamath and Gupta, (1972) (Fig. 6B), however, male of *C. moellerii* shows variation of fore wing areolet, either present or absent (Fig. 8A, B) same as male *C. mesopyrrha* (Kamath and Gupta 1972).

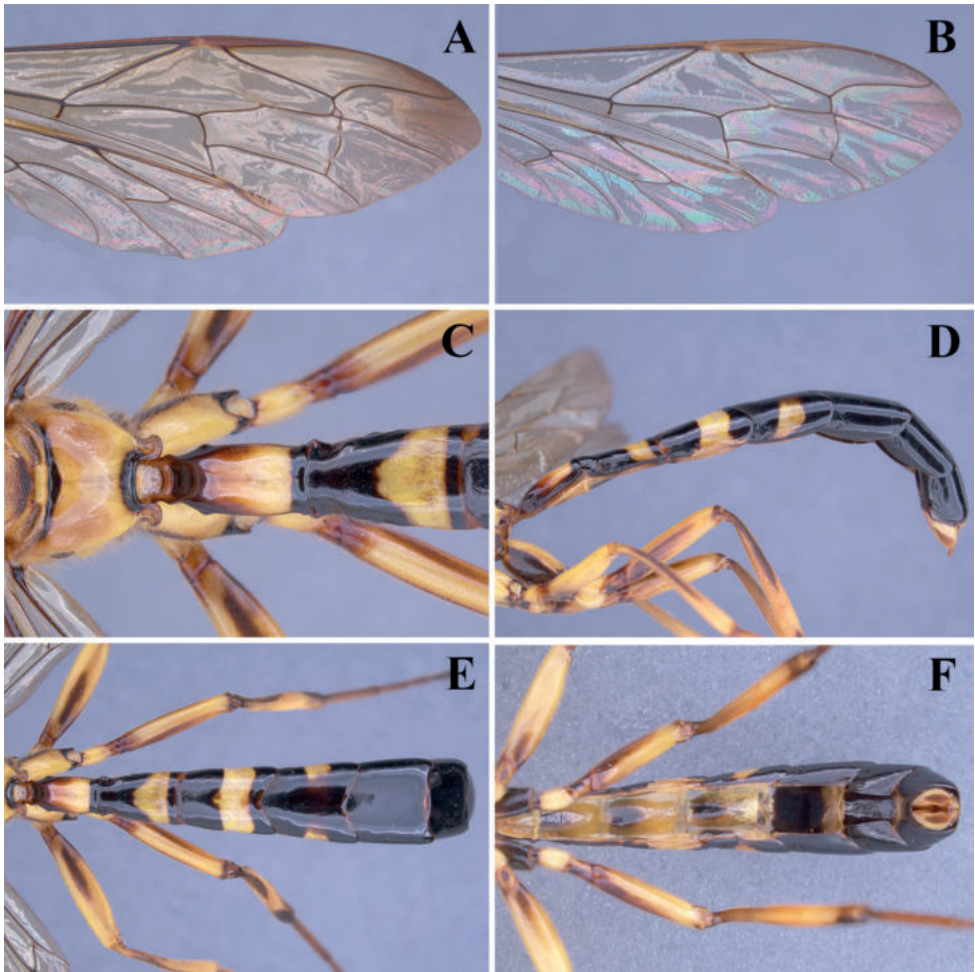


Figure 8. Light micrograph of male *C. moellerii* fore wing areolet present morph (A), fore wing areolet absent morph (B), dorsal view of propodeum (C), lateral view of metasoma (D), dorsal view of metasoma (E), ventral view of metasoma (F).

Phylogenetic analyses

A preliminary molecular phylogeny based on the available DNA barcodes of the rhyssines is shown in Fig. 9. *Cyrtorhyssa* was recovered as sister group to *Myllenyxis* but with low bootstrap support (37%), and the two together as derived from within *Epirhyssa*, with 75% support.

The ML phylogeny including the new sequence from the host *Encaustes opaca* with other available erotyloid sequences is shown in Fig. 10. Dacninae, Eucaustinae, Megalodacninae and Trominae+Erotylinae were each recovered as monophyletic with strong bootstrap support (84–100%). *Encaustes opaca* was recovered in a polytomy with the only other represented congener *Encaustes cruenta formosama*, and the genus *Aulacochilus*, the only other member of Eucaustinae included represented by two species (Fig. 10).

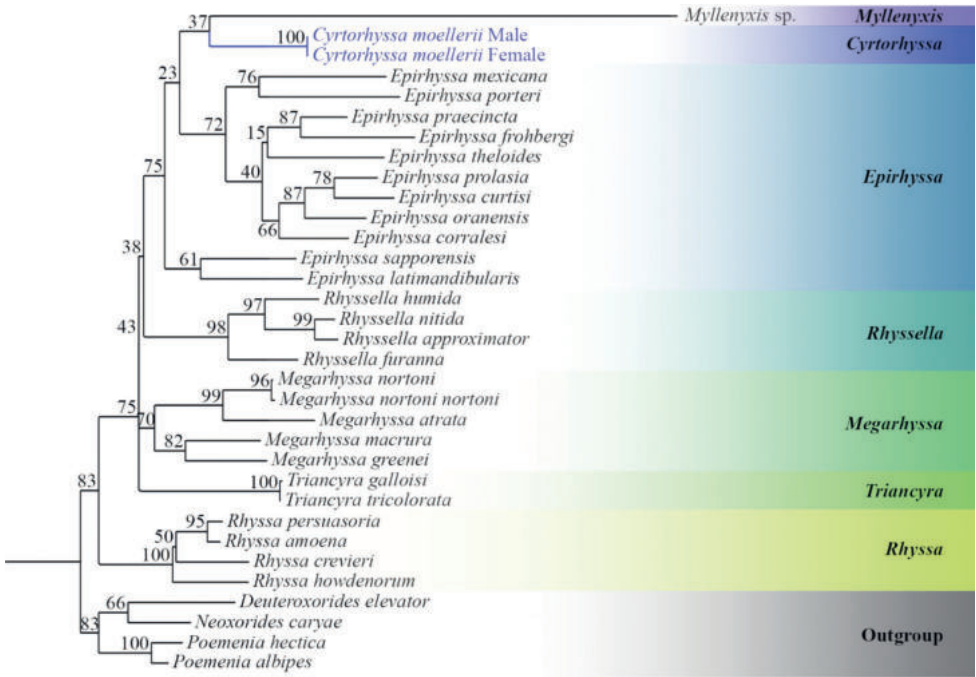


Figure 9. Maximum likelihood tree of *C. moellerii* and other rhyssine wasps based on the barcoding region of cytochrome oxidase subunit 1 (COI) with RaxML rapid bootstrap support values.

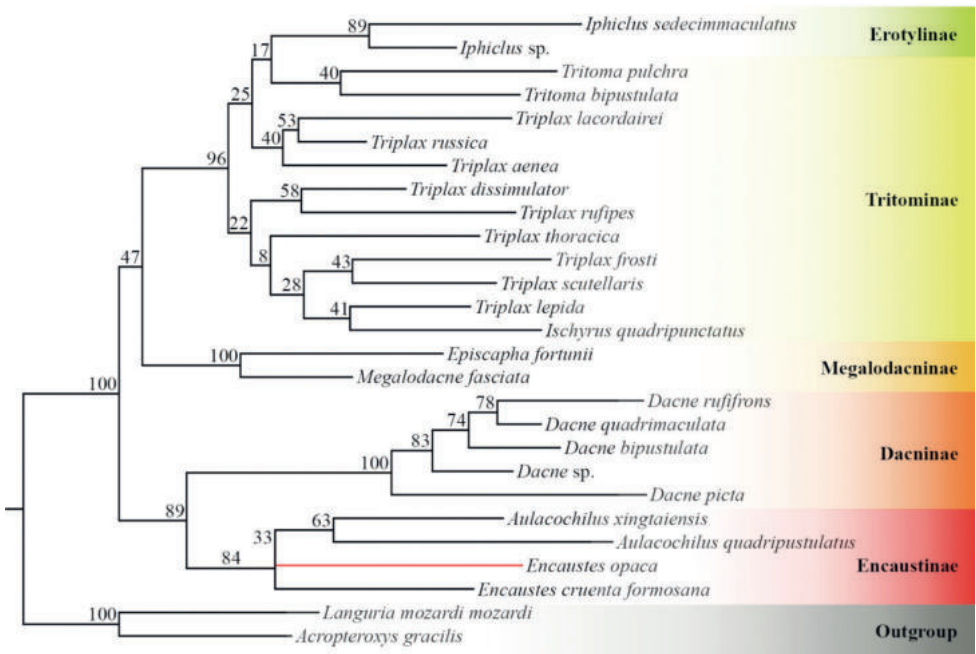


Figure 10. Maximum likelihood tree of *E. opaca* (Encaustinae) and other erotyloid beetles based on the barcoding region of cytochrome oxidase subunit 1 (COI) with RaxML rapid bootstrap support values.

Discussion

The protandry observed in *C. moellerii* is similar to what is known for other rhyssine wasps. Most males were observed aggregating in the area where a female was about to emerge (Baker 1992; Eggleton 1991). Tergal stroking behaviour has previously been reported for the males of the genus *Megarhyssa* (Matthews et al. 1979) and here we report it for the first time in *Cyrtorhyssa*. Male rhyssines that have long slender metasomas, e.g. *Megarhyssa rixator* (Schellenberg, 1802), are able to insert their abdomens into the female emergence tunnel for mating (Quicke 2015). However, males of *C. moellerii* are not so slender. Further, in *C. moellerii* only the larger males have a sufficiently long metasoma that can be inserted into the emergence tunnel to achieve copulation. The observed adult lifespan of *C. moellerii* is comparable to that reported for *Megarhyssa* spp. which can live at least 27 days (Heatwole and Davis 1965).

Our molecular study is the first to include a substantial number of representative rhyssines since Klopstein et al. (2019), which included representatives of only three genera. In agreement with that study, we recovered *Rhyssa* as sister group to the remaining included genera (Fig. 9). We recovered *Cyrtorhyssa* and *Myllenyxis* as sister groups nested within *Epirhyssa*, however, additional molecular data would be needed before any conclusions can be drawn about possible non-monophyly of the latter. Both are endemic Asian genera, being known from in India, southern China and both mainland and island of Southeast Asia (Kamath and Gupta 1972; Wang 1972). In contrast, the genera *Epirhyssa* and *Megarhyssa* have considerably more cosmopolitan distributions. *Myllenyxis* is the only genus of Rhyssinae that has the upper tooth of the mandible subdivided thus appearing tridentate. Moreover, fore wing areolet is always present in *Megarhyssa* and *Rhyssella* and always absent in *Epirhyssa*, but some variation in this character is found in males of *C. moellerii* and *C. mesopyrrha*.

The host genus *Encaustes* is widespread in the Old-World tropics and subtropics being reported from Africa, South Asia, East Asia, Southeast Asia to Australia (Chujo 1968a; Chujo 1968b; Chujo 1969; Chujo 1973; Chujo and Chujo 1987; Chujo and Chujo 1988; Chujo et al. 1993). Its distribution completely overlaps that of *Cyrtorhyssa*. Only two species of *Encaustes* have been recorded in Thailand previously, *E. cruenta montana* Schenkling, 1919 and *E. opaca* Crotch, 1876, both from Chiang Mai province in 1957 (Chujo 1968b; Chujo and Chujo 1988). The relationships between the subfamilies of Erotylidae recovered here using just COI (Fig. 10) are essentially identical to those obtained by Robertson (2004) using combined 16S and 28S data.

Acknowledgements

We are grateful to Mr Surachit Waengsothorn for providing facilities at the Sakaerat Environmental Research Station; Samai Sewakhonburi and Arthit Janthadee for identification of the tree; Sakaerat bird team for collecting insect specimens; and Dr Michael Geiser, The Natural History Museum (London) for confirming identification of the beetle. We also thank Shen-Horn Yen (National Sun Yat-sen University, Taiwan) and Zhipang

Huang (Insitute of Eastern-Himalaya Biodiversity Research) for help with literature. This research was funded by National Research Council of Thailand (NRCT) (N42A650262) and Chulalongkorn University, RSPG-Chula to BAB; DLJQ was supported by Rachadaphiseksomphot Fund, Graduate School, Chulalongkorn University; KC was supported by CU Graduate School Thesis Grant (GCUGR1225641025D), the Overseas Research Experience Scholarship for Graduate Student from CU Graduate School and Faculty of Science; and The Second Century Fund (C2F), Chulalongkorn University.

References

- Baker BR (1992) Emergence and pairing of *Rhyssa persuasoria* L. (Hymenoptera: Ichneumonidae). *British Journal of Entomology and Natural History* 5: 184–185.
- Bennett AMR, Cardinal S, Gauld ID, Wahl DB (2019) Phylogeny of the subfamilies of Ichneumonidae (Hymenoptera). *Journal of Hymenoptera Research* 71: 1–156. <https://doi.org/10.3897/jhr.71.32375>
- Bocak L, Barton C, Crampton-Platt ALEX, Chesters D, Ahrens D, Vogler AP (2014) Building the Coleoptera tree-of-life for > 8000 species: composition of public DNA data and fit with Linnaean classification. *Systematic Entomology* 39: 97–110. <https://doi.org/10.1111/syen.12037>
- Broad G, Shaw M, Fitton M (2018) *The Ichneumonid Wasps of Britain and Ireland* (Hymenoptera: Ichneumonidae). Royal Entomological Society, Telford.
- Cao LM, Achterberg CV, Tang YL, Wang XY, Yang ZQ (2020) Revision of parasitoids of *Massicus raddei* (Blessig Solsky) (Coleoptera, Cerambycidae) in China, with one new species and genus. *Zootaxa* 4881: 104–130. <https://doi.org/10.11646/zootaxa.4881.1.7>
- Chujo M (1968a) Erotylid beetles from south-China, Hainan, Taiwan and the Ryukyus. *Studies on the erotyloid beetles* (20). *Pacific Insects* 10: 539–550.
- Chujo M (1968b) Erotylid beetles from Thailand, Laos and Viet-Nam. *Studies on the erotyloid beetles* (21). *Pacific Insects* 10: 551–573.
- Chujo M (1969) Erotylidae (Insecta: Coleoptera). *Fauna Japonica, Insecta Coleoptera Erotylidae*. Academic Press of Japan, Tokyo.
- Chujo M (1973) Coleoptera: Erotylidae and Languriidae from Ceylon. *Entomologica Scandinavica. Supplementum* 4: 195–198.
- Chujo M, Chujo M (1987) Erotylidae from New Guinea and her adjacent islands I (Coleoptera). *Esakia* 25: 5–36. <https://doi.org/10.5109/2492>
- Chujo M, Chujo M (1988) A catalog of the Erotylidae (Insecta, Coleoptera) from the Old World (excl. the Ethiopian Region). *Esakia* 26: 139–185. <https://doi.org/10.5109/2510>
- Chujo M, Chujo M, Lee CE (1993) Erotylidae from Korea (Insecta, Coleoptera). *Esakia* 33: 99–108. <https://doi.org/10.5109/2567>
- Cline AR, Smith TR, Miller K, Moulton M, Whiting M, Audisio P (2014) Molecular phylogeny of Nitidulidae: assessment of subfamilial and tribal classification and formalization of the family Cybocephalidae (Coleoptera: Cucujoidea). *Systematic Entomology* 39: 758–772. <https://doi.org/10.1111/syen.12084>

- Couturier A (1949) Observations sur *Rhyssa approximator* F. cleptoparasite de *Rh. persuasoria* L. (Hym. Ichneumonidae). Bulletin de la Société Entomologique de France 54: 62–63. <https://doi.org/10.3406/bsef.1949.18366>
- Crotch GR (1876) A revision of the coleopterous family Erotylidae. Cistula Entomologica [1869–1876]: 359–572.
- Deelder CL (1942) Revision of the Erotylidae (Coleoptera) of the Leiden Museum. Zoologische Mededelingen 24: 49–115.
- DeWaard JR, Ratnasingham S, Zakharov EV, Borisenko AV, Steinke D, Telfer AC, Perez KH, Sones JE, Young MR, Levesque-Beaudin V, Sobel CN (2019) A reference library for Canadian invertebrates with 1.5 million barcodes, voucher specimens, and DNA samples. Scientific data 6: 1–12. <https://doi.org/10.1038/s41597-019-0320-2>
- Eagalle T (2014) Latitudinal Effects on Diversity and Body Size: A Case Study with Parasitoid and Parasitic Wasps. Unpublished Ph.D. thesis, University of Guelph.
- Eggleton P (1991) Patterns in male mating strategies of the Rhyssini: a holophyletic group of parasitoid wasps (Hymenoptera: Ichneumonidae). Animal Behaviour 41: 829–838. [https://doi.org/10.1016/S0003-3472\(05\)80350-1](https://doi.org/10.1016/S0003-3472(05)80350-1)
- Hanson HS (1939) Ecological notes on *Sirex* wood wasps and their parasites. Bulletin of Entomological Research 30: 27–65. <https://doi.org/10.1017/S0007485300004399>
- Heatwole H, Davis DM (1965) Ecology of three sympatric species of parasitic insects of the genus *Megarhyssa* (Hymenoptera: Ichneumonidae). Ecology 46: 140–150. <https://doi.org/10.2307/1935265>
- Hebert PDN, Cywinska A, Ball SL, DeWaard JR (2003) Barcoding animal life: cytochrome c oxidase subunit I divergences among closely related species. Proceedings of the Royal Society of London, Series B: Biological Science 270(suppl_1): S96–S99. <https://doi.org/10.1098/rsbl.2003.0025>
- Hebert PDN, Ratnasingham S, Zakharov EV, Telfer AC, Levesque-Beaudin V, Milton MA, Pedersen S, Jannetta P, DeWaard JR (2016) Counting animal species with DNA barcodes: Canadian insects. Philosophical Transactions of the Royal Society B: Biological Sciences 371: e20150333. <https://doi.org/10.1098/rstb.2015.0333>
- Kamath MK, Gupta VK (1972) Ichneumonologia Orientalis, Part II. The Tribe Rhyssini (Hymenoptera: Ichneumonidae). Oriental Insects Monographs 2: 1–300.
- Klopfstein S, Langille B, Spasojevic T, Broad GR, Cooper SJ, Austin AD, Niehuis O (2019) Hybrid capture data unravel a rapid radiation of pimpliform parasitoid wasps (Hymenoptera: Ichneumonidae: Pimpliformes). Systematic Entomology 44: 361–383. <https://doi.org/10.1111/syen.12333>
- Matthews RW, Matthews JR, Crankshaw O (1979) Aggregation in male parasitic wasps of the genus *Megarhyssa*: I. Sexual discrimination, tergal stroking behavior, and description of associated anal structures. The Florida Entomologist 62: 3–8. <https://doi.org/10.2307/3494037>
- National Center for Biotechnology Information [NCBI] (2023) [Internet]. Bethesda (MD): National Library of Medicine (US), National Center for Biotechnology Information; [1988] – [cited 2023 Sep 14]. <https://www.ncbi.nlm.nih.gov/>

- Park DS, Suh SJ, Oh HW, Hebert PDN (2010) Recovery of the mitochondrial COI barcode region in diverse Hexapoda through tRNA-based primers. *BMC Genomics* 11: 1–7. <https://doi.org/10.1186/1471-2164-11-423>
- Pentinsaari M, Hebert PDN, Mutanen M (2014) Barcoding beetles: a regional survey of 1872 species reveals high identification success and unusually deep interspecific divergences. *PLoS ONE* 9: e108651. <https://doi.org/10.1371/journal.pone.0108651>
- Porter CC (1978) A revision of the genus *Epirhyssa* (Hymenoptera: Ichneumonidae). *Studia Entomologica* 20: 297–411.
- Quicke DLJ (2015) *The Braconid and Ichneumonid Parasitic Wasps: Biology, Systematics, Evolution and Ecology*. Wiley Blackwell, Chichester, 681 pp. <https://doi.org/10.1002/9781118907085>
- Quicke DLJ, Laurence NM, Fitton, MG Broad GR (2009) A thousand and one wasps: a 28S rDNA and morphological phylogeny of the Ichneumonidae (Insecta: Hymenoptera) with an investigation into alignment parameter space and elision. *Journal of Natural History* 43: 1305–1421. <https://doi.org/10.1080/00222930902807783>
- Quicke DLJ, Smith MA, Janzen DH, Hallwachs W, Fernandez-Triana J, Laurence NM, Zaldivar-Riveron A, Shaw MR, Broad GR, Klopstein S, Shaw SR, Hrccek J, Hebert PD, Miller SE, Rodriguez JJ, Whitfield JB, Sharkey MJ, Sharanowski BJ, Jussila R, Gauld ID, Chesters D, Vogler AP (2012) Utility of the DNA barcoding gene fragment for parasitic wasp phylogeny (Hymenoptera: Ichneumonoidea): data release and new measure of taxonomic congruence. *Molecular Ecology Resources* 12: 676–685. <https://doi.org/10.1111/j.1755-0998.2012.03143.x>
- Robertson JA, McHugh JV, Whiting MF (2004) A molecular phylogenetic analysis of the pleasing fungus beetles (Coleoptera: Erotylidae): evolution of colour patterns, gregariousness and mycophagy. *Systematic Entomology* 29: 173–187. <https://doi.org/10.1111/j.0307-6970.2004.00242.x>
- Roslin T, Somervuo P, Pentinsaari M, Hebert PD, Agda J, Ahlroth P, Anttonen P, Aspi J, Blagoev G, Blanco S, Chan D 2022. A molecular-based identification resource for the arthropods of Finland. *Molecular Ecology Resources* 22: 803–822. <https://doi.org/10.1111/1755-0998.13510>
- Sharkey MJ, Wharton RA (1997) Morphology and terminology. In: Wharton RA, Marsh PM, Sharkey MJ (Eds) *Identification manual to the New World genera of Braconidae*. Special Publication of the International Society of Hymenopterists 1: 19–37.
- Sheng ML, Sun SP (2010) *Parasitic Ichneumonids on Woodborers in China* (Hymenoptera: Ichneumonidae). Science Press, Beijing, 338 pp. [in Chinese with English summary]
- Sikes DS, Bowser M, Morton JM, Bickford C, Meierotto S, Hildebrandt K (2017) Building a DNA barcode library of Alaska's non-marine arthropods. *Genome* 60: 248–259. <https://doi.org/10.1139/gen-2015-0203>
- Sire L, Gey D, Debruyne R, Noblecourt T, Soldati F, Barnouin T, Parmain G, Bouget C, Lopez-Vaamonde C, Rougerie R (2019) The challenge of DNA barcoding saproxylic beetles in natural history collections—exploring the potential of parallel multiplex sequencing with Illumina MiSeq. *Frontiers in Ecology and Evolution* 7: e495. <https://doi.org/10.3389/fevo.2019.00495>

- Spasojevic T, Broad GR, Sääksjärvi IE, Schwarz M, Ito M, Korenko S, Klopstein S (2021) Mind the outgroup and bare branches in total-evidence dating: a case study of pimpliform Darwin wasps (Hymenoptera, Ichneumonidae). *Systematic Biology* 70: 322–339. <https://doi.org/10.1093/sysbio/syaa079>
- Stamatakis A (2006) RAxML-VI-HPC: Maximum likelihood-based phylogenetic analyses with thousands of taxa and mixed models. *Bioinformatics* 22: 2688–2690. <https://doi.org/10.1093/bioinformatics/btl446>
- Telfer AC, Young MR, Quinn J, Perez K, Sobel CN, Sones JE, Levesque-Beaudin V, Derbyshire R, Fernandez-Triana J, Rougerie R, Thevanayagam A (2015) Biodiversity inventories in high gear: DNA barcoding facilitates a rapid biotic survey of a temperate nature reserve. *Biodiversity Data Journal* 3: e6313. <https://doi.org/10.3897/BDJ.3.e6313>
- Wang SF (1982) A new species of the genus *Cyrtorhyssa* (Ichneumonidae: Ephialtinae). *Sinozoologia* 2: 59–60. [in Chinese with English summary]

Supplementary material 1

Video Online Resource 1

Authors: Kittipum Chansri, Kanoktip Somsiri, Donald L. J. Quicke, Buntika A. Butcher

Data type: mp4

Explanation note: Tergal stroking behaviour of male *Cyrtorhyssa moellerii*.

Copyright notice: This dataset is made available under the Open Database License (<http://opendatacommons.org/licenses/odbl/1.0/>). The Open Database License (ODbL) is a license agreement intended to allow users to freely share, modify, and use this Dataset while maintaining this same freedom for others, provided that the original source and author(s) are credited.

Link: <https://doi.org/10.3897/jhr.96.107196.suppl1>

Supplementary material 2

Video Online Resource 3

Authors: Kittipum Chansri, Kanoktip Somsiri, Donald L. J. Quicke, Buntika A. Butcher

Data type: mp4

Explanation note: Aggressive guarding behaviour of male *Cyrtorhyssa moellerii*.

Copyright notice: This dataset is made available under the Open Database License (<http://opendatacommons.org/licenses/odbl/1.0/>). The Open Database License (ODbL) is a license agreement intended to allow users to freely share, modify, and use this Dataset while maintaining this same freedom for others, provided that the original source and author(s) are credited.

Link: <https://doi.org/10.3897/jhr.96.107196.suppl2>

Supplementary material 3

Video Online Resource 2

Authors: Kittipum Chansri, Kanoktip Somsiri, Donald L. J. Quicke, Buntika A. Butcher

Data type: mp4

Explanation note: Mating behaviour of male *Cyrtorhysa moellerii*.

Copyright notice: This dataset is made available under the Open Database License (<http://opendatacommons.org/licenses/odbl/1.0/>). The Open Database License (ODbL) is a license agreement intended to allow users to freely share, modify, and use this Dataset while maintaining this same freedom for others, provided that the original source and author(s) are credited.

Link: <https://doi.org/10.3897/jhr.96.107196.suppl3>

Supplementary material 4

Video Online Resource 4

Authors: Kittipum Chansri, Kanoktip Somsiri, Donald L. J. Quicke, Buntika A. Butcher

Data type: mp4

Explanation note: Emergence of female *Cyrtorhysa moellerii*.

Copyright notice: This dataset is made available under the Open Database License (<http://opendatacommons.org/licenses/odbl/1.0/>). The Open Database License (ODbL) is a license agreement intended to allow users to freely share, modify, and use this Dataset while maintaining this same freedom for others, provided that the original source and author(s) are credited.

Link: <https://doi.org/10.3897/jhr.96.107196.suppl4>

New suggestion of the species group reconstruction of genus *Nomada* Scopoli, 1770 (Hymenoptera, Apidae) from Korea

Kayun Lim^{1,2}, Seunghwan Lee^{2,3}

1 Utah State University, Department of Biology, 5305 Old Main Hill, Logan, UT 84322-5305, USA **2** Insect Biosystematics Laboratory, Research Institute for Agriculture and Life Sciences, Seoul National University, Seoul 151-921, Republic of Korea **3** Department of Agricultural Biotechnology, Seoul National University, Seoul 151-921, Republic of Korea

Corresponding author: Seunghwan Lee (seung@snu.ac.kr)

Academic editor: Michael Ohl | Received 16 May 2023 | Accepted 5 October 2023 | Published 13 October 2023

<https://zoobank.org/DEFCAACD-E148-4CD6-8B29-24CE995C9D79>

Citation: Lim K, Lee S (2023) New suggestion of the species group reconstruction of genus *Nomada* Scopoli, 1770 (Hymenoptera, Apidae) from Korea. Journal of Hymenoptera Research 96: 805–816. <https://doi.org/10.3897/jhr.96.106452>

Abstract

Genus *Nomada*, which includes approximately 800 species, is the largest genus in the subfamily Nomadinae and the sole genus in the tribe Nomadini. Its taxonomic classification is particularly challenging due to high morphological variations, making it one of the most controversial groups in the subfamily. In order to shed light on the complex classification of *Nomada* species and their tribal position, this study conducted a multi-locus phylogeny using one mitochondrial gene (COI) and five nuclear protein-coding genes (EF1 α , Nak, Opsin, Pol II, Wingless). The study focused on expanding the knowledge of some East Palearctic species, with the ultimate goal of reviewing species groups of *Nomada* present in Korea. In this study, we suggest that the *ruficornis* species group is polyphyletic. Some species should be moved to more appropriate species groups as follows: *N. tsunekiana*, *N. emarginata*, and *N. flavopicta* into the *basalis* species group; *N. asvensis*, *N. kaguya*, and *N. taicho* into the *armata* species group.

Keywords

Bees, Cleptoparasite, *Nomada*, Nomadinae, Molecular phylogeny, Multi-locus

Introduction

Nomada, the only genus in the tribe Nomadini and the largest genus in the subfamily Nomadinae, is composed of around 800 species (Smit 2018). This genus has a predominantly Holarctic distribution in all continents except Antarctica (Alexander 1994). Due to the high morphological diversity exhibited by this genus, its classification into subgroups has been a contentious issue, particularly at the species level, where identification is challenging. For example, the genus has been divided into various subgenera or even designated as new genera by Nearctic taxonomists, while most Palearctic taxonomists have insisted on the species group concept (Snelling 1986; Alexander 1994). Thereafter, Alexander (1994) reconstructed the genus using the species group concept in *Nomada* which are *adducta*, *armata*, *basalis*, *belfragei*, *bifasciata*, *erigeronis*, *furva*, *gigas*, *integra*, *odontophora*, *roberjeotiana*, *ruficornis*, *superba*, *trispinosa*, *vegana*, and *vincta*. Of these, the *ruficornis* species group, which is the largest among the 16 established groups, may be a paraphyletic group due to the lack of apomorphic characters (Alexander 1994). Moreover, he designated *Nomada ruficornis* Linnaeus as the type species of the *ruficornis* species group, but *N. ruficornis* has an apomorphic character that cannot be a common trait to the species group. For instance, the type species has a bifurcated mandible, while most species in the species group have a simple one. As such, the species that belong to the *ruficornis* species group are more like the remnants of the species that cannot be merged into the other species group (Mitai and Tadauchi 2007).

Nomada species from Korea have been classified into species groups primarily based on the work of Mitai and Tadauchi (Mitai and Tadauchi 2003, 2004, 2005, 2006, 2007, 2008), with an update by Won and Kim (Won and Kim 2013). Initially, molecular phylogenetics using a COI marker was employed by Won to resolve the species group complex of the *Nomada* in his Ph.D. dissertation (Won 2006). However, as the number of recorded species within Korea has increased and with improvements in molecular phylogenetics, further research is necessary to expand upon the previous study, which was limited in scope by analyzing 12 species and using a single marker.

Recently, with the advancement of phylogenomics and the use of ultra-conserved elements (UCEs), Sless et al. (2022) provided the new classification of the subfamily Nomadinae using UCE and Odanaka et al. (2022) showed paraphyly of *ruficornis* species group. On the other hand, Lim et al. (2022) noted that with variations in taxon sampling, the *ruficornis* species group is polyphyletic. However, the taxon sampling of the study was mainly focused on the species that have host information. In this study, the species group concept validity of the genus *Nomada* proposed by Alexander (1994) was tested using the molecular phylogenetic approach with an increased sampling of the *ruficornis* species group from Korea, which is currently subject to incomplete and controversial systematic classifications.

Methods

Taxon sampling

For this study, we included 74 species as an ingroup and selected 6 species from Ammobatoidini, Neolarrini, and Hexepeolini as an outgroup (See Suppl. material 1). Outgroup species were chosen due to its close relationship with *Nomada* based on Sless et al. (2022) and availability in NCBI database. To clarify the validity of the species group concept by Alexander (1994), we included *Nomada ruficornis*, *N. roberjeotiana*, *N. bifasciata*, *N. armata*, *N. furva*, as they represent the type species of various species groups. In total, sampling in this study encompasses 8 species groups out of the 16 species groups. We added 44 more *Nomada* species from Lim et al. (2022), out of which 17 species were newly sequenced for this study, and the remaining sequences were obtained from NCBI (Suppl. material 1).

DNA extraction, PCR amplification, and sequencing

To extract total genomic DNA, we ground up either the detached midleg, head of the alcohol vouchers or dried specimens. The wet lab work protocol was consistent with the supplementary information 3 from Lim et al. (2022). We utilized one mitochondrial protein-coding gene, namely the cytochrome oxidase subunit I gene (COI), and five nuclear protein-coding genes (EF-1 α , long-wavelength rhodopsin (opsin), NaK, pol II, and wingless) to maintain consistency with Lim et al. (2022). All DNA vouchers were deposited in the Insect Biosystematics Laboratory at Seoul National University.

Sequencing alignments

We utilized SeqMan Pro version 7.1.0 (DNASTAR, Inc., Madison, WI, U.S.A.) to assemble, check, and trim the raw sequence data. The sequence alignment of all six genes was conducted using MAFFT version 7 (<https://mafft.cbrc.jp/alignment/server/>), and the sequences were adjusted in Mega 7 with the amino acid translation option. In cases where the length of certain genes differed between the NCBI data and the newly obtained sequences, longer sequences were removed. Finally, the aligned sequences were combined using SequenceMatrix Windows ver. 1.8 (Vaidya et al. 2011).

Phylogenetic analyses

We conducted phylogenetic analyses using two methods, Bayesian inference (BI) and Maximum likelihood (ML). Different potential partitioning schemes, considering codon position and genes, and nucleotide substitution models were assessed using ModelFinder2 (Kalyaanamoorthy et al. 2017) within IQ-TREE 2.2.3 (Minh et al. 2020) using “TEST-

NEWMERGE” option. Following the implementation of the most suitable partitioning scheme and substitution models, IQ-TREE2 generated a ML tree, and nodal supports were determined through 1000 ultrafast bootstrap replicates (Hoang et al. 2018).

On the other hand, because some models, such as TIM, TNe, TN models, were not applicable in MrBayes 3.2.7 for BI (Ronquist et al. 2012), we excluded the unavailable models in MrBayes by using the “-mset” option to restrict the testing procedure with the “TESTMERGEONLY” (See Suppl. material 2). To conduct the MrBayes analysis, we ran 20 million Markov chain Monte Carlo (MCMC) generations, and trees were sampled every 100 generations. We executed one cold chain and three heated chains for each MCMC analysis. We examined the outcome with Tracer 1.7.1 (Rambaut et al. 2018) and discarded the first 2,500,000 sampled trees as burned in.

Results

The dataset used for the phylogenetic reconstruction contained 660 bp of COI, 442 bp of *ef1a*, 870 bp of *Nak*, 459 bp of *Opsin*, 840 bp of *Pol2*, 456 bp of *Wng*, for a total of 3727 bp of the nucleotide sequence. Phylogenies obtained through BI and ML support for the monophyly of *Nomada*.

Although the monophyly of the tribe Nomadini remains notably stable, the *ruficornis* species group showed polyphyly, which is consistent with Lim et al. (2022). For example, *N. imbricata* and *N. lathburiana*, previously categorized within the *ruficornis* species group, were nested within the *bifasciata* species group. Similarly, *N. tsunekiana*, *N. emarginata*, and *N. flavopicta* were clustered with the *basalis* species group. Furthermore, the *roberjeotiana* species group showed paraphyly in both ML and BI. Notably, the *bifasciata* species group formed a well-supported subclade (BS=88, PP=97) with *N. lathburiana* and *N. imbricata*, previously considered part of the *ruficornis* species group.

When it comes to the *armata* species group, it was also revealed as paraphyletic due to the *N. kaguya* and *N. aswensis*, which were previously treated as the *ruficornis* species group as well, and *N. taicho*, formerly treated as *furva* species group according to the Alexander and Schwarz (1994). Because multiple species that were originally placed within the *ruficornis* species group radiated into multiple species groups, a polyphyly of this species group was confirmed in this study.

Discussion

Phylogeny of subfamily Nomadinae

Alexander first conducted species group classification in the genus *Nomada* in 1994. There has been a range of prior attempts to proceed with the comprehensive reconstruction of the entire genus *Nomada*, but after he reconstructed the genus into 16 species groups via cladistic analysis, this classification has been commonly used in its

morphological taxonomy (Alexander 1994; Mitai and Tadauchi 2007; Proshchalykin and Lelej 2010; Smit 2018; Lim et al. 2022; Odanaka et al. 2022; Lim and Lee 2023). However, he mentioned that one of the species groups, the *ruficornis* species group, may be a paraphyletic group that belongs to a remnant of a more comprehensive clade without relatively distinct apomorphic subunits such as in *armata* and *basalis* species group (Alexander 1994; Mitai and Tadauchi 2007). Because of this uncertainty, there was confusion about which species was included in which groups. For example, *Nomada ginran* Tsuneki, 1973 was treated as a *bifasciata* species group (Mitai and Tadauchi 2004). However, it was reconstructed as a member of the *armata* species group later (Mitai and Tadauchi 2007). Won also indicated in his PhD thesis that the *bifasciata* species group, *trispinosa* species group, and partial *ruficornis* species group were not clearly congruent with the classification by Alexander (1994) using mitochondrial COI gene (Won 2006). Nevertheless, he did not propose a newly modified classification.

In Odanaka et al. (2022), the largest number of *Nomada* was exploited for phylogenetic analysis compared to the previous investigations and suggested that the *ruficornis* species group is paraphyletic, with highlighting potential new species group. In this study, we suggest that the *ruficornis* species group is polyphyletic, which is congruent with Lim et al. (2022) but with the expanded sampling of East Palearctic species. The discrepancy between the previous classification and redesignation will be discussed below based on Fig. 1.

Node A.

Nomada tsunekiana Schwarz, 1999, which is distributed only in Korea has been considered as the *ruficornis* species group (Won and Kim 2013). However, it formed a subclade within the *basalis* species group in this study. According to Alexander (1994), the diagnostic characters of the *basalis* species group were as follows: 1) mandible simple and round at tip; 2) first flagellar segment, evidently longer than the second or the first two flagella equal in length; 3) malar space closed posteriorly; 4) pygidial plate rounded; 5) margin of the hind tibia with dense straight hair. Among these characters, the 2nd characteristic is the most distinctive character to distinguish the species group from the *ruficornis* species group. In *N. tsunekiana*, most of the mentioned characters can be applied to its description except the 5th character as the setae are absent on its hind tibial setae. However, the species is more likely to be placed in the *basalis* species group rather than the *ruficornis* species group since it should have a distinctly shorter first flagella to belong to the *ruficornis* species group (Fig. 2). Therefore, *N. tsunekiana*, *N. emarginata*, *N. flavopicta* should be moved to *basalis* species group and the absent of hind tibial setae should be accepted as an exception because *N. emarginata* is also historically placed in the *ruficornis* species group and possess no setae on the hind tibiae (Smit 2018). The complexity of the *roberjeotiana* species group might have arisen due to the sampling limitation because the analyses for *N. obtusifrons* and *N. argentata* were based on only COI data. Therefore, a more comprehensive taxon sampling should be conducted to enhance the resolution of the *roberjeotiana* species group.

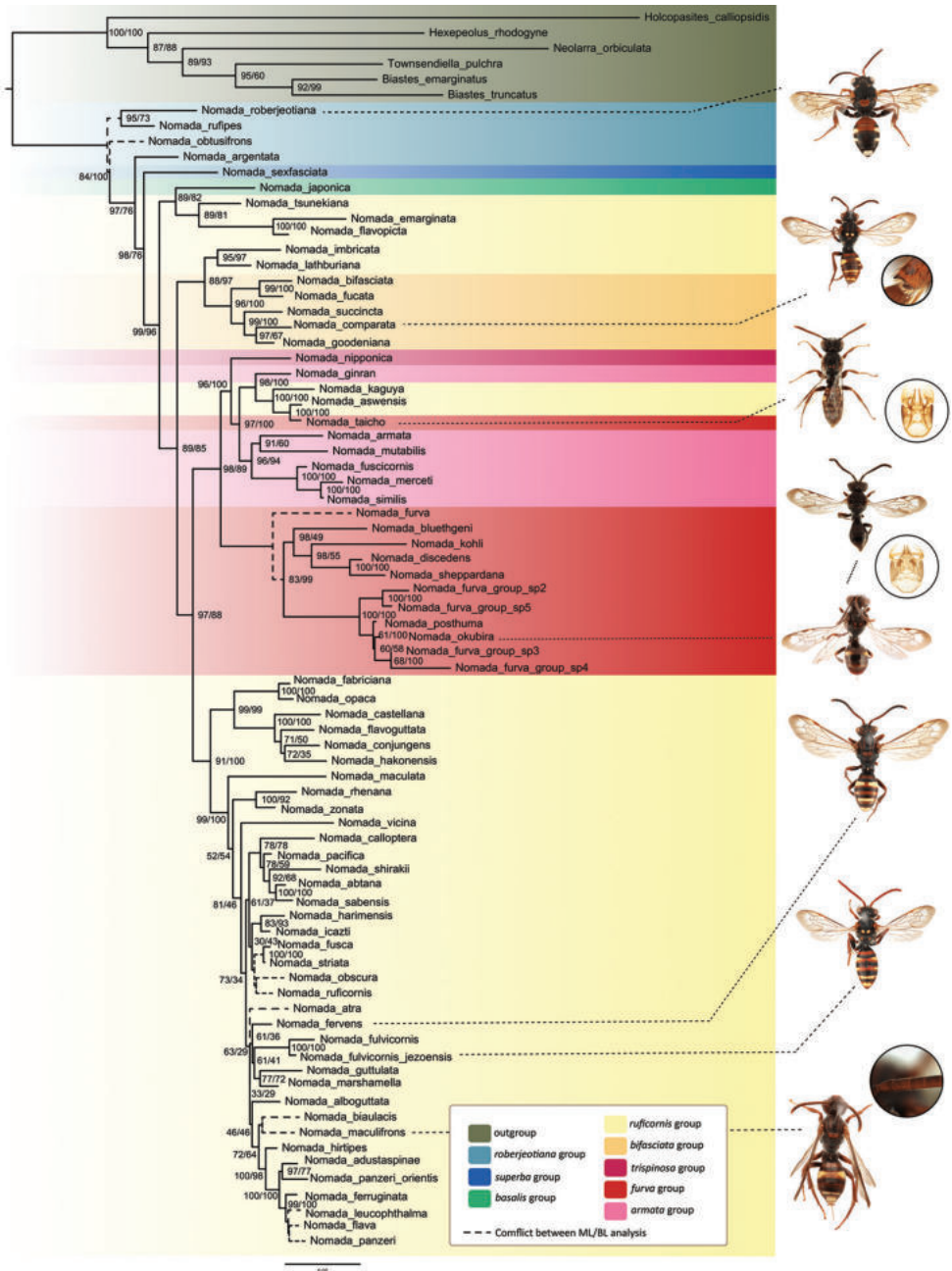


Figure 1. Phylogenetic trees (ML/ BI) of genus *Nomada* (Photo: Kayun Lim).

Node B.

The *bifasciata* species group comprises 21 species worldwide and one of the well-known apomorphic characters is distinctly produced and backwardly curved setae, which is two or three in number on the margin of hind tibiae of the females (Alexander 1994).

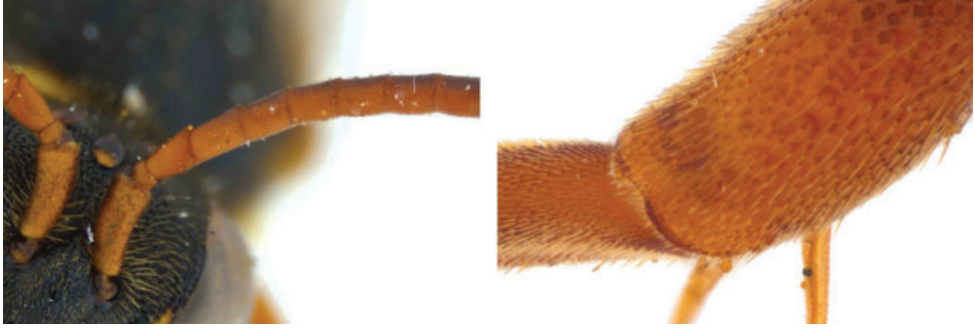


Figure 2. *N. tsunekiana* female. left, antennae in ventral view; right, hind tibiae (Photo: Kayun Lim).

However, the species group formed the subclade with *N. lathburiana*, and *N. imbricata*, which were placed in the *ruficornis* species group (Alexander 1994), indicating the classification of *bifasciata* species group may need modification as the apomorphic character for it cannot be applied to these two species. Otherwise, the new species group must be designated with *N. lathburiana* and *N. imbricata*. For example, the females of *N. lathburiana* possess three or four stout and straight setae (Smit 2018), and females of *N. imbricata* usually have about three, posteriorly curved setae on their hind tibiae (Personal observation). Alexander (1994) agreed that *N. imbricata* has a similar appearance to the species in the *bifasciata* species group, but he did not include the *N. imbricata* in the *bifasciata* species group because males did not have the apomorphic morphology. Consequently, further investigation of morphology with the increased taxon sampling must be conducted to resolve these species group complexes.

Node C.

The expanded multi-gene phylogeny in this study supports the designation of *N. ginran* within the *armata* species group, as proposed by Mitai and Tadauchi (2007) because the *N. ginran* forms the same clade with *Nomada armata* Herrich-Schäffer, 1839, which is the type species of the *armata* species group. On the other hand, *N. aswensis* and *N. kaguya* were previously treated as the *ruficornis* species group, and *N. nipponica*, which was previously considered as the *trispinosa* species group, also formed the same clade with *N. armata*. Moreover, *N. taicho*, formally classified as the *furva* species group by Alexander and Schwarz (1994), was nested in the *armata* species group. Therefore, it might be plausible to move *N. aswensis* and *N. kaguya* to the *armata* species group. Traditionally, the *ruficornis* species group has been considered to have evidently shorter first flagellum than the second, while it is nearly equal in length in *N. aswensis* females (Mitai and Tadauchi 2007). Also, *N. kaguya* shares morphological characteristics with *N. aswensis* and *N. ginran*, such as stout setae and a generally small body size of less than 8 mm (Won and Kim 2013). However, its first flagellum is distinctly shorter than the second one, suggesting that flagellum length may not serve as a definitive apomorphic character for the *ruficornis* species group. Therefore, the redesignation of

the *ruficornis* species group with vast sampling of the East Palearctic species must be conducted. When it comes to the *N. taicho*, it should be moved into the *armata* species group because of both morphological and molecular evidence. To be specific, it lacks the strongly curved gonostylus with sinuate hair to be *furva* species group according to the classification by Alexander (1994) and does not form the same subclade with the other species of the *furva* species group.

Conclusion

In this study, the review of species groups in genus *Nomada*, with a particular focus on the East Palearctic species, was conducted. Most of the species groups from the traditional classification by Alexander (1994) did not form monophyly. However, this discrepancy may not necessarily stem from inaccuracies in the traditional classification but rather from exceptions found among East Palearctic species, especially those from Northeast Asia. This is attributed to Alexander's limited examination of collections by Tsuneki, a *Nomada* taxonomist from Japan. Consequently, the current classification must be expanded with these exceptions as described in the discussion and some species should be moved to the appropriate species group, including *N. tsunekiana*, *N. emarginata*, and *N. flavopicta* into the *basalis* species group, and *N. aswensis*, *N. kaguya*, and *N. taicho* into the *armata* species group. When it comes to the *bifasciata* species group complex, future study must be proceeded with a broad array of taxa to confirm if the two species, *N. lathburiana* and *N. imbricata* manifestly form an independent subclade with the *basalis* species group or remain nested within the *bifasciata* group. The updated species list with species group reconstruction can be found in Table 1.

Table 1. Species list of *Nomada* from Korea with new suggestion of the species group designation.

No.	Recorded species	Previous species group	This study
1	<i>Nomada abtana</i> Tsuneki, 1973	<i>ruficornis</i>	<i>ruficornis</i>
2	<i>Nomada adustaspinae</i> Lim & Lee, 2023	<i>ruficornis</i>	<i>ruficornis</i>
3	<i>Nomada amurensis</i> Radoszkowski, 1876	<i>ruficornis</i>	<i>ruficornis</i>
4	<i>Nomada aswensis</i> Tsuneki, 1973	<i>ruficornis</i>	<i>armata</i>
5	<i>Nomada atra</i> Lim & Lee, 2023	<i>ruficornis</i>	<i>ruficornis</i>
6	<i>Nomada biaulacis</i> Lim & Lee, 2023	<i>ruficornis</i>	<i>ruficornis</i>
7	<i>Nomada calloptera</i> Cockerell, 1918	<i>ruficornis</i>	<i>ruficornis</i>
8	<i>Nomada comparata</i> Cockerell, 1911	<i>bifasciata</i>	<i>bifasciata</i>
9	<i>Nomada esana</i> Tsuneki, 1973	<i>ruficornis</i>	<i>ruficornis</i>
10	<i>Nomada fervens</i> Smith, 1873	<i>ruficornis</i>	<i>ruficornis</i>
11	<i>Nomada flavoguttata</i> (Kirby, 1802)	<i>ruficornis</i>	<i>ruficornis</i>
12	<i>Nomada fulvicornis jezoensis</i> Matsumura, 1912	<i>ruficornis</i>	<i>ruficornis</i>
13	<i>Nomada fusca</i> Schwarz, 1986	<i>ruficornis</i>	<i>ruficornis</i>
14	<i>Nomada galloisi</i> Yasumatsu & Hirashima, 1953	<i>roberjeotiana</i>	<i>roberjeotiana</i>
15	<i>Nomada ginran</i> Tsuneki, 1973	<i>armata</i>	<i>armata</i>
16	<i>Nomada guttulata</i> Schenck, 1861	<i>ruficornis</i>	<i>ruficornis</i>
17	<i>Nomada hakonensis</i> Cockerell, 1911	<i>ruficornis</i>	<i>ruficornis</i>

No.	Recorded species	Previous species group	This study
18	<i>Nomada hokusana hokusana</i> Tsuneki, 1973	<i>roberjeotiana</i>	<i>roberjeotiana</i>
19	<i>Nomada harimensis</i> Cockerell, 1914	<i>ruficornis</i>	<i>ruficornis</i>
20	<i>Nomada icazti</i> Tsuneki, 1976	<i>ruficornis</i>	<i>ruficornis</i>
21	<i>Nomada japonica</i> Smith, 1873	<i>basalis</i>	<i>basalis</i>
22	<i>Nomada kaguya</i> Hirashima, 1953	<i>ruficornis</i>	<i>ruficornis</i>
23	<i>Nomada koreana</i> Cockerell, 1926	<i>ruficornis</i>	<i>ruficornis</i>
24	<i>Nomada lathburiana</i> (Kirby, 1802)	<i>ruficornis</i>	<i>ruficornis</i>
25	<i>Nomada leucophthalma</i> (Kirby, 1802)	<i>ruficornis</i>	<i>ruficornis</i>
26	<i>Nomada maculifrons</i> Smith, 1869	<i>ruficornis</i>	<i>ruficornis</i>
27	<i>Nomada montverna</i> Tsuneki, 1973	<i>ruficornis</i>	<i>ruficornis</i>
28	<i>Nomada nipponica</i> Yasumatsu & Hirashima, 1951	<i>trispinosa</i>	<i>armata</i>
29	<i>Nomada okamotonis</i> Matsumura, 1912	<i>roberjeotiana</i>	<i>roberjeotiana</i>
30	<i>Nomada okubira</i> Tsuneki, 1973	<i>furva</i>	<i>furva</i>
31	<i>Nomada opaca</i> Alfken, 1913	<i>ruficornis</i>	<i>ruficornis</i>
32	<i>Nomada pacifica</i> Tsuneki, 1973	<i>ruficornis</i>	<i>ruficornis</i>
33	<i>Nomada panzeri orientis</i> Tsuneki, 1973	<i>ruficornis</i>	<i>ruficornis</i>
34	<i>Nomada pekingensis</i> Tsuneki, 1986	<i>trispinosa</i>	<i>trispinosa</i>
35	<i>Nomada pulawskii</i> Tsuneki, 1973	<i>furva</i>	<i>furva</i>
36	<i>Nomada pyrifer</i> Cockerell, 1918	<i>ruficornis</i>	<i>ruficornis</i>
37	<i>Nomada roberjeotiana aino</i> Tsuneki, 1973	<i>roberjeotiana</i>	<i>roberjeotiana</i>
38	<i>Nomada sabaensis</i> Tsuneki, 1973	<i>ruficornis</i>	<i>ruficornis</i>
39	<i>Nomada sexfasciata</i> Panzer, 1799	<i>superba</i>	<i>superba</i>
40	<i>Nomada shirakii</i> Yasumatsu & Hirashima, 1951	<i>ruficornis</i>	<i>ruficornis</i>
41	<i>Nomada shoyozana</i> Tsuneki, 1986	<i>roberjeotiana</i>	<i>roberjeotiana</i>
42	<i>Nomada striata</i> Fabricius, 1793	<i>ruficornis</i>	<i>ruficornis</i>
43	<i>Nomada taicho</i> Tsuneki, 1973	<i>furva</i>	<i>armata</i>
44	<i>Nomada temmasana temmasana</i> Tsuneki, 1986	<i>roberjeotiana</i>	<i>roberjeotiana</i>
45	<i>Nomada tsunekiana</i> Schwarz, 1999	<i>ruficornis</i>	<i>basalis</i>

Acknowledgement

We extend our sincere thanks to Mr. Jan Smit, the *Nomada* taxonomist from the Netherlands, for his invaluable guidance and the west Palearctic specimens he provided. We also express our deep appreciation to Mr. Keiichi Otsui for contributing the valuable Japanese specimens. Lastly, we deeply thank to Michael Branstetter, Jeremy Jensen, and Jaeseok Oh for improving the manuscript with valuable comments and suggestions.

The study received assistance through various sources. Firstly, it was conducted with assistance from the R&D Program for Forest Science Technology (Project No. 2021362B10-2223-BD01), which was provided by the Korea Forest Service (Korea Forestry Promotion Institute). Additionally, this study was partially supported by the Korea National Arboretum (project no. KNA 1-2-44, 23-2). Moreover, this research received support from the Basic Science Research Program through the National Research Foundation of Korea (NRF), funded by the Ministry of Education (NR-F2020R111A2069484). Lastly, this work was supported by a grant from the National Institute of Biological Resources (NIBR) funded by the Ministry of Environment (MOE) of the Republic of Korea (NIBR202307202).

Reference

- Alexander BA (1994) Species-groups and cladistic analysis of the cleptoparasitic bee genus *Nomada* (Hymenoptera: Apoidea). The University of Kansas Science Bulletin 55: 175–238. <https://doi.org/10.5962/bhl.part.776>
- Alexander BA, Schwarz M (1994) A catalog of the species of *Nomada* (Hymenoptera: Apoidea) of the world. The University of Kansas Science Bulletin 55: 239–270. https://digitalcommons.usu.edu/bee_lab_a/100/
- Hoang DT, Chernomor O, Von Haeseler A, Minh BQ, Vinh LS (2018) UFBoot2: improving the ultrafast bootstrap approximation. Molecular biology and evolution 35(2): 518–522. <https://doi.org/10.1093/molbev/msx281>
- Lim K, Lee S (2023) A key to species of *Nomada ruficornis* species-group (Hymenoptera: Apidae) of South Korea, with descriptions of three new species. Zootaxa 5228(1): 44–60. <https://doi.org/10.11646/zootaxa.5228.1.2>
- Lim K, Lee S, Orr M, Lee S (2022) Harrison's rule corroborated for the body size of cleptoparasitic cuckoo bees (Hymenoptera: Apidae: Nomadinae) and their hosts. Scientific Reports 12(1): 10984. <https://doi.org/10.1038/s41598-022-14938-9>
- Minh BQ, Schmidt HA, Chernomor O, Schrempf D, Woodhams MD, Von Haeseler A, Lanfear R (2020) IQ-TREE 2: new models and efficient methods for phylogenetic inference in the genomic era. Molecular Biology and Evolution 37(5): 1530–1534. <https://doi.org/10.1093/molbev/msaa015>
- Mitai K, Tadauchi O (2004) Taxonomic notes on the *bifasciata* species group of the genus *Nomada* (Hymenoptera: Apidae) in Japan. Esakia 44: 91–101. <https://doi.org/10.5109/2685>
- Mitai K, Tadauchi O (2005) Systematic notes on the *basalis* and *trispinosa* species groups of the genus *Nomada* (Hymenoptera, Apidae) in Japan. Japanese Journal of Systematic Entomology 11: 1–10.
- Mitai K, Tadauchi O (2006) Taxonomic notes on Japanese species of the *Nomada furva* species group (Hymenoptera: Apidae). Entomological science 9: 239–246. <https://doi.org/10.1111/j.1479-8298.2006.00169.x>
- Mitai K, Tadauchi O (2007) Taxonomic study of the Japanese species of the *Nomada ruficornis* species group (Hymenoptera, Apidae) with remarks on Japanese fauna of the genus *Nomada*. Esakia 47: 25–167. <https://doi.org/10.5109/8324>
- Mitai K, Hirashima Y, Tadauchi O (2003) A systematic study of the *roberjeotiana* species group of the genus *Nomada* in Japan (Hymenoptera, Apidae). Japanese Journal of Systematic Entomology 9: 297–318.
- Mitai K, Schwarz M, Tadauci O (2008) Redescriptions and taxonomic positions of three little known species of the genus *Nomada* (Hymenoptera, Apidae). Japanese Journal of Systematic Entomology 14: 107–119.
- Odanaka KA, Branstetter MG, Tobin KB, Rehan SM (2022) Phylogenomics and historical biogeography of the cleptoparasitic bee genus *Nomada* (Hymenoptera: Apidae) using ultraconserved elements. Molecular Phylogenetics and Evolution 170: 107453. <https://doi.org/10.1016/j.ympev.2022.107453>

- Proshchalykin MY, Lelej AS (2010) Review of the *Nomada roberjeotiana* species-group (Hymenoptera: Apidae) of Russia, with description of new species. *Zootaxa* 2335 (1): 1–15. <https://doi.org/10.11646/zootaxa.2335.1.1>
- Rambaut A, Drummond AJ, Xie D, Baele G, Suchard MA (2018) Posterior summarization in Bayesian phylogenetics using Tracer 1.7. *Systematic biology* 67(5): 901–904. <https://doi.org/10.1093/sysbio/syy032>
- Ronquist F, Teslenko M, Van Der Mark P, Ayres DL, Darling A, Höhna S, Larget B, Liu L, Suchard MA, Huelsenbeck JP (2012) MrBayes 3.2: efficient Bayesian phylogenetic inference and model choice across a large model space. *Systematic biology* 61(3): 539–542. <https://doi.org/10.1093/sysbio/sys029>
- Sless TJ L, Branstetter MG, Gillung JP, Krichilsky EA, Tobin KB, Straka J, Rozen JG, Freitas FV, Martins AC, Bossert S, Searle JB, Danforth BN (2022) Phylogenetic relationships and the evolution of host preferences in the largest clade of brood parasitic bees (Apidae: Nomadinae). *Molecular Phylogenetics and Evolution* 166: 107326. <https://doi.org/10.1016/j.ympev.2021.107326>
- Smit J (2018) Identification key to the European species of the bee genus *Nomada* Scopoli, 1770 (Hymenoptera: Apidae), including 23 new species. *Entomofauna* 3: 1–253. https://www.zobodat.at/publikation_volumes.php?id=54546
- Snelling RR (1986) Contributions toward a revision of the new world Nomadine bees. A partitioning of the genus *Nomada* (Hymenoptera: Anthophoridae). *Natural history museum Los Angeles County* 376: 1–32. <https://doi.org/10.5962/p.208119>
- Won HS (2006) Systematics of the genus *Nomada* (Hymenoptera: Apidae) in Korea. PhD thesis. Korea University (Seoul).
- Won HS, Kim JK (2013) Arthropoda: Insecta: Hymenoptera: Apidae: Nomadinae: *Nomada*: cuckoo bees. *Insect Fauna of Korea* 13: 1–89.
- Vaidya G, Lohman DJ, Meier R (2011) SequenceMatrix: concatenation software for the fast assembly of multi-gene datasets with character set and codon information. *Cladistics* 27: 171–180. <https://doi.org/10.1111/j.1096-0031.2010.00329.x>

Supplementary material I

NCBI accession numbers

Authors: Kayun Lim, Seunghwan Lee

Data type: docx

Copyright notice: This dataset is made available under the Open Database License (<http://opendatacommons.org/licenses/odbl/1.0/>). The Open Database License (ODbL) is a license agreement intended to allow users to freely share, modify, and use this Dataset while maintaining this same freedom for others, provided that the original source and author(s) are credited.

Link: <https://doi.org/10.3897/jhr.96.106452.suppl1>

Supplementary material 2

Model selection for BI

Authors: Kayun Lim, Seunghwan Lee

Data type: docx

Copyright notice: This dataset is made available under the Open Database License (<http://opendatacommons.org/licenses/odbl/1.0/>). The Open Database License (ODbL) is a license agreement intended to allow users to freely share, modify, and use this Dataset while maintaining this same freedom for others, provided that the original source and author(s) are credited.

Link: <https://doi.org/10.3897/jhr.96.106452.suppl2>

Discovery of the velvet ant genus *Orientilla* Lelej from Laos (Hymenoptera, Mutillidae, Dasylabrinae), with description of a related new species from India

Juriya Okayasu¹

¹ *Systematic Entomology, Graduate School of Agriculture, Hokkaido University, Sapporo, 060-8589, Japan*

Corresponding author: Juriya Okayasu (mutiphiidae@gmail.com)

Academic editor: Michael Ohl | Received 5 August 2023 | Accepted 5 October 2023 | Published 17 October 2023

<https://zoobank.org/08EC5550-C847-4BE8-A66C-CDDA50BE8BDA>

Citation: Okayasu J (2023) Discovery of the velvet ant genus *Orientilla* Lelej from Laos (Hymenoptera, Mutillidae, Dasylabrinae), with description of a related new species from India. *Journal of Hymenoptera Research* 96: 817–834. <https://doi.org/10.3897/jhr.96.110590>

Abstract

The genus *Orientilla* Lelej, 1979 is newly recorded from Laos based on *O. tamaderai* **sp. nov.** (Xieng Khouang) and *O. vietnamica* Lelej, 1979 (Vientiane). One additional new species, *O. nitens* **sp. nov.**, is described from India (Tamil Nadu). These three species share many diagnostic features within *Orientilla*, but they are distinguished by the body coloration and shape of clypeus, hypostomal carina, humeral carina, and metasomal terga 1–2. An identification key to females of the genus is provided.

Keywords

Aculeata, biodiversity, Oriental Region, taxonomy

Introduction

Velvet ants (Mutillidae and Myrmosidae) are large groups of aculeate wasps including more than 4600 species, which predominantly occur in tropical regions (Lelej 2005, 2007; Pagliano et al. 2020). Southeast Asia is known for the rich but hidden velvet ant diversity (Williams et al. 2019; Okayasu et al. 2021b). In this region, Laos is one of the most unsampled countries, with only 21 species so far recorded (see Appendix 1). This number is nearly one-third to half the number of species known from Thailand

and Vietnam, even though these adjacent countries share many terrestrial ecoregions (Olson et al. 2001; Wikramanayake et al. 2002; Dinerstein et al. 2017).

The genus *Orientilla* Lelej, 1979 presently includes 13 species from the eastern Palearctic, Oriental, and Australasian Regions (Lelej 1979, 1996a, 2005; Das and Girish Kumar, 2016a; Zhou et al. 2018; Pagliano et al. 2020; Brothers 2022). This genus is widespread in mainland Southeast Asia but has never been found in Laos, presumably due to inadequate sampling. After extensive museum surveys, only two *Orientilla* specimens from Laos were discovered, which are treated in this paper. Additionally, one new species from India is described, because this species shows diagnostic features suggesting close relationship with the Laotian species.

Material and methods

The material examined in this study is deposited in the following institutes: Ehime University Museum, Matsuyama, Japan (**EUM**); Hokkaido University Insect Collection, Sapporo, Japan (**SEHU**); Thailand Natural History Museum, National Science Museum, Pathum Thani, Thailand (**THNHM**). Specimens were examined under a Leica M205C stereomicroscope (7.8–160× magnification). Habitus photographs were taken using a Canon EOS 6D Mark II digital camera equipped with a Canon MP-E 65mm f/2.8 1–5× Macro Photo lens. External morphological features were imaged with a Canon EOS 6D Mark II attached to a Leica M205C. Focus stacking was done using Zerene Stacker (Zerene Systems LLC, Richland, WA, USA). Images were post-processed using Adobe Photoshop and assembled into plates using Adobe Illustrator (Adobe Inc., San Jose, CA, USA). Terminology mostly follows the Hymenoptera Anatomy Consortium (2023). The following abbreviations are used in the description: **F**, flagellomere; **S**, metasomal sternum; **T**, metasomal tergum.

Taxonomy

Orientilla Lelej, 1979

Orientilla Lelej, 1979: 1066, ♀; Lelej 1996a: 103, ♂♀; Lelej 2002: 101; Lelej 2005: 111; Lelej and Brothers 2008: 42; Pagliano et al. 2020: 131. Type species: *Orientilla vietnamica* Lelej, 1979 (♀), by original designation.

Diagnosis. Male. Frons lacking medial longitudinal carina between antennal tubercles; eye oval, slightly projecting from head capsule; wings fully developed; tegula posteriorly reaching mesoscuto-scutellar articulation; mesoscutellum laterally longitudinally carinate; tibial spurs pale; metasomal segment 1 petiolate; T1 with distinct dorsal and anterior faces; lateral felt line present on S2 but absent on T2; S6 flat, lacking medial tubercles; genital paramere with short inner setae. **Female.** Frons lacking me-

dial process; F1 depressed; F1 length subequal to its width and F2 length; mesopleuron strongly expanded laterally; protarsus with short outer spines; metasomal segment 1 petiolate; T1 with distinct dorsal and anterior faces; lateral felt line present on S2 but absent on T2; pygidial plate convex, lacking lateral carina.

Species included. This genus includes the following 15 species: *O. aureorubra* (Sichel & Radoszkowski, 1870), ♂♀ (India, Sri Lanka); *O. chinensis* (Zavattari, 1922), ♂♀ (China); *O. croma* (Zavattari, 1914), ♂ (Myanmar); *O. desponsa* (Smith, 1855), ♂♀ (China, Taiwan, Myanmar, Vietnam); *O. jabalpurensis* Das & Girish Kumar, 2016, ♀ (India); *O. kallata* (Nurse, 1902), ♂ (India, Sri Lanka); *O. krombeini* Lelej, 1996, ♂♀ (Vietnam); *O. manni* (Krombein, 1971), ♀ (Solomon Islands); *O. nitens* sp. nov., ♀ (India); *O. nobilis* (Smith, 1855), ♂ (India); *O. remota* (Cameron, 1897), ♀ (Sri Lanka); *O. schmideggeri* Lelej, 2005, ♀ (India); *O. sejugooides* (Magretti, 1892), ♂ (Myanmar); *O. tamaderai* sp. nov., ♀ (Laos); *O. vietnamica* Lelej, 1979, ♀ (Laos, Myanmar, Thailand, Vietnam).

Remarks. This genus was initially established to include East Asian species of the predominantly Afrotropical and western Palaearctic genus *Stenomutilla* André, 1896 (Lelej 1979). Later, this genus was recorded from South Asia and the Australasian Region (Lelej 2005; Das and Girish Kumar 2016ab; Terine et al. 2020; Brothers 2022). The females of *Orientilla* and *Stenomutilla* are recognized in DasyLabrinae by having the metasomal segment 1 petiolate and lateral felt line present only on S2. However, the *Orientilla* females have the F1 depressed, its length subequal to F1 width and F2 length (F1 cylindrical, its length 2.2–2.3× F1 width and 1.2× F2 length in *Stenomutilla*) (Lelej 1979, 1996a).

Orientilla tamaderai sp. nov.

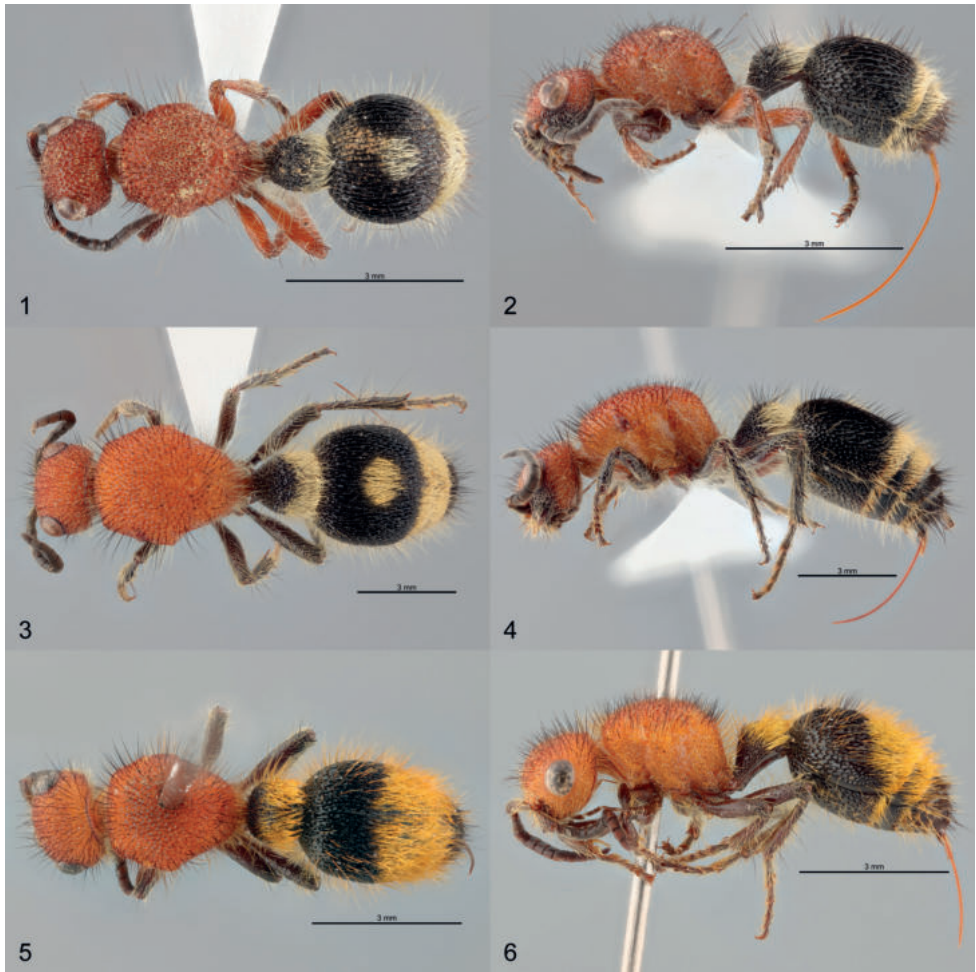
<https://zoobank.org/834489D9-ED8E-4D30-9ECB-FD89C6FF6C96>

Figs 1, 2, 7, 10

Diagnosis. Female. Head mostly red; clypeal medial elevation forming subtriangular area; clypeal subtriangular area dorso-medially delimited by carina (Fig. 7); hypostomal carina sharp; antenna dark; humeral carina sharp; mesopleuron evenly convex, not spinose (Fig. 1); legs largely red; T1 and T2 posterior margins with complete pale setal bands; T1 long and slender, with dorsal T1 length 0.97× T1 width and 0.46× T2 length (Fig. 10); T2 broad, 2.26× wider than T1, with lateral margins strongly convex (Fig. 10); T2 with medial pale setal spot, distance between medial spot and posterior band subequal to spot diameter; T3 with pale setal band; S1 carina short, reaching anterior 1/4 of S1; S2 felt line short. **Male.** Unknown.

Description. Female. Body length. 7.09 mm.

Color and setae. Frons, vertex, dorsal half of gena, and mesosoma dark red; antennal rim, meso- and metafemora, and meso- and metatibiae except apices yellowish red; clypeus, mandible apex, T1–3, and S2–S3 black; ventral half of gena including malar space, postgenal bridge, scape except apex, pedicel, mandible except apex, coxae,



Figures 1–6. *Orientilla* spp., ♀, habitus **1, 2** *O. tamaderai* sp. nov., holotype **3, 4** *O. vietnamica* Lelej, Laos **5, 6** *O. nitens* sp. nov., holotype **1, 3, 5** dorsal view **2, 4, 6** lateral view.

trochanters, profemur, protarsus, and meso- and metatibial apices dark brown; prementum, stipes, F1, F2–10 dorsally, meso- and metatarsi, S1, T4–6, and S4–6 brownish black; scape apex, F2–10 ventrally, maxillary and labial palpi, and protibia brown; tibial spurs yellow.

Frons, vertex, gena, scape, and mesosomal dorsum with sparse short recumbent pale golden and sparse erect to suberect brownish black setae; clypeus, postgenal bridge, mandible, pronotal neck, propleuron, lateral mesosomal face, dorsal propodeal face, T1 anterior and lateral faces, T1 posterior margin, S1, T2 lateral and posterior margins, T3, and S2–4 with sparse long erect pale golden setae; pedicel and F1 with sparse short recumbent pale golden setae; F2–10 with sparse very short appressed pale golden setae; prementum, stipes, and maxillary and labial palpi with sparse short erect pale golden setae; coxae, trochanters, and tibiae with sparse long recumbent and sparse long erect

pale golden setae; tarsi with sparse long appressed pale golden setae; T1 dorsal face, T2 disc, T4–6, and S5–6 with sparse short recumbent and sparse long erect brownish black setae; posterior 2/5 of T1 dorsal face covered with band of dense appressed pale golden setae; T2 with medial circular (0.92× longer than wide) spot of dense appressed pale golden setae and with posterior narrow band of dense appressed pale golden setae; distance between T2 spot and band 0.82× spot length; T2 lacking lateral felt line; S2 with short lateral felt line of pale golden setae; distance between S2 felt line and posterior fringe 0.55× felt line length; T3 with wide uniform band of dense appressed pale golden setae; S2–S3 with posterior fringe of dense appressed pale golden setae.

Structure. Head 1.35× wider than long with lateral margins strongly convergent behind eye; gena narrow, 0.78× eye breadth in lateral view; eye height:eye breadth = 58:50; distance between eyes 1.72× eye height; eye height 1.23× malar distance; frons and vertex without medial carina or groove; occipital carina complete, dorsally strongly protruding from posterior margin of vertex; antennal scrobe lacking dorsal carina; genal carina wavy, ventrally separated from hypostomal carina and lacking hypostomal tooth; postgenal bridge laterally delimited by sharp carina extending from occiput; hypostomal carina sharp; eye semicircular, convex, distinctly protruding from head capsule; clypeus dorso-medially strongly elevated nearly to level of antennal rim; clypeus with subventral transverse ridge extending along entire width of clypeus, with anterior margin crenulate; medial elevation limited on dorsal half of clypeus and forming medial subtriangular area; medial subtriangular area dorso-medially delimited by carina; mandible worn out, apically rounded and lacking preapical tooth; mandible dorsal face with sharp ridge basally, ventral margin straight; prementum flattened; scape bending medially; length and width of pedicel:F1:F2 = 10:15:18:18:20:20; F2–9 almost same in length and width; F10 slightly longer than F1 and F9, conical; F3–10 depressed.

Mesosoma broadest at mesothorax; lateral margins of mesosoma weakly crenulate, lacking carina; head width:humeral width:mesonotal width:T2 width = 83:63:87:100; mesosomal length 1.20× mesothoracic width; anterior margin of pronotal dorsum nearly straight; pronotal and propodeal spiracles without distinct tubercle; humeral carina sharp, reaching pronotal dorsum, rounded at dorsal end; scutellar scale obliterated; scutellar area without scales; metanotal-propodeal suture obliterated; mesopleuron evenly convex; propodeum lacking distinct dorsal and posterior faces; dorsal propodeal face vertical, without medial carina; mesopleural lamella absent; mesopleural ventral face with sharp precoxal transverse carina.

Protarsus lacking outer spines; protarsomere 1 apically truncate, not protruding outward; tibiae lacking outer spines; metacoxa armed with weak inner carina along its entire length.

Metasomal segment 1 petiolate; T1 with distinct dorsal and anterior faces; T1 dorsal length:T1 width:T2 dorsal length:T2 width = 38:39:82:88; T2 weakly convex, dorsally flattened; T2 lateral margin strongly convex; S1 medial carina present only on anterior 1/4 of sternum, anteriorly tuberculate; S2 with distinct anterior face, without medial carina; S6 posterior margin bidentate; pygidial plate obscurely defined, convex, lacking lateral carina.

Frons, vertex, mesosomal dorsum, T1 dorsal face, T2 lateral margin, and S1 with large dense punctures, with intervals distinct and smooth; gena with large confluent punctures, punctures larger and coarser ventrally; postgenal bridge densely transversely striate; antennal rim, clypeus lateral portion, pedicel, flagellum, and prementum with minute dense punctures; clypeal subtriangular area with large dense shallow punctures; scape, legs, T4–6, and S4–6 with small sparse punctures; stipes with small dense punctures; pronotal collar anteriorly with minute sparse punctures; pronotal collar posteriorly smooth; mesosomal lateral face and dorsal propodeal face with large confluent punctures; T1 anterior face, T3, and S2–3 with large sparse punctures; T2 disc longitudinally coarsely puncto-striate.

Male. Unknown.

Type material. Holotype: LAOS • ♀; Xieng Khouang Prov., Ban Vang, Ban Tha; 19°44'15.2"N, 103°35'16.6"E; 1239 m alt.; 30 Apr. 2018; Yutaka Tamadera leg. [SEHU].

Distribution. Laos: Xieng Khouang.

Etymology. The specific name is dedicated to the type collector, Yutaka Tamadera, an expert in the systematics of jewel beetles (Coleoptera: Buprestidae).

Remarks. The area of the type locality (Figs 13–15) is composed of two low mountains densely covered with forests and a trail between them, and surrounded by a village and a swidden (Y. Tamadera, pers. comm. 2023). The collector is not sure about the habitat (forest or swidden) where the holotype female was collected.

Orientilla tamaderai sp. nov. can be easily confused with *O. vietnamica* Lelej, 1979 by sharing the following combination of character states: head and mesosoma red, clypeus with a medial subtriangular area, mesopleuron evenly convex, T1 and T2 posterior margins with complete pale setal bands, and T2 with a medial pale setal spot. However, this new species is distinguished from the latter by the clypeal subtriangular area delimited by carinae only dorso-medially (subtriangular area delimited by carinae along its entire width in *O. vietnamica*; Figs 7, 8), T1 as long as wide (T1 wider than long in *O. vietnamica*; Figs 10, 11), and T2 lateral margins strongly convex (T2 lateral margins weakly convex in *O. vietnamica*; Figs 10, 11). Also, the female of *O. tamaderai* sp. nov. is smaller than that of *O. vietnamica* (8.0–14.9 mm; Lelej 1996a; Williams et al. 2019; supplemented by the specimens examined in this study).

Orientilla vietnamica Lelej, 1979

Figs 3, 4, 8, 11

Orientilla vietnamica Lelej, 1979: 1066, ♀, holotype ♀ (Nha Trang, S. Annam, Vietnam) [Zoological Institute, Russian Academy of Sciences, St. Petersburg, Russia]; Lelej 1996a: 105, ♀; Lelej 2005: 113; Okayasu et al. 2018: 309, ♀; Williams et al. 2019: 11, ♀; Pagliano et al. 2020: 132; Thaochan et al. 2022: 164, ♂♀.

Diagnosis. Female. Head red; clypeal medial elevation forming subtriangular area; clypeal subtriangular area delimited by carina extending nearly to clypeal lateral margin

(Fig. 8); hypostomal carina sharp; antenna dark; humeral carina sharp; mesopleuron evenly convex, not spinose (Fig. 3); legs black; T1 and T2 posterior margins with complete pale setal bands; T1 short and broad, with dorsal T1 length $0.64\text{--}0.76\times$ T1 width and $0.33\text{--}0.40\times$ T2 length (Fig. 11); T2 slender, $1.80\text{--}2.03\times$ wider than T1, with lateral margins weakly convex (Fig. 11); T2 with medial pale setal spot, distance between medial spot and posterior band subequal to spot diameter; T3 with pale setal band; S1 carina short, reaching anterior $1/4$ of S1; S2 felt line short. **Male.** Unknown.

Material examined. LAOS • 1♀; Vientiane; May 1995 [EUM]. THAILAND • 1♀; Khon Kaen; 15 Oct. 1972; M. Sato leg. [EUM] • 1♀; Chiang Mai, Omkoi District; $17^{\circ}50'49.9''\text{N}$, $98^{\circ}22'33.0''\text{E}$; 950–1010 m alt.; 10 Sep. 2016; R. Mizuno; Dry dipterocarp forest [THNHM] • 1♀; same collection data as for preceding; 27 Jun. 2017 [THNHM] • 1♀; same collection data as for preceding; 28 Jun. 2017 [THNHM] • 1♀; same collection data as for preceding; 18 Jul. 2019 [THNHM] • 1♀; same collection data as for preceding; 19 Jul. 2019 [THNHM] • 1♀; same collection data as for preceding; 20 Jul. 2019 [THNHM] • 1♀; same collection data as for preceding; 21 Jul. 2019 [THNHM].

Distribution. LAOS: Vientiane (new record). Myanmar: additional data unavailable (Lelej 2005; Williams et al. 2019). Thailand: Chiang Mai, Khon Kaen, Phetchaburi, Ubon Ratchathani (Williams et al. 2019). Vietnam: Khanh Hoa (Lelej 1979; Williams et al. 2019).

Remarks. At Omkoi District, this species was collected on a trail through a dry dipterocarp forest during the rainy season (Mizuno et al. 2019; R. Mizuno, pers. comm. 2017).

Orientilla nitens sp. nov.

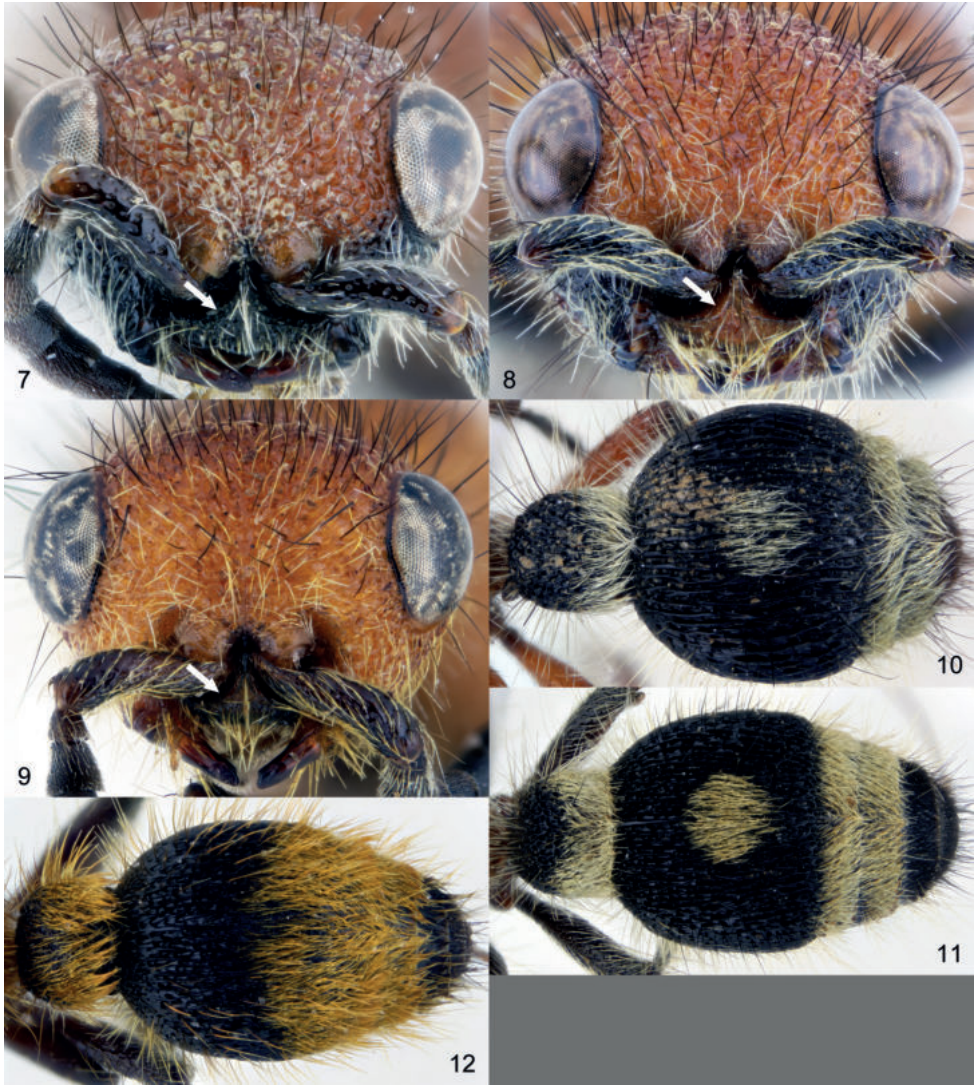
<https://zoobank.org/78D44215-5330-473B-9AB9-59A6B9860707>

Figs 5, 6, 9, 12

Diagnosis. Female. Head red; clypeal medial elevation forming subtriangular area; clypeal subtriangular area dorso-medially delimited by carina (Fig. 9); hypostomal carina lamellately projecting; antenna dark; humeral carina obliterated; mesopleuron evenly convex, not spinose (Fig. 5); legs black; T1 posterior margin with complete pale setal band and T2 posterior half covered with dense appressed golden setae; T1 short and broad, with dorsal T1 length $0.68\times$ T1 width and $0.32\times$ T2 length (Fig. 12); T2 slender, $1.96\times$ wider than T1, with lateral margins weakly convex (Fig. 12); T2 lacking medial spot; T3 with golden setal band; S1 carina short, reaching anterior $1/4$ of S1; S2 felt line short. **Male.** Unknown.

Description. Female. Body length. 8.51 mm.

Color and setae. Head except clypeus, mesosoma, and meso- and metacoxae basal $1/3$ yellowish red; clypeus, mandible except apex, scape, pedicel, maxillary and labial palpi, and legs except meso- and metacoxal bases dark brown; mandible apex, flagellum dorsal face, prementum, and stipes black; flagellum ventral face and tibial spurs brown; metasoma brownish black.



Figures 7–12. *Orientilla* spp., ♀ **7, 10** *O. tamaderai* sp. nov., holotype **8, 11** *O. vietnamica* Lelej, Laos **9, 12** *O. nitens* sp. nov., holotype **7–9** face **10–12** metasoma, dorsal view. White arrows indicate the subtriangular area on the clypeus.

Frons, vertex, mesosomal dorsum, and tibiae with sparse short recumbent golden and sparse long erect black setae; gena, coxae, and femora with sparse long recumbent and sparse erect golden setae; postgenal bridge, clypeus, mandible, pronotal collar, lateral mesosomal face, dorsal propodeal face, T1, T2 except medial portion, T3, T4–5 lateral portions, and S1–S6 with sparse long erect golden setae; eye dorsal and posterior margins edged with long erect black setae; scape with sparse long recumbent golden setae; pedicel and F1 with sparse short recumbent golden setae; F2–10 with sparse very

short appressed golden setae; prementum, stipes, and maxillary and labial palpi with sparse short erect golden setae; tarsi with sparse long appressed golden setae; T2 and T4–5 medial portions with sparse short recumbent black and sparse long erect golden setae; T6 with sparse short recumbent and sparse long erect golden setae; T1 dorsal face entirely covered with band of dense appressed golden setae; T2 posterior half covered with semicircular spot of dense appressed golden setae; T2 lacking lateral felt line; S2 with short lateral felt line of pale golden setae; distance between S2 felt line and posterior fringe $0.46\times$ felt line length; T3 with wide uniform band of dense appressed golden setae; S2–S3 with posterior fringe of dense appressed golden setae.

Structure. Head $1.39\times$ wider than long with lateral margins strongly convergent behind eye; gena narrow, $0.73\times$ eye breadth in lateral view; eye height:eye breadth = 62:50; distance between eyes $1.75\times$ eye height; eye height $1.49\times$ malar distance; frons and vertex without medial carina or groove; occipital carina complete, dorsally strongly protruding from posterior margin of vertex; antennal scrobe lacking dorsal carina; genal carina weakly developed, wavy, ventrally separated from hypostomal carina and lacking hypostomal tooth; postgenal bridge laterally delimited by sharp carina extending from occiput; eye semicircular, convex, distinctly protruding from head capsule; clypeus dorso-medially strongly elevated nearly to level of antennal rim; clypeus with subventral transverse ridge extending along entire width of clypeus, with anterior margin shallowly concave; medial elevation limited on dorsal half of clypeus and forming medial subtriangular area; medial subtriangular area dorso-medially delimited by carina; mandible apically bidentate; mandible dorsal face with sharp ridge basally, ventral margin straight; prementum flattened; scape bending medially; length and width of pedicel:F1:F2 = 10:14:20:18:20:20; F2–9 almost same in length and width; F10 slightly longer than F1 and F9, conical; F3–10 depressed.

Mesosoma broadest at mesothorax; lateral margins of mesosoma weakly crenulate, lacking carina; head width:humeral width:mesonotal width:T2 width = 91:75:98:100; mesosomal length $1.14\times$ mesothoracic width; anterior margin of pronotal dorsum nearly straight; pronotal and propodeal spiracles without distinct tubercle; humeral carina obliterated; scutellar scale obliterated; scutellar area without scales; metanotal-propodeal suture obliterated; mesopleuron evenly convex; propodeum lacking distinct dorsal and posterior faces; dorsal propodeal face vertical, without medial carina; mesopleural lamella absent; mesopleural ventral face with sharp precoxal transverse carina.

Protarsus lacking outer spines; protarsomere 1 apically truncate, not protruding outward; tibiae lacking outer spines; metacoxa armed with weak inner carina along its entire length.

Metasomal segment 1 petiolate; T1 with distinct dorsal and anterior faces; T1 dorsal length:T1 width:T2 dorsal length:T2 width = 32:47:100:92; T2 weakly convex, dorsally flattened; T2 lateral margin weakly convex; S1 medial carina present only on anterior $1/4$ of sternum, anteriorly rounded; S2 with distinct anterior face, without medial carina; S6 posterior margin truncate; pygidial plate obscurely defined, convex, lacking lateral carina.



Figures 13–15. The type locality of *Orientilla tamaderai* sp. nov. **13** type locality seen from the south **14** type locality and a swidden seen from the north **15** the access to the forest trail. Photo by Y. Tamadera.

Frons, vertex, mesosomal dorsum, T2 lateral margin, and S1 with large dense punctures, with intervals distinct and smooth; gena, mesosomal lateral face, and dorsal propodeal face with large confluent punctures; postgenal bridge, antennal rim, clypeus lateral portion, scape, legs except coxae, T3–T6, and S3–S6 with small sparse punctures; clypeal subtriangular area with small sparse punctures, with intervals wrinkled; pedicel, flagellum, and prementum with minute dense punctures; stipes with minute sparse punctures; pronotal collar transversely wrinkled on anterior half and smooth on posterior half, with minute sparse punctures; coxae with small dense punctures; T1 anterior face and S2 with large sparse punctures; T1 dorsal face and T2 posteriorly with large shallow dense punctures interspersed with small punctures; T2 anteriorly to setal patch longitudinally coarsely puncto-striate.

Male. Unknown.

Type material. Holotype: INDIA • ♀; Tamil Nadu, Anaimalai, Top Slip; 550–800 m alt.; 2–5 Dec. 1978; JAP-IND CO TR [SEHU].

Distribution. India: Tamil Nadu.

Etymology. The specific name *nitens* is a Latin feminine adjective in the nominative case meaning bright. It refers to the metasoma of this new species ornamented with golden setal bands.

Remarks. By having the red head, dark legs, and slender T2, this new species is similar to *O. jabalpurensis* Das & Girish Kumar, 2016 and *O. vietnamica*. This new species differs from these two species by having the clypeal subtriangular area delimited by carinae only dorso-medially (subtriangular area delimited by carinae along its entire width in *O. vietnamica*; Figs 8, 9), hypostomal carina lamellately

projecting (sharp but not projecting in *O. vietnamica*), humeral carina obliterated (well developed in *O. jabalpurensis* and *O. vietnamica*), T1 with a complete pale setal band (T1 band medially interrupted in *O. jabalpurensis*; Fig. 12), T2 lacking medial spot (T2 with a medial pale setal spot in *O. jabalpurensis* and *O. vietnamica*; Figs 11, 12), T2 posterior half covered with dense appressed golden setae (T2 with a complete or medially interrupted setal band on posterior margin in *O. jabalpurensis* and *O. vietnamica*; Figs 11, 12), and T3 with a golden setal band (T3 with sparse erect black setae in *O. jabalpurensis*; Fig. 12).

Key to females of *Orientilla*

- 1 Mesopleuron evenly convex 2
- Mesopleuron laterally strongly produced to form large spine 9
- 2 Body black; mesopleuron with vertical carina extending from in front of mesocoxa to midway of mesopleuron; body punctures sparse. Solomon Islands.....
..... ***O. manni* (Krombein, 1971)**
- Body black with mesosoma or both head and mesosoma red; mesopleuron lacking vertical carina; body punctures large dense, longitudinally punctostriate on T2 3
- 3 Clypeal medial elevation and subventral transverse ridge forming T-shaped area; T2 lacking pale setal spot. China ***O. chinensis* (Zavattari, 1922)**
- Clypeal medial elevation forming subtriangular area (Fig. 8); T2 with medial pale setal spot (Fig. 11), if absent, then posterior half of T2 covered with dense golden setae (Fig. 12) 4
- 4 Head mostly red 5
- Head black 8
- 5 Legs largely red (Fig. 2); T1 as long as wide (Fig. 10); T2 lateral margin strongly convex (Fig. 10). Laos ***O. tamaderai* sp. nov.**
- Legs brownish to black; T1 wider than long (Figs 11, 12); T2 lateral margin weakly convex (Figs 11, 12) 6
- 6 Humeral carina obliterated; T2 lacking medial spot (Fig. 12); T2 posterior half covered with dense golden setae (Fig. 12). India..... ***O. nitens* sp. nov.**
- Humeral carina sharp; T2 with medial pale setal spot (Fig. 11); T2 posterior margin with complete or medially interrupted pale setal band (Fig. 11) 7
- 7 T1 and T2 posterior pale setal bands medially interrupted (Das and Girish Kumar 2016a: fig. 4); T2 medial pale setal spot small, distance between medial spot and posterior band apparently exceeding spot diameter (Das and Girish Kumar 2016a: fig. 4). India.....
..... ***O. jabalpurensis* Das & Girish Kumar, 2016**
- T1 and T2 posterior pale setal bands complete (Fig. 11); T2 medial pale setal spot large, distance between medial spot and posterior band subequal to spot diameter (Fig. 11). Laos, Myanmar, Thailand, Vietnam
..... ***O. vietnamica* Lelej, 1979**

- 8 Head lateral margins weakly convergent posteriorly (Lelej 1996a: fig. 1); length of S2 lateral felt line 1.2–1.3× distance between felt line and S2 posterior band. China, Taiwan, Myanmar (?), Vietnam ***O. desponsa* (Smith, 1855)**
- Head lateral margins strongly convergent posteriorly (Lelej 1996a: Fig. 2); length of S2 lateral felt line 0.4–0.6× distance between felt line and S2 posterior band. Vietnam ***O. krombeini* Lelej, 1996**
- 9 Body black with mesosoma red; T3 except lateral portion with black setae. India ***O. schmideggeri* Lelej, 2005**
- Body entirely black or with head and mesosoma red; T3 with pale setal band **10**
- 10 Head and mesosoma red (de Saussure 1867: fig. 1); scape black. India, Sri Lanka ***O. aureorubra* (Sichel & Radoszkowski, 1870)**
- Head and mesosoma black (Pagliano et al. 2020: fig. 190); scape reddish. Sri Lanka ***O. remota* (Cameron, 1897)**

Discussion

The genus *Orientilla* is closely related to *Stenomutilla*, only differing in the male mesoscutellum, tibial spurs, genital paramere, and female flagellum (Lelej 1996a). This hypothesis is supported by Waldren et al. (2023) in which the sister relationship of *Orientilla* and *Stenomutilla* was recovered by a phylogenomic framework examining seven out of ten dasylabrine genera. The *Stenomutilla* species parasitize on bees and wasps constructing their nests with mud or in pre-existing cavities (Bradley and Bequaert 1928; Ronchetti and Polidori 2020; Weaving 1994, 1995), except for few sub-Saharan and Malagasy species utilizing moth cocoons (Limaconidae, Lepidoptera) in the soil or on twigs (Bezzi 1924; Seyrig 1936; Paulian 1950; Bowden 1967; Krombein 1972). Like *Stenomutilla* (excluding some Malagasy species; Krombein 1972), the females of *Orientilla* lack the protarsal rake and defined pygidial plate, suggesting that they do not utilize ground-nesting hosts (Krombein 1972; Bayliss and Brothers 2001; Pitts and Manley 2004; Bartholomay et al. 2015; Brothers 2018; Taylor et al. 2019; Okayasu 2020).

In addition to the character states listed above, *O. nitens* sp. nov. and *O. tamaderai* sp. nov. are similar in their small body size. Specifically, *O. tamaderai* sp. nov. is the second smallest *Orientilla* species ever described after *O. manni* which measures only 5.4 mm (Krombein 1971). The body length of other *Orientilla* females ranges from 7.5 to 29 mm (de Saussure 1867; Sichel and Radoszkowski 1869–1870; Smith 1879; Cameron 1897; Nurse 1904; Chen 1957; Lelej 1979, 1996a; Das and Girish Kumar 2016a; Williams et al. 2019). Morphologically, *O. nitens* sp. nov. and *O. tamaderai* sp. nov. resemble *O. vietnamica*. However, these new species are comparable to or even smaller than the smallest specimen of *O. vietnamica*. Of the nine *O. vietnamica* females examined herein, only one specimen was 9.05 mm long and others exceeded

12 mm. Given that the body size of adult mutillids correlates with that of the host (Mickel 1924; Ferguson 1962), the size difference of those *Orientilla* species likely reflects utilization of different sized hosts. Additional data are apparently needed to test this hypothesis. I hope the key and descriptions in this paper will facilitate discovery of more *Orientilla* species and their hosts from the Oriental Region.

Acknowledgements

I thank: Kazunori Yoshizawa (Hokkaido University, Sapporo) for his comments on this paper; Riou Mizuno (Kagawa University, Takamatsu) and Yutaka Tamadera (Kyoto Prefectural University, Kyoto) for offering the material. This work was supported by Japan Society for the Promotion of Science under Grant-in-Aid for JSPS Fellows (Grant Number 23KJ0038).

References

- André E (1896) Notes pour servir a la connaissance de mutilles paléarctiques et description de quelques espèces nouvelles. Deuxieme partie (I). Mémoires de la Société Zoologique de France 9: 261–277.
- Bartholomay PR, Williams KA, Luz DR, Morato EF (2015) *Frigitilla* gen. nov., a new genus of Amazonian Mutillidae (Hymenoptera). Zootaxa 3957(1): 49–58. <https://doi.org/10.11646/zootaxa.3957.1.3>
- Bayliss PS, Brothers DJ (2001) Behaviour and host relationships of *Dolichomutilla scyrorax* (Smith, 1855) (Hymenoptera: Mutillidae, Sphecidae). Journal of Hymenoptera Research 10: 1–9.
- Bezzi M (1924) The Bombyliidae of the Ethiopian region based on material in the British museum (Natural History). British Museum (Natural History), 1–390.
- Bowden J (1967) Studies in African Bombyliidae. VI. A provisional classification of the Ethiopian Systropinae with descriptions of new and little known species. Journal of the Entomological Society of Southern Africa 30(2): 126–173.
- Bradley JC, Bequaert J (192) Synopsis of the Mutillidae of the Belgian Congo. Bulletin of the American Museum of Natural History 58(2): 63–122.
- Brothers DJ (2018) *Aglaotilla*, a new genus of Australian Mutillidae (Hymenoptera) with metallic coloration. Zootaxa 4415(2): 357–368. <https://doi.org/10.11646/zootaxa.4415.2.6>
- Brothers DJ (2022) Critical analysis of the type material of Mutillidae described from the Australasian Region (Hymenoptera). Zootaxa 5140(1): 1–215. <https://doi.org/10.11646/zootaxa.5140.1.1>
- Brothers DJ, Lelej AS (2017) Phylogeny and higher classification of Mutillidae (Hymenoptera) based on morphological reanalyses. Journal of Hymenoptera Research 60: 1–97. <https://doi.org/10.3897/jhr.60.20091>

- Cameron P (1897) Hymenoptera orientalia, or contributions to a knowledge of the Hymenoptera of the Oriental Zoological Region. Part V. Memoirs and Proceedings of the Manchester Literary and Philosophical Society 41(4): 1–144. [pls 3–4]
- Chen C-w (1957) A revision of the velvety ants or Mutillidae of China (Hymenoptera). Quarterly Journal of the Taiwan Museum 10(3–4): 135–224. [+ 6 pls]
- Das D, Girish Kumar P (2016a) Description of a new species of *Orientilla* Lelej, 1979 (Hymenoptera: Mutillidae: Dasytibrinae) from India. Journal of Entomological Research 40(1): 113–116. <https://doi.org/10.5958/0974-4576.2016.00021.9>
- Das D, Girish Kumar P (2016b) Velvet ants (Hymenoptera: Mutillidae) from Chhattisgarh, India. Records of the Zoological Survey of India 116(1): 89–92.
- de Saussure H (1867) Mutillarum novarum species aliquot. Annales de la Société Entomologique de France, quatrième série 7: 351–364. [pl. 8]
- Dinerstein E, Olson D, Joshi A, Vynne C, Burgess ND, Wikramanayake E, Hahn N, Palminteri S, Hedao P, Noss R, Hansen M, Locke H, Ellis EC, Jones B, Barber CV, Hayes R, Kormos C, Martin V, Crist E, Sechrest W, Price L, Baillie JEM, Weeden D, Suckling K, Davis C, Sizer N, Moore R, Thau D, Birch T, Potapov P, Turubanova S, Tyukavina A, De Souza N, Pintea L, Brito JC, Llewellyn OA, Miller AG, Patzelt A, Ghazanfar SA, Timberlake J, Klöser H, Shennan-Farpón Y, Kindt R, Lillesø JB, Van Breugel P, Graudal L, Vogé M, Al-Shammari KF, Saleem M (2017) An ecoregion-based approach to protecting half the terrestrial realm. BioScience 67(6): 534–545. <https://doi.org/10.1093/biosci/bix014>
- Ferguson WE (1962) Biological characteristics of the mutillid subgenus *Photopsis* Blake and their systematic values. University of California Publications in Entomology 27: 1–92.
- Hymenoptera Anatomy Consortium (2023) The Hymenoptera Glossary. <http://glossary.hy-mao.org/> [accessed 20 July 2023]
- Krombein KV (1971) A monograph of the Mutillidae of New Guinea, Bismarck Archipelago and Solomon Islands. Part 1: Mutillinae (Hymenoptera Aculeata). In: Asahina S, Linsley Gressitt J, Hidaka Z, Nishida T, Nomura K (Eds) Entomological Essays to Commemorate the Retirement of Professor K. Yasumatsu. Hokuryukan, Tokyo, 25–60.
- Krombein KV (1972) Monograph of the Madagascan Mutillidae (Hymenoptera). Part I: Myrmillini, Mutillini and Smicromyrmini. Annales, Musée Royal de l’Afrique Centrale, Série in 8°, Sciences Zoologiques 199: 1–61.
- Lelej AS (1979) A new genus of velvet ants (Hymenoptera, Mutillidae) from south-east Asia. Zoologicheskii Zhurnal 58(7): 1065–1067. [in Russian]
- Lelej AS (1996a) A review of the East Asian species of *Orientilla* (Hymenoptera, Mutillidae). Memoirs of the Entomological Society of Washington 17: 103–107.
- Lelej AS (1996b) A review of the East Asian species of *Mickelomyrme* Lelej, 1995 (Hymenoptera, Mutillidae). Entomofauna 17(15): 277–292.
- Lelej AS (2002) Catalogue of the Mutillidae (Hymenoptera) of the Palaearctic Region. Dalnauka, 1–172.
- Lelej AS (2005) Catalogue of the Mutillidae (Hymenoptera) of the Oriental Region. Dalnauka, 1–252.
- Lelej AS (2007) Biogeography of mutillid wasps (Hymenoptera, Mutillidae). In: Rasnitsyn AP, Gokhman VE (Eds) Studies on Hymenopterous Insects. Collection of Scientific Papers. KMK Scientific Press Ltd., Moscow, 82–111. [in Russian]

- Lelej AS (2023) Review of the tribe Ctenotillini (Hymenoptera: Mutillidae) from Oriental and Palaearctic Regions. *Far Eastern Entomologist* 480: 1–22. <https://doi.org/10.25221/fee.480.1>
- Lelej AS, Brothers DJ (2008) The genus-group names of Mutillidae (Hymenoptera) and their type species, with a new genus, new name, new synonymies, new combinations and lectotypifications. *Zootaxa* 1889: 1–79. <https://doi.org/10.11646/zootaxa.1889.1.1>
- Lelej AS, Williams KA, Terine JB, Okayasu J, Parikh G, Girish Kumar P (2023) Review of the tribe Mutillini (Hymenoptera: Mutillidae) from the Oriental Region. *Zootaxa* 5228(4): 455–476. <https://doi.org/10.11646/zootaxa.5228.4.5>
- Lelej AS, Zhou HT, Loktionov VM, Xu ZF (2016) Review of the genus *Promecidia* Lelej, 1996, with description of two new species from China (Hymenoptera, Mutillidae, Trogaspidiini). *ZooKeys* 641: 103–120. <https://doi.org/10.3897/zookeys.641.10765>
- Magretti P (1892) Viaggio di Leonardo Fea in Birmania e regioni vicine XLIII. Imenotteri. Parte prima. Mutillidei, Scoliidei, Tifidei, Tinnidei colla descrizione di parecchie nuove specie. *Annali del Museo Civico di Storia Naturale di Genova Serie 2* 12(32): 197–266. [+ pl. V.]
- Mickel CE (1924) An analysis of a bimodal variation in size of the parasite *Dasyutilla bioculata* Cresson (Hymen.: Mutillidae). *Entomological News* 35(7): 236–242.
- Mizuno R, Suttiprapan P, Jaitrong W, Ito F (2019) Daily and seasonal foraging activity of the Oriental non-army ant doryline *Cerapachys sulcinodis* species complex (Hymenoptera: Formicidae). *Sociobiology* 66(2): 239–246. <https://doi.org/10.13102/sociobiology.v66i2.3775>
- Nurse CG (1902) New species of Indian Hymenoptera. *Journal of the Bombay Natural History Society* 14(1): 79–92. [+ 1 pl]
- Nurse CG (1904) New species of Indian Hymenoptera. *Journal of the Bombay Natural History Society* 16(1): 19–26.
- Okayasu J (2018) Taxonomic review of Chin-wen Chen's species described in the genus *Smicromyrme* (Hymenoptera: Mutillidae: Smicromyrmini). *Acta Entomologica Musei Nationalis Pragae* 58(2): 479–494. <https://doi.org/10.2478/aemnp-2018-0036>
- Okayasu J (2020) Velvet ants of the tribe Smicromyrmini Bischoff (Hymenoptera: Mutillidae) of Japan. *Zootaxa* 4723(1): 1–110. <https://doi.org/10.11646/zootaxa.4723.1.1>
- Okayasu J (2023) Love is in the air and beyond the ocean: Taxonomic review of *Neotrogaspidia* Lelej (Hymenoptera: Mutillidae: Trogaspidiini) in Northeast Asia highlights its unique distributional pattern. *Entomological Science* 26(1): e12532. <https://doi.org/10.1111/ens.12532>
- Okayasu J, Lelej AS, Williams KA (2021a) Review of *Eotrogaspidia* Lelej (Hymenoptera: Mutillidae: Trogaspidiini). *Zootaxa* 4920(1): 56–90. <https://doi.org/10.11646/zootaxa.4920.1.2>
- Okayasu J, Williams KA, Lelej AS (2018) A remarkable new species of the genus *Sinotilla* Lelej (Hymenoptera: Mutillidae: Smicromyrmini) from Taiwan and an overview of color diversity in East Asian mutillid females. *Zootaxa* 4446(3): 301–324. <https://doi.org/10.11646/zootaxa.4446.3.1>
- Okayasu J, Williams KA, Lelej AS, Pham TH (2021b) Review of female *Andreimyrme* Lelej (Hymenoptera: Mutillidae: Smicromyrmini). *Zootaxa* 5061(1): 1–38. <https://doi.org/10.11646/zootaxa.5061.1.1>
- Olson DM, Dinerstein E, Wikramanayake ED, Burgess ND, Powell GVN, Underwood EC, D'Amico JA, Strand HE, Morrison JC, Loucks CJ, Allnutt TF, Lamoreux JF, Ricketts TH, Itoua I, Wettengel WW, Kura Y, Hedao P, Kassem K (2001) Terrestrial ecoregions

- of the world: A new map of life on Earth. *BioScience* 51(11): 933–938. [https://doi.org/10.1641/0006-3568\(2001\)051\[0933:TEOTWA\]2.0.CO;2](https://doi.org/10.1641/0006-3568(2001)051[0933:TEOTWA]2.0.CO;2)
- O'Toole C (1975) The systematics of *Timulla oculata* (Fabricius) (Hymenoptera, Mutillidae). *Zoologica Scripta* 4(1): 229–251. <https://doi.org/10.1111/j.1463-6409.1975.tb00733.x>
- Pagliano G, Brothers DJ, Cambra R, Lelej AS, Lo Cascio P, Matteini Palmerini M, Scaramozzino PL, Williams KA, Romano M (2020) Checklist of names in Mutillidae (Hymenoptera), with illustrations of selected species. *Bollettino del Museo Regionale di Scienze Naturali di Torino* 36(1–2): 5–425.
- Paulian R (1950) Recherches sur les insectes d'importance biologique de Madagascar. IX. *Stenomutilla splendida* OLS. (Hymen. Mutill.). Mémoires de l'Institut Scientifique de Madagascar, Série A 3(3): 389–391.
- Pitts JP, Manley DG (2004) A revision of *Lomachaeta* Mickel, with a new species of *Smicromutilla* Mickel (Hymenoptera: Mutillidae). *Zootaxa* 474: 1–27. <https://doi.org/10.11646/zootaxa.474.1.1>
- Ronchetti F, Polidori C (2020) A sting affair: A global quantitative exploration of bee, wasp and ant hosts of velvet ants. *PLoS ONE* 15(9): e0238888. <https://doi.org/10.1371/journal.pone.0238888>
- Seyrig A (1936) Un Mutillide parasite d'un Lépidoptère: *Stenomutilla freyi*. In: Livre Jubilaire de M. Eugène-Louis Bouvier, membre de l'Institut, professeur honoraire au Muséum. Firmin-Didot: 313–316. [+ pl. 14]
- Sichel J, Radoszkowski O (1869–1870) Essai d'une monographie des Mutilles de l'Ancion Continent. *Horae Societatis Entomologicae Rossicae* 6(3): 139–172. [(1869); 6(4): 173–309 + tabs; 6–11 (1870)]
- Smith F (1855) Catalogue of hymenopterous insects in the collection of the British Museum. Part III. Mutillidae and Pompilidae. Taylor and Francis: 1–206. [5 pls.] <https://doi.org/10.5962/bhl.title.20858>
- Smith F (1879) Descriptions of new species of Hymenoptera in the collection of the British Museum. Taylor and Francis, 1–240. <https://doi.org/10.5962/bhl.title.60089>
- Taylor CK, Murphy MV, Hitchen Y, Brothers DJ (2019) Four new species of Australian velvet ants (Hymenoptera: Mutillidae, *Aglaotilla*) reared from bee and wasp nests, with a review of Australian mutillid host records. *Zootaxa* 4609(2): 201–224. <https://doi.org/10.11646/zootaxa.4609.2.1>
- Terine JB, Das D, Girish Kumar P (2020) New distributional records of two species of *Orientilla* Lelej, 1979 (Hymenoptera: Mutillidae) from different Indian states. *Devagiri Journal of Science* 6(1): 15–20.
- Thaochan N, Williams KA, Thoawan K, Jeenthong T, Sittichaya W (2022) Three new species and one new country record of velvet ants (Hymenoptera, Mutillidae) from Thailand. *Journal of Hymenoptera Research* 93: 151–165. <https://doi.org/10.3897/jhr.93.94727>
- Waldren GC, Sadler EA, Murray EA, Bossert S, Danforth BN, Pitts JP (2023) Phylogenomic inference of the higher classification of velvet ants (Hymenoptera: Mutillidae). *Systematic Entomology* 48(3): 463–487. <https://doi.org/10.1111/syen.12588>
- Weaving AJS (1994) Nesting behaviour in three Afrotropical trap-nesting wasps, *Chalybion laevigatum* (Kohl), *Proepipona meadewaldoi* Bequaert and *Tricarinydynerus guerinii* (Sausure), (Hymenoptera: Sphecidae: Eumenidae). *The Entomologist* 113: 183–197.

- Weaving AJS (1995) A comparison of nesting success and nesting habitats in some Afrotropical aculeate wasps, with particular reference to nest parasites (Hymenoptera: Sphecidae, Eumenidae). *Annals of the Cape provincial Museums Natural History* 19(4): 181–224.
- Wikramanayake E, Dinerstein E, Loucks CJ, Olson DM, Morrison J, Lamoreux J, McKnight M, Hedao P (2002) *Terrestrial ecoregions of the Indo-Pacific: A conservation assessment*. Island Press, 1–643.
- Williams KA, Lelej AS, Okayasu J, Borkent CJ, Malee R, Thoawan K, Thaochan N (2019) The female velvet ants (aka modkhong) of southern Thailand (Hymenoptera: Mutillidae), with a key to the genera of southeast Asia. *Zootaxa* 4602(1): 1–69. <https://doi.org/10.11646/zootaxa.4602.1.1>
- Zavattari E (1914 [1913]) Mutille Austro-Malesi. *Bolletino della Societa Entomologica Italiana* 45: 61–114.
- Zavattari E (1922) Eine neue Mutille von China (Hym). *Entomologische Mitteilungen* 11(4): 1–192. <https://doi.org/10.5962/bhl.part.3338>
- Zhou HT, Lelej AS, Liu JX (2018) New records of velvet ants (Hymenoptera: Mutillidae) from China with taxonomic notes. *Far Eastern Entomologist* 354: 23–28. <https://doi.org/10.25221/fee.354.4>

Appendix I

Synoptic list of Mutillidae of Laos

Dasylabrinae

1. *Orientilla tamaderai* sp. nov.: Xieng Khouang (this paper).
2. *Orientilla vietnamica* Lelej, 1979: Vientiane (this paper).

Mutillinae: Ctenotillini

3. *Williamstillia guangdongensis* (Lelej, 1992): Bolikhamsay, Champasak (Williams et al. 2019; Lelej 2023).

Mutillinae: Mutillini

4. *Kurzenkotilla harmandi* (André, 1898): Sayaboury, Vientiane (Okayasu et al. 2018; Lelej et al. 2023).

Mutillinae: Smicromyrmini

5. *Andreimyrmex substriolata* (Chen, 1957): Houa Phan, Xieng Khouang (Okayasu 2020; Okayasu et al. 2021b).
6. *Andreimyrmex yotoi* Okayasu, 2021: Attapeu (Okayasu et al. 2021b).
7. *Mickelomyrme athalia* (Pagden, 1949): additional data unavailable (Lelej 2005).

8. *Mickelomyrme chinensis* (Smith, 1855): additional data unavailable (Brothers and Lelej 2017).
9. *Mickelomyrme exiloides* (Magretti, 1892): Vientiane (Lelej 1996b).
10. *Mickelomyrme kuznetsovi* Lelej, 1996: additional data unavailable (Brothers and Lelej 2017).
11. *Mickelomyrme pusillaeformis* (Hammer, 1962): Attapeu, Bolikhamsay, Luang Phabang (Okayasu 2018; Williams et al. 2019).
12. *Physetopoda thai* Lelej, 1995: Bolikhamsay (Williams et al. 2019).
13. *Smicromyrme triguttatus* Mickel, 1933: Lak Sao (Okayasu 2018).

Mutillinae: Trogaspidiini

14. *Eotrogaspidia auroguttata* (Smith, 1855): Houa Phan, Luang Phabang, Xieng Khouang (Okayasu et al. 2021a).
15. *Eotrogaspidia oryzae* (Pagden, 1934): Bolikhamsay (Okayasu et al. 2021a).
16. *Neotrogaspidia circumcincta* (André, 1896): Houa Phan, Xaisomboun, Xieng Khouang (Okayasu 2023).
17. *Promecidia birmanica* (Dalla Torre, 1897): additional data unavailable (Lelej 2005; Lelej et al. 2016).
18. *Trogaspidia lingnani* (Mickel, 1933): Attapeu, Khammouan (Williams et al. 2019).
19. *Trogaspidia pagdeni* Mickel, 1933: Attapeu, Bolikhamsay (Williams et al. 2019).
20. *Trogaspidia pittsi* Williams, 2019: Bolikhamsay (Williams et al. 2019).
21. *Trogaspidia wilsoni* Williams, 2019: Attapeu (Williams et al. 2019).
22. *Wallacidia oculata* (Fabricius, 1804): Bolikhamsay, Vientiane (O’Toole 1975; Williams et al. 2019).

Odontomutillinae

23. *Odontomutilla uranioides* Mickel, 1933: additional data unavailable (Okayasu et al. 2018).

Note: Pagliano et al. (2020) included *Sinotilla boheana* (Chen, 1957) in the Laotian fauna, but this species has not yet been formally recorded from this country.

An unexpected new species of *Anachrysis* Krombein, 1986 (Hymenoptera, Chrysididae, Amiseginae) from the Arabian Peninsula

Milo van Loon¹, Ahmed M. Soliman²

1 *Naturalis Biodiversity Center, P.O. 9517, 2300 RA, Leiden, Netherlands* **2** *Plant Protection Department, College of Food and Agriculture Sciences, King Saud University, P.O. BOX 2460, Riyadh 11451, Saudi Arabia*

Corresponding author: Milo van Loon (milo.vanloon@naturalis.nl)

Academic editor: Volker Lohrmann | Received 6 June 2023 | Accepted 22 August 2023 | Published 17 October 2023

<https://zoobank.org/9055C93D-232B-4032-BB4A-ACF3990349F9>

Citation: van Loon M, Soliman AM (2023) An unexpected new species of *Anachrysis* Krombein, 1986 (Hymenoptera, Chrysididae, Amiseginae) from the Arabian Peninsula. *Journal of Hymenoptera Research* 96: 835–846. <https://doi.org/10.3897/jhr.96.107489>

Abstract

Anachrysis arabica **sp. nov.**, a new chrysidid species from Saudi Arabia and Yemen, is described and illustrated. The new species represents the first record of the subfamily Amiseginae in the Arabian Peninsula. A key to species of the genus is provided. The phylogenetic position of *Anachrysis* within the subfamily is briefly discussed.

Keywords

Afrotropics, description, key, Saudi Arabia, Yemen

Introduction

The Amiseginae are an unusual group of chrysidids with a pantropical distribution. Together with the related subfamily Loboscelidiinae, they are the only aculeate wasps known to parasitize phasmid eggs (Kimsey and Bohart 1991). Due to their parasitoid lifestyle, the distribution of Amiseginae is bound to that of their phasmid hosts. Krombein (1983) charted the zoogeography of the Amiseginae, as well as the distribution of the Phasmatodea. Notably, the Amiseginae are absent from the Mediterranean

subregion, as well as from the Arabian Peninsula (Rosa et al. 2020), although some species of Phasmatodea are recorded. Despite extensive collecting in these regions, no Amiseginae had been collected and their absence in the aforementioned regions seemed to be well established. Recent collecting carried out in Southwestern Saudi Arabia and Yemen revealed an undescribed species of *Anachrysis* Krombein. Despite the southern part of the Arabian Peninsula having strong ties to the Afrotropical fauna (e.g. Olmi and van Harten 2000; van Achterberg 2011; Fernández-Triana and van Achterberg 2017; Saure et al. 2017), the presence of *Anachrysis* is nonetheless unexpected considering the known distribution of the genus. The *Anachrysis* was described from a single species, *Anachrysis paradoxa* Krombein, one male from Transvaal, South Africa, and four females from Serowe, Botswana (Krombein 1986). A second species was recognized by Kimsey and Bohart (1991) from the same collecting event in Transvaal and later described by Krombein (1994) as *Anachrysis spanglerorum* which is known from the holotype male only. Both species were collected in open savannah. *Anachrysis* differs quite drastically from the other Afrotropical Amiseginae, in which both the female and male are apterous and possess a highly modified mesosoma. The fully winged state of both sexes and the short metanotum of *Anachrysis* are reminiscent of the morphology of the plesiomorphic New World Amiseginae, which include *Adelphé* Mocsáry, 1890, *Amisega* Cameron, 1888, *Anadelphé* Kimsey, 1987, and *Duckeia* Costa Lima, 1936.

Material and method

The present study is based on *Anachrysis* specimens collected from Jazan region (Southwestern Saudi Arabia) and Lahj and Sana'a governorates (Yemen), using Malaise traps. The specimens were examined using a MEIJI-EMZ-10 stereomicroscope (up to 180× magnification) fitted with an ocular micrometer for measurements and an Olympus SZ40 stereomicroscope.

Photographs, except that of male genitalia, were taken with a Canon EOS 70D camera attached to a LEICA MZ 125 stereomicroscope. Individual source images were then stacked using the extended depth-of-field software Helicon Focus (ver. 7.6). The male genitalia are imaged using an auto-montage software system (Syncroscopy, Cambridge, UK) attached to a phase contrast microscope (DM2500, Leica, Germany). Further image processing was completed with Adobe Photoshop CS5.1 (ver. 12.1.0.0) and Adobe Photoshop Lightroom 5.2 × 64 (ver. 5.2.0.10) software programs.

Morphological terminology largely follows Kimsey and Bohart (1991). The “scrobal sulcus” and “omalus” in Kimsey & Bohart are instead named oblique posterior sulcus following Mita (2022) for the former and prepectal carina for the latter in the present description. The terminology adopted for wing cells and veins follows Huber and Sharkey (1993). Body sculpture terminology follows Harris (1979).

The following abbreviations are used: **AOD**, anterior ocellus diameter; **F1**, **F2**, **F3**, **etc.**, first, second, third, etc. antennal flagellomeres; **IOL**, interocular distance at minimum width; **MT**, malaise trap; **OOL**, inner distance between posterior ocellus

and eye; **OPL**, minimal distance between posterior ocellus and occiput; **POL**, inner distance between posterior ocelli; **S1, S2, S3, etc.**, first, second, third, etc. metasomal sterna; **T1, T2, T3, etc.**, first, second, third, etc. metasomal terga. **Forewing cells and veins**: **2R1**, second radial 1 cell; **R**, radial cell; **1m-cu**, first median-cubital cross-vein; **Cu**, cubital vein; **cu-a**, cubital-anal cross-vein; **M**, median vein; **M+Cu**, median+cubital vein; **Rs+M**, radial sector+median vein.

A single slash (/) represents a new line on the same label, whereas a double slash (//) represents the separation of labels. The material belongs to the following depositories: **KSMA**, King Saud University Museum of Arthropods, Riyadh, Saudi Arabia; **PRPC**, Paolo Rosa private collection, Bernareggio (Italy); **RMNH**, Naturalis Biodiversity Center, Leiden, the Netherlands.

Results

Genus *Anachrysis* Krombein, 1986

Type species. *Anachrysis paradoxa* Krombein, 1986 by original designation.

Diagnosis. Antennal flagellum fusiform (female) or filiform (male). Malar space with vertical sulcus. Male mandible broad basally and foliaceous (Γ -shaped in lateral view), edentate apically. Occipital carina absent. Pronotum flattened, with a furrow posteromedially. Metanotum short, without median enclosure. Propodeum posterolaterally rounded, not angulate. Mesopleuron with prepectal carina, without posterior oblique sulcus. Rs stub of forewing extended by more or less curved dark streak.

Anachrysis arabica van Loon & Soliman, sp. nov.

<https://zoobank.org/6FF256F7-9C68-4D21-A11B-4727D4AC4C55>

Figs 1–4

Type material. **Holotype** ♂: SAUDI ARABIA / Jazan / Ahad Almasarhah / Alkhoms [16°46'14.42"N, 42°46'15.94"E, alt. 20 m] // 21.v.2022, MT / Leg. Ahmed M. Soliman [KSAM]; **Paratypes**: 2♂ and 3♀ same data as holotype [KSAM]; 1♂ and 1♀ same data as holotype [PRPC]; 1♂, SAUDI ARABIA / Jazan / Farasan Island / site 2, 14.iv.2016, MT / Leg. H. Dawah [KSMA]; 1♂, YEMEN / Lahj, xi.2000, MT / no. 5202, Leg. A. v. Harten / & A. Sallam [RMNH]; 1♂ and 3♀, YEMEN (7585) / 12 km NW Manakhah / 15.v–23.vi.2003, MT / Leg. A. v. Harten [RMNH].

Diagnosis. Vertex with two large impunctate and polished swellings (Figs 1C, 2A, 3B). Gena narrowing gradually from mandibular base to upper limit of eye (Figs 1D, 3A). Scapal basin deep, transversally ridged (Figs 1C, 3C). Lateral lobe of male clypeus lamellate, acute at apex and translucent white in color (Fig. 1C). Pronotum and mesoscutum coarsely and densely setiferous foveate, interspaces polished (Figs 2A, B, 4A, B). Pronotum posteromedially with deep short groove (Figs 2A, 4A). Scutellum sparsely

setiferous punctate, interspaces polished (Figs 2A, 4A). Propodeum with longitudinal median fine carina (Figs 2A, 4A). T1–4 densely punctate (punctures on T4 minute), interspaces polished (Figs 2D, E, 3B, 4C). Body metallic blue, with reddish to reddish brown tint on mesepisternum, metasomal venter and legs (Figs 1A, B, 2F, 3A, B, 4E).

Description. Male (Figs 1–2): Body length 3–4 mm; forewing length 2.2–2.5 mm.

Head. In frontal view about as long as wide, distinctly narrowed ventrally, somewhat triangular (Fig. 1C). Vertex with two large polished swellings directly behind posterior ocelli, posteriorly moderately declivous and setiferous foveate-subreticulate, foveae about $0.3\times$ AOD (Figs 1D, 2A). Ocellar triangle equilateral (Fig. 1C). OOL $1.5\times$ AOD; POL $2\times$ AOD; OPL about $5\times$ AOD (Figs 1C, 2A). Occiput without occipital carina (Fig. 2A). Temple evenly rounded behind eye, about $1.5\times$ AOD (Fig. 1D). Frons setiferous foveate-subreticulate (foveae about $0.5\times$ AOD), bulging on either side of scapal basin; scapal basin relatively small but deeply depressed and transversally ridged, with longitudinal median ridge (Fig. 1C). IOL $0.4\times$ as long as head width (Fig. 1C). Eyes distinctly diverging ventrally, bare, about $1.25\times$ as high as wide (Fig. 1C, D). Subantennal distance relatively long, $2.8\text{--}3.0\times$ AOD (Fig. 1C). Clypeus broad, about $2\times$ as wide as long, slightly convex and punctulate on disc, depressed and polished along subapical rim, trilobate apically; median lobe acutely rounded apically; lateral lobe moderately large and thin (lamellate), broadly triangular and pointed towards apical end (Fig. 1C). Malar space long, $4.5\text{--}5.0\times$ AOD, sparsely punctate, with well-developed vertical sulcus (Fig. 1D). Gena gradually narrowed towards the temple, its width about $1.5\times$ AOD at its mid-length, densely foveate (Fig. 1D). Flagellum long, filiform, flagellomeres cylindrical and gradually decreasing in length distally; F1 longest, $5.0\text{--}5.2\times$ as long as wide; F2 $3.5\text{--}3.8\times$ as long as wide; F3 about $3.5\times$ as long as wide; F11 about $4.5\times$ as long as wide (Fig. 1E). Mandible flattened, broad and incised near base, tapering and edentate apically (Fig. 1C, D). Palpal formula $3/4$.

Mesosoma. About $2.5\times$ as long as maximum width at the level of mesopleuron (Fig. 2A), relatively flat in lateral view (Fig. 2B). Pronotum wider than long, about $1.2\times$ (Fig. 2A), with anterior shelf longitudinally ridged, dorsal face setiferous foveate-reticulate to subreticulate (foveae about $0.7\times$ AOD), humeral angles evenly rounded (Fig. 2A) and lateral lobe not reaching tegula (Fig. 2B), posteromedially with deep short groove (Fig. 2A). Mesoscutum shorter than pronotum, about $0.7\times$, setiferous foveate-subreticulate (Fig. 2A); notauli complete, anteriorly strongly diverging towards pronotal lobes (Fig. 2A); parapsides reaching anterior fourth of mesoscutum (Fig. 2B). Tegula oval and polished (Fig. 2A). Scutellum about $0.7\times$ as long as mesoscutum, setiferous sparsely punctate (Fig. 2A); interspaces between foveae and punctures on pronotum, scutum and scutellum polished (Fig. 2A, B); metanotum about $0.3\times$ as long as scutellum, longitudinally ridged (Fig. 2A). Propodeum areolate, posterolaterally evenly rounded (without lateral angle), with longitudinal median fine carina extended on both faces (Fig. 2A, D), propodeal dorsal face about $0.9\times$ as long as scutellum and metanotum combined (Fig. 2A), posterior face in lateral view rather abruptly declivitous (Fig. 2B). Mesopleuron gradually differs from being foveate on dorsal face to sparsely punctate on ventral face (Fig. 2B, F), with prepectal carina (Fig. 2B).

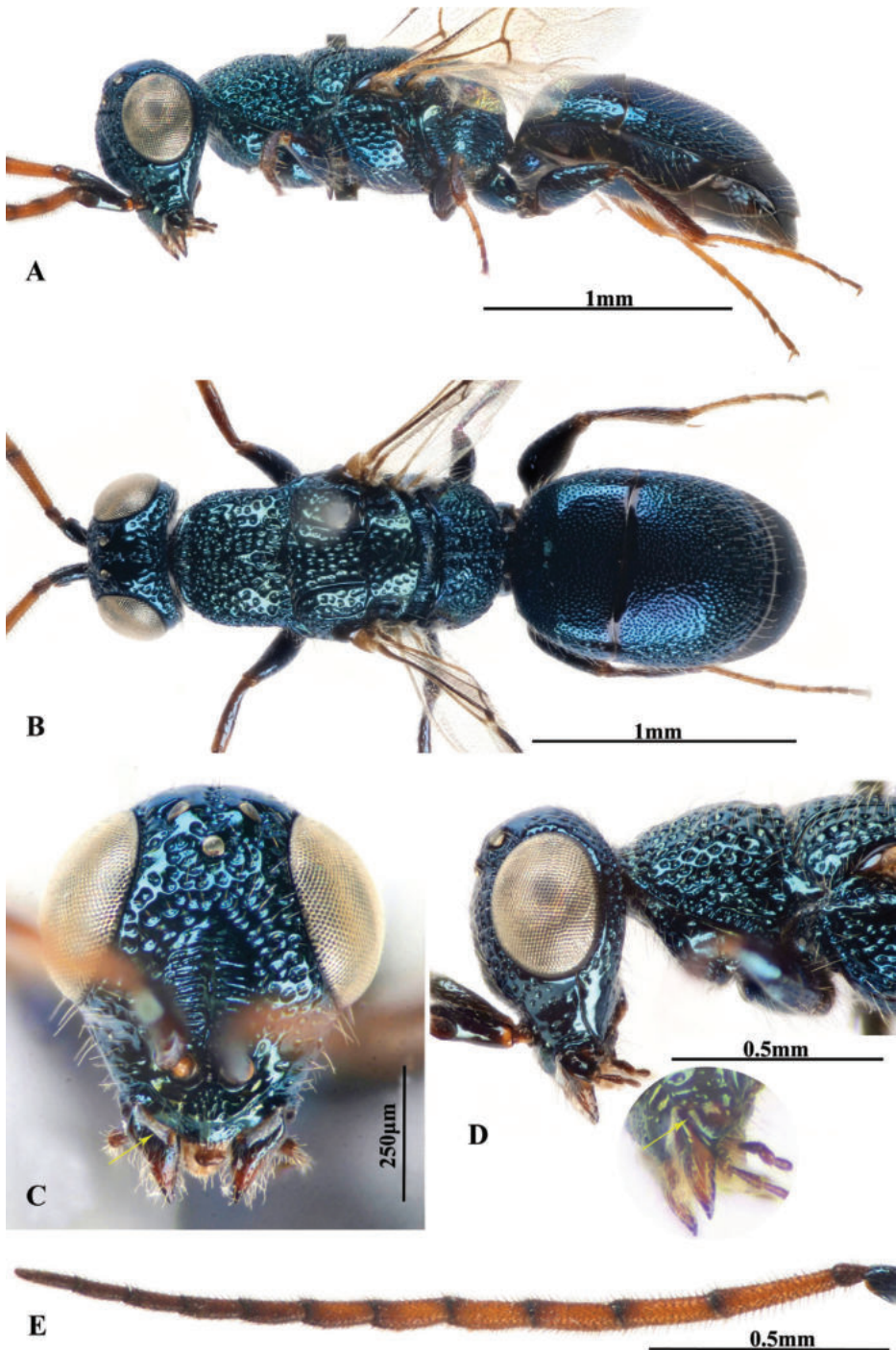


Figure 1. *Anachrysis arabica* van Loon & Soliman, sp. nov., holotype ♂ **A** habitus, lateral view **B** habitus, dorsal view **C** head, frontal view (clypeal lateral lamella indicated) **D** head and pronotum, lateral view (mandible is magnified, mandibular subbasal incision indicated) **E** antenna (part of scape).

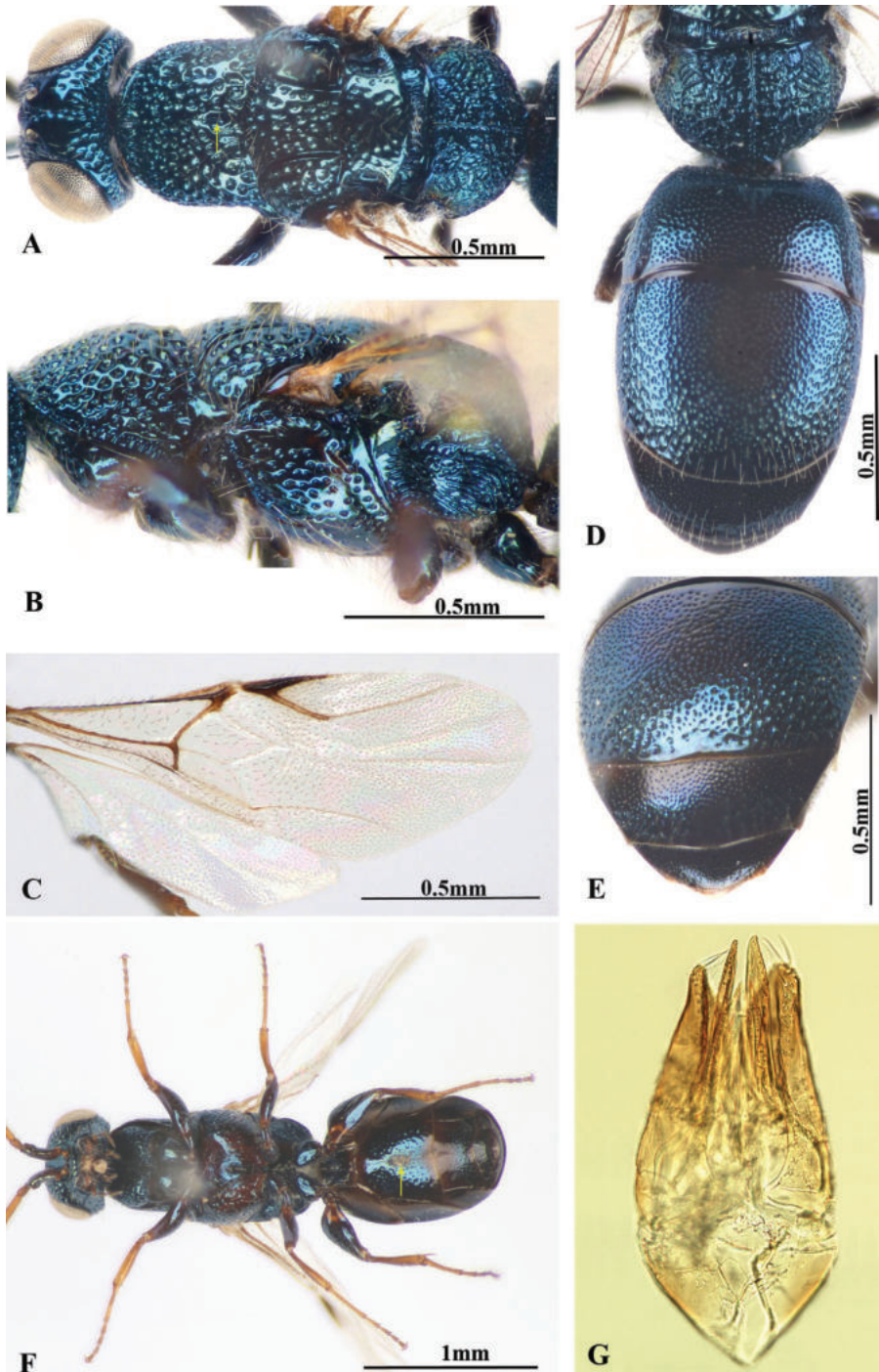


Figure 2. *Anachrysis arabica* van Loon & Soliman, sp. nov., holotype ♂ **A** head and mesosoma, dorsal view (pronotal posteromedian groove indicated) **B** mesosoma, lateral view **C** wings **D** propodeum and metasoma, dorsal view **E** metasomal T2–5, dorsal view **F** habitus, ventral view **G** genitalia, ventral view.

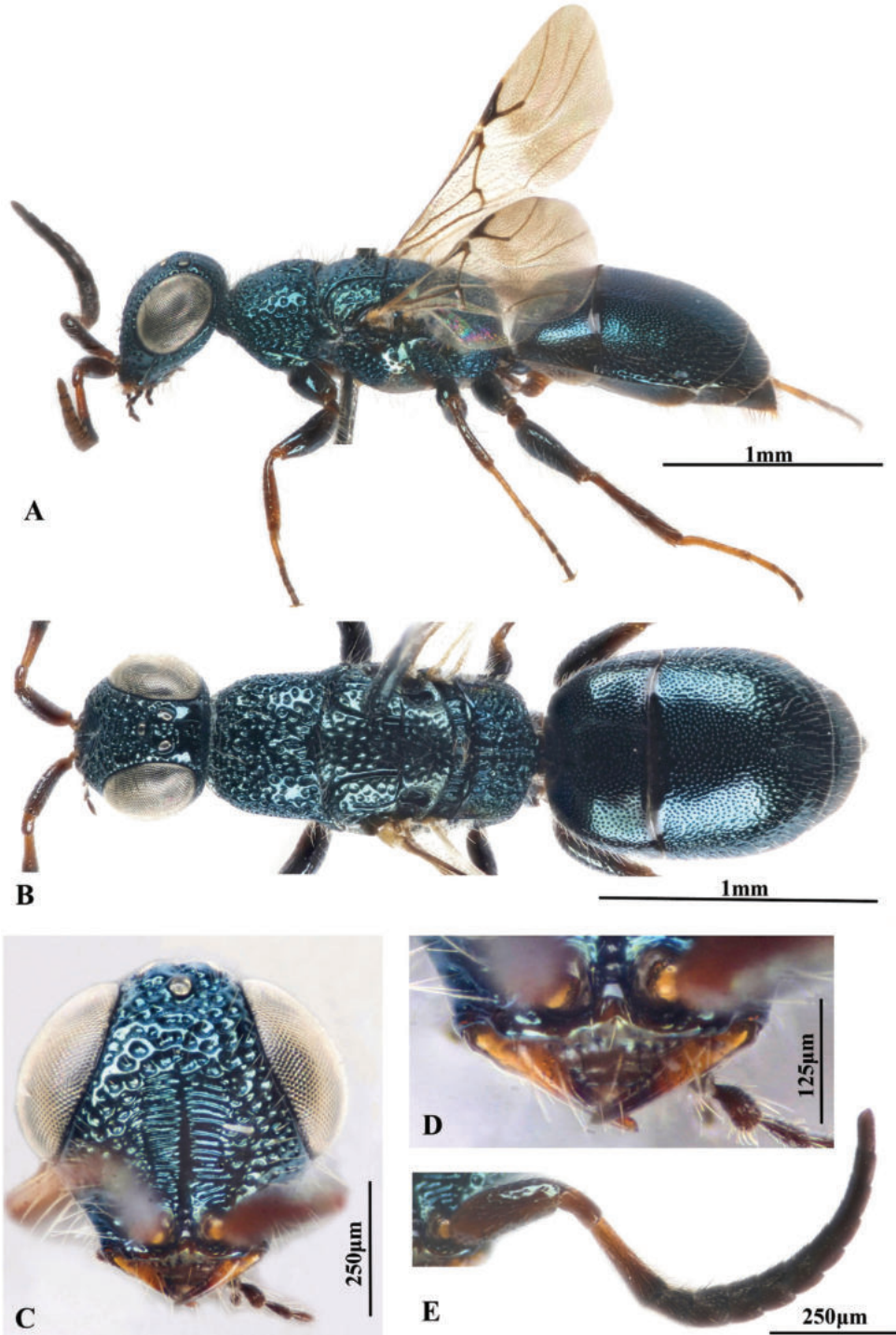


Figure 3. *Anachrysis arabica* van Loon & Soliman, sp. nov., paratype ♀ from Saudi Arabia **A** habitus, lateral view **B** habitus, dorsal view **C** head, frontal view **D** mandibles and clypeus **E** antenna.

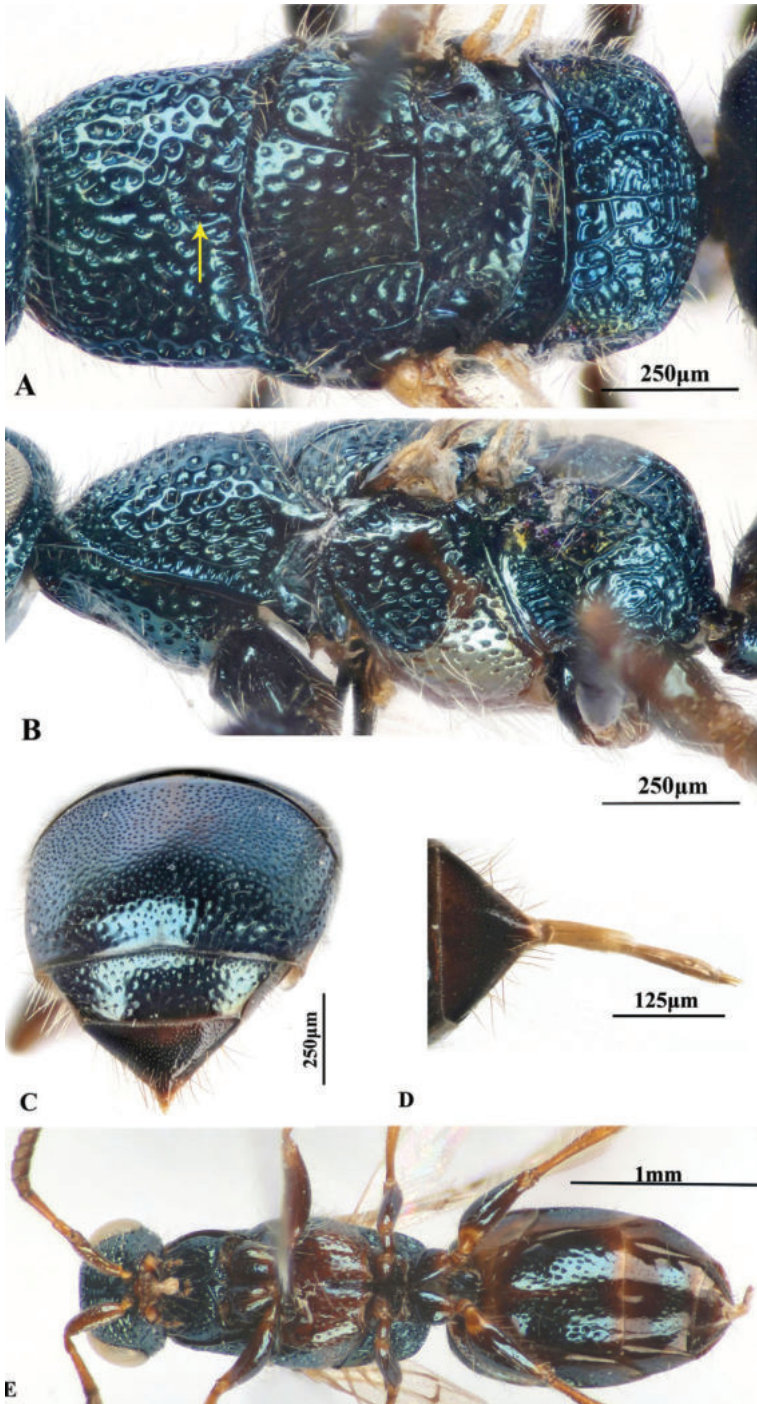


Figure 4. *Anachrysis arabica* van Loon & Soliman, sp. nov., paratype ♀ from Saudi Arabia **A** mesosoma, dorsal view (pronotal posteromedian groove indicated) **B** mesosoma, lateral view **C** metasomal T2–5, dorsal view **D** T4 and ovipositor **E** habitus, ventral view.

Forewing (Fig. 2C). R and 1Cu cells fully sclerotized. M1 cell delimited with faint veins except proximal M well sclerotized. Stub of Rs particularly well sclerotized (thick), about 0.7× as long as pterostigma and R1 combined. M vein slightly curved, meets M+Cu before cu-a.

Hind leg (Figs 1A, 2F). Femur 2.3–2.5× as long as its maximum width, with dorsal margin basally strongly swollen then gradually narrowing towards apical end.

Metasoma. T1 about 0.5× and 1.5× as long as T2 and T3 respectively, anterolaterally gently rounded (Fig. 2D). T1–4 punctulate (punctures on anterior half of T3 and T4 minute), interspaces polished (Fig. 2D, E). T2 with posterior margin strongly convex (Fig. 2D). T5 extremely small, greatly concealed (Fig. 2E). S2 punctulate on disc, polished on edges, with posterior margin slightly emarginate medially (Fig. 2F). S3–4 minutely punctate, S3 polished on anterior half (Fig. 2F).

Genital capsule. As in Fig. 2G.

Pilosity. Body rather sparsely setose throughout, with erect to suberect white fine setae (about 1.5–2× AOD in length) (Figs 1A, C, D, 2B, D), except male antennal flagellomeres particularly with dense short reddish setae (Fig. 1E) and male S2 with circular central area of dense recumbent setae (Fig. 2F). Setae longest on fore coxa and femur and hind femur. Wings with brown macrotrichiae on both sides, denser on distal half than elsewhere (Fig. 2C).

Color. Body metallic blue (Figs 1A, B, 2F), except following parts: apical half of mandible (Fig. 1C), labial and maxillary palps (Fig. 1D), F7–11 (Fig. 1E), small to large marking on mesepisternum and metasomal sternal borders reddish to reddish brown (Fig. 2F); ventral aspect of tibiae, entire tarsi and F1–6 orange (Figs 1A, E, 2F); lateral lamella of clypeus whitish and largely translucent (Fig. 1C); anterior rim of T2, anterior half of T3 and T4 with black tint (Fig. 2D, E). Wings hyaline, veins and pterostigma brown to dark brown (Fig. 2C).

Female (Figs 3, 4): Body length 3–3.5 mm; forewing length about 2.3 mm.

Similar to male, but differs as follows: Subantennal distance distinctly shorter, 0.9–1.0× AOD (Fig. 3C); clypeus without lateral lamella (apically not trilobate), with free margin truncate (Fig. 3D); mandible simple, rather slender and subbasally entire (without incision) (Fig. 3D); flagellum fusiform and distinctly shorter (F2–8 widened, at least as long as wide), ventral surface of F3–11 flattened, pedicel and F1 reddish brown, F2–11 dark brown to blackish (Fig. 3E); frons in lateral view more strongly bulging (Fig. 3A); reddish marking on mesepisternum extensive and lighter (Fig. 4E); forewing slightly infumate, brown, on distal half (Fig. 3A); distal veins, Cu, Rs+M and 1 m-cu of M1 cell extremely faint (nearly absent) (Fig. 3A); S2 sparsely setose throughout (without central area of dense recumbent setae) (Fig. 4E); metasoma with slender ovipositor (Fig. 4D).

Distribution. Southwestern Saudi Arabia and Yemen.

Etymology. The specific name *arabica* is a Latin adjective derived from Arabian Peninsula, referring to the subregion where the species has been found.

The following key can be used for differentiation between *Anachrysis* species: the new species *A. arabica* (Saudi Arabia and Yemen), *A. paradoxa* Krombein, 1986 (Botswana and South Africa) and *A. spanglerorum* Krombein, 1994 (South Africa).

Key to the species of *Anachrysis* Krombein

Males

- 1 Vertex with impunctate and polished swellings behind posterior ocelli. Punctuation of body sparse to subreticulate, not reticulate. Pronotum posteriorly without transverse carina..... *Anachrysis arabica* **sp. nov.**
- Vertex entirely foveate-reticulate, without such swellings. Punctuation of body dense and reticulate, especially on head. Pronotum posteriorly with a transverse carina on each side of posteromedian groove **2**
- 2 Clypeus without lateral reflexed lamella, with median lobe gently arched. Mesepisternum largely reddish to reddish brown. T2 with a narrow polished longitudinal median streak on anterior two-thirds.....
..... *Anachrysis spanglerorum* **Krombein**
- Clypeus with distinct lateral reflexed lamella and median lobe sharply arched. Mesepisternum uniformly metallic blue. T2 evenly punctate, without polished longitudinal median streak..... *Anachrysis paradoxa* **Krombein**

Females (female of *A. spanglerorum* Krombein unknown)

- 1 Vertex with impunctate and polished swellings behind posterior ocelli. Clypeal apical margin truncate. Gena evenly curved behind eye, not angulate. Pronotum posteriorly without transverse carina. Mesoscutum and scutellum in lateral view flattened, the latter sparsely punctate. Mesepisternum ventrally and laterally partially reddish to reddish-brown *Anachrysis arabica* **sp. nov.**
- Vertex entirely foveate-reticulate, without such swellings. Clypeal apical margin evenly rounded. Gena abruptly widened, with obtuse angulation, behind lower third of eye height. Pronotum posteriorly with transverse carina on each side of posteromedian groove. Mesoscutum and scutellum in lateral view convex, the latter foveate-reticulate. Mesepisternum uniformly metallic blue *Anachrysis paradoxa* **Krombein**

Discussion

All specimens of *Anachrysis arabica* sp. nov. were collected in southwestern Saudi Arabia (Jazan and Farasan Island) and western Yemen (Lahj and Sana'a). The position of the Arabian Peninsula in relation to the faunal regions of the world is rather unique, as it is situated at the junction of three different biogeographical realms with the southern part of the Peninsula having Afrotropical affinities (Gadallah and Brothers 2020). Conditions in west Yemen superficially resemble those of the African savanna, with the average annual rainfall in the western highlands ranging between 200 to 500 mm (Hadden 2012), which is about the same as the annual rainfall in the southern Afrotropical open savanna where *Anachrysis paradoxa* Krombein was collected. Hosts of any species of *Anachrysis* are un-

known, but since all female Amiseginae have narrow and pointed mandibles, presumably used to pierce the tough outer layer of phasmid eggs, it is likely that *Anachrysis* also parasitizes phasmid eggs. *Anachrysis* shares the lateral lamellate process of the clypeus and the foliaceous mandibles of the male with *Adelphæ* Mocsáry and possibly *Anadelphæ* Kimsey. These features are not seen in any other Amiseginae and are likely synapomorphic traits. The alleged lack of a lateral lamellate process of the male clypeus in *Anachrysis spanglerorum* is notable. Nevertheless, since it is present in both the closely related *A. paradoxa* and the relatively more distantly related *A. arabica*, its absence is very likely not plesiomorphic. This new discovery reaffirms the notion by Krombein (1986) that *Anachrysis* is a relict genus lacking synapomorphies with the more derived Afrotropical Amiseginae and instead shares synapomorphies (e.g. the derived mandible shape of the males and the short metanotum) with the New World Amiseginae. The discovery of a species of *Anachrysis* in the Arabian Peninsula and its previous known presence in southern Africa indicate that the distribution of *Anachrysis* is much broader than previously thought. The Amiseginae very likely had a northern origin (Kimsey 1990) and fossil evidence, of which primitive species have been exclusively found in the Northern Hemisphere, seems to support this hypothesis (Krombein 1986; Martynova and Perkovsky 2017). The presence of *Anachrysis* in the Northern Hemisphere might provide us with a better understanding of how those basal lineages spread to the Southern Hemisphere. Further sampling with malaise traps in the Arabian Peninsula as well as southern and particularly eastern Africa is recommended and will almost certainly lead to the discovery of more species of *Anachrysis*.

Acknowledgements

Sincere gratitude to Paolo Rosa (University of Mons, Belgium), Flor Rhebergen (University of Amsterdam, The Netherlands), Cees van Achterberg (Naturalis Biodiversity Center, The Netherlands), Simon van Noort (Iziko Museums, South Africa), Lynn Kimsey (University of California, United States of America) and an anonymous reviewer for their critical comments, which helped improve the quality of the manuscript. The authors thank Tony van Harten (Vaiamonte, Portugal) for providing additional information regarding the type localities and Hathal Al Dhafer (King Saud University, Saudi Arabia) for his support in collecting specimens. This study was supported financially by Stichting Fonds Pontium.

References

- Fernández-Triana J, van Achterberg C (2017) Order Hymenoptera, family Braconidae. Subfamily Microgastrinae from the Arabian Peninsula. In: van Harten A (Ed.) Arthropod fauna of the United Arab Emirates 6: 275–321.
- Gadallah NS, Brothers DJ (2020) Biodiversity of the aculeate wasps (Hymenoptera: Aculeata) of the Arabian Peninsula: Overview. *Zootaxa* 4754(1): 8–16. <https://doi.org/10.11646/zootaxa.4754.1.4>

- Hadden RL (2012) *The Geology of Yemen: An Annotated Bibliography of Yemen's Geology, Geography and Earth Science*. Army Geospatial Center, US Army Corps of Engineers, Alexandria, Virginia, 330 pp.
- Harris RA (1979) A glossary of surface sculpturing. *California Department of Food & Agriculture Occasional Papers in Entomology* 28: 1–31. <https://doi.org/10.5281/zenodo.26215>
- Huber J, Sharkey MJ (1993) Chapter 3 Structure. In: Goulet A, Huber JT (Eds) *Hymenoptera of the World. An Identification Guide to Families*. Agriculture Canada, 13–59.
- Krombein KV (1983) *Biosystematic Studies of Ceylonese Wasps, XI: A Monography of the Amiseginae and Loboscelidiinae (Hymenoptera: Chrysididae)*. *Smithsonian Contributions to Zoology* 376: 1–79. <https://doi.org/10.5479/si.00810282.376>
- Krombein KV (1986) A remarkable new African amisegine wasp (Hymenoptera: Chrysididae: Amiseginae). *Proceedings of the Entomological Society of Washington* 88: 509–514.
- Krombein KV (1994) A new *Anachrysis* from South Africa (Hymenoptera: Chrysididae: Amiseginae). *Proceedings of the Entomological Society of Washington* 96: 339–341.
- Kimsey LS (1990) Zoogeography of the Amiseginae and a remarkable new chrysidid wasp from Chile (Hymenoptera). *Psyche* 97: 141–146. <https://doi.org/10.1155/1990/48413>
- Kimsey LS, Bohart RM (1991) *The Chrysidid Wasps of the World*. Oxford Science Publications, New York.
- Martynova KV, Perkovsky EE (2017) Two new genera of cuckoo wasps (Chrysididae: Amiseginae) from Rovno and Baltic ambers. *Paleontological Journal* 51(4): 382–390. <https://doi.org/10.1134/s0031030117040074>
- Mita T (2022) Taxonomy of *Perissosega* Krombein (Hymenoptera: Chrysididae, Amiseginae), with description of a new species from Japan. *Zootaxa* 5169(3): 279–285. <https://doi.org/10.11646/zootaxa.5169.3.4>
- Olm M, van Harten T (2000) Dryinidae, Embolemidae and Sclerogibbidae (Hymenoptera: Chrysididae) of Yemen, with revised keys to the species of the Arabian Peninsula. *Fauna of Arabia* 21: 307–337.
- Rosa P, Gadallah NS, Brothers DJ (2020) Biodiversity of the aculeate wasps (Hymenoptera: Aculeata) of the Arabian Peninsula: Chrysididae, Chrysididae. *Zootaxa* 4754(1): 101–121. <https://doi.org/10.11646/zootaxa.4754.1.10>
- Saure C, Schmid-Egger C, van Achterberg C (2017) Order Hymenoptera, family Gasterurptidae. In: van Harten A (Ed.) *Arthropod fauna of the United Arab Emirates* 6: 190–224.
- van Achterberg C (2011) Order Hymenoptera, family Braconidae. The subfamily Agathidinae from the United Arab Emirates, with a review of the fauna of the Arabian Peninsula. *Arthropod fauna of the UAE* 4: 286–352.

Three new species of *Amphibulus* Kriechbaumer (Hymenoptera, Ichneumonidae, Phygadeuontinae) from China with a key to species known from the Oriental and Eastern Palaearctic Regions

Tao Li¹, Zai-Hua Yang², Shu-Ping Sun¹, Mao-Ling Sheng¹

1 Center for Biological Disaster Prevention and Control, National Forestry and Grassland Administration, 58 Huanghe North Street, Shenyang 110034, China **2** Guizhou Academy of Forestry, Guiyang, Guizhou, 550005, China

Corresponding author: Mao-Ling Sheng (shengmaoling@163.com)

Academic editor: Tamara Spasojevic | Received 4 July 2023 | Accepted 15 October 2023 | Published 20 October 2023

<https://zoobank.org/5F7DA036-1B00-4FCF-9FE4-A8ACA8253992>

Citation: Li T, Yang Z-H, Sun S-P, Sheng M-L (2023) Three new species of *Amphibulus* Kriechbaumer (Hymenoptera, Ichneumonidae, Phygadeuontinae) from China with a key to species known from the Oriental and Eastern Palaearctic Regions. Journal of Hymenoptera Research 96: 847–862. <https://doi.org/10.3897/jhr.96.108825>

Abstract

Three new species of *Amphibulus* Kriechbaumer, 1893, collected from the northern border of the Oriental part of China, are described and illustrated: *A. areolaris* Sheng, Li & Yang, **sp. nov.**, *A. rufithorax* Sheng, Li & Yang, **sp. nov.** collected from Guizhou province, and *A. guiiicus* Sheng, Li & Sun, **sp. nov.** collected from Guangxi Zhuang Autonomous Region. A key to the species of the genus known in the Oriental and Eastern Palaearctic Regions is provided.

Keywords

Asia, Endaseina, Guangxi, Guizhou, taxonomy

Introduction

The subfamily Phygadeuontinae (Hymenoptera, Ichneumonidae) was raised to subfamily status from within Cryptinae by Santos (2017), which was corroborated by Bennett et al. (2019) and followed by other authors (e.g., Broad et al. 2018).

Amphibulus Kriechbaumer is a relatively small genus belonging to the subfamily Phygadeuontinae (Hymenoptera, Ichneumonidae) currently comprising 27 species (Yu et al. 2016), of which four are from the Eastern Palaearctic (one of which also occurring in the Oriental Region), two from the Western Palaearctic, six from the Nearctic, two from the Oriental Region (Luhman 1991), one from the Afrotropical and 15 from the Neotropical Region (Yu et al. 2016).

Sawoniewicz (1990) revised the European species of the genus. More species and a revision and a key to the species of the world *Amphibulus* was reported by Luhman (1991). Three species, *A. albimaculatus* Sheng, 1999, *A. melanarius* Zong, Sun & Sheng, 2013, and *A. orientalis* Luhman 1991, are known from China.

In the last five years the authors, Sheng, Li and their research group, have been exploring the forests in Guizhou province and Guangxi Zhuang Autonomous Region, in the Oriental part of China, and collected large numbers of ichneumonids. In this article three new species of *Amphibulus*, collected in these areas, are described.

Materials and methods

Specimens were collected with intercept traps (Li et al. 2012) in the forests of Fanjingshan and Leigongshan National Natural Reserves, Guizhou, and Shiwandashan National Natural Reserve, Guangxi Zhuang Autonomous Region, the Oriental part of China in 2018 to 2022.

Images were taken using a Leica M205A stereomicroscope with LAS Montage MultiFocus software. Morphological terminology is based on Broad et al. (2018). All type specimens are deposited in the Insect Museum, Center for Biological Disaster Prevention and Control (CBDPC), National Forestry and Grassland Administration, Shenyang, P. R. China.

Results

Amphibulus Kriechbaumer, 1893

Amphibulus Kriechbaumer, 1893:122. Type species: *Amphibulus gracilis* Kriechbaumer.

Complete diagnosis. Provided in Townes (1970), Luhman (1991) and Zong et al. (2013).

Summary diagnosis. The genus is characterized by clypeus large, apical margin thick and slightly raised. Lower tooth of mandible shorter than upper tooth. Dorsal edge of face with small, rounded median tubercle. Occipital carina reaching hypostomal carina above base of mandible. Posterior edge of mesoscutum with transverse suture. Scutoscutellar groove without median longitudinal carina. Epicnemial carina approaching anterior edge of mesopleuron. Sternaulus reaching to posterior margin of mesopleuron, usually sculptured anterior portion. Latero-median carinae of first

tergite weak or absent. Tip of ovipositor (Figs 3E, 6C, 8H) elongate lanceolate, nodus indistinct (Luhman 1991, Zong et al. 2013).

Key to the species of *Amphibulus* Kriechbaumer known from the Oriental and Eastern Palaearctic Regions

- 1 Male 2
- Female 7
- 2 Clypeus about 2.5 × as wide as long, apical margin distinctly lifted. Postpetiole 2.0 × as wide as long. Tergites 2–6 orange. (Pakistan) ***A. salicis* Luhman, 1991**
- Clypeus about 3.0 × as wide as long, apical margin not or only slightly lifted. Postpetiole less than 2.0 × as wide as long. Tergites 2–6 black, or at most tergites 2–3 orange 3
- 3 Lower end of occipital carina reaching hypostomal carina at mandibular base 4
- Lower end of occipital carina reaching hypostomal carina distinctly above mandibular base 5
- 4 Fore wing with ramulus present. Clypeus white or pale yellow. Tergites 2–3 mostly orange. (Female unknown). (Korea) ***A. bicolor* Luhman, 1991**
- Fore wing without ramulus. Clypeus and tergites 2–3 black. (China) ***A. guiiicus* Sheng, Li & Sun, sp. nov.**
- 5 Propodeum without apophysis. Flagellomeres 10 and 11 with distinct tyloids. Apices of tergites 2–6 yellowish. (China, Japan) ***A. orientalis* Luhman, 1991**
- Propodeum with apophysis. Flagellomeres at least 10 to 12 with distinct tyloids. Apices of tergites 2–6 almost entirely black 6
- 6 Area basalis and superomedia separated by strong carina, with distinct sculpture. Posterior end of first sternite distinctly basad of spiracle. Mesosoma black ***A. areolaris* Sheng, Li & Yang, sp. nov.**
- Area basalis and superomedia almost entirely confluent, smooth, shiny. Posterior end of first sternite reaching level of spiracle. Mesopleuron and propodeum darkish red. (Female unknown) (China) ***A. albimaculatus* Sheng, 1999**
- 7 Posterior end of first sternite distinctly basad of spiracle. All coxae brown to reddish brown 8
- Posterior end of first sternite reaching level of spiracle. Coxae with different coloration 9
- 8 Area basalis and superomedia entirely confluent. Propodeal spiracle almost circular. Postpetiole with dense longitudinal wrinkles and indistinct punctures. (Male unknown) (China) ***A. melanarius* Zong, Sun & Sheng, 2013**
- Area basalis and superomedia (Fig. 3C) separated by strong carina. Propodeal spiracle 3.0 × as long as wide. Postpetiole (Fig. 3D) smooth, without wrinkles, sparsely indistinctly punctate ***A. areolaris* Sheng, Li & Yang, sp. nov.**

- 9 Clypeus about 2.5 × as wide as long. Median portion of flagellomeres brownish. Coxae black. Tergites 2–6 orange.....*A. salicis* **Luhman, 1991**
- Clypeus about 3.0 × as wide as long. Flagellum with median white band. Coxae red, orange or brown, or at least with orange or brown spots. Tergites 2–6 black, dark orange or brown **10**
- 10 Lower end of occipital carina reaching hypostomal carina at mandibular base. Tergites 2–5 black..... **11**
- Lower end of occipital carina reaching hypostomal carina distinctly above mandibular base. Tergites 2–5 dark orangish or brownish
.....*A. orientalis* **Luhman, 1991**
- 11 Malar space 0.4 × as long as basal width of mandible. Propodeum (Fig. 5D) with distinct apophysis. Area superomedia 0.6 × as wide as long. First tergite (Fig. 6A) reddish brown. (China).....*A. guicus* **Sheng, Li & Sun, sp. nov.**
- Malar space 0.6 × as long as basal width of mandible. Propodeum (Fig. 8D) without apophysis. Area superomedia wider than its length. First tergite (Fig. 8E) almost entirely black. (Male unknown). (China)
.....*A. rufithorax* **Sheng, Li & Yang, sp. nov.**

***Amphibulus areolaris* Sheng, Li & Yang, sp. nov.**

<https://zoobank.org/A1208338-9876-4FF6-B80C-ECB92CA80AE4>

Figs 1–3

Diagnosis. Gena (Figs 1C, 2B) slightly convex medio-longitudinally, with dense punctures. Postocellar line 0.7 × as long as ocular-ocellar line. Areolet (Figs 1A, 3B) receiving vein 2m-cu at posterior 0.2. Metapleuron with coarse dense punctures. Propodeum with area basalis distinctly wider than long, reversed trapezoidal. Area superomedia (Fig. 3C) wider than long. Tergites smooth. Posterior end of first sternite distinctly basad of spiracle. Flagellomeres 10–12 (13) of male with tyloids. Head, mesosoma and tergites 16 entirely black.

Description. Female. Body length 8.6–10.1 mm. Fore wing length 6.8–8.0 mm. Ovipositor sheath length approximately 2.1–2.3 mm.

Head. Inner eye orbits divergent ventrally. Face (Fig. 1B) 2.0 × as wide as long, convex medially, with dense longitudinal punctures; dorsal margin with median small tubercle. Anterior tentorial pit relatively large, transversely elliptic. Median point of clypeal sulcus below line reaching ventral margins of eyes. Clypeus (Fig. 1B) shiny, distinctly convex, with sparse irregular punctures, 3.1 × as wide as long, apical margin weakly evenly arched forward, distinctly convex medially. Mandible (Fig. 2A) with transverse wrinkles, dense yellow brown setae and sparse punctures; teeth strong, upper tooth 1.5 × longer than lower tooth. Subocular sulcus indistinct. Malar space 0.5 × as long as basal width of mandible. Gena (Figs 1C, 2B) in dorsal view 0.8–0.9 × as long as width of eye, slightly convex median-longitudinally, with more or less dense punctures, distance between punctures mainly 0.2 to 1.0 × their diameter. Vertex (Fig. 2B) and frons with

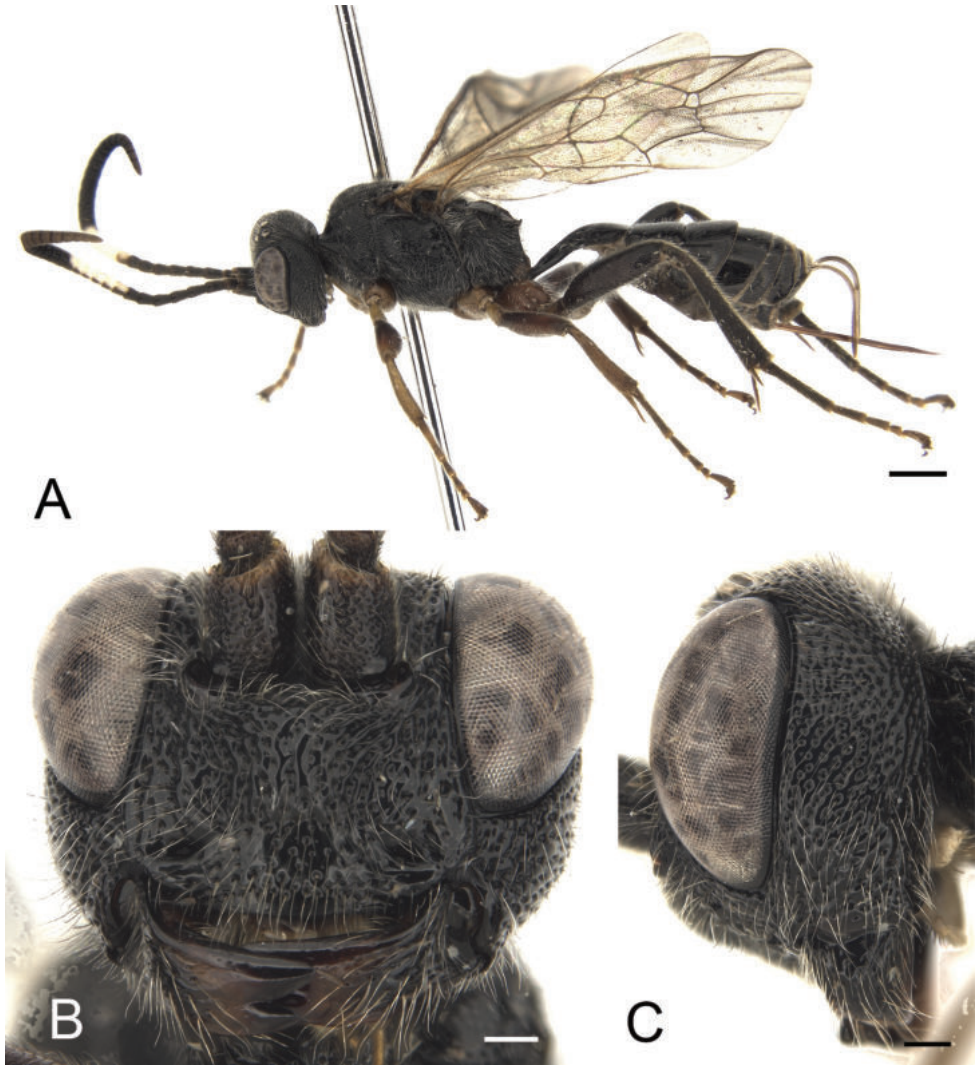


Figure 1. *Amphibulus areolaris* Sheng, Li & Yang, sp. nov., ♀, holotype (CBDPC) **A** habitus, lateral view **B** head, anterior view **C** head, lateral view. Scale bars: 1.0 mm (**A**); 0.2 mm (**B, C**).

texture as gena. Postocellar line $0.7 \times$ as long as ocular-ocellar line. Antenna with 27–28 flagellomeres. Flagellomeres 11 to 25 slightly wider than long, slightly flattened in ventral profile. Ratios of lengths from first to fifth flagellomeres: 1.1:1.2:1.1:1.1:1.0. Occipital carina complete, reaching hypostomal carina distinctly above base of mandible.

Mesosoma. Pronotum (Fig. 2C) with yellow brown setae; dorsal posterior area shiny, with distinct punctures; lower portion with dense oblique transverse wrinkles. Epomia long, strong. Mesoscutum (Fig. 2D) shiny, with uneven punctures, postero-median portion with irregular longitudinal wrinkles. Notauli distinct anteriorly. Scutoscutellar groove steep, with distinct longitudinal wrinkles. Scutellum slightly

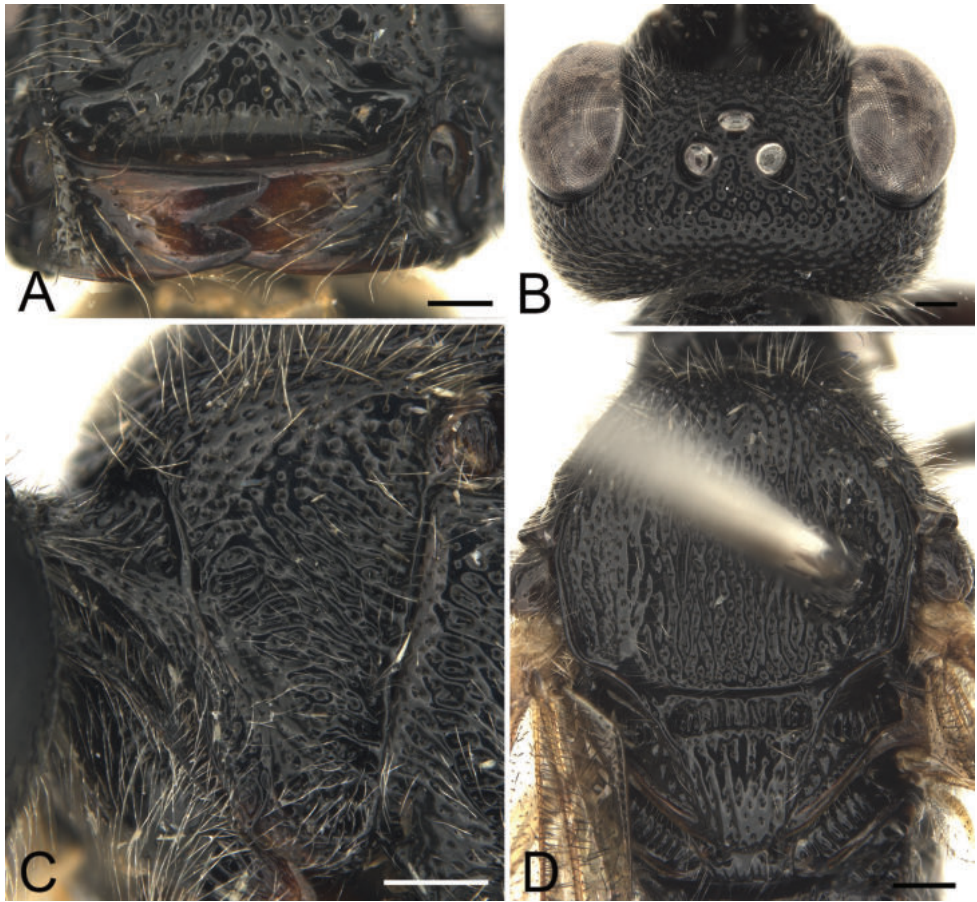


Figure 2. *Amphibulus areolaris* Sheng, Li & Yang, sp. nov., ♀, holotype (CBDPC) **A** mandibles **B** head, dorsal view **C** pronotum, lateral view **D** mesoscutum and scutellum, dorsal view. Scale bars: 0.2 mm (**A**, **B**); 0.3 mm (**C**, **D**).

convex, with irregular punctures and weak longitudinal wrinkles; lateral carina reaching almost to apex. Antero-lateral portion of postscutellum with deep concavity, posterior portion distinctly convex transversely. Mesopleuron (Fig. 3A) with irregular transverse wrinkles, median portion with uneven punctures; speculum small. Dorsal end of epicnemial carina closing anterior margin of mesopleuron, almost reaching to 0.5 distance to subtegular ridge. Metapleuron slightly convex, with dense punctures and yellow brown setae; juxtacoxal carina almost complete. Anterior portion of submetapleural carina strongly convex. Fore wing (Figs 1A, 3B) with vein 1cu-a almost opposite 1/M. Areolet pentagonal, lateral veins convergent forwardly, receiving vein 2m-cu approximately at posterior 0.2. Postnervulus intercepted distinctly below middle. Hind wing vein 1-cu strongly inclivous, $3.0 \times$ as long as cu-a. Ratio of length of hind tarsomeres from first to fifth: 6.4:2.8:2.0:1.0:2.5. Propodeum (Fig. 3C) completely areolated; apophysis distinct; area basalis reversed trapezoid, anterior half smooth, posterior with sparse punctures. Area superomedia wider than long, receiving

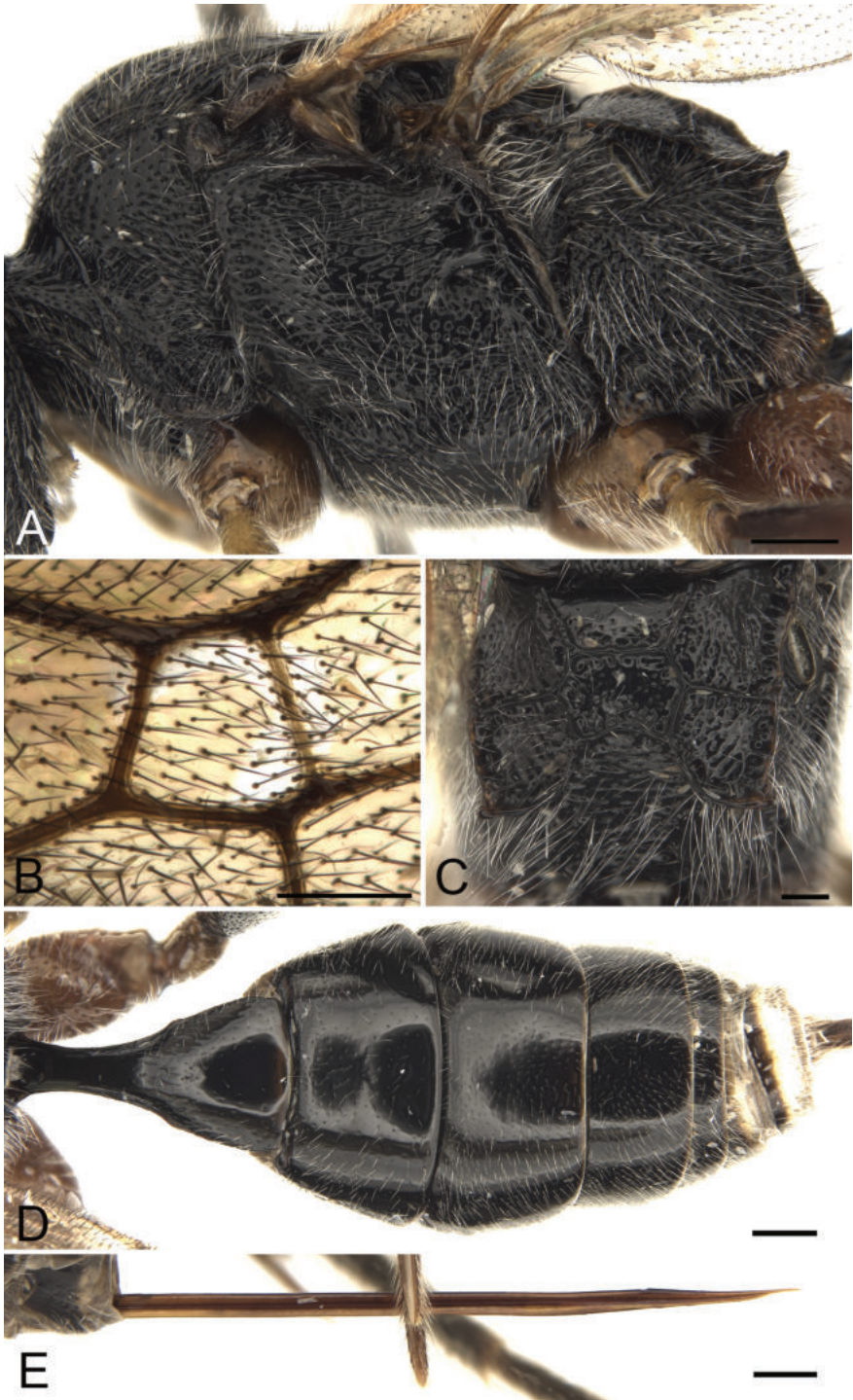


Figure 3. *Amphibulus areolaris* Sheng, Li & Yang, sp. nov., ♀, holotype (CBDPC) **A** mesosoma, lateral view **B** areolet **C** propodeum **D** metasoma, dorsal view **E** ovipositor, lateral view. Scale bars: 0.4 mm (**A, D**); 0.2 mm (**B, C**); 0.3 mm (**E**).

costula slightly before its middle, with indistinct punctures. Remainder areas with indistinct punctures, irregular weak wrinkles and yellow brown setae. Propodeal spiracle relatively larger, obliquely elliptic, approximate $3.0 \times$ as long as wide.

Metasoma (Fig. 3D). First tergite approximately $1.9 \times$ as long as posterior width, smooth, shiny. Postpetiole distinctly widened posteriorly, posterior width approximately $1.3 \times$ as its length, anterior and lateral portions with weak sparse punctures; latero-median carina indistinct; dorso-lateral and ventro-lateral carinae complete. Posterior end of first sternite distinctly basad of spiracle. Spiracle circular, small, located approximately at posterior 0.4 of first tergite. Tergites 2–4 shiny. Second tergite smooth, $0.5 \times$ as long as posterior width, with sparse indistinct fine punctures. Third tergite $0.47 \times$ as long as maximum width, with texture as second tergite, punctures denser than on second tergite. Fourth tergite with distinct fine punctures, denser than on third tergite. Ovipositor sheath $0.8 \times$ as long as hind tibia. Ovipositor (Fig. 3E) compressed, with indistinct subapical nodus and weak notch; ventral valve with three weak teeth.

Coloration (Fig. 1A). Black, except the following: dorsal profiles of flagellomeres 7–12 white, ventrally slightly brownish black; apical portion of flagellum brown to dark brown. Median portion of mandible, maxillary and labial palpi darkish red. Fore and mid coxae brown to darkish brown; femora, basal portions of tibiae and tarsi predominantly dark brown. Hind coxa and trochanter brown; tarsomeres brownish black. Posterior margins of tergites 6–8 white medially.

Male. Body length 8.8–11.2 mm. Fore wing length 6.4–8.4 mm. Antenna with 26–28 flagellomeres. Flagellomeres 10–12 (13) with tyloids. Face $1.6 \times$ as wide as long. Clypeus $2.6 \times$ as wide as long. Median portion of mesopleuron smooth. Area superomedia of propodeum $2.0 \times$ as wide as long. Apophysis indistinct. Black, except for following: Ventral profiles of flagellomeres 1–5, maxillary and labial palpi, fore tibia and first tarsomere yellowish brown. Flagellomeres 6–13, hind tarsomeres 1 apically and 2–4 white. Fore and mid femora reddish brown. Remainder of characteristics similar to female.

Etymology. The specific name is derived from the area superomedia being wider.

Material examined. Holotype. CHINA • ♀; Guizhou Province, Fanjingshan National Natural Reserve; 31 May 2019; leg. Tao Li; CBDPC.

Paratypes. CHINA • 1 ♀, 5 ♂♂; same data as holotype except: Fanjingshan National Natural Reserve, Yapanlin; 15 May to 7 July 2019; IT by Mao-Fei Tian; CBDPC • 1 ♂; same data as holotype except: Fanjingshan National Natural Reserve, Lengjiaba; 11 September 2019; IT by Zheng-Hai Yang; CBDPC.

***Amphibulus guicus* Sheng, Li & Sun, sp. nov.**

<https://zoobank.org/D69A3A6B-1698-45DF-A8DE-BB0F25235279>

Figs 4–6

Diagnosis. Gena (Figs 4C, 5A) evenly convergent posteriorly, with sparse uneven punctures. Clypeus smooth, shiny, subanterior margin with fine indistinct punctures. Propodeum (Fig. 5D) almost smooth, shiny, with indistinctly finely punctate. Area

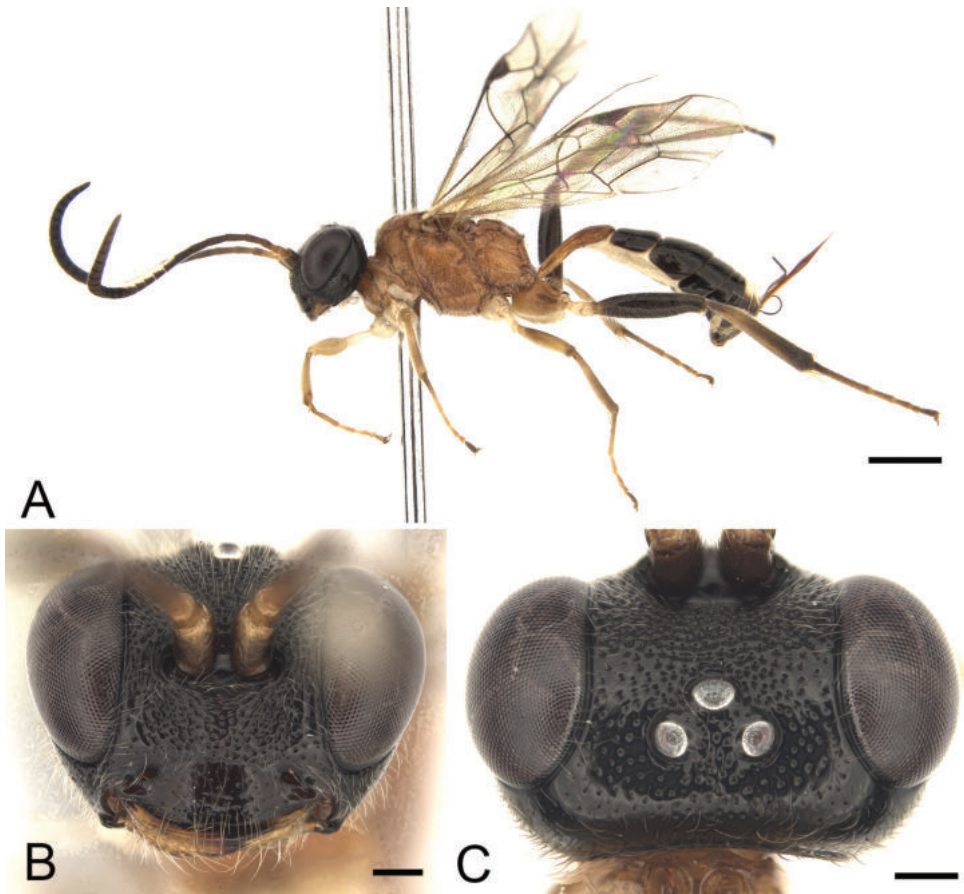


Figure 4. *Amphibulus guicus* Sheng, Li & Sun, sp. nov., ♀, holotype (CBDPC) **A** habitus, lateral view **B** head, anterior view **C** head dorsal view. Scale bars: 1.0 mm (**A**); 0.2 mm (**B, C**).

superomedia $0.6 \times$ as wide as long. Tergites (Fig. 6A) shiny, with sparse fine punctures. First sternite reaching level of spiracle. Head and tergites 2–5 entirely black; Mesosoma and first tergite reddish to yellowish brown.

Description. Female. Body length 6.8–7.0 mm. Fore wing length 4.5–4.8 mm. Ovipositor sheath length approximately 1.2–1.4 mm.

Head. Face (Fig. 4B) $2.2 \times$ as wide as long, slightly convex medially, with weak punctures, distance between punctures mainly 0.5 to $1.5 \times$ their diameter, sparser laterally. Anterior tentorial pit relatively large, almost circular. Median point of clypeal sulcus above level of line reaching lower margins of eyes. Clypeus smooth, $3.2 \times$ as wide as long, evenly convex, with sparse indistinct punctures and long brown hairs; apical margin evenly arched forward. Mandible with fine punctures; upper tooth $3.3 \times$ as long as lower tooth. Malar space $0.4 \times$ as long as basal width of mandible. Gena (Figs 4C, 5A) shiny, in dorsal view 0.3 – $0.4 \times$ as long as width of eye, evenly convergent posteriorly, with sparse uneven punctures. Vertex (Fig. 4C) with distinct punctures,

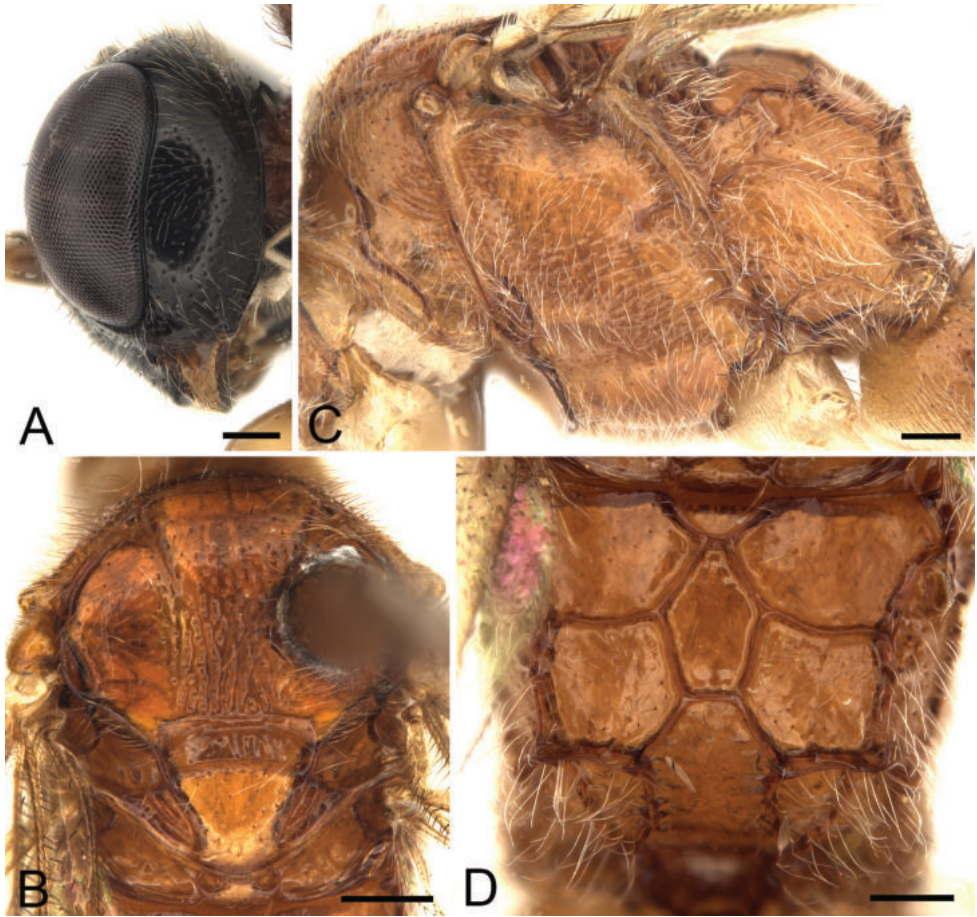


Figure 5. *Amphibulus guiiicus* Sheng, Li & Sun, sp. nov., ♀, holotype (CBDPC) **A** head, lateral view **B** mesoscutum and scutellum, dorsal view **C** mesosoma, lateral view **D** propodeum. Scale bars: 0.2 mm (**A, C, D**); 0.3 mm (**B**).

denser on stemmaticum than lateral and posterior portion. Postocellar line $0.8 \times$ as long as ocular-ocellar line. Frons with dense punctures. Antenna with 23–26 flagellomeres. Flagellomeres 11 to 22(23) almost wider than long, ventral slightly flattened in ventral view. Ratios of lengths from first to fifth flagellomeres: 1.0:1.2:1.3:1.3:1.2. Occipital carina complete, reaching hypostomal carina almost near base of mandible.

Mesosoma. Dorsal and anterior portion of pronotum (Fig. 5C) shiny, medio-posterior with indistinct oblique wrinkles, dorsal posterior portion with distinct fine punctures. Epomia long, strong, lower end reaching to anterior margin of pronotum, dorsal end almost reaching dorsal margin. Mesoscutum (Fig. 5B) shiny, lateral and anterior portions almost smooth, with sparse indistinct fine punctures, posteromedian portion with indistinct longitudinal wrinkles and fine punctures. Anterior portion of notaulus distinct. Scutoscutellar groove shiny, with indistinct longitudinal wrinkles. Scutellum with texture as lateral portion of mesoscutum, basal portion of lateral ca-

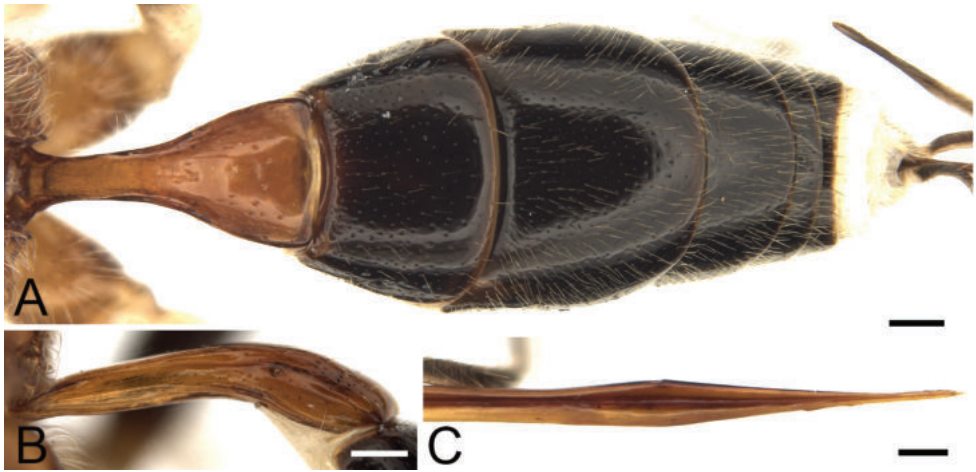


Figure 6. *Amphibulus guiticus* Sheng, Li & Sun, sp. nov., ♀, holotype (CBDPC) **A** metasoma, dorsal view **B** tergite 1, lateral view **C** posterior portion of ovipositor, lateral view. Scale bars: 0.2 mm (**A, B**); 0.1 mm (**C**).

rina present anteriorly. Postscutellum transverse, smooth, with deep antero-lateral pits. Dorsal portion of mesopleuron (Fig. 5C) almost smooth, shiny, with sparse indistinct punctures; median portion with indistinct oblique wrinkles; lower slightly convex. Speculum indistinct. Metapleuron (Fig. 5C) evenly convex, with sparse fine punctures; lower portion with indistinct wrinkles. Juxtacoxal carina complete. Anterior portion of submetapleural carina distinctly convex. Ratio of length of hind tarsomeres from first to fifth: 6.9:2.6:1.9:1.0:1.8. Fore wing with vein 1cu-a opposite 1/M. Areolet pentagonal, lateral veins weakly convergent forward, receiving vein 2m-cu approximately at posterior 0.4. Hind wing vein 1-cu strongly inclivous, 3.0 × as long as cu-a. Propodeum (Fig. 5D) almost completely areolated, carinae strong; almost smooth, shiny, with sparse indistinct fine punctures. Area basalis almost triangular. Area superomedia 0.6 × as wide as long, receiving costula slightly before its middle. Apophysis distinct. Propodeal spiracle obliquely elliptic, approximate 3.2 × as long as wide.

Metasoma (Fig. 6A). First tergite (Fig. 6A, B) smooth, shiny, approximately 2.1 × as long as posterior width, median portion somewhat prismatic. Postpetiole evenly widened posteriorly, posterior width distinctly longer than its length. Latero-median carina weakly present; Dorso-lateral and ventro-lateral carinae present. First sternite reaching level of spiracle. Spiracle small, circular, located approximately at posterior 0.3 of first tergite. Tergites 2–4 (Fig. 6A) shiny. Second tergite smooth, strongly widened posteriorly, 0.6 × as long as posterior width, lateral with sparse indistinct fine punctures. Third tergite almost parallel laterally, with distinct even setae. Remaining tergites with dense short setae. Ovipositor sheath 0.8 × as long as hind tibia. Ovipositor (Fig. 6C) slightly compressed, subapical nodus indistinct, with weak notch; ventral valve with two weak teeth.

Coloration (Fig. 4A). Mainly black, reddish brown and white. Head black; maxillary and labial palpi yellowish white; mandible, scape and pedicel brownish yellow; dorsal profiles of flagellomeres 7–11 (12) white. Mesosoma reddish brown. Fore and mid-

dle coxae and all trochanters whitish yellow; remainder of fore and middle legs, hind coxa and subbase of tibia and tarsus predominantly yellowish brown; hind femur and posterior portion of tibia brownish black. First tergite reddish brown; tergites 2–6 black; tergites 7–8 white, blackish brown laterally. Pterostigma and wing veins brownish black.

Male. Body length 4.1–7.0 mm. Fore wing length 3.4–4.8 mm. Antenna with 22–25 flagellomeres. Flagellomeres 10–12 with tyloids. Face $2.1 \times$ as wide as long. Clypeus $2.8 \times$ as wide as long. Occipital carina reaching hypostomal carina above base of mandible. Area superomedia 1.0 – $1.2 \times$ as wide as long, receiving costula at its anterior 0.3 . Apophysis indistinct. Basal and ventral profiles of flagellomeres yellowish brown, dorsal profiles dark brown. Remainder of characteristics similar to female.

Etymology. The specific name is derived from the type locality, gui, the Chinese abbreviation for Guangxi Zhuang Autonomous Region.

Material examined. Holotype. CHINA • ♀; Guangxi Zhuang Autonomous Region, Shiwandashan National Natural Reserve; 275 m; 13 November 2018; IT by Qing-Tang Huang; CBDPC.

Paratypes. CHINA • 1 ♀; same data as holotype; CBDPC • 7 ♂♂; same data as holotype except: 20 November to 4 December 2018; CBDPC • 3 ♀♀; same data as holotype except: 29 April to 15 May 2019; CBDPC • 1 ♀; same data as holotype except: Dayaoshan National Natural Reserve, Shengtangshan; 1520 m; 30 January 2019; IT by Tao Li; CBDPC • 8 ♂♂; same data as holotype; CBDPC.

***Amphibulus rufithorax* Sheng, Li & Yang, sp. nov.**

<https://zoobank.org/1A98A643-78BD-4895-BE43-3A1801AB121B>

Figs 7, 8

Diagnosis. Frons (Fig. 8A) with coarse dense punctures. Fore wing (Fig. 7A) vein 1cu-a distinctly distal to M&RS; areolet receiving vein 2m-cu approximately at its middle. Lateral carinae of area basalis (Fig. 8D) mostly vestigial. Area superomedia almost as wide as long, receiving costula at anterior 0.3 . First sternite reaching level of spiracle. Head and tergites 2–6 almost entirely black; First tergite predominantly black. Mesosoma reddish brown.

Description. Female. Body length 4.9–6.7 mm. Fore wing length 4.1–5.1 mm. Ovipositor sheath length 1.1–1.2 mm.

Head. Face (Fig. 7B) $2.3 \times$ as wide as long, evenly convex medially, dense punctures and irregular indistinct longitudinal wrinkles medially; lateral side smooth, sparsely punctate. Anterior tentorial pit relatively large, obliquely elliptic. Median point of clypeal sulcus above level of line reaching lower margins of eyes. Clypeus smooth, shiny, $2.9 \times$ as wide as long, evenly convex apically; with sparse fine punctures; apical margin weakly arched forward. Mandible with dense fine punctures; upper tooth $3.0 \times$ as long as lower tooth. Malar space $0.6 \times$ as long as basal width of mandible. Gena in dorsal view 0.62 – $0.65 \times$ as long as width of eye, evenly slightly convergent backwardly, with irregular punctures, distance between punctures 0.5 to $3.0 \times$ their diameter. Vertex (Fig. 7C) with sparse punctures and long brown setae. Stemmaticum with relatively dense punctures. Postocellar line $0.7 \times$ as long as ocular-ocellar line. Frons (Fig. 8A) with dense punctures,

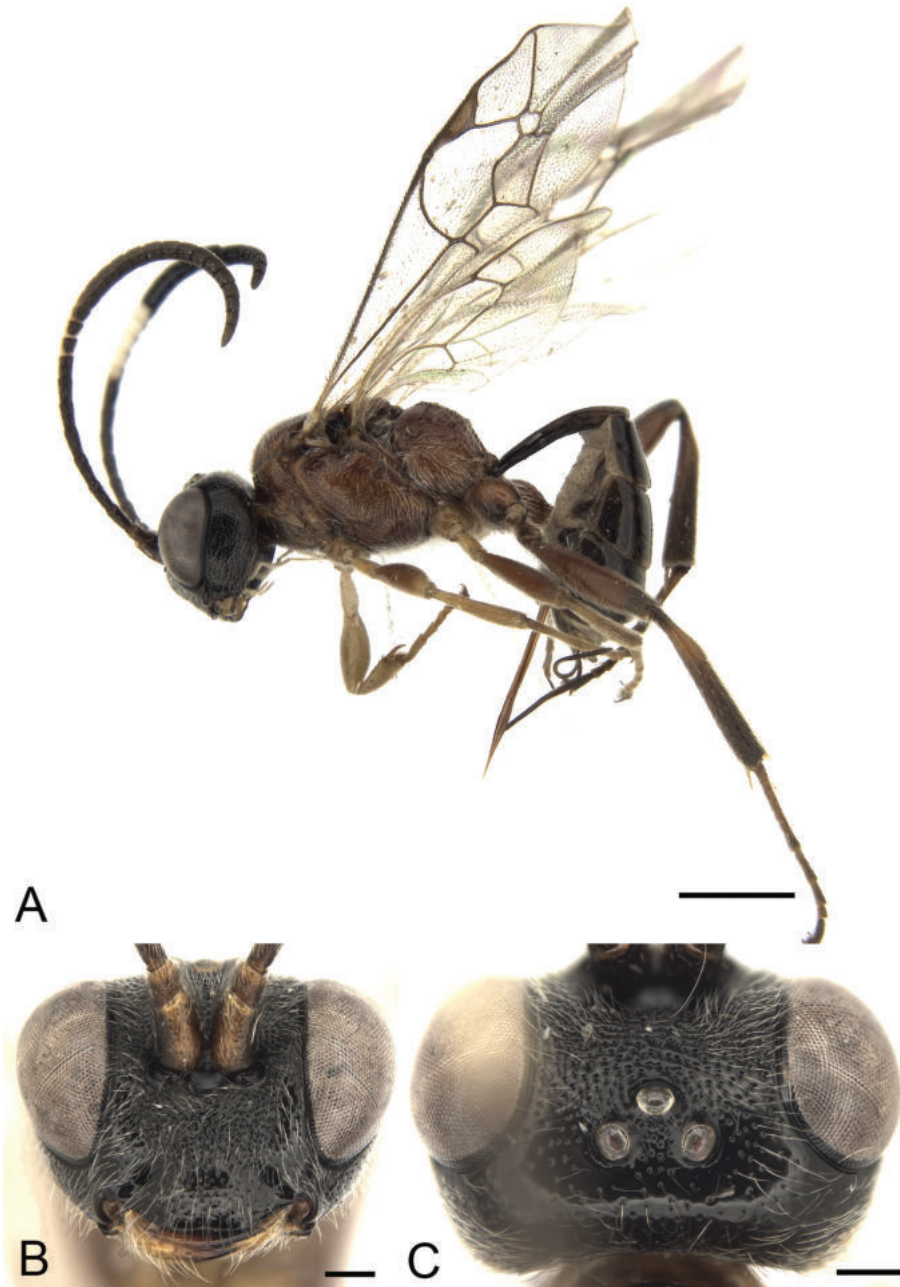


Figure 7. *Amphibulus rufithorax* Sheng, Li & Sun, sp. nov., ♀, holotype (CBDPC) **A** habitus, lateral view **B** head, anterior view **C** head, dorsal view. Scale bars: 1.0 mm (**A**); 0.2 mm (**B, C**).

distance between punctures at most $0.5 \times$ their diameter, lateral sparser than median portion. Antenna with 23–25 flagellomeres. Flagellomeres 11 to 23 (26) slightly flattened in ventral view. Ratios of lengths from first to fifth flagellomeres: 5.5:6.1:5.7:5.5:5.2. Occipital carina complete, reaching hypostomal carina at base of mandible.

Mesosoma. Pronotum (Fig. 8C) almost shiny, with indistinct fine punctures; lower portion with indistinct fine oblique wrinkles. Epomia long, lower end almost reaching to lower-anterior margin of pronotum, dorsal end almost reaching dorsal margin. Mesoscutum (Fig. 8B) shiny, lateral and anterior portions almost smooth, with shallow punctures; posteromedian portion with short irregular longitudinal wrinkles and fine punctures. Anterior end of notaulus distinct. Scutoscutellar groove deep, with distinct longitudinal wrinkles. Scutellum shiny, almost smooth, with few punctures; lateral carina present anteriorly. Postscutellum smooth, shiny, with deep antero-lateral pits. Anterior and lower portions of mesopleuron (Fig. 8C) with dense punctures and setae, dorsal posterior shiny, with sparse fine punctures. Speculum small, indistinct. Dorsal end of epicnemial carina almost reaching to 0.5 distance to subtegular ridge. Meta-pleuron (Fig. 8C) weakly convex, with dense setae and relatively sparse fine punctures. Median portion of juxtacoxal carina vestigial. Anterior portion of submetapleural carina strongly lobe-shaped convex. Ratio of length of hind tarsomeres from first to fifth:

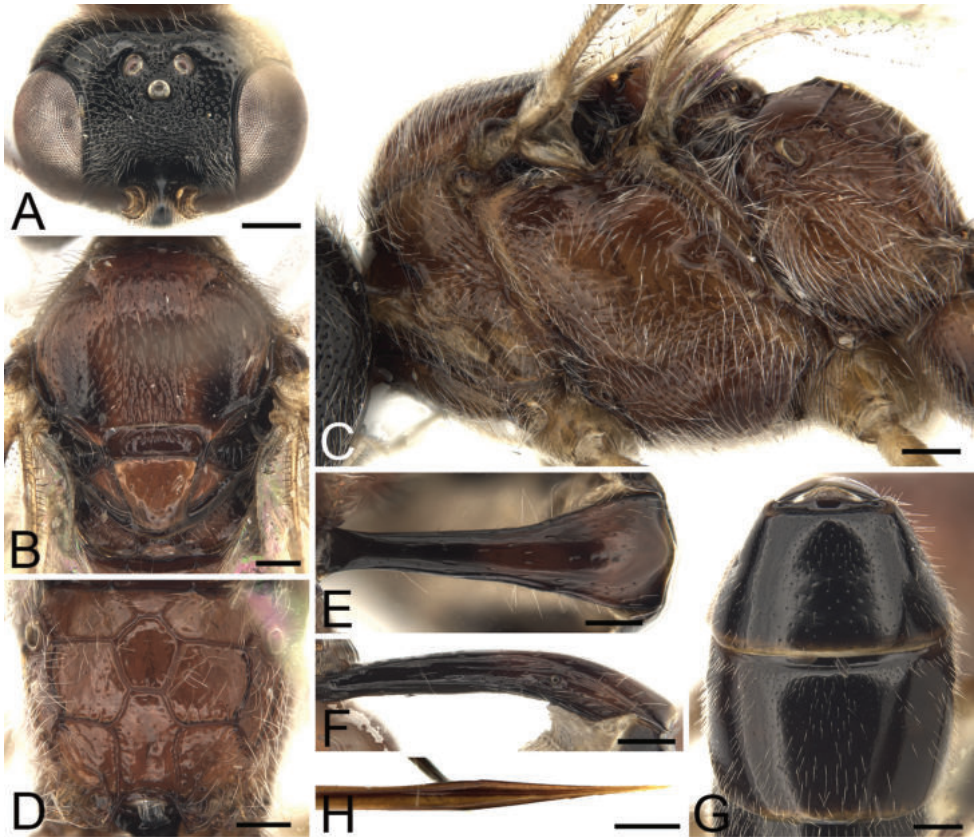


Figure 8. *Amphibulus rufithorax* Sheng, Li & Yang, sp. nov., ♀, holotype (CBDPC) **A** head, dorso-anterior view **B** mesoscutum and scutellum, dorsal view **C** mesosoma, lateral view **D** propodeum **E** tergite 1, dorsal view **F** tergite 1, lateral view **G** tergites 2–3, dorsal view **H** posterior portion of ovipositor, lateral view. Scale bars: 0.3 mm (**A**); 0.2 mm (**B–H**).

5.8:2.2:1.6:1.0:1.8. Wings slightly gray, hyaline; vein 1cu-a distinctly distal to M&RS. Areolet pentagonal, lateral veins strongly convergent forwardly, receiving vein 2m-cu approximately at its middle. Postnervulus intercepted at lower 0.3. Hind wing vein 1-cu strongly inclivous, $3.0 \times$ as long as cu-a. Propodeum (Fig. 8D) smooth, shiny, indistinctly punctate peripherally, completely areolated. Apophysis indistinct. Area basalis reversed trapezoidal, lateral carina mostly vestigial. Area superomedia hexagonal, maximum width slightly wider than its length, reaching costula at anterior 0.35. Propodeal spiracle elongate, approximate $1.4 \times$ as long as wide.

Metasoma. First tergite (Fig. 8E, F) approximately $3.0 \times$ as long as posterior width, smooth, shiny, with very sparse punctures; posterior half evenly widened posteriorly. Postpetiole approximately as long as its width. Latero-median carina indistinct; dorso-lateral and ventro-lateral carinae weak, complete. First sternite reaching level of spiracle. Spiracle circular, small, located approximately at posterior 0.4 of first tergite. Tergites 2–3 (Fig. 8G) almost smooth, shiny. Second tergite $0.6 \times$ as long as posterior width, with sparse indistinct fine punctures. Third tergite approximately $0.5 \times$ as long as maximum width, slightly convergent posteriorly. Remainder tergites with fine punctures and distinct setae. Ovipositor sheath $0.8 \times$ as long as hind tibia. Ovipositor (Fig. 8H) compressed, with indistinct subapical nodus and weak notch; ventral valve with two indistinct teeth.

Coloration (Fig. 7A). Head black; ventral profiles of scape and pedicel, mandible, maxillary and labial palpi yellowish brown; flagellomeres 7–11 white dorsally. Mesosoma almost entirely red brown. Fore and middle legs dark brown, except coxae and trochanters, fore femur apically and tibia whitish yellow. Hind coxa predominantly, trochanter, femur (apex black) darkish red, subbase of tibia brownish yellow. Posterior half of first tergite irregularly brown. Tergites 2–6 black, apical margins narrowly yellow. Tergites 7–8 white medially, black brown laterally. Wing veins brownish black; Pterostigma brown medially.

Male. Unknown.

Etymology. The specific name is derived from the mesosoma being entirely red brown.

Material examined. Holotype. CHINA • ♀; Guizhou Province, Fanjingshan National Natural Reserve, Yapanlin; 1250 m; 15 May 2019; IT by Mao-Fei Tian; CBDPC.

Paratypes. CHINA • 2 ♀♀; same data as holotype except: Lengjiaba; 840 m; 14 to 21 October 2019; IT by Zheng-Hai Yang; CBDPC • 1 ♀; same data as holotype; CBDPC • 8 ♀♀; Guizhou Province, Leigongshan National Natural Reserve; 1760 m; 17 June to 6 August 2019; IT by Wan-Xin Pan; CBDPC.

Acknowledgements

The authors are deeply grateful to Drs Tamara Spasojevic (Natural History Museum Basel, Switzerland), Bernardo F. Santos (Center for Integrative Biodiversity Discovery, Museum für Naturkunde, Leibniz Institute for Evolution and Biodiversity Science, Berlin, Germany) and Maryam Zardouei Heydari (Iran) for reviewing this manuscript. The authors thank Mr. Qing-Tang Huang (Forestry bureau of Shangsi, Guangxi

Zhuang Autonomous Region, China) for his help in the course of exploration in Shiwandashan National Forest Park, Shangsi. This research was supported by National Key R & D Program of China (No. 2022YFD1401000) and the National Natural Science Foundation of China (NSFC, No. 31501887).

References

- Bennett AMR, Cardinal S, Gauld ID, Wahl DB (2019) Phylogeny of the subfamilies of Ichneumonidae (Hymenoptera). *Journal of Hymenoptera Research* 71: 1–156. <https://doi.org/10.3897/jhr.71.32375>
- Broad GR, Shaw MR, Fitton MG (2018) *Ichneumonid Wasps (Hymenoptera: Ichneumonidae): their Classification and Biology*. Royal Entomological Society and the Field Studies Council. *Handbooks for the Identification of British Insects* 7(12): 1–418.
- Kriechbaumer J (1893) *Cryptiden-Studien*. *Entomologische Nachrichten* 19(8): 119–127.
- Li T, Sheng M-L, Sun S-P, Chen G-F, Guo Z-H (2012) Effect of the trap color on the capture of ichneumonids wasps (Hymenoptera). *Revista Colombiana de Entomología* 38(2): 338–342. <https://doi.org/10.25100/socolen.v38i2.9015>
- Luhman JC (1991) A revision of the world *Amphibulus* Kriechbaumer (Hymenoptera: Ichneumonidae, Phygadeuontinae). *Insecta Mundi* 5(3–4): 129–152.
- Santos BF (2017) Phylogeny and reclassification of Cryptini (Hymenoptera, Ichneumonidae, Cryptinae), with implications for ichneumonid higher-level classification. *Systematic Entomology* 42: 650–676. <https://doi.org/10.1111/syen.12238>
- Sawoniewicz J (1990) Revision of European species of the subtribe Endaseina (Hymenoptera, Ichneumonidae), II. Genus *Amphibulus* Kriechbaumer, 1893. *Annales Zoologici* 43(11): 287–291.
- Sheng M-L, Sun S-P (1999) Two new species of tribe Endaseini from Funiu Mountains (Hymenoptera: Ichneumonidae: Phygadeuontinae). In: Shen XC, Pei HC (Eds) *The Fauna and Taxonomy of Insects in Henan*. Vol. 4. *Insects of the Mountains Funiu and Dabie Regions*. China Agricultural Sciencetech Press, 74–78.
- Sheng M-L, Sun S-P (2009) *Insect fauna of Henan, Hymenoptera: Ichneumonidae*. Science Press, Beijing, 340 pp. [In Chinese with English summary]
- Sheng M-L, Sun S-P (2013) *Ichneumonid fauna of Jiangxi (Hymenoptera: Ichneumonidae)*. Science Press, Beijing, 569 pp. [In Chinese with English summary]
- Townes HK (1970) The genera of Ichneumonidae, Part 2. *Memoirs of the American Entomological Institute* 12(1969): 1–537.
- Yu DS, van Achterberg C, Horstmann K (2016) *Taxapad 2016, Ichneumonoidea 2015*. Database on flash-drive. Nepean, Ontario.
- Zong S-X, Sun S-P, Sheng M-L (2013) A new species of *Amphibulus* Kriechbaumer (Hymenoptera, Ichneumonidae, Cryptinae) from Beijing with a key to species known from the Oriental and Eastern Palaearctic regions. *ZooKeys* 312: 89–95. <https://doi.org/10.3897/zookeys.312.5294>

First record and characterization of *Aganaspis daci* (Weld, 1951) (Hymenoptera, Figitidae, Eucoilinae), a parasitoid of fruit flies, from Italy

Umberto Bernardo¹, Feliciano Pica¹, Carmela Carbone¹,
Francesco Nugnes¹, Gennaro Viggiani²

1 Institute for Sustainable Plant Protection – National Research Council (IPSP-CNR), Ple E. Fermi, 1, 80055 Portici, NA, Italy **2** Via Madonna della Salute, 4, 80055, Portici, NA, Italy

Corresponding author: Francesco Nugnes (francesco.nugnes@ipsp.cnr.it)

Academic editor: Miles Zhang | Received 31 July 2023 | Accepted 25 September 2023 | Published 23 October 2023

<https://zoobank.org/511C3297-0A4F-4BDD-B594-4F873F8C075D>

Citation: Bernardo U, Pica F, Carbone C, Nugnes F, Viggiani G (2023) First record and characterization of *Aganaspis daci* (Weld, 1951) (Hymenoptera, Figitidae, Eucoilinae), a parasitoid of fruit flies, from Italy. Journal of Hymenoptera Research 96: 863–877. <https://doi.org/10.3897/jhr.96.110000>

Abstract

Aganaspis daci, a larval-pupal parasitoid of several tephritid species, was unexpectedly recovered in the Campania region (Southern Italy), where it had not been intentionally released. An integrative approach was used to conduct a comprehensive characterization of this parasitoid, confirming its identification through a comparison with specimens obtained from laboratory rearing. While *A. daci* emerged from puparia of *Ceratitis capitata* during this study, its original association was recorded with *Bactrocera dorsalis*. The presence of *A. daci* in Italy highlights its successful establishment, possibly facilitated by the recent invasive process of its host, *B. dorsalis*, offering promising prospects for future tephritids control strategies. It is intriguing to note that the mt-haplotypes found in Italy were only partially shared with those observed in specimens originating from a Spanish rearing, suggesting likely distinct origins for at least part of the Italian population.

Keywords

Bactrocera dorsalis, biological control, *Ceratitis capitata*, Medfly, oriental fruit fly, Tephritids

Introduction

The family Tephritidae (Diptera) commonly recognized as fruit flies, includes numerous damaging and invasive pests that pose a serious concern for agricultural production worldwide (Scolari et al. 2021). These fruit flies have the potential to establish into new areas, leading to ecological imbalances and environmental and economic consequences (Szyniszewska et al. 2014). People movements and import-export trade activities are the main factors that allow the transportation of arthropods from one continent to another (Lichtenberg and Olson 2018; Pace et al. 2022).

Among the fruit flies, *Ceratitis capitata* (Wiedemann, 1824) and *Bactrocera dorsalis* (Hendel, 1912) (Diptera: Tephritidae), along with other species belonging to the *B. dorsalis* complex, exhibit particularly high invasive potential. These entities share common biological traits such as high polyphagy, short life cycles, and excellent adaptive capacities (Pieterse et al. 2020).

Ceratitis capitata, commonly known as the Mediterranean fruit fly (Medfly), is native to sub-Saharan Africa. Since its initial discovery in some Southern European countries in the 19th century, this species has rapidly spread to several countries worldwide, often using European countries as bridgeheads. Additionally, this species is increasingly being detected in areas formerly free of infestation, such as Florida and California, where control and eradication strategies are being implemented (Calla et al. 2014; Szyniszewska et al. 2014).

On the other hand, *B. dorsalis*, native to Asia, has invaded a significant portion of the African continent (Goergen et al. 2011). It was first intercepted in Italy (Campania Region) in 2018 (Nugnes et al. 2018) and subsequently in 2019 (Gargiulo et al. 2021). However, active infestations of this species on different fruits were recorded in Italy for the first time in 2022, indicating a considerable shift in the scenario, and posing a significant challenge to the agriculture of several European countries (Mertens et al. 2022; Bernardo et al. 2023a; Nugnes et al. 2023). Both entities, *B. dorsalis* complex and *C. capitata* exhibit a wide host range, causing damage to 300 plant species including various fruits and vegetables (Gilioli et al. 2022). However, it is important to heed that the accurate host range of the *B. dorsalis* complex remains a challenge due to possible confusion with related species (Mertens et al. 2022).

The damage caused by these species is mainly due to larval trophic activity, which ultimately leads to fruit collapse and can result in the loss of fruits of high commercial value such as *Citrus* spp., *Malus* spp., *Diospyros* spp., and *Prunus* spp. (Shelly 2014).

Implementing phytosanitary measures is crucial for controlling these harmful species. Furthermore, as the number of active ingredients and the amounts allowed in cultivation continually decrease, an integrated approach that includes parasitoids has become essential (Jacquet et al. 2022).

Classical biological control, accomplished through the introduction of one or more parasitoids from the native area of the phytophagous pest, often represents the most effective and cost-efficient approach (Moore 2021). However, the effectiveness

of natural enemies can vary and be influenced by abiotic conditions, with the species' thermal requirements determining their success or failure (Adly 2016).

Biological control offers significant advantages, including enhanced security and cost-effectiveness. Numerous successful cases of tephritids management using parasitoids have already been documented, particularly in subtropical and tropical regions (Wharton 1997; Purcell 1998; Ovruski and Aluja 2000).

However, the introduction of exotic parasitoids for biological control purposes is a complex process that involves strict regulations and extensive preliminary studies. Conducting risk assessments can be time-consuming and expensive, resulting in bureaucratic challenges and delays in obtaining authorization for the release of biocontrol agents (Gay 2012; Barratt et al. 2018; Bernardo et al. 2023b).

However, the initial step of this lengthy process involves studying the indigenous parasitoid complex that has rapidly adapted to invasive pests. In addition, the parasitoid complex, both on endemic and invasive species, is constantly evolving, both qualitatively (different species) and quantitatively (varying percentages of relative parasitisation over time and space) (Mirchev et al. 2004). The parasitoid complex associated with tephritids present in Europe (Clausen et al. 1965; Papadopoulos and Katsoyannos 2003; Viggiani et al. 2006; Sasso et al. 2019) has been strongly influenced by the release of numerous parasitoids by Professor Silvestri (Silvestri 1916; Silvestri 1938) and other scientists (Marucci et al. 1952; Bokonon-Ganta et al. 2019; Wang et al. 2021; Coelho et al. 2023).

The aims of this study were manifold. First, we aimed to report the results of a survey conducted on parasitoids developing on *C. capitata* and/or *B. dorsalis* in Campanian fields. Second, we aimed to characterize the recorded parasitoid using a comprehensive integrative approach. This included a comparison with specimens obtained from a laboratory rearing in Spain, which, in turn, allowed us to infer the possible origins of the Italian population. Therefore, we assessed the establishment and distribution of this parasitoid in Campania (Italy), with a particular focus on territories affected by the recent invasive process of *B. dorsalis*. Lastly, the potential implications of the presence of the parasitoid in Italy for future tephritids control strategies are discussed.

Materials and methods

Monitoring sites and fruit samplings

As part of the compulsory monitoring of *B. dorsalis* and other non-European fruit flies from 2022 to the May of 2023, a fruit sampling with damages ascribable to fruit flies was conducted in various locations within the Campania region. Most samples were collected in mixed fruit-trees fields where the sampled fruit species varied with the progression of the seasons (Table 1). In each monitored area twenty fruits were collected from the ground and twenty directly from trees. The date and place of collection, along with the host plant species, were recorded for each sample.

Table 1. Locality, date of collection, sex, mt-haplotype, and Genbank accession number of *A. daci* specimens studied in the present work (codes in italics: molecularly characterised samples).

Locality	Coordinates	Date of collection	Specimen code	Number of specimens and sex	Mt-haplotype	Genbank accession number COI	ITS2-28S
Palma Campania (Na, Italy)	40°50'15"N, 14°32'54"E	13-Jan-23	Ad_1-Ad_7	5♀, 2♂	-	-	-
	40°51'36"N, 14°33'20"E	25-Oct-22	Ad_8, Ad_9, Ad_11-Ad_21 <i>Ad_10</i>	6♀, 7♂ 1♀	- Ha	- OR157906	- OR166972
	40°51'52"N, 14°33'7"E	24-Oct-22	Ad_22, Ad_24-Ad_26 <i>Ad_23</i>	2♀, 2♂ 1♀	- Hb	- OR157907	- OR166973
	40°52'46"N, 14°32'59"E	14-Sep-22	Ad_27, Ad_28	2♂	-	-	-
	40°51'41"N, 14°33'19"E	19-Oct-22	Ad_29	1♀	-	-	-
	40°52'5"N, 14°33'8"E	21-Sep-22 19-May-23	Ad_30 Ad_31	1♀ 1♀	- -	- -	- -
Portici (Na, Italy)	40°48'50"N, 14°20'47"E	4-Jul-23	Ad_60-Ad_62 <i>Ad_59</i>	1♀, 2♂ 1♂	- Hc	- OR536574	- OR539752
Quindici (Av, Italy)	40°52'12"N, 14°38'32"E	9-Nov-22	Ad_40-Ad_42, Ad_44 <i>Ad_43</i> <i>Ad_45</i>	2♀, 2♂ 1♀ 1♂	- Hb Hb	- OR157909 OR157910	- OR166975 OR166976
Sant'Agnello (Na, Italy)	40°37'4"N, 14°24'19"E	13-Jan-23 25-Oct-22	Ad_32-Ad_33 Ad_34-Ad_37, Ad_39 <i>Ad_38</i>	2♀ 3♀, 2♂ 1♀	- - Ha	- - OR157908	- - OR166974
Sant'Egidio del Monte Albino (Sa, Italy)	40°43'45"N, 14°35'15"E	03-Nov-22	Ad_46, Ad_47 <i>Ad_48</i>	1♀, 1♂ 1♂	- Ha	- OR157911	- OR166977
Moncada (Spain) rearing	39°35'21"N, 0°23'43"E	06-Mar-23	<i>Ad_49</i> <i>Ad_50</i> <i>Ad_51</i> <i>Ad_52</i> <i>Ad_53</i> Ad_54-Ad_58	1♀ 1♀ 1♀ 1♀ 1♀ 5♂	Hc Hc Hc Hc Hc -	OR157912 OR157913 OR157914 OR157915 OR157916 -	OR166978 OR166979 OR166134 OR166980 OR166981 -

The samples were transported in double-sealed bags to the CNR-IPSP laboratory. To allow mature larvae to pupate, infested fruits were isolated in plastic bugdorms (45×45×45 cm) and placed in a climatic chamber with the following conditions: 25±2 °C, 65±10% relative humidity and a 16:8 (L:D) photoperiod. Puparia were individually isolated in glass vials under the previously mentioned environmental conditions, and species and sex of the emerged tephritids and/or natural parasitoids were recorded. When a parasitoid emerged from an isolated puparium, the host species was identified by examining the mandible shape of the mature larva inside (Sabatino 1974; Balmès and Mouttet 2017). Sex ratio of parasitoids was calculated as in de Pedro et al. (2017a).

Morphological identification

Both tephritids and emerged parasitoid specimens (Table 1) were examined under a Leica M165C auto montage microscope (Leica Microsystems, Mannheim, Germany)

equipped with a Leica DFC450 digital photo camera. The multifocal images were assembled using the Leica Application Suite software version 3.8.0 (Leica 2011). Some adult parasitoids were slide-mounted in Canada balsam phenol and observed under a Zeiss Axiophot 2 microscope (Carl Zeiss, Oberkochen, Germany).

To determine the genus of the emerged parasitoids, the key by Forshage and Nordlander (2008) was used. For species level, the keys Lin (1987) and Diaz and Gallardo (2001) were used. After the initial identification, a morphological comparison was conducted between the Italian specimens and twelve (6 males and 6 females) Spanish adults of *Aganaspis daci* (Weld 1951) (Hymenoptera: Figitidae: Eucoilinae).

The Spanish samples were provided in absolute alcohol, each contained within its own individual vial, and were obtained from the laboratory colony of the Valencian Institute of Agrarian Research (IVIA, Valencia, Spain). This colony was established in 2010 using several specimens obtained from medfly larvae collected from figs in a village near Valencia (Bétera, Spain) (de Pedro et al. 2016).

DNA extraction, amplification and sequencing

Twelve adults (Table 1) were selected for molecular analysis and were singularly placed in Eppendorf containing 95% ethanol and preserved at -20 °C until use.

The DNA extraction from metasoma and legs (which do not present taxonomic characters at species level) was performed using a destructive method based on Chelex–proteinase K- protocol described in Gebiola et al. (2009). Part of the mitochondrial cytochrome oxidase C subunit I (COI) gene was targeted as it is a widely used marker for species-level systematics. PCR amplifications were performed in a 10 µl reaction volume on an Eppendorf Nexus GX2 thermocycler using primers as in Schulmeister et al. (2002) and the primer pair LepF1/LepR1 as described in Hajibabaei et al. (2006). The thermocycler conditions were set according to Nugnes et al. (2017). Furthermore, the inclusion of additional markers (ITS2-28S_D1_D2) for specimen characterization is motivated by situations where COI is shared among different species, thus necessitating the use of extra markers to distinguish between these entities (Nugnes et al. 2017; Bernardo et al. 2021; Wacławik et al. 2021).

Hence, the ribosomal gene ITS2, along with the expansion segments D1-D2 of the 28S ribosomal subunit (ITS2-28S_D1_D2) (~ 1200 bp), was amplified with primers ITS2F and D2R (Campbell et al. 1993) using the PCR cycling program reported in de Benedetta et al. (2022).

PCR products were checked on a 1.2% agarose gel stained with SYBR Safe (Invitrogen) and directly sequenced.

Chromatograms were assembled using BioEdit 7.0 (Hall 1999) and edited manually. The obtained sequences were compared with each other and with sequences in the genetic databases GenBank and BOLD (www.ncbi.nlm.nih.gov/genbank/; www.boldsystems.org; last accessed on 28 May 2023) and, subsequently, were submitted to GenBank.

Results

Monitoring activities

Parasitoids emerged exclusively from oranges infested by *C. capitata*, collected from 9 orchards located in three Campanian provinces. A total of 52 adult parasitoids (29 females and 23 males) were obtained from the sampled fruits, resulting in a female-biased sex ratio (0.56). The fruits were harvested between September 14, 2022 and December 15, 2022 and subsequently in May and July 2023 from sites where adults of *B. dorsalis* were trapped, except for Sant’Agnello and Portici (Naples), where the pest has not been detected previously (Bernardo et al. 2023a CNIE). Details of the emerged parasitoids are summarized in Table 1.

The maximum distance between the most extreme recorded localities was approximately 35 Km. The geographical distribution is depicted in Fig. 1.

Morphological identification

All collected specimens exhibited morphological characteristics consistent with *A. daci* (Fig. 2A–E) as diagnosed in Diaz and Gallardo (2001).

In the genus *Aganaspis* Lin, 1987, two species groups are recognised: *A. pelleranoi* group, [comprising *A. pelleranoi* (Brèthes, 1924) and *A. nordlander* Wharton (1998)], and *A. contracta* group, [comprising *A. contracta* Lin, 1987, *A. ocellata* (Lin, 1987), *A. major* (Lin, 1987), and *A. daci*]. The second group is characterized by eyes with setae and a conspicuous antennal club.

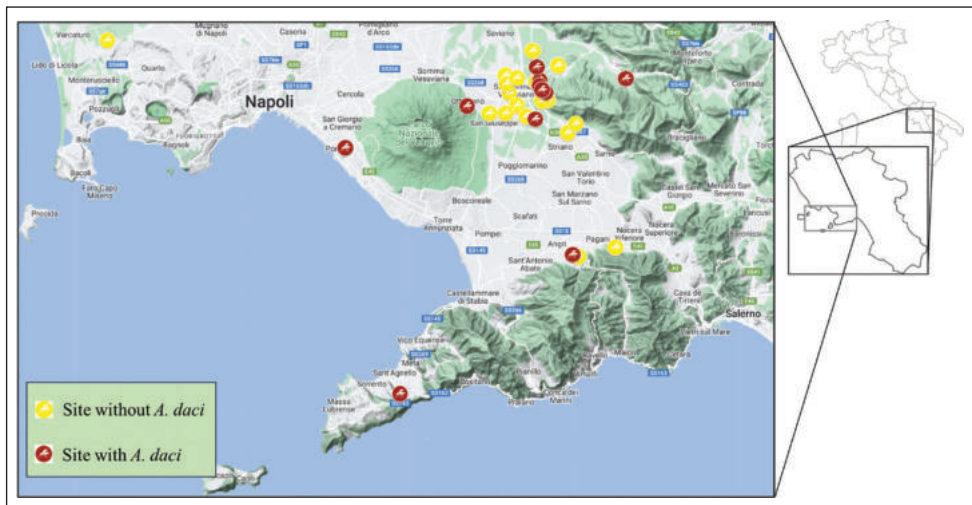


Figure 1. Sampling sites for *A. daci*: sites where *A. daci* emerged (red dots) or not (yellow dots) from puparia of *C. capitata*.

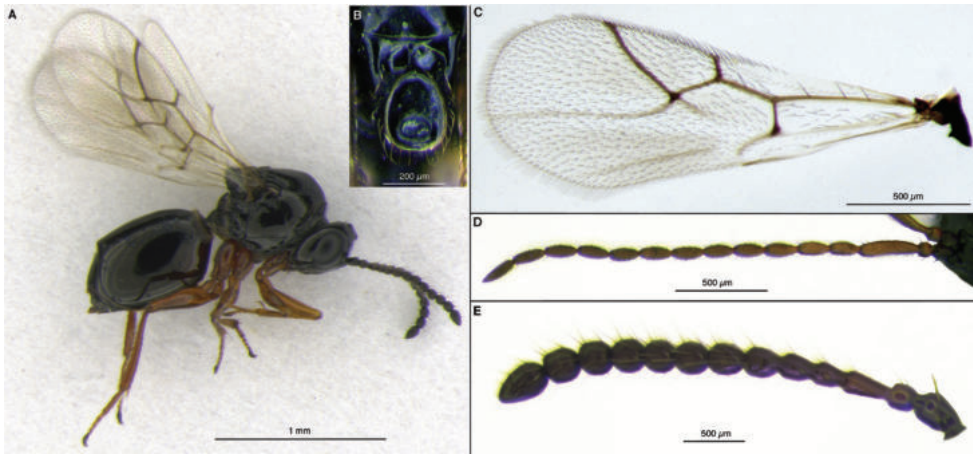


Figure 2. *A. daci* **A** female **B** scutellar plate **C** female forewing **D** male antenna **E** female antenna.

Aganaspis daci can be identified by the 9-segmented antennal club in females, featuring spherical segments (Fig. 2E). In males, antenna segment 3 is distinctly longer than segment 4 (Fig. 2D). The scutellar plate is oblong-ovate, very large, and extends beyond the disc (Fig. 2B). The black body exhibits weak bilateral compression in both sexes (Fig. 2A). When viewed from the dorsal perspective, the head is distinctly wider than long in both sexes, and the ocelli are always arranged in a broad triangle in both sexes (Diaz and Gallardo 2001). The comparison of the specimens obtained from field sampling with those obtained from the IVIA rearing confirmed that all specimens share the same morphological characteristics.

Molecular characterization

The sequences, corresponding to the COI barcoding region, were obtained solely using the LepF1/LepR1 primer pair, resulting in a length of 632 bps, after editing and trimming. Sequencing analyses of *A. daci* specimens revealed the presence of at least three mitochondrial haplotypes (Ha, Hb, and Hc) where Ha and Hb differ each other by 1 bp and Hc showed 0.32% and 0.47% difference with Ha and Hb respectively. In Italian samples all the three mt-haplotypes were recorded (Table 1) while in the whole Spanish samples a single mt-haplotype (Hc) was found. However, these differences (2 or 3 out of 632 bp) do not infer any variations at the amino-acid level.

A BLAST search in the GenBank database showed an 88% similarity with samples identified as *Eucoilinae* sp. (without specific species information). The BOLD system did not find any similarities with sequences in the database since the only available sequences, belonging to *Aganaspis* sp., was short and referred to another COI region.

All specimens collected both in Italy and Spain shared the same nuclear gene sequence (ITS2-28S_D1_D2) with a single exception of the Spanish specimen *Ad_52* that shows a three bases indel.

Discussion and conclusion

Aganaspis daci is a solitary larval-pupal endoparasitoid of tephritids, recognized as an effective biocontrol agent (de Pedro et al. 2021). It was recorded for the first time in Malaysia and Taiwan as a parasitoid of *B. dorsalis* and subsequently released in Hawaii for the biocontrol of the same pest (Weld 1951; Clausen et al. 1965).

Additional releases of *A. daci* were carried out in various countries for the biological control of fruit flies such as *B. dorsalis*, and species belonging to the genus *Anastrepha* Shiner (Diptera: Tephritidae) (Clausen et al. 1965; Andleeb et al. 2010; Adly 2016; El-Heneidy 2019). Due to successful laboratory assay, the parasitoid has also been released in Egypt for the biocontrol of *Bactrocera zonata* (Saunders) (Diptera: Tephritidae), the peach fruit fly (Adly 2016; El-Heneidy 2019).

In Europe, *A. daci* was introduced in France in the 1970s to control *C. capitata*, but the results were inconclusive (de Pedro et al. 2021). Subsequently, it was recorded in the Greek Island of Chios and Spain, as a parasitoid of medfly, and its presence has not been reported in other European countries (Papadopoulos and Katsoyannos 2003; Verdú et al. 2011).

During the monitoring of *B. dorsalis* and other fruit flies, a few individuals of *A. daci* were found in the medfly-infested fruits in Italy. This discovery of *A. daci* represents the first documented finding of this Figitidae species in the country and highlights the expansion of its distribution range in Europe. The intricate history of its releases and findings, both in Europe and other countries within the Mediterranean region, complicates the reconstruction of its diffusion process, leaving its arrival and establishment unclear. Nevertheless, certain evidence permits to formulate hypotheses. Morphological and molecular analyses confirmed that the Italian and Spanish populations belong to the same species. However, mitochondrial studies suggest that only a single haplotype is shared (Hc) between Italian and Spanish individuals. This indicates a potential difference in the origin of at least a part of the Italian population. However, it is essential to consider that this difference might also be linked to the bottleneck phenomenon, particularly in terms of rearing practices, leading to a decrease in the variety of haplotypes (Prentis et al. 2008). Nevertheless, due to the limited number of Spanish specimens analysed, this result may not be conclusive.

Moreover, consistently with other instances of invasive Hymenoptera, where genetic analysis has indicated that invasive events are frequently attributable to populations comprising a solitary or a few haplotypes, the conducted analyses have revealed the presence of at least three haplotypes in Italy (Nugnes et al. 2015; Nugnes et al. 2016; Sabbatini et al. 2019; Sthal et al. 2019). Nonetheless, it is important to note that these analyses have been conducted on a relatively small number of specimens. Thus, the presence of other haplotypes could not be excluded a priori. Furthermore, the absence of similar sequences in the genetic databases prevented a comparison with other samples from different regions. For this reason, it is not possible to estimate the possible origin of the adult wasp here studied. The absolute absence of genetic sequences belonging to a species found and studied in multiple countries is highly unusual. Therefore, the molecular characterization of *A. daci* presented here, using a

mitochondrial region (COI) and two nuclear regions (ITS2-28S_D1_D2), not only represents the characterization of the entities found in Italian areas but also serves as a starting point for potential identifications and genetic studies by other researchers engaged in studies on this species and its congeneric entities.

The hypotheses regarding the arrival of *A. daci* in Italy include independent migration from neighbouring countries where the species is already present (Papadopoulos and Katsoyannos 2003; Verdú et al. 2011; Viggiani 2001; Beltrá and Soto 2011; Nugnes et al. 2016), host-tracking, following the invasion of its host fruit fly species (Radeghieri et al. 2002; Gebiola et al. 2014), or a combination of both. It is indeed plausible that *A. daci* may have arrived in Italy even together with its major host (*B. dorsalis*) which has been recently and repeatedly intercepted in recent years in Europe (Nugnes et al. 2018; Egartner et al. 2019; Vitiello et al. 2020).

The polyphagy of *A. daci* suggests that it could have established in Italy by reproducing on *C. capitata*. However, taking into account the number of Italian tephritids, which were probably not studied in depth because they are not related to agriculture, it cannot be excluded that *A. daci* may have adapted and reproduced on other hosts. Further investigations are required to determine the exact pathway of introduction and establishment.

The recorded sex ratio (0.56) is consistent with the previously calculated range (0.54–0.61) when the parasitoid was reared on *C. capitata*, as reported by de Pedro et al. (2017a).

The performance of *A. daci* as a biocontrol agent has been extensively studied (de Pedro et al. 2016, 2017a; El-Heneidy et al. 2019). Despite its female low fertility and longevity, *A. daci* can induce pupal mortality, resulting in significant reductions of pest populations. However, its effectiveness depends on environmental conditions, with high temperatures (30–35 °C) and low temperatures (about 15 °C) adversely affecting its development and survival (de Pedro et al. 2016). Conflicting reports exist regarding its field activity, with higher parasitism rates observed in some areas compared to others, and several reports indicating very low parasitisation percentages (Papadopoulos and Katsoyannos 2003; Ali et al. 2016; De Pedro et al. 2017b; El-Heneidy et al. 2019; Moraiti et al. 2020; de Pedro et al. 2021).

The presence of *A. daci* in Italy from September to December and again in May and July suggests that the parasitoid may be capable of completing more than one generation per year, particularly during seasons with favourable environmental conditions for its development. The observations made in May and July, following the winter period, further confirm its establishment in Italy.

The expansion of *C. capitata* northward in Italy, driven by climate change, may potentially enable *A. daci* to shift its distribution to other suitable environments.

The Mediterranean region has proven to be conducive to the establishment of *A. daci*, as demonstrated by its presence in Spain, Greece, and now Italy (Papadopoulos and Katsoyannos 2003; de Pedro et al. 2016; this work). The discovery of *A. daci* in Italy not only highlights its natural expansion in Europe, as we have previously discussed, but also its association with *C. capitata*, which presents a potential additional control strategy not only for this pest but also due to its polyphagy for other fruit fly species.

In the coming years, it will be intriguing to assess the stability of the parasitoid population, its spatial and temporal distribution, and the host range of *A. daci*, especially in certain Italian locations where another of its host, *B. dorsalis*, is also found.

It is important to note that European legislation currently imposes restrictions on the introduction of parasitoids for pest control into non-native areas. Despite such regulations, the discovery of *A. daci* in Italy underscores the ability of natural enemies to traverse the globe and establish in distant territories.

Comparable cases are becoming increasingly frequent (Radeghieri et al. 2002; Beltrá et al. 2011; Gebiola et al. 2014; Gebiola et al. 2015a, 2015b; Nugnes et al. 2016; Stahl et al. 2019).

Therefore, it is essential to reconsider some of these regulations in light of the fact that the arrival of any parasitoid, capable of controlling a phytophagous insect and released in a nearby country, can be prevented. Indeed, the delays caused by the mandatory studies only result in a period in which the alien species can develop undisturbed, leading to the massive use of chemicals that are probably more dangerous for the environment and humans than any parasitoid.

Considering the challenges associated with the importation of *B. dorsalis* parasitoids, the significance of this discovery cannot be understated. The presence and widespread distribution of its parasitoid in Italy greatly facilitate the implementation of a viable biological control strategy.

Acknowledgements

The authors are thankful to Francisco Beitia for providing specimens for this study and Fortuna Miele, Laura Figlioli, Giovanna Avventura, Giovanna Ceriello, for their precious technical help.

This study was carried out within the Agritech National Research Center and received funding from the European Union Next-GenerationEU (Piano Nazionale di Ripresa e Resilienza (PNRR) – missione 4 componente 2, investimento 1.4 – d.d. 1032 17/06/2022, cn00000022). This manuscript reflects only the authors' views and opinions, neither the European Union nor the European Commission can be considered responsible for them. Furthermore, this research was supported by the Campania Region-funded URCoFi project (Unità Regionale Coordinamento Fitosanitario) and by the project ComPLEMEntS (Piante complementari: modulazione dei sistemi entomologici) funded by CNR-DISBA.

References

- Ali AY, Ahmad AM, Amar JA, Darwish RY, Izzo AM, Al-Ahmad SA (2016) Field parasitism levels of *Ceratitidis capitata* larvae (Diptera: Tephritidae) by *Aganaspis daci* on different host fruit species in the coastal region of Tartous, Syria. *Biocontrol Science and Technology* 26(12): 1617–1625. <https://doi.org/10.1080/09583157.2016.1229756>

- Adly D (2016) Thermal requirements of the Peach Fruit Fly, *Bactrocera zonata* (Saunders) (Diptera: Tephritidae), and its exotic parasitoid species *Aganaspis daci* (Weld) (Hymenoptera: Eucolilidae). Egyptian Academic Journal of Biological Sciences (A. Entomology) 9(2): 89–96. <https://doi.org/10.21608/eajbsa.2016.12848>
- Andleeb S, Shahid MS, Mehmood R (2010) Biology of parasitoid *Aganaspis daci* (Weld) (Hymenoptera: Eucolilidae). Pakistan Journal of Scientific and Industrial Research 53(4): 201–204.
- Balmès V, Mouttet R (2017) Development and validation of a simplified morphological identification key for larvae of tephritid species most commonly intercepted at import in Europe. EPPO Bulletin 47(1): 91–99. <https://doi.org/10.1111/epp.12369>
- Barratt BI, Moran VC, Bigler F, Van Lenteren JC (2018) The status of biological control and recommendations for improving uptake for the future. BioControl 63: 155–216. <https://doi.org/10.1007/s10526-017-9831-y>
- Beltrá A, Soto A (2011) Primera cita del parasitoide “*Thripobius semiluteus*” Bouček (Hymenoptera: Eulophidae) en España. Boletín de Sanidad Vegetal Plagas 37: 3–8.
- Bernardo U, Miele F, Ascolese R, Carbone C, Griffó R, Nugnes F (2023a) La genesi del processo invasivo di *Bactrocera dorsalis* in Italia. Un evento ineludibile? CNIE 12–16. June 2023 Palermo.
- Bernardo U, Nugnes F, Carbone C, Figlioli L, Viggiani G (2023b) *Aganaspis daci*, parassitoide di *Ceratitis capitata*: benvenuta in Italia! CNIE 12–16. June 2023 Palermo.
- Bernardo U, Nugnes F, Gargiulo S, Nicoletti R, Becchimanzi A, Stinca A, Viggiani G (2021) An integrative study on *Asphondylia* spp. (Diptera: Cecidomyiidae), causing flower galls on Lamiaceae, with description, phenology, and associated fungi of two new species. Insects 12(11): e958. <https://doi.org/10.3390/insects12110958>
- Bokonon-Ganta AH, Ramadan MM, Messing RH (2019) Insectary production and synopsis of *Fopius caudatus* (Hymenoptera: Braconidae), parasitoid of tephritid fruit flies indigenous to Africa. Journal of Asia-Pacific Entomology 22(1): 359–371. <https://doi.org/10.1016/j.aspen.2019.01.018>
- Calla B, Hall B, Hou S, Geib SM (2014) A genomic perspective to assessing quality of mass-reared SIT flies used in Mediterranean fruit fly (*Ceratitis capitata*) eradication in California. BMC Genomics 15(1): e98. <https://doi.org/10.1186/1471-2164-15-98>
- Campbell BC, Steffen-Campbell JD, Werren JH (1993) Phylogeny of the *Nasonia* species complex (Hymenoptera: Pteromalidae) inferred from an internal transcribed spacer (ITS2) and 28S rDNA sequences. Insect Molecular Biology 2: 225–237. <https://doi.org/10.1111/j.1365-2583.1994.tb00142.x>
- Clausen CP, Clancy PW, Chock QC (1965) Biological control of the oriental fruit fly (*Dacus dorsalis*, Hendel) and other tropical fruit flies in Hawaii. United States Department of Agriculture Technical Bulletin 1322: 1–102.
- Coelho RS, Pec M, Silva ALR, Peñaflo MFGV, Marucci RC (2023) Predation potential of the earwig *Euborellia annulipes* on fruit fly larvae and trophic interactions with the parasitoid *Diachasmimorpha longicaudata*. Journal of Applied Entomology 147(2) 147–156. <https://doi.org/10.1111/jen.13091>
- de Benedetta F, Gargiulo S, Miele F, Figlioli L, Innangi M, Audisio P, Nugnes F, Bernardo U (2022) The spread of *Carpophilus truncatus* is on the razor’s edge between an outbreak and a pest invasion. Scientific Reports 12: e18841. <https://doi.org/10.1038/s41598-022-23520-2>

- de Pedro L, Beitia F, Sabater-Munoz B, Asís JD, Tormos J (2016) Effect of temperature on the developmental time, survival of immatures and adult longevity of *Aganaspis daci* (Hymenoptera: Figitidae), a natural enemy of *Ceratitis capitata* (Diptera: Tephritidae). *Crop Protection* 85: 17–22. <https://doi.org/10.1016/j.cropro.2016.03.010>
- de Pedro L, Beitia F, Ferrara F, Asís JD, Sabater-Muñoz B, Tormos J (2017a) Effect of host density and location on the percentage parasitism, fertility and induced mortality of *Aganaspis daci* (Hymenoptera: Figitidae), a parasitoid of *Ceratitis capitata* (Diptera: Tephritidae). *Crop Protection* 92: 160–167. <https://doi.org/10.1016/j.cropro.2016.11.007>
- de Pedro L, Beitia F, Sabater-Muñoz B, Harbi A, Ferrara F, Polidori C, Asís JD, Tormos J (2017b) Parasitism of *Aganaspis daci* against *Ceratitis capitata* under Mediterranean climate conditions. *Entomologia Experimentalis et Applicata* 163(3): 287–295. <https://doi.org/10.1111/eea.12585>
- de Pedro L, Harbi A, Tormos J, Sabater-Muñoz B, Beitia F (2021) A minor role of host fruit on parasitic performance of *Aganaspis daci* (Hymenoptera: Figitidae) on medfly larvae. *Insects* 12: e345. <https://doi.org/10.3390/insects12040345>
- Diaz NB, Gallardo FE (2001) *Aganaspis* Lin, 1987: generic enlargement and a key for the species of neotropical region (Cynipoidea: Figitidae: Eucoilinae). *Physis* 58(134–135): 91–95.
- Egartner A, Lethmayer C, Gottsberger RA, Blümel S (2019) Survey on *Bactrocera* spp. (Tephritidae, Diptera) in Austria. *EPPO Bulletin* 49(3): 578–584. <https://doi.org/10.1111/epp.12604>
- El-Heneidy AH, Hosni ME, Ramadan MM (2019) Identity and biology of *Aganaspis daci* (Weld) (Hymenoptera: Figitidae), recently introduced to Egypt for biological control of *Bactrocera zonata* (Diptera: Tephritidae). *Entomologist's Monthly Magazine* 155(1): 17–37. <https://doi.org/10.31184/m00138908.1551.3958>
- Forshage M, Nordlander G (2008) Identification key to European genera of Eucoilinae (Hymenoptera, Cynipoidea, Figitidae). *Insect Systematics and Evolution* 39(3): 341–359. <https://doi.org/10.1163/187631208794760885>
- Gargiulo S, Nugnes F, De Benedetta F, Bernardo U (2021) *Bactrocera latifrons* in Europe: The importance of the right attractant for detection. *Bulletin of Insectology*: 74: 311–320.
- Gay H (2012) Before and after silent spring: From chemical pesticides to biological control and integrated pest management-Britain, 1945–1980. *Ambix* 59(2): 88–108. <https://doi.org/10.1179/174582312X13345259995930>
- Gebiola M, Bernardo U, Monti MM, Navone P, Viggiani G (2009) *Pnigalio agraulis* (Walker) and *Pnigalio mediterraneus* Ferrière and Delucchi (Hymenoptera: Eulophidae): Two closely related valid species. *Journal of Natural History* 43(39–40): 2465–2480. <https://doi.org/10.1080/00222930903105088>
- Gebiola M, Bernardo U, Ribes A, Gibson GA (2015a) An integrative study of *Necremnus Thomson* (Hymenoptera: Eulophidae) associated with invasive pests in Europe and North America: taxonomic and ecological implications. *Zoological journal of the Linnean Society* 173(2): 352–423. <https://doi.org/10.1111/zoj.12210>
- Gebiola M, Garonna AP, Bernardo U, Belokobylskij SA (2015b) Molecular phylogenetic analyses and morphological variation point to taxonomic problems among four genera of parasitoid Doryctine wasps (Hymenoptera: Braconidae). *Invertebrate Systematics* 29(6): e591. <https://doi.org/10.1071/IS14064>

- Gebiola M, Lopez-Vaamonde C, Nappo AG, Bernardo U (2014) Did the parasitoid *Pnigalio mediterraneus* (Hymenoptera: Eulophidae) track the invasion of the horse chestnut leafminer? *Biological Invasions* 16(4): 843–857. <https://doi.org/10.1007/s10530-013-0542-8>
- Gilioli G, Sperandio G, Colturato M, Pasquali S, Gervasio P, Wilstermann A, Dominic AR, Schrader G (2022) Non-linear physiological responses to climate change: the case of *Ceratitis capitata* distribution and abundance in Europe. *Biological Invasions* 24(1): 261–279. <https://doi.org/10.1007/s10530-021-02639-9>
- Goergen G, Vayssières JF, Gnanvossou D, Tindo M (2011) *Bactrocera invadens* (Diptera: Tephritidae), a new invasive fruit fly pest for the afrotropical Region: Host plant range and distribution in West and Central Africa. *Environmental Entomology* 40(4): 844–854. <https://doi.org/10.1603/EN11017>
- Hajibabaei M, Smith MA, Janzen DH, Rodriguez JJ, Whitfield JB, Hebert PDN (2006) A minimalist barcode can identify a specimen whose DNA is degraded. *Molecular Ecology Notes* 6: 959–964. <https://doi.org/10.1111/j.1471-8286.2006.01470.x>
- Hall TA (1999) BioEdit: a user-friendly biological sequence alignment editor and analysis program for Windows 95/98/NT. *Nucleic Acids Symposium Series* 41: 95–98.
- Jacquet F, Jeuffroy MH, Jouan J, le Cadre E, Litrico I, Malausa T, Reboud X, Huyghe C (2022) Pesticide-free agriculture as a new paradigm for research. In *Agronomy for Sustainable Development* 42(1): 1–8. <https://doi.org/10.1007/s13593-021-00742-8>
- Lichtenberg E, Olson LJ (2018) The fruit and vegetable import pathway for potential invasive pest arrivals. *PLoS ONE* 13(2): e0192280. <https://doi.org/10.1371/journal.pone.0192280>
- Lin KS (1987) *Aganaspis*, a new genus of Eucolidae (Hymenoptera: Cynipoidea). *Taiwan Agricultural Research. Institute Taipei Special Publication* 22: 67–79.
- Marucci PE, Van Den Bosch R, Chong M, Clancy DW (1952) Notes on Parasites of Fruit Flies. *Proceedings of the Hawaiian Entomological Society* 14(03): 371–375.
- Mertens J, Schenk M, Delbianco A, Graziosi I, Vos S (2022) Pest survey card on *Bactrocera dorsalis*. *EFSA Supporting Publications* 18(1): 1–28. <https://doi.org/10.2903/sp.efsa.2021.EN-1999>
- Mirchev PG, Schmidt H, Tsankov G, Avc M (2004) Egg parasitoids of *Thaumatopoea pityocampa* (Den.&Schiff.) (Lepidoptera: Thaumatopoeidae) and their impact. *Journal of Applied Entomology* 128(8): 533–542. <https://doi.org/10.1111/j.1439-0418.2004.00837.x>
- Moore SD (2021) Biological control of a phytosanitary pest (*Thaumatotibia leucotreta*): A case study. *International Journal of Environmental Research and Public Health* 18: e1198. <https://doi.org/10.3390/ijerph18031198>
- Moraiti CA, Kyritsis GA, Papadopoulos NT (2020) Effect of the olive fruit size on the parasitism rates of *Bactrocera oleae* (Diptera: Tephritidae) by the figitid wasp *Aganaspis daci* (Hymenoptera: Figitidae), and first field releases of adult parasitoids in olive grove. *Hellenic Plant Protection Journal* 13(2): 66–77. <https://doi.org/10.2478/hppj-2020-0007>
- Nugnes F, Bernardo U, Viggiani G (2017) An integrative approach to species discrimination in the *Anagrus atomus* group sensu stricto (Hymenoptera: Mymaridae), with a description of a new species. *Systematics and Biodiversity* 15(6): 582–599. <https://doi.org/10.1080/14772000.2017.1299811>
- Nugnes F, Gebiola M, Gualtieri L, Russo E, Sasso R, Bernardo U (2016) When exotic biocontrol agents travel without passport: first record of *Quadrastichus mendeli*, parasitoid of the blue-gum chalcid *Leptocybe invasa*, in Italy. *Bulletin of Insectology* 69(1): 85–91.

- Nugnes F, Gebiola M, Monti MM, Gualtieri L, Giorgini M, Wang J, Bernardo U (2015) Genetic diversity of the invasive gall wasp *Leptocybe invasa* (Hymenoptera: Eulophidae) and of its *Rickettsia* endosymbiont, and associated sex-ratio differences. PLoS ONE 10(5): e0124660. <https://doi.org/10.1371/journal.pone.0124660>
- Nugnes F, Miele F, Carbone C, Ascolese R, Figlioli L, Bernardo U (2023) Studi preliminari sulla variabilità genetica di *Bactrocera dorsalis* e dinamica dell'infestazione in Campania. CNIE 12–16. June 2023 Palermo.
- Nugnes F, Russo E, Viggiani G, Bernardo U (2018) First record of an invasive fruit fly belonging to *Bactrocera dorsalis* complex (Diptera: Tephritidae) in Europe. Insects 9(4): e182. <https://doi.org/10.3390/insects9040182>
- Ovruski S, Aluja M (2000) Hymenopteran parasitoids on fruit-infesting Tephritidae (Diptera) in Latin America and the southern United States: Diversity, distribution, taxonomic status and their use in fruit fly biological control. Integrated Pest Management Reviews 5: 81–107. <https://doi.org/10.1023/A:1009652431251>
- Pace R, Ascolese R, Miele F, Russo E, Griffò RV, Bernardo U, Nugnes F (2022) The bugs in the bags: the risk associated with the introduction of small quantities of fruit and plants by airline passengers. Insects 13: e617. <https://doi.org/10.3390/insects13070617>
- Papadopoulos NT, Katsoyannos BI (2003) Field parasitism of *Ceratitidis capitata* larvae by *Aganaspis daci* in Chios, Greece. Biocontrol 48: 191–196. <https://doi.org/10.1023/A:1022651306249>
- Pieterse W, Manrakhan A, Terblanche JS, Addison P (2020) Comparative demography of *Bactrocera dorsalis* (Hendel) and *Ceratitidis capitata* (Wiedemann) (Diptera: Tephritidae) on deciduous fruit. Bulletin of Entomological Research 110: 185–194. <https://doi.org/10.1017/S0007485319000592>
- Prentis PJ, Wilson JRU, Dormontt EE, Richardson DM, Lowe AJ (2008) Adaptive evolution in invasive species. Trends in Plant Science 13: 288–294. <https://doi.org/10.1016/j.tplants.2008.03.004>
- Purcell MF (1998) Contribution of biological control to integrated pest management of tephritid fruit flies in the tropics and subtropics. Integrated Pest Management Reviews 3: 63–83. <https://doi.org/10.1023/A:1009647429498>
- Radeghieri P, Santi F, Maini S (2002) New record species for the Italian fauna: *Cirrospilus talitzkii* (Hymenoptera Eulophidae), a new parasitoid of *Cameraria ohridella* (Lepidoptera Gracillariidae) (Preliminary note). Bulletin of Insectology 55(1–2): 63–64.
- Sabatino A (1974) Caratteri morfologici distintivi delle larve di *Dacus oleae* Gmel., *Ceratitidis capitata* Wied., *Rhagoletis cerasi* L. (Dipt., Tephritidae). Entomologica 10: 109–116.
- Sabbatini Peverieri G, Mitroiu MD, Bon MC, Balusu R, Benvenuto L, Bernardinelli I, Talamas EJ (2019) Surveys of stink bug egg parasitism in Asia, Europe and North America, morphological taxonomy, and molecular analysis reveal the Holarctic distribution of *Acroclisoides sinicus* (Huang & Liao) (Hymenoptera, Pteromalidae). Journal of Hymenoptera Research 74: 123–151. <https://doi.org/10.3897/jhr.74.46701>
- Sasso R, Gualtieri L, Russo E, Nugnes F, Gebiola M, Bernardo U (2020) The establishment of a rearing technique for the fruit fly parasitoid *Baryscapus silvestrii* increases knowledge of biological, ecological and behavioural traits. BioControl 65(1): 47–57. <https://doi.org/10.1007/s10526-019-09984-8>

- Schulmeister S, Wheeler WC, Carpenter JM (2002) Simultaneous analysis of the basal lineages of Hymenoptera (Insecta) using sensitivity analysis. *Cladistics* 18: 455–484. <https://doi.org/10.1111/j.1096-0031.2002.tb00287.x>
- Scolari F, Valerio F, Benelli G, Papadopoulos NT, Vaníčková L (2021) Tephritid fruit fly semiochemicals: current knowledge and future perspectives. *Insects* 12: 408. <https://doi.org/10.3390/insects12050408>
- Shelly T, Epsky N, Jang EB, Reyes-Flores J, Vargas R (2014) Trapping tephritid fruit flies. lures, area-wide programs, and trade implications; Eds.; Springer: Berlin, Germany, 2014, 643 pp.
- Silvestri F (1916) Descrizione di alcuni Imenotteri Braconidi parassiti di Ditteri Tripaneidi. *Bollettino del Laboratorio di zoologia generale e agraria della Regia Scuola superiore d'agricoltura in Portici* 11: 160–169.
- Silvestri F (1938) La lotta biologica contro le mosche dei frutti della famiglia Trypetidae. *Verh. VII Int. Kongr. F. Ent. Berlin* 4: 2396–2418.
- Stahl J, Tortorici F, Pontini M, Bon MC, Hoelmer K, Marazzi C, Hays T (2019) First discovery of adventive populations of *Trissolcus japonicus* in Europe. *Journal of Pest Science* 92: 371–379. <https://doi.org/10.1007/s10340-018-1061-2>
- Szyniszewska AM, Tatem AJ (2014) Global assessment of seasonal potential distribution of mediterranean fruit fly, *Ceratitis capitata* (Diptera: Tephritidae). *PLoS ONE* 9(11): e111582. <https://doi.org/10.1371/journal.pone.0111582>
- Verdú MJ, Falcó JV, Beitia F, Sabater-Muñoz B (2011) Identificación de un nuevo agente de control biológico de *Ceratitis capitata* en España, el himenóptero eucoilino *Aganaspis daci*. *Proceedings of the XXVIII Jornadas de la Asociación Española de Entomología (AeE)*, Book of Abstracts, Ponferrada, Spain, 6–8.
- Viggiani G (2001) Una svolta nel controllo biologico della minatrice fogliare degli agrumi. *Informatore Agrario* 57(4): 53–55.
- Viggiani G, Bernardo U, Sasso R (2006) Description of *Baryscapus silvestrii*, n. sp. (Hymenoptera: Eulophidae), a new gregarious parasitoid of the olive fly *Bactrocera oleae* (Gmelin) (Diptera: Tephritidae) in southern Italy. *Bollettino del Laboratorio di Entomologia Agraria Filippo Silvestri Portici* 61: 63–70.
- Vitiello M, de Benedetta F, Gargiulo S, Griffò R, Nugnes F, Bernardo U (2020) *Bactrocera dorsalis* in Campania: Insediamento o Incursione? *Entomata* 13: 83–92.
- Wacławik B, Nugnes F, Bernardo U, Gebiola M, Przybycien, M, Lachowska-Cierlik D (2021) An integrative revision of the subgenus *Liophloeodes* (Coleoptera: Curculionidae: Entiminae: Polydrusini): Taxonomic, systematic, biogeographic and evolutionary insights. *Arthropod Systematic Phylogeny* 79: 419–441.
- Wang X, Ramadan MM, Guerrieri E, Messing RH, Johnson MW, Daane KM, Hoelmer KA (2021) Early-acting competitive superiority in opiine parasitoids of fruit flies (Diptera: Tephritidae): Implications for biological control of invasive tephritid pests. *Biological Control* 162: e104725. <https://doi.org/10.1016/j.biocontrol.2021.104725>
- Weld LH (1951) A new species of *Tribliographa* (Hymenoptera: Cynipidae). *Proceedings Hawaiian Entomological Society* 14: 331–332.
- Wharton RA (1997) Classical biological control of fruit Tephritidae. In: Robinson A, Harper G (Eds) *World Crop Pests, Fruit Flies: Their Biology, Natural Enemies, and Control* (Vol. 3b). Elsevier, Amsterdam, 303–313.

At the dawn of megadiversity – Protoitidae, a new family of Chalcidoidea (Hymenoptera) from Lower Cretaceous Lebanese amber

Jonah M. Ulmer^{1,2}, Petr Janšta^{1,3}, Dany Azar^{4,5}, Lars Krogmann^{1,2}

1 Department of Entomology, State Museum of Natural History Stuttgart, Rosenstein 1, 70191 Stuttgart, Germany **2** Institute of Biology, Biological Systematics (190w), University of Hohenheim, Stuttgart, Germany **3** Department of Zoology, Faculty of Science, Charles University, Prague, Czech Republic **4** State Key Laboratory of Palaeobiology and Stratigraphy, Nanjing Institute of Geology and Palaeontology, Chinese Academy of Sciences, Nanjing, China **5** Lebanese University, Faculty of Sciences II, Department of Natural Sciences, Fanar, Matn, Lebanon

Corresponding author: Jonah M. Ulmer (jonah.ulmer@gmail.com)

Academic editor: Ankita Gupta | Received 25 April 2023 | Accepted 7 August 2023 | Published 23 October 2023

<https://zoobank.org/DB845B36-62BA-4DA1-8370-5B36E5916BBO>

Citation: Ulmer JM, Janšta P, Azar D, Krogmann L (2023) At the dawn of megadiversity – Protoitidae, a new family of Chalcidoidea (Hymenoptera) from Lower Cretaceous Lebanese amber. *Journal of Hymenoptera Research* 96: 879–924. <https://doi.org/10.3897/jhr.96.105494>

Abstract

The earliest representatives of Chalcidoidea are described from Barremian age Early Cretaceous Lebanese amber and classified in Protoitidae Ulmer & Krogmann, **fam. nov.** (Hymenoptera: Chalcidoidea). Protoitidae exhibits a high morphological diversity of the terminal metasomal tergum which may indicate a broad spectrum of oviposition capabilities and the ability to occupy a diverse range of ecological niches. Protoitidae comprises two genera, *Protoita* Ulmer & Krogmann, **gen. nov.**, and *Cretaxenomerus* Nel & Azar, 2005 based on *C. jankotejai* Nel & Azar, 2005, which is transferred from Scelionidae (Hymenoptera: Platygastroidea) to Protoitidae. Together, 10 new species, all by Ulmer and Krogmann, are described in the two included genera—*Protoita bidentata*, *P. istvani*, *P. noyesi*, *P. petersi*, *Cretaxenomerus brevis*, *C. curvus*, *C. deangelis*, *C. mirari*, *C. tenuipenna*, and *C. vitreus*. Keys to the genera and species of Protoitidae are provided. In addition, we examine the postulated plesiomorphies and apomorphies within Chalcidoidea with respect to the fossil record, and provide additional hypotheses on their biogeographic origins.

Keywords

Barremian age, Palaeoentomology, plesiomorphic, taxonomy

Introduction

Today, chalcid wasps (Hymenoptera: Chalcidoidea) are among the most diverse lineages of life, following a megaradiation event in the Late Cretaceous (Heraty and Darling 2009; Peters et al. 2018; Cruaud et al. 2023). This diversification however can obfuscate much of the early morphology and homology of the group's origins with rapid radiation often leading to high degrees of homoplasy in groups (Çıplak et al. 2021). Despite their current abundance, the described fossil record of chalcids is sparse. However, those known from prior to the radiation boundary are increasingly important for understanding of the group's evolutionary paths and phylogenetic dating.

Due to its extreme diversification, Chalcidoidea has been the subject of numerous phylogenetic studies since the end of the last century (e.g., Gibson 1986; Heraty et al. 2013; Peters et al. 2018; Cruaud et al. 2023). Chalcidoidea's diversity can be partly attributed to its occupation of nearly every niche and life history strategy for parasitoids, exhibiting thirteen of the fifteen feeding habits of insects (Grissel and Shauff 1990). The rapid diversification which has led to staggering morphological diversity, has also resulted in a high level of morphological convergences (Krogmann and Vilhelmsen 2006). Gibson (1986) began an era of morphologically based phylogenetic studies for the group, as the first to formally examine hypotheses of character evolution within a cladistic concept. He postulated autapomorphies of Chalcidoidea in several additional papers expanding on the understanding of both internal and external anatomy and sister-group relationships (Gibson 1985; Gibson et al. 1999). The three autapomorphies of Chalcidoidea proposed by Gibson (1986) were the presence of a specialized structure of multiporous plate sensillae (MPS) on the flagellar segments, a laterally exposed, free prepectus, and position of the mesothoracic spiracle at the lateral level of the mesoscutum. The loss of the posterior condyle leading to flexible mandibles was recently postulated as an additional autapomorphy (van de Kamp et al. 2022). All of these above-mentioned morphological studies were based heavily, and often solely, on extant crown-group taxa leaving the identity of extinct stem-group chalcids and the ancestral states of morphological characters speculative.

The early pattern of evolution of Chalcidoidea is still uncertain, in part because of the low number of fossils ($n \approx 154$ species) (from paleobioDB; McClennen et al. 2017) relative to the sheer species abundance of extant taxa, more than 22,700 described (Huber 2017a), and an estimated true diversity of 500,000 (Heraty et al. 2013). Likewise, the megaradiation of crown-group Chalcidoidea is shrouded by the 'taxon gap' of the Early Paleocene, which can be clearly seen in the trends of the chalcid fossil record (Fig. 1) as well as from recent molecular studies (Cruaud et al. 2023). The advent of genomics and subsequent introduction of fossils into research of extant taxa, as a tool for calibration of phylogenies, has generated new found interest into the fossil record of Chalcidoidea. The known paleofauna of Chalcidoidea is mostly Eocene taxa that can be associated with extant groups (Fig. 1), however, the relative few described Cretaceous taxa ($n = 27$ species) have been invaluable resources for understanding the timeline of early divergence.

Chalcidoidea is a notoriously difficult group to assess for statements of homology (Krogmann and Vilhelmsen 2006; Heraty et al. 2013). This is only more so the case when working with exclusively extinct lineages relative to extant ones, which can lead to “ambiguous ambiguity” in analysis and interpretation of phylogenies based on fragmentary records (Kearny and Clark 2003). Taphonomy of many fossils, often though not exclusively, those not preserved in amber can also lead to functional ambiguity with structures damaged or obscured leading to fragmentary information in a given fossil itself. All of these variables have made the introduction and interpretation of fossil chalcids into superfamily level studies a difficult task, with studies only in the past decade beginning to integrate early extinct lineages for calibrating phylogenies.

Peters et al. (2018) suggested a late Jurassic origin for Chalcidoidea, with the earliest distinct lineages emerging during early to mid-Cretaceous (129–81 MYA), and the extant crown groups not forming until the Early Paleogene (75–53 MYA). The earliest root node taxon, which was utilized to provide a minimum age for the superfamily, is here described as *Protoita petersi*, gen. et. sp. nov. It came from Lebanese amber and was initially associated with Chalcidoidea only by possession of the apomorphy of specialized MPS along the flagellomeres. An even earlier divergence of crown Chalcidoidea was established by Cruaud et al. (2023) at 162 MYA with the initial split from the hypothesized sister lineage of Chalcidoidea, Mymarommatoidea, occurring in the Early-Middle Jurassic boundary (174 MYA). Subsequent splitting of the major extant clades was determined during the late Jurassic to mid Cretaceous (153–80 MYA), aligning reasonably with the fossil record, in which Mymarommatoidea are often found in Lebanese deposits (Rasnitsyn et al. 2022).

While no Chalcidoidea have previously been described from Lebanese amber, several undoubtedly chalcid taxa have been uncovered from mid-Cretaceous amber deposits, which coincides with the diversification of the superfamily (Fig. 1). *Minutoma yathribi* Kaddumi, 2005, described as the oldest chalcid from Jordanian amber (115 MYA) was initially placed in Mymaridae, the sister family to all Chalcidoidea (Gibson et al. 1999; Munro et al. 2011; Peters et al. 2018; Cruaud et al. 2023). Later, Heraty et al. (2013) suggested this might be a member of the subfamily Bouceklytinae Yoshimoto 1975, a fossil subfamily of Tetracampidae known already from Campanian Cretaceous Canadian amber (83.5–70.6 MYA) (Yoshimoto 1975). Kaddumi (2005) also mentioned a eupelmid (Chalcidoidea: Euplemidae) wasps in the same amber (lower Cretaceous amber deposits of the Zarqa river basin), but based on wing venation and a dorsoventrally compressed metasoma it is very likely Scelionidae (Platygasteroidea).

This uncertainty of fossil placement is further seen in the description of the putative pteromalid, *Parviformosus wohlabeae* Barling et al. (2013), which was described from a compression fossil from a late Aptian Crato deposit in Brazil (110 MYA). Due to the nature of compression fossils, many of the necessary diagnostic characters of Chalcidoidea are not visible and its placement was based purely on a comparable gestalt to the subfamily Sycophaginae (Agaonidae). The species was subsequently moved to Proctotrupomorpha *incertae sedis* by Haas et al. (2020).

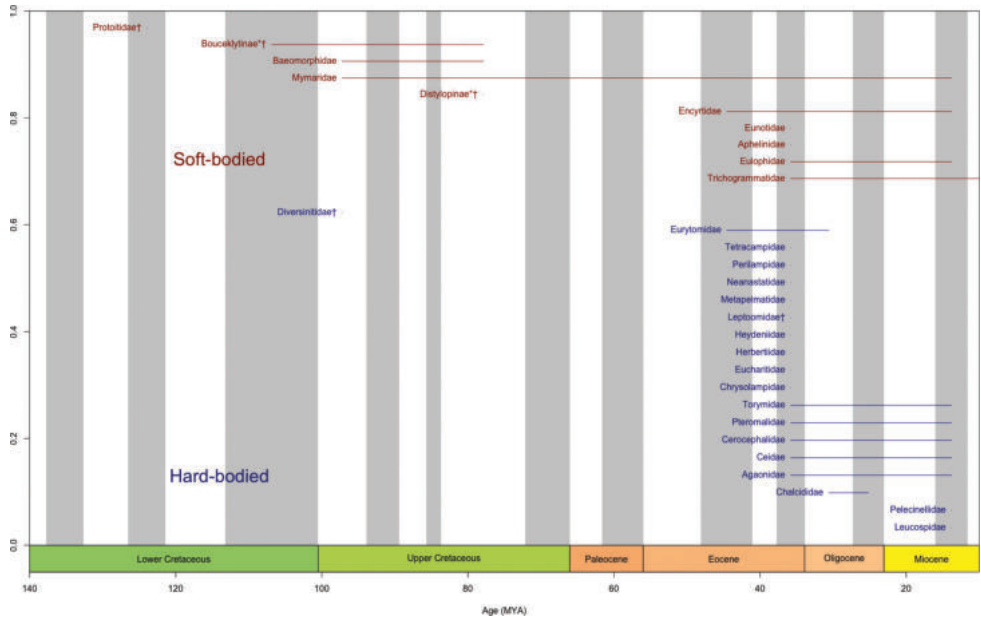


Figure 1. Graph of identified Chalcidoidea families along the fossil record. Points are singleton taxa known only within the fossil record from one time period, whereas those with a fossil record extending multiple ages are shown as a line through the ages in which they are represented. Alternating gray and white bands represent geological eras. Extinct families are denoted by †. Boucekytinae and Distylopinae are noted with an asterisk (*) because their familial placement is uncertain. Taxa in red correspond to the “soft-bodied” clade (Soft-bodied), while taxa in blue correspond to the “hard-bodied” (Hard-bodied) lineages based on Cruaud et al. (2023). Data sourced from Paleodb. Family names adopted from Burks et al. (2022) and Gibson and Fusu (2023).

Fossil “true” Chalcidoidea are more prevalent within the Upper Cretaceous (Burmese) deposits, although the sister group Mymarommatoidea is known already from Lebanese amber (Rasnitsyn et al. 2022). The earliest confirmed chalcids are *Myanmymar areconoides* Poinar & Huber, 2011 (Mymaridae) and *Baeomorpha liorum* Huber, Shih & Ren, 2019 (Baeomorphidae), both from Burmese amber (99 MYA) (Poinar and Huber 2011; Huber et al. 2019). These taxa are consistent with the current calibrated superfamily phylogeny (Cruaud et al. 2023) as Mymaridae and Baeomorphidae are the oldest known extant lineages of Chalcidoidea. *Baeomorpha* Yoshimoto, 1975 was originally described from Campanian Canadian Cretaceous amber (83.5–70.6 MYA) and classified within Tetracampidae, but was later transferred to the small extant, relictual family Baeomorphidae by Gumovsky et al. (2018). Baeomorphidae was previously known as Rotoitidae, which contained two extant genera prior to being synonymized under Baeomorphidae due to priority in subfamilial names (Burks et al. 2022). Gumovsky et al. (2018) subsequently described 10 additional species of *Baeomorpha* as well as a new fossil genus, *Tai-*

myromorpha, within Baeomorphidae, all from Upper-Santonian Yantardakh amber (85.8–83.5 MYA). This makes Mymaridae and Baeomorphidae, the two basalmost lineages (Cruaud et al. 2023), one of the most prevalent chalcids within the fossil record from Lower Cenomanian through the Miocene (paleoDB 2022; Fig. 1). Unlike Mymaridae, no Baeomorphidae are known between the Cretaceous fauna and the two extant genera.

Excluding Bouceklytinae (uncertain subfamily), Diversitinidae was the only valid extinct family of Chalcidoidea described from Cretaceous (Burmese) amber (Haas et al. 2018). The family consists of three monotypic genera, *Diversinitus attenboroughi*, *Burminata caputaeria*, and *Glabilia barbata* Haas, Burks & Krogmann. Its placement as a chalcid is well supported by the presence of multiporous plate sensillae (MPS) on the flagellum as well as a laterally distinct prepectus, though its phylogenetic placement within Chalcidoidea is uncertain. Despite its age, it shares few symplesiomorphic characters with Mymaridae and Baeomorphidae such as an exposed labrum and MPS on the flagellomere 1 (fl1) in males and some females. While it retains many putative plesiomorphies of the superfamily (well-developed fl1, presence of a frenum, and peg-like cerci), this could indicate a ‘gap’ in the fossil record of potentially transitional taxa between the early lineages of Chalcidoidea from the Cretaceous and their descendants (Gibson 2003; Krogmann and Vilhelmsen 2006; Heraty et al. 2013; Haas et al. 2018).

The Chalcidoidea fossil record prior to this work consists of approximately 154 described species (Suppl. material 1). Of that, only 27 species have been described from the Cretaceous, with the vast majority (n=127) being from the Eocene onward (Fig. 1). Hong (2002) also described two new chalcid families from Ypresian Xilutian amber from China (56–47 MYA), but all the species names, and hence the two new families are considered as unavailable because the author provided no explicit statement of the depository of the primary type material (see ICZN 1999, Article 16.4.2; Noyes 2021).

Lebanese amber is one of the oldest fossil sources, dating to the Barremian age of the Lower Cretaceous (~130 MYA) (Azar et al. 2010; Granier et al. 2016; Maksoud and Azar 2020; Maksoud et al. 2017, 2022). Due to its age, Lebanese amber includes some of the earliest representatives of the extant lineages of insects, as well as extinct families which are likely ancestors of known groups. Lebanese amber likewise provides one of the only examinations of the earliest radiations of major insect lineages over northeastern Gondwana (Poinar and Milki 2001). The study of the different Lebanese amber inclusions has allowed for the reconstruction of the palaeoenvironment. The information provided by well-preserved inclusions including palynology data corroborate the palaeoenvironment of the resin deposits as a tropical dense, warm, and humid forest with a very complex fluvial system, altogether close to the sea (Poinar and Milki 2001). In addition, most of the fauna entombed in Lebanese amber was living on the lower to mid-parts of trees. This could be explained by the fact that this type of fauna has more chance to be trapped because normally all resin-drops falling

from a tree pass inevitably and more frequently through these zones (Azar et al. 2010; Maksoud and Azar 2020; Maksoud et al. 2022). The environment of the Barremian age is comparable to the younger and more commonly studied Burmese amber of Eastern Gondwana.

Because the most recent paleobiogeographic models suggest a Southern Gondwana origin for chalcids (Cruaud et al. 2022), with multiple northward dispersals between 150 and 100 MYA, the examination of older northeastern Gondwanan fauna can provide novel insights into the earliest range expansions of a fledgling group. Herein, we provide the description of a new family of Chalcidoidea from Lebanese amber, the earliest currently known, based on 15 fossils. The new family is classified as two genera (one described as a new) and 11 species, of which ten are newly described. Postulated plesiomorphies and hypotheses about the early diversification of Chalcidoidea pre-radiation are discussed.

Methods

Specimens

Among the 450 different outcrops of amber-bearing sediment from the Lower Cretaceous in Lebanon, 29 outcrops provide biological inclusions. In the present study we examined 15 specimens from two outcrops:

1. Hammana / Mdeyrij, Caza Baabda, Mouhafazet Mount Lebanon; lower Barremian (Granier et al. 2016; Maksoud et al. 2017, 2021)
2. Roum – Aazour – Homsiyeh, Caza Jezzine, Mouhafazet South Lebanon; lower Barremian (Granier et al. 2016; Maksoud et al. 2017, 2021).

Of the examined specimens, all but one, *Protoita istvani*, sp. nov., are from the Hammana outcrop.

All the material was previously deposited at the National Museum of Natural History, Paris, France (MNHN) and is now deposited at the Natural History Museum of the Lebanese University, Faculty of Sciences II, Fanar, Lebanon.

Imaging

Relevant material was prepared following (Azar et al. 2003) between two coverslips, using Canada balsam as a mounting medium. Specimens were examined and scored under a Leica M205C stereo microscope with a 7.8–320× magnification. Imaging of specimens was performed with a Keyence VHX 5000 digital microscope. Images were stacked and scale bars placed using the proprietary software. Measurements were taken based on the stacked images in ImageJ (v. 2.1.0). All measurements are in micrometers (µm). Plates were generated in Adobe Photoshop 2022.

Fossil biodiversity analysis

Fossil data for Chalcidoidea was pulled from the paleobioDB (McClennen et al. 2017), data was subsequently checked for errors and harmonized across all taxa for analysis in OpenRefine. Time series plots at the genus and family level were generated in R, with the DivDyn package (Kocsis et al. 2019). Fossil data was set based on its earliest possible age rather than oldest when an interval range is given for its occurrence, following the reasoning of Klopstein (2021).

Terminology

Terminology follows the Hymenoptera Anatomy Ontology (HAO) (Yoder et al. 2010), all term abbreviations will be noted at their first time of use in figure captions or in text. Additional wing terminology is derived from Heraty et al. (2013; Fig. 2), with modifications for clarity of venation variation present in the taxon based on HAO preferred synonyms. Measurements are given in micrometers.

Notes on rationale for discretization of uncertain characters

Some morphological characters are of a continuous or difficult to discretize nature (e.g., clavomere segments) or their physical boundaries are not clearly defined in some taxa (e.g., marginal wing venation). The need for consistency and checkpoints of characters amongst all taxa are critical for their interpretation, especially within paleotaxonomy where structures can be degraded or obscured. Here we provide our rationale for discretizing such characters within Protoitidae.

Marginal vein (mv)—The marginal vein of Chalcidoidea is usually delimited between either the end of the costal cell (cc) proximally or the junction of the hyaline break and the point of intersection of the stigmal vein and postmarginal vein. In several specimens of Protoitidae the costal cell is not visible or folded in a way that it does not provide clear indication of the proximal starting point of the marginal vein. In these specimens we use the presence of a weakening of the wing venation at a junction similar to the hyaline break in higher chalcids, which often has sensilla that mark the beginning of the marginal vein (hb; Fig. 2A).

Flagellomere (fl)/ funicle (fu)/ clavomere (cl)—Within chalcid antennal terminology, flagellomeres are all the antennomeres beyond the pedicel, whereas funicular segments are defined as the flagellomeres located between the anellus or anelli (often ring-like segment(s) directly distal of pedicel that always lack MPS) and clava. Protoitidae lack an anellus, the basal flagellomere being longer than wide and having MPS, so for the sake of clarity when discussing antennal segments “flagellomere” is used for all segments beyond the pedicel including clavomere(s), and funicle for all segments between pedicel and clava. The claval segments of several taxa are often difficult to discern because of a gradual increase in flagellomere width through the entire length of the flagellum. Likewise, many fossil taxa described are based on singletons so shape and closeness of antennal segments are difficult

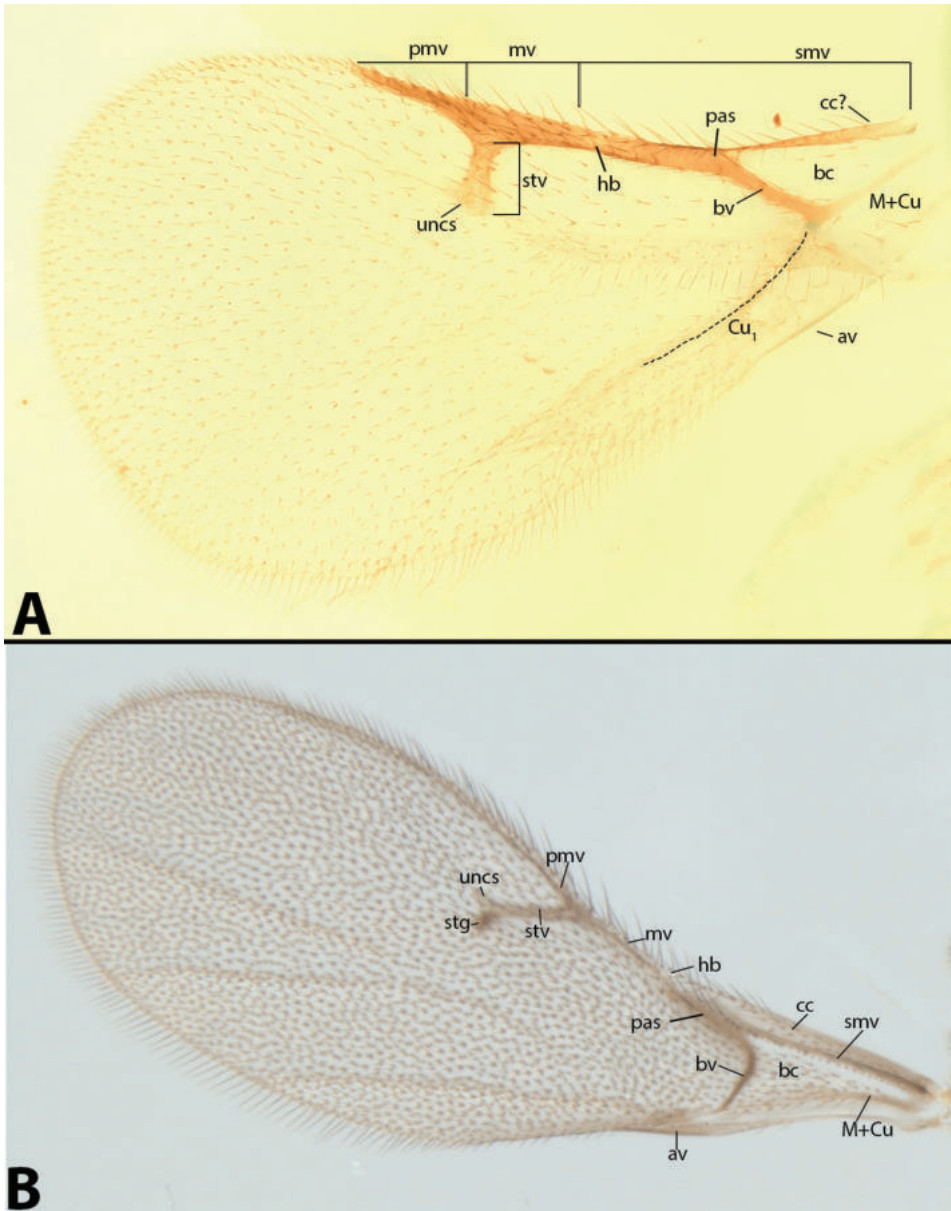


Figure 2. Fore wing morphology and terminology **A** *Cretaxenomerus vitreus*, sp. nov. **B** *Rotoita* sp. (Baeomorphidae). **av** = anal vein; **bc** = basal cell; **bv** = basal vein; **cc** = costal cell; **Cu₁** = cubital vein; **hb** = hyaline break; **M+Cu** = medio-cubital crossvein; **mv** = marginal vein; **pas** = parastigma; **pmv** = postmarginal vein; **smv** = submarginal vein; **stv** = stigmal vein; **uncs** = unicus.

to state as true or as taphonomic artifacts. Within this work, we assign and count claval segments starting at those without a clear ‘gap’ at the joint with the subsequent segment (Fig. 3A, B). Nearly all protoitids have at minimum a 2-segmented clava due to the partial fusion of fl_{11} and fl_{12} (Fig. 3A, B: cl_1, cl_2). *Cretaxenomerus vitreus* and *C. tenuipenna* have no

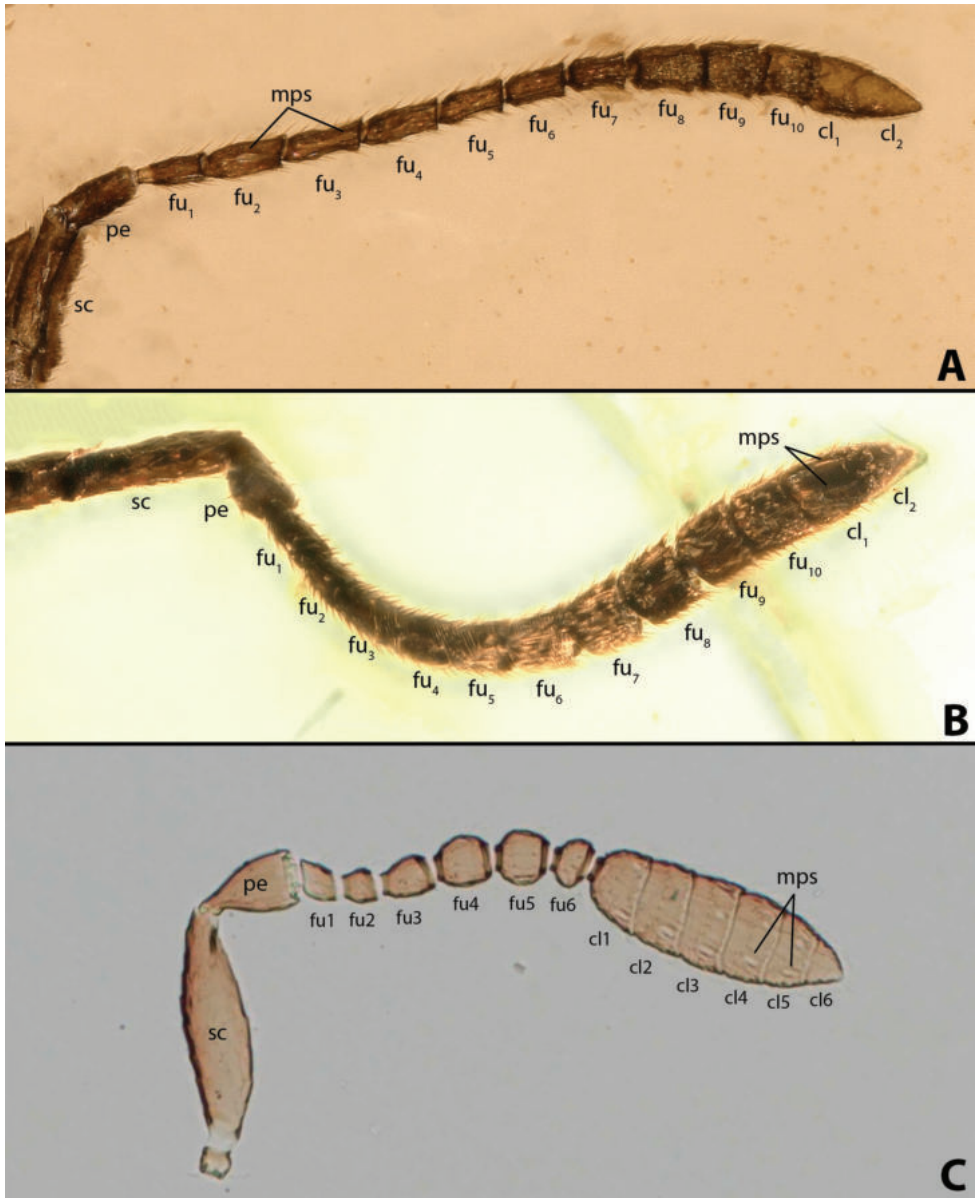


Figure 3. Antennal morphology **A** *Protoita noyesi*, sp. nov. **B** *Cretaxenomerus curvus*, sp. nov. **C** *Rotoita basalis* (Baeomorphidae). **cl_n** = claval segment n; **fu_n** = funicular segment n; **mps** = multiporous plate sensilla; **pe** = pedicel; **sc** = scape.

distinction or fusion in the terminal flagellomeres and thus the terminal flagellomere (fl_{12}) is considered the clava. In many species there is a dimensional variation in the terminal five or six flagellomeres, however consistent identification of these as claval segments is difficult within fossils where the angle of the antennae may obfuscate the closeness of two segments (for comparison with Baeomorphidae antennae see Fig. 3C).

Results

Systematic palaeontology

Order Hymenoptera Linnaeus, 1758

Superfamily Chalcidoidea

Family Protoitidae Ulmer & Krogmann, fam. nov.

<https://zoobank.org/D3E42A23-E578-4343-87E7-78A4B0B86E55>

Type genus. *Protoita*, gen. nov.

Diagnosis. Antenna 14-segmented (Fig. 3A, B); clava 1–3 segmented, terminal two flagellomeres differentiated by a line of weakness (partially fused) when clava multi-segmented (Fig. 3A, B); MPS present on all flagellomeres. Clypeus inflected dorsally and laterally with an arched groove at margin (Figs 6G, 7C, 8E, 10C). Malar sulcus present. Lower tentorial bridge present, about as broad as distance between lower margin of occipital foramen and dorsal margin of hypostomal foramen. Postgenal bridge absent (Fig. 5A). Pronotum dorsally narrow, almost entirely concealed by mesonotum medially in dorsal view (Figs 5D, 6C, 7A, 8B, 10D, 11D); lateral panel externally reaching base of tegula. Mesonotum about 4× as long as mesoscutellum (Figs 4D, 5D, 6C, 7A, 8B, 11D, 13A, 14A). Prepectus laterally evident as elongate, vertical sclerite partly covered by posterior-most margin of lateral panel of pronotum (Fig. 16A, B). Mesopleuron oriented dorsoventrally, abutting ventrally on a lower plane than coxae (Fig. 8B); mesodiscrimen deeply invaginated. Fore wing with basal vein completely sclerotized (Fig. 2A). M+Cu pigmented at least distally and usually sclerotized. Marginal vein strongly sclerotized and 2–3× as wide as submarginal vein. Parastigma usually as wide as or nearly as wide as marginal vein (Fig. 2A). Costal cell reaching far beyond junction of submarginal vein and basal vein. Retinaculum pigmented. Hind wing with three hamuli of equal length and orientation, the distal hamulus not extending beyond midpoint of hind wing. Meso- and metacoxae abutting, separated widely from procoxa by mesopleuron (Figs 6A, C, 8B, 11D, 13A). Protibial spur curved and apically cleft; probasitarus with basitarsal comb nearly always present (Figs 4C, 7D, 10E, 11F, 14D:cal). Metatibia with two apical spurs with shorter spur about 1/3 length of longer spur (Figs 8A, 9A, 11C). All tarsi 5-segmented; basitarsi about as long as or slightly shorter than tarsomeres 2–4 (Figs 4A, 5A, 6A, 8A, 10E, 11F, 15C). Metasoma with short petiole. Hypopygium reaching end of metasoma.

Key to genera of Protoitidae, fam. nov.

- 1 Metasoma in dorsal view triangular in shape and broadly attached to mesosoma (Figs 4A, 5A, 7A); syntergum approximately equal in length to preceding tergite (Figs 4G, 6F); cerci digitiform. Body length less than 1 mm ***Protoita* gen. nov.**
- Metasoma in dorsal view ovoid, with distinct constriction between meta- and mesosoma (Figs 9A, 12A, 13A, 14A); syntergum nearly always elongate (single

exception *Cretaxenomerus deangelis* with syntergum very short and narrow) (Figs 8D, 10F, 12D, 13B, 15B); cerci button-like. Body length greater than 1 mm. *Cretaxenomerus* Nel & Azar, 2005

***Protoita* Ulmer & Krogmann, gen. nov.**

<https://zoobank.org/7B0689EB-29B3-4D83-AB1C-3C32F8EC1CF2>

Diagnosis. Small, less than 1 mm in length. Head transverse in dorsal view, wider than mesosoma and with temple narrow. Metasoma sessile, broadly associated with mesosoma, and in dorsal view triangular in shape; syntergum no longer than preceding tergite; cerci digitiform. Female with exerted ovipositor at most $\frac{1}{4}$ as long as length of metasoma.

Key to species of *Protoita*, gen. nov.

- 1 Head globular or of about equal dimensions (Figs 4E, 7A)..... **2**
- Head narrowed antero-posteriorly in dorsal view (Figs 5A, 6D, G). **3**
- 2 Terminal clavomere equal in length to preceding clavomere (Fig. 4B). Head in lateral view triangular (Fig. 4A); occiput deeply impressed (Fig. 4E). with basitarsal comb sparse, only present on proximal half of tarsomere (Fig. 4C) ***Protoita noyesi* sp. nov.**
- Terminal clavomere $\frac{1}{2}$ length of preceding clavomere (Fig. 7B); head in dorsal and anterior view globular, slightly broader than long (Fig. 7A, C). Foreleg with basitarsal comb present along entire length (Fig. 7D)..... ***Protoita petersi* sp. nov.**
- 3 Antenna with clava 3-segmented; funicular segments all about equal in dimensions (Fig. 5A, C). Mandibles bidentate (Fig. 5E). Foreleg without basitarsal comb. Stigmal vein at 90° angle with marginal vein (Fig. 5A). Male (Fig. 5B)..... ***Protoita bidentata* sp. nov.**
- Antenna with clava 2-segmented; funicular segments 1–3 $4\times$ as long as wide (Fig. 6A, B). Mandibles tridentate (Fig. 6G). Fore leg with basitarsal comb. Stigmal vein at 45° angle with marginal vein (Fig. 6A, C). Female (Fig. 6F)..... ***Protoita istvani* sp. nov.**

***Protoita noyesi* Ulmer & Krogmann, sp. nov.**

<https://zoobank.org/DD237DE0-0F2D-447F-933C-4008D1B1ABBC>

Figs 3A, 4, 16B

Diagnosis. The female of *Protoita noyesi* differs from those of other species in the genus by the following combination of characters: occiput impressed relative to vertex (Fig. 4E). Flagellomere 8–12 with micropilosity on ventrum. Ovipositor sheaths broadened at midpoint before tapering distally (Fig. 4G).

Description. Female. Body length 876. Body uniformly brown except legs light brown. Wings with light brown infumation, uniformly setose. Right mesopleuron

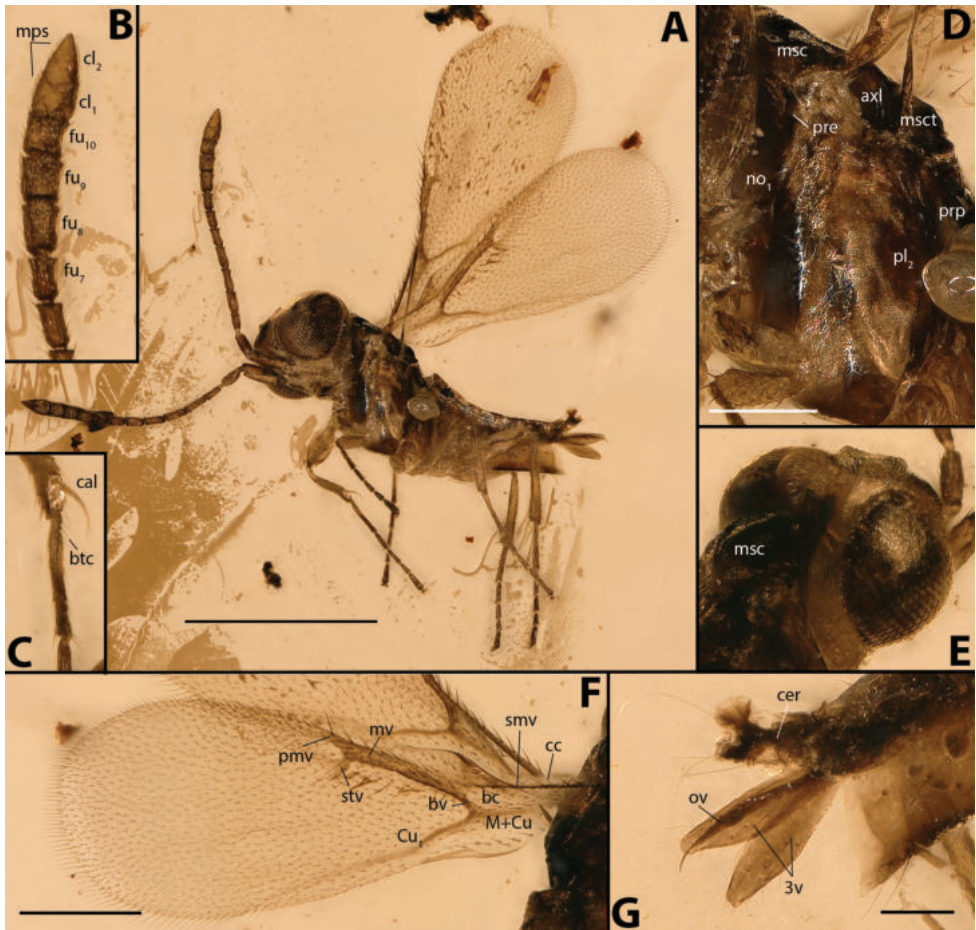


Figure 4. *Protoita noyesi*, holotype **A** lateral habitus **B** apical part of antenna **C** fore leg basitarsus **D** mesosoma, lateral **E** head, posterior **F** fore wing **G** ovipositor complex and terminal metasomal segments. Scale bars: 500 μm (**A**); 200 μm (**F**); 100 μm (**D**); 50 μm (**G**). **3v** = 3rd valvulae; **axl** = axillula; **btc** = basitarsal comb; **cal** = calcar; **cer** = cerci; **msc** = mesoscutum; **msct** = mesoscutellum; **no₁** = pronotum; **ov** = ovipositor; **pl₂** = mesopleuron; **pre** = prepectus; **prp** = propodeum.

with bluish metallic tint. **Head** wedge shaped in lateral view, wider than mesosoma in dorsoventral view (Fig. 4A, E), width 301, length 249. Postorbital carina present. Temple very narrow (Fig. 4E). Vertex concave. Occiput impressed. Antennal scrobes depressed. Toruli closer to inner margin of eye than each other. Antennal insertion at midline of eye. Genal margin with 3 setae on ventral edge. Clypeus inflexed, dorsally merging with interantennal projection. Mandibles on higher plane from face. Mandibular dentition 3:3. Maxillary palps 2–3 segmented (specimen position makes exact count impossible). Labial palps damaged. **Antenna** length 586. Radicle as long as basal width of scape. Scape distally laterally compressed, 2.5 \times as long as wide. Pedicel 2.25 \times as long as wide. Funicles 1–4 at least 2.6 \times as long as wide; fu7 2 \times as long as wide. Clava at least

2 segmented. All clavomeres with micropilosity on ventral side. **Mesosoma** (Fig. 4D) length 263. Lateral panel of pronotum narrow, not touching tegula. Mesonotum length 185. Mesoscutum partially collapsed. Prepectus present as vertically narrow triangular sclerite. Mesopleuron about 2.6× as long as wide (281:105); pleural suture present as depression. Axillae relatively small; axillulae with dorsal flange extending over wing base slightly (Fig. 4D). Mesoscutellum posteriorly sloped. Dorsellum band-like, width 28. Propodeum sloping posteriorly, at 45° angle relative to dorsal plane of mesosoma. **Wings** (Fig. 4F). Fore wing length 826, width 330. Longest marginal seta of fore wing 42. Submarginal vein length 350. Marginal vein wide and strongly sclerotized, length 69, width 22. Cubital vein sclerotized along basal 1/3 of its length, then present as pigmented fold, length 200. Basal vein sclerotized, length 27. Stigmal vein short, length 30. Uncus elongate, extending distally further than postmarginal vein (possible artifact); 5 uncal sensillae present. Postmarginal vein slightly shorter than marginal vein. Basal cell with 2–3 rows of setae. Hind wing slender; length 598, width 35. Length of longest marginal seta of hind wing 37. **Legs** with barsitarsal comb of fore leg present as sparse setation only on proximal half of tarsomere (Fig. 4C:btc). Trochanter of mid leg elongate relative to fore- and metatrochanter. **Metasoma** length 410. Gaster wedge-like. Metasoma broadly associated with mesosoma; petiole (Mt₁) not visible. Mt_{2,9} visible. 4 sternal segments visible with hypopygium equal in length to preceding 3 segments, protruding laterally and reaching end of metasoma. Ovipositor slightly extruded; ovipositor sheaths flattened and broadest in middle (Fig. 4G).

Male. Unknown.

Holotype. Female. Hammana / Mdeyrij, Caza Baabda, Mouhafazet Mount Lebanon; lower Barremian. In amber mounted in Canada Balsam. Deposited at Natural History Museum of the Lebanese University, accession/specimen number: 407AB.

Type condition. Specimen in good condition with slight detachment from amber along the mesopleuron, and bubble formed around propodeal spiracle.

Etymology. The specific epithet is a patronym in honor of Dr John Noyes for his lifelong contributions to chalcidology.

***Protoita bidentata* Ulmer & Krogmann, sp. nov.**

<https://zoobank.org/35C89B66-DAA3-4CE6-9DD5-9F9D1716E03B>

Fig. 5

Diagnosis. *Protoita bidentata*, the only species of the genus known from the male, differs from all other species in the genus by the following combination of characters: Body and antenna bicolored (Fig. 5A). Mandibular formula 2:2 (Fig. 5E:md). Clava 3-segmented (Fig. 5C). Stigmal vein of fore wing extending at a right angle to wing margin (Fig. 5A). Basitarsal comb of fore leg lacking.

Description. Male. Body length 855. Head, scape, pedicel and fu₁–fu₄ brown. Mesosoma, metasoma and fu₅ to tip of clava dark brown. Legs pale. Sculpture on head, meso- and metasoma alutaceous. Wings hyaline, uniformly pilose, damaged beyond postmarginal

vein (Fig. 5A). **Head** strongly transverse, $2\times$ as wide as long in dorsal view (360/179). Temples very short, about $0.15\times$ as long as eye length. Lower tentorial bridge wide, about as wide as long; postgenal bridge absent; hypostomal carina complete (Fig. 5E:hyc). Occipital carina present (Fig. 5E). Antennal scrobe slightly depressed. Interantennal region convex. Antennal insertion closer to inner eye margin than each other (Fig. 5A). Clypeus not visible. Dentition 2:2, extending out from facial plane (Fig. 5E:md). Maxillary palps 3-segmented (Fig. 5E:mxp). Labial palps 2-segmented (Fig. 5E:lbp). Maxilla wider than labium. **Antenna** length 533. Pedicel and scape partly damaged. Fu_1 about or slightly less as wide as pedicel, other flagellomeres gradually widening distally, fu_{1-6} not less than $2\times$ as long as wide, fu_{7-9} less than $2\times$ as long as wide. Clava 3-segmented, clava length 85 (Fig. 5C). MPS present on all segments including terminal segment; MPS extend beyond the distal edge of the segment. Claval segments equilateral and closely associated relative to funicle segments; clava without micropilosity (Fig. 5C). **Mesosoma** length 346. Transcutal articulation present as weak line of separation (Fig. 5D:tsc). Mesopleuron large, partially obscured by bubble (Fig. 5D:pl₂); separated from metapleuron by suture. Axillae not pronounced; axillulae slightly flanged (Fig. 5D). Mesonotum length 224. Mesoscutellum convex, length 44, $2\times$ as long as wide (Fig. 5D:msct). Metanotum narrow, band-like, width 21 (Fig. 5D:no₃). Propodeum partially obscured by abdomen, relatively short, as long as or slightly longer than mesoscutellum (Fig. 5D:prp); propodeal spiracle visible, oval, posteriorly angled, closer to anterior margin of propodeum than its diameter (Fig. 5D:psp). **Wings**. Fore wing damaged beyond midline. Fore wing width 323. Longest marginal seta length 46. Submarginal vein length 379. Marginal vein narrow, length 81, width 24. Cubital vein narrow, weakly pigmented. Basal vein sclerotized, length 60. Stigmal vein straight, 90° relative to dorsal wing margin, stigmal vein length 44. Uncus present with ephemeralline extending distally. Postmarginal vein length 53. Hind wing length 440, width 28. Longest marginal seta of hind wing 35 (Fig. 5A). **Legs**. Protibial calcar long, curved, apically bifurcate. Basitarsus of fore leg ventrally curved; no basitarsal comb. **Metasoma** length 313. Metasoma broadly associated with mesosoma; petiole obscured (Fig. 5A). Mt_{2-9} visible; all equal in length except Mt_2 , dorsally slightly shorter. 3 sternal segments visible, each about $2\times$ as long as tergal segment average length. Cerci between Mt_8 and Mt_9 , digitiform, about $2\times$ as long as digitiform base. **Genitalia** length externally 97. Genital capsule externally protruding. Paramere present; single apical parameral setae present. Intervosellar process broad, extends equally in length to aedeagus. Aedeagus broad with 2 sets of sensillae (Fig. 5B:aed). Digitus with 2 digital processes (Fig. 5B:dig).

Female. Unknown.

Specimens examined. *Holotype*: male, Hammana / Mdeyrij, Caza Baabda, Mouhafazet Mount Lebanon; lower Barremian. In amber mounted in Canada Balsam. Deposited at Natural History Museum of the Lebanese University, accession/specimen number: 182.

Type condition. Specimen with distal $\frac{1}{3}$ of its wings missing and basal antennomeres damaged.

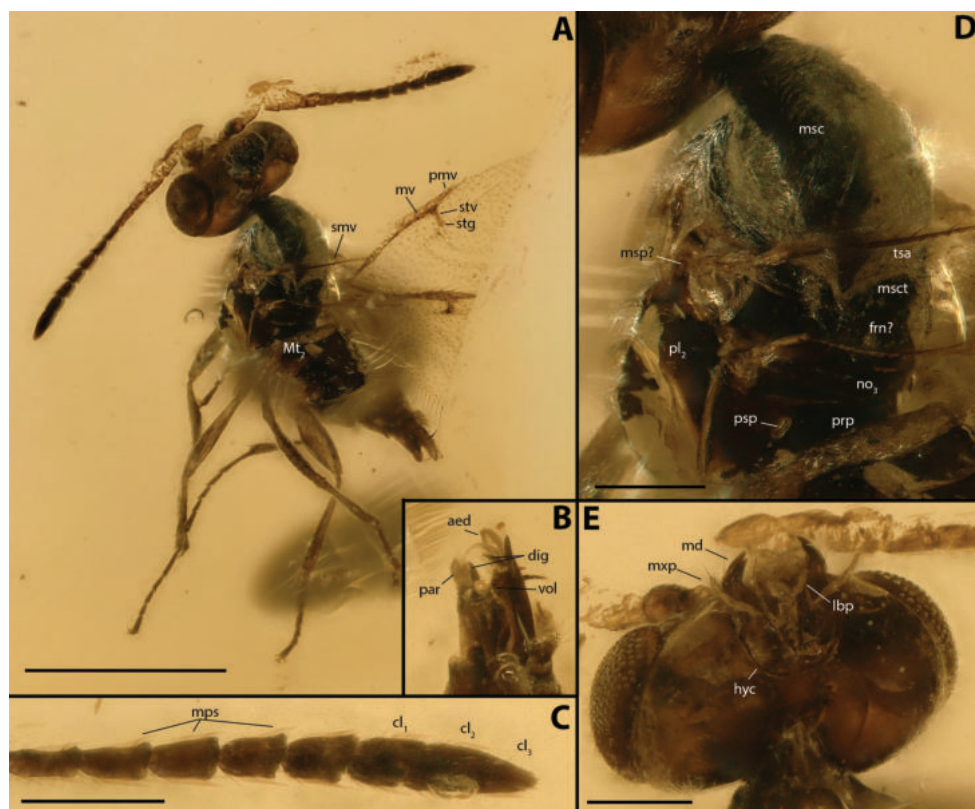


Figure 5. *Protoita bidentata*, holotype **A** dorsolateral habitus **B** male genitalia, ventral **C** terminal funicular segments and clava **D** mesosoma, dorsolateral **E** head, posteroventral. Scale bars: 500 μm (**A**); 100 μm (**C–E**). **aed** = aedeagus; **dig** = digitus; **frn** = frenum; **hyc** = hypostomal carina; **lbp** = labial palp; **md** = mandible; **msp** = mesothoracic spiracle; **Mt_n** = metasomal tergum; **mxp** = maxillary palp; **no₃** = metanotum; **par** = paramere; **psp** = propodeal spiracle; **tsa** = transcutal articulation; **vol** = volsella.

Etymology. The specific epithet is derived from the mandibular formula of the species.

Notes. *Protoita bidentata* is the only species in the genus described from a male. While it is the only taxon with two mandibular teeth, sexual dimorphism in this character is very rare in Chalcidoidea, likely the female of *P. bidentata* is also bidentate. Unlike dentition, antennal shape and claval segments are quite often sexually dimorphic in extant chalcids, and in *Cretaxenomerus curvus* where the male is known we can see a drastic variation in flagellar shape and claval number. *P. bidentata* is the only species known within *Protoita* with 3 claval segments, and within all of Protoitidae only *C. deangelis* is also known to have 3 claval segments however that species is described from a female.

***Protoita istvani* Ulmer & Krogmann, sp. nov.**

<https://zoobank.org/7550D3A4-0E73-444C-9692-E6AFA6915815>

Fig. 6

Diagnosis. The female of *P. istvani* differs from all others in the genus by the following combination of characters: Head flattened antero posteriorly, disc-like (Fig. 6D, G). Fl₁₋₃ elongate, about 4× as long as wide (Fig. 6B). Clava 2-segmented (Fig. 6B).

Description. Female. Body length 918. Coloration auburn with dark antennae. Eyes white. Wings hyaline, uniformly setose. Metasoma damaged, tergal segments detached from body (Fig. 6A). **Head** broad, wider than mesosoma in dorsal view, anteroposteriorly narrow, head longer than wide in lateral view (Fig. 6D, G). Frons 2× as long as face (Fig. 6F, G). Eyes large, 0.8× height of head, about 1.6× as high as long. Malar sulcus present; malar space short, only about 0.15× as long as eye height (Fig. 6D). POL slightly shorter than LOL. Toruli equal in distance from each other as to inner eye margin. Maxillary palps 3-segmented (Fig. 6G:mxp) **Antenna** length 676. Scape 2× as long as pedicel, gradually broadened from base (Fig. 6B). Pedicel same length or slightly shorter than fu₁, about 1.5× as wide as fu₁ width. Flagellomeres gradually widening; fu₁₋₃ about 4× as long as wide, fu₆ 3× as long as wide, fu₇₋₁₀ elongated, but less than 2× as long as wide. Clava 2 segmented. MPS present on all segments (Fig. 6B). **Mesosoma** length 299. Mesosoma in lateral view heavily sloped; nearly 135° relative to mesosoma (Fig. 6C). Mesonotum roughly 0.5× as long as mesosoma. Notauli present as simple depressions. Mesopleuron dorsoventrally elongate, 2.4× as long as wide (Fig. 6C:pl₂). Axilla not advanced, not extending beyond the anterior margin of mesoscutellum (Fig. 6A:axl). Mesoscutellum 1/3× as long as mesonotum. Metanotum band-like, 0.3× as long as mesoscutellum (Fig. 6C:no₃). Propodeum is only slightly longer than mesoscutellum (Fig. 6C:prp). **Wings.** Fore wing length roughly 1.1× as long as body, 3.2× as long as wide. Marginal setae of fore wing short, length of longest seta 26. Cubital vein ephemeral, roughly 1.8× as long as basal vein. Basal vein pigmented. Submarginal vein long and narrow, length 393. Marginal vein narrow, about 0.2× as long as submarginal vein. Postmarginal vein short and tapering, slightly shorter than marginal vein (63:77) (Fig. 6E). Stigmal vein at 80° angle to wing margin. Uncus present. Hind wing obscured by fore wing. **Legs.** Tarsomere 4 on all tarsi very short relative to other tarsal segments (Fig. 6A). Basitarsal comb of fore leg present. Hindtibia elongate, equal in length to tarsi (Fig. 6A). Forecoxa greatly impressed into prosternum (possibly an artifact). Hind coxa elongated, about 3.1× as long as broad (Fig. 6C:cx₃). **Metasoma** 1.3× as long as mesosoma. Metasoma broadly associated with mesosoma; remnants of Mt₂ visible (Fig. 6C). Most of tergal and sternal segments damaged. Only 3 tergites countable, all with transverse setal row posteromedially. Two elongate sensillae visible off of terminal sternite. Metasomal cerci digitiform (visible only on left side ; Fig. 6F:cer). Ovipositor length 140, not extending beyond distal point of ovipositor sheath; ovi-

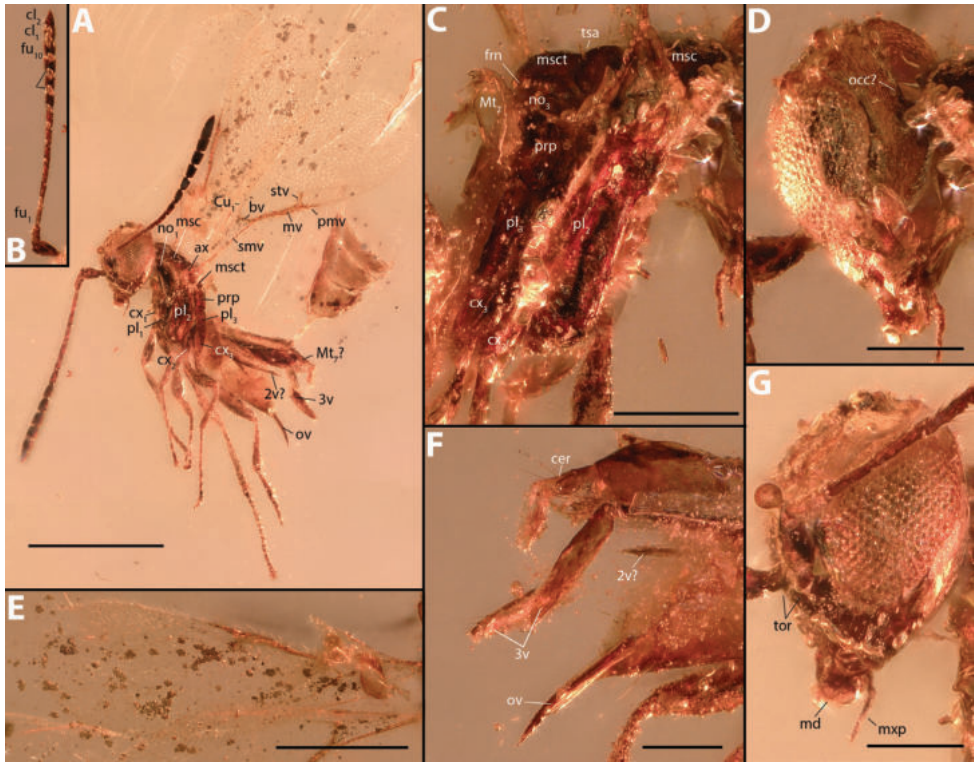


Figure 6. *Protoita istvani*, holotype **A** lateral habitus **B** antenna, lateral **C** mesosoma, lateral **D** head, posterior **E** fore wing **F** ovipositor complex and terminal metasomal segments **G** head, lateral. Scale bars: 500 μm (**A**); 250 μm (**E**); 150 μm (**C**); 100 μm (**D**, **F**, **G**). **2v** = 2nd valvifer; **cx_n** = coxa; **occ** = occipital carina; **pl₃** = metapleuron; **tor** = toruli.

positor sheaths roughly equal in length to ovipositor, uniform width along entire length, about 4.2 \times as long as wide (Fig. 5F:3v).

Male. Unknown

Material examined. *Holotype:* female, Roum – Aazour – Homsiyeh, Caza Jezzine, Mouhafazet South Lebanon; lower Barremian. In amber mounted in Canada Balsam. Deposited at Natural History Museum of the Lebanese University, accession/specimen number: HAR26.

Type condition. Specimen with bubbles surrounding MPS on several flagellomeres, mesosoma detached from the amber, and metasomal tergites damaged because they are detached.

Etymology. The specific epithet is a patronym in honor of István Mikó, the first author's mentor and close friend who instilled in him his passion for entomology and morphology.

***Protoita petersi* Ulmer & Krogmann, sp. nov.**

<https://zoobank.org/F7E6DB52-8F17-4151-994D-706B2AEB3808>

Fig. 7

Diagnosis. The female of *P. petersi* differs from others of the genus by the following combination of characters: Head not as transverse as in other species, only about 1.6× as wide as long in dorsal view (Fig. 7A). Clava 2 segmented; terminal clavomere 0.5× as long as preceding clavomere (Fig. 7B). Postmarginal vein of fore wing equal in length to stigmal vein, both short; and basal vein very short and wide (Fig. 7E). Hind wing marginal setae not longer than width of hind wing.

Description. Female. Body length 913. Body dark brown legs, except coxae, and part of mesepimeron. Head, especially frons, vertex and back of head, base of fu_1 light brown to dark yellow. Wings hyaline, uniformly pilose. **Head** ovular, only 1.6× as wide as long, wider than widest point of meso- or metasoma in dorsal view (Fig. 7A). Frons 1.5× as long as face. Ocelli equilateral, POL=OOL. Malar sulcus faintly present. Antennal scrobe weakly defined (Fig. 7A, C). Interantennal projection pronounced (Fig. 7C). Toruli near lower eye margin, slightly sunken into face. Toruli more than one diameter from eye margin and about same distance from one another (Fig. 7C). Dental formula 3:3. Maxillary palp at least 2 segmented (Fig. 7C). **Antenna** length 549. Scape about 3.5× as long as wide, gradually broadening from base to end. Pedicel 1.8× as long as wide. Fu_1 tapering proximally at insertion into pedicel, fu_{1-4} about 2.3× as long as wide, fu_7 only about 1.2× as long as wide (Fig. 7A). Clava at least 2 segmented, cl_1 wider than fu_7 , claval length 187; all clavomeres with sensillary patch ventrally (Fig. 7B). MPS present on all segments in one row lengthwise (Fig. 7B). Pilosity uniform along all flagellomeres. **Mesosoma** length 359. Lateral panel of pronotum with 4 setae along dorsolateral margin. Mesoscutum convex, obscuring pronotum medially in dorsal view. Mesonotum large, $\frac{3}{5}$ x as long as mesosoma in dorsal view (Fig. 5A). Notauli not externally visible (when a strong underlight is used distinct strips of thickened sclerite may be seen corresponding to notauli and mesoscutal sulcus, possibly an artifact). Transcutal articulation complete. Mesoscutellum convex, band-like approximately $\frac{1}{3}$ x as long as mesonotum. Axillae advanced (Fig. 7A). Metano-propodeal complex obscured by wings and bubbles. **Wings.** Fore wing 2.9× as long as wide. Longest marginal seta 38. Cubital vein 211. Basal vein short, 0.17× as long as cubital vein. Submarginal vein 229. Marginal vein slightly less than $\frac{1}{2}$ as long as submarginal vein (104), width only 17. Stigma oriented at 40° angle with wing margin. Uncus present as cluster of uncil sensillae (Fig. 7E). Postmarginal vein approximately equal in length to stigmal vein (38:39) (Fig. 7E). Hind wing elongate, 0.66× as long as fore wing, 7.75× as long as wide. Marginal setae of hind wing long, 1.5× as long as width of hind wing, length of longest visible sensilla 58. Marginal vein of hind wing less than $\frac{1}{2}$ x as long as hind wing. **Legs.** Basitarsal comb of fore leg present (Fig. 7D:btc); slight basitarsal notch present. (Fig. 7D:btn) **Metasoma.** Metasoma roughly equal to mesosoma in length, attached broadly to mesosoma; petiole obscured. Mt_2 as broad as broadest point of mesosoma and only about 0.5× as long as Mt_3 ; Mt_3 - Mt_8 about same length (Fig. 7F). 7 tergal segments countable. Ovipositor length 148, only partially extruded, enveloped by ovipositor sheaths (Fig. 7F:3v).

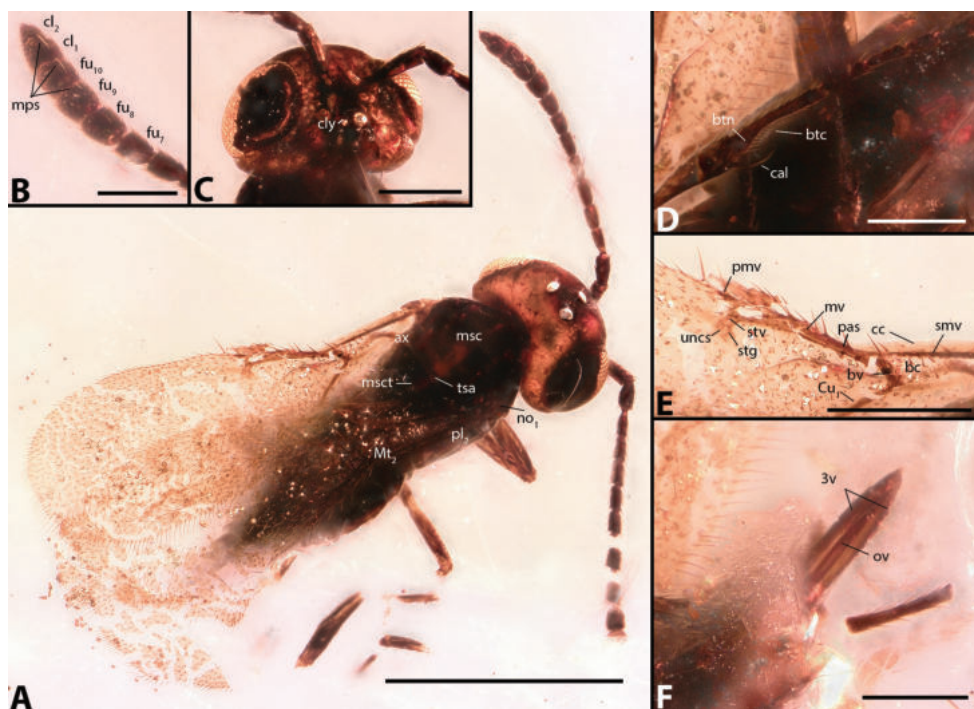


Figure 7. *Protoita petersi*, holotype **A** dorsal habitus **B** apical flagellomeres, lateral **C** head, ventral **D** fore leg **E** fore wing venation **F** ovipositor complex. Scale bars: 500 μm (**A**); 150 μm (**E**); 100 μm (**B–D**). **ax** = axilla; **btn** = basitarsal notch; **cly** = clypeus.

Male. Unknown

Specimens examined. *Holotype*: female, Hammana / Mdeyrij, Caza Baabda, Mouhafazet Mount Lebanon; lower Barremian. In amber mounted in Canada Balsam. Deposited at Natural History Museum of the Lebanese University, accession/specimen number: 874A.

Type condition. Specimen with right antenna damaged beyond flagellomere 5, right hind leg damaged at midpoint of femur, and right fore wing damaged beyond midpoint of marginal vein.

Etymology. The specific epithet is a patronym in honor of our friend and colleague Dr Ralph Peters, for his work on the early diversification of Chalcidoidea.

Cretaxenomerus Nel & Azar, 2005

Diagnosis. Body larger than 1 mm. Head usually long in dorsal view with temples well developed. Metasoma separated from mesosoma by distinct petiole or constriction, and in dorsal view ovoid; female with an elongate syntergum, longer than preceding tergite (Mt_7) (except *C. deangelis*).

Key to species of *Cretaxenomerus*

- 1 Syntergum longer than 1/2 length of ovipositor (Figs 8D, 12D, 15B). Ovipositor sheaths spatulate distally (Figs 8D, 12D) **2**
- Syntergum shorter than or equal to 1/2 length of ovipositor (Figs 10F, 13B). Ovipositor sheaths uniformly broad (Figs 10F, 13B) **4**
- 2 Syntergum articulating with preceding tergum at an angle (Fig. 8A, D). Cubital vein extending beyond tip of postmarginal vein (Figs 8F, 9D) ***Cretaxenomerus curvus* sp. nov.**
- Terminal tergum not articulating with preceding tergum at an angle (Figs 10F, 12D, 13B). Cubital vein extending to tip of or less than length of postmarginal vein (Figs 10B, 11A, 12C, 13D) **3**
- 3 Head at least 2× as broad as long (Fig. 15A). Terminal tergum broadening posteriorly (Fig. 15B). Hind basitarsus with only sparse setation (Fig. 15C). Fu_1 - fu_3 2× as long as wide (Fig. 15A). ***Cretaxenomerus jankotejai***
- Head about as broad as long, globular. Terminal tergum of uniform width along entire length (Fig. 12D). Hind basitarsus with dense setation (Fig. 12D). Fu_1 - fu_3 3× as long as wide (Fig. 12B). ***Cretaxenomerus mirari* sp. nov.**
- 4 Flagellum with 1-segmented clava (Figs 11B, 13C). **5**
- Flagellum with 2–3 segmented clava (Figs 10C, 14C) **6**
- 5 Fore wing spatulate, 2.5× as long as wide (Fig. 11A). Basitarsal comb absent (Fig. 11F) ***Cretaxenomerus vitreus* sp. nov.**
- Fore wing narrow, 3.5× as long as wide (Fig. 13D). Basitarsal comb present (Fig. 13A). ***Cretaxenomerus tenuipenna* sp. nov.**
- 6 Head longer than wide (Fig. 14A). Clava 3-segmented (Fig. 14C). Basitarsal comb of fore leg present (Fig. 14D). Fore wing with costal cell about equal in width to marginal vein (Fig. 14B). Syntergum not longer than preceding tergite (Fig. 14A). ***Cretaxenomerus deangelis* sp. nov.**
- Head wider than long (Fig. 10C). Clava 2-segmented (Fig. 10C). Basitarsal comb of fore leg absent (Fig. 10E). Fore wing costal cell narrower than marginal vein (Fig. 10B). Syntergum nearly 2× as long as preceding tergite (Fig. 10A, F) ***Cretaxenomerus brevis* sp. nov.**

***Cretaxenomerus curvus* Ulmer & Krogmann, sp. nov.**

<https://zoobank.org/CF8C92D9-DD42-4E47-AA86-78ED85561736>

Figs 3B, 8, 9, 16B

Diagnosis. Female. Females differ from those of all other species within the genus by the following combination of characters: Syntergum hinged at joint with elongated Mt_7 , reaching more than $\frac{3}{4}$ length of ovipositor sheath (Fig. 8D: $Mt_{8,9}$); fore wing with postmarginal vein about equal in length to stigmal vein and cubital vein extending beyond tip of postmarginal vein (Fig. 8F). **Male.** Same as female except flagellomeres all as wide as long; clava 2-segmented (Fig. 9B).

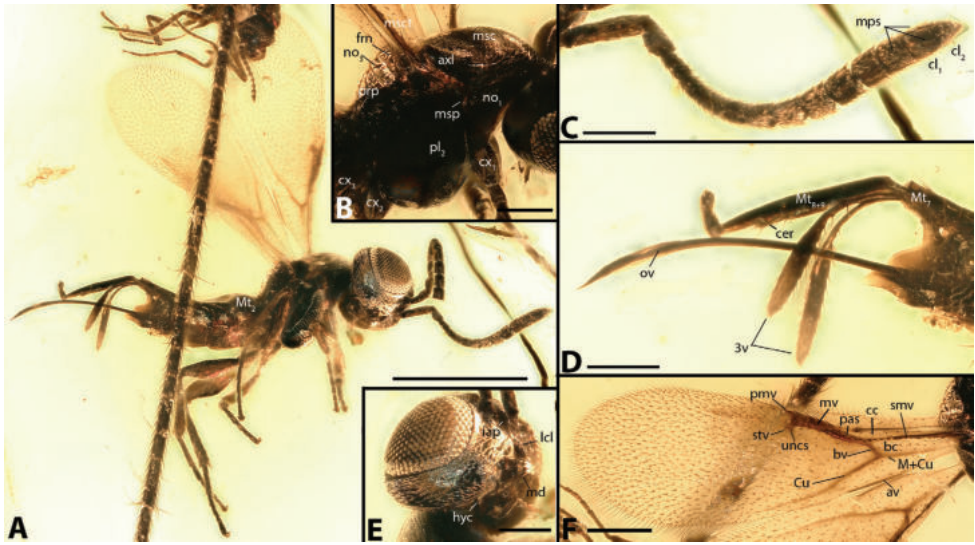


Figure 8. *Cretaxenomerus curvus*, holotype (874D) **A** lateral habitus **B** mesosoma, lateral **C** antenna, lateral **D** ovipositor complex and terminal abdominal segments **E** head, lateroventral **F** fore wing. Scale bars: 500 μm (**A**); 150 μm (**F**); 100 μm (**B–E**). **iap** = interantennal process; **lcl** = lateral clypeal line; **Mt**_{8,9} = syntergum.

Description. Female. Body length 1314 (HT) – 1407 (PT). Overall body color black with a blue sheen on the gena of HT when examined at certain angles except tegulae, legs excluding coxae, and second half of ovipositor sheath dark brown, tip of ovipositor sheath light brown, and with legs almost black. Wings hyaline except fore wing slightly brownish in HT (possible artifact) and partly brownish in PT 881B; with sparser pilosity proximally on wing surface. Head, mesosoma and metasoma coriaceous to alutaceous except areolate posterior part of mesoscutellum and propodeum. **Head** ovate, 1.5 \times as wide as long (Fig. 8E). Vertex and temple of head curved strongly, back of head concave, closely associated with mesosoma. Temple about 0.3–0.25 \times as long as eye length. Eye broadly oval, almost as long as high. Ocellar triangle equilateral, POL=LOL=OOL. Malar sulcus faint, but present. Shallow internantennal projection (Fig. 8E:iap). Toruli closer to inner margin of eye than each other and very close to dorsal margin of clypeus, well below center of eye, hence lower face short. Clypeus dorsally with raised rim, inwardly inflexed, with row of setae just below dorsal clypeal margin (Fig. 8E). Anterior tentorial pits situated well below dorsal margin of clypeus. Dentition 3:3, mandibles on different plane from face (Fig. 8E). Maxillary palp 3 segmented, distal segment longer than basal segment (Fig. 8E). **Antenna** length 637 (HT)–671 (PT). Antenna 14-segmented. Radicle raised from face. Fu1-2 at least 2 \times as long as wide. Clava 2-segmented (Fig. 8C); clava 1.5 \times as long as wide. MPS present on all flagellomeres with single row on each segment; MPS on terminal segment not extending beyond tip. All segments uniformly pilose (Fig. 8C). **Mesosoma** length 380 (PT)–401 (HT). Pronotum with bristle on posterolateral corner. Mesoscutum obscuring pronotum medially in

dorsal view. Lateral part of prepectus slender and straight, dorsally covered by posteriormost corner of lateral pronotum, slightly broadened ventrally (Fig. 16A:pre). Mesonotum large, roughly $2/3\times$ as long as mesosoma. Notauli present and simple impressions. Mesopleuron $2\times$ as high as long in lateral view (Fig. 8,B). Suture present between meso- and metapleuron (Fig. 8A). Transcutal articulation present and complete. Axillae reduced, axillulae extending further anterior than posterior edge of mesonotum (Fig. 8B:axl). Mesoscutellum short, about $1/5$ length of mesonotum. Dorsellum band like. Propodeum strongly sloped. **Wings.** Fore wing $2.4\times$ (PT)– $2.7\times$ (HT) as long as wide. Pilosity sparse in basal part of wing relative to disc (Fig. 8F). Basal cell dorsally with one median row of hairs only. Longest marginal seta of fore wing 38. Cubital vein extending beyond length of postmarginal vein, length 377 (Fig. 8F). Basal vein short, length 43. Submarginal vein length 342. Marginal vein strongly sclerotized and broad, length 96, width 29; marginal vein with 6 marginal sensillae present. Stigmal vein present, equal in length to postmarginal vein, at 45° angle with wing margin (Fig. 8F). Uncus present; 5 uncal sensillae in cluster. Postmarginal vein very short, about $0.25\times$ as long as marginal vein (Fig. 8F). Hind wing elongate and narrow $6.8\times$ as long as wide. Hamuli count 3, proximal hamular hook longer than other 2. Hamuli and venation of hind wing only extend $1/3$ length of hind wing. **Legs.** Hind femur slightly broadened medially (Fig. 8A). Fore tibia with curved clefted spur. Hind tibia with two spurs, shorter spur about $0.75\times$ as long as longer one. Basitarsus of fore leg ventrally curved; basitarsal comb present, bristles of comb very short (Fig. 8A). **Metasoma** length 407, nearly equal in length to mesosoma. Six (Mt_{2-7}) tergal segments and syntergum (Mt_8+Mt_9) countable, except the Mt_{3-7} all roughly equal in length from lateral view (Fig. 8A). Six sternal segments visible. Hypopygium flanged, extending beyond Mt_7 . Syntergum articulating with Mt_7 and covering ovipositor sheaths dorsally, syntergum length 273, Mt_7 length 51 (Fig. 8A, D). Ovipositor $1.2\times$ as long as metasoma; tip of ovipositor with 5 teeth; ovipositor sheaths stalk-like at base, distally spatulate with sensillae along margin, sheaths approximately equal in length to syntergum (Fig. 8D:3v). **Male.** Similar to female except the head is not as long (Fig. 9A). Interantennal process reaching over the $2/3$ of eye height, antenna with only Fl_1 about $2\times$ as long as wide (Fig. 9B). Clava 2-segmented (Fig. 9B). Postmarginal vein slightly longer than stigmal vein (Fig. 9D). Male genitalia extended; digitus with single digital spine (Fig. 9C:dig)

Specimens examined. Holotype: female, Hammana / Mdeyrij, Caza Baabda, Mouhafazet Mount Lebanon; lower Barremian. In amber mounted in Canada Balsam. Deposited at Natural History Museum of the Lebanese University, accession/specimen number: 874D. Locality information and depository of paratypes same as for holotype (Female–881B,146U; Male–1614FA).

Type condition. Right antenna of holotype with terminal 3 segments missing. The amber piece of the holotype included a single inclusion of a Ceratopogonidae (Diptera).

Etymology. The specific epithet is derived from the Latin ‘curvus’ meaning curved or bent, in regards to the articulation of the syntergum of the species.

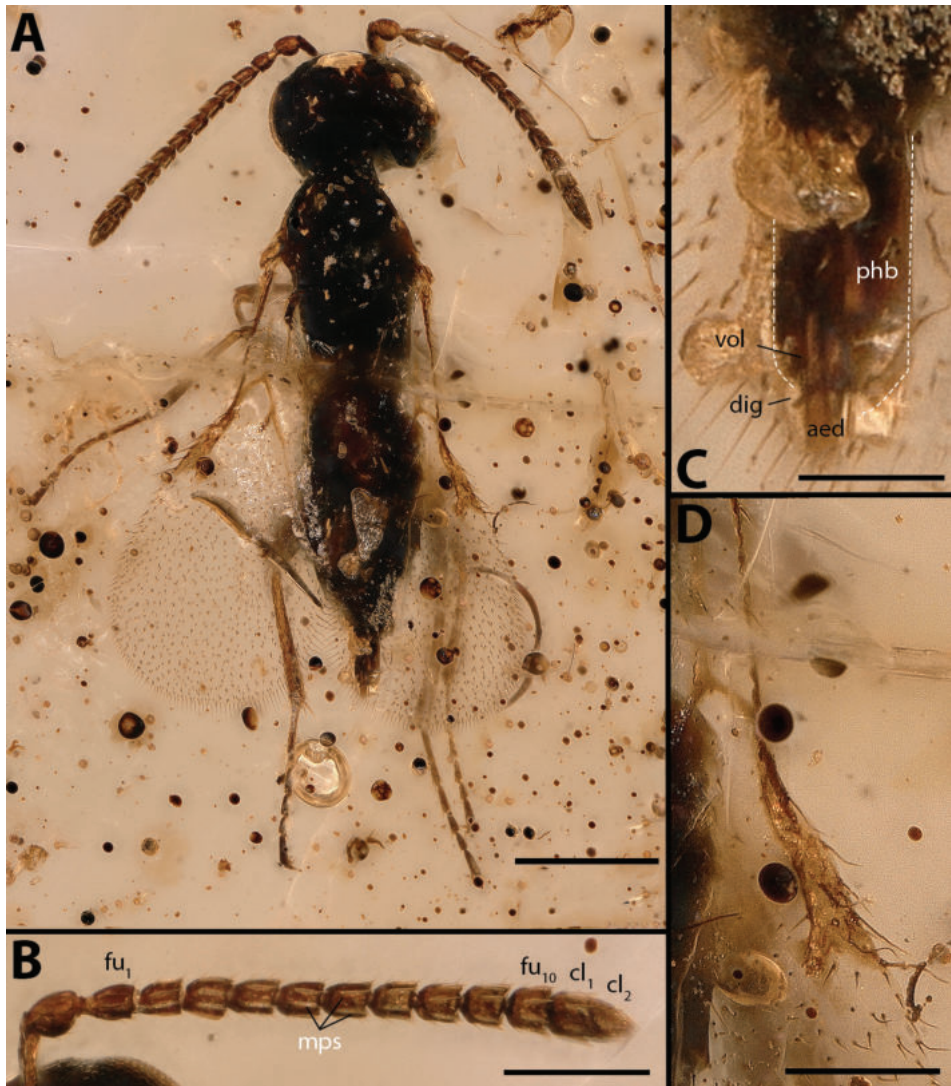


Figure 9. *Cretaxenomerus curvus*, male paratype (1614F) **A** dorsal habitus **B** antenna, lateral **C** male genitalia, ventral **D** fore wing venation. Scale bars: 250 μm (**A**); 100 μm (**B**, **D**); 50 μm (**C**). **phb** = phallobase.

Notes. The metasoma of paratype specimen 146U is damaged, preventing examination of the syntergum, however the wing venation and head shape place it as *C. curvus*. This is the only species described based on both sexes which provides some insight into the putative sexual dimorphisms within the genus. Notably, the variation in antennal shape and claval size which is a prolific form of dimorphism within extant chalcids. The female of *C. curvus* has a clear clava with multiple claval segments relative to the male which has all flagellar segments relatively stout and uniform with only the partial fusion of the terminal segments indicating a clava.

***Cretaxenomerus brevis* Ulmer & Krogmann, sp. nov.**

<https://zoobank.org/1BAEE43E-EAFA-4921-8B80-A4824EAA9B35>

Fig. 10

Diagnosis. Female. *Cretaxenomerus brevis* differs from all other species in the genus by the following combination of characters: scape laterally flattened, only 2.25× as long as broad; antenna with at least fu₁–fu₄ conspicuously longer than broad, fl₁ about 3.75× as long as broad. Anterolateral margin of mesoscutum flanged. Arolium elongated and extending beyond tip of tarsal claws. Syntergum relatively short, extending about 1/3 length of ovipositor sheath.

Description. Female. Body length 1145. Uniformly dark brown, legs light brown, eyes white (likely an artifact of amber deposition) (Fig. 10A). **Head.** Ovular in shape, wider than long, length 201, width 313. Eye almost circular. Ocelli large, equilateral, POL=LOL=OOL. Temples relatively short, at most about 0.2× as long as eye length. Gena large, about 0.5× as long as eye length; no genal carina or sulcus present. Toruli closer to inner margin of eye than each other and very close to dorsal margin of clypeus, well below center of eye, hence lower face short (Fig. 10C). Clypeus dorsally with raised rim, inwardly inflexed; lower clypeal margin wide. Anterior tentorial pits situated well below dorsal margin of clypeus. Dentition 3:3. Maxillary palp count 2. **Antenna** length 706. Radicle pronounced. Scape laterally flattened, only 2.25× as long as broad. Pedicel semiglobular, only 1.5× as long as broad (possible artifact of compression), 0.5× as long as scape (Fig. 10C). All flagellomeres are longer than wide with fu₁ longest one, length 98, about 3.75 as long as wide, fu₁₀ about 1.5× as long as broad. Clava 2-segmented, 2.8× as long as broad (Fig. 10C). Micropilosity present on all claval segments (Fig. 10C). **Mesosoma** length 334. Notch in posterior most part of lateral panel of pronotum dorsal to prepectus with prothoracic spiracle (?) (Fig. 10D:mSP). Mesonotum 238. Prepectus externally visible, thin, dorsally overlapped by lateral panel of pronotum, ventral portion curved anteriorly (Fig. 10C:pre). Notauli present as depression (Fig. 10D). Mesopleuron elongate, 1.5× as long as wide (250:164). Axillular rim with sharp carina delimiting mesoscutellum from frenum. Bubble obscuring propodeo-metanotal complex. **Wings.** Fore wing 2.8× longer than wide (981:343). Longest marginal seta 31. Cubital vein 174 (sclerotized part) and extending as pigmented fold beyond length of postmarginal vein. Basal vein 43, strongly sclerotized. Submarginal vein length 372, with 7 admarginal setae, basalmost 2 being longest. Marginal vein length 110, width 27, with 6 admarginal setae. Stigmal vein 61, at ≈85° to wing edge. Uncus with 5 uncal sensillae. Postmarginal vein 0.8× as long as marginal vein, tapering. Costal cell of fore wing very narrow. Hind wing slender, 10.6× longer than wide (647:61) (Fig. 10B). **Legs.** Basitarsomere equal in length to tarsomere 2–4; basitarsal comb absent. Arolium of pretarsus elongate, extending further distally than tarsal claws (Fig. 10E:aro). **Metasoma** length 555. Petiole obscured by bubble, however slendering of propodeum and expanding of metasoma suggests a constricted petiole. Metasoma with 6 countable tergal segments (Mt₂₋₇) and syntergum (Mt₈₊₉);

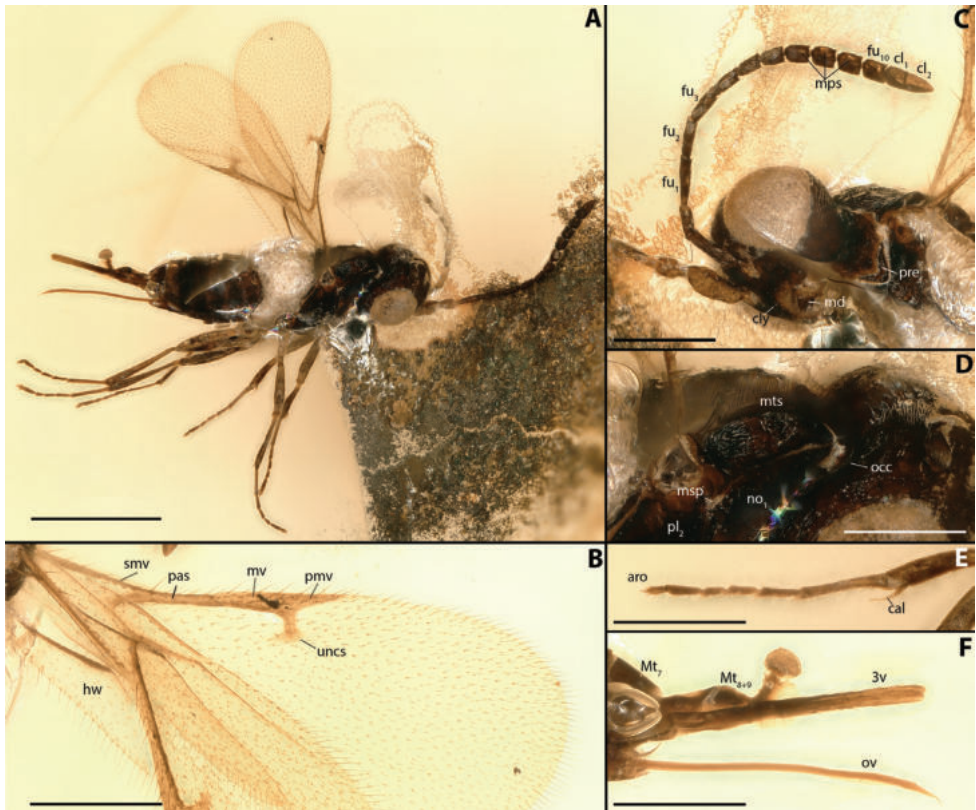


Figure 10. *Cretaxenomerus brevis*, holotype **A** lateral habitus **B** fore and hind wing **C** head, ventrolateral, and antenna **D** mesonotum, dorsolateral **E** fore leg **F** ovipositor complex and terminal abdominal segments. Scale bars: 500 μm (**A**); 200 μm (**B**, **C**); 150 μm (**D–F**). **aro** = arolium; **hw** = hind wing.

2 enlarged sternal segments countable. Hypopygium with longitudinal row of 6 setae along edge, concave distally and reaching end of Mt_7 . Syntergum relatively short (141), only $\frac{1}{3}$ length of extruded ovipositor (Fig. 10F). Ovipositor length 383, tip of ovipositor with 5 teeth (Fig. 10F:ov); ovipositor sheaths equal in length to ovipositor, ovipositor sheath flattened but equal width along entire length (Fig. 10F:3v).

Male. Unknown.

Material examined. *Holotype:* female, Hammana / Mdeyrij, Caza Baabda, Mouhafazet Mount Lebanon; lower Barremian. In amber mounted in Canada Balsam. Deposited at Natural History Museum of the Lebanese University, accession/specimen number: 1228.

Type condition. A large bubble obscures the posterior of the propodeum and petiole. The head is damaged at the lateral clypeal line.

Etymology. The specific epithet is derived from the Latin word for ‘short’, referring to the comparatively short syntergum relative to the other species in the genus.

***Cretaxenomerus vitreus* Ulmer & Krogmann, sp. nov.**

<https://zoobank.org/A147EFF9-9000-4983-BD3F-1D2C927B7607>

Figs 2A, 11

Diagnosis. *Cretaxenomerus vitreus* differs from all other species in the genus by the following combination of characters: fore wings broadly spatulate, with postmarginal vein about 2× as long as stigmal vein (Fig. 2A). All tarsi with manubrium broadly spatulate (Fig. 11F:man).

Description. Female. Body length 1381. Body bilaterally damaged with some internal sclerite structures visible (Fig. 11A). Most of the right part of the specimen is missing including both scapes and right pedicel, the whole mouth complex, entire right hind leg, right midcoxa, forecoxa and femur and base of right fore wing and entire hind wing. Metasoma damaged with only Mt_{2,5} and ovipositor sheaths and ovipositor present. Body light brown in coloration, eyes red. Wings hyaline, speculum less pilose than wing disc. **Head.** Head broad, approximately 1.4× as wide as long, posteromedially depressed. Eyes large, broadly oval, slightly taller than wide (Fig. 11A). Ocellar triangle equilateral, ocelli raised and angled from head capsule; ocelli large (Fig. 11A). No facial sulci or occipital carina present. **Antenna** length 805. All flagellomeres longer than broad, fu_{1,2} about 2.8× as long as broad, fu₃ 2.0× as long as broad (Fig. 11A). Clava 1-segmented (Fig. 11B). MPS present on all segments, extending beyond distal margin of segment, including on apical segment; MPS at least on fu₁₋₄ in two rows. Pilosity sparse and uniform on all flagellomeres. **Mesosoma** length 480, pronotum medially obscured, with setal line along mesonotal margin. Mesoscutum 0.7× length of mesosoma. Prepectus elongate and slender, overlapped anteriorly by lateral pronotal panel (Fig. 11D, E:pre). TSA complete across mesonotum (Fig. 11D:tsa). Mesopleuron large, 1.75× as long as wide; transpimeral line present as narrow line. Metapleuron small, differentiated from mesopleuron by carina. Axillae not well defined. Mesoscutellum narrow and band-like, 1/3 length of mesoscutum. Frenum discernable as shift in scutellar sculpturing with marginal foveal rim, roughly 1/4 length of mesoscutellum (Fig. 11D:fre). Dorsellum damaged. Propodeum 1/3 length of mesoscutum; supracoxal flange developed, but very narrow; propodeal spiracle ovoid (Fig. 11D:psp). **Wings.** Fore wing spatulate, 3× longer than wide. Longest marginal seta length 40. Costal cell narrow. Submarginal vein broad and distally tapering, length 458. Cubital vein pigmented and tubular after intersection with basal vein for about length of basal vein then ephemeral distally, tubular portion equal in length to basal vein (Fig. 2A). Basal vein strongly pigmented and broad, 2/3 length of entire cubital vein. Marginal vein strongly pigmented, ≈ 1/3 length of submarginal vein. Width of marginal vein 1/2 length of marginal seta. Stigmal vein broad, 1/2 length of postmarginal vein, oriented 90° relative to wing margin. Stigma spatulate with distinct uncus; uncal sensillae count 4 (Fig. 2A:uncs). Postmarginal vein elongate and tapering, equal in length to marginal vein. Hind wing approximately 1/2 length of fore wing, 16× as long as wide. Longest marginal seta of hind wing longer than width of hind wing. Marginal vein of hind wing 1/2 length of hind wing. **Legs.** Hindlegs slightly longer than mid



Figure 11. *Cretaxenomerus vitreus*, holotype **A** lateral habitus **B** apical flagellomeres, lateral **C** metasoma, lateral **D** mesosoma, lateral **E** prepectus **F** fore leg. Scale bars: 500 μ m (**A**); 100 μ m (**C–F**).

and fore legs which are equal in length (Fig. 11A). Basitarsus of all legs roughly equal in length to tarsomere 2–4; basitarsal comb of fore leg absent (Fig. 11F). Legs with sparse pilosity. Tarsal manubrium spatulate, as broad as tarsal claws (Fig. 11F:man). **Metasoma.** Only $Mt_{2,5}$ preserved, all equal in length (Fig. 11C). Medial longitudinal setal line present on all tergal segments, counting of setal lines retained in the amber indicate 6 tergal segments countable (Fig. 11C). Ovipositor length 248. Ovipositor sheath equal in length to ovipositor, broadened along entire length; setae arising from surface of ovipositor sheath, margin bare.

Male. Unknown.

Material examined. Holotype: female, Hammana / Mdeyrij, Caza Baabda, Mouhafazet Mount Lebanon; lower Barremian. In amber mounted in Canada Balsam. Deposited at Natural History Museum of the Lebanese University, accession/specimen number: 534C.

Type condition. Face and mandibles absent from specimen. Mesosoma bisected and cleared with scleritic components visible on left side, internal components visible on right. Metasoma with first few terga present, and marginal setal line of other segments still present to indicate placement. Right hind leg with only distal tarsomeres remaining.

Etymology. The specific epithet is the Latin word for ‘glassy’ or ‘transparent’ in regards to the unique taphonomy of the specimen that appears as though it were cleared.

Notes. Damage to the specimen provides for a unique examination of both external and internal scleritic structures; however, damage to the abdomen has resulted in the loss of the terminal segments and syntergum. The lack of a multi-segmented clava is shared with *Cretaxenomerus tenuipenna* sp. nov.; however, the distinct difference in wing shape and venation separates these two specimens into distinct species.

***Cretaxenomerus mirari* Ulmer & Krogmann, sp. nov.**

<https://zoobank.org/CA9573B0-4C46-443C-9000-03F57E442982>

Fig. 12

Diagnosis. *Cretaxenomerus mirari* differs from all other species in the genus by the following combination of characters: Head very transverse in dorsal view. Clypeus not as inflexed. Mesoscutum broader than long. Hind basitarsus with dense comb-like setation (Fig. 12D). Syntergum straight, and longer than $\frac{3}{4}$ the length of the ovipositor (Fig. 12D). Fore wing with a pronounced costal cell which is broader than the marginal vein, and cubital vein equal in length to distal tip of postmarginal vein (Fig. 12C).

Description. Female. Body length 1212. Coloration dark brown to black, slight metallic coloration on abdomen may be an artifact. Scape, legs and ovipositor sheaths dark brown, tip of ovipositor sheaths light brown. Wings lightly brownish infumated, wing venation brown. **Head.** Unusually long and low, about 1.5× as wide as long and low, about 0.5× as high as broad (Fig. 12A). Eye broadly ovoid, but horizontally oriented (longer than height). Temple about $\frac{1}{4}$ as long as eye. Clypeus not deeply inflected. Epistomal sulcus and malar sulcus present. Toruli closer to inner eye margin than to each other.

Antenna. Length 699, approximately 0.6× as long as body. Scape 2.85× as long as broad. All flagellomeres longer than wide, fu_{1-3} 3.0× as long as wide, fu_{4-10} about 2.0× as long as wide (Fig. 12B). Clava 2-segmented, length 88 (Fig. 12B). MPS present on all segments, slightly askew, not extending beyond apical edge of segment. Micropilosity laterally on cl_{1-2} and fu_{9-10} . **Mesosoma.** Length 342. Mesonotum wider than long and 0.6× length of mesosoma. Prepectus narrow, dorsally hidden from dorsoposterior edge of lateral panel of pronotum. Axillae advanced. Mesopleuron obscured due to angle of specimen. Mesoscutellum short, 0.2× as long as mesonotum (Fig. 12A:msct). Dorsellum narrow and band-like, $\frac{3}{4}$ length of mesoscutellum. Propodeum sloped, roughly 2× as long as mesonotum (Fig. 12A:prp). **Wings.** Base of the fore wing including speculum with sparser pilosity than disc. Fore wing length 1046, 2.7× as long as wide. Longest marginal seta of fore wing 39. Costal cell about 2× as long as marginal vein and postmarginal vein (Fig. 12C).

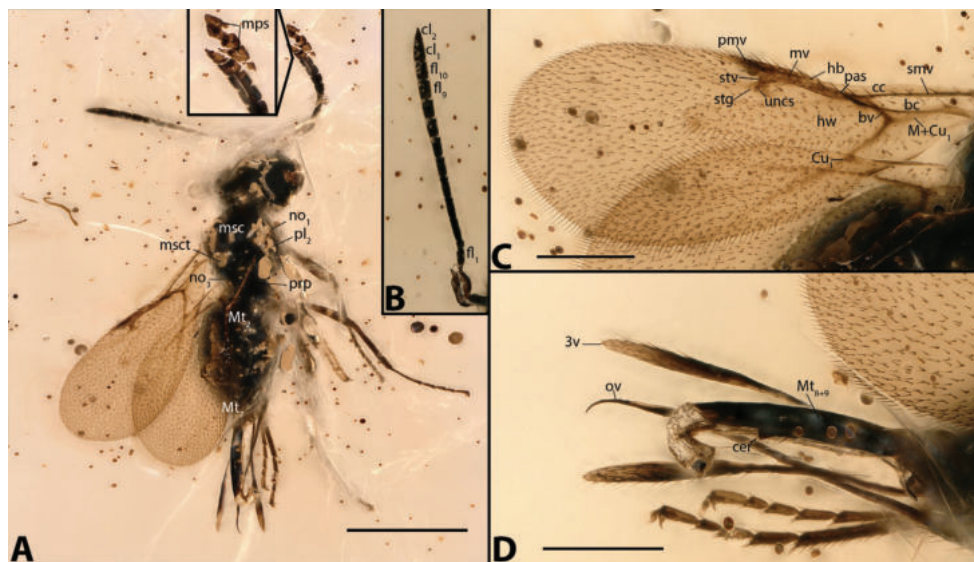


Figure 12. *Cretaxenomerus mirari*, holotype **A** dorsal habitus with magnified view of clava **B** antenna, lateral **C** fore wing **D** ovipositor complex and terminal metasomal segments. Scale bars: 500 μm (**A**); 200 μm (**C, D**).

Cubital vein very long, approximately $\frac{1}{3}$ length of fore wing, strongly pigmented. Basal vein length 44, strongly pigmented. Submarginal vein length 367, costal cell of fore wing well developed. Marginal vein slightly longer than $\frac{1}{4}$ length of submarginal vein; strongly pigmented and broad, width 23. Stigmal vein short, length 33. Uncus with 4 uncal sensillae (Fig. 12C). Postmarginal vein tapering towards wing margin, $\frac{2}{3}$ length of marginal vein. Hind wing $\frac{3}{5}$ length of fore wing, $6.7\times$ longer than wide. Longest marginal seta of hind wing 34. Venation and hamuli of hind wing not further than $\frac{1}{2}$ length of wing (Fig. 12C). **Legs.** Basitarsal comb present on fore leg. Basitarsomere equal in length to tarsomere 2–4 on fore leg. Dense setation along hind basitarsus (Fig. 12D). **Metasoma** length 563, $\approx 1.6\times$ as long as mesosoma. Constricted petiole. Mt_{2-7} countable. Hypopygium elongate, reaching nearly to end of metasoma. Elongate, medial, longitudinal setal row down ventrum of metasoma. Syntergum about $0.5\times$ as long as metasoma and reaching up to about $\frac{3}{4}$ of ovipositor sheath length, broadened after insertion of cerci, spatulate (Fig. 12D). Ovipositor ejected, about equal in length to metasoma; ovipositor tip with 3 teeth; ovipositor sheaths equal in length to ovipositor, stalk-like basally before widening distally and becoming spatulate with marginal setation (Fig. 12D).

Male. Unknown.

Material examined. Holotype: female, Hammana / Mdeyrjij, Caza Baabda, Mouhafazet Mount Lebanon; lower Barremian. In amber mounted in Canada Balsam. Deposited at Natural History Museum of the Lebanese University, accession/specimen number: 157G.

Type condition. Specimen complete, but terminal segments of the right antenna fragmented, and tarsal segments of the left fore leg longitudinally split; partial detachment from the amber along the right side of thorax and eye margin. Streaks in the amber make it difficult to clearly assess some characters.

Etymology. The specific epithet is derived from the Latin ‘mirari’, which is the origin of the English ‘mirage’ in regards to the haziness of the specimen within the amber from the taphonomic process.

Notes. *Cretaxenomerus mirari* shares several characters with *P. curvus*, namely the presence of 3 claval segments and a syntergal protrusion which is roughly $\frac{3}{4}$ of length of the ovipositor. While it is possible that *P. mirari* has an articulating syntergum which is simply not observable due to taphonomic processes, a postmarginal vein that is longer than the stigmal vein and a clear costal cell, would suggest that *P. mirari* is a distinct species for the sake of identification and until more specimens are discovered which may contradict its current placement.

***Cretaxenomerus tenuipenna* Ulmer & Krogmann, sp. nov.**

<https://zoobank.org/021F799C-F0BD-48D4-B803-B207B9DDC43D>

Fig. 13

Diagnosis. *Cretaxenomerus tenuipenna* can be differentiated from all other species in the genus by the following combination of characters: scape conspicuously long, about as long as eye height, fu_{1-2} about 2× as long as wide, especially fu_1 much narrower than pedicel, at least fu_4 only slightly longer than wide and wider than pedicel, terminal claval segments loosely associated, without distinct fusion between cl_1 and fl_{11} . Fore wing slender, 3.5× longer than wide. Foretibia without basitarsal comb. Propodeum not strongly sloped.

Description. Female. Body length 1256. Body dark brown, appendages light brown, may be taphonomic artifact. Wings hyaline with some slight brown infumation distally from basal vein, uniformly pilose. Right fore leg tarsal segments except about half of basitarsus and left hind tarsal segments 25 are missing, left antenna after pedicel and ovipositor broken on several places, both antennae with some cracks on scape and pedicel. **Head.** Globular, approximately equal in length and width (Fig. 13A). Face equal in length to frons. Temple rather short, about $\frac{1}{5}$ as long as eye length. Eye circular, about as high as pedicel length (Fig. 13A). Toruli equal distance from one another as to inner eye margin. No scrobal depression. Dental formula 3:3; mandibles on higher plane than face. Maxillary palps at least 2-segmented. **Antenna** long, more than half the length of body (712). Scape elongated, about 3.4× as long as wide and 4× as long as length of pedicel (Fig. 13A). Fu_{1-2} elongate relative to other funicles, both segments about 2× as long as wide, length of fu_1 72 (Fig. 13C). Fu_1 much narrower than pedicel; at least fu_4 only slightly longer than wide and wider than pedicel. Clava 1-segmented, undifferentiated from prior flagellomeres (Fig. 13C). MPS extending past apical margin of flagellomeres. Pilosity uniform on all segments.

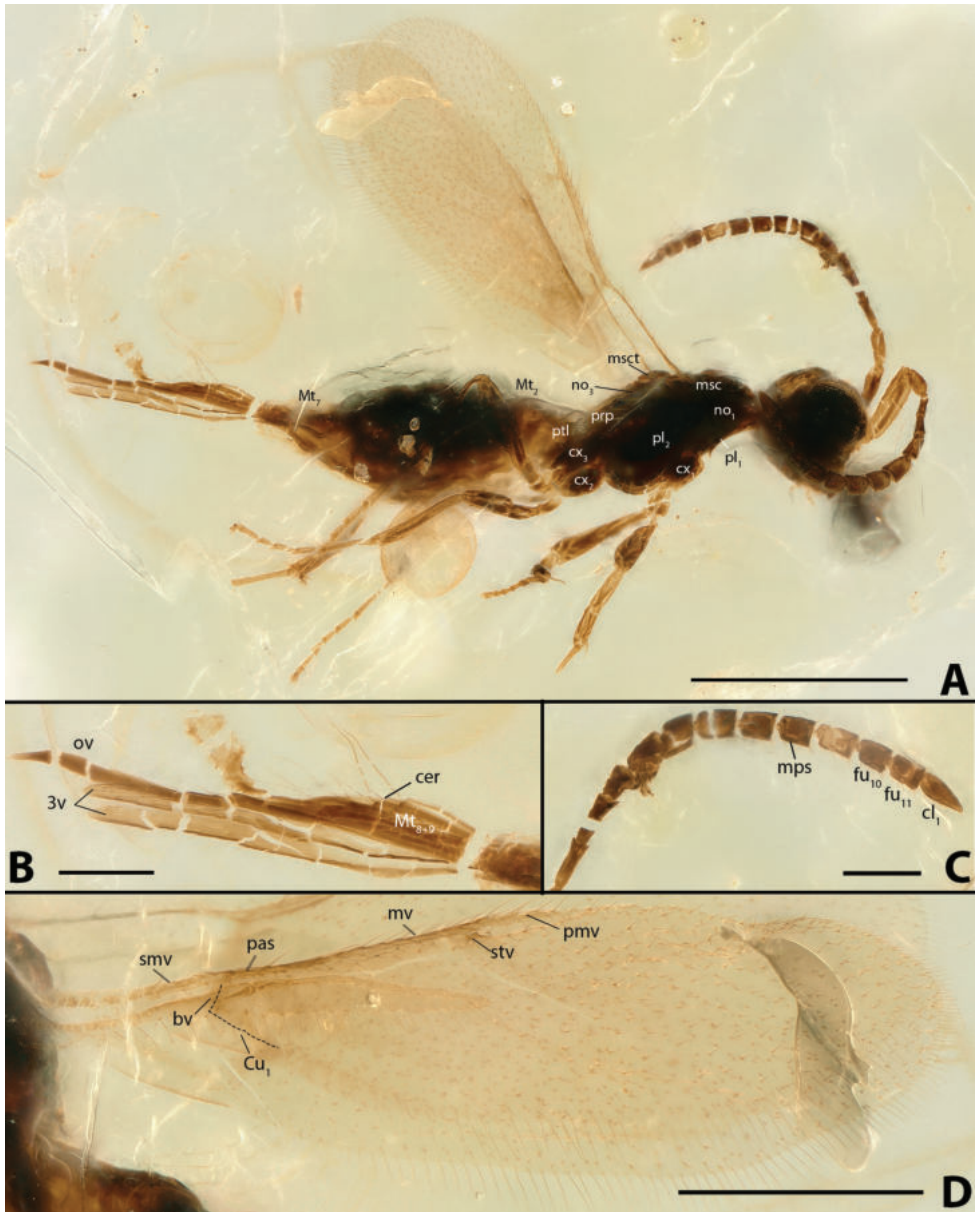


Figure 13. *Cretaxenomerus tenuipenna*, holotype **A** lateral habitus **B** ovipositor and terminal metasomal segments **C** antenna, lateral **D** fore and hind wing (showing beneath fore wing). Scale bars: 500 μm (**A**); 250 μm (**D**); 100 μm (**B**, **C**). pl_1 = propleuron; ptl = petiole.

Mesosoma elongate, longer than high; length 390. Mesonotum roughly $\frac{1}{2}$ length of mesosoma. Mesoscutum convex. Mesopleuron elongate, $1.6\times$ as long as wide. Mesoscutellum $0.4\times$ length of mesonotum. Metanotum band-like, $0.4\times$ length of mesoscutellum (Fig. 13A). Propodeum elongate and sloped roughly 30° , roughly $\frac{1}{2}$ length of

mesonotum. **Wings.** Fore wings elongate, 3.5× longer than wide, length 1041, width 292. Longest marginal seta 44. Basal vein and cubital vein ephemeral (Fig. 13D). Basal vein length 47. Submarginal vein length 399. Marginal vein about $\frac{3}{8}$ length of submarginal vein and narrow; width 19. Stigma short, length 28. Postmarginal vein narrow, $\frac{1}{2}$ length of marginal vein. Hind wing slender and elongate, 13× as long as wide, 0.5× as long as fore wing length (Fig. 13D). Ventral marginal setae of hind wing long, 0.8× width of hind wing. **Legs.** Basitarsus curved in first third; basitarsal comb of fore leg not visible. Hind trochanter as long as hindcoxa (Fig. 13A:cx₃). **Metasoma** elongate, 1.5× as long as mesosoma. Attached to mesosoma narrowly by clear petiole (Fig. 13A:ptl). Mt₂₋₆ tergal segments countable. Syntergum 0.6× length of metasoma. Ovipositor length 620, 1.2× length of gaster; ovipositor about 2× as long as syntergum (Fig. 13B); ovipositor tip with at least 3 teeth visible; ovipositor sheaths uniformly flattened along its entire length (Fig. 13B).

Male. Unknown.

Material examined. Holotype: female, Hammana / Mdeyrij, Caza Baabda, Mouhafazet Mount Lebanon; lower Barremian. In amber mounted in Canada Balsam. Deposited at Natural History Museum of the Lebanese University, accession/specimen number: 623I.

Type condition. Specimen relatively complete; antennal segments partly fragmented and separated from taphonomic process; syntergum and ovipositor complex also fragmented; tarsal segments missing beyond basitarsus on left fore- and hind leg. Streaks and ripples in the amber obscured some characters during imaging.

Etymology. The specific epithet is a portmanteau of the Latin ‘*tenuis*’ for narrow and ‘*penna*’ for feather in regards to its slender wings.

Notes. *Cretaxenomerus tenuispenna* has several similarities with *C. brevis*, most pronounced being the shortened syntergum as well as *C. vitreus* in antennal structure. However, the wing shape would indicate it is likely a closely associated but distinct species.

Cretaxenomerus deangelis Ulmer & Krogmann, sp. nov.

<https://zoobank.org/A30ADD01-7CA5-42D0-99A9-F16B6EE8669A>

Fig. 14

Diagnosis. *Cretaxenomerus deangelis* differs from all other species in the genus by the following combination of characters: shape of its head capsule, longer than wide in dorsal view. Mesoscutum with notauli. Fore wing basal cell narrow and marginal setation short. Syntergum short.

Description. Female. Body length 1179. Head capsule light-brown, body and appendages dark brown, aside from first two flagellomeres. Wing venation dark brown. Wing's damaged just distal to junction of smv and bv, first 2 flagellomeres damaged. Wings with slight brown infumation, uniform pilosity. **Head** elongate, about 1.3× as long as wide, wider than mesosoma in dorsal view (Fig. 14A). Temple large, at most $\frac{1}{4}$ as long as eye length. Occiput very narrow and concave, about $\frac{1}{3}$ as wide as head width.

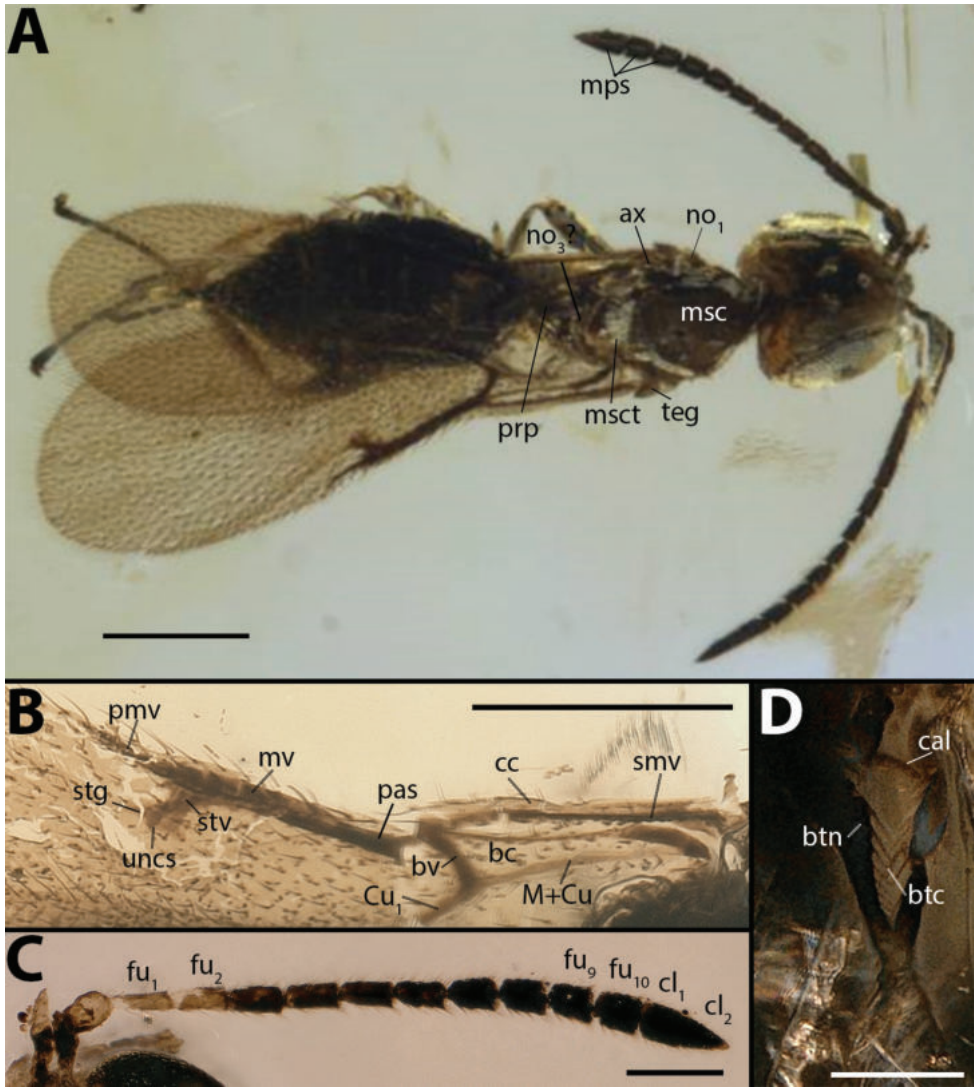


Figure 14. *Cretaxenomerus deangelis*, holotype **A** dorsal habitus **B** fore wing venation and cells **C** antenna, lateral **D** fore leg basitarsus and tibia. Scale bars: 250 μm (**A**); 200 μm (**B**); 100 μm (**C**); 50 μm (**D**).

Malar sulcus well developed, connecting lower margin of eye and oral fossa. Antenna insertion around midline of eye. Frons protruding, on higher plane than face. Clypeus inflected. Mandibles on higher plane than clypeal margin. *Antennae* length 743. Scape probably short and broad, not visible due to damage. Fu_{1-6} narrow, longer than wide, but not elongate, equal in length to fu_{7-10} . Clava 2-segmented, claval length 95. MPS present on all segments (Fig. 14C). Fine pilosity present, adpressed at 45° on all segments aside from pedicel and scape relative to surface. *Mesosoma* length 466. Mesoscutum $2.4\times$ as long as mesoscutellum. Notauli well visible for its entire length. Prepectus narrow, dor-

sally overlapped by posterior-most corner of lateral panel of pronotum, laterally seen as narrow sclerite, well separated from mesonotum. Transscutal articulation medially present. Mesodiscrimen deeply invaginated. Tegula visible, bare of setation (Fig. 14A:teg). Lateral panel of metanotum with flange. Propodeum approximately equal in length to mesoscutellum (Fig. 14A). **Wings.** Fore wing length 1047, 3.3× as long as wide. Longest marginal seta length 22. Costal cell present, nearly equal in width to basal cell (Fig. 14B). Cubital vein length 229, pigmented along the entire length. Basal vein $\frac{1}{5}$ length of cubital vein, strongly pigmented and distally curved. Basal cell of fore wing proximally narrowed, wider at junction of M+Cu. Submarginal length 380. Marginal vein with uniform thickness along its length, short, about 0.2 as long as submarginal vein (Fig. 14B). Stigmal vein length 42, stigma and uncus present; 6 uncal sensillae present. Postmarginal vein equal in length to marginal vein; tapering distally (Fig. 14B). Hind wings obscured by fore wings. **Legs.** Basitarsomere of all legs elongate, slightly shorter than tarsomere 2–4. Basitarsal comb of fore leg present (Fig. 14D:btc) with a blunt protuberance present laterobasally (Fig. 14D:btn). **Metasoma** length 505. Mt_{2,7} plus syntergum visible, syntergum about 0.15× as long as the rest of gaster, broadly attached to Mt₇, articulation not visible (Fig. 14A). **Genitalia.** Ovipositor only slightly extended from body and slightly longer than syntergum, no more than Mt₇ plus syntergum length (Fig. 14A).

Male. Unknown.

Material examined. Holotype: female, Hammana / Mdeyrij, Caza Baabda, Mouhafazet Mount Lebanon; lower Barremian. In amber mounted in Canada Balsam. Deposited at Natural History Museum of the Lebanese University, accession/specimen number 810H.

Type condition. Due to the taphonomic process both antennae are detached from the head and both scapes, pedicels and first two flagellomeres are broken; the mesosoma is slightly deformed dorsolaterally; both wings are broken, the left wing just before the basal vein and the right wing beyond the basal vein, and with some additional ruptures on the disc of both wings.

Etymology. The specific epithet is a patronym in honor of Eric Deangelo, an early mentor and professor of one of the authors (JU) who introduced him to biology and research.

Notes. Due to the orientation of the specimen in the amber, the tip of the metasoma is obscured, so the syntergum could not be clearly examined, but there does not appear to be an elongate syntergum. Because *C. deangelis* apparently lacks an elongate syntergum, similar to *Protoita* but unlike other *Cretaxenomerus* females, this feature might support its placement into a third genus, although it shares more similarities with *Cretaxenomerus* species than *Protoita*. Without additional specimens to examine, we consider it premature to erect a third genus for the specimen due to its damaged state and obscured syntergum and place it tentatively in *Cretaxenomerus*. Even though the lack of an elongate syntergum is shared with *Protoita*, this lack of an apomorphy does not justify placement within *Protoita* as it shares more diagnostic features with *Cretaxenomerus* such as body length, a petiolar constriction at the waist and a head which is not wider than long in dorsal view.

***Cretaxenomerus jankotejai* Nel & Azar, 2005**

Fig. 15

Diagnosis. *Cretaxenomerus jankotejai* can be differentiated from all other species in the genus by the following combination of characters: large body length, broad head, which is nearly 2× as wide as long (Fig. 15A), and a distinctly broadened posterior portion of its elongate syntergum (Fig. 15B: Mt_{8,9}).

Redescription. Female. Body length 1490, uniformly dark brown in coloration, eyes white, wings hyaline with dense pilosity along wing disc, sparser at speculum. **Head** globulose, length 160, 2× as wide as long (Fig. 15A). Ocelli large, LOL about equal to OOL. Toruli slightly closer to one another than inner eye margin. Malar sulcus present. Maxillary palps 2–3 segments. **Antenna** length 776. Fu₁₋₃ 2× as long as wide, fu₄₋₁₀ about 1.5× as long as wide (Fig. 15A). Clava 2 segmented, undifferentiated from funicles (Fig. 15A-inset). MPS present on all flagellomeres, as single long sensillae around circumference of segment in single row (Fig. 15A-inset). **Metasoma** length 370. Lateral panel of pronotum large and triangular. Mesonotum without notauli. Mesoscutum about 1.5× as long as mesoscutellum. Prepectus visible as a narrow strip in anterior half of mesopleuron. Mesopleuron dorsoventrally elongate. Axillulae striate. Metanotum short, length 30, medially overlapped by mesoscutellum (Fig. 15A).

Wings. Obscured by malformation around specimens, make measurements of wing length not possible. Costal cell narrow. Basal vein short, strongly pigmented. Cubital vein lightly pigmented anterior to junction with basal vein and more strongly pigmented posterior to junction. Submarginal vein length 259. Marginal vein broad, 1/3 length of submarginal vein (Fig. 15A). Postmarginal vein very short, equal in length to shortened stigmal vein. **Legs.** Basitarsomere of all legs very long, approximately equal in length to following 4 tarsomeres combined (Fig. 15C). Tarsomere 4 noticeably shorter than others on all legs. Protibial calcar simple; basitarsal comb of fore leg present. **Metasoma** length 553, 917 with syntergum. Clear number of metasomal segments obscured. Metasoma connected with mesosoma by narrow petiolus (Fig. 15A). Syntergum widest in the posterior 1/3 of its length (Fig. 15B). Cerci with 3 cercal sensillae (Fig. 15B:ccs). Ovipositor extending only slightly beyond length of syntergum; ovipositor sheaths narrow basally before becoming spatulate in the posterior 1/4 of its length.

Male. Unknown.

Material examined. Holotype: female, Hammana / Mdeyrij, Caza Baabda, Mouhafazet Mount Lebanon; lower Barremian. In amber mounted in Canada Balsam. Deposited at Natural History Museum of the Lebanese University, accession/specimen number: 972A.

Type condition. Specimen complete; dorsum of head partially detached; a large transverse crack in the amber obscures portions of the metasoma distally.

Notes. Nel and Azar (2005) described the elongate syntergum and associated ovipositor complex as a “tubular structure”, and suggested it was an early variant of the unique telescoping ovipositor system of Platygastroidea. Reexamination of the specimens indicates that this structure is not tubular but shaped as a narrow channel and



Figure 15. *Cretaxenomerus jankotejai*, holotype **A** dorsal habitus, with inset showing close up of terminal flagellomeres **B** ovipositor complex with elongate syntergum **C** mesotibia and tarsus showing tarsal length. Scale bars: 500 µm (**A**); 100 µm (**B**, **C**). **ccs** = cercal sensilla.

the presence of frass at the end of it suggests it is the true ending of the abdomen and alimentary canal rather than the ovipositor, which is clearly seen on (Fig. 15B). Along with the wing venation and tarsal characters we transfer *Cretaxenomerus jankotejai* from Scelionidae to Protoitidae.

Discussion

The classification of Protoitidae within Chalcidoidea is based on at least two of three putative external synapomorphies for the superfamily, with the most conspicuous being the specialized morphology and placement of MPS along all flagellar segments. Although multiporous plate sensilla occur within several lineages of Proctotrupomorpha, Chalcidoidea are unique in having the MPS raised, ridge-like, along the flagellomere and with the apical end of the sensilla raised above and often projecting beyond the apical margin of the flagellomere (Figs 5C, 7B, 9B, 11B) (Barlin and Vinson 1981; Basibuyuk and Quicke 1999). Likewise, the MPS of Protoitidae can be seen in lateral view as raised above the surface of the flagellum and often extending beyond the distal apices of the segment, including the distalmost clavomere (best seen in Fig. 9B). A second external synapomorphy that supports superfamilial placement of the newly described family is the presence of a free prepectus that is external between the pronotum and mesopleuron (Fig. 16). The structure and evolution of the prepectus within Chalcidoidea was examined in great detail by Gibson (1986, 1999). A free, external prepectus was hypothesized as the derived structure relative to the rest of Proctotrupomorpha, in which the prepectus is fused with the posterior margin of the pronotum to form a



Figure 16. Prepectus of Protoitidae **A** *Cretaxenomerus curvus*, mesosoma, lateral **B** *Protoita noyesi*, mesosoma, ventrolateral. Scale bars: 100 μm (**A, B**).

“tongue and groove” articulation with the anterior margin of the mesopleuron (Gibson 1999, fig. 2) such that the pronotum is immovable relative to the mesopleuron and typically is more or less triangular in shape in lateral view. Because most Chalcidoidea have a free prepectus between the pronotum and mesopleuron (secondarily fused with the pronotum in most Perilampidae and Eucharitidae) the pronotum is moveable relative to the mesothorax and not laterally triangular in shape, at least if the prepectus is comparatively large between the pronotum and mesopleuron. A comparatively narrow and partially concealed prepectus is found in Baeomorphidae and some Mymaridae and this structure is hypothesized as the groundplan structure for the superfamily (Gibson 1986; Heraty et al. 2013). The prepectus of Protoitidae is likewise a vertically elongate sclerite that is partially overlapped dorsally by the posteriormost edge of the lateral panel of the pronotum. It is visible in only a few specimens, most clearly in *P. vitreus* (Fig. 11E) and *P. noyesi* (Fig. 16B), in part due to the unique taphonomy of the specimen, but the structure of the pronota in all the fossil taxa indicates the prepectus is small and narrow because the pronotum is very short dorsally so not readily visible in dorsal view and is much more extensive laterally (e.g. Figs 7A, 8B, 11D).

It should be noted that the prepectus is free, external and triangular in Diversinitidae, which represents the condition in most larger “hard-bodied chalcids” (Haas et al. 2018) and putatively the most-derived condition within Chalcidoidea. The occurrence of Diversinitidae in Upper Cretaceous Burmese amber is significant because the only other lineages represented in the Cretaceous fossil record are smaller “soft-bodied” families that lack a distinctly triangular, external prepectus, such as Baeomorphidae and some Mymaridae. This indicates that the shift from stem- to crown-group lineages in Chalcidoidea occurred much earlier than previously anticipated. Based on fossil evidence we find a minimum age of this shift well within the Lower Cretaceous period at a time period between 130 million years (occurrence of Protoitidae) and 100

million years (occurrence of Diversinitidae) rather than at the Paleocene-Eocene thermal maximum as suggested by previous authors (e.g., Heraty and Darling 2009; Peters et al. 2018). An earlier crown-group diversification during the late Jurassic was recently suggested by Cruaud et al. (2023).

Within Chalcidoidea, Protoitidae cannot be included in Mymaridae, which are regarded as the earliest extant lineage of Chalcidoidea, morphologically by the structure of the ovipositor (Quicke et al. 1994; Gibson and Huber 2000) and more recently by molecular studies (Heraty et al. 2013; Peters et al. 2018; Cruaud et al. 2023). Putative mymarids are also found in Lebanese amber (Azar pers. comm.), further confirming Mymaridae as being present under its current concept at that time. Likewise, classification of protoitids in Baeomorphidae is unfounded based on tarsal formula (four in Baeomorphidae vs. five in Protoitidae), and shape of the protibial spur, short and straight in Baeomorphidae, while elongate and curved in Protoitidae. Based on outgroup comparisons (selected from Blaimer et al. 2023), a 5-segmented tarsi is likely the groundplan feature in Chalcidoidea with 4 segments being the derived state. 5-segments being most common in both Mymarommatoida and Diaprioidea. Within Mymaridae both 4- and 5-segmented tarsi may be found. The number of flagellomeres vary greatly in extinct baeomorphid species (Gumovsky et al. 2018), but extant baeomorphid females and males of *Baeomorpha* have 12-flagellomere antennae as do Protoitidae. Protoitidae in general have a putatively small breadth of claval numbers (1–3 segmented) which is a similar range to the extinct *Baeomorpha*. Despite the similar range, *Baeomorpha* have a larger number of claval segments (4–6 segmented clava) (Gumovsky et al. 2018). Likewise, the curvature of the basal vein in Baeomorphidae is chalcid like (basally-curved), and the marginal vein is much thinner than in Protoitidae (Fig. 2). Moreover, some specimens of Protoitidae have traces of metallic coloration on the gena or laterally on the mesonotum, which might indicate a relationship of Protoitidae to crown-group hard-bodied lineages rather than to Mymaridae or Baeomorphidae (Fig. 16B).

Protoitidae do share some features with Baeomorphidae and some Mymaridae, namely the shape of the prepectus, which is comparatively narrow, dorsoventrally elongated and anteriorly overlapped by the lateral panel of the pronotum (Fig. 16). The presence of MPS on the 1st flagellomere is known only for male Mymaridae within extant Chalcidoidea (Heraty et al. 2013). A probable hypothesis is that MPS on flagellomere 1 in both sexes was the groundplan state within Chalcidoidea, with subsequent loss in mymarid females and both sexes of other chalcids. The MPS present on flagellomere 1 in both sexes of Protoitidae is likely a retained symplesiomorphy of the family. Absence of flagellar MPS from Mymarommatoida, the hypothesized sister lineage of Chalcidoidea, and irregular presence and structure of MPS for other Proctotrupomorpha prevents any definitive statement of character polarity more broadly.

Gibson (1986) regarded the possession of 13 antennomeres as a ground plan feature for Chalcidoidea and interpreted 14 antennomeres in *Diglochis* (Pteromalidae) and some males of Eucharitidae as secondarily derived. Some authors have considered a terminal spine or what has been termed a terminal button on the antennal clava as remnants of a 14th antennomere and have thus considered a 14-segmented antenna as the ground

plan condition for Chalcidoidea (Graham 1969; Onagbola and Fadamiro 2008b). The presence of a 14-segmented antennae in the oldest known chalcid fossils supports this view, i.e., that a flagellum consisting of 12 flagellomeres was the ground plan structure of Chalcidoidea and the terminal button of some extant chalcids is, indeed, a highly reduced 12th flagellomere. A 12-segmented flagellum has been previously hypothesized as a grouplan character in Gibson (1986). Even at the early stage of Lower Cretaceous diversification of Chalcidoidea there has been a reduction in number of flagellomeres to 7 (as exhibited by *Baeomorpha caeleps* Gumovsky (2018)), a derived character state which is otherwise not known from Cretaceous Chalcidoidea. Cretaceous mymarids have 8 (*Enneagmus*, *Carpenteriana*), 10 (*Myanmymar*) or 11 (*Macalpina*, *Triadomerus*) flagellomeres (Poinar and Huber 2011). Diversinitidae females have an 11-segmented flagellum, whereas males have a 12-segmented flagellum, suggesting the fusion of the terminal segments occurred early in the evolution of Chalcidoidea in at least females (Haas et al. 2018). This partial fusion of the terminal button along with MPS on the terminal button of, for example, *Chromeurytoma* (Megastigmidae) or *Pseudotorymus* (Torymidae), a character shared with Protoitidae and Diversinitidae, provides further evidence that this was previously a separate segment. The initial indicators of this fusion can be seen in several species of Protoitidae based on the simple line of weakness dividing the terminal two flagellomeres (Fig. 3A, B).

All species of Protoitidae, aside from *P. bidentata*, have tridentate mandibles. Although there has been no formal investigation of the character polarity of mandibular dentition for Chalcidoidea, variation in the mandibular formula amongst the most basal lineages, Mymaridae and Baeomorphidae, makes it a structure difficult to assess for phylogenetic significance. The extinct genera of Mymaridae have no consistent pattern in dentition, varying from 2–4 teeth (Huber 2017b). Among extant Baeomorphidae, *Rotoita* Bouček & Noyes has bidentate mandibles (Bouček and Noyes 1987, fig. 2) similar to those of *P. bidentata* (Fig. 5D), whereas *Chiloe* Gibson & Huber has bidentate mandibles but with the upper tooth broad and serrate (Gibson and Huber 2000, fig. 4). Within the extinct Baeomorphidae, both bidentate (*Baeomorpha popovi*) and tridentate (*Baeomorpha liorum*) mandibles have been observed (Gumovsky et al. 2018; Huber et al. 2019). Amongst extinct lineages, the mandibles of all diversinitids are bidentate (Haas et al. 2018), indicating 2 or 3 teeth certainly are the most common mandibular structures amongst early chalcids, and perhaps supporting bidentate mandibles as the groundplan structure for Chalcidoidea.

Both the basal and cubital veins of Protoitidae are sclerotized or at least pigmented, unlike for most other Chalcidoidea. Within Chalcidoidea, basal and cubital fore wing veins are also pigmented in Baeomorphidae, a few Pteromalidae (Miscogasterinae, Trigonoderinae), a few Melanosomellidae, Leucospidae, some Megastigmidae and sporadically in many other groups (Krogmann and Burks 2009). However, other chalcids have the basal vein curved strongly basally (Fig. 2B), whereas the basal vein in protoitids joins the cubital vein at a straight angle without curving or curving only slightly proximally (Fig. 2A). A straight or proximally oriented basal vein is most common in the relictual lineages of Proctotrupomorpha (Rasnitsyn and Kühnle 2020) such as Peleciniidae, Vanhorniidae,

Heloridae and Roproniidae, and the Australasian genera of Proctotrupidae, such as *Austroserphus* and *Austrocodrus*. This straight or proximal curvature of the Rs+M vein (putatively homologous with the basal vein of Chalcidoidea) is seen for Evaniomorpha when venation is not reduced as well as for Ichneumonoidea and Symphyta (Sharkey and Roy 2002), which would indicate a proximally curving Rs+M vein as plesiomorphic with the redirection of the vein occurring in more derived Proctotrupomorpha.

All protoitids are characterized by a syntergum which results from the fusion of Mt₈ and Mt₉. This is a derived feature found also in most extant Chalcidoidea, but which likely evolved convergently multiple times (Krogmann and Burks 2009). The unique shape of the elongated syntergum is an autapomorphy of *Cretaxenomerus* among extinct chalcids.

We observed in several *Cretaxenomerus* females six distinct metasomal tergal sclerites preceding the syntergum, with Mt₇ being slightly elongate to articulate with the syntergum (Mt₈₊₉). The point of fusion between Mt₈₊₉ is likely at about the posterior 1/3 of the elongated tergum where there is a pair of lateral notches before the structure abruptly narrows slightly again, corresponding to the position of the cerci (Fig. 8D:cer).

The syntergum is sexually dimorphic, being elongate only in females, and likely functioning as a dorsal protection for the elongate ovipositor sheaths. In several females, such as a paratype of *P. curvus*, where the ovipositor is extended, the syntergum is shifted up, articulating with the base of the ovipositor, and terminal tergite (Mt₇). The membranous anal tube can be seen projecting from the apex of the syntergum, suggesting it to be the true distal point of the abdomen (Figs 8D, 10F, 12D). This is in contrast to the platygastroid ovipositor system (Austin and Field 1997), with which the structure was initially mistaken for in the original description of *Cretaxenomerus jankotejai* Nel & Azar, 2005.

Within *Cretaxenomerus* there is continuous variation in the structure of the syntergum. Within the “short-syntergum” species, consisting of *C. brevis* and *C. tenuipenna*, the ovipositor sheaths are continuous in width along their entire length (Figs 10F, 13B), compared to the spatulate-like sheaths of the “long-syntergum” group, such as *C. curvus* and *C. mirari*, which broaden distally into paddle-like structures along a narrow proximal stalk (Figs 8D, 12D). The structural diversity of the metasoma indicates a broad spectrum of oviposition capabilities and that the early Chalcidoidea described herein were able to occupy a diverse range of ecological niches. The function of the modified syntergum is uncertain, in part due to lacking comparison in extant taxa, although likely involved in assisting with oviposition or protection of the ovipositor. Egg parasitism is known from early chalcid lineages of Mymaridae and putatively in Baemorphidae (Munro et al. 2011; Peters et al. 2018). The additional presence of micropilosity along the claval and distal flagellar segments in Protoitidae, provides some support for parasitism of concealed hosts, character often associated with the lifestyle Podagrioninae, mantid eggs parasitoids (Janšta et al. 2018).

There is a clear divide in the Chalcidoidea fossil record between the Cretaceous and Eocene, corresponding with the division of early “soft-bodied” chalcids and the larger “hard-bodied” lineages (Fig. 1). Cruaud et al. (2023) places the divergence points of

the major chalcid lineages within the Lower Cretaceous, which corresponds with the fossil record, with Mymaridae persisting as an early crown-group lineage from the Cretaceous throughout the fossil record but Baeomorphae presenting itself as a “Lazarus taxon”, with a disjointed record between the Cretaceous and extant lineages (Jablonski 1986). The presence of Protoitidae and Diversinitidae in the Lower Cretaceous also confirms an early crown group diversification, with the two families likely representing late stem group lineages. Diversinitidae shares several synapomorphies with other members of the younger “hard-bodied” clade that provides further support for an Upper Cretaceous diversification. One hypothesis based on the known fossil record is an early diversification of Chalcidoidea within the Cretaceous, followed by the extinction of several lineages (including Protoitidae and Diversinitidae), possibly during the subsequent K-T extinction (Labandeira 2005), and then a subsequent radiation of other chalcidoid lineages during the paleocene-eocene thermal maximum. This secondary radiation corresponds with the diversification of herbivorous insects (Curanno et al. 2008), which led to the rapid diversification of parasitoids (Nyman et al. 2007). This may also provide some rationale for the seemingly disjunct apomorphies of surviving lineages of the earlier diversification event (Baeomorphae and Mymaridae) relative to the rest of Chalcidoidea. Research into fossils within the paleocene may elucidate this transition and provide better resolution to the stem-group to crown-group transition.

The most recent biogeographic theories on the origin of Chalcidoidea suggest an Eastern Gondwanan origin for the group with the rapid radiation of the group occurring in Southern Gondwana (Cruaud et al. 2023). This is based quite heavily on the density of early lineages occurring in Burmese amber such as Mymaridae and Baeomorphae (Gumovsky et al. 2018), with crown group taxa appearing with more regularity in the southern gondwanan Cenozoic records. The presence of Protoitidae in Northeastern Gondwanan Lebanese amber presents a new piece of evidence for an Eastern Gondwanan origin. Lebanese amber also contains early putative Mymaridae (Azar pers. comm.), which suggests *Cretaxenomerus* was at least present in tandem with an extant lineage. We suggest an addendum to the present theory of Cruaud et al. (2023) based on this new evidence. An Eastern Gondwanan origin to Chalcidoidea led to the presence of early crown groups and relictual families of Chalcidoidea, including the “hard-bodied clade”. These groups spread both north and south. Northern lineages such as the fossil *Baeomorpha* and Protoitidae were not successful and disappeared early in the evolution of Chalcidoidea whereas southern groups proliferated during the climatic shifts of the early Cenozoic. This would also account for the curious distribution of Baeomorphae, which has a purely Southern Gondwanan extant distribution (New Zealand and Chile) and heavily Laurasian fossil record. Likewise, the presence of Diversinitidae in mid Cretaceous Burmese deposits (Haas et al. 2020) may suggest an early unsuccessful radiation attempt in Chalcidoidea prior to the eocene-paleocene thermal boundary with the bottleneck leading to the morphological “gap” between early relictual lineages such as Baeomorphae, Mymaridae, Diversinitidae, and Protoitidae and the larger post gap megaradiation event. Only with continued investigation of the fossil record of Chalcidoidea can we begin to uncover the true origins and early diversification of one of the largest insect lineages.

Acknowledgements

The authors would like to thank André Nel for providing the initial specimens for this study and for hosting several research stays of LK at MNHN. Thanks to MNHN for granting a research fellowship to LK. We thank Roger Burks, John Huber, and Gary Gibson for comments and suggestions on early drafts of this manuscript. JMU would like to thank Mihaela Tanas and Ekatarina Pirvu for assistance with imaging.

References

- Azar D, Perrichot V, Néraudeau D, Nel A (2003) New psychodids from the Cretaceous ambers of Lebanon and France, with a discussion of *Eophlebotomus connectens* Cockerell, 1920 (Diptera Psychodidae). *Annals of the Entomological Society of America* 96(2): 117–126. [https://doi.org/10.1603/0013-8746\(2003\)096\[0117:NPFTCA\]2.0.CO;2](https://doi.org/10.1603/0013-8746(2003)096[0117:NPFTCA]2.0.CO;2)
- Azar D, Gèze R, Acra F (2010) Chapter 14: Lebanese amber. In: Penney D (Ed.) *Biodiversity of Fossils in Amber*. Siri Scientific Press, 271–298. [ISBN 978-0-9558636-4-6]
- Barlin MR, Vinson SB (1981) The multiporous plate sensillum and its potential use in braconid systematics (Hymenoptera: Braconidae) 1. *The Canadian Entomologist* 113(10): 931–938. <https://doi.org/10.4039/Ent113931-10>
- Barling N, Heads SW, Martill DM (2013) A new parasitoid wasp (Hymenoptera: Chalcidoidea) from the lower Cretaceous Crato formation of Brazil: the first mesozoic Pteromalidae. *Cretaceous Research* 45: 258–264. <https://doi.org/10.1016/j.cretres.2013.05.001>
- Basibuyuk HH, Quicke DL (1999) Gross morphology of multiporous plate sensilla in the Hymenoptera (Insecta). *Zoologica Scripta* 28(1–2): 51–67. <https://doi.org/10.1046/j.1463-6409.1999.00007.x>
- Blaimer BB, Santos BF, Cruaud A, Gates MW, Kula RR, Mikó I, Rasplus J-Y, Smith DR, Talamas EJ, Brady SG, Buffington ML (2023) Key innovations and the diversification of Hymenoptera. *Nature Communications* 14(1): e1212. <https://doi.org/10.1038/s41467-023-36868-4>
- Burks R, Mitroiu M-D, Fusu L, Heraty JM, Janšta P, Heydon S, Papilloud ND-S, Peters RS, Tselikh EV, Woolley JB, van Noort S, Baur H, Cruaud A, Darling C, Haas M, Hanson P, Krogmann L, Rasplus J-Y (2022) From hell's heart I stab at thee! A determined approach towards a monophyletic Pteromalidae and reclassification of Chalcidoidea (Hymenoptera). *Journal of Hymenoptera Research* 94: 13–88. <https://doi.org/10.3897/jhr.94.94263>
- Çıplak B, Yahyaoglu Ö, Uluar O (2021) Revisiting Pholidopterini (Orthoptera Tettigoniidae): Rapid radiation causes homoplasy and phylogenetic instability. *Zoologica Scripta* 50(2): 225–240. <https://doi.org/10.1111/zsc.12463>
- Cruaud A, Rasplus J-Y, Zhang J, Burks R, Delvare G, Fusu L, Fusu L, Gumovsky A, Huber JT, Janšta P, Mitroiu M-D, Noyes JS, van Noort S, Baker A, Böhmová J, Baur H, Blaimer BB, Brady SG, Bubeníková K, Chartois M, Copeland RS, Dale-Skey Papilloud N, Dal Molin A, Dominguez C, Gebiola M, Guerrieri E, Kresslein RL, Krogmann L, Lemmon EM, Murray ES, Nidelet S, Nieves-Aldrey JL, Perry RK, Peters RS, Polaszek A, Sauné L, Torrén

- J, Triapitsyn S, Tselikh EV, Yoder M, Lemmon AR, Woolley JB, Heraty JM (2023) The Chalcidoidea bush of life—a massive radiation blurred by mutational saturation. *Systematic Entomology*. <https://doi.org/10.1101/2022.09.11.507458>
- Currano ED, Wilf P, Wing SL, Labandeira CC, Lovelock EC, Royer DL (2008) Sharply increased insect herbivory during the Paleocene-Eocene Thermal Maximum. *Proceedings of the National Academy of Sciences* 105(6): 1960–1964. <https://doi.org/10.1101/2022.09.11.507458>
- Gibson GA (1985) Some pro- and mesothoracic structures important for phylogenetic analysis of Hymenoptera, with a review of terms used for the structures. *The Canadian Entomologist* 117(11): 1395–1443. <https://doi.org/10.4039/Ent1171395-11>
- Gibson GA (1986) Evidence for monophyly and relationships of Chalcidoidea Mymaridae, and Mymarommatidae (Hymenoptera: Terebrantes) 1. *The Canadian Entomologist* 118(3): 205–240. <https://doi.org/10.4039/Ent118205-3>
- Gibson GA (1999) Sister-group relationships of the Platygastroidea and Chalcidoidea (Hymenoptera)—an alternate hypothesis to Rasnitsyn (1988) *Zoologica Scripta* 28(1–2): 125–138. <https://doi.org/10.1046/j.1463-6409.1999.00015.x>
- Gibson GA (1989) Phylogeny and classification of Eupelmidae, with a revision of the world genera of Calosotinae and Metapelmatinae (Hymenoptera: Chalcidoidea). *The Memoirs of the Entomological Society of Canada* 121(S149): 3–121. <https://doi.org/10.4039/ent-m121149fv>
- Gibson GA, Heraty JM, Woolley JB (1999) Phylogenetics and classification of Chalcidoidea and Mymarommatoidea—a review of current concepts (Hymenoptera Apocrita). *Zoologica Scripta* 28(1–2): 87–124. <https://doi.org/10.1046/j.1463-6409.1999.00016.x>
- Gibson GA, Huber JT (2000) Review of the family Rotoitidae (Hymenoptera: Chalcidoidea), with description of a new genus and species from Chile. *Journal of Natural History* 34(12): 2293–2314. <https://doi.org/10.1080/002229300750037901>
- Gibson GA (2003) Phylogenetics and classification of Cleonyminae (Hymenoptera: Chalcidoidea: Pteromalidae). Associated Publishers.
- Graham MWRV (1969) The Pteromalidae of north-western Europe (Hymenoptera: Chalcidoidea). *Bulletin of the British Museum (Natural History). Entomology. Supplement* 16: 1–908. <https://doi.org/10.5962/p.258046>
- Granier B, Toland C, Gèze R, Azar D, Maksoud S (2016) Some steps toward a new story for the Jurassic–Cretaceous transition in Mount Lebanon. *Carnets de Géologie* 16(8): 247–269. <https://doi.org/10.4267/2042/59924>
- Grissell EE, Schauff ME (1990) A handbook of the families of Nearctic Chalcidoidea (Hymenoptera). Entomological Society of Washington (Washington D.C.) Handbook 1: 1–85.
- Gumovsky A, Perkovsky E, Rasnitsyn A (2018) Laurasian ancestors and “Gondwanan” descendants of Rotoitidae (Hymenoptera: Chalcidoidea): what a review of late cretaceous *Baeomorpha* revealed. *Cretaceous Research* 84: 286–322. <https://doi.org/10.1016/j.cretres.2017.10.027>
- Haas M, Burks RA, Krogmann L (2018) A new lineage of Cretaceous jewel wasps (Chalcidoidea: Diversinitidae). *PeerJ* 6: e4633. <https://doi.org/10.7717/peerj.4633>
- Haas M, Burks RA, Janša P, Krogmann L (2020) Redescription and phylogenetic placement of the Cretaceous wasp *Parviformosus wohltrabeae* (Hymenoptera: Proctotrupomorpha). *Palaeontologia Electronica* 23(1): 1–10. <https://doi.org/10.26879/1031>

- Heraty JM, Darling DC (2009) Fossil eucharitidae and perilampidae (Hymenoptera: Chalcidoidea) from Baltic amber. *Zootaxa* 2306(1): 1–16. <https://doi.org/10.11646/zootaxa.2306.1.1>
- Heraty JM, Burks RA, Cruaud A, Gibson GA, Liljeblad J, Munro J, Rasplus J-Y, Delvare G, Janšta P, Gumovsky A, Huber J, Woolley JB, Krogmann L, Heydon S, Polaszek A, Schmidt S, Darling DC, Gates MW, Mottern J, Murray E, Molin AD, Triapitsyn S, Baur H, Pinto JD, van Noort S, George J, Yoder M (2013) A phylogenetic analysis of the megadiverse Chalcidoidea (Hymenoptera). *Cladistics* 29(5): 466–542. <https://doi.org/10.1111/cla.12006>
- Hong YC (2002) Amber insects of China. Beijing Science and Technology Publishing House Beijing.
- Huber JT (2017) Biodiversity of hymenoptera. *Insect biodiversity: Science and Society*, 419–461. <https://doi.org/10.1002/9781118945568.ch12>
- Huber JT (2017) *Eustochomorpha* Girault, *Neotriadomerus* gen. n., and *Proarescon* gen. n. (Hymenoptera Mymaridae), early extant lineages in evolution of the family. *Journal of Hymenoptera Research* 57: 1–87. <https://doi.org/10.3897/jhr.57.12892>
- Huber JT, Shih C, Dong R (2019) A new species of *Baeomorpha* (Hymenoptera Rotoitidae) from mid-Cretaceous Burmese amber. *Journal of Hymenoptera Research* 72: 1–10. <https://doi.org/10.3897/jhr.72.35502>
- Jablonski D (1986) Background and mass extinctions: the alternation of macroevolutionary regimes. *Science* 231(4734): 129–133. <https://doi.org/10.1126/science.231.4734.129>
- Janšta P, Cruaud A, Delvare G, Genson G, Heraty J, Křížková B, Rasplus JY (2018) Torymidae (Hymenoptera Chalcidoidea) revised: molecular phylogeny, circumscription and reclassification of the family with discussion of its biogeography and evolution of life-history traits. *Cladistics* 34(6): 627–651. <https://doi.org/10.1111/cla.12228>
- Kaddumi HF (2005) Amber of Jordan. *The Oldest Prehistoric Insects in Fossilised Resins*. Eternal River Museum of Natural History Jordan, 168 pp.
- Kearney M, Clark JM (2003) Problems due to missing data in phylogenetic analyses including fossils: a critical review. *Journal of Vertebrate Paleontology* 23(2): 263–274. [https://doi.org/10.1671/0272-4634\(2003\)023\[0263:PDTMDI\]2.0.CO;2](https://doi.org/10.1671/0272-4634(2003)023[0263:PDTMDI]2.0.CO;2)
- Klopfstein S (2021) The age of insects and the revival of the minimum age tree. *Austral Entomology* 60(1): 138–146. <https://doi.org/10.1111/aen.12478>
- Krogmann L, Vilhelmsen L (2006) Phylogenetic implications of the mesosomal skeleton in Chalcidoidea (Hymenoptera Apocrita)—tree searches in a jungle of homoplasy. *Invertebrate Systematics* 20(6): 615–674. <https://doi.org/10.1071/IS06012>
- Krogmann L, Burks RA (2009) *Doddifoenus wallacei*, a new giant parasitoid wasp of the subfamily Leptofoeninae (Chalcidoidea: Pteromalidae), with a description of its mesosomal skeletal anatomy and a molecular characterization. *Zootaxa* 2194(1): 21–36. <https://doi.org/10.11646/zootaxa.2194.1.2>
- Labandeira CC (2005) The fossil record of insect extinction: new approaches and future directions. *American Entomologist* 51(1): 14–29. <https://doi.org/10.1093/ae/51.1.14>
- Maksoud S, Azar D, Granier B, Gèze R (2017) New data on the age of the Lower Cretaceous amber outcrops of Lebanon. *Palaeoworld* 26(2): 331–338. <https://doi.org/10.1016/j.palwor.2016.03.003>

- Maksoud S, Azar D (2020) Lebanese amber: latest updates. *Palaeoentomology* 3(2): 125–155. <https://doi.org/10.11646/palaeoentomology.3.2.2>
- Maksoud S, Granier BR, Azar D (2022) Palaeoentomological (fossil insects) outcrops in Lebanon. *Carnets Geol.* 22(16): 699–743. <https://doi.org/10.2110/carnets.2022.2216>
- Matthews S (1973) Notes on Open Nomenclature and on Synonymy Lists. *Paleontology* 16: 713–719.
- McClennen M, Jenkins J, Uhen M (2017) Paleobiology Database.
- Kocsis ÁT, Reddin CJ, Alroy J, Kiessling W (2019) The R package divDyn for quantifying diversity dynamics using fossil sampling data. *Methods in Ecology and Evolution* 10(5): 735–743. <https://doi.org/10.1111/2041-210X.13161>
- Munro JB, Heraty JM, Burks RA, Hawks D, Mottern J, Cruaud A, Jansta P (2011) A molecular phylogeny of the Chalcidoidea (Hymenoptera). *PLoS ONE* 6(11): e27023. <https://doi.org/10.1371/journal.pone.0027023>
- Nel A, Azar D (2005) The oldest parasitic Scelionidae: Teleasinae (Hymenoptera: Platygastroidea). *Polskie Pismo Entomologiczne* 74(3): 333–338.
- Nyman T, Bokma F, Kopelke JP (2007) Reciprocal diversification in a complex plant-herbivore-parasitoid food web. *Bmc Biology* 5(1): 1–9. <https://doi.org/10.1186/1741-7007-5-49>
- Onagbola EO, Fadamiro HY (2008) Scanning electron microscopy studies of antennal sensilla of *Pteromalus cerealellae* (Hymenoptera: Pteromalidae). *Micron* 39(5): 526–535. <https://doi.org/10.1016/j.micron.2007.08.001>
- Peters RS, Niehuis O, Gunkel S, Bläser M, Mayer C, Podsiadlowski L, Kozlov A, Donath A, van Noort S, Liu S, Zhou X, Misof B, Heraty J, Krogmann L (2018) Transcriptome sequence-based phylogeny of chalcidoid wasps (Hymenoptera: Chalcidoidea) reveals a history of rapid radiations, convergence, and evolutionary success. *Molecular Phylogenetics and Evolution* 120: 286–296. <https://doi.org/10.1016/j.ympev.2017.12.005>
- Poinar GO, Milki R (2001) Lebanese amber. Oregon State University Press, USA.
- Poinar Jr G, Huber JT (2011) A new genus of fossil Mymaridae (Hymenoptera) from Cretaceous amber and key to Cretaceous mymarid genera. *ZooKeys* 130: 461–472. <https://doi.org/10.3897/zookeys.130.1241>
- Quicke DLJ, Fitton MG, Tunstead JR, Ingram SN, Gaitens PV (1994) Ovipositor structure and relationships within the Hymenoptera, with special reference to the Ichneumonoidea. *Journal of Natural History* 28(3): 635–682. <https://doi.org/10.1080/00222939400770301>
- Rasnitsyn AP, Maalouf M, Maalouf R, Azar D (2022) New Serphitidae and Gallorommatidae (Insecta: Hymenoptera: Microprocta) in the Early Cretaceous Lebanese amber. *Palaeoentomology* 5(2): 120–136. <https://doi.org/10.11646/palaeoentomology.5.2.4>
- Rasnitsyn AP, Öhm-Kühnle C (2021) Non-acute hymenoptera in the Cretaceous ambers of the world. *Cretaceous Research* 124: e104805. <https://doi.org/10.1016/j.cretres.2021.104805>
- Sharkey MJ, Roy A (2002) Phylogeny of the Hymenoptera: a reanalysis of the Ronquist et al.(1999) reanalysis, emphasizing wing venation and apocritan relationships. *Zoologica Scripta* 31(1): 57–66. <https://doi.org/10.1046/j.0300-3256.2001.00081.x>
- Spasojevic T, Broad GR, Bennett AM, Klopstein S (2018) Ichneumonid parasitoid wasps from the Early Eocene Green River Formation: five new species and a revision of the known

fauna (Hymenoptera Ichneumonidae). *PalZ* 92(1): 35–63. <https://doi.org/10.1007/s12542-017-0365-5>

Spasojevic T, Broad GR, Klopfstein S (2022) Revision of 18 ichneumonid fossil species (Hymenoptera, Ichneumonidae) highlights the need for open nomenclature in palaeontology. *Fossil Record* 25(1): 187–212. <https://doi.org/10.3897/fr.25.83034>

van de Kamp T, Mikó I, Staniczek AH, Eggs B, Bajerlein D, Faragó T, Hagelstein L, Hamann E, Spiecker R, Baumbach T, Janšta P, Krogmann L (2022) Evolution of flexible biting in hyperdiverse parasitoid wasps. *Proceedings of the Royal Society B* 289(1967): e20212086. <https://doi.org/10.1098/rspb.2021.2086>

Yoder MJ, Mikó I, Seltmann KC, Bertone MA, Deans AR (2010) A gross anatomy ontology for Hymenoptera. *PLoS ONE* 5(12): e15991. <https://doi.org/10.1371/journal.pone.0015991>

Yoshimoto CM (1975) Cretaceous chalcidoid fossils from Canadian amber. *The Canadian Entomologist* 107(5): 499–527. <https://doi.org/10.4039/Ent107499-5>

Supplementary material I

Fossil Chalcidoidea occurrence data

Authors: Jonah M. Uimer

Data type: csv

Explanation note: Curated occurrence and metadata of fossil Chalcidoidea taxa used for generating time series plots.

Copyright notice: This dataset is made available under the Open Database License (<http://opendatacommons.org/licenses/odbl/1.0/>). The Open Database License (ODbL) is a license agreement intended to allow users to freely share, modify, and use this Dataset while maintaining this same freedom for others, provided that the original source and author(s) are credited.

Link: <https://doi.org/10.3897/jhr.96.105494.suppl1>

Notes on the parasitoids found within the nests of *Delta dimidiatipenne* (Hymenoptera, Vespidae)

Alfred Daniel Johnson¹, Tamir Rozenberg¹, Michal Segoli¹

¹ *Mitrani Department of Desert Ecology, The Jacob Blaustein Institutes for Desert Research, Ben-Gurion University of the Negev, Sde Boker Campus, Midreshet Ben Gurion, Israel*

Corresponding author: Alfred Daniel Johnson (danieljalfred@gmail.com)

Academic editor: Volker Lohrmann | Received 19 February 2023 | Accepted 16 October 2023 | Published 24 October 2023

<https://zoobank.org/729CA528-1CB4-4804-A7AD-BEA38D8094DE>

Citation: Johnson AD, Rozenberg T, Segoli M (2023) Notes on the parasitoids found within the nests of *Delta dimidiatipenne* (Hymenoptera, Vespidae). *Journal of Hymenoptera Research* 96: 925–936. <https://doi.org/10.3897/jhr.96.102336>

Abstract

An examination of parasitoids that had completed their development but were trapped within *Delta dimidiatipenne* nests revealed 15 species of insect parasitoids, belonging to eight families under two orders. A new association of Miltogramminae (Diptera: Sarcophagidae) with this wasp is also reported.

Keywords

Diptera, Miltogramminae, parasitoids, potter wasps, Sarcophagidae

Introduction

Potter wasps (Eumeninae) are the largest vespid wasp subfamily in the world, comprising nearly 3800 species in more than 210 currently described genera (Pickett and Carpenter 2010; Auko et al 2014; Pannure et al. 2016; Tan et al. 2018). Nevertheless, the ecology and phylogenetic relationships of this mega-diverse lineage is poorly studied (Carpenter and Marques 2001; Pickett and Carpenter 2010; Hermes et al. 2013; Bank et al. 2017). Adult Eumeninae feed on nectar while the larvae are predatory. Females build nests made of mud, deposit eggs, and hunt for prey, usually larvae of Lepidoptera, Curculionidae, and Chrysomelidae (Júnior et al. 2012), to provide food for their own larvae (Evans 1956; Krombein 1979; Carpenter and Marques 2001; Hunt et al. 2003). The females usually sting to paralyze the prey before carrying it to the nest and

depositing it in the cell. The wasp larvae develop by feeding on the prey externally, thereby completing their development inside the cell, and they emerge as adults by breaking open the nest cell (Matthews and González 2004; Prezoto et al. 2007; Matthews and Matthews 2009). In some studies, potter wasps were reported to be effective generalist predators of some economically important Lepidoptera (Boesi et al. 2005; Buschini and Buss 2010; Abarca et al. 2012; Udayakumar et al. 2022).

Eumeninae's main natural enemies are birds, ants, bats, and parasitoids (West-Eberhard et al. 1995). Some parasitoids of potter wasps have adapted to infest the nest while it is under construction, whereas others infest it after the nest has been built and sealed, using their mandibles or ovipositors to puncture the nest cell wall (Berland and Bernard 1938; Krombein 1979; Gauld and Hanson 1995; West-Eberhard et al. 1995; Liu et al. 2014). Regardless of the infestation timing, parasitoids that specialize on potter wasp nests, after completing their development, normally have morphological adaptations to break open the nests (Martynova 2020). Nevertheless, occasionally parasitoids may fail to emerge from the nest cells (Buschini and Buss 2010).

Apart from these nest parasitoids, several studies have also reported the occurrence of parasitized prey and parasitoids of the prey insects trapped in the nests of solitary wasps. This may occur when the potter wasps collect and bring to the nest already parasitized prey (Bohart et al. 1982; Jennings and Houseweart 1984; Tschardt et al. 1998; Buschini and Buss 2010; Auko et al. 2015; Segoli et al. 2020; Leduc et al. 2022). In contrast to the nest parasitoids, the parasitoids of the prey species are not likely to have adaptations to break out of the mud cells, as most commonly, they do not develop inside a potter wasp nest. In this context, we documented the parasitoids of the potter wasps and of their prey species that were trapped inside potter wasp nests in Israel's Negev and Judean Deserts.

We focused on the wasp species *Delta dimidiatipenne* de Saussure, 1852 (Hymenoptera, Vespidae, Eumeninae), which has been recorded in Afghanistan, Algeria, Chad, Djibouti, Egypt, Eritrea, Ethiopia, India, Iran, Israel, Jordan, Mauritania, Morocco, Nepal, Niger, Oman, Pakistan, Qatar, Saudi Arabia, Spain, Somalia, South Africa, Sudan, Syria, Tajikistan, Turkey, Turkmenistan, the United Arab Emirates, Uganda, and Yemen, mainly in desert habitats (Rafi et al. 2017; Hamzavi et al. 2019; Segoli et al. 2020). These wasps construct nests, composed of multiple mud cells, on rock surfaces. Females lay a single egg per cell (usually) and provision it with several caterpillars. In Israel, the wasps can be found in drier areas, from the center to the south of the country, and they are active mostly between March and June (Alon and Kugler 1989). The wasp's most common prey species in the deserts of Israel are caterpillars of noctuid moths, especially *Heliothis nubigera* Herrich-Schäffer, 1851, which are often found on the desert shrub *Zygophyllum dumosum* Boiss. (Segoli et al. 2020; Leduc et al. 2022). Evidence for the occurrence of caterpillars parasitized by *Copidosoma primum* (Mercet 1921) in *D. dimidiatipenne* nests has been documented in multiple sites in the Negev Desert, and in ca. 70–80% of the observed newly constructed nests (Segoli et al. 2020; Leduc et al. 2022). These authors also found that potter wasp larvae that develop with parasitized caterpillars had lower developmental success, probably because the parasitized prey is of lower quality. We recorded the content of *D. dimidiatipenne* nests from previous years and identified the dead parasitoids found within them.

Materials and methods

The current study was conducted in Israel's Negev and Judean Deserts during 2021–22. The climate is characterized by hot, dry summers, with an average maximum daily temperature of around 36 °C (Judean Desert) and 27 °C (Negev Desert) in July–August, and cold winters, with an average minimum daily temperature of around 18 °C (Judean Desert) and 9 °C (Negev Desert) in January–February. Annual precipitation is ca. 100 mm (data retrieved from the Israel Meteorological Service, <https://ims.gov.il/en>). A total of 11 field sites were selected, especially ones in proximity to temporary water holes that are used by potter wasps for drinking and nest construction. *Delta dimidiatipenne* normally build nests under rock ledges and in concealed rock surfaces, presumably to avoid direct insolation by the sun, which may result in overheating of the brood cell, and also to avoid the nest from being washed away by the heavy rains that occasionally occur during the nesting season. In each of the field sites, we sampled from five to 10 nests. However, it was difficult to estimate the exact number of nests that were sampled because the nests sometimes partially overlapped. In each nest, we sampled between three to 18 cells. This is again a rough estimation as some cells were partially disintegrated or contained secondary residences such as spiders, beetles or bees. We located nests from previous years, which can easily be recognized by the presence of emergence holes. Some nests had emergence holes in each cell, suggesting complete successful emergence, while other nests had some emergence holes and some intact cells, suggesting partial emergence success. In a few cases, we also found nests that were completely sealed without any emergence holes, suggesting that neither parasitoids nor potter wasps emerged successfully. Wherever feasible, we opened the cells by carefully dampening them with water and gently breaking the cell walls open using forceps and collecting all the parasitoids within. Apart from the focal study species, *D. dimidiatipenne*, we also collected and documented other vespid potter wasps in the study area by sweeping with nets near the water hole. We identified all the collected insects to the lowest taxonomic level possible, using keys published by Broad (2011) for Ichneumonidae and by van Achterberg (1990a) for Braconidae, and we confirmed the identities by consulting respective experts for each group and by comparing the specimens with the available reference collections at the Steinhardt Museum of Natural History, Tel Aviv, Israel. Geographic coordinates are given in WGS84. The specimens were then deposited in the Steinhardt Museum.

Results and discussion

Potter wasp species, other than *D. dimidiatipenne*, that were collected include the following: *Delta asina mixtum* (Giordani Soika, 1944), *Delta hottentotum elegans* (De Saussure, 1852), *Katamenes niger* (Brullé, 1839), *Katamenes dimidiativentris* (Giordani Soika, 1941), *Katamenes jenjouristei* (Kostylev, 1939), and *Ancistrocerus biphaleratus* (de Saussure, 1852). We identified *D. dimidiatipenne* nests based on their distinctive pot-shaped entrance with a size of approximately 1 cm in diameter. Moreover,

Table I. List of parasitoids found within *Delta dimidiatipenne* nests.

Order	Family	Taxon/ Species	No. of individuals	Place of collection	Potential host
Diptera	Sarcophagidae	Miltogramminae	1	Nahal Peres (31°00'31.52"N, 35°28'39.95"E)	Wasp larva (Spofford et al. 1989; Pape 1996)
	Tachinidae	Undetermined	1	Mamshit (31°02'31.47"N, 35°06'70.13"E)	Could be prey or wasp larva (Belshaw 1994)
Hymenoptera	Ichneumonidae	<i>Netelia fuscicornis</i> (Holmgren, 1860)	1	Ein Bokek (31°19'86.72"N, 35°35'03.57"E)	Prey (Townes 1965)
		<i>Barylypa rufa</i> (Holmgren, 1857)	1	Nahal Shoalim (30°95'29.57"N, 34°91'39.78"E)	Prey (Ahmed 1950)
		<i>Ophion similis</i> (Szépligeti, 1905)	1	Nahal Daroch (30°86'09.39"N, 34°85'96.41"E)	Prey (Gauld 1988)
	Braconidae	<i>Cotesia vanessae</i> (Reinhard, 1880)	17 individuals from three nests	Nahal Gov (30°90'38.30"N, 35°12'77.89"E) & Nahal Shoalim (30°95'29.57"N, 34°91'39.78"E) & Ein Zik (30°80'36.54"N, 34°85'10.00"E)	Prey (a gregarious parasitoid) (Hervet et al. 2014)
		<i>Microplitis</i> sp.	9	Nahal Gov (30°90'38.30"N, 35°12'77.89"E) & Nahal Afran (30°86'38.14"N, 34°92'71.31"E)	Prey (Takasu and Lewis 1995)
		<i>Schoenlandella deserta</i> (Telenga, 1955)	1	Nahal Mador (30°86'99.66"N, 34°96'40.56"E)	Prey (Huddleston and Walker 1988)
		<i>Chelonus</i> sp.	4	Mamshit (31°02'31.47"N, 35°06'70.13"E), Nahal Afran (30°86'38.14"N, 34°92'71.31"E)	Prey (Jourdie et al. 2008)
		<i>Rogas</i> sp.	1	Nahal Shoalim (30°95'29.57"N, 34°91'39.78"E)	Prey (Reardon 1973)
		<i>Phanerotoma</i> sp.	11	Ein Bokek (31°19'86.72"N, 35°35'03.57"E)	Prey (van Achterberg 1990b)
		Encyrtidae	<i>Copidosoma primulum</i> (Mercet, 1921)	Hundreds emerging out of 28 mummified caterpillars	In all the collection sites

Order	Family	Taxon/ Species	No. of individuals	Place of collection	Potential host
Hymenoptera	Torymidae	<i>Monodontomerus</i> sp.	3	Nahal Afran (30°86'38.14"N, 34°92'71.31"E)	Could be prey or wasp larva (Grissell 2000, 2007)
	Eulophidae	<i>Melittobia acaosta</i> (Walker, 1839)	4	Nahal Zafit (30°97'21.47"N, 35°29'69.26"E)	Wasp larva (a gregarious parasitoid) (Gonzalez et al. 2004)
	Chrysididae	<i>Stilbum</i> sp.	1	Saraf (30°78'72.25"N, 35°02'99.82"E)	Wasp larva (Gess and Gess 2014)

D. dimidiatipenne adults are the largest (approximately 2.5 cm long) of all the above-mentioned potter wasp species, and they construct the largest nests, comprising ca. 20 cells. Also, whenever we collected fresh cells (e.g., as part of our other published studies), this species always emerged from them. We have also recorded 12 imagines of *D. dimidiatipenne* that were trapped within the cell. This reaffirms that we have sampled only the nests of *D. dimidiatipenne*.

Our collections from the nests resulted in a total of 15 parasitoid species, belonging to two orders and eight families of insects. Based on the literature, most of them are probably parasitoids of species that the potter wasps collect as prey, while some are nest parasitoids of the potter wasps themselves. The details are presented in Table 1.

Though Bombyliidae is one of the most commonly occurring parasitoids in potter wasp nests (Yeates and Greathead 1997), we did not collect any of them, but we witnessed pupal cases that were most likely of bombyliids (Fig. 1a) in some nests, suggesting that they were able to emerge out of the nest successfully. Apart from the below list, we found some interesting secondary inhabitants of the nests, *viz.*, a neuropteran larva, many different species of spiders and bees, earwigs, and a scorpion exuvium. We also observed fully developed adult potter wasps that had failed to break open the cell and died within (Fig. 1d).

Caterpillar parasitoids

Based on their known ecology, all the ichneumonids, braconids, and the encyrtid that were documented in this study, *i.e.*, 10 out of 15 recorded species, are parasitoids of the prey caterpillars brought by the potter wasps to the nests. In this sense, it is perhaps not surprising to find them trapped within potter wasp nests, as they are not likely to have adaptations that enable them to emerge successfully through the hardened mud cell walls. Moreover, the occurrence of most of these prey parasitoids seems to be rare. Such low occurrence could perhaps represent a generally low parasitism rate on the prey by these parasitoid species in the field. In addition, some predatory insects are known to



Figure 1. Interior of some opened nests showing trapped parasitoids and unemerged wasps **a** *Netelia fuscicornis* **b** Miltogramminae **c** emerged fly pupal cases **d** *Copidosoma primulum* infested caterpillars and an unemerged male of *Delta dimidiatipenne*.

discriminate against parasitized prey, which are often of lower quality (e.g., Aparicio et al. 2020; Leduc et al. 2022; Perier et al. 2022). The fact that some of these parasitoids were not consumed by the potter wasp larvae and were able to complete their development inside the cell could perhaps also support the interpretation that they are not a good food source for the developing potter wasp larvae.

An exception was the high occurrence of *Copidosoma primulum*, which was found in all 11 study sites and was the most abundant of all the parasitoids that we documented. This accords with previous studies conducted on these species (Segoli et al. 2020; Leduc et al. 2022), suggesting that *D. dimidiatipenne* frequently collects caterpillars that are already parasitized by this gregarious parasitoid, possibly due to the lower susceptibility of the parasitized caterpillars to predation risk (Leduc et al. 2022).

In such cases, the parasitoid larvae feed on the caterpillar internally, depleting the food required for *D. dimidiatipenne* development, thereby reducing the probability that the wasp larvae can survive and successfully pupate (Segoli et al. 2020; Leduc et al. 2022).

Nest parasitoids

Out of the eight families that were collected, five families, *viz.*, Sarcophagidae, Tachinidae, Torymidae, Eulophidae, and Chrysididae, were most likely to be nest parasitoids, each represented by one species. These species and, more importantly, the potter wasp adults are all presumably well adapted to complete their development inside a potter wasp nest, and hence, it may be surprising that they were trapped within the nest. One possible explanation is that the occurrence of prey parasitized by *Copidosoma*, or other low-quality prey, led to the development of malnourished potter wasps, which were too small or not strong enough to break open the nest cell. This could potentially also be true for some of the other trapped nest parasitoids. Another possibility could be that the extreme desert conditions, such as exceptionally high temperatures or extremely dry conditions, occurring in this region, caused insect death inside the nests.

Miltogramminae (Diptera, Sarcophagidae) are primarily kleptoparasites of wasps and bees (Spofford et al. 1989; Pape 1996). The host range of Miltogramminae is wide, including many families of wasps (Crabronidae, Pompilidae, Sphecidae, and Vespidae) and bees belonging to the families Andrenidae, Apidae, Colletidae, and Halictidae. Some Miltogramminae were reported to parasitize Orthoptera and Diptera, and some invade termite and ant nests as well (Thompson and Love 1979; Verves 1979; Pape 1987; Spoford and Kurczewski 1990; O'Neill 2001; Pape 2006; Evans and O'Neill 2007; Polidori et al. 2009; Sinha 2012; Polidori 2017). The current study adds *D. dimidiatipenne* as a newly discovered host of Miltogramminae (Fig. 1b).

Usually, Miltogramminae are termed “satellite flies” as they wait on perching sites close to the entrance of a host’s nest for a nest-returning host female and then follow it, in flight, at a fixed distance behind. Some Miltogramminae are termed “hole searchers” as they patrol the host’s nesting site and enter the host’s nest, and some are dubbed “stalkers” as they enter the host’s nest after having detected the female host entering it (Newcomer 1930; Ristich 1956; Alcock 2000; Polidori et al. 2022). However, we cannot determine the behavior of the collected species as we did not directly observe them and were unable to identify them beyond subfamily level.

Future research based on host-parasitoid rearing can shed more light on factors causing different parasitoid species’ emergence failure, their developmental nutritional requirements, and their ability to break open the nest successfully.

Acknowledgements

We thank Ofir Altstein, Ishai Hoffman, and Tamar Sinai, the enthusiastic technicians from the Mitrani Department of Desert Ecology, for their help during the field trips.

We also thank the taxonomists from the Steinhardt Museum of Natural History for all their assistance in identifying/confirming the identity of the specimens: Gideon Pisanty (for Braconidae), Wolf Kuslitzky (for Ichneumonidae), Ariel Leib Friedman (for Sarcophagidae and Tachinidae), Sergei Zonstein (for Chrysididae), Miriam Kishinevsky (for Encyrtidae and Torymidae), and Zoya Yefremova (for Eulophidae). Our thanks are due to Prof. Yael Lubin, Dr. Efrat Gavish-Regev, Dr. Monica Mowery, and Valeria Arabesky for their moral support and comments on this manuscript.

References

- Abarca FM, Mundaca EA, Vargas HA (2012) First remarks on the nesting biology of *Hypodynerus andeus* (Packard) (Hymenoptera, Vespidae, Eumeninae) in the Azapa valley, northern Chile. *Revista Brasileira de Entomologia* 56(2): 240–243. <https://doi.org/10.1590/S0085-56262012005000033>
- Ahmed MK (1950) The External Morphology and Biology of *Barylypa rufa* Holmgren (Hymenoptera: Ichneumonidae). Doctoral dissertation, Fouad 1st University, Giza.
- Alcock J (2000) The natural history of a miltogrammine fly, *Miltogramma rectangularis* (Diptera: Sarcophagidae). *Journal of the Kansas Entomological Society* 73(4): 208–219.
- Alon A, Kugler J (1989) Plants and animals of the land of Israel: an illustrated encyclopedia. Publishing House Society for Protection of Nature.
- Aparicio Y, Gabarra R, Arno J (2020) Interactions among *Myzus persicae*, predators and parasitoids may hamper biological control in Mediterranean peach orchards. *Entomologia Generalis* 40: 217–228. <https://doi.org/10.1127/entomologia/2020/0946>
- Auko TH, Trad BM, Silvestre R (2014) Five new associations of parasitoids in potter wasps (Vespidae, Eumeninae). *Revista Brasileira de Entomologia* 58: 376–378. <https://doi.org/10.1590/S0085-56262014005000004>
- Auko TH, Trad BM, Silvestre R (2015) Bird dropping masquerading of the nest by the potter wasp *Minixi suffusum* (Fox, 1899) (Hymenoptera: Vespidae: Eumeninae). *Tropical Zoology* 28(2): 56–65. <https://doi.org/10.1080/03946975.2015.1027103>
- Bank S, Sann M, Mayer C, Meusemann K, Donath A, Podsiadlowski L, Kozlov A, Petersen M, Krogmann L, Meier R, Rosa P (2017) Transcriptome and target DNA enrichment sequence data provide new insights into the phylogeny of vespid wasps (Hymenoptera: Aculeata: Vespidae). *Molecular Phylogenetics and Evolution* 116: 213–226. <https://doi.org/10.1016/j.ympev.2017.08.020>
- Belshaw R (1994) Life history characteristics of Tachinidae (Diptera) and their effect on polyphagy. In: Hawkins BA, Sheehan W (Eds) *Parasitoid community ecology*. Oxford University Press, Oxford, 145–162.
- Berland L, Bernard F (1938) Hyménoptères vespiformes. (Cleptidae, Chrysidae, Trigonalidae). *Faune de France* (Lechevalier, Paris, 1938) 34: 1–145.
- Boesi R, Polidori C, Tormos J, Bevacqua S, Asis JD, Andrietti F (2005) Trapnesting *Ancistrocers sikhimensis* (Hymenoptera: Eumenidae) in Nepal: Nest structure and associates

- (Hymenoptera: Chrysididae; Acarina: Saprogllyphidae). Florida Entomologist 88(2): 135–140. [https://doi.org/10.1653/0015-4040\(2005\)088\[0135:TASHEI\]2.0.CO;2](https://doi.org/10.1653/0015-4040(2005)088[0135:TASHEI]2.0.CO;2)
- Bohart GE, Parker FD, Tepedino VJ (1982) Notes on the biology of *Odynerus dilectus* [Hym.: Eumenidae], a predator of the alfalfa weevil, *Hypera postica* [Col.:Curculionidae]. Entomophaga 27: 23–31. <https://doi.org/10.1007/BF02371934>
- Broad GR (2011) Keys for the identification of British and Irish nocturnal Ichneumonidae. Natural History Museum, London, 1–42.
- Buschini MLT, Buss CE (2010) Biological aspects of different species of *Pachodynerus* (Hymenoptera; Vespidae; Eumeninae). Brazilian Journal of Biology 70(3): 623–629. <https://doi.org/10.1590/S1519-69842010000300020>
- Carpenter JM, Marques OM (2001) Contribuição ao estudo dos vespídeos do Brasil. Série publicações digitais, 3 pp.
- Evans HE (1966) The behavior patterns of solitary wasps. Annual Review of Entomology 11(1): 123–154. <https://doi.org/10.1146/annurev.en.11.010166.001011>
- Evans HE, O'Neill KM (2007) The sand wasps: Natural history and behavior. Harvard University Press, 360 pp. <https://doi.org/10.4159/9780674036611>
- Gauld ID (1988) A survey of the Ophioninae (Hymenoptera: Ichneumonidae) of tropical Mesoamerica with special reference to the fauna of Costa Rica. Bulletin of the British Museum, Natural History. Entomology 57(1): 1–309.
- Gess SK, Gess FW (2014) Wasps and bees in southern Africa, SANBI Biodiversity ser. 24, South African National Biodiversity Institute, Pretoria, 327 pp.
- Gonzalez JM, Teran JB, Matthews RW (2004) Review of the biology of *Melittobia acasta* (Walker) (Hymenoptera: Eulophidae) and additions on development and sex ratio of the species. Caribbean Journal of Science 40(1): 52–61.
- Grissell EE (2000) A revision of New World *Monodontomerus* Westwood (Hymenoptera: Chalcidoidea: Torymidae). Contributions of the American Entomological Institute 32(1): 1–90.
- Grissell EE (2007) Torymidae (Hymenoptera: Chalcidoidea) associated with bees (Apoidea), with a list of chalcidoid bee parasitoids. Journal of Hymenoptera Research 16(2): 234–265.
- Hamzavi F, Carpenter JM, Ting-Jing L (2019) A contribution to the study of Eumeninae (Hymenoptera, Vespidae) in South-Eastern Iran. Journal of Insect Biodiversity and Systematics 5(4): 393–398. <https://doi.org/10.52547/jibs.5.4.393>
- Hanson PE, Gauld ID (1995) The Hymenoptera of Costa Rica (Vol. 1). Oxford University Press, Oxford, 893 pp.
- Hermes MG, Somavilla A, Garcete-Barrett BR (2013) On the nesting biology of *Pirhosigma Giordani Soika* (Hymenoptera, Vespidae, Eumeninae), with special reference to the use of vegetable matter. Revista Brasileira de Entomologia 57: 433–436. <https://doi.org/10.1590/S0085-56262013005000044>
- Hervet VAD, Murillo H, Fernández-Triana JL, Shaw MR, Laird RA, Floate KD (2014) First report of *Cotesia vanessae* (Hymenoptera: Braconidae) in North America. The Canadian Entomologist 146(5): 560–566. <https://doi.org/10.4039/tce.2014.9>
- Huddleston T, Walker AK (1988) *Cardiochiles* (Hymenoptera: Braconidae), a parasitoid of lepidopterous larvae, in the Sahel of Africa, with a review of the biology and host relationships

- of the genus. *Bulletin of Entomological Research* 78(3): 435–461. <https://doi.org/10.1017/S0007485300013201>
- Hunt JH, Buck NA, Wheeler DA (2003) Storage proteins in vespid wasps: characterization, developmental pattern, and occurrence in adults. *Journal of Insect Physiology* 49: 785–794. [https://doi.org/10.1016/S0022-1910\(03\)00115-X](https://doi.org/10.1016/S0022-1910(03)00115-X)
- Jennings DT, Houseweart MW (1984) Predation by eumenid wasps (Hymenoptera: Eumenidae) on spruce budworm (Lepidoptera: Tortricidae) and other lepidopterous larvae in spruce-fir forests of Maine. *Annals of the Entomological Society of America* 77(1): 39–45. <https://doi.org/10.1093/aesa/77.1.39>
- Jourdie V, Alvarez N, Turlings TC (2008) Identification of seven species of hymenopteran parasitoids of *Spodoptera frugiperda*, using polymerase chain reaction amplification and restriction enzyme digestion. *Agricultural and Forest Entomology* 10(2): 129–136. <https://doi.org/10.1111/j.1461-9563.2008.00362.x>
- Júnior PAS, Gonring AHR, Picanço MC, Ramos RS, Martins JC, Ferreira DO (2012) Natural biological control of *Diaphania* spp. (Lepidoptera: Crambidae) by social wasps. *Sociobiology* 59(2): 561–572. <https://doi.org/10.13102/sociobiology.v59i2.618>
- Korb J, Linsenmair KE (1999) The architecture of termite mounds: a result of a trade-off between thermoregulation and gas exchange? *Behavioral Ecology* 10(3): 312–316. <https://doi.org/10.1093/beheco/10.3.312>
- Krombein KV, Hurd PD, Smith DR, Burks BD (1979) *Catalog of Hymenoptera in America north of Mexico* (Vol. 1). Smithsonian Institution Press, Washington, 1199–2209. <https://doi.org/10.5962/bhl.title.5074>
- Leduc S, Rosenberg T, Johnson AD, Segoli M (2022) Nest provisioning with parasitized caterpillars by female potter wasps: costs and potential mechanisms. *Animal Behaviour* 188: 99–109. <https://doi.org/10.1016/j.anbehav.2022.03.020>
- Liu MH, Blamires SJ, Liao CP, Tso IM (2014) Evidence of bird dropping masquerading by a spider to avoid predators. *Scientific Reports* 4: 1–5. <https://doi.org/10.1038/srep05058>
- Martynova KV (2020) Cocoons of cuckoo wasps (Hymenoptera: Chrysididae): First overview of morphology reveals unexpected traces of taxonomy. *Zoologischer Anzeiger* 285: 122–138. <https://doi.org/10.1016/j.jcz.2020.02.002>
- Matthews JR, Matthews RW (2018) Nesting biology of an Australian potter wasp, *Delta latreillei* (Saussure) (Hymenoptera: Vespidae: Eumeninae). *The Australian Entomologist* 45(1): 93–104.
- Matthews RW, González JM (2004) Nesting biology of *Zeta argillaceum* (Hymenoptera: Vespidae: Eumeninae) in southern Florida, US. *Florida Entomologist* 87(1): 37–40. [https://doi.org/10.1653/0015-4040\(2004\)087\[0037:NBOZAH\]2.0.CO;2](https://doi.org/10.1653/0015-4040(2004)087[0037:NBOZAH]2.0.CO;2)
- Newcomer EJ (1930) Notes on the habits of a digger wasp and its inquiline flies. *Annals of the Entomological Society of America* 23(3): 552–563. <https://doi.org/10.1093/aesa/23.3.552>
- O'Neill KM (2001) *Solitary Wasps: Natural History and Behavior*. Cornell University Press, 424 pp. <https://doi.org/10.7591/9781501737367>
- Pannure A, Belavadi VV, Carpenter JM (2016) Taxonomic studies on potter wasps (Hymenoptera: Vespidae: Eumeninae) of south India. *Zootaxa* 4171(1): 1–50. <https://doi.org/10.11646/zootaxa.4171.1.1>

- Pape T (1987) The Sarcophagidae (Diptera) of Fennoscandia and Denmark. *Fauna Entomologica Scandinavica* 19: 1–203. <https://doi.org/10.1163/9789004273436>
- Pape T (1996) Catalogue of the Sarcophagidae of the world (Insecta: Diptera), *Memoirs of Entomology*. Associated Publishers 8, 1–558.
- Pape T (2006) A new species of *Hoplcephala* Macquart (Diptera: Sarcophagidae) from Namibia, with a discussion of generic monophyly. *Zootaxa* 1183: 57–68. <https://doi.org/10.11646/zootaxa.1183.1.4>
- Perier JD, Haseeb M, Kanga LHB, Meagher RL, Legaspi JC (2022) Intraguild interactions of three biological control agents of the fall armyworm *Spodoptera frugiperda* (JE Smith) in Florida. *Insects* 13: 815. <https://doi.org/10.3390/insects13090815>
- Pickett KM, Carpenter JM (2010) Simultaneous analysis and the origin of eusociality in the Vespidae (Insecta: Hymenoptera). *Arthropod Systematics & Phylogeny* 68(1): 3–33. <https://doi.org/10.3897/asp.68.e31707>
- Polidori C (2017) Interactions between the social digger wasp, *Cerceris rubida*, and its brood parasitic flies at a Mediterranean nest aggregation. *Journal of Insect Behaviour* 30: 86–102. <https://doi.org/10.1007/s10905-017-9601-9>
- Polidori C, Ouadrageou M, Gadallah N, Andrietti F (2009) Potential role of evasive fights and nest closures in an African sand wasp, *Bembix* sp. near *capensis* Lepeletier 1845 (Hymenoptera Crabronidae), against a parasitic satellite fly. *Tropical Zoology* 22: 1–14.
- Polidori C, Piwczynski M, Ronchetti F, Johnston NP, Szpila K (2022) Host-trailing satellite flight behaviour is associated with greater investment in peripheral visual sensory system in miltogrammine flies. *Scientific Reports* 12(1): 1–17. <https://doi.org/10.1038/s41598-022-06704-8>
- Prezoto F, Ribeiro Júnior C, Cortes SAO, Elisei T (2007) Manejo de vespas e marimbondos em ambiente urbano. In: Pinto AS, Rossi MM, Salmeron E (Eds) *Manejo de Pragas Urbanas*, 123–126.
- Rafi MA, Carpenter JM, Qasim M, Shehzad A, Zia A, Khan MR, Mastoi MI, Naz F, Yas M, Shah M, Bhati AR (2017) The vespidae fauna of Pakistan. *Zootaxa* 4362(1): 1–28. <https://doi.org/10.11646/zootaxa.4362.1.1>
- Reardon RC, Statler MW, McLane WH (1973) Rearing techniques and biology of five gypsy moth parasites. *Environmental Entomology* 2(1): 124–127. <https://doi.org/10.1093/ee/2.1.124>
- Ristich SS (1956) The host relationship of a Miltogrammid fly *Senotainia trilineata* (V&W). *Ohio Journal of Science* 56: 271–274.
- Segoli M, Leduc S, Meng F, Hoffmann I, Kishinevsky M, Rozenberg T (2020) Frequency and consequences of the collection of already parasitized caterpillars by a potter wasp. *Scientific Reports* 10(1): 1–9. <https://doi.org/10.1038/s41598-020-65096-9>
- Sinha SK (2012) Report of some satellite flies (Diptera, Miltogramminae) in West Bengal, India, for the first time. North Bengal University. *Journal of Animal Science* 6: 1–7.
- Spofford MG, Kurczewski FE, Downes Jr WL (1989) Nearctic species of Miltogrammini (Diptera: Sarcophagidae) associated with species of Aculeata (Hymenoptera: Vespoidea, Pompiloidea, Sphecoidea, Apoidea). *Journal of the Kansas Entomological Society* 254–267.

- Spoford MG, Kurczewski FE (1990) Comparative larvipositional behaviors and cleptoparasitic frequencies of Nearctic species of Miltogrammini (Diptera, Sarcophagidae). *Journal of Natural History* 24: 731–755. <https://doi.org/10.1080/00222939000770511>
- Takasu K, Lewis WJ (1995) Importance of adult food sources to host searching of the larval parasitoid *Microplitis croceipes*. *Biological Control* 5(1): 25–30. <https://doi.org/10.1006/bcon.1995.1003>
- Tan JL, Carpenter JM, van Achterberg C (2018) Most northern Oriental distribution of *Zethus* Fabricius (Hymenoptera, Vespidae, Eumeninae), with a new species from China. *Journal of Hymenoptera Research* 62: 1–13. <https://doi.org/10.3897/jhr.62.23196>
- Townes H (1965) A catalogue and reclassification of the eastern Palearctic Ichneumonidae. *Mem American Entomological Institute* 5: 1–660.
- Tscharntke T, Gathmann A, Steffan-Dewenter I (1998) Bioindication using trap-nesting bees and wasps and their natural enemies: community structure and interactions. *Journal of Applied Ecology* 35(5): 708–719. <https://doi.org/10.1046/j.1365-2664.1998.355343.x>
- Udayakumar A, Aravindaram K, Shivalingaswamy TM (2022) Nesting and predatory behaviour of potter wasp, *Rhynchium brunneum brunneum* (Eumeninae: Vespidae: Hymenoptera) in an urban farm landscape. *Biocontrol Science and Technology* 32(7): 794–810. <https://doi.org/10.1080/09583157.2022.2047612>
- van Achterberg C (1990a) Illustrated key to the subfamilies of the Holarctic Braconidae (Hymenoptera: Ichneumonoidea). *Zoologische Mededelingen* 64(1): 1–20.
- van Achterberg C (1990b) Revision of the western Palaeartic Phanerotomini (Hymenoptera: Braconidae). *Zoologische Verhandelingen* 255(1): 1–106.
- Verves YG (1979) A review of the subfamily Miltogrammatinae (Diptera, Sarcophagidae) in Sri Lanka. *Entomologicheskoe obozrenie* 58: 883–897.
- West-Eberhard MJ, Carpenter JM, Hanson PE (1995) The vespidae wasps (Vespidae). In: Hanson PE, Gauld ID (Eds) *The Hymenoptera of Costa Rica* Oxford, Oxford Science Publications, The Natural History Museum, 561–587.
- Yeates DK, Greathead D (1997) The evolutionary pattern of host use in the Bombyliidae (Diptera): a diverse family of parasitoid flies. *Biological Journal of the Linnean Society* 60(2): 149–185. <https://doi.org/10.1111/j.1095-8312.1997.tb01490.x>

First record of the pine sawfly *Neodiprion warreni* (Hymenoptera, Diprionidae) in the state of Tennessee and on *Pinus virginiana*

Ryan D. Ridenbaugh^{1*}, Ashleigh N. Glover^{1*}, Catherine R. Linnen¹

¹ Department of Biology, University of Kentucky, 675 Rose St., Lexington, KY 40506, USA

Corresponding authors: Ryan D. Ridenbaugh (rdri228@uky.edu); Ashleigh N. Glover (angl226@uky.edu)

Academic editor: Marko Prous | Received 7 September 2023 | Accepted 11 October 2023 | Published 6 November 2023

<https://zoobank.org/C3D5DEF4-8555-4168-8218-3EF565C527B5>

Citation: Ridenbaugh RD, Glover AN, Linnen CR (2023) First record of the pine sawfly *Neodiprion warreni* (Hymenoptera, Diprionidae) in the state of Tennessee and on *Pinus virginiana*. Journal of Hymenoptera Research 96: 937–947. <https://doi.org/10.3897/jhr.96.112395>

Abstract

Pine sawflies in the genus *Neodiprion* Rohwer are widely distributed across the Northern Hemisphere and are pests of commercially important conifer trees. While sampling for *Neodiprion* species in eastern North America, two colonies of *Neodiprion warreni* Ross were discovered in Tennessee feeding on *Pinus virginiana* Mill. These are the first records of *N. warreni* in Tennessee and on the host *P. virginiana*. Here, we use a combination of larval and adult female morphology to confirm species identification. We also discuss two potential explanations for these observations: *N. warreni* was always present in Tennessee and feeding on *P. virginiana* but, until now, has gone unreported or these new records are attributable to a recent range expansion and host shift. We also discuss potential economic and evolutionary implications of range expansions and host shifts in plant-feeding insect pest species.

Keywords

Distribution, *Neodiprion*, new host, new record

* These authors contributed equally to this work.

Introduction

Pine sawflies in the genus *Neodiprion* Rohwer, 1918 (Hymenoptera, Diprionidae) are pests of pine trees and other conifers of commercial importance (Coppel and Benjamin 1965; Welch 1991; Darr et al. 2022; Davis et al. 2023). This genus consists of 50 species that, collectively, are widely distributed across the Northern Hemisphere and are found on a wide variety of conifer hosts in the family Pinaceae (Coppel and Benjamin 1965; Taeger et al. 2018; Davis et al. 2023). All parts of the *Neodiprion* life cycle are dependent upon their coniferous hosts. The adults meet and mate on the host. The mated female then uses her saw-like ovipositor to carve pockets into the needle tissue, where she deposits her eggs. The eggs develop in the needle tissue, hatch, and feed on the needles. After undergoing several molts, the larvae spin a fibrous cocoon either on or near the host tree. Inside the cocoon, pupation occurs, and the adult emerges from the cocoon to repeat the cycle (Dixon 2004). Although the sequence of life cycle events is the same for all *Neodiprion* species, there is variation among species in details for each stage of the life cycle that have implications for pest status (Davis et al. 2023). For example, species that spend the winter months as prepupae in cocoons and that tend to have multiple generations per year cause more damage to their hosts than species that spend the winter months as eggs in the needle tissue and that have only one generation per year (Kulman 1971; Lyytikäinen-Saarenmaa and Tomppo 2002).

Neodiprion warreni Ross, 1961 is a cocoon-overwintering pine sawfly that tends to have multiple generations per year (Wilkinson 1968; Dixon 2004). The previously published distribution of *N. warreni* includes Florida, Louisiana, Arkansas, and Georgia (Ross 1961; Wilkinson 1968; Baker 1972; Smith 1979; Linnen and Farrell 2007, 2010). Previously reported hosts of *N. warreni* include *Pinus echinata* Mill., *Pinus glabra* Walt., *Pinus clausa* (Chapm. ex Engelm.) Vasey ex Sarg., and *Pinus taeda* L. (Ross 1961; Wilkinson 1968; Baker 1972; Smith 1979; Dixon 2004; Linnen and Farrell 2007, 2010), with one recorded outbreak on *P. echinata* in Union County, Arkansas in 1957 (Warren 1958). Here, we provide the first verified records of *N. warreni* in the state of Tennessee, the furthest northeast this species has been recorded, and on *Pinus virginiana* Mill., a newly reported host for this species. These new records could represent new information on an understudied species or could represent evidence of a recent range expansion and host shift. Thus, we also discuss potential implications of range expansions and host shifts.

Methods

Collection and species identification

On September 13, 2022, two separate colonies of *N. warreni* were found in Tennessee by authors ANG and RDR. The first colony of approximately 30–50 mid-late instars was found in Knoxville, Tennessee (36.0050, -83.7782) and was assigned the colony ID “AG170”. The second colony of approximately 15 early-mid instars was found in Crossville, Tennessee (35.9293, -84.9127) and was assigned the colony ID “AG171”. Colony

AG170 was preliminarily identified in the field as *N. warreni* based on larval pigmentation and photographed using an Apple iPhone X (Fig. 1). Because complete larval pigmentation pattern was not yet developed, a preliminary species identification of colony AG171 was not made in the field. Both colonies were determined to be feeding on mature *P. virginiana* based on needle and bark morphology (Petrides and Wehr 1998). To confirm species identity, both colonies were collected and brought back to the lab by clipping the branch containing the feeding larval colony and placing the clipping in a labeled paper bag.

To confirm the species identity of both colonies, we first photographed a single larva from colony AG170 using a Canon EOS Rebel T6 with a Canon EF 100 mm Macro lens (Fig. 2A, B) and used a *Neodiprion* key based on larval morphology (Davis et al.



Figure 1. *Neodiprion warreni* colony feeding on *Pinus virginiana*. A *Neodiprion warreni* Ross colony (colony ID: AG170) found in Knoxville, Tennessee feeding on a *Pinus virginiana* Mill. tree.

2023). We later used this key to confirm colony AG171 as *N. warreni* on September 22, 2022, once larvae had developed a diagnostic pigmentation pattern. Because adult female coloration and ovipositor morphology is also diagnostic (Ross 1961), we also reared the larvae of both colonies to adulthood using standard lab protocols (Harper et al. 2016; Bendall et al. 2017). Upon emergence from their cocoons, a single adult female from colony AG170 was photographed using a Canon EOS Rebel T6 with a Canon EF 100 mm Macro lens (Fig. 3A, B). From the AG170 colony two adult females and one male were preserved in 100% ethanol for pinning and ovipositor mounting. An ovipositor was dissected from one of the females, mounted, and photographed using a Zeiss DiscoveryV8 stereomicroscope with an Axiocam 105 color camera and ZEN lite 2012 Software (Carl Zeiss Microscopy, LLC Thornwood, NY) after Bendall et al. (2017). The AG171 colony was heavily parasitized and as such we were unable to rear *Neodiprion* adults for preservation. All pinned specimens are stored at the University of Kentucky (UKIC).



Figure 2. *Neodiprion warreni* larva. The lateral (A) and dorsal (B) view of a *Neodiprion warreni* Ross larva (colony ID: AG170) collected from Knoxville, Tennessee.

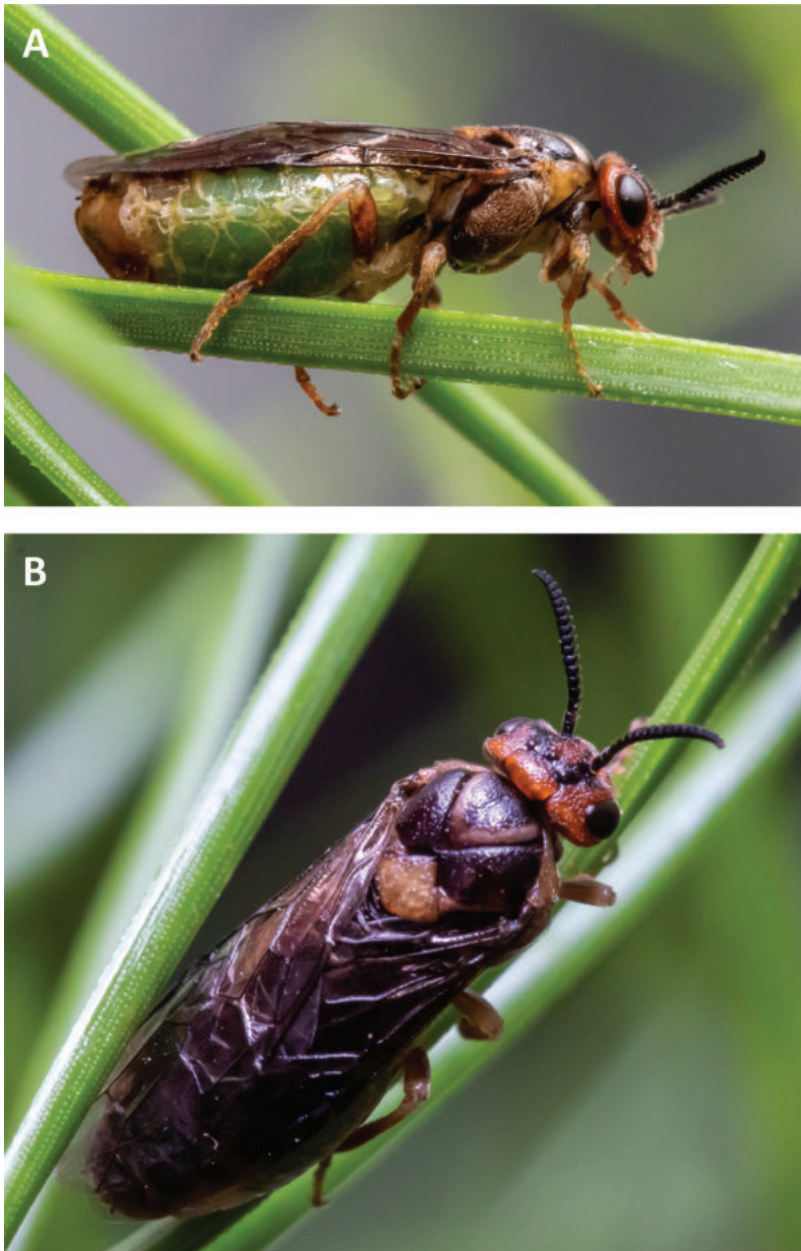


Figure 3. *Neodiprion warreni* adult female. The lateral (A) and dorsal (B) view of an adult *Neodiprion warreni* Ross female collected from Knoxville, Tennessee (colony ID: AG170).

Material deposited

Female (UKIC), “36.00496, -83.77818, 13-Sep-22, Knoxville, TN”; “AG170 ♀, NW23-V001, Ovipositor A”; “*Neodiprion warreni*, col. on *Pinus virginiana*, det. Ashleigh Glover”, “UKIC_0056864”. Female (UKIC) “36.00496, -83.77818, 13-

Sep-22, Knoxville, TN”; “AG170 ♀, NW23-V002”; “*Neodiprion warreni*, col. on *Pinus virginiana*, det. Ashleigh Glover”, “UKIC_0056813”. Male (UKIC), “36.00496, -83.77818, 13-Sep-22, Knoxville, TN”; “AG170 ♂, *N. warreni*; “*Neodiprion warreni*, col. on *Pinus virginiana*, det. Ashleigh Glover”, “UKIC_0056720”. Mounted Ovipositor (UKIC), “AG170, *Neodiprion warreni*, saw”, “RDR, 06/06/23, A”.

Neodiprion warreni distribution

To describe the current known distribution of *N. warreni*, we searched for the locations of all recorded *N. warreni* observations. These records were obtained from museum specimens (Linnen and Farrell 2010), research grade observations from iNaturalist (inaturalist.org), and our own collections (including the two new records above). The distribution map was created using the ggplot2 package (Wickham 2016) in R version 4.1.0 (R Core Team 2021). We also plotted the native range of *P. virginiana* on the map using the sf package (Pebesma 2018) to visualize the potential for further *N. warreni* range expansion. The *P. virginiana* shape files were downloaded from the USGS (<https://web.archive.org/web/20170127093428/https://gec.cr.usgs.gov/data/little/>).

Results

Using a *Neodiprion* key based on larval morphology (Davis et al. 2023), we confirmed that the two colonies collected on September 13, 2022 in Tennessee are *N. warreni*. Briefly, the larvae have a pale body, a completely black head, two black dorsal stripes, a row of thick black spots along each lateral side of the body that appear to bleed together, a black line above the prolegs, and a distinct black marking on the dorsal side of the last body segment (Fig. 2A, B). Additionally, adult female coloration and ovipositor morphology, as described by Ross (1961), further confirm that colony AG170 is *N. warreni*. The females are generally brownish in color, with an orange brown head (except for the eyes and antennae, which are black), a thorax that is a slightly paler brown with some darker areas on the dorsal side, an abdomen that contains some blackish areas and is greenish on the lateral side, and legs that are primarily light brown with a lighter straw coloration at the basal part of the tibiae (Fig. 3A, B). Finally, the ovipositors have unusually long and narrow lancets as well as numerous saw teeth that are unusually small, especially on annuli 2, 3, and 4 (Fig. 4), characteristics that are unlike other species in the *Neodiprion virginianus* complex to which this species belongs (Ross 1961).

Neodiprion warreni was previously reported as being distributed only in the southernmost parts of the United States (Georgia, Arkansas, Louisiana, and Florida; Ross 1961; Wilkinson 1968; Baker 1972; Smith 1979; Dixon 2004; Linnen and Farrell 2007, 2010). However, our collections in Tennessee provide evidence that the range of *N. warreni* extends further north than previously known (Fig. 5). Our Tennessee collections also provide evidence of a wider host range than has been reported: these collections are the first recorded occurrences of *N. warreni* using *P. virginiana* as a host.

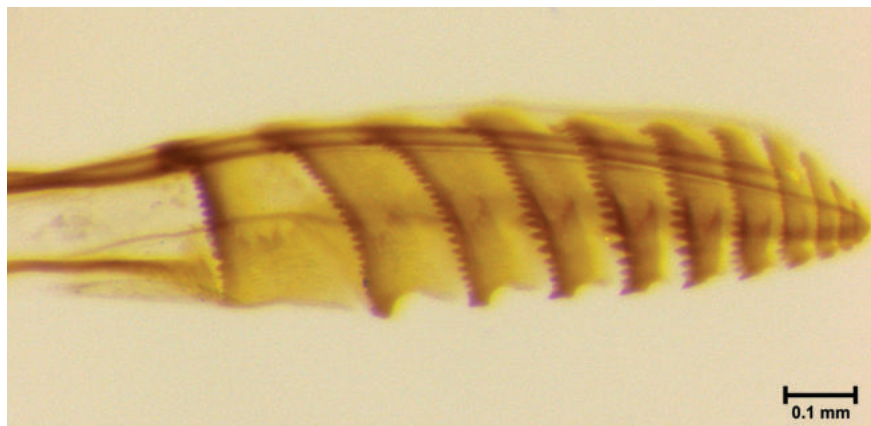


Figure 4. *Neodiprion warreni* female ovipositor. A mounted ovipositor from *Neodiprion warreni* Ross adult female individual “UKIC_0056864” (colony AG170) collected from Knoxville, Tennessee.

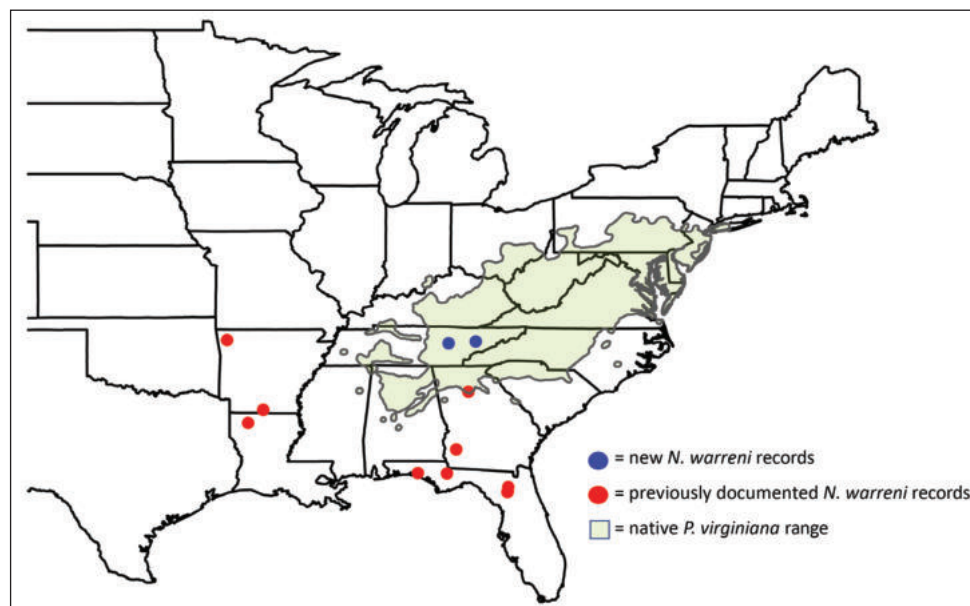


Figure 5. Currently known *Neodiprion warreni* distribution and native *Pinus virginiana* range. All recorded locations of *Neodiprion warreni* Ross observations in the eastern United States. Previously reported *N. warreni* observations are in red and the new recorded observations of *N. warreni* in this report are in blue. The native range of *Pinus virginiana* Mill. (newly reported host of *N. warreni*) is shown in green.

Discussion

With the documentation of our new *N. warreni* records, two possibilities arise. One possibility is that *N. warreni* has always been present in Tennessee and feeding on *P. virginiana* but has gone unreported until now. Thus, our new records enhance our knowledge of the

geographical and host range of an understudied species. Alternatively, our new records may be evidence of a recent range expansion and host shift for *N. warreni*. Currently, we do not have enough data to distinguish between these two possibilities. In general, range expansions of many organisms are becoming more common as humans continue to modify the environment. These range expansions can have important impacts on insect pest species, such as the ability for insect pest species to hybridize upon secondary contact (Grabenstein and Taylor 2018; Larson et al. 2019; Ottenburghs 2021). One potential outcome of hybridization is adaptive introgression, or the exchange of genetic material between lineages via backcrossing that confers an adaptive advantage (Payseur 2010; Pfennig et al. 2016). If hybridization results in adaptive introgression, pest population dynamics can quickly change so that they evade established integrative pest management strategies (Correa et al. 2019). It is currently unknown whether *N. warreni* is expanding its range and whether this will lead to hybridization between *N. warreni* and other *Neodiprion* species that they come into secondary contact with. However, in no-choice mating assays performed in the lab, *Neodiprion virginiana* Rowher males mated with *N. warreni* females (Glover and Linnen, unpublished data). Interestingly, Tennessee and North Carolina comprise the southernmost part of *N. virginiana*'s published range (Smith 1979; Dixon 2004). Thus, our finding of *N. warreni*'s presence in Tennessee is notable because it verifies that *N. warreni* and *N. virginiana* co-occur, providing an opportunity for hybridization between these two species in nature.

Another important finding of our Tennessee *N. warreni* collections is their use of *P. virginiana* as hosts. This finding can have important economic and evolutionary implications. From an economic perspective, *N. warreni* now represents another potential pest species of *P. virginiana*, which has commercial value as Christmas trees (Belanger and Bramlett 1975). Because *N. warreni* is a cocoon-overwintering species with the potential to have multiple generations per year (Wilkinson 1968; Dixon 2004), large, destructive outbreaks are possible (Kulman 1971). Thus, identification of this new *P. virginiana* insect pest is important for effective management. From an evolutionary perspective, host shifts have initiated speciation in several plant-feeding insect systems (Bush 1975; Berlocher and Feder 2002; Drès and Mallet 2002; Matsubayashi et al. 2010). When plant-feeding insects rely on their host plant for most or all of their life cycle (as is the case for *Neodiprion*), colonization of a new host plant can result in strong selection on traits required to utilize the new host (Forbes et al. 2017). If different traits are favored on different hosts, reproductive isolation can rapidly evolve between host-associated populations (Glover et al. 2023). It is unknown whether the finding of *N. warreni* on *P. virginiana* indicates a host shift, and if so, whether the shift onto *P. virginiana* will result in a speciation event in *N. warreni*. However, this finding of *N. warreni* on a newly reported host provides another opportunity to study the relationship between plant-feeding insects and their hosts. This information can help shed light on why plant-feeding insects are so unusually diverse (Mitter et al. 1988; Farrell 1998; Wiens et al. 2015; Vertacnik and Linnen 2017).

While more work is needed to determine the consequences of broader geographical and host ranges in *N. warreni*, the first step is knowledge of these ranges. In this regard,

community involvement, such as via recording observations of *N. warreni* and its hosts on iNaturalist (inaturalist.org), is valuable for facilitating the documentation of current and changing distributions of *N. warreni* and other *Neodiprion* species. Notably, only one record on iNaturalist of *N. warreni* exists to date, and this observation was recorded by the authors in 2019. Therefore, this report provides a valuable foundation for future work to investigate the possibility and consequences of *N. warreni* range expansions and host shifts.

Acknowledgments

The author order was decided through a handicapping competition of five races at Churchill Downs the weekend of the 2023 Kentucky Derby and Oaks. The result of that competition is as follows: In the Grade 2 Edgewood Stakes Papilio (ANG) finished 4th, six lengths ahead of Preliminary (RDR) who finished 11th; In the Grade 1 Kentucky Oaks Pretty Mischievous (ANG) finished 1st, three lengths ahead of Wet Paint (RDR) who finished 4th; In the Grade 2 Pat Day Mile Stakes Echo Again (RDR) finished 6th beating Kangaroo Court (ANG) by twelve lengths, who finished 11th; In the Grade 2 American Turf Stakes Major Dude (RDR) finished 3rd ahead of Mo Stash (ANG) in 4th by a length; and in the Grade 1 Kentucky Derby Angel of Empire (RDR) finished in 3rd, beating 7th place Tapit Trice (ANG) by seven and three quarter lengths. ANG and RDR wish to thank the equine and human athletes who helped us decide which author was to be listed first. We would also like to thank members of the Linnen lab for help with insect rearing.

This work was funded by a USDA National Institute of Food and Agriculture Predoctoral Fellowship (2021-09497) to ANG and the National Science Foundation DEB-CAREER-1750946 to CRL.

References

- Baker WL (1972) Eastern forest insects, vol 116. US Forest Service. <https://doi.org/10.5962/bhl.title.65893>
- Belanger RP, Bramlett DL (1975) Virginia pine as a Christmas tree, vol 223. US Department of Agriculture, Forest Service, Southeastern Forest Experiment Station.
- Bendall EE, Vertacnik KL, Linnen CR (2017) Oviposition traits generate extrinsic postzygotic isolation between two pine sawfly species. *BMC Evolutionary Biology* 17(1): 26. <https://doi.org/10.1186/s12862-017-0872-8>
- Berlocher SH, Feder JL (2002) Sympatric speciation in phytophagous insects: Moving beyond controversy? *Annual Review of Entomology* 47(1): 773–815. <https://doi.org/10.1146/annurev.ento.47.091201.145312>
- Bush GL (1975) Modes of animal speciation. *Annual Review of Ecology and Systematics* 6: 339–364. <https://doi.org/10.1146/annurev.es.06.110175.002011>
- Coppel H, Benjamin DM (1965) Bionomics of Nearctic pine-feeding diprionids. *Annual Review of Entomology* 10(1): 69–96. <https://doi.org/10.1146/annurev.en.10.010165.000441>

- Correa AS, Cordeiro EMG, Omoto C (2019) Agricultural insect hybridization and implications for pest management. *Pest Management Science* 75(11): 2857–2864. <https://doi.org/10.1002/ps.5495>
- Darr MN, Coyle DR, Jetton RM (2022) Arthropod and disease management in Fraser fir (Pinales: Pinaceae) Christmas trees in the southeastern United States. *Journal of Integrated Pest Management* 13(1): 8. <https://doi.org/10.1093/jipm/pmac001>
- Davis JS, Glover AN, Everson KM, Coyle DR, Linnen CR (2023) Identification, biology, and management of conifer sawflies (Hymenoptera: Diprioninae) in eastern North America. *Journal of Integrated Pest Management* 14(1): 1–16. <https://doi.org/10.1093/jipm/pmad011>
- Dixon WN (2004) Pine sawfly larvae, *Neodiprion* spp. (Insecta: Hymenoptera: Diprionidae). University of Florida IFAS Extension.
- Drès M, Mallet J (2002) Host races in plant-feeding insects and their importance in sympatric speciation. *Philosophical Transactions of the Royal Society B: Biological Sciences* 357(1420): 471–492. <https://doi.org/10.1098/rstb.2002.1059>
- Farrell B (1998) “Inordinate Fondness” explained: why are there so many beetles? *Science* 281(5376): 555–559. <https://doi.org/10.1126/science.281.5376.555>
- Forbes AA, Devine SN, Hippee AC, Tvedte ES, Ward AKG, Widmayer HA, Wilson CJ (2017) Revisiting the particular role of host shifts in initiating insect speciation. *Evolution* 71(5): 1126–1137. <https://doi.org/10.1111/evo.13164>
- Glover AN, Bendall EE, Terbot II JW, Payne N, Webb A, Filbeck A, Norman G, Linnen CR (2023) Body size as a magic trait in two plant-feeding insect species. *Evolution* 77(2): 437–453. <https://doi.org/10.1093/evolut/qpac053>
- Grabenstein KC, Taylor SA (2018) Breaking barriers: causes, consequences, and experimental utility of human-mediated hybridization. *Trends in Ecology & Evolution* 33(3): 198–212. <https://doi.org/10.1016/j.tree.2017.12.008>
- Harper KE, Bagley RK, Thompson KL, Linnen CR (2016) Complementary sex determination, inbreeding depression and inbreeding avoidance in a gregarious sawfly. *Heredity* 117(5): 326–335. <https://doi.org/10.1038/hdy.2016.46>
- Kulman HM (1971) Effects of insect defoliation on growth and mortality of trees. *Annual Review of Entomology* 16(1): 289–324. <https://doi.org/10.1146/annurev.en.16.010171.001445>
- Larson EL, Tinghitella RM, Taylor SA (2019) Insect hybridization and climate change. *Frontiers in Ecology and Evolution* 7: 348. <https://doi.org/10.3389/fevo.2019.00348>
- Linnen CR, Farrell BD (2007) Mitonuclear discordance is caused by rampant mitochondrial introgression in *Neodiprion* (Hymenoptera: Diprionidae) sawflies. *Evolution* 61(6): 1417–1438. <https://doi.org/10.1111/j.1558-5646.2007.00114.x>
- Linnen CR, Farrell BD (2010) A test of the sympatric host race formation hypothesis in *Neodiprion* (Hymenoptera: Diprionidae). *Proceedings of the Royal Society B Biological Sciences* 277(1697): 3131–3138. <https://doi.org/10.1098/rspb.2010.0577>
- Lyytikäinen-Saarenmaa P, Tomppo E (2002) Impact of sawfly defoliation on growth of Scots pine *Pinus sylvestris* (Pinaceae) and associated economic losses. *Bulletin of Entomological Research* 92(2): 137–140. <https://doi.org/10.1079/BER2002154>

- Matsubayashi KW, Ohshima I, Nosil P (2010) Ecological speciation in phytophagous insects. *Entomologia Experimentalis et Applicata* 134(1): 1–27. <https://doi.org/10.1111/j.1570-7458.2009.00916.x>
- Mitter C, Farrell B, Wiegmann B (1988) The phylogenetic study of adaptive zones: has phytophagy promoted insect diversification? *The American Naturalist* 132(1): 107–128. <https://doi.org/10.1086/284840>
- Ottenburghs J (2021) The genic view of hybridization in the Anthropocene. *Evolutionary Applications* 14(10): 2342–2360. <https://doi.org/10.1111/eva.13223>
- Payseur BA (2010) Using differential introgression in hybrid zones to identify genomic regions involved in speciation. *Molecular Biology Resources* 10(5): 806–820. <https://doi.org/10.1111/j.1755-0998.2010.02883.x>
- Pebesma E (2018) Simple features for R: standardized support for spatial vector data. *The R Journal* 10(1): 439–446. <https://doi.org/10.32614/RJ-2018-009>
- Petrides GA, Wehr J (1998) *A Peterson Field Guide to Eastern Trees: Eastern United States and Canada, Including the Midwest*. HarperCollins (New York), 1–448.
- Pfennig KS, Kelly AL, Pierce AA (2016) Hybridization as a facilitator of species range expansion. *Proceedings of the Royal Society B Biological Sciences* 283(1839): 20161329. <https://doi.org/10.1098/rspb.2016.1329>
- R Core Team (2021) *R: A language and environment for statistical computing*. R Foundation for Statistical Computing. <https://www.R-project.org/>
- Ross HH (1961) Two new species of *Neodiprion* from southeastern North America (Hymenoptera: Diprionidae). *Annals of the Entomological Society of America* 54(3): 451–453. <https://doi.org/10.1093/aesa/54.3.451>
- Smith DR (1979) Symphyta. In: Krombein PD, Hurd Jr PD, Smith DR, Burks BD (Eds) *Catalog of Hymenoptera in America north of Mexico*. Smithsonian Institution Press (Washington, DC), 3–137.
- Taeger A, Liston AD, Prous M, Groll EK, Gehroldt T, Blank SM (2018) ECatSym - electronic world catalog of Symphyta (Insecta, Hymenoptera). Program version 5.0 (19 Dec 2018), data version 40 (23 Sep 2018) – Senckenberg Deutsches Entomologisches Institut (SDEI), Müncheberg; 2018. [Accessed Aug 2023]
- Vertacnik KL, Linnen CR (2017) Evolutionary genetics of host shifts in herbivorous insects: insights from the age of genomics. *Annals of the New York Academy of Sciences* 1389(1): 186–212. <https://doi.org/10.1111/nyas.13311>
- Warren LO (1958) Pine sawflies in Arkansas. *Arkansas Farm Research* (Jan. – Feb.): 8.
- Welch HJ (1991) Classification and nomenclature. In: *The Conifer Manual*. Forestry Sciences, vol 34. Springer (Dordrecht), 44–61. https://doi.org/10.1007/978-94-011-3704-1_5
- Wickham H (2016) *ggplot2: Elegant Graphics for Data Analysis*. Springer-Verlag, New York. <https://ggplot2.tidyverse.org>
- Wiens JJ, Lapoint RT, Whiteman NK (2015) Herbivory increases diversification across insect clades. *Nature communications* 6(1): 8370. <https://doi.org/10.1038/ncomms9370>
- Wilkinson RC (1968) Record of *Neodiprion warreni* (Hymenoptera: Diprionidae) in Florida. *Florida Entomologist* 51(3): 199. <https://doi.org/10.2307/3493554>



Male-biased night foraging by bumblebees (Hymenoptera, Apidae, *Bombus* spp.) in Taiwan

Yun-Chen Hsieh^{1,2*}, Joe Chun-Chia Huang^{3*}, Wen-Chi Yeh²,
Chun-Yang Tsai⁴, Chien-Jung Lin⁵, Sheng-Shan Lu⁵

1 Institute of Ecology and Evolutionary Biology, National Taiwan University, Taipei City, Taiwan **2** Forest Protection Division, Taiwan Forestry Research Institute, Taipei City, Taiwan **3** Department of Life Science, National Taiwan Normal University, Taipei City, Taiwan **4** Department of Forestry and Natural Resources, National Ilan University, Yilan City, Taiwan **5** Fushan Research Center, Taiwan Forestry Research Institute, Yuanshan Township, Taiwan

Corresponding author: Sheng-Shan Lu (sslu@tfri.gov.tw)

Academic editor: C. K. Starr | Received 29 September 2023 | Accepted 28 October 2023 | Published 7 November 2023

<https://zoobank.org/DC2BCDC6-B278-4FAD-A2EB-C9B1D1437A10>

Citation: Hsieh Y-C, Huang JC-C, Yeh W-C, Tsai C-Y, Lin C-J, Lu S-S (2023) Male-biased night foraging by bumblebees (Hymenoptera, Apidae, *Bombus* spp.) in Taiwan. Journal of Hymenoptera Research 96: 949–954. <https://doi.org/10.3897/jhr.96.113486>

Abstract

Known nocturnal behaviors of bees in the superfamily Apoidea, including the genus *Bombus*, were almost exclusively of females. Here we report observations of active free-ranging male *Bombus* at night in the plant nursery of the Fushan Research Center, Taiwan, in April 2022. Nectar feeding by males at inflorescences was confirmed by tongue-licking in the absence of pollen collecting. The numbers of active female and male bumblebees during the daytime were close to equal. In contrast, only males were found to be active in the night. Our observations suggest that such nocturnal activity is facultative. This finding not only provides a rare case of nocturnal activity in free-ranging *Bombus*, but also demonstrates that such behaviors can vary between the sexes.

Keywords

Bombus flavescens, nocturnal behavior, sex-biased

Circadian rhythm represents a key mechanism regulating temporal patterns of activity and physiological processes in animals. Given species tend to be diurnal, nocturnal or crepuscular, depending on whether their main active times are during daylight hours, at night or in twilight. The timing of daily activity may involve distinct selection forces on account of

* These authors contributed equally to this research and share first authorship.

light conditions, weather, the distribution of important resources, and predation risk. Furthermore, synchronization with conspecifics of daily activity may be important in social and reproductive interactions (Sullivan 1981; Frisch and Koeniger 1994). On the other hand, asynchronization of daily activity among conspecifics could favor individuals via avoidance of severe intraspecific competition for critical resources (Alanärä et al. 2001).

Bumblebees (Hymenoptera; Apidae; *Bombus*) are a group of large social bees. The genus is most abundant in the northern hemisphere, where it provides critical pollination services to many crops and wild plants (Prys-Jones and Corbet 2011). While observations to date show both sexes to be active mainly or exclusively in the daytime, Chittka et al. (1999) recorded nocturnal feeding by *B. impatiens* workers in captive condition. Here we report observations of nocturnal activity in free-ranging male *Bombus* from northeastern Taiwan.

The observations were mainly made at the plant nursery of Fushan Research Center (24.7556°N, 121.5959°E) in Yilan County, Taiwan, from early to mid-April 2022. The climate is characterized by a strong seasonality that is mainly driven by the north-east monsoon in the winter and occasional typhoons in the late summer and early fall. The weather is generally mild and humid with a mean annual temperature of 18.2 °C and precipitation of 3,888 mm (Tu et al. 2023). The surrounding vegetation is primarily submontane evergreen broadleaf forest (Su et al. 2010). The plant nursery was established by Taiwan Forestry Research Institute (T.F.R.I.) to conserve endemic and threatened native plants. Since the observation area in the plant nursery had no insect exclusion nets, bumblebees can access the plants freely. An additional 1.6-km transect line was set along a trail of the nearby Fushan Botanical Garden in the later phase of the study, when many dicot plants were in bloom.

Bees' nocturnal behavior was initially noted by direct visual observation with lights from torch and headlamp. Later we utilized a night-vision video cam recorder (Canon XA40, Japan) with an 850 nm infrared torch (Nightfox NB5, U.K.) in order to record nocturnal activity without presenting a visual light stimulus. Bees found to be walking, flying, wing fluttering, or showing leg movements or nectar feeding were considered active. Nectar feeding is evidenced by extension of the tongues and licking movements at flowers, along with the absence of pollen-collecting movements.

Three bumblebee species have been reported from the Fushan area: *B. bicoloratus*, *B. eximius*, and *B. flavescens* (S.S.L., Y.C.H., and W.C.Y. unpublished data). We identified bees to species according to a key of the three species (Suppl. material 1) based on Starr (1992). However, the diagnostic traits to distinguish *B. eximius* and *B. flavescens* cannot be applied with confidence to active individuals, so that the two species are combined in our data as *B. eximius/B. flavescens*.

Six male bumblebees were spotted in active status on *Ligustrum pricei* during a night walk in the plant nursery between 20:50 and 21:00 on April 5th, 2022. All active bumblebees walked slowly among the branches and inflorescences and inspected both opened and unopened flowers during most of the observation time. One individual flew with wings slowly fluttering, from *L. pricei* to a neighboring plant. While the bees were in contact with stigma and pistil, they often extended their tongues in the typical nectar licking behavior (Fig. 1). No pollen collection actions were performed by the bees, consistent with feeding on nectar.

Additional observations of *B. eximius*/*B. flavescens* were made at the plant nursery and botanical garden (Table 1). While active bumblebees of both sexes had been seen at both sites in the daytime, nocturnal foraging behavior was again recorded solely from male bumblebees at the plant nursery (Suppl. material 2). No active females were observed in the three additional survey nights, but one inactive worker was recorded with two males on *Ajuga dictyocarpa*. In the only daytime observation, we recorded a similar number of male and worker *B. eximius*/*B. flavescens*, feeding at *L. pricei* and *A. dictyocarpa*.

Diurnality is considered the predominant habit in bees. Nocturnal and crepuscular activities have been reported from several genera of Apidae and Halictidae, including *Apis*, *Bombus*, *Lasioglossum*, *Megalopta* and *Xylocopa*, but exclusively from females (Chittka et al. 1999; Burgett and Sukumalanand 2000; Wcislo et al. 2004; Kelber et al. 2006; Tierney et al. 2008; Young et al. 2021). Our observation of facultative nocturnal foraging by *B. eximius*/*B. flavescens* provides a case of male bees showing considerable plasticity in daily activity pattern.

Night light has been suggested as a critical environmental factor driving nocturnal activities in bees (Kelber et al. 2006; Warrant 2008). In our case, the *B. eximius*/*B. flavescens* in Fushan were attracted by and licked unopened flowers of *L. pricei* (Suppl.



Figure 1. A male bumblebee at *Ligustrum pricei* flowers at night.

Table 1. Numbers of active and inactive *B. eximius*/*B. flavescens* individuals of each sex in each survey. Two males (FACT-00215031, FACT-00215032) identified as *B. flavescens* were deposited at the Forest Arthropod Collection of Taiwan (F.A.C.T.) in T.F.R.I. This survey session included both at the botanical garden and the plant nursery.

Date	Active bees	Inactive bees
2022 April 5 th – night	6♂♂	–
2022 April 6 th – night	–	–
2022 April 14 th – day	12♂♂, 10♀♀	–
2022 April 14 th – night	2♂♂	1♂, 1♀
2022 April 16 th – night	–	7 (unknown sex)

material 3) and the white flower tags that we labeled on the tree several times. The misrecognition suggests that the bees used visual cues when targeting food resources. However, the two nights when active bees were observed were cloudy and dark, suggesting that *B. eximius*/*B. flavescens* may also use chemical cues for foraging in addition to vision (Chittka et al. 1999; Kulahci et al. 2008; Lawson et al. 2018).

Studies have shown that consumption of nutrient supplements could increase low temperature tolerance and survivorship from acute cold (Owen et al. 2013; Abou-Shaara 2017). In the low elevation mountainous areas (<1000 m a.s.l.) of Taiwan, male bumblebees, especially *B. flavescens*, emerge in spring (Sung et al. 2011). Unlike the females feeding on nectar and collecting pollen, male bumblebees were found feeding exclusively on nectar. They feed in the day and usually stay on inflorescences in the night (Prys-Jones and Corbet 2011). Both *Ligustrum pricei* and *Ajuga dictyocarpa* blossom in the day, and their flowers last for around 24 hours. Nectar-feeding behaviors in bumblebees suggest that the nectar is available throughout the day.

On the other hand, only half of the surveyed nights showed male bumblebees on plants. During the study period, bumblebees reduced their nocturnal activity when the wind became stronger and temperature dropped, becoming active again when the wind speed lowered. It might be too energetically costly for the bees to remain active during bad weather conditions.

We thank E-Ping Rau, Ping-Hsin Wang, Sz-yi Tsai, and Yider Hsu for assistance in the field, Ellen McArthur and Christopher K. Starr for the language review, Ace Kevin S. Amarga for the format review, Christopher K. Starr and an anonymous reviewer for their useful comments on a previous version. This study was supported financially by T.F.R.I. (grant number 110AS-7.1.3-FI-G3)

References

- Abou-Shaara HF (2017) Effects of various sugar feeding choices on survival and tolerance of honey bee workers to low temperatures. *Journal of Entomological and Acarological Research* 49: e6200. <https://doi.org/10.4081/jear.2017.6200>
- Alanärä A, Burns MD, Metcalfe NB (2001) Intraspecific resource partitioning in brown trout: the temporal distribution of foraging is determined by social rank. *Journal of Animal Ecology* 70(6): 980–986. <https://doi.org/10.1046/j.0021-8790.2001.00550.x>

- Burgett DM, Sukumalanand P (2000) Flight activity of *Xylocopa* (*Nyctomelitta*) *tranquebarica*: a night flying carpenter bee (Hymenoptera: Apidae). *Journal of Apicultural Research* 39: 75–83. <https://doi.org/10.1080/00218839.2000.11101024>
- Chittka L, Williams NM, Rasmussen H, Thomson JD (1999) Navigation without vision: bumblebee orientation in complete darkness. *Proceedings of the Royal Society (B)* 266: 45–50. <https://doi.org/10.1098/rspb.1999.0602>
- Frisch B, Koeniger N (1994) Social synchronization of the activity rhythms of honeybees within a colony. *Behavioral Ecology and Sociobiology* 35: 91–98. <https://doi.org/10.1007/BF00171498>
- Kelber A, Warrant EJ, Pfaff M, Wallén R, Theobald JC, Wcislo WT, Raguso RA (2006) Light intensity limits foraging activity in nocturnal and crepuscular bees. *Behavioral Ecology* 17: 63–72. <https://doi.org/10.1093/beheco/arj001>
- Kulahci IG, Dornhaus A, Papaj DR (2008) Multimodal signals enhance decision making in foraging bumble-bees. *Proceedings of the Royal Society B: Biological Sciences* 275(1636): 797–802. <https://doi.org/10.1098/rspb.2007.1176>
- Lawson DA, Chittka L, Whitney HM, Rands SA (2018) Bumblebees distinguish floral scent patterns, and can transfer these to corresponding visual patterns. *Proceedings of the Royal Society B: Biological Sciences* 285(1880): e20180661. <https://doi.org/10.1098/rspb.2018.0661>
- Owen EL, Bale JS, Hayward SAL (2013) Can winter-active bumblebees survive the cold? Assessing the cold tolerance of *Bombus terrestris audax* and the effects of pollen feeding. *PLoS ONE* 8(11): e80061. <https://doi.org/10.1371/journal.pone.0080061>
- Prys-Jones OE, Corbet SA (2011) *Bumblebees* (3rd edn.). Pelagic Publishing, Exeter, 130 pp.
- Starr CK (1992) The bumble bees (Hymenoptera: Apidae) of Taiwan. *Bulletin of the National Museum of Natural Science* 3: 139–157.
- Su SH, Hsieh CF, Chang-Yang CH, Lu CL, Guan BT (2010) Micro-topographic differentiation of the tree species composition in a subtropical submontane rainforest in northeastern Taiwan. *Taiwan Journal of Forestry Science* 25: 63–80. https://www.tfri.gov.tw/en/News_Content2.aspx?n=7589&cs=14070
- Sullivan RT (1981) Insect swarming and mating. *Florida Entomologist* 64: 44–65. <https://doi.org/10.2307/3494600>
- Sung IH, Lu SS, Chan ML, Lin MY, Chiang CH, Li CC, Yang PS (2011) A study on the size and morphological difference, seasonal occurrence and distribution features of four bumblebees from Taiwan (Hymenoptera, Apidae). *Formosan Entomology* 31: 309–323. <https://doi.org/10.6661/TESEFE.2011020>
- Tierney SM, Gonzales-Ojeda T, Wcislo WT (2008) Biology of a nocturnal bee, *Megalopta atra* (Hymenoptera: Halictidae; Augochlorini), from the Panamanian highlands. *Journal of Natural History* 42: 1841–1847. <https://doi.org/10.1080/00222930802109124>
- Tu FJ, Lin CL, Huang HH (2023) Weather data from Fushan Research Center of Taiwan Forestry Research Institute – Nursery Weather Station. Taiwan Forestry Research Institute. [accessed 16 August 2023] <https://metacat.tfri.gov.tw/tfri/view/TFRIWMT.11.19>
- Warrant EJ (2008) Seeing in the dark: vision and visual behaviour in nocturnal bees and wasps. *Journal of Experimental Biology* 211(11): 1737–1746. <https://doi.org/10.1242/jeb.015396>
- Wcislo WT, Arneson L, Roesch K, Gonzalez V, Smith A, Fernández H (2004) The evolution of nocturnal behaviour in sweat bees, *Megalopta genalis* and *M. ecuadoria* (Hymenoptera:

Halictidae): an escape from competitors and enemies? *Biological Journal of the Linnean Society* 83: 377–387. <https://doi.org/10.1111/j.1095-8312.2004.00399.x>

Young AM, Kodabalagi S, Brockmann A, Dyer FC (2021) A hard day's night: Patterns in the diurnal and nocturnal foraging behavior of *Apis dorsata* across lunar cycles and seasons. *PLoS ONE* 16(10): e0258604. <https://doi.org/10.1371/journal.pone.0258604>

Supplementary material 1

Identification keys to bumblebee species of the Fushan area

Authors: Yun-Chen Hsieh, Joe Chun-Chia Huang

Data type: docx

Copyright notice: This dataset is made available under the Open Database License (<http://opendatacommons.org/licenses/odbl/1.0/>). The Open Database License (ODbL) is a license agreement intended to allow users to freely share, modify, and use this Dataset while maintaining this same freedom for others, provided that the original source and author(s) are credited.

Link: <https://doi.org/10.3897/jhr.96.113486.suppl1>

Supplementary material 2

Behavior of a male bumblebee on the inflorescences of *Ligustrum pricei* at night

Authors: Joe Chun-Chia Huang

Data type: mov

Copyright notice: This dataset is made available under the Open Database License (<http://opendatacommons.org/licenses/odbl/1.0/>). The Open Database License (ODbL) is a license agreement intended to allow users to freely share, modify, and use this Dataset while maintaining this same freedom for others, provided that the original source and author(s) are credited.

Link: <https://doi.org/10.3897/jhr.96.113486.suppl2>

Supplementary material 3

A bumblebee worker licking unopened flowers of *Ligustrum pricei*

Authors: Joe Chun-Chia Huang

Data type: mov

Copyright notice: This dataset is made available under the Open Database License (<http://opendatacommons.org/licenses/odbl/1.0/>). The Open Database License (ODbL) is a license agreement intended to allow users to freely share, modify, and use this Dataset while maintaining this same freedom for others, provided that the original source and author(s) are credited.

Link: <https://doi.org/10.3897/jhr.96.113486.suppl3>

On the specific epithet “*vaccinii*” of Ashmead, 1887 and Burks, 1979 (Hymenoptera, Cynipidae)

Juli Pujade-Villar^{1,2}, Y. Miles Zhang³, Matthew L. Buffington⁴,
Denis J. Brothers⁵, Irene Lobato-Vila^{1,2}, Victor Cuesta-Porta^{1,2}

1 *Departament de Biologia Evolutiva, Ecologia i Ciències Ambientals (Secció Invertebrats), Facultat de Biologia, Universitat de Barcelona, Avinguda Diagonal 643, 08028 Barcelona, Spain* **2** *Institut de Recerca de la Biodiversitat (IRBio), Facultat de Biologia, Universitat de Barcelona, Avinguda Diagonal 643, 08028 Barcelona, Spain* **3** *Institute of Ecology and Evolution, University of Edinburgh, Edinburgh, UK* **4** *Systematic Entomology Laboratory, ARS-USDA c/o National Museum of Natural History, Smithsonian Institution, 10th & Constitution Ave NW, 20013 Washington D.C., USA* **5** *School of Life Sciences, University of KwaZulu-Natal, Pietermaritzburg, Private Bag X01, 3209 Scottsville, South Africa*

Corresponding author: Irene Lobato-Vila (i.lobatovila@gmail.com)

Academic editor: T. Spasojevic | Received 7 August 2023 | Accepted 24 October 2023 | Published 9 November 2023

<https://zoobank.org/8CC595CC-BE3C-43F8-80F5-40312B5A6DB2>

Citation: Pujade-Villar J, Zhang YM, Buffington ML, Brothers DJ, Lobato-Vila I, Cuesta-Porta V (2023) On the specific epithet “*vaccinii*” of Ashmead, 1887 and Burks, 1979 (Hymenoptera, Cynipidae). *Journal of Hymenoptera Research* 96: 955–965. <https://doi.org/10.3897/jhr.96.110687>

Abstract

Ashmead (1887) provided descriptions of two species of Cynipidae with “*vaccinii*” as the specific epithet: *Solenozopheria vaccinii* Ashmead, 1887 and *Acraspis vaccinii* Ashmead, 1887. There are numerous nomenclatural issues that have arisen from these descriptions. To resolve them, we have examined all relevant primary types and provide images of these specimens, as well as their labels. We recognize as valid the two “*vaccinii*” species, *Loxaulus vaccinii* (Ashmead, 1887) and *Zopheroteris vaccinii* (Ashmead, 1887), and list their synonyms. We also include the following new nomenclatural and taxonomic acts: *Acraspis vaccinii* Ashmead, 1887: lectotype by present designation; *Callirhytis vaccinii* Burks, 1979: species *incertae sedis*; *Andricus impositus* Beutenmüller, 1918: revalidated status; *Andricus verifactor* Kinsey, 1922: new status.

Keywords

Acraspis, *Andricus*, *Callirhytis*, gall wasps, *Loxaulus*, nomenclature, *Solenozopheria*, taxonomy, *Zopheroteris*

Introduction

Oak gall wasps (Hymenoptera, Cynipidae, Cynipini) are by far the most species-rich group of gall wasps, with about 1,000 known species in 50 genera worldwide (Melika and Abrahamson 2002; Csóka et al. 2005; Ronquist et al. 2015; Péntzes et al. 2018; Pujade-Villar et al. 2020; Melika et al. 2021; Melika and Nicholls 2021). The oak gall wasp tribe Cynipini induces galls on host plants within both *Quercus* L. and non-*Quercus* genera of Fagaceae [such as *Chrysolepis* Hjelmq. and *Notholithocarpus* Manos, Cannon and S.H.Oh in North America (Burks 1979; Csóka et al. 2005; Péntzes et al. 2018; Melika et al. 2021)].

About 680 species of oak gall wasps are known from the Nearctic region (Burks 1979; Melika and Abrahamson 2002; Melika and Nicholls 2021). Many of these species have been repeatedly transferred to other genera over time by different authors, which has inevitably led to numerous nomenclatural issues – for example, misplacements and misassociations of species with the same specific epithet. These nomenclatural problems worsen when a species originally described solely from galls, that is, without obtaining the adult wasps, is later associated with the wrong adults. This is what has happened with the species that share the epithet “*vaccinii*”.

Ashmead (1887) described two species of Cynipidae with “*vaccinii*” as the specific epithet: *Solenozopheria vaccinii* Ashmead, 1887: 149 and *Acraspis vaccinii* Ashmead, 1887: 136. There are numerous nomenclatural issues that have arisen from these descriptions, so our intent here is to bring clarity and resolution to these problems. To this aim, we have traced the usage of the epithet “*vaccinii*” throughout history to clarify the affiliation of the species involved.

Material and methods

We have examined the original descriptions of the species involved and all relevant primary types. A total of nine species is addressed in this revision: *Acraspis vaccinii* Ashmead, 1887; *Andricus chapmanii* Melika & Abrahamson, 2021; *And. impositus* Beutenmüller, 1918; *And. lustrans* Beutenmüller, 1913; *And. robustus* Weld, 1926; *And. verifactor* Kinsey, 1922; *Callirhytis vaccinii* Burks, 1979; *Cynips vacciniiformis* Beutenmüller, 1913, and *Solenozopheria vaccinii* Ashmead, 1887.

The type material and other material examined are deposited in the following institutions: the American Museum of Natural History (AMNH), New York, USA; the Academy of Natural Sciences of Drexel University (ANSP), Philadelphia, Pennsylvania, USA; the National Museum of Natural History (USNM), Washington, D.C., USA.

Results and discussion

Solenozopheria Ashmead, 1887 was synonymized with *Loxaulus* Mayr, 1881 by Weld (1951: 643); hence *Solenozopheria vaccinii* was then recognized as *Loxaulus vaccinii* (Ashmead). This species had been described based on adult wasps reared from the wild low-

bush blueberry *Vaccinium angustifolium* Ait. (as *V. pennsylvanicum* Lam.) and the northern highbush blueberry *V. corymbosum* L. Melika and Abrahamson (2000) determined that Ashmead (1887) had incorrectly associated the galls with the adult gall wasps, and that the real gall inducer on blueberries was *Hemadas nubilipennis* (Ashmead, 1887) [Chalcidoidea, Ormyridae (after Burks et al. 2022)]. The actual hosts of *L. vaccinii* are oaks, *Quercus chapmanii* Sarg. and *Q. stellata* Wangenh. (Weld 1921). Also, Melika and Abrahamson (2000: 209) synonymized *Loxaulus humilis* (Weld, 1921) with *L. vaccinii*. For future reference in the text, *L. vaccinii*, an oak galler that does not gall blueberry, has not undergone any other taxonomic change and has never been included in *Callirhytis* Foerster, 1869. This information is critical for assigning hosts for parasitoid species (see below).

A chronological summary of these changes is presented here:

***Loxaulus vaccinii* (Ashmead, 1887)**

Solenozopheria vaccinii Ashmead, 1887: 134, 149 (only asexual females);

Compsodryoxenus humilis Weld, 1921: 190, 193 (asexual female and gall);

Loxaulus vaccinii (Ashmead); Weld (1951: 643);

Loxaulus humilis (Weld); Weld (1951: 643) [synonymized by Melika and Abrahamson (2000: 209)].

The history of *Acraspis vaccinii* is far more complicated. Osten-Sacken (1862: 255) characterized a gall from post oak, *Q. stellata* (as *Q. obtusiloba* Michx.), found by him on a tree in Washington (p. 241) in October 1861, but did not provide a name, nor rear any adult wasps. Later, Ashmead (1887: 127, 136) provided a name for this species, duplicating Osten-Sacken’s (1862) description of the gall, and adding a short description of the apterous adult wasps. Ashmead’s unfortunate choice of “*vaccinii*” as specific epithet for this species was in reference to Osten-Sacken’s (1862) mention of the gall shape: “their shape may be compared to that of the flowers of *Vaccinium*”. *Acraspis vaccinii* was later transferred to *Zopheroteras* Ashmead, 1897 (Ashmead 1897: 261). Later, Ashmead (1903: 148) formally designated *A. vaccinii* as the type species of *Zopheroteras*; this act referred only to adults and did not mention the galls.

Almost in parallel, Kieffer (1902: 97) assigned *Acraspis vaccinii* to *Trigonaspis* Hartig, 1840 and, later, Dalla-Torre and Kieffer (1910: 393) considered *Zopheroteras* (galls and adults) a junior synonym of *Trigonaspis*. Weld (1922: 9) resurrected *Zopheroteras* and synonymized *Parateras* Ashmead, 1887 under *Zopheroteras*. In the same study, Weld (1922) mentioned that the gall that Ashmead (1887) had described for *Acraspis vaccinii* corresponded to galls of a winged species which Beutenmüller (1918: 329) had previously described as *Andricus impositus* Beutenmüller, 1918, and stated that the true gall of *Zopheroteras vaccinii* had not yet been described; this was supported by the observation that Ashmead’s *A. vaccinii* adult wasps were apterous (Fig. 1). Hence, Weld (1922) concluded that Ashmead (1887) had misidentified the gall and misassociated adults of his new genus *Zopheroteras* with the galls described as *Acraspis vaccinii*.

However, the name confusion of these wasps was still developing. Based on gall, adult morphology and host, Weld (1926: 95) synonymised *Andricus impositus* with *Andricus lustrans*

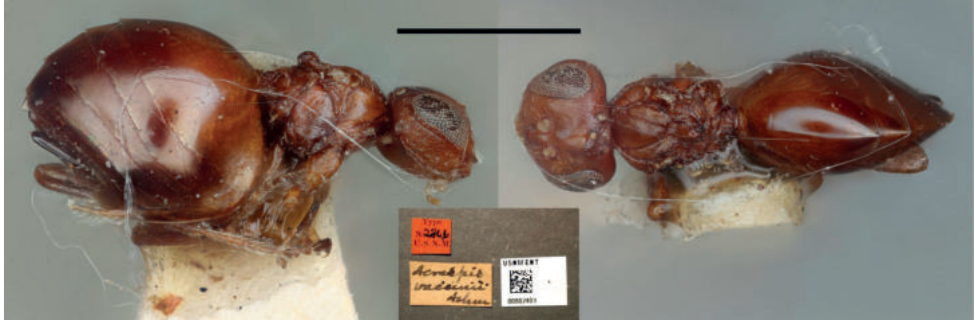


Figure 1. Habitus and labels of Lectotype of *Acraspis vaccinii* Ashmead, 1887, deposited in the USNM (<https://collections.nmnh.si.edu/search/ento/>). Scale bar: 1 mm.

and transferred *A. lustrans* (= *A. impositus*) to the genus *Callirhytis* Foerster, 1869. In the same paper, *Andricus dimorphus* var. *verifactor* Kinsey, 1922 was synonymized under *Callirhytis lustrans* and the galls of *Acraspis vaccinii* were identified as those of *C. lustrans*.

Weld (1951: 650) considered *Acraspis vaccinii* (galls only) as a *nomen nudum*, under *C. lustrans*. However, we consider that this *nomen nudum* assignment was an error as the galls were described under that name, but erroneously associated with the adults described therein, resulting in a mixed type series. Weld (1951: 643) indicated *Acraspis vaccinii* (adult female only) as the type species of *Zopheroteras*.

More recently, Burks (1979: 1095, 1106) considered the adult wasps of *Acraspis vaccinii* as *Zopheroteras vaccinii*, but the galls as *Callirhytis vaccinii* Burks, 1979, listing *Andricus lustrans*, *A. impositus* and *A. dimorphus* var. *verifactor* as junior synonyms of the latter, thus mysteriously regarding Ashmead's name as valid for two different taxa. It can, however, be considered that Burks (1979) effectively established a new species, *Callirhytis vaccinii*, for the galls since he referred to Ashmead's description of them, complying with Article 13.1.2 of the International Code of Zoological Nomenclature (ICZN 1999). Finally, Zhang et al. (2022: 69) re-established the name *Andricus lustrans* as a valid species, removing it from *Callirhytis*.

The International Code of Zoological Nomenclature (ICZN 1999: Article 72.4.1) specifies that the type series includes all specimens that the author included in the new taxon "whether directly or by bibliographic reference" (except any disclaimed by the author). Article 73.2.1 reinforces this broad concept of syntypes, including specimens representing the work of an animal if described before 1931 (Article 1.2.1). Ashmead (1887: 136) quoted Osten-Sacken's description of the gall, rather than writing his own, but also described two adult specimens (implied to have been reared from similar galls), so both components were properly described. He also stated that he had seen similar galls "on the Post Oak at Asheville, N.C." Consequently, the type series must include the two adult female specimens, both labelled as "type 2866" (deposited in USNM and ANSP), plus the gall specimens that Ashmead saw from Asheville, and the gall specimens from Washington that Osten-Sacken used for his description. The USNM has several collections of galls, identified as *Callirhytis vaccinii* and matching the description, and collected on "*Q. obtusiloba*", some from Florida, and others card-mounted without further data but labelled as "type 2866" (Fig. 2A); the latter may very well represent the Asheville specimens, but we cannot assume this since

the type labels were undoubtedly later additions, and we thus do not consider them to be syntypes. Further galls in the USNM, also labelled as *Callirhytis vaccinii*, were collected by Ashmead in Florida, but on “*Q. minor*”, and so cannot be syntypes (although they have erroneously been labelled as cotypes, Fig. 2B). To add to the confusion, there are five galls in ANSP labelled as “type” of *Acraspis vaccinii* in a similar style to some of the USNM galls, but collected in Florida on “*Q. obtusiloba*”, and so also not syntypes. Unfortunately, the syntype galls are thus presumed to be lost, misplaced or unidentifiable as such. We hereby formally designate the USNM type 2866 (USNMENT802403) as the lectotype of *Acraspis vaccinii* Ashmead, 1887 (Fig. 1), and the specimen (also labelled as a type, number 2866) deposited in ANSP as a paralectotype. This fixes the name as applicable to the adult only.

A chronological summary of these changes is provided here:

***Andricus lustrans* Beutenmüller, 1913**

Acraspis vaccinii Ashmead, 1887: 136 (only galls) [synonymized by Weld (1926: 95)];
Andricus lustrans Beutenmüller, 1913: 244; Zhang et al. (2022: 69);
Andricus impositus Beutenmüller, 1918: 329 [synonymized by Weld (1926: 95)];
Andricus dimorphus verifactor Kinsey, 1922: 15 [synonymized by Weld (1926: 95)];
Callirhytis lustrans (Beutenmüller); Weld (1926: 95);
Callirhytis vaccinii Burks, 1979: 1106 (only galls).

***Zopheroteras vaccinii* (Ashmead, 1887)**

Acraspis vaccinii Ashmead, 1887: 136 (only adults). Lectotype by present designation;
Zopheroteras vaccinii (Ashmead) Ashmead (1897: 261); Weld (1922: 9);
Trigonaspis vaccinii (Ashmead) Kieffer (1902: 97); Dalla-Torre and Kieffer (1910: 397).

The galls of *Andricus lustrans* (? = “*Callirhytis vaccinii*” galls) are similar to those of a recently described new species, *Andricus chapmanii* Melika & Abrahamson, 2021 (Melika et al. 2021), and also to the galls of *Andricus vacciniiformis* (Beutenmüller, 1913) and *Andricus robustus* Weld, 1926. In fact, Beutenmüller (1918) mentioned that the mature galls of *A. lustrans* resembled those of *A. vacciniiformis*, and Weld (1926) wrote that the gall of *A. robustus* had previously been described in connection with the adult of *A. vacciniiformis*, which must then have come from a gall of a different sort accidentally included in the breeding cage. So, what are the “*Callirhytis vaccinii*” galls (Fig. 2)? The oak host of *A. lustrans* is unknown, according to the original description, but the galls of *A. impositus* (junior synonym of *A. lustrans*) occur on *Quercus stellata* (as *Q. minor* (Marsh.) Sarg.), as do the galls of *A. vacciniiformis* and *A. robustus*, while *A. chapmanii* occurs on *Q. chapmanii*. Osten-Sacken’s (1862) galls, and the others mentioned in Ashmead (1897), occurred on *Quercus stellata* (as *Q. obtusiloba*) as shown in the labels visible in Fig. 2A, thus those galls could belong to *A. lustrans*, *A. vacciniiformis* or *A. robustus*. The gall of *A. lustrans* is unknown according to the original description, but has recently been photographed (Zhang et al. 2022). According to the descriptions of these galls, the shape is globular with a nipple at the apex, while those of *A. chapmanii* are truncate at the apex and depressed centrally;



Figure 2. Galls deposited in USNM collection **A** on *Quercus stellata* (as *Q. obtusiloba*) similar to Osten-Sacken galls, confusingly described by Ashmead as “The Huckleberry-like Gall”; card-mounted galls are labelled “Type 2866” but are not syntypes (explanation in text) **B** similar galls, erroneously labelled as cotypes of *Zopherothesa vaccinii*, collected by Ashmead in Florida on *Q. stellata* (as *Q. minor*). Photos by M. L. Buffington.

Beutenmüller (1913) mentioned that *A. vacciniiformis* galls are similar to the huckleberry fruit or to *Celtis occidentalis* L. fruit, but these fruits have different shapes; huckleberry fruit is truncated distally and depressed centrally and *C. occidentalis* has a pointed fruit.

To this point, the identity of the huckleberry-flower-like galls (truncated distally and depressed centrally) from Osten-Sacken (1862), erroneously associated with the adults used by Ashmead (1887) in his description of *Acraspis vaccinii* (Fig. 2), is uncertain. Since there are no adult samples reared from Osten-Sacken (1862) galls, we cannot associate those galls with any of the species mentioned. We therefore designate *Callirhytis vaccinii* Burks, 1979 as a species *incertae sedis*.

Examining the adults, we found important differences (Table 1). Adults of *A. vacciniiformis* have all metasomal segments pubescent (Fig. 3D), while in *A. lustrans*, *A. impositus* and *A. robustus* the pubescence is restricted to the second metasomal segment only (Fig. 3A–C); which may be the reason why both Weld (1926: 81) and Kinsey (1922: 17) mentioned that the “*vacciniiformis*” gall was incorrectly associated. Additionally, Kinsey (1922) affirmed that “*verifactor*” galls are undoubtedly “*vacciniiformis*” galls, and described

the former as a variety of *A. dimorphus* (both are clustered leaf galls), even though both the adults and the galls of *A. dimorphus* (spherical galls) and *A. dimorphus* var. *verifactor* (urn-shaped galls) are different. Also, the synonymy of *A. lustrans* and *A. impositus* is doubtful because the length of the ventral spine of the hypopygium is different (Fig. 3A, B). *Andricus dimorphus* var. *verifactor* has the metasomal terga micropunctate, similar to *A. chapmanii*, so it is not a synonym of *A. lustrans*. Finally, *A. lustrans* has simple tarsal claws (type mate-

Table 1. Characters differentiating members of the *Andricus lustrans* group mentioned in the text. (*) *Andricus verifactor* has mesoscutum and mesopleuron punctate while in *A. chapmanii* these are not punctate.

Species	Metasomal pubescence	Metasomal punctation	Tarsal claw	Ventral spine
<i>A. chapmanii</i> *	Only 2 nd segment	Present	Simple	Long
<i>A. impositus</i>	Only 2 nd segment	Absent	Toothed	Short
<i>A. lustrans</i>	Only 2 nd segment	Absent	Simple	Long
<i>A. robustus</i>	Only 2 nd segment	Absent	Toothed	Long
<i>A. vacciniiformis</i>	All segments	Present	Toothed	Long
<i>A. verifactor</i> *	Only 2 nd segment	Present	Simple	Long

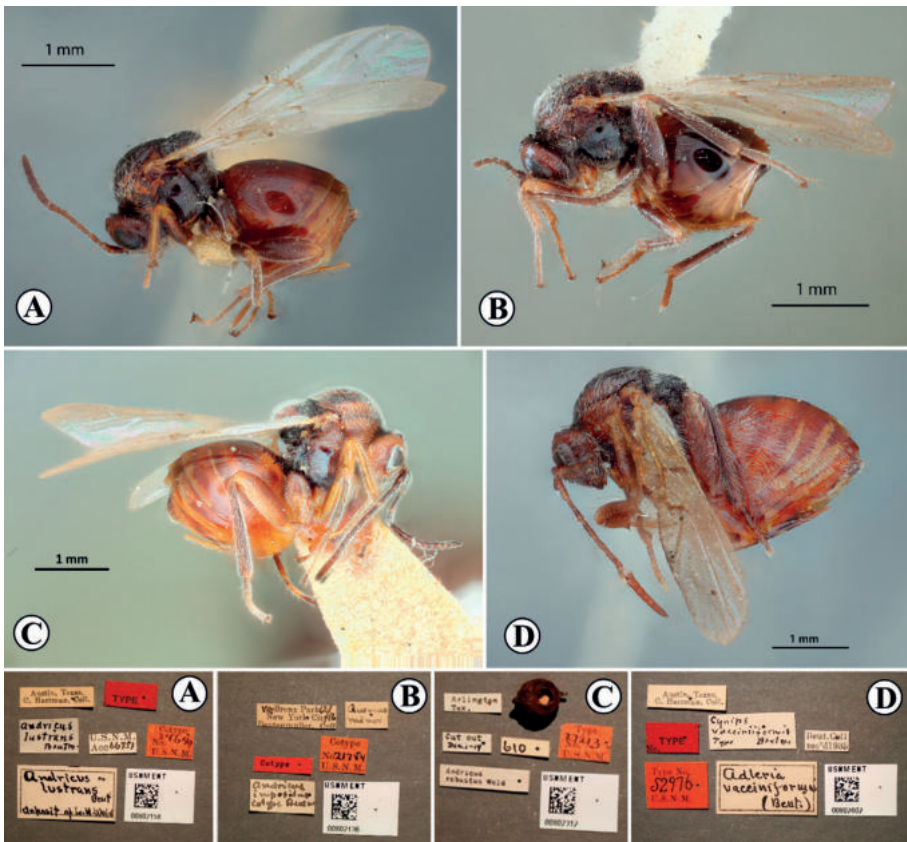


Figure 3. Habitus and labels of type specimens, deposited in the USNM, representing species of concern in this paper **A** *Andricus lustrans*, syntype **B** *Andricus impositus*, syntype **C** *Andricus robustus*, holotype **D** *Cynips vacciniiformis*, syntype. (<https://collections.nmnh.si.edu/search/entof/>). Scale bars: 1 mm.

rial examined), while in *A. impositus* and *A. robustus* they are toothed. Concerning the tarsal claws, *A. impositus* is a valid species, and not a synonym of *A. lustrans*: *Andricus impositus* Beutenmüller, 1918 status revalidated. Regarding the metasomal sculpture, *A. dimorphus* var. *verifactor* (with micropunctures on metasoma) is a valid species, not a synonym of *A. lustrans* (with smooth metasoma): *Andricus verifactor* Kinsey, 1922, stat. nov.

In summary, the species mentioned (in alphabetical order) have the following status and synonymic names:

***Andricus chapmanii* Melika & Abrahamson in Melika et al. (2021)**

Andricus chapmanii Melika & Abrahamson in Melika et al. (2021: 18). Type material deposited in USNM.

***Andricus impositus* Beutenmüller, 1918, status revalidated**

Andricus impositus Beutenmüller, 1918: 329. Type material deposited in USNM.

***Andricus lustrans* Beutenmüller, 1913**

Andricus lustrans Beutenmüller, 1913: 244; Zhang et al. (2022: 69). Type material deposited in USNM and ANSP;
Callirhytis lustrans (Beutenmüller); Weld (1926: 95).

***Andricus robustus* Weld, 1926**

Andricus robustus Weld, 1926: 81. Type material deposited in USNM.

***Andricus vacciniiformis* (Beutenmüller, 1913)**

Cynips vacciniiformis Beutenmüller, 1913: 247. Type material deposited in USNM;
Adleria vacciniiformis (Beutenmüller); Weld (1951: 630);
Andricus vacciniiformis (Beutenmüller); Melika and Abrahamson (2002: 160);

***Andricus verifactor* Kinsey, 1922, stat. nov.**

Andricus dimorphus var. *verifactor* Kinsey, 1922: 15. Type material deposited in AMNH and USNM;
Andricus dimorphus verifactor Kinsey; Weld (1926: 95).

Callirhytis vaccinii* Burks, 1979, *incertae sedis

Acraspis vaccinii Ashmead, 1887: 136 (part, only galls); Weld (1926: 95). Type material presumably lost or unidentifiable as such;
Callirhytis vaccinii Burks, 1979: 1106 (only galls).

***Loxaulus vaccinii* (Ashmead, 1887)**

Solenozopheria vaccinii Ashmead, 1887: 134, 149 (part, only asexual females). Type material deposited in USNM and ANSP;

Loxaulus vaccinii (Ashmead); Weld (1951: 643, only adults); Weld (1926: 95);

Compsodryoxenus humilis Weld, 1921: 190, 193 (asexual female and gall);

Loxaulus humilis (Weld); Weld (1951: 643) [synonymized by Melika and Abrahamson (2000: 209)].

***Zopheroteras vaccinii* (Ashmead, 1887)**

Acraspis vaccinii Ashmead, 1887: 136 (only adults). Type material deposited in USNM and ANSP (see above). Lectotype by present designation;

Zopheroteras vaccinii (Ashmead); Ashmead (1897: 261); Weld (1922: 9);

Trigonaspis vaccinii (Ashmead); Kieffer (1902: 97); Dalla-Torre and Kieffer (1910: 397).

Conclusions

After this revision, the following species are considered to be valid: *Andricus chapmanii* Melika & Abrahamson, 2021; *A. impositus* Beutenmüller, 1918, status revalidated; *A. lustrans* Beutenmüller, 1913; *A. robustus* Weld, 1926; *A. vacciniiformis* (Beutenmüller, 1913); *A. verifactor* Kinsey, 1922, stat. nov; *Loxaulus vaccinii* (Ashmead, 1887); and *Zopheroteras vaccinii* (Ashmead, 1887). *Callirhytis vaccinii* Burks, 1979 is considered as *incertae sedis*.

The specific epithet “*vaccinii*” has given rise to many nomenclatural and taxonomic problems that have persisted over time. Therefore, it was imperative to clarify its status for the sake of future research. For instance, a catalogue of oak-gall parasitoids is currently in preparation, for which accurate identifications are required. The final purpose of this contribution was to clarify the identities of some of the gall makers and their associated galls so as to be able correctly to assign their parasitoids to each determined species of gall. Various authors cite parasitoids of “*Callirhytis vaccinii*” (e.g., Hanson, 1992: 1340), not recognizing that the identity of the true species involved is currently unknown, as shown above.

Acknowledgements

DJB is grateful for funding and facilities from the University of KwaZulu-Natal, Scottsville, South Africa. YMZ was supported by the European Union’s Horizon 2020 research and innovation programme under the Marie Skłodowska-Curie grant agreement no. 101024056. This research was funded by the project “PID2021-128146NB-I00/MCIN/AEI/10.13039/501100011033/” and “FEDER una manera de hacer Europa” from the Ministry of Science and Innovation of Spain and the European Region-

al Development Fund (ERDF). The authors have declared that no competing interests exist. Mention of trade names or commercial products in this publication is solely for the purpose of providing specific information and does not imply recommendation or endorsement by the USDA. USDA is an equal opportunity provider and employer.

References

- Ashmead WH (1887) On the cynipidous galls of Florida, with descriptions of new species and synopses of the described species of North America. *Transactions of the American Entomological Society* 14: 125–158. <https://doi.org/10.2307/25076487>
- Ashmead WH (1897) Descriptions of five new genera in the family Cynipidae. *Canadian Entomologist* 29: 260–263. <https://doi.org/10.4039/Ent29260-11>
- Ashmead WH (1903) Classification of the gall-wasps and the parasitic cynipoids, or the superfamily Cynipoidea. III. *Psyche* 10: 140–155. <https://doi.org/10.1155/1903/83423>
- Beutenmüller W (1913) Description on new Cynipidae. *Transactions of the American Entomological Society* 39(3–4): 243–248. <https://www.jstor.org/stable/25076912>
- Beutenmüller W (1918) Notes on Cynipidae, with description of a new species (Hym.). *Entomological News* 29(9): 327–330. <https://www.biodiversitylibrary.org/item/84955#page/13/mode/1up>
- Burks BD (1979) Superfamily Cynipoidea. In: Krombein K, Hurd P, Smith D Burks B (Eds) *Catalog of Hymenoptera in America of North of Mexico* (Vol. 1). Symphyta and Apocrita. Smithsonian Institution Press, Washington, 1045–1107. <https://www.biodiversitylibrary.org/item/24831#page/1065/mode/1up>
- Burks R, Mitroiu M-D, Fusu L, Heraty JM, Janšta P, Heydon S, Papilloud ND-S, Peters RS, Tselikh EV, Woolley JB, van Noort S, Baur H, Cruaud A, Darling C, Haas M, Hanson P, Krogmann L, Rasplus J-Y (2022) From hell's heart I stab at thee! A determined approach towards a monophyletic Pteromalidae and reclassification of Chalcidoidea (Hymenoptera). *Journal of Hymenoptera Research* 94: 13–88. <https://doi.org/10.3897/jhr.94.94263>
- Csóka G, Stone GN, Melika G (2005) Biology, Ecology and Evolution of gall-inducing Cynipidae. In: Raman A, Schaefer CW, Withers TM (Eds) *Biology, Ecology and Evolution of Gall-Inducing Arthropods*. Science Publishers, Inc. Enfield, New Hampshire, 569–636.
- Dalla-Torre KW von, Kieffer JJ (1910) Cynipidae. *Das Tierreich* (Vol. 24). Friedländer & Sohn, Berlin, 891 pp. <https://doi.org/10.5962/bhl.title.1077>
- Hanson P (1992) The Nearctic species of *Ormyrus* Westwood (Hymenoptera: Chalcidoidea: Ormyridae). *Journal of Natural History* 26: 1333–1365. <https://doi.org/10.1080/00222939200770761>
- ICZN (International Commission on Zoological Nomenclature) (1999) *International Code of Zoological Nomenclature* (4th edn.). International Trust for Zoological Nomenclature, London, 306 pp. <https://www.iczn.org/the-code/the-code-online/>
- Kieffer JJ (1902) Révision du genre *Aulax* et des genres limitrophes d'*Aulax* avec quelques notes sur divers autres cynipides. *Bulletin de la Société d'Histoire Naturelle de Metz* 22: 91–97. <https://www.biodiversitylibrary.org/item/105303#page/101/mode/1up>
- Kinsey A (1922) Studies of some new and described Cynipidae (Hymenoptera). *Indiana University Studies* 9(53): 3–141. <https://www.biodiversitylibrary.org/item/162121#page/65/mode/1up>

- Melika G, Abrahamson WG (2000) Review of the cynipid gall wasps of the genus *Loxaulus* Mayr (Hymenoptera: Cynipidae) with descriptions of new species. *Proceedings of the Entomological Society of Washington* 102(1): 198–211. <https://www.biodiversitylibrary.org/item/54792#page/204/mode/1up>
- Melika G, Abrahamson WG (2002) Review of the world genera of oak cynipid wasps (Hymenoptera: Cynipidae: Cynipini). In: Melika G, Thuróczy C (Eds) *Parasitic Wasps: Evolution, Systematics, Biodiversity and Biological Control*. Agroinform, Budapest, 150–190.
- Melika G, Nicholls JA (2021) A new genus of Nearctic oak gall wasp, *Grahamstoneia* Melika & Nicholls, gen. nov. (Hymenoptera: Cynipidae, Cynipini). *Zootaxa* 4999(5): 456–468. <https://doi.org/10.11646/zootaxa.4999.5.4>
- Melika G, Nicholls JA, Abrahamson WG, Buss EA, Stone GN (2021) New species of Nearctic oak gall wasps (Hymenoptera: Cynipidae, Cynipini). *Zootaxa* 5084(1): 1–131. <https://doi.org/10.11646/zootaxa.5084.1.1>
- Osten-Sacken R (1862) Additions and corrections to the paper entitled: “On the CYNIPIDAE of the North American Oaks and their Galls”. *Proceedings of the Entomological Society of Philadelphia* 1(8): 241–259. <https://www.biodiversitylibrary.org/item/22852#page/283/mode/1up>
- Pérez Z, Tang C-T, Stone GN, Nicholls JA, Schwéger S, Bozsó M, Melika G (2018) Current status of the oak gallwasp (Hymenoptera: Cynipidae: Cynipini) fauna of the Eastern Palearctic and Oriental Regions. *Zootaxa* 4433(2): 245–289. <https://doi.org/10.11646/zootaxa.4433.2.2>
- Pujade-Villar J, Wang Y, Guo R, Sala-Nishikava A, Cuesta-Porta V, Arnedo MA, Melika G (2020) A new species of *Cerroneuroterus* Melika & Pujade-Villar from the Eastern Palearctic (Hymenoptera, Cynipidae, Cynipini). *Zootaxa* 4869(4): 515–528. <https://doi.org/10.11646/zootaxa.4869.4.3>
- Ronquist F, Nieves-Aldrey J-L, Buffington ML, Liu Z, Liljeblad J, Nylander JAA (2015) Phylogeny, evolution and classification of gall wasps: The plot thickens. *PLoS ONE* 10: e0123301. <https://doi.org/10.1371/journal.pone.0123301>
- Weld LH (1921) American gallflies of the family Cynipidae producing subterranean galls on oak. *Proceedings of the United States National Museum* 59(2368): 187–246. [+ 10 pls.] <https://doi.org/10.5479/si.00963801.59-2368.187>
- Weld LH (1922) Notes on cynipid wasps, with descriptions of new North American species. *Proceedings of the United States National Museum* 61(2439): 1–29. [+ 1 pl.] <https://doi.org/10.5479/si.00963801.61-2439.1>
- Weld LH (1926) Field notes on gall-inhabiting cynipid wasps with descriptions of new species. *Proceedings of the United States National Museum* 68(2611): 1–131. [+ 8 pls.] <https://doi.org/10.5479/si.00963801.68-2611.1>
- Weld LH (1951) Superfamily Cynipoidea. In: Muesebeck CFW, Krombein KV, Townes HK (Eds) *Hymenoptera of America North of Mexico, Synoptic Catalog*. Agricultural Monograph No. 2. United States Government Printing Office, Washington, 594–654. <https://www.biodiversitylibrary.org/page/41966767#page/604/mode/1up>
- Zhang YM, Sasan K, O’Kennon R, Kranz A (2022) Discovery through iNaturalist: new species and new records of oak gall wasps (Hymenoptera: Cynipidae: Cynipini) from Texas, USA. *Zootaxa* 5168(1): 063–074. <https://doi.org/10.11646/zootaxa.5168.1.5>

The wing interference patterns (WIPs) of *Parapanteles* (Braconidae, Microgastrinae): demonstrating a powerful and accessible tool for species-level identification of small and clear winged insects

Shuyang Jin¹, Kyle S. Parks², Daniel H. Janzen³,
Winnie Hallwachs³, Lee A. Dyer⁴, James B. Whitfield⁵

1 Department of Neurobiology, Duke University, Durham NC 27708, USA **2** Department of Physical and Biological Sciences, Western New England University, Springfield MA 01119, USA **3** Department of Biology, University of Pennsylvania, Philadelphia, PA 19104, USA **4** Department of Biology, University of Nevada, Reno NV 89557, Nevada, USA **5** Department of Entomology, University of Illinois Urbana-Champaign, Urbana IL 61801, USA

Corresponding author: Kyle S. Parks (kyle.parks@wne.edu)

Academic editor: J.M. Jasso-Martínez | Received 19 September 2023 | Accepted 25 October 2023 | Published 13 November 2023

<https://zoobank.org/5D12BB28-CFEF-4360-BF27-B0C761D938A0>

Citation: Jin S, Parks KS, Janzen DH, Hallwachs W, Dyer LA, Whitfield JB (2023) The wing interference patterns (WIPs) of *Parapanteles* (Braconidae, Microgastrinae): demonstrating a powerful and accessible tool for species-level identification of small and clear winged insects. Journal of Hymenoptera Research 96: 967–982. <https://doi.org/10.3897/jhr.96.111382>

Abstract

Wing interference patterns (WIPs) are color patterns of insect wings caused by thin film interference. Thin film interference is the same phenomenon responsible for the refracted spectral colors sometimes visible on soap bubbles. Insect WIPs are static patterns due to the variable thickness of wing membranes and the colors produced depend on the thicknesses of wing membranes. While WIPs have been studied in several taxa of small insects, they have not been broadly adopted by insect taxonomists. We surveyed WIPs in one moderate-sized genus of parasitoid wasps, *Parapanteles* (Braconidae: Microgastrinae). Using an inexpensive microscope camera set-up and free imaging and analysis software, we detected consistent WIP differences between *Parapanteles* species. In some cases, WIPs can be used to diagnose sibling species that would otherwise require SEM images to differentiate or DNA barcodes. Wing interference patterns are an underemployed character that may be similarly useful in many other taxa of small clear-winged insects.

Keywords

Braconidae, color patterns, Microgastrinae, *Parapanteles*, WIP, Wing interference patterns

Introduction

Wing interference patterns (WIPs), the rainbow colors that can appear on clear insect wings against dark background, have not been broadly adopted by insect taxonomists as morphological characters. Shevtsova et al. (2011) comprehensively investigated and called attention to these patterns, discovering that they are stable non-iridescent color patterns produced by thin film interference, where light that is reflected off of the upper or lower surface of a clear membrane constructively or destructively interferes with light approaching the membrane. The perceived color pattern is primarily caused by the varying thickness of the wing itself, and are, unlike iridescent colors from butterfly wing scales, static at a range of viewing angles (Shevtsova et al. 2011).

Wing interference patterns are under-used in species descriptions and as a tool for species-level identification of small clear-winged insects. Since their discovery as stable color patterns, they have rarely been reported in taxonomic works and even less frequently been used in species diagnoses or identification keys. In addition to discovering them, Shevtsova et al. (2011) comprehensively described the physical phenomenon that causes them and documented examples of WIPs in several Diptera and Hymenoptera taxa. Since then, WIPs have been documented in just 20 taxonomic or descriptive works (Hansson 2011; Shevtsova and Hansson 2011; Buffington and Sandler 2012; Hansson 2012; Hansson and Shevtsova 2012; Hernández-López et al. 2012; Simon 2012; Stigenberg 2012; Buffington and Condon 2013; Mitroiu 2013; Buffington and Forshage 2014; Drohojowska and Szwedo 2015; Zhang et al. 2014a, 2014b, 2016; Hosseini et al. 2019, 2020, 2021 2021; Pielowska-Ceranowska and Szwedo 2020; Butterworth et al. 2021; Conrow and Gelhaus 2022) and five experimental studies (Katayama et al. 2014; Brydegaard et al. 2018; Hawkes et al. 2019; Dong et al. 2020; White et al. 2021). Most of these studies focus on Hymenoptera (161 species), followed by Diptera (58 species), Hemiptera (8 species), and Odonata (1 species) (Suppl. material 1).

Because WIPs are a function of the varying thickness of wings, some authors have speculated that color may vary intraspecifically because overall wing thickness may be correlated to individual size (Shevtsova and Hansson 2011; Hernández-López et al. 2012). Therefore, they concluded that the colors of WIPs are less important than the patterns they form. Despite this, the majority of taxonomic works that document WIPs describe them in terms of qualitative colors and the relative portion of the wing those colors occupy (e.g., distal 1/3 magenta). Wing interference patterns have been used as characters in species diagnoses in only three publications to date (Hansson 2011; Shevtsova and Hansson 2011; Hansson and Shevtsova 2012), and have been used in a taxonomic key only three times (Mitroiu 2013; Zhang et al. 2014b; Hosseini et al. 2021). Efforts to quantify and compare WIPs have generally found them to be species-specific but rarely sexually dimorphic (Hawkes et al. 2019; Hosseini et al. 2019; Hosseini et al. 2020; Butterworth et al. 2021; White et al. 2021). To-date, WIPs have not been broadly adopted by taxonomists of small insects.

Microgastrinae (Hymenoptera: Braconidae) is a hyper-diverse subfamily of small parasitoid wasps that attack Lepidoptera (Mardulyn and Whitfield 1999). Microgastrinae currently has 2,999 described species (Fernández-Triana et al. 2020), representing roughly 5–10% of the estimated worldwide diversity of this group (Rodríguez et al. 2012; Fernández-Triana and Ward 2015). Their diminutive adult size and small number of morphological characters have made the generic-level taxonomy of this group difficult, and species-level diagnoses, absent DNA barcoding, often rely on subtly variable or minute characters that often require SEM imaging to observe (e.g., Valerio et al. 2009). Wing interference patterns have never been reported for microgastrines but are readily visible in living wasps in a container (DHJ, WH, personal communication).

Parapanteles Ashmead is a small genus of Microgastrinae with several species that are morphologically very similar to other genera (*Dolichogenidea* and *Glyptapanteles*) and frequently misdiagnosed (Valerio et al. 2009; Parks et al. 2020). Here, we document the WIPs of 7 described and 12 putative undescribed *Parapanteles* species from Costa Rica and Ecuador and present a simple and inexpensive method for quantifying and comparing WIPs that can contribute to identification keys and rapid species diagnosis.

Here we present the first study of WIPs in Microgastrinae (Hymenoptera: Braconidae), and an attempt to quantitatively compare the WIPs of closely related species using materials and methods already common in or freely available to most taxonomic laboratories that focus on small clear-winged insects.

Methods

Adult wasps used in this study were collected by two long-term Lepidoptera/parasitoid rearing projects: Área de Conservación Guanacaste (ACG) in Costa Rica (Janzen and Hallwachs 2009, 2016) and Yanayacu Biological Station in Ecuador (Dyer et al. 2017). A list of specimens used in this study is available in Table 1.

One set of fore and hind wings were removed from each adult wasp from samples stored in ethanol. Where available, wings from one male and one female per brood were removed and slide mounted on temporary slides. All species sampled are gregarious (i.e. the female lays multiple eggs in a single host) except *Parapanteles* sp. J and *Parapanteles* sp. K, which are solitary (i.e. females lay a single egg per host). We assume that all wasps eclosing from the cocoons from one caterpillar are siblings. Wings were sandwiched between two microscope slides which were taped together at the ends. This flattens wings more reliably than using a standard slide cover. As in Shevtsova and Hansson 2011, a drop of black India ink was spread on one slide to create a uniform black background behind the wings.

Wings were photographed at 50× magnification using a Cannon Rebel Xsi camera and an Amscope LED-144A-YK 144 LED ring light at maximum brightness. Wing images were not visually adjusted. Materials examined and qualitative descriptions of WIPs are available in Suppl. material 2. Images used in our analyses are available in Suppl. material 3.

Table 1. Materials examined for *Parapanteles* species included in this study from Área de Conservación Guanacaste (ACG), Costa Rica and Yanayacu Biological Station (YBS), Ecuador. Identification numbers for ACG specimens reflect voucher codes for COI DNA barcoding sequences on the Barcode of Life Database (BOLD).

Species	Source	ID #
<i>Parapanteles continua</i>	ACG, Costa Rica	DHJPAR0013724, DHJPAR0013810, DHJPAR0013718, DHJPAR0013733, DHJPAR0020230, DHJPAR0013716, DHJPAR0013725, DHJPAR0020228, DHJPAR0013723, DHJPAR0013717, DHJPAR0020236, DHJPAR0004196, DHJPAR0004192, DHJPAR0004189, DHJPAR0004190, DHJPAR0002808, DHJPAR0004798, DHJPAR0005102, DHJPAR0020859, DHJPAR0020911, DHJPAR0030974, DHJPAR0020231
<i>Parapanteles em</i>	ACG, Costa Rica	DHJPAR0004212, DHJPAR0004543, DHJPAR0004535, DHJPAR0004539, DHJPAR0002757, DHJPAR0020573, DHJPAR0020466, DHJPAR0020785, DHJPAR0020788, DHJPAR0020261, DHJPAR0002802
<i>Parapanteles paradoxus</i>	ACG, Costa Rica	DHJPAR0000248, DHJPAR0012335, DHJPAR0030924, DHJPAR0004544, DHJPAR0004209, DHJPAR0004534, DHJPAR0000246, DHJPAR0004194, DHJPAR0004541, DHJPAR0005103, DHJPAR0004796, DHJPAR0004800
<i>Parapanteles sicpolus</i>	ACG, Costa Rica	DHJPAR0004542, DHJPAR0000204, DHJPAR0000199, DHJPAR0004201, DHJPAR0004200, DHJPAR0004537, DHJPAR0004198, DHJPAR0004187
<i>Parapanteles tessares</i>	ACG, Costa Rica	DHJPAR0030744, DHJPAR0020916, DHJPAR0030733, DHJPAR0030762, DHJPAR0020905, DHJPAR0020850, DHJPAR0020849, DHJPAR0030752, DHJPAR0020904, DHJPAR0020852, DHJPAR0020857, DHJPAR0030773, DHJPAR0030975
<i>Parapanteles tinea</i>	ACG, Costa Rica	DHJPAR0004188
<i>Parapanteles</i> sp. “valerio05”	ACG, Costa Rica	DHJPAR0020792, DHJPAR0012000, DHJPAR0020574, DHJPAR0020570, DHJPAR0020568, DHJPAR0020569, DHJPAR0031011
<i>Parapanteles</i> sp. “B”	YBS, Ecuador	45714, 26049, 37474, 20919, 24670
<i>Parapanteles</i> sp. “C”	YBS, Ecuador	12105, 45981, 48054
<i>Parapanteles</i> sp. “D”	YBS, Ecuador	8275, 35934, 37263, 37275, 37791, 44117
<i>Parapanteles</i> sp. “E”	YBS, Ecuador	36197, 36198, 36520
<i>Parapanteles</i> sp. “H”	YBS, Ecuador	2365, 2366, 2466, 4503
<i>Parapanteles</i> sp. “I”	YBS, Ecuador	42069, 43211, 46466, 66971
<i>Parapanteles</i> sp. “J”	YBS, Ecuador	27850, 27851, 34403, 34413, 36533
<i>Parapanteles</i> sp. “K”	YBS, Ecuador	28620, 32234, 36406, 36534, 38844

The average RGB (red, green, and blue) values of pixels in each fore wing image were measured using the “RGB Measure” feature in ImageJ v1.49 (Schneider et al. 2012). The value for each color component was divided by the average of all three average color values to calculate the relative “redness,” “greenness,” and “blueness” of each fore wing image (e.g., redness= $R / ((R + G + B) / 3)$). This averages out the contribution of black (R/G/B=0/0/0), white (R/G/B=255/255/255), and grey (R/G/B are all equal) pixels.

Arrays of relative redness, greenness, and blueness for each species were tested for normality in R v4.2.2 (R Core Team 2017) using the ‘agricolae’ and ‘nortest’ packages

(Gross and Ligges 2015; de Mendiburu and Yaseen 2020) via the Shapiro-Wilk test and for skewness, and then compared across species via ANOVA and Tukey's HSD test and visualized with ggplot2 (Beck 2017). Species with sample size lower than 3 were excluded from our statistical analysis. Data files and R code are available in Suppl. material 4.

Several metrics of fore wing size were measured to test whether they correlated with WIP patterns, because if they do then species-level differences in WIPs may simply be caused by some species being larger than others. Fore wing length (measured from the junction of C+Sc+R and M+Cu to the distal end of 3/M) and area were compared to each color array. In addition, overall fore wing shape was measured by dividing length by width (measured from the junction of r-rs and the stigma to the distal end of the anal lobe) to test if wing narrowness has any effect on wing thickness. Measurements were done in ImageJ v1.49 (Schneider et al. 2012) and tested for correlation via the Pearson Correlation test in R v4.2.2 (R Core Team 2017) using the 'hmisc' package (Harrell and Dupont 2019).

Linear discriminate function analyses were used to test how useful our quantification of microgastrine WIPs were by themselves for identifying species. Linear discrimination analyses were done in R v4.2.2 (R Core Team 2017). Several subsets of models were tested, and variables included the relative redness/greenness/blueness values for both fore wing and hind wing for all species, fore wing only for all species, hind wing only for all species, fore wing and hind wing data for each subclade containing two or more taxa, fore wing and hind wing data for species collected in the same country (Costa Rica or Ecuador), and fore wing and hind wing data for species that attack the same host family (Erebidae, Geometridae, Notodontidae, or Saturniidae). In each case 50% of the dataset was used to train the model and 50% of the dataset was used for validation. R code and data files are available in Suppl. material 4.

Results

Inter- and intraspecific variation in WIPs

The wing interference patterns of the species surveyed are generally consistent within species, although intraspecific consistency does vary. Both qualitatively (Suppl. material 3) and in terms of relative redness, greenness, and blueness (R.RGBs) (Table 2, Fig. 1), the species with purplish WIPs (*Parapanteles tessares*, *P. continua*, *P. sicpolus*, and *P. sp. H*) have the most consistent WIPs, while species with reddish or yellowish WIPs are more variable, especially *Parapanteles sp. J* and *Parapanteles sp. K*.

All R.RGB arrays were normally distributed except two *P. continua* arrays, one *Parapanteles sp. E*, one *P. paradoxus*, one *P. sicpolus*, and four *P. tessares* arrays (Table 2). The distributions of fore wing and hind wing R.RGBs among closely related species are often similar with one or two parameters significantly different (Fig. 1). For example, the R.RGBs of the sister species *P. tessares* and *P. continua* are not significantly different except for fore wing relative redness (higher in *P. continua*) and relative blueness

Table 2. Average relative redness (RR), greenness (RG), and blueness (RB) of the fore and hind wings of fifteen *Parapanteles* species plus or minus one standard deviation, with results of Tukey's HSD test, skewness, and Shapiro-Wilks' test for normality.

Wing	Species	n	Ave. RR	HSD	Skew	P-value	Ave. RG	HSD	Skew	P-value	Ave. RB	HSD	Skew	P-value
Fore	<i>Parapanteles continua</i>	41	1.05 ± 0.021	e	0.22	0.44	0.864 ± 0.018	bc	-1.19	0.01	1.086 ± 0.025	b	0.22	0.75
	<i>Parapanteles em</i>	16	1.149 ± 0.025	c	-0.52	0.60	0.836 ± 0.038	cd	1.21	0.09	1.016 ± 0.031	c	-0.22	0.96
	<i>Parapanteles paradoxus</i>	16	1.199 ± 0.023	ab	-0.29	0.91	0.912 ± 0.022	ab	-0.38	0.25	0.89 ± 0.033	f	0.43	0.05
	<i>Parapanteles sicpulus</i>	14	1.042 ± 0.013	ef	-0.78	0.25	0.884 ± 0.009	ab	0.59	0.55	1.074 ± 0.017	b	0.90	0.13
	<i>Parapanteles</i> sp. B	8	1.216 ± 0.029	a	-0.55	0.45	0.897 ± 0.051	ab	-0.75	0.10	0.887 ± 0.063	f	1.13	0.52
	<i>Parapanteles</i> sp. C	3	1.119 ± 0.018	cd	0.21	0.92	0.832 ± 0.018	cd	-0.72	0.73	1.049 ± 0.03	bc	-1.64	0.21
	<i>Parapanteles</i> sp. D	10	1.169 ± 0.029	bc	-0.15	0.86	0.834 ± 0.044	cd	0.57	0.54	0.997 ± 0.051	cd	0.59	0.50
	<i>Parapanteles</i> sp. E	3	1.183 ± 0.017	abc	0.51	0.81	0.915 ± 0.028	ab	-1.71	0.11	0.902 ± 0.013	ef	0.54	0.80
	<i>Parapanteles</i> sp. H	9	1.088 ± 0.022	d	1.13	0.19	0.813 ± 0.026	d	0.09	0.73	1.099 ± 0.039	b	-1.04	0.35
	<i>Parapanteles</i> sp. I	4	1.214 ± 0.05	ab	-0.71	0.87	0.929 ± 0.026	a	0.47	0.28	0.857 ± 0.037	f	0.01	0.06
	<i>Parapanteles</i> sp. J	5	1.212 ± 0.015	ab	1.07	0.50	0.887 ± 0.029	ab	-0.03	0.25	0.9 ± 0.04	ef	-0.70	0.25
	<i>Parapanteles</i> sp. K	5	1.142 ± 0.078	c	-0.58	0.90	0.889 ± 0.026	ab	-0.17	0.42	0.968 ± 0.069	cde	1.52	0.25
	<i>Parapanteles</i> sp. valerio05	7	1.178 ± 0.032	abc	-0.98	0.44	0.868 ± 0.041	bc	0.33	0.41	0.954 ± 0.06	de	0.82	0.58
	<i>Parapanteles</i> sp. tessares	25	1.012 ± 0.025	f	0.43	0.38	0.827 ± 0.025	cd	1.17	0.01	1.161 ± 0.036	a	-2.11	0.00
	<i>Parapanteles thinea</i>	3	1.163 ± 0.026	bc	1.19	0.52	0.915 ± 0.026	ab	-1.57	0.28	0.922 ± 0.043	def	-1.05	0.58
Hind	<i>Parapanteles continua</i>	41	1.049 ± 0.026	f	0.03	0.84	0.89 ± 0.012	a	-0.63	0.31	1.062 ± 0.025	ab	1.02	0.02
	<i>Parapanteles em</i>	16	1.129 ± 0.023	cd	-0.60	0.29	0.84 ± 0.034	b	1.09	0.10	1.031 ± 0.046	bc	-0.54	0.39
	<i>Parapanteles paradoxus</i>	16	1.168 ± 0.026	bcd	1.06	0.26	0.863 ± 0.023	ab	0.53	0.71	0.969 ± 0.034	def	-0.14	0.70
	<i>Parapanteles sicpulus</i>	14	1.045 ± 0.012	f	2.16	0.00	0.894 ± 0.009	a	-0.64	0.47	1.062 ± 0.016	ab	-0.73	0.68
	<i>Parapanteles</i> sp. B	8	1.169 ± 0.032	abcd	0.04	1.00	0.872 ± 0.031	ab	0.24	0.23	0.959 ± 0.047	def	-0.82	0.11
	<i>Parapanteles</i> sp. C	3	1.106 ± 0.018	de	-0.69	0.74	0.839 ± 0.005	b	1.62	0.23	1.055 ± 0.016	abc	1.60	0.25
	<i>Parapanteles</i> sp. D	10	1.151 ± 0.042	bcd	0.14	0.87	0.835 ± 0.029	b	-0.09	0.35	1.014 ± 0.046	bcd	0.61	0.74
	<i>Parapanteles</i> sp. E	3	1.172 ± 0.052	abcd	1.73	0.03	0.895 ± 0.014	a	-1.48	0.35	0.933 ± 0.066	ef	-1.72	0.06
	<i>Parapanteles</i> sp. H	9	1.07 ± 0.014	ef	0.11	0.18	0.839 ± 0.018	b	0.09	1.00	1.091 ± 0.015	a	0.89	0.22
	<i>Parapanteles</i> sp. I	4	1.222 ± 0.043	a	1.23	0.55	0.875 ± 0.029	ab	-1.14	0.29	0.904 ± 0.065	f	-0.34	0.30
	<i>Parapanteles</i> sp. J	5	1.191 ± 0.039	ab	0.54	0.93	0.854 ± 0.043	ab	0.20	0.71	0.955 ± 0.078	def	-1.63	0.18
	<i>Parapanteles</i> sp. K	5	1.142 ± 0.041	bcd	0.72	0.81	0.867 ± 0.038	ab	0.40	0.41	0.99 ± 0.03	cde	0.19	0.27
	<i>Parapanteles</i> sp. valerio05	7	1.17 ± 0.033	abcd	0.22	0.75	0.891 ± 0.034	a	0.20	0.46	0.939 ± 0.06	ef	-0.34	0.73
	<i>Parapanteles tessares</i>	25	1.067 ± 0.019	ef	-0.58	0.02	0.853 ± 0.022	ab	1.46	0.00	1.081 ± 0.026	a	0.94	0.06
	<i>Parapanteles thinea</i>	3	1.186 ± 0.039	abc	0.45	0.83	0.874 ± 0.033	ab	-1.12	0.55	0.94 ± 0.072	def	0.20	0.93

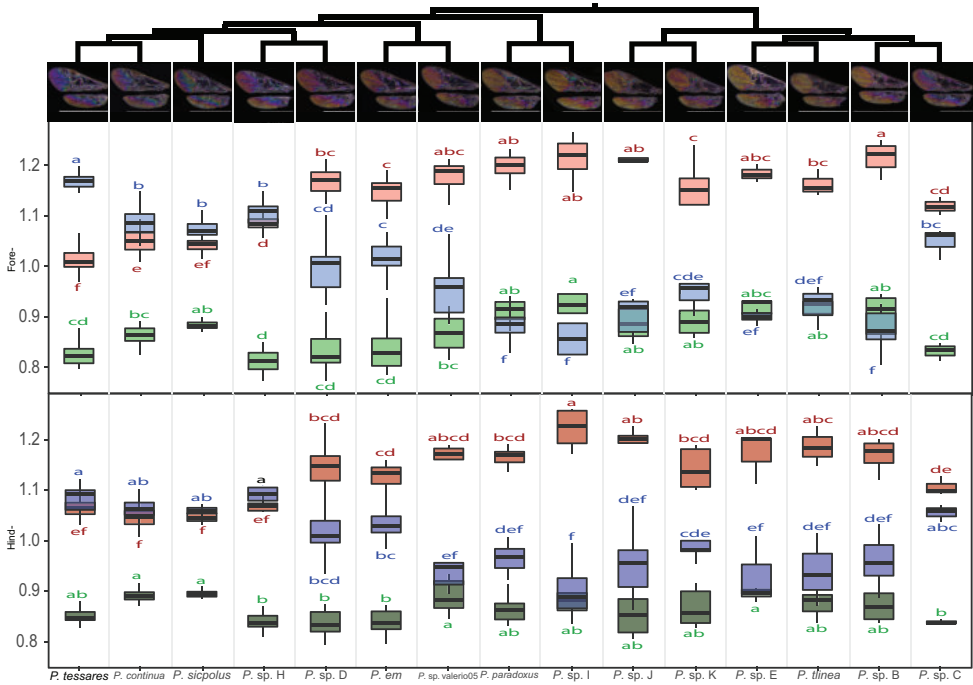


Figure 1. Box-and-whiskers plots of forewing and hind wing wing interference pattern relative redness (RR), greenness (RG), and blueness (RB) shown in phylogenetic order. The cladogram above the figure is based on results from Parks et al. 2020. RR box-and-whiskers are shown in red, RB in blue, and RG in green (for colorblind: all RR values are greater than their corresponding RG values, so all red box-and-whisker plots are above green box-and-whisker plots in the figure). Results of Tukey’s HSD test are displayed above or below each box-and-whisker. The white horizontal bar below each wing image represents 2 mm.

(higher in *P. tessares*), which corroborates the more uniformly purple appearance of *P. tessares*’s WIP.

We did not find evidence of sexual dimorphism in *Parapanteles* WIPs. Males and females of most species have similar WIPs, although in *Parapanteles* sp. D and *P. em* male WIPs are slightly more yellowish (Suppl. material 3: f and g.). Sexual dimorphism could not be assessed for 6 species: only females were available for *Parapanteles* sp. C, sp. J, sp. K, and sp. Valerio05, and only males were available for *Parapanteles* sp. I and sp. E.

Relative redness, greenness, and blueness and wing size

The majority of R.RGB arrays were not significantly correlated with wing length, area, or shape. Eleven of the 33 R.RGB tested were significantly correlated with wing length and 8 of 33 were significantly correlated with wing area. In each case the slope of the line of regression was slight and no R.RGB arrays were correlated with wing shape (Table 3).

Table 3. Average length, area, and shape (length/height) of the fore wings of fifteen *Parapanteles* species plus or minus one standard deviation, with coefficient of determination and the *p*-value of Pearson correlation tests of each measurement for each fore wing color array (relative redness (RR), greenness (RG), and blueness (RB)).

Species	n	Fore wing measurement	Average	*/RR r ²	<i>p</i>	*/RG r ²	<i>p</i>	*/RB r ²	<i>p</i>
<i>Parapanteles continua</i>	41	Length* (mm)	2.5 ± 0.18	0.09	0.06	0.16	0.01	0.29	0.00
		Height (mm)	0.67 ± 0.05	—	—	—	—	—	—
		Area* (mm ²)	0.67 ± 0.05	0.06	0.13	0.15	0.01	0.24	0.00
		Shape* (L/H)	3.76 ± 0.13	0.01	0.56	0.01	0.51	0.03	0.33
<i>Parapanteles em</i>	16	Length* (mm)	2.36 ± 0.21	0.45	0.00	0.79	0.00	0.29	0.03
		Height (mm)	0.64 ± 0.06	—	—	—	—	—	—
		Area* (mm ²)	0.64 ± 0.06	0.42	0.01	0.85	0.00	0.35	0.02
		Shape* (L/H)	3.71 ± 0.14	0.00	0.84	0.01	0.71	0.03	0.55
<i>Parapanteles paradoxus</i>	16	Length* (mm)	2.36 ± 0.21	0.08	0.28	0.04	0.49	0.01	0.76
		Height (mm)	0.62 ± 0.05	—	—	—	—	—	—
		Area* (mm ²)	0.62 ± 0.05	0.08	0.28	0.12	0.19	0.00	0.92
		Shape* (L/H)	3.81 ± 0.23	0.00	0.88	0.01	0.73	0.01	0.73
<i>Parapanteles sicpulus</i>	14	Length* (mm)	2.74 ± 0.13	0.24	0.08	0.07	0.34	0.24	0.07
		Height (mm)	0.74 ± 0.04	—	—	—	—	—	—
		Area* (mm ²)	0.74 ± 0.04	0.25	0.07	0.04	0.47	0.23	0.08
		Shape* (L/H)	3.7 ± 0.18	0.03	0.53	0.03	0.53	0.04	0.47
<i>Parapanteles</i> sp. B	8	Length* (mm)	2.11 ± 0.1	0.00	0.87	0.86	0.00	0.49	0.05
		Height (mm)	0.51 ± 0.03	—	—	—	—	—	—
		Area* (mm ²)	0.51 ± 0.03	0.08	0.49	0.69	0.01	0.28	0.18
		Shape* (L/H)	4.16 ± 0.15	0.37	0.11	0.04	0.65	0.18	0.30
<i>Parapanteles</i> sp. D	10	Length* (mm)	3.59 ± 0.15	0.00	0.95	0.66	0.00	0.48	0.03
		Height (mm)	0.93 ± 0.06	—	—	—	—	—	—
		Area* (mm ²)	0.93 ± 0.06	0.01	0.79	0.76	0.00	0.49	0.02
		Shape* (L/H)	3.88 ± 0.14	0.00	0.98	0.13	0.30	0.10	0.36
<i>Parapanteles</i> sp. H	9	Length* (mm)	3.11 ± 0.47	0.06	0.53	0.00	0.88	0.01	0.82
		Height (mm)	0.82 ± 0.13	—	—	—	—	—	—
		Area* (mm ²)	0.82 ± 0.13	0.06	0.51	0.00	0.00	0.02	0.72
		Shape* (L/H)	3.81 ± 0.08	0.10	0.42	0.37	0.08	0.34	0.10
<i>Parapanteles</i> sp. J	5	Length* (mm)	2.96 ± 0.21	0.02	0.82	0.02	0.83	0.00	0.95
		Height (mm)	0.78 ± 0.07	—	—	—	—	—	—
		Area* (mm ²)	0.78 ± 0.07	0.03	0.77	0.03	0.77	0.00	0.93
		Shape* (L/H)	3.81 ± 0.12	0.62	0.11	0.01	0.85	0.16	0.50
<i>Parapanteles</i> sp. K	5	Length* (mm)	2.66 ± 0.47	0.62	0.11	0.02	0.83	0.74	0.06
		Height (mm)	0.7 ± 0.12	—	—	—	—	—	—
		Area* (mm ²)	0.7 ± 0.12	0.09	0.16	0.02	0.82	0.61	0.12
		Shape* (L/H)	3.81 ± 0.17	0.16	0.51	0.05	0.71	0.29	0.35
<i>Parapanteles</i> sp. valerio05	7	Length* (mm)	2.4 ± 0.13	0.07	0.58	0.48	0.09	0.10	0.48
		Height (mm)	0.62 ± 0.04	—	—	—	—	—	—
		Area* (mm ²)	0.62 ± 0.04	0.02	0.77	0.55	0.06	0.18	0.35
		Shape* (L/H)	3.87 ± 0.2	0.30	0.20	0.10	0.49	0.25	0.25
<i>Parapanteles tessares</i>	25	Length* (mm)	2.33 ± 0.09	0.04	0.37	0.18	0.03	0.18	0.03
		Height (mm)	0.61 ± 0.04	—	—	—	—	—	—
		Area* (mm ²)	0.61 ± 0.04	0.00	0.89	0.13	0.08	0.07	0.19
		Shape* (L/H)	3.83 ± 0.15	0.00	0.91	0.00	0.73	0.00	0.78

Linear discriminate function analysis

Results for linear discriminate function analyses varied widely and are available in Suppl. material 4. Linear discriminate function analysis using our complete dataset predicted species accurately only 34% of the time, but was more accurate with some subsets of species separated by subclade, geography, or host use (e.g., species prediction of species found in Costa Rica was 83% and species parasitizing saturniids was 75%).

Discussion

The wing interference patterns of *Parapanteles* are consistent within species and distinct between species, often enough to be diagnostic by themselves. Among the species surveyed, the WIPs of *Parapanteles tessares*, *P. continua*, *P. sicpolus*, *P. sp. H*, and *P. sp. C* were the most distinct. These species tended to have more green and purple in their WIPs, while the remaining species' WIPs were predominantly red and/or yellow.

Wing interference patterns are directly related to the thickness of wing membranes, and previous publications have speculated that WIP colors should change as individuals get larger because cuticle thickness may increase with body size (Shevtsova and Hansson 2011; Hernández-López et al. 2012). We are not aware of any studies investigating the allometry of body or wing cuticle thickness. Among the species we surveyed, some relative redness, greenness, and/or blueness arrays were significantly correlated with wing size and/or area in some species, but in each of these cases the slope of the corresponding linear regression was very slight (Table 3). Correlation with wing size (as a proxy for body size) alone does not account for the differences between the WIPs of closely related *Parapanteles* species. We were not able to use WIPs alone to reliably predict the identity of an unknown specimen from a large number of species, but were able to discriminate between species in some subclades or subsets of species defined by location or host use (Suppl. material 4). Wing interference patterns are not likely to be useful for automated species identification for many taxa, but are useful as an additional and generally overlooked morphological character to be used in conjunction with other characters for species diagnosis, as any morphological character traditionally would be. When viewed this way they are often one of the most conspicuous and accessible morphological characters of the physically small taxa on which they appear.

Wing interference patterns are directly related to the wavelength of the light passing through the wing membrane, which is a major weakness for using any measurement derived from RGB values for diagnostic purposes. The relative RGB values we measured in this study were not consistent if the wing was illuminated with a different light source. This limitation can be solved by using a consistent light source, and the light source which we used for all WIP photographs in this study, an Amscope LED-144A-YK 144 LED ring light, is widely available and relatively inexpensive. Using one or more lasers of specific wavelengths to illuminate WIPs could offer a more replicable

and standardizable method for documenting WIPs, although using one or a few wavelengths would result in less data than full spectrum white light. Wing interference patterns can be observed *in situ* on pinned specimens, but these are of little use compared to WIPs observed on slide-mounted wings. Including WIP slides (wing slides with India Ink painted on the back) of at least a few paratype individuals with the type series of small winged insects would ameliorate most of the problem posed by variations between light sources, and expand the usefulness of WIPs for future studies.

Experiments in *Drosophila* have repeatedly shown WIPs to be subject to sexual selection (Katayama et al. 2014; Hawkes et al. 2019). While this has not been experimentally tested in other taxa, this and other studies have found that WIPs are frequently species-specific (Shevtsova et al. 2011; Buffington and Sandler 2012; Zhang et al. 2014b, 2016; Hosseini et al. 2019; Butterworth et al. 2021; Hosseini et al. 2021). Similarly to the *Drosophila* species used in the sexual selection experiments, microgastrinae males also display their wings to females during courtship (Bredlau and Kester 2019). The colors of WIPs are visible *in situ* and in natural settings whenever insect wings are displayed in front of a dark background (e.g. green leaves), and the colors that compose them occur in spectra visible to most insects (Shevtsova et al. 2011; Brydegaard et al. 2018; Butterworth et al. 2021). Anecdotally, we found that closely related sympatric species tended to be more subjectively different (i.e. (*Parapanteles tessares*, *P. continua*), *P. sicpolus*) and (*P. em*, *P. valerio05*) from Costa Rica and (*P. sp. B*, *P. sp. C*) from Ecuador), while closely related allopatric species tended to be less distinct (i.e. (*P. paradoxus*, *P. sp. I*) and (*P. sp. E*, *P. tinea*) (Fig. 2). This suggests that WIPs may be used by microgastrines for conspecific recognition, but this is entirely speculative and would require a broader survey of microgastrine WIPs to test. We only included two solitary species (i.e. females oviposit a single egg into each host, *P. sp. J* and *P. sp. K*) in our study. These two species had the most variable WIPs and wing sizes. The relationship to host quality and adult wasp size may be more direct in solitary

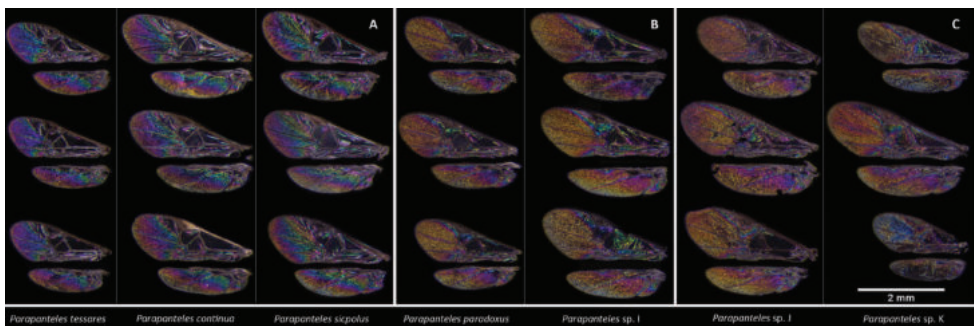


Figure 2. Right wings of three different individuals from seven *Parapanteles* species showing wing interference patterns. A shows three gregarious sympatric sister species ((*P. tessares*, *P. continua*), *P. sicpolus*) from Area de Conservación Guanacaste (ACG) in Costa Rica. B shows two gregarious allopatric sister species, one from AVG (*P. paradoxus*) and one from Yanayacu Biological Station in Ecuador (*P. sp. I*). C shows two solitary sister species from Yanayacu Biological Station.

species that use small host caterpillars than gregarious species attacking larger caterpillars. In such solitary species, poor quality hosts may have less resources available for parasitoids and result in smaller adults, while gregarious species can oviposit fewer eggs to account for poor quality hosts which may result in more consistent adult wasp sizes. Even so, *P.* sp. J fore wings are significantly redder than *P.* sp. K (Figs 1, 2).

Conclusions

In general, WIPs can be observed and documented with very little additional effort for most taxonomists who work on small winged insects. We predict that they can be a large source of new morphological characters for the taxonomy and systematics of these tiny animals. The only materials required are a dissecting microscope with a camera attachment, a ring light, glass slides, and India Ink. Wing interference patterns are often species-specific and useful for *Parapanteles* wasps, and will likely be for most other microgastrine wasps.

Acknowledgments

This work was supported in part by the National Science Foundation grant DEB 1146119 and DEB 1442103. We thank the National Institute of Biodiversity – Ecuador (INABIO) for support and the Ministry of the Environment of Ecuador for providing permits under the genetic access contract MAE-DNB-CM-2016-0045 and the project “Interacciones entre plantas, orugas, y parasitoides de los Andes del Ecuador.” All specimens were collected, exported and to be DNA barcoded under Costa Rican government permits issued to BioAlfa (Janzen and Hallwachs 2019) (R-054-2022-OT-CONAGEBIO; R-019-2019-CONAGEBIO; National Published Decree #41767), JICA-SAPI #0328497 (2014) and DHJ and WH (ACG-PI-036-2013; R-SINAC-ACG-PI-061-2021; Resolución N°001-2004 SINAC; PI-028-2021). We thank the GDFCF/ACG parataxonomist team of Area de Conservacion Guanacaste, northwestern Costa Rica for finding and rearing the caterpillar hosts of these parasites, which are documented individually by their DHJPAR..... voucher codes at <http://janzen.sas.upenn.edu/caterpillars/database.lasso>.

References

- Beck MW (2017) Ggord: Ordination Plots with ggplot2. R packages version 1.0.0. <https://zenodo.org/badge/latest/doi/35334615>
- Buffington ML, Sandler RJ (2012) The occurrence and phylogenetic implication of wing interference patterns in Cynipoidea (Insecta: Hymenoptera). *Invertebrate Systematics* 25: 586–597. <https://doi.org/10.1071/IS11038>

- Buffington ML, Condon M (2013) The description and bionomics of *Tropideucoila blepharoneurae* Buffington and Condon, new species (Hymenoptera: Figitidae: Zaeucoilini), parasitoid of *Blepharoneura* Loew fruit flies (Tephritidae). *Proceedings of the Entomological Society of Washington* 115(4): 349–357. <https://doi.org/10.4289/0013-8797.115.4.349>
- Buffington ML, Forshage M (2014) The Description of *Gurudella* Buffington and Forshage, new genus (Hymenoptera: Figitidae: Eucoilinae). *Proceedings of the Entomological Society of Washington* 116(3): 225–242. <https://doi.org/10.4289/0013-8797.116.3.225>
- Bredlau JP, Kester KM (2019) Evolutionary relationships of courtship songs in the parasitic wasp genus, *Cotesia* (Hymenoptera: Braconidae). *PLoS ONE* 14(1): e0210249. <https://doi.org/10.1371/journal.pone.0210249>
- Brydegaard M, Jansson S, Schulz M, Runemark A (2018) Can the narrow red bands of dragonflies be used to perceive wing interference patterns? *Ecology and Evolution* 8: 5369–5384. <https://doi.org/10.1002/ece3.4054>
- Butterworth NJ, White TE, Byrne PG, Wallman JF (2021) Love at first flight: wing interference patterns are species-specific and sexually dimorphic in blowflies (Diptera: Calliphoridae). *Journal of Evolutionary Biology* 34: 558–570. <https://doi.org/10.1111/jeb.13759>
- Conrow RT, Gelhaus JK (2022) Wing interference patterns are consistent and sexually dimorphic in the four families of crane flies (Diptera, Tipuloidea). *ZooKeys* 1080: 1356–163. <https://doi.org/10.3897/zookeys.1080.69060>
- de Mendiburu F, Yaseen M (2020) *Agricolae: Statistical Procedures for Agricultural Research*. R package version 1.4.0. <https://myaseen208.github.io/agricolae/https://cran.r-project.org/package=agricolae>
- Dong W, Gao YH, Zhang XB, Moussian B, Zhang JZ (2020) Chitinase 10 controls chitin amounts and organization in the wing cuticle of *Drosophila*. *Insect Science* 27: 1198–1207. <https://doi.org/10.1111/1744-7917.12774>
- Drohojowska J, Szewo J (2015) Early Cretaceous Aleyrodidae (Hemiptera: Sternorrhyncha) from the Lebanese amber. *Cretaceous Research* 52: 368–389. <https://doi.org/10.1016/j.cretres.2014.03.015>
- Dyer LA, Miller JS, Rab Green SB, Gentry GL, Greeney HF, Walla TW (2017) Caterpillars and parasitoids of the Eastern Andes in Ecuador. <http://www.caterpillars.org>
- Fernández-Triana JL, Ward D (2015) *Microgastrinae Wasps of the World*. <http://microgastrinae.myspecies.info> [6/8/2017]
- Fernández-Triana JL, Shaw MR, Boudreault C, Beaudin M, Broad GR (2020) Annotated and illustrated world checklist of Microgastrinae parasitoid wasps (Hymenoptera, Braconidae). *ZooKeys* 920: 1–1089. <https://doi.org/10.3897/zookeys.920.39128>
- Gross J, Ligges U (2015) *Nortest: Tests for Normality*. <https://cran.r-project.org/package=nortest>
- Janzen DH, Hallwachs W (2009) Dynamic database for an inventory of the macrocaterpillar fauna, and its food plants and parasitoids, of Área de Conservación Guanacaste (ACG), northwestern Costa Rica (nn-SRNP-nnnnn voucher codes). <http://janzen.sas.upenn.edu>
- Janzen DH, Hallwachs W (2016) DNA barcoding the Lepidoptera inventory of a large complex tropical conserved wildland, Área de Conservación Guanacaste, northwestern Costa Rica. *Genome* 59: 641–660. <https://doi.org/10.1139/gen-2016-0005>

- Hansson C (2011) *Cornugon* (Hymenoptera: Eulophidae: Entedoninae) a new genus from tropical America including ten new species. *Zootaxa* 2873: 1–26. <https://doi.org/10.11646/zootaxa.2873.1.1>
- Hansson C (2012) *Achrysocharoides* Girault (Hymenoptera, Eulophidae) new to tropical America, with eight new species. *Zookeys* 173: 79–108. <https://doi.org/10.3897/zookeys.173.2653>
- Hansson C, Shevtsova E (2012) Revision of the European species of *Omphale* Haliday (Hymenoptera, Chalcidoidea, Eulophidae). *ZooKeys* 232: 1–157. <https://doi.org/10.3897/zookeys.232.3625>
- Harrel Jr F, Dupont CH (2019) Hmisc: Harrell Miscellaneous. R Package Version 4.2-0. <https://CRAN.R-project.org/package=Hmisc>
- Hawkes MF, Duffy E, Joag R, Skeats A, Radwan J, Wedell N, Sharma MD, Hosken DJ, Troschianko J (2019) Sexual selection drives the evolution of male wing interference patterns. *Proceedings of the Royal Society B* 286: e20182850. <https://doi.org/10.1098/rspb.2018.2850>
- Hernández-López A, Rougerie R, Augustin S, Lees DC, Tomov R, Kenis M, Çota E, Kullaj E, Hansson C, Grabenweger G, Rogues A, López-Vaamonde C (2012) Host tracking or cryptic adaptation? Phylogeography of *Pediobius saulius* (Hymenoptera, Eulophidae), a parasitoid of the highly invasive horse-chestnut leafminer. *Evolutionary Applications* 5(3): 256–269. <https://doi.org/10.1111/j.1752-4571.2011.00220.x>
- Hosseini F, Lotfalizadeh H, Norouzi M, Dadpour M (2019) Wing interference colours in *Eurytoma* (Hymenoptera: Eurytomidae): variation in patterns among populations and sexes of five species. *Systematics and Biodiversity* 17(7): 679–689. <https://doi.org/10.1080/14772000.2019.1687603>
- Hosseini F, Lotfalizadeh H, Norouzi M, Dapour M (2020) Wing interference patterns and colours of *Oomyzus sokolowskii* (Kurdjomov) (Hymenoptera: Eulophidae). *International Journal of Environmental Studies* 78(3): 484–490. <https://doi.org/10.1080/00207233.2020.1824729>
- Hosseini F, Lotfalizadeh H, Rakhshani E, Norouzi M, Butterworth NJ, Dadpour M (2021) Significance of wing interference patterns as taxonomic characters in Aphidiinae (Hymenoptera: Braconidae). *Journal of Zoological Systematics and Evolutionary Research* 59: 1481–1490. <https://doi.org/10.1111/jzs.12542>
- Katayama N, Abbott JK, Kjærandsen J, Takahashi Y, Svensson EI (2014) Sexual selection on wing interference patterns in *Drosophila melanogaster*. *Proceedings of the National Academy of Sciences* 111(42): 15144–15148. <https://doi.org/10.1073/pnas.1407595111>
- Mardulyn P, Whitfield JB (1999) Phylogenetic signal in the COI, 16S, and 28S genes for inferring relationships among genera of Microgastrinae (Hymenoptera; Braconidae): evidence of a high diversification rate in this group of parasitoids. *Molecular Phylogenetics and Evolution* 12(3): 282–294. <https://doi.org/10.1006/mpev.1999.0618>
- Mitroiu MD (2013) Taxonomic review of Afrotropical *Watshamia* Bouček (Hymenoptera: Pteromalidae), with description of a new species. *Entomological Science* 166: 191–195. <https://doi.org/10.1111/j.1479-8298.2012.00554.x>
- Parks KS, Janzen DH, Hallwachs W, Fernández-Triana J, Dyer LA, Rodriguez JJ, Arias-Penna DC, Whitfield JB (2020) A five-gene molecular phylogeny reveals *Parapanteles* Ashmead

- (Hymenoptera: Braconidae) is polyphyletic as currently composed. *Molecular Phylogenetics and Evolution* 150: e106859. <https://doi.org/10.1016/j.ympev.2020.106859>
- Pielowska-Ceranowska A, Szewdo J (2020) Wing interference Patterns in patterned wings of *Culicoides* Latreille, 1809 (Diptera: Ceratopogonidae)-exploring potential identification tool. *Zootaxa* 4868(3): 389–407. <https://doi.org/10.11646/zootaxa.4868.3.4>
- R Core Team (2017) R: A Language and Environment for Statistical Computing, R Foundation for Statistical Computing, Vienna. <https://www.R-project.org>
- Rodríguez JJ, Fernández-Triana JL, Smith MA, Janzen DH, Hallwachs W, Erwin TL, Whitfield JB (2012) Extrapolations from field studies and known faunas converges on dramatically increased estimates of global microgastrine parasitoid wasp species richness (Hymenoptera: Braconidae). *Insect Conservation and Diversity* 6(4): 530–536. <https://doi.org/10.1111/icad.12003>
- Schneider CA, Rasband WS, Eliceiri KW (2012) NIH Image to ImageJ: 25 years of image analysis. *Nature Methods* 9(7): 671–675. <https://doi.org/10.1038/nmeth.2089>
- Shevtsova E, Hansson C (2011) Species recognition through wing interference patterns (WIPs) in *Achrysocharoides* Girault (Hymenoptera, Eulophidae) including two new species. *ZooKeys* 154: 9–30. <https://doi.org/10.3897/zookeys.154.2158>
- Shevtsova E, Hansson C, Janzen DH, Kjærandsen J (2011) Stable structural color patterns displayed on transparent insect wings. *Proceedings of the National Academy of Sciences* 108(2): 668–673. <https://doi.org/10.1073/pnas.1017393108>
- Simon E (2012) Preliminary study of wing interference patterns (WIPs) in some species of soft scale (Hemiptera, Sternorrhyncha, Coccoidea, Coccidae). *ZooKeys* 319: 269–281. <https://doi.org/10.3897/zookeys.319.4219>
- Stigenberg J (2012) *Spathicopis* van Achterberg, 1977 (Braconidae, Euphorinae) a new wasp genus for Sweden, with a spoon shaped ovipositor. *Entomologisk Tidskrift* 133(4): 1–4.
- Valerio AA, Whitfield JB, Janzen DH (2009) Review of the world *Parapanteles* Ashmead (Hymenoptera: Braconidae: Microgastrinae), with description of fourteen new Neotropical species and the first description of the final instar larvae. *Zootaxa* 2084: 1–49. <https://doi.org/10.11646/zootaxa.2084.1.1>
- White TE, Locke A, Latty T (2021) Heightened condition dependent expression of structural colouration in the faces, but not wings, of male and female flies. *Current Zoology* 2021: 1–8. <https://doi.org/10.1101/2021.06.09.447681>
- Zhang M, Chen J, Gao X, Pape T, Zhang D (2014a) First description of the female *Sarcophage* (*Sarcorohdendorfia*) *gracilior* (Chen, 1975) (Diptera, Sarcophagidae). *ZooKeys* 396: 43–53. <https://doi.org/10.3897/zookeys.396.6752>
- Zhang M, Chu WW, Pape T, Zhang D (2014b) Taxonomic review of the *Sphecapatodes ornate* group (Diptera: Sarcophagidae: Miltogramminae), with description of one new species. *Zoological Studies* 53: e48. <https://doi.org/10.1186/s40555-014-0048-9>
- Zhang D, Ge YQ, Li XY, Liu XH, Zhang M, Wang RR (2016) Review of the *Lispe caesia*-group (Diptera: Muscidae) from Palaearctic and adjacent regions, with redescrptions and one new synonymy. *Zootaxa* 4098(1): 043–072. <https://doi.org/10.11646/zootaxa.4098.1.2>

Supplementary material 1

Taxonomic summary of published wing interference pattern images and/or descriptions

Authors: Shuyang Jin, Kyle S. Parks, Daniel H. Janzen, Winnie Hallwachs, Lee A. Dyer, James B. Whitfield

Data type: xlsx

Copyright notice: This dataset is made available under the Open Database License (<http://opendatacommons.org/licenses/odbl/1.0/>). The Open Database License (ODbL) is a license agreement intended to allow users to freely share, modify, and use this Dataset while maintaining this same freedom for others, provided that the original source and author(s) are credited.

Link: <https://doi.org/10.3897/jhr.96.111382.suppl1>

Supplementary material 2

Qualitative descriptions and materials examined for *Parapanteles* species included in this study

Authors: Shuyang Jin, Kyle S. Parks, Daniel H. Janzen, Winnie Hallwachs, Lee A. Dyer, James B. Whitfield

Data type: docx

Copyright notice: This dataset is made available under the Open Database License (<http://opendatacommons.org/licenses/odbl/1.0/>). The Open Database License (ODbL) is a license agreement intended to allow users to freely share, modify, and use this Dataset while maintaining this same freedom for others, provided that the original source and author(s) are credited.

Link: <https://doi.org/10.3897/jhr.96.111382.suppl2>

Supplementary material 3

Wing interference patterns

Authors: Shuyang Jin, Kyle S. Parks, Daniel H. Janzen, Winnie Hallwachs, Lee A. Dyer, James B. Whitfield

Data type: zip

Explanation note: Wing interference patterns of *Parapanteles tessares* (a), *P. continua* (b and c), *P. sicpolus* (d), *P. sp. H* (e), *P. sp. D* (f), *P. em* (g), *P. sp. valerio05* (h), *P. paradoxus* (i), *P. sp. I* (j), *P. sp. J* (k), *P. sp. K* (l), *P. sp. E* (m), *P. tlinea* (n), *P. sp. B* (o), and *P. sp. C* (p). Female wings are shown to the left and males to the right. Horizontal pairs of wing images are of sibling wasps from the same reared brood while each vertical set is from a distinct brood.

Copyright notice: This dataset is made available under the Open Database License (<http://opendatacommons.org/licenses/odbl/1.0/>). The Open Database License (ODbL) is a license agreement intended to allow users to freely share, modify, and use this Dataset while maintaining this same freedom for others, provided that the original source and author(s) are credited.

Link: <https://doi.org/10.3897/jhr.96.111382.suppl3>

Supplementary material 4

Data files and R code

Authors: Shuyang Jin, Kyle S. Parks, Daniel H. Janzen, Winnie Hallwachs, Lee A. Dyer, James B. Whitfield

Data type: zip

Explanation note: Data files and R code used to calculate mean, standard deviation, ANOVA, Tukey's HSD, Skewness, Shapiro-Wilks normality test, and linear discriminate functions analysis of forewing and hindwing relative redness, greenness, and blueness, and Pearson's correlation of forewing length, forewing area, and forewing shape (H/L) to forewing relative redness, greenness, and blueness.

Copyright notice: This dataset is made available under the Open Database License (<http://opendatacommons.org/licenses/odbl/1.0/>). The Open Database License (ODbL) is a license agreement intended to allow users to freely share, modify, and use this Dataset while maintaining this same freedom for others, provided that the original source and author(s) are credited.

Link: <https://doi.org/10.3897/jhr.96.111382.suppl4>

A new small carder bee species from the eastern Canary Islands (Hymenoptera, Megachilidae, Anthidiini)

Nicolas J. Vereecken¹, Carlos Ruiz², Leon Marshall¹, Mónica Pérez-Gil³, Jean-Marc Molenberg¹, Bernhard Jacobi⁴, Francisco La Roche⁵, Jessica R. Litman⁶

1 Université libre de Bruxelles (ULB), Agroecology Lab, Avenue F.D. Roosevelt 50, B-1050 Brussels, Belgium
2 Department of Animal Biology, Edaphology and Geology, University of La Laguna, 38206 La Laguna de Tenerife, Canary Islands, Spain **3** Calle Guaticea 20, Playa Honda, Lanzarote, Canary Islands, Spain
4 Dieckerstraße 26, 46047 Oberhausen, Germany **5** Department of Mathematical Analysis, University of La Laguna, 38206 La Laguna de Tenerife, Canary Islands, Spain **6** Muséum d'Histoire Naturelle de Neuchâtel, Terreaux 14, 2000 Neuchâtel, Switzerland

Corresponding author: Nicolas J. Vereecken (nicolas.vereecken@ulb.be)

Academic editor: Jack Neff | Received 12 September 2023 | Accepted 17 October 2023 | Published 22 November 2023

<https://zoobank.org/5BE4EBEB-4D7D-41FA-93D1-12AD64AC73AD>

Citation: Vereecken NJ, Ruiz C, Marshall L, Pérez-Gil M, Molenberg J-M, Jacobi B, La Roche F, Litman JR (2023) A new small carder bee species from the eastern Canary Islands (Hymenoptera, Megachilidae, Anthidiini). *Journal of Hymenoptera Research* 96: 983–1015. <https://doi.org/10.3897/jhr.96.111550>

Abstract

Recent field surveys in the eastern Canary Islands (Spain), followed by contributions of new occurrence records through the citizen science platform iNaturalist.com and the social media photo repository Flickr.com have revealed the presence of an overlooked small carder bee species (genus *Pseudoanthidium* Friese (Megachilidae: Anthidiini)) on the islands of Lanzarote and Fuerteventura. Here, we combined morphology, DNA barcodes (mitochondrial cytochrome *c* oxidase subunit I, *COI*) and ecological data (distribution, altitudinal ranges and environmental niche classification) to describe this species as *Pseudoanthidium (Pseudoanthidium) jacobii* **sp. nov.** We provide an illustrated description along with diagnostic morphological characters to separate it from *P. (P.) canariense* (Mavroumoustakis, 1954), the only other congeneric species known from the neighbouring islands of La Gomera, Tenerife and Gran Canaria and from which it is separated by a genetic distance of 2.7%. We also evaluated the extent of shared environmental niche space among the two *Pseudoanthidium* species, and our results show a significant difference in elevation range as well as a very small (less than 1%) overlap between the modelled climatic niche of *P. jacobii* and that of *P. canariense*. Given the extremely restricted geographic distribution and the fragile and isolated nature of the habitat and host plants of this new island endemic species, we assign it an IUCN conservation status of “EN” (endangered) and discuss avenues for future research on the ecology and conservation of wild bees in the Canary Islands and neighbouring regions.

Keywords

Archipelago, biogeography, Canary Islands, COI mtDNA, genetic divergence, IUCN assessment, Red List, taxonomy

Introduction

Within Macaronesia and its oceanic islands, the Canary Islands (CI) archipelago encompasses seven islands with contrasting climates, topography, and geological history. Among the many fascinating facets of the CI archipelago for the island biogeographer is the diversity of environmental conditions, as well as the ecological and geological gradients observed within and among the islands. The CI are a well-known hotspot of biological endemism ever since Von Humboldt's first visit in 1799, for both plants and animals (Kunkel 1976; Fernández-Palacios et al. 2004; Fernández-Palacios and Whittaker 2008; Bowler 2018): to some naturalists, including the entomologist WM Wheeler, author of a review on the ants of the CI in the early 20th century, the Canaries “bear much the same relation to the south Palearctic fauna that [...] the Galapagos bear to those of South and Central America” (Wheeler 1927). The CI have long been a popular destination for European entomologists, including lepidopterists who by the end of the 19th century had already listed all butterfly species inhabiting the archipelago (Wiemers 1995 and references therein). Likewise, coleopterists have investigated the fauna of the archipelago for decades, including in some relict communities of laurel forest (*Laurisilva*) and thermophilous vegetation on the island of Fuerteventura (Machado 1976).

By contrast, historical surveys across the CI by hymenopterists (except myrmecologists), have lagged behind for decades. Although there are early reports on wild bees tracing back to the early 20th century, it was not until 1993 that the first comprehensive and annotated catalogue of the 127 species and subspecies of wild bees (of which 38% are strict CI endemics) was published (Hohmann et al. 1993), at a time when most European regions and countries still lacked species checklists. The availability of this 1993 “baseline” represents a cornerstone piece of information, as well as one of the pillars of contemporary research, and it has stimulated more surveys in the CI and the collection of biological occurrence records by Canarian and continental European entomologists ever since (Tkalčič 1993, 2001a, 2001b; Kuhlmann 2000; Dupont and Skov 2004; Pesenko and Pauly 2005; Smit 2007; Pérez and Marcías-Hernández 2012; Suarez et al. 2017; Kratochwil and Schwabe 2018, 2020; Kratochwil 2020). This, along with the development of citizen science projects (iNaturalist.com 2023) and standardised field surveys by and with local institutions, has radically improved our knowledge on the biodiversity and biogeography of wild bees in the CI archipelago.

Despite these advances, it is clear that gaps in our knowledge on CI bees are persistent, as demonstrated by the new island records of native species (Jacobi and Suárez 2018), or recent reports on exotic species reaching the archipelago (Pérez and Hernández 2012; Ortiz et al. 2016; Strudwick and Jacobi 2018; Ruiz et al. 2020; Lugo et al.

2022). Even locally intensive surveys on the most species-rich islands are likely still incomplete and have missed a certain number of species, opening the door for new discoveries. Photographs posted on online platforms such as iNaturalist.com or observations.org, as well as on Flickr.com and other similar online repositories, have recently served as the first evidence of new species in other parts of the world (Jaiswara et al. 2022; Masson Rosa et al. 2022; Zhang et al. 2022). These online portals represent an important new source of biological records for bees and other organisms, and an effective tool to engage anyone willing to produce new observations, armed with a camera, a little luck and some time spent in the field.

Here, we report on the results of recent field surveys focusing on wild bees in the CI archipelago, followed by observations shared through the citizen science platform iNaturalist.com and the social media photo repository Flickr.com. By combining detailed morphological analysis, DNA barcodes (mitochondrial cytochrome *c* oxidase subunit I, *COI*) and ecological data (distribution, altitudinal ranges and environmental niche classification), we concluded that specimens of a solitary bee belonging to the genus *Pseudoanthidium* (Megachilidae, Anthidiini) collected and photographed *in situ* in Lanzarote and Fuerteventura on multiple occasions in recent years, represents a hitherto unknown species of small carder bee that we describe below.

Materials and methods

Specimen collection and preparation, collection of occurrence records

As part of an ongoing collaboration between the Université libre de Bruxelles (NJV, LM, JMM) and the Departamento Biología Animal, Edafología y Geología of the University of La Laguna (CR) on apple tree pollinators, as well as the biogeography of the Canary Islands bees and the development of new taxonomic tools on the bees of Europe, field surveys have been conducted on the islands of Tenerife, Fuerteventura and Lanzarote in April 2021.

On 18.iv.2021, a male *Pseudoanthidium* was photographed by NJV (Fig. 1A, B) and collected with a hand net at Haría (Lanzarote); a female was collected with a hand net at the same site on the same day by JMM. The following day, on 19.iv.2021, two male *Pseudoanthidium* specimens were collected at Tegüise (Lanzarote). All specimens were first assumed to be new island records of *P. canariense*, until a closer examination of pinned specimens under the microscope challenged this view. The type specimens curated at the ULB Agroecology Lab entomological collection (Brussels, Belgium) will be transferred to the DZUL entomological collection curated by CR at the University of La Laguna (Tenerife) upon the publication of this manuscript.

On 12.ii.2023, a female *Pseudoanthidium* was photographed at Bco. Valle del Palomo (Lanzarote) by MPG, and two female specimens were collected by MPG at Haría (Lanzarote), one on 21.ii.2023 (Bco. Valle del Palomo), and another one on 16.iv.2023 (Bco. de Elvira Sánchez). These specimens were sent to CR to be pinned,

prepared for identification and deposited at the entomological collection curated by CR at the University of La Laguna (Tenerife). On 19.iv.2023, CR collected one female *Pseudoanthidium* species at Bco. de Elvira Sánchez (Haría, Lanzarote) now included in the DZUL entomological collection at the University of La Laguna (Tenerife). Publicly available occurrence data on wild bees across the Canary Islands reveal a significant disparity in sampling (GBIF 2023a): Tenerife (3,211 records), Gran Canaria (787), La Palma (560), Lanzarote (449), La Gomera, (383), Fuerteventura (263) and El Hierro (16). These figures are consistent with the historical patterns published by Hohmann et al. (1993). As a result, although additional collection efforts are needed across the entire island group, we can reasonably conclude that the range of the new *Pseudoanthidium* species does not include Gran Canaria and Tenerife.

On 12.iii.2023 and on 16.iii.2023, two female *Pseudoanthidium* specimens were photographed by BJ at Mácher (Lanzarote) (Fig. 1C, D).

Finally, G. Peña Tejera notified CR of another observation made and published on Flickr.com on 7.iii.2020 at Betancuria (Fuerteventura) by photographer L. Mullins.

DNA extraction, polymerase chain reaction (PCR) and sequencing of COI sequences

DNA extractions were performed on single legs from one male and one female specimen of this new species using Nucleospin tissue DNA extraction kits (Macherey - Nagel). A 658 base pair fragment of the mitochondrial gene cytochrome c oxidase (COI) was amplified using the primers Lep-F1 and Lep-R1 under the PCR conditions described in Hebert et al. (2004). PCR products were purified using a combination of exonuclease and FastAP thermosensitive alkaline phosphatase (Fermentas) and sequencing was performed using the same primers as those used for PCR reactions.

Sequence alignment and phylogenetic analysis of COI

Sequences were edited using Geneious (Kearse et al. 2012) and aligned with eight other COI sequences representing the closely related species *Pseudoanthidium canariense* (Mavromoustakis, 1954), *P. scapulare* (Latreille, 1809), *P. nanum* (Mocsáry, 1880), *P. palestinicum* (Mavromoustakis, 1938), *P. tenellum* (Mocsáry, 1880), *P. cribratum* (Morawitz, 1875) and *P. stigmaticorne* (Dours, 1873), as well as the more distantly related *P. reticulatum* (Mocsáry, 1884) as an outgroup (see Suppl. material 1 for taxon list). Alignments were performed using MAFFT v7.520 (Katoh and Standley 2013) and were verified visually using Mesquite v3.81 (Maddison and Maddison 2023). Data were divided into two partitions, with first and third codon positions in one partition and second codon positions in another. Model testing and maximum likelihood analyses were performed using the IQTree web server (Trifinopoulos et al. 2016). One thousand bootstrap replicates were performed on the partitioned dataset using the models TIM2+F+I (first and third codon positions) and HKY+F+G4 (second codon positions). Calculations of genetic distance were performed under a K2P model using Mesquite v3.81 (Maddison and Maddison 2023).

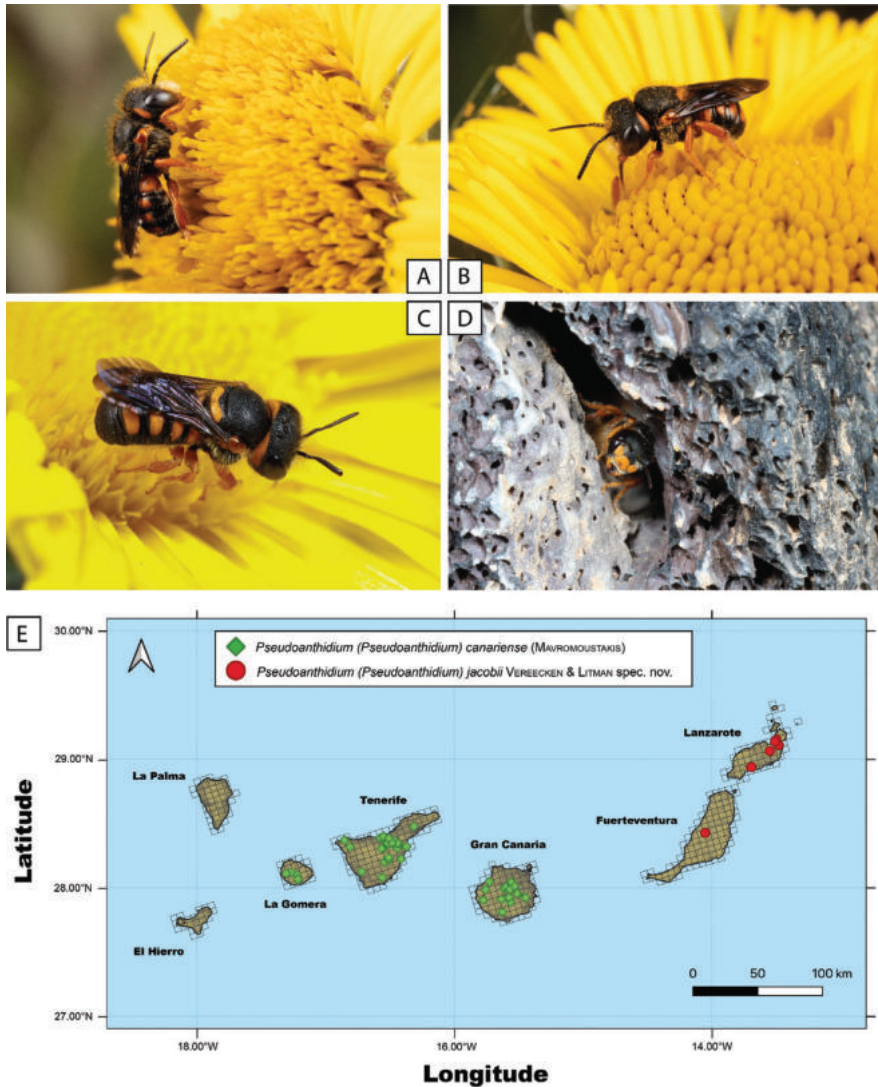


Figure 1. Ecology and distribution of *Pseudoanthidium jacobii* in the Canary Islands **A, B** male nectaring on an inflorescence of *Asteriscus intermedius* (*Asteraceae*) (Photos NJ Vereecken) **C** female collecting pollen on an inflorescence of *A. intermedius* (Photo B Jacobi) **D** female nesting in a pre-existing cavity located in a volcanic lava rock (Photo B Jacobi) **E** distribution map showing all occurrence records available to us and relevant to both *P. canariense* and *P. jacobii* in the Canary Islands.

Specimen depositories

- ULB** Agroecology Lab, Brussels School of Bioengineering, Université libre de Bruxelles, Belgium
- DZUL** Departamento Biología Animal, Edafología y Geología of the University of La Laguna, Tenerife, Spain
- FLR** Private collection of F. La Roche, San Cristóbal de La Laguna, Tenerife, Spain

Morphological diagnosis

The morphological terminology used in the description follows Michener (2007), Litman et al. (2021), Niu et al. (2021) as well as Kasperek and Ebmer (2023). All absolute measurements are made in millimetres (mm) and are used for body length. For all other structures, relative measurements are used. Abbreviations used in the description and diagnosis section below are as follows:

- BL** (body length): measured as the shortest absolute distance from the base of the antennal socket to the apex of the metasoma (see Niu et al. 2021);
- ITD** (inter-tegular distance): measured as the shortest absolute distance between the tegulae (scale-like structure covering the insertion point of the wings on the thorax) in dorsal view;
- OOD** (ocellar-occiput distance): assessed in dorsal view, under a stereomicroscope with continuous LED light, as a ratio between the distance separating the lateral ocelli and the posterior occiput (dorsal margin of the vertex) on one hand, and the ocellar diameter on the other hand;
- MPD** (median punctuation density): assessed as the ratio between the distance separating neighbouring points in the median region of the tergites and the puncture diameter;
- LPD** (lateral punctuation density): measured as the ratio between the distance separating neighbouring points in the lateral region of the tergites, particularly on T2 (second tergite) and T3 (third tergite), and the puncture diameter;
- SSPD** (scutum and scutellum punctuation density): measured under a stereomicroscope with continuous LED light as the distance between neighbouring points on the scutum (dorsal side of the thorax/mesonotum) and on the scutellum (dorso-apical plate of the thorax/mesonotum) on one hand, and the puncture diameter;
- TEG** (tegulae): colour of the scale-like structures covering the insertion point of the wings on the thorax/mesonotum;
- ProN** (pronotum): colour of the dorsal lobe of the first thorax/mesonotum segment;
- ProLo** (pronotal lobe): colour of the pronotal lobe (also known as “humeral tubercles”) located just next to the tegulae, towards the anterior site of the thorax/mesonotum;
- TCP** (tergite colour patches): colour, size and delineation between the orange colour patches on the tergites and the surrounding black cuticle;
- FACE** (face): colour of the clypeus, mandibles, lower part of paraocular region;
- LEGS** (legs): colour of the coxae, femurs, tibiae on each pair of legs.

Photographs of the type material were taken using a Leica S8APO equipped with a Leica MC190 HD digital camera and a Leica LED3000 DI light dome. Series of shots were taken by manually adjusting the precision dial to cover the sharpness of the target body parts. The specialized hooked and waved hairs on the metasomal sterna

(S3-S4-S5) in males were photographed using a Canon 5DS R equipped with a Canon MP-E 65mm lens at 5× and (set at $f/3.2$ and ISO 100), mounted on a StackShot macro rail (distance/step = 0.01mm) and lit with two custom diffused, IR-operated Godox 860vii cobra flashes. All resulting photos were stacked with Helicon Focus (version 8.2.6.) using the software's "Depth Map mode (Method B)". Resulting stacked shots were slightly edited in Adobe Lightroom and cleaned in Adobe Photoshop 2023.

Mapping of occurrence records

Shapefiles and map data derived from OpenStreetMap (copyrighted OpenStreetMap contributors and available from <https://www.openstreetmap.org>) were downloaded from GeoFabrik (<https://download.geofabrik.de>). Species distribution points were plotted using QGIS 3.22 -Białowieża (QGIS Development Team 2023). We have included a series of 35 "research-grade" occurrence records of *P. canariense* from GBIF.org (GBIF 2023b) and we have estimated the coordinates of another 15 conspecific specimens cited by Hohmann et al. (1993) based on the approximate center of the most specific locality given from the island of Gran Canaria. All new *Pseudoanthidium* records relevant to the islands of Lanzarote and Fuerteventura resulting from specimens collected in the field or macrophotographs exhibiting enough detail to allow for an identification at the species level were included on the map too.

Finally, we used the *elevatr* package (version 0.4.2.) (Hollister 2022) to compute the elevation associated with each occurrence record of both *Pseudoanthidium* species. Boxplots of all records were prepared with the "ggplot2" package (Wickham 2016). All records, including their latitude/longitude coordinates in decimal degrees (WGS84), their elevation, the date of each record and their source are compiled in Suppl. material 2. All analyses were performed with RStudio (RStudio Team 2020) for R (version 4.2.2; R Core Team 2022).

Ecological niche characterisation

To evaluate the extent of shared environmental niche space among the two *Pseudoanthidium* species, we conducted an analysis of ecological niche characteristics. Significant niche differentiation is anticipated owing to the contrasting habitats between the eastern islands of Lanzarote and Fuerteventura and the western islands. The comparison is intended to illustrate the prevailing climatic conditions for the two species. For each occurrence record of the two species, we extracted environmental data from a 200m buffer. BIOCLIM data was obtained from CHELSA (Climatologies at High resolution for the Earth's Land Surface Areas) climate dataset at 30 arc seconds resolution (Karger et al. 2017). We selected 4 bioclim variables to cover precipitation and temperature range, and variation (mean annual temperature/precipitation, temperature/precipitation seasonality). Elevation data was obtained from the "elevatr" package as described above. The background niche space was calculated based on 2,000 randomly generated points within the Canary Islands. These data were then used to classify the ecological niche space

occupied by the two *Pseudoanthidium* species. Following Broennimann et al. (2012), we used a principal component analysis (PCA) that was calibrated based on the complete environmental space encompassing the Canary Islands, that applies smoothers to the species presences in environmental space for the purpose of selecting and weighting the environmental variables. We then computed niche overlap between the two species with Schoener's *D* statistic (Schoener 1968; Warren et al. 2008). Finally, we tested whether the niche overlap of the two species is less equivalent than random by means of a niche equivalence test with 1,000 repetitions (Broennimann et al. 2012). These analyses were conducted with RStudio (RStudio Team 2020) for R (version 4.2.2; R Core Team 2022) using the “ecospat” package (version 3.5.1; Broennimann et al. 2023).

EOO, AOO and extinction risk assessment using IUCN criteria

We used the “red” package (version 1.5.0) (Cardoso 2017) and all occurrence records to compute the extent of occurrence (EOO) and area of occupancy (AOO) of *P. canariense* and the newly discovered *Pseudoanthidium* species described below. EOO encompasses the total geographic range of a species, while AOO focuses on the current occupied area of a species within its known habitat; both metrics are vital for assessing a species' conservation status and can influence its IUCN Red List categorization. We then used the *rCAT* package (version 0.1.6) (Moat 2020) to calculate the IUCN rating of each species based on their EOO in km².

Assessing the extinction risk of a species, including of hitherto overlooked, or newly described taxa, requires using a series of criteria listed by the International Union for the Conservation of Nature (IUCN) Red List (IUCN Standards and Petitions Committee 2022). These criteria are based on indicators of extinction risk and ultimately help assign a ranked threat category, such as critically endangered (CR), endangered (EN) and vulnerable (VU) (Mace et al. 2008; Nieto et al. 2014). In a nutshell, the five key components of an IUCN extinction risk assessment are: population reduction (Criterion A), restricted geographic range (Criterion B), small population size and decline (Criterion C), very small or restricted population size (abundance) (Criterion D) and a quantitative analysis of decline (Criterion E). For each criterion, threshold values are defined and associated with different threat categories; we performed the assessment for the new *Pseudoanthidium* species following practical guidelines (Rodríguez et al. 2015) and using as much direct (and to some extent, indirect) evidence as possible (Le Breton et al. 2019).

Results

Our study reveals the presence of a hitherto overlooked species within the subgenus *Pseudoanthidium* (*Pseudoanthidium*) in the Canary Islands. A closer examination of the only earlier and unpublished record of a *Pseudoanthidium* from Lanzarote, a female specimen collected by F. La Roche in Lanzarote 1997, curated in the private collection

of F. La Roche (San Cristóbal de La Laguna, Spain) and identified by the late Czech entomologist B. Tkalčů as *P. stigmaticorne*, revealed that this specimen also belongs to the species we describe here below.

***Pseudoanthidium (Pseudoanthidium) jacobii* Vereecken & Litman, sp. nov.**

<https://zoobank.org/BD67A8C7-F34B-45AB-9E85-45813F167E33>

Type material. Holotype. SPAIN • 1♂; Lanzarote, Haría, 19 Apr. 2021; NJ Vereecken leg.; DZUL.

Paratypes. SPAIN • 1♀; Lanzarote, Haría, 18 Apr. 2021; J-M Molenberg leg.; ULB • SPAIN • 1♂; same collection data as for preceding, 19 Apr. 2021; J-M Molenberg leg.; ULB • 1♂; same collection data as for preceding, 18 Apr. 2021; J-M Molenberg leg.; DZUL.

Other material. SPAIN • 1♂; Lanzarote, Haría; 21 Feb. 2023; M Pérez-Gil leg.; DZUL • 1♀; Haría, 16 Apr. 2023; M Pérez-Gil leg.; DZUL • 1♀; Haría, 19 Apr. 2023; C Ruiz leg.; DZUL • 1♀; Lanzarote, Guatiza, 25 Mar. 1997, F La Roche leg.; FLR.

Diagnosis. Besides differences in their distribution pattern across the Canary Islands archipelago (Fig. 1), males and females of *P. canariense* and the newly described *P. jacobii* can be unambiguously identified based on a number of morphological criteria described below, including their relative size, as well as the density of the punctuation, the colour and the shininess of their cuticle as shown on Figs 2–4. Fig. 5 illustrates the structure of specialized hooked and waved hairs on the metasomal sterna (S3–S4–S5) in males, as well as their apicolateral combs on each lateral arm of S5.

Female. The female of *P. jacobii* may be distinguished from *P. canariense* by the following combination of characters: **BL** minimally only half size (4–7 mm in *P. jacobii*, 6–9 mm in *P. canariense*), **ITD** shorter (on average: 2.13 mm in *P. jacobii*, 2.91 mm in *P. canariense*), **OOD** shorter (~ 1 ocellar diameter in *P. jacobii*, ~ 1.5–2 ocellar diameters in *P. canariense*), **TPD** lower (spaces between points at least ~ 1–1.5 diameter of a single point in *P. jacobii*, < 0.5 diameter of a single point in *P. canariense*), **SSPD** slightly higher (~ 0.5 diameter of a single point in *P. jacobii*, < 0.5 diameter of a single point in *P. canariense*), **TEG** brighter (orange-yellow in *P. jacobii*, black in *P. canariense*), **ProN** brighter (orange-yellow in *P. jacobii*, black in *P. canariense*), **ProLo** mostly brighter (orange-yellow like the tegulae in *P. jacobii*, black in *P. canariense*, but more specimens of each species should be examined), **TCP** wider, brighter (wide and orange-yellow in *P. jacobii*, narrower and dark orange in *P. canariense*), and with a better defined maculation margin (gradual infiltration of the black colour into the orange yellow maculations of the integument in *P. jacobii*, well-defined colour boundary/contrast between darker orange maculations and black cuticle in *P. canariense*), **FACE** brighter (orange-yellow clypeus, mandibles, lower part of paraocular region in *P. jacobii*, all black in *P. canariense*) and wider (face broader than long in *P. jacobii*, face longer than broad in *P. canariense*), **LEGS** brighter (all legs black only from the coxa to the very base of the femur black, the rest of the femur and other leg segments are orangish yellow in *P. jacobii*, all coxae, femurs but only posterior tibiae black in *P. canariense*).

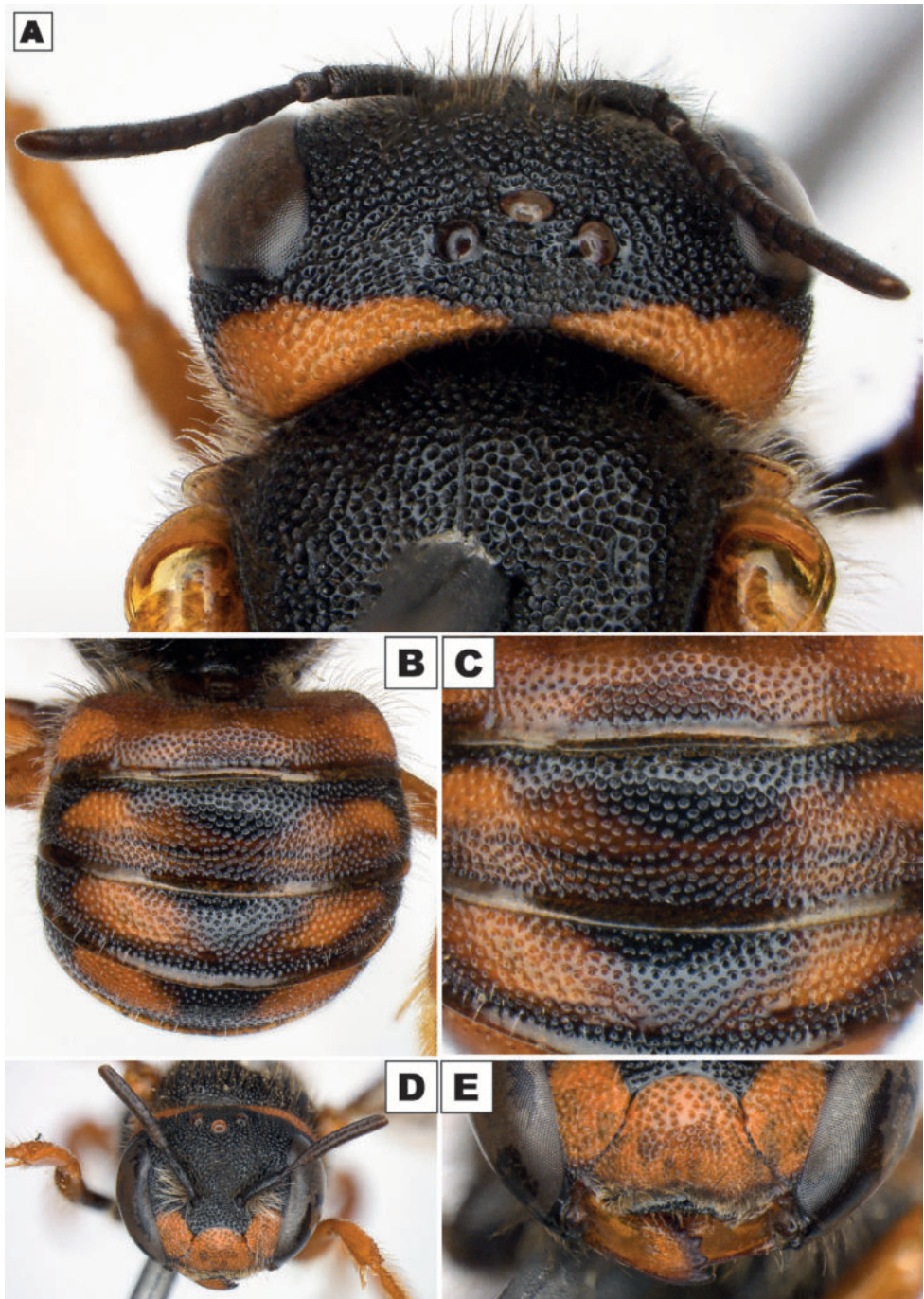


Figure 2. Illustration of some key morphological traits that characterise females of *Pseudoanthidium jacobii* **A** head capsule and first half of the mesonotum in dorsal view **B** abdomen in dorsal view **C** tergites 1-2 (from top to bottom) in dorsal view **D** face in frontal view **E** mandibles and clypeus in frontal view. Photos NJ Vereecken; see description of each sex and the diagnosis in the text for more details.

Male. The male of *P. jacobii* may be distinguished from *P. canariense* by the following combination of characters: **BL** minimally only half size (4–6 mm in *P. jacobii*, 6–8 mm in *P. canariense*), **ITD** shorter (on average: 2.22 mm in *P. jacobii*, 2.95 mm in *P. canariense*), **OOD** shorter (~ 1 ocellar diameter in *P. jacobii*, ~ 1.5–2 ocellar diameters in *P. canariense*), **TPD** lower (spaces between points at least ~ 1–1.5 diameter of a single point in *P. jacobii*, < 0.5 diameter of a single point in *P. canariense*), **SSPD** slightly higher (~ 0.5 diameter of a single point in *P. jacobii*, < 0.5 diameter of a single point in *P. canariense*), **TEG** brighter (orange-yellow in *P. jacobii*, black in *P. canariense*), **ProN** brighter (orange-yellow in *P. jacobii*, black in *P. canariense*), **ProLo** mostly brighter (orange-yellow like the tegulae in *P. jacobii*, black in *P. canariense*, but more specimens of each species should be examined), **TCP** wider, brighter (wide and orange-yellow in *P. jacobii*, narrower and dark orange in *P. canariense*), and with a better defined maculation margin (gradual infiltration of the black colour into the orange yellow maculations of the integument in *P. jacobii*, well-defined colour boundary/contrast between darker orange maculations and black cuticle in *P. canariense*), **FACE** brighter (orange-yellow clypeus, mandibles, lower part of paraocular region in *P. jacobii*, all black in *P. canariense*) and wider (face broader than long in *P. jacobii*, face longer than broad in *P. canariense*), **LEGS** brighter (all legs black only from the coxa to the very base of the femur black, the rest of the femur and other leg segments are orangish yellow in *P. jacobii*, all coxae, femurs but only posterior tibiae black in *P. canariense*). Brushes of thickened, wavy hairs on S3, as well as the lateral dark brown comb of S5, identical in both species.

Description. Female. Head: Mandible orange-yellow, except for teeth and apex of anterior margin, which are reddish-brown. Pilosity on clypeus and tufts at base of antenna white; on anterior margin of clypeus off-white, and on vertex blond. Clypeus dark yellow with black anterior margin. Punctures of clypeus dense and small anteriorly and laterally, with interspaces not larger than diameter of one-half puncture. Punctures become sparser and larger medially and posteriorly, where the maximum distance between punctures reaches two puncture diameters or more in the posterior-medial zone. Interspaces between punctures on clypeus shiny, most notably so where punctures are least dense. Paraocular area dark yellow and densely punctate, with interspaces not over the diameter of one-half puncture. Antenna with scape and pedicel black; flagellar segments dark brown. Flagellar segments shorter than wide, except for the first and the last, which are longer than wide. Frons with punctuation nearly honeycomb areolate, punctuation becoming slightly less dense toward the vertex, with shiny interspaces. Vertex with dark yellow triangle behind each eye, meeting or nearly meeting at midline of vertex. Vertex densely punctate, with interspaces not over 0.5 puncture diameter wide. Punctuation on vertex mostly homogenous, with punctures just posterior to median ocellus slightly larger. Gena densely, evenly punctate, with spaces between points less than 0.25 puncture diameter wide.

Mesosoma: Scutum black. Punctuation dense, with spaces between punctures shiny, not more than one-quarter puncture diameter wide. Tegula dark yellow anteriorly, translucent yellow posteriorly. Pronotal lobe dark yellow apically, black basally.

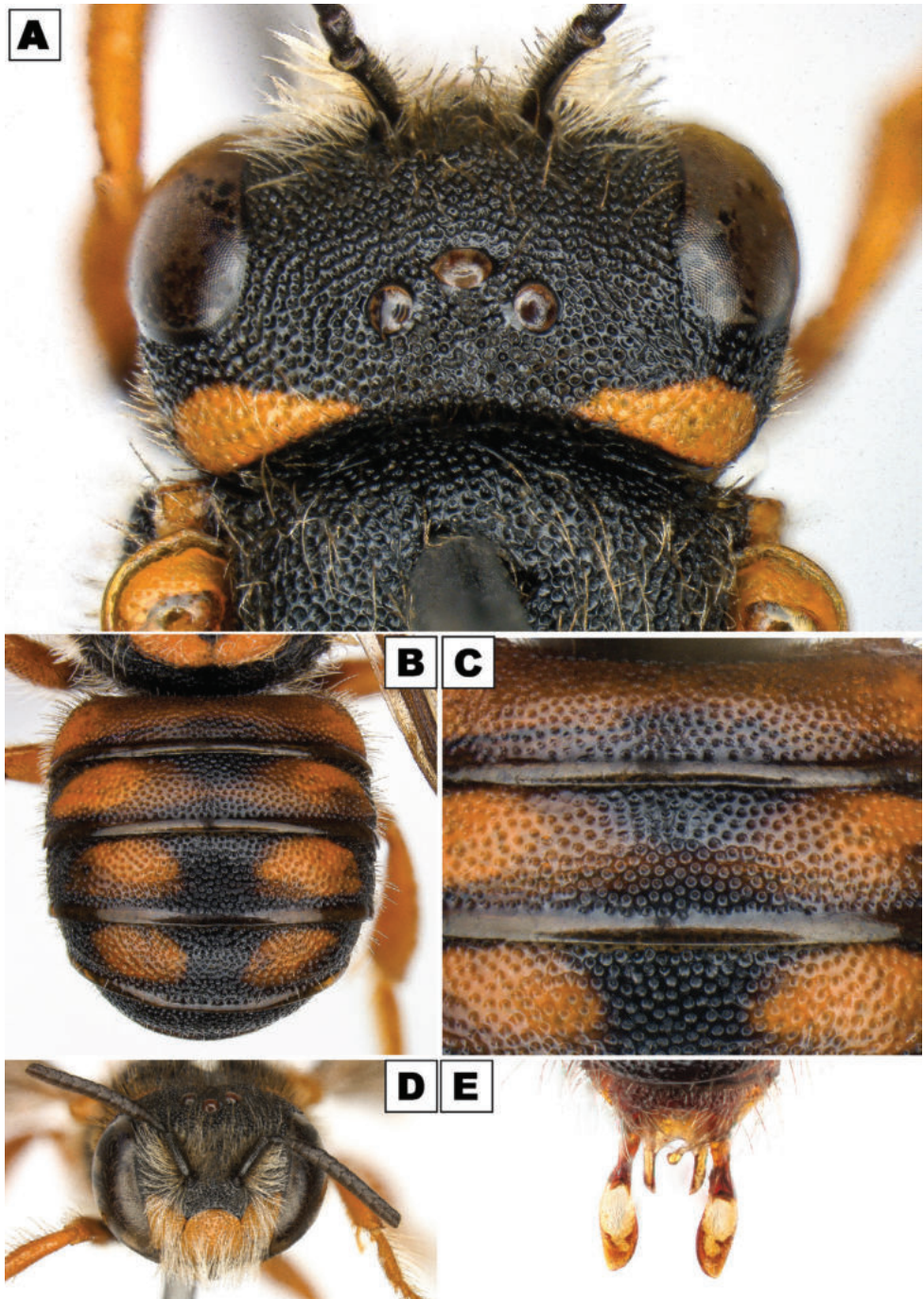


Figure 3. Illustration of some key morphological traits that characterise males of *Pseudoanthidium jacobii* **A** head capsule and first half of the mesonotum in dorsal view **B** abdomen in dorsal view **C** tergites 1-2-3 (from top to bottom) in dorsal view **D** face in frontal view **E** gonostyli in dorsal view. Photos NJ Vereecken; see description of each sex and the diagnosis in the text for more details.

Scutellum black with dark yellow band medially on posterior margin. Punctures on black part of scutellum slightly larger and less dense than on scutum, with spaces between punctures on the median part of the scutellum shiny and up to one half a puncture diameter wide; punctation on yellow part of scutellum even less dense, with spaces between punctures over one puncture diameter wide. Mesepisternum densely punctate, punctures becoming smaller and less dense around episternal groove; spaces between punctures shiny. Propodeum laterally and anteriorly finely, densely punctate; medially shiny and without punctuation. On all legs, coxa, trochanter and base of femur black; the rest of the femur, tibia and tarsal segments orange-yellow. Wings infusate.

Metasoma: T1 anteriorly brownish-yellow, posteriorly reddish-brown. A dark yellow spot present laterally, slightly masked by the colour of the anterior margin of the tergite. Lateral spots vaguely joined medially on the tergite by a faint yellow band connecting the posterior margin of each spot. Punctuation relatively dense, even laterally, with spaces between punctures not greater than the diameter of half a puncture. T1 with unpunctured, shiny, translucent brown posterior margin measuring about two punctures wide. T2 anteriorly black with diffuse dark yellow lateral spots; posteriorly, T2 brownish-yellow. Lateral spots on T2 placed slightly medially to those on T1. Punctuation on T2 dense but less so than on T1, with spaces between punctures laterally up to nearly one puncture diameter. Diameter of punctures of T2 greater than those of T1. T2 with unpunctured, shiny, translucent brown posterior margin measuring about two punctures wide. T3 like T2 in colour, with punctuation slightly less dense. Punctuation of T4 similar to that of T3; T4 mostly black with yellow spots laterally and with shiny, translucent brown posterior margin; anterior edge of this margin with a single row of punctures medially. T5 black, densely punctate, with spaces between punctures shiny and measuring less than 0.25 puncture diameter. T6 black, densely punctate, spaces between punctures less shiny than those of T5 and measuring less than 0.25 puncture diameter, overall texture T6 somewhat rough.

Male. Head: Mandible orange-yellow, except for teeth and apex of anterior margin, which are reddish-brown. Pilosity on clypeus and tufts at base of antenna white; on anterior margin of clypeus off-white, and on vertex dark blond to brown. Clypeus rugose-punctate, orange-yellow with black anterior margin. Paraocular area orange-yellow and rugose-punctate, with interspaces not over the diameter of half a puncture. Antenna with scape and pedicel black; flagellar segments dark brown. Flagellar segments shorter than wide, except for the first and the last, which are longer than wide. Frons with punctuation nearly honeycomb areolate, punctuation becoming slightly less dense toward the vertex, with shiny interspaces. Vertex with orange-yellow triangle behind each eye, widely interrupted towards the midline of the vertex by a black punctured space. Vertex densely punctate, with interspaces not over 0.5 puncture diameter wide. Punctuation on vertex mostly homogenous, with interspaces between punctures increasing towards the eye margin and the latero-posterior part of the vertex. Gena densely, evenly punctate, with spaces between points less than 0.25 puncture diameter wide.



Figure 4. Illustration of some structural diagnostic morphological traits that help discriminate between *Pseudoanthidium canariense* (Mavromoustakis) (**A, C**) and *P. jacobii* (**B, D**). Photos NJ Vereecken; see description of each sex and the diagnosis in the text for more details.

Mesosoma: Scutum black. Punctuation dense, with spaces between punctures shiny, not more than one-quarter puncture diameter wide. Tegula orange-yellow anteriorly, translucent orange brown posteriorly. Pronotal lobe orange-yellow apically, black basally. Scutellum black with orange-yellow band medially on posterior margin. Punctures on black part of scutellum slightly larger and less dense than on scutum, with spaces between punctures on the median part of the scutellum shiny and up to one half a puncture diameter wide; punctuation on yellow part of scutellum even less dense, with spaces between punctures over one puncture diameter wide. Mesepisternum densely punctate, punctures becoming smaller and less dense around episternal groove; spaces between punctures shiny. Propodeum laterally and anteriorly finely, densely punctate; medially shiny and without punctuation. On all legs, coxa, trochanter and base of femur black; the rest of the femur, tibia and tarsal segments orange-yellow. Wings infuscate.

Metasoma: T1 brownish-orange on its anterior half, with an orange-yellow spot present laterally, slightly masked by the colour of the anterior margin of T1. Lateral spots joined medially on the tergite by a brownish-orange band connecting each spot.



Figure 5. Both *Pseudoanthidium jacobii* and *P. canariense* share the same overall structure of specialized hooked and waved hairs on their metasomal sternite (S3-S4-S5) in males, as well as their dark brown to black apicolateral combs on each lateral arm of S5. The present photo illustrates the structure in a male *P. jacobii* where S3 also exhibits a short, dense, velvety pubescence anteriorly, posteriorly with pre-marginal brush of hairs, hooked at the tips, as well as an underlying comb of thickened, wavy hairs (Photo NJ Vereecken).

Punctuation relatively dense, even laterally, with spaces between punctures not greater than the diameter of half a puncture. T1 with unpunctured, shiny, translucent brown posterior margin measuring about two punctures wide. T2 anteriorly black with diffuse orange-yellow lateral spots; posteriorly, T2 brownish. Lateral spots on T2 placed slightly medially to those on T1. Punctuation on T2 dense but less so than on T1, with spaces between punctures laterally up to nearly one puncture diameter. Diameter of punctures of T2 greater than those of T1. T2 with unpunctured, shiny, translucent brown posterior margin measuring about two punctures wide. Lateral spots on T3 placed slightly medially to those on T2. T3 similar to T2 in colour, with punctuation slightly less dense. Punctuation of T4 similar to that of T3; T4 mostly black with less diffuse orange-yellow spots laterally and with shiny, translucent brown posterior margin; anterior edge of this margin with a single row of punctures medially. T5 black, densely punctate, with spaces between punctures shiny and measuring less than 0.25 puncture diameter. T6 black, densely punctate, spaces between punctures less shiny than those of T5 and measuring less than 0.25 puncture diameter, overall texture T6 somewhat rough. T7 black, densely punctate, with rounded notch on posterior margin. Genitalia with semi-translucent, apically rounded (i.e., unnotched) and flattened

gonostyli; penis valves flattened and rounded. S3 with short, dense, velvety pubescence anteriorly, posteriorly with premarginal brush of hairs, hooked at the tips, as well as an underlying comb of thickened, wavy hairs. S5 laterally with dark brown comb.

Etymology. *Pseudoanthidium (Pseudoanthidium) jacobii* is dedicated to Mr. Bernhard Jacobi (Oberhausen, Germany), naturalist extraordinaire and talented macro-photographer who has a genuine and boundless passion for wild bees, particularly for species found in Europe and Australia. Bernhard's interest for the Canary Islands has grown steadily and uninterrupted ever since the publication of Hohmann et al.'s (1993) landmark volume on the bees, wasps and ants of the archipelago. He has since then investigated the entomofauna of all of the Canary Islands *in situ*, reporting and illustrating the occurrence and distribution of the European Beewolf, *Philanthus triangulum* (Fabricius, 1775) on the archipelago (Jacobi et al. 2013), as well as new records on the distribution and phenology of *Colletes perezi* Morice, 1904 on Fuerteventura (Jacobi and Suárez 2018) and the first record of the American species *Megachile (Chelostomoides) otomita* Cresson, 1878 established on Tenerife (Strudwick and Jacobi 2018). Bernhard and his wife have been regular visitors to Lanzarote for over three decades, particularly during the winter months, and he was the third person (after authors NJV on 18.iv.2021 and MPG 12.ii.2023) to photograph a live specimen of *P. jacobii* in Lanzarote on 12.iii.2023 (Fig. 1D). Bernhard has also recently contributed new occurrence records of the widespread small carder bee *P. nanum* near his home in the German state of North Rhine-Westphalia (Jacobi et al. 2021).

Genetic differentiation between *P. jacobii* and other *Pseudoanthidium* species

The results of CO1 analyses demonstrate that *P. jacobii* is strongly supported as the sister species to *P. canariense* (ML bootstrap value = 96%) (Fig. 6). The two species are separated by a K2P-corrected genetic distance of 2.7%. Furthermore, *P. jacobii* exhibits an average K2P-corrected genetic distance of 5.9% from the clade consisting of *P. nanum* - *P. scapulare* - *P. palestinicum*; of 5.1% from *P. stigmaticorne*; and of 5.3% from the clade consisting of *P. tenellum* - *P. cribratum*.

Ecology, distribution and ecological niche differentiation

Habitat and host plant associations

In Lanzarote, the vegetation at the localities of Haría and Bco. de Elvira Sánchez where males and females of *P. jacobii* were recorded was composed of a chamaephytic substitutional flowering plant community established on old agricultural land with deep soils, generally on eroded slopes and on stony slopes, ravines, ledges physiognomically characterised by the presence of *Asteriscus intermedius* (DC.) Pit. & Proust (Asteraceae) and *Lavandula pinnata* L. (Lamiaceae) among others (see also Ramón Arévalo et al. 2016). By contrast, the localities of Teguisse and Macher are peri-urban

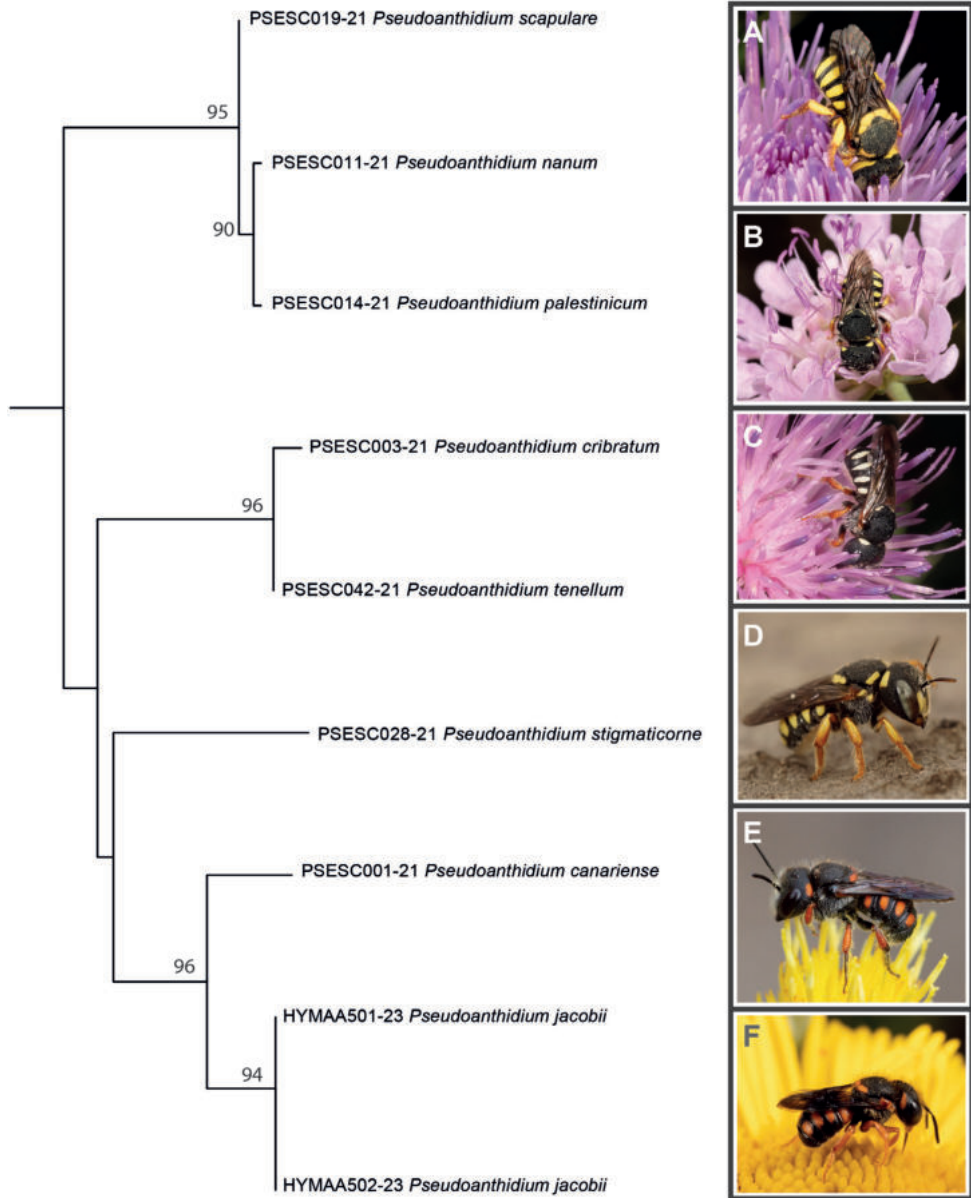


Figure 6. Maximum likelihood-based tree based on analysis of a 658 base pair fragment of COI sequenced from selected *Pseudoanthidium* species in the *P. scapulare* complex. Maximum likelihood bootstrap support values, based on 1,000 replicates, are shown over nodes; only nodes with support values >90% are shown. Terminals are labelled with species names, as well as the BOLD sample IDs corresponding to each specimen. Outgroup removed from figure for convenience. Individuals shown in photographs were not those sequenced for analysis **A** *P. scapulare* (Photo NJ Vereecken) **B** *P. nanum* (Photo NJ Vereecken) **C** *P. tenellum* (Photo B Jacobi) **D** *P. stigmaticorne* (Photo H Wallays) **E** *P. canariense* (Photo G Peña); and **F** *P. jacobii* (Photo NJ Vereecken).

or rural anthropic areas with sparse natural vegetation, and the locality of Valle del Palomo is composed of xeric shrubland with a physiognomy of dendroid spurge shrubland, dominated by *Euphorbia regis-jubae* J. Gay (Euphorbiaceae). This is secondary vegetation typically found on abandoned arable or pastureland, roadsides and watercourse-beds (Reyes-Betancourt et al. 2001). In Fuerteventura, the locality of Betancuria where a female of *P. jacobii* was photographed is characterised by a flowering plant community consisting of dwarf chamaephytes exposed to strong winds and heavily grazed, where *Helianthemum canariense* (Jacq.) Pers. (Asteraceae) and *Spergularia fimbriata* Boiss. & Reut. (Caryophyllaceae) are dominant (del Arco Aguilar et al. 2018). Females of *P. (P.) jacobii* were observed collecting pollen on *A. intermedius* (DC.) Pit. & Proust (endemic to Fuerteventura and Lanzarote) (Fig. 1), *Pulicaria canariensis* subsp. *lanata* (Font Quer & Svent.) Bramwell & G. Kunkel (endemic to Lanzarote), and *Glebionis coronaria* (L.) Cass. ex Spach (syn. *Chrysanthemum coronarium* L., native and of Mediterranean origin) (Asteraceae). Males were also observed nectaring and patrolling for females on and around the same flowering plant species.

Nesting behaviour

A single observation by co-author BJ in Lanzarote on 16.iii.2023 of a female nesting in a pre-existing cavity formed in a lava rock (Fig. 1D). All *Pseudoanthidium* species are reported to nest in pre-existing cavities or in pithy plant stems (see Litman et al. 2021 and references therein; Bogusch et al. 2022).

Ecological niche differentiation

The environmental niche space occupied by *P. canariense* encompasses a large part of the total environmental niche space available in the Canary Islands, covering wide elevation (from 70 m to 2,046 m with a mean of 952 m), mean annual temperature (8.3 °C to 20.9°C, $\mu=15.2$ °C), and mean annual rainfall (135 kg m⁻² to 534 kg m⁻², $\mu=354.7$ mm) gradients with greater temperature (1.9 °C to 2.2 °C, $\mu=2.1$ °C) and lower precipitation seasonality (73 kg m⁻², 90 kg m⁻², $\mu=81.2$ kg m⁻²) gradients and occupying a variety of land cover types (Fig. 7). The environmental niche space of *PB* is almost entirely separate from the niche space occupied by *P. canariense* and is driven by low elevation (204 m to 460 m, $\mu=268$ m) (Fig. 7), warmer (17.6 °C to 19.5 °C, $\mu=18.7$ °C), and drier (101 kg m⁻² to 170 kg m⁻², $\mu=138.9$ kg m⁻²) areas with less variation in temperature (1.9 °C to 2.0°C, $\mu=2.0$ °C) and more varied rainfall (92 kg m⁻², 100 kg m⁻², $\mu=96.9$ kg m⁻²) (Fig. 7). This comparison, as hypothesised, strongly represents the climatic and elevational differences between the islands where the species occur. The overlap between the two species represents the limits of the niche for *P. canariense*. As shown on Fig. 8, overall niche overlap between the two species is less than 1% and we can accept the alternative hypothesis that the two niches are less equivalent than random ($p<0.001$).

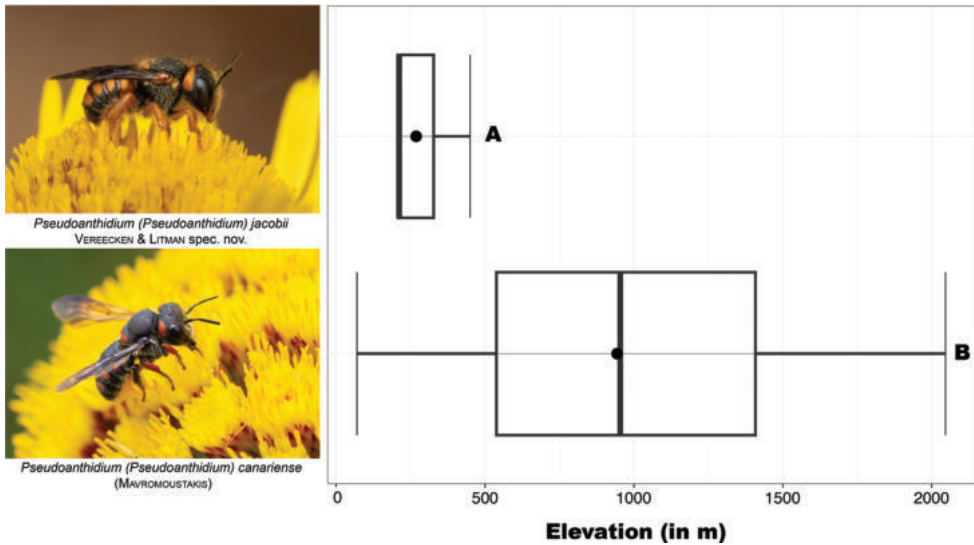


Figure 7. Distribution of elevation records relevant to **A** *Pseudoanthidium jacobii* and **B** *P. canariense* in the Canary Islands. Different letters right to the boxplots indicate highly significant differences in the elevation range and mean elevation of occurrence (black dot in boxplots) of both species (Kruskal-Wallis test: $\chi^2 = 12.425$, $df = 1$, p -value < 0.0005). Photo of *P. jacobii* M Pérez-Gil and of *P. canariense* G Peña.

Distribution and threats

Due to a lack of historical baseline data, we could not evaluate *P. jacobii* using IUCN Criterion A (population reduction). However, with an EOO of 326 km² and an AOO of 28 km², *P. jacobii* fulfils both Criteria B1 and B2 (restricted geographic range; EOO < 5,000 km² and AOO < 500 km², respectively) (IUCN 2023).

Our current knowledge suggests that *P. jacobii* is known only from Mediterranean type shrubland vegetation localities on the islands of Lanzarote and Fuerteventura (Fig. 1). The key host plants exclusively visited by *P. jacobii* females for the collection of pollen include the herbaceous single-island endemic *Pulicaria canariensis* subsp. *lanata* (Font Quer & Svent.) Bramwell & G. Kunkel (endemic to Lanzarote), the archipelago endemic *Asteriscus intermedius* (DC.) Pit. & Proust (endemic to Fuerteventura and Lanzarote) and the native non-endemic *Glebionis coronaria* (L.) Cass. ex Spach, all belonging to the family Asteraceae. According to a recent study by Hanz et al. (2023), climate change will severely restrict the climatically suitable area of Canarian herbaceous plant species, particularly archipelago endemics and single-island endemic species, and particularly on the islands of Lanzarote and Fuerteventura, which are expected to experience less annual precipitation in the future. This phenomenon along with the negative impacts of invasive flowering plant species in the archipelago (del Arco Aguilar et al. 2018; but see Fernandez-Palacios et al. 2022), is very likely going to affect the availability of floral resources used by *P. jacobii* females, with cascading impacts on their population size and distribution.

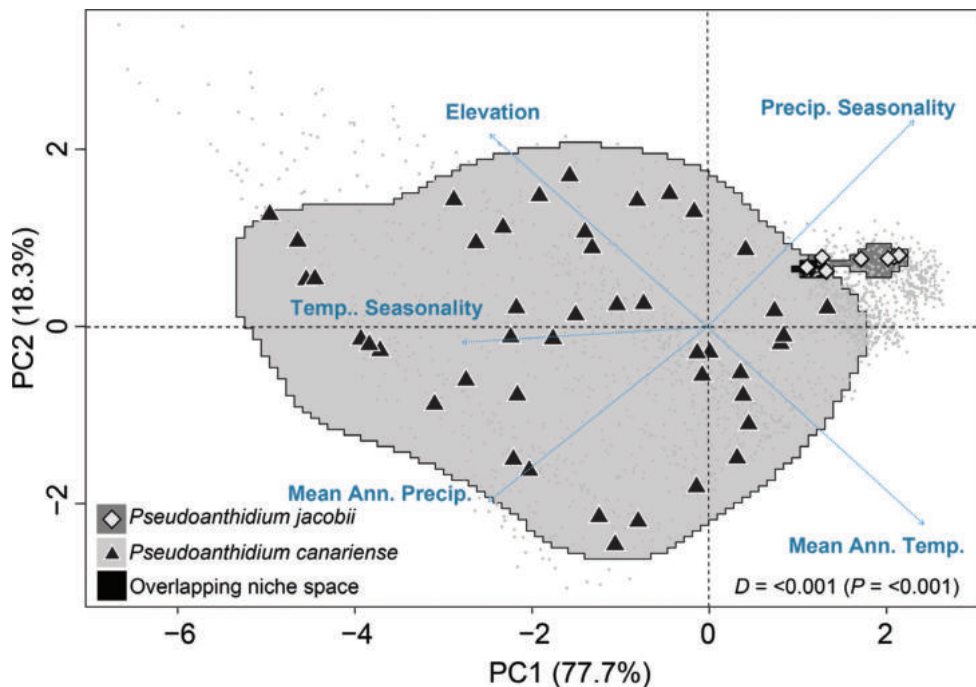


Figure 8. Ecological niche overlap between *Pseudoanthidium jacobii* and *P. canariense* in the Canary Islands represented by a principal component analysis (PCA). Light grey diamonds represent occurrence records of *P. jacobii*, and the small underlying dark grey area represents its niche space. Black triangles represent occurrence records of *P. canariense* and the light grey underlying area represents its niche space. The small black area represents shared niche space between the two species. Small grey dots are background environmental samples from the Canary Islands. Schoener's *D* statistics and the *p*-value from the niche equivalence test are also shown. See methods and results sections for more details.

According to the IUCN, populations are considered “severely fragmented” if most individuals are found in small and relatively isolated subpopulations, where the probability of recolonization is reduced, should these subpopulations go extinct (IUCN 2023). Under this strict definition, populations of *P. jacobii*, restricted to extremely isolated pockets on Lanzarote and Fuerteventura, may be considered severely fragmented, thus fulfilling both criteria B1a and B2a. Furthermore, the continuous development of touristic infrastructures on both islands, the increase of pollution brought about by new roads facilitating transport and tourism across the islands (Martín-Cejas and Ramírez Sánchez 2010), the increase in car ownership and usage (Martín-Cejas 2015), and other pervasive forms of anthropogenic disturbance such as irresponsible off-roading practices (with associated pollution, damages on plant and animal life, and increased soil erosion rates), sand extraction, wind farms, and increased goat grazing (Nogales et al. 2006; Banos-González et al. 2016; Cubas et al. 2019) are all likely to have a severely negative impact on the extent and/or the quality of Mediterranean-type

shrubland vegetation favoured by *P. jacobii* and its key host plants. This, in turn, might lead to a continuous reduction of EOO, AOO, the number of subpopulations and the number of mature individuals stemming from a reduction in foraging resources. Following this scenario, *P. jacobii* also fulfils criteria B1ab(i,ii,iii,iv,v) and B2ab(i,ii,iii,iv,v).

Our field experience further suggests that *P. jacobii* is characterised by very small population sizes: this can be argued based on the fact (i) that we failed to collect more than two specimens at each sampled locality when the number of specimens should have been at its peak, (ii) that *P. jacobii* has been completely overlooked up to the present day, and (iii) that females and males are relatively conspicuous in colour, sharing their pollen host plant species with other Canarian bee species active at the same time of the year, namely in early Spring. Hence, *P. jacobii* also fulfils Criterion C2a(i) based on a conservative estimation of the total number of mature individuals < 2,500 across its distribution, as well as an estimated, projected, or inferred decline for reasons detailed above and < 250 mature specimens per subpopulation (IUCN 2023).

Because of a lack of population size estimation or comprehensive evaluation of the number of extant populations and their trends, we were unable to classify *P. jacobii* under Criteria D and E (IUCN 2023).

Last, we obtained convergent results through the parallel calculation of the IUCN rating based on EOO Area (in km²) with the “EOORating” function in the *rCAT* package, which suggests that *P. jacobii* should be classified as “EN” (endangered).

Given the above results, *P. jacobii* thus qualifies for “EN” (endangered) conservation status under IUCN Criteria B1ab(i,ii,iii,iv,v), B2ab(i,ii,iii,iv,v) and Criterion C2a(i); this status is also supported by the results of the “EOORating” analysis mentioned above. We thus propose an IUCN conservation status of “EN” (endangered) for this species.

Discussion

A new species of *Pseudoanthidium* from the Canary Islands

Twenty-two years after the last description of two new Megachilidae bee species in the CI archipelago, *Osmia palmae* Tkalčů (Tkalčů 2001a) and the cuckoo *Dioxys lanzarotensis* Tkalčů (Tkalčů 2001b), we provide evidence for the presence of a hitherto overlooked species of *Pseudoanthidium* on the islands of Fuerteventura and Lanzarote, the archipelago’s “Eastern Islands”. We describe this new species as *Pseudoanthidium* (*Pseudoanthidium*) *jacobii* Vereecken & Litman spec. nov., and we illustrate its close evolutionary relatedness to the Canarian endemic *P. canariense*. We have highlighted key diagnostic morphological traits to discriminate between the two Canarian *Pseudoanthidium* for each sex (Figs 1–5) and a degree of genetic divergence of 2.7%, lower than, yet still in keeping with, the genetic distances observed between other major clades in the *P. scapulare* complex (Litman et al. 2021). Last, our results illustrate that these two small carder bee species are allopatric in their contemporary distribution (Fig. 1),

they exhibit a significant differentiation in elevation range (Fig. 6), as well as a very low overlap (1%) in their respective ecological niches (Figs 7, 8), due in large part to the different climate of the islands on which they occur. Collectively, and in light of the criteria generally used to delineate species in this genus (Litman et al. 2021; Niu et al. 2021), our observations therefore suggest that *P. jacobii* deserves its own species status.

Most females in the subgenus *Pseudoanthidium* (*Pseudoanthidium*), and particularly in the *P. scapulare* species complex, appear to have a strong preference for host plants in the family Asteraceae (Litman et al. 2021; Niu et al. 2021; Kasperek and Ebmer 2023). A strong preference of *P. jacobii* for host plants in the family Asteraceae might therefore reflect a phylogenetic conservatism of pollen diet, a phenomenon already described in several other groups of wild bees in Europe (Müller and Kuhlmann 2008; Sedivy et al. 2008; Dötterl and Vereecken 2010; Wood et al. 2021; Dorchin et al. 2022).

Canarian *Pseudoanthidium* species and other members of the *P. scapulare* complex

The *Pseudoanthidium scapulare* complex of species is distributed throughout the Palearctic region. Certain members of the complex represent closely related species pairs that are sympatric throughout a part of their distributions, including *P. nanum* - *P. scapulare* and *P. tenellum* - *P. cribratum*. Both of these pairs are morphologically distinct but exhibit relatively low levels of genetic differentiation in analyses of CO1 (0.35% and 0.59%, respectively) (Litman et al. 2021). In recent analyses, however, neither *P. nanum* - *P. scapulare* nor *P. tenellum* - *P. cribratum* showed evidence of barcode-sharing and in both cases, historical mitochondrial introgression was deemed the most likely explanation for the low levels of genetic differentiation observed in these species pairs (Litman et al. 2021). This argument was further supported by a UCE analysis of *P. nanum* and *P. scapulare* that provided strong evidence of two genetically distinct lineages (Litman et al. 2021). In comparison, *P. canariense* and *P. jacobii* show consistent morphological differences but a K2P-corrected genetic distance of 2.7% at the CO1 locus, somewhat higher than the distances separating *P. nanum* - *P. scapulare* and *P. tenellum* - *P. cribratum*. *Pseudoanthidium canariense* and *P. jacobii* may thus represent species whose genetic divergence was facilitated by the reproductive barrier imposed by their distributions on different islands. Further analyses of genomic-level data are needed to better understand the evolutionary history of these taxa.

Our morphological analysis and that of Litman et al. (2021) illustrate that both *P. canariense* and *P. jacobii* have gonostyli that are approximately parallel-sided and exhibit a rounded (i.e., unnotched) apex. This is in marked contrast to other species in the *P. scapulare* complex (except *P. tropicum* (Warncke, 1982) known only from Iran so far, see Litman et al. (2021)), which have an obvious U-shaped notch at the apex of their gonostyli). Interestingly, the absence of a notch is also a feature shared with non-*scapulare* complex *Pseudoanthidium* species (see Niu et al. 2021; Kasperek and Ebmer 2023), which calls into question the ancestral or derived nature of the gonostylus notch in small carder bees.

Given the lack of resolution in our analyses of CO1, namely regarding the phylogenetic relationships among different clades within the complex, we can only propose hypotheses to explain the presence of a rounded gonostylus in *P. jacobii* and *P. canariense*. If the clade represented by these two species is the sister group to all other members of the *P. scapulare* complex, then one possible explanation is that the common ancestor of *P. jacobii* and *P. canariense* colonised the Canary Islands prior to the origin of other members of the *P. scapulare* complex (Litman et al. 2021), i.e., the presence of the rounded gonostylus may represent the plesiomorphic state for the complex. If this clade, however, turns out to be nested within the complex, another possible explanation is that the gonostylus in the common ancestor of *P. jacobii* and *P. canariense* may have undergone a reversion to an ancestral state. If speciation may be driven, at least partially, by morphological barriers to reproduction (Oneal and Knowles 2013; Huang et al. 2020), perhaps the marked differences in the shape of the gonostylus in other, closely related members of the *P. scapulare* complex (i.e., *P. nanum* and *P. scapulare*) may have been significant drivers of speciation, especially in sympatric populations. On the Canary Islands, where the diversity of closely related species is considerably lower than on the mainland, selective pressure on the shape of the gonostylus may be less intense, thus facilitating a reversion to an ancestral state. A future phylogenomic approach to an analysis of this genus using more samples of each species from across their distribution should shed light on the evolution of this and other traits in the genus *Pseudoanthidium* and contribute to improving our knowledge on the diversification and historical biogeography of small carder bees.

Diversity and endemism in Lanzarote and Fuerteventura

Ever since Antiquity, historians, traders and (bio)geographers have acknowledged the peculiar nature of Lanzarote and Fuerteventura, these “Eastern Islands” of the Canary archipelago. Although they form two islands today, they are, geologically speaking, the oldest emerging part of the archipelago that used to be merged during the Pleistocene glacial cycles, forming the paleo-island of Mahan (Rijsdijk et al. 2014). These two islands were also historically referred to as the “Islas Purpurarias” (Garcia-Talavera 2016). The origin of this name supposedly traces back to the peak trade period of *Roccella canariensis* Darb. (Roccellaceae), a lichen species endemic to the Canary Islands and locally known as *orchilla*. This lichen grew on the cliffs of Lanzarote and Fuerteventura at the seashore and was unique as a natural source of the red-purple pigment orcein, a highly sought-after resource in the textile industry up until the end of the 19th century.

By describing *P. jacobii* as an endemic species from the Purpurarias, we provide further evidence for the peculiar environmental conditions met on the islands of Lanzarote and Fuerteventura within the Canary Islands archipelago, and how original life forms have evolved solely on these two islands. Single-island endemics are reported in the eastern CI, such as *Tetralonia lanzarotensis* Tkalçü, 1993 (Apidae) and *Dioxys (Dioxys) lanzarotensis* Tkalçü, 2001 (Megachilidae) from Lanzarote, or *Megachile (Eutricharaea) hohmanni* Tkalçü, 1993 (Megachilidae) and *Dufourea fortunata* Ebmer, 1993 (Halictidae), both recorded exclusively from Fuerteventura within the CI archipelago (Hohmann et al. 1993).

Examples of other wild bee species sharing a distribution restricted to these two islands include *Anthophora purpuraria* Westrich, 1993 (Apidae) (whose specific epithet derives directly from the “Purpurarias”), as well as other Anthophorini species like *A. (Heliophila) lanzarotensis* (Tkalčů, 1993), *A. (Heliophila) lieftincki* (Tkalčů, 1993), *A. (Pyganthophora) porphyrea* Westrich, 1993 (all endemic to Lanzarote and Fuerteventura) and some of their associated cuckoos such as *Melecta (Melecta) caroli* Lieftinck, 1958, and *M. (Melecta) prophanta* Lieftinck, 1980 (on Lanzarote only) (Hohmann et al. 1993). Other cuckoos of these narrow endemic and other more ubiquitous Anthophorini species might include *Thyreus histronicus* (Illiger, 1806) and *T. ramosus* (Lepeletier, 1841) that have a Circum-Mediterranean distribution (Michez et al. 2019; Leclercq et al. 2022). Likewise, the family Megachilidae has a few endemic representatives, such as *Hoplitis (Tkalcula) zandeni* (Teunissen & van Achterberg, 1992) that nests in empty snail shells (Müller and Mauss 2016), *Megachile (Chalicodoma) fuerteventurae* (Tkalčů, 1993) and *M. (Eutricharaea) binominata* Smith, 1853 (Hohmann et al. 1993). The Andrenidae fauna of the Canary Islands also includes narrow endemics to Lanzarote and Fuerteventura, such as *Andrena (Chlorandrena) damara* Warncke, 1968 or *A. (Aciandrena) hillana* Warncke, 1968 (Hohmann et al. 1993).

It is important to note that some species originally described from a single island (such as *A. (H.) lanzarotensis* or *M. (C.) fuerteventurae*, as their specific epithet suggests) turned out to be discovered on both islands after a few decades of field surveys. These recent records contribute to the emergence of distribution patterns among closely related, endemic species in different groups of wild bees, with some restricted to the eastern islands and others present only in the central (and western) islands. For example, the three *Megachile (Chalicodoma)* species recorded in the archipelago exhibit such a distribution pattern similar to the *Pseudoanthidium* species discussed here, with *M. (C.) canescens* (Brullé, 1840) restricted to the central and western islands, whereas *M. (C.) sicula* (Rossi, 1794) and *M. (C.) fuerteventurae* are found only on the eastern islands (Lanzarote and Fuerteventura) (Hohmann et al. 1993). Likewise, *Megachile (Eutricharaea) canariensis* Pérez, 1902 is restricted to the central and western islands, whereas *M. (E.) binominata* is endemic to Lanzarote and Fuerteventura.

Interestingly, no species in the families Colletidae or Melittidae is endemic to Lanzarote and Fuerteventura: these families encompass CI endemic species distributed across the eastern, central and western islands, but none are restricted to eastern islands. Those that are found on these islands have a much wider distribution encompassing Morocco and sometimes extending to the Levant and even the Arabian Peninsula (e.g., for *Melitta schmiedeknechti* Friese, 1898 (Melittidae); see Shebl et al. (2016)).

At their nearest point, Lanzarote and Fuerteventura are located just under 100 km (60 miles) off the coasts of Morocco (García Talavera 1999; Florencio et al. 2021). This relative proximity is therefore likely to have favoured faunal exchanges across families of bees between the Canary Islands archipelago and the African continent. For example, *Andrena (Distandrena) mariana* s.str. Warncke, 1968 (Andrenidae) was described from the island of Fuerteventura in the Canary Islands, and its description was associated with a remark that the species could potentially be found in Morocco as well (Warncke 1968). A similar distribution bridging the Canary Islands archipelago and

the south-western coasts of Morocco has already been found in *Lasioglossum* (*Evylaeus*) *phoenicurum* (Warncke, 1975) (Pauly 2016), in *Nomioides* (*Nomioides*) *fortunatus* Blüthgen, 1937 (Pauly 2017) (both Halictidae), as well as in *Haetosmia circumventa* (Peters, 1974) (Müller 2022), and these findings could probably be echoed in different genera of the diverse family Apidae among others (A. Dorchin, pers. comm. July 2023; P. Rasmont, pers. comm. July 2023). More surveys along the coasts of south-western Morocco are needed to determine if other species considered as endemic to the Canary Islands, including *P. jacobii*, show similar patterns “bridging” the distribution gap with the African continent.

Threats to a new bee species and the Canary Islands bee fauna

Are newly discovered species at a higher risk of extinction than those first described long ago? According to Liu et al. (2022), the trend is positive and significant across major vertebrate groups (amphibians, birds, fish, mammals, and reptiles), and it is driven by several factors, including their often-smaller population numbers and restricted distribution range making them vulnerable to habitat loss and fragmentation. Whether this applies to less intensively investigated groups of organisms like insects, and wild bees in particular, has not been adequately tested so far. Yet, these results suggest that extinction risk assessments that are based on overall threat status of all species combined may seriously underestimate the true number of species threatened with extinction (McKinney 1999).

Here, we classified the new species *P. jacobii* as Endangered (EN) according to IUCN Criteria B1ab(i,ii,iii,iv,v), B2ab(i,ii,iii,iv,v) and Criterion C2a(i), as well as based on the parallel calculation of the IUCN rating based on EOO Area (in km²). In other words, and practically speaking, this means that *P. jacobii* is threatened with extinction and might experience continuous decline unless conservation efforts are made. The results of our extinction risk assessment are also motivated by the fact that *P. jacobii*, similarly to other threatened wild bee species, typically occurs within a few small patches rather than a spatially continuous area of uniform presence. This patchy distribution implies that *P. jacobii* is exposed to comparatively higher extinction risks, because there is a greater chance that one or several of the identified threats will act in concert and will affect all or most of the distribution within a certain time frame. How imminent the identified risks are has remained elusive for a long time, but in recent years the Canary Islands and the “Purpurarias” in particular have seen droughts and heatwaves, just like large parts of the drought-stricken mainland. These changing weather patterns are the direct outcome of climate change operating in real time, and in the worst-case scenario they have even combined with environmental hazards like the 2021 Cumbre Vieja volcano eruption on the island of La Palma, followed in 2023 by massive wildfires breaking out and threatening all terrestrial forms of life on several of the Western Canary Islands. Such wildfires are less likely on Fuerteventura and Lanzarote due to their scarce vegetation and lack of forested areas (Carillo et al. 2022).

The Canary Islands archipelago, like many other insular ecosystems renowned for their breath-taking natural beauty, faces major challenges in achieving a delicate

balance between promoting recreational activities and preserving its fragile biodiversity as the effects of climate change become increasingly pronounced. Our study illustrates that our understanding of biodiversity in the archipelago is far from complete, and that international scientific collaborations with local experts and citizen science projects can help gain significant insights into species distribution and ecological interactions. This paper also confirms the vivid interest of the international scientific community towards the Canary Islands bee fauna and its conservation (see also Monasterio León et al. 2023), and highlights that more targeted field surveys and increased sampling efforts, primarily in the eastern and less sampled western islands, but also slightly before or after the typical “bee season” of January–April, and in high altitude ecosystems found on Gran Canaria and Tenerife still have the potential to reveal other unique taxa and contribute to refine our understanding of the spatial taxonomic, functional and phylogenetic patterns of diversity and endemism of the CI wild bees.

Author contribution statement

NJV: Conceptualization; Data curation; Formal analysis; Funding acquisition; Investigation; Methodology; Project administration; Resources; Software; Validation; Visualization; Writing - original draft; Writing - review & editing. **CR:** Data curation; Project administration; Resources; Supervision; Validation; Writing - review & editing. **CJP:** Formal analysis; Funding acquisition; Investigation; Resources; Software; Visualization; Writing - review & editing. **MPG:** Data curation; Investigation; Visualization; Writing - review & editing. **BJ:** Data curation; Investigation; Writing - review & editing. **JMM:** Data curation; Investigation; Project administration; Resources. **LM:** Conceptualization; Data curation; Formal analysis; Funding acquisition; Investigation; Resources; Software; Visualization; Writing - review & editing. **FLR:** Data curation; Writing - review & editing. **JRL:** Conceptualization; Data curation; Investigation; Methodology; Resources; Supervision; Validation; Writing - review & editing.

Acknowledgements

NJV and JMM are grateful to the FNRS/FWO joint program “EOS—Excellence of Science” for the financial support to the project “CliPS: Climate change and its impact on Pollination Services” (project 30947854). LM and NJV are grateful to the F.R.S.-FNRS (Belgium) for their financial support to LM for his “Chargé de Recherches” mandate on the global bee island biogeography. Our warmest thanks are also due to C.J. Praz for sequencing COI barcode using our specimens of *P. jacobii*, and to L. Mullins for letting us use the metadata of his *P. jacobii* photographic record from Fuerteventura in this study. Last but not least, we are grateful to S.P.M. Roberts for his constructive comments on our IUCN assessment in an earlier version of the manuscript, as well as to A. Müller and an anonymous referee for their positive and constructive comments that helped improve the quality of the manuscript.

References

- Banos-González I, Terrier C, Martínez-Fernández J, Esteve-Selma MA, Carrascal LM (2016) Dynamic modelling of the potential habitat loss of endangered species: the case of the Canarian houbara bustard (*Chlamydotis undulata fuerteventurae*). *European Journal of Wildlife Research* 62: 263–275. <https://doi.org/10.1007/s10344-016-0997-x>
- Bogusch P, Houfková Marešová P, Astapenkova A, Heneberg P (2022) Nest structure, associated parasites and morphology of mature larvae of two European species of *Pseudoanthidium* Friese, 1898 (Hymenoptera, Megachilidae). *Journal of Hymenoptera Research* 92: 285–304. <https://doi.org/10.3897/jhr.92.87215>
- Bowler J (2018) *Wildlife of Madeira and the Canary Islands*. Princeton University Press, 224 pp. <https://doi.org/10.1515/9781400889266>
- Broennimann O, Fitzpatrick MC, Pearman PB, Petitpierre B, Pellissier L, Yoccoz NG, Thuiller W, Fortin M, Randin C, Zimmermann NE, Graham CH, Guisan A (2012) Measuring ecological niche overlap from occurrence and spatial environmental data. *Global Ecology and Biogeography* 21: 481–497. <https://doi.org/10.1111/j.1466-8238.2011.00698.x>
- Broennimann O, Di Cola V, Guisan A (2023) *ecospat: Spatial Ecology Miscellaneous Methods*. R package version 3.5.1. <https://CRAN.R-project.org/package=ecospat>
- Cardoso P (2020) *red: IUCN Red listing Tools*. R package version 1.5.0. <https://CRAN.R-project.org/package=red>
- Carillo J, Pérez JC, Expósito FJ, Díaz JP, González A (2022) Projections of wildfire weather danger in the Canary Islands. *Scientific Reports* 12: 8093. <https://doi.org/10.1038/s41598-022-12132-5>
- Cubas J, Irl SD, Villafuerte R, Bello-Rodríguez V, Rodríguez-Luengo JL, Del Arco M, Martín-Esquível JL, González-Mancebo JM (2019) Endemic plant species are more palatable to introduced herbivores than non-endemics. *Proceedings of the Royal Society B, Biological Sciences* 286(1900): 20190136. <https://doi.org/10.1098/rspb.2019.0136>
- del Arco Aguilar MJ, Rodríguez Delgado O, del Arco Aguilar MJ, Rodríguez Delgado O (2018) *Vegetation of the Canary Islands*. Springer Verlag, Germany, 429 pp. <https://doi.org/10.1007/978-3-319-77255-4>
- Dötterl S, Vereecken NJ (2010) The chemical ecology and evolution of bee–flower interactions: a review and perspectives. *Canadian Journal of Zoology* 88(7): 668–697. <https://doi.org/10.1139/Z10-031>
- Dorcin A, Shafir A, Neumann FH, Langgut D, Vereecken NJ, Mayrose I (2021) Bee flowers drive macroevolutionary diversification in long-horned bees. *Proceedings of the Royal Society B, Biological Sciences* 288(1959): 28820210533 <https://doi.org/10.1098/rspb.2021.0533>
- Dupont YL, Skov C (2004) Influence of geographical distribution and floral traits on species richness of bees (Hymenoptera: Apoidea) visiting *Echium* species (Boraginaceae) of the Canary Islands. *International Journal of Plant Sciences* 165(3): 377–386. <https://doi.org/10.1086/382806>
- Fernández-Palacios JM, Arévalo JR, Delgado JD, Otto R (2004) *Canarias: ecología, medio ambiente y desarrollo*. Centro de la Cultura Popular de Canarias, La Laguna, 171 pp.
- Fernández-Palacios JM, Whittaker RJ (2008) The Canaries: an important biogeographical meeting place. *Journal of Biogeography* 35(3): 379–387. <https://doi.org/10.1111/j.1365-2699.2008.01890.x>

- Fernández-Palacios JM, Schrader J, de Nascimento L, Irl SDH, Sánchez-Pinto L, Otto R (2023) Are plant communities on the Canary Islands resistant to plant invasion? Diversity and Distributions 29: 51–60. <https://doi.org/10.1111/ddi.13650>
- Florencio M, Patiño J, Nogué S, Traveset A, Borges PA, Schaefer H, Amorim IR, Arnedo M, Ávila SP, Cardoso P, de Nascimento L, Fernández-Palacios JM, Gabriel SI, Gil A, Gonçalves V, Haroun R, Illera JC, López-Darias M, Martínez A, Martins GM, Neto AI, Nogales M, Oromí P, Rando JC, Raposeiro PM, Rigal F, Romeiras MM, Silva L, Valido A, Vanderpoorten A, Vasconcelos R, Santos AMC (2021) Macaronesia as a fruitful arena for ecology, evolution, and conservation biology. *Frontiers in Ecology and Evolution* 9: 718169. <https://doi.org/10.3389/fevo.2021.718169>
- García Talavera F (1999) Consideraciones geológicas, biogeográficas y paleoecológicas. In: Fernández-Palacios JM, Bacallado JJ and Belmonte JA (Eds) *Ecología y Cultura en Canarias*. Cabildo Insular de Tenerife, Santa Cruz de Tenerife, 39–63.
- García-Talavera F (2016) Guanches ayer, hoy Canarios. *Apuntes de la historia e identidad de un pueblo Macaronésio*. Idea Ediciones, 314 pp.
- GBIF (2023a) GBIF Occurrence Download. <https://doi.org/10.15468/dl.x6cwjx>
- GBIF (2023b) GBIF Occurrence Download. <https://doi.org/10.15468/dl.4hgjkb>
- Hanz DM, Cutts V, Barajas-Barbosa MP, Algar A, Beierkuhnlein C, Collart F, Fernández-Palacios JM, Field R, Karger DN, Kienle DR, Kreft H, Patiño J, Schrodt F, Steinbauer MJ, Weigelt P, Irl SDH (2023) Effects of climate change on the distribution of plant species and plant functional strategies on the Canary Islands. *Diversity and Distributions* 29(9): 1157–1171. <https://doi.org/10.1111/ddi.13750>
- Hebert PDN, Penton EH, Burns JM, Janzen DH, Hallwachs W (2004) Ten species in one: DNA barcoding reveals cryptic species in the neotropical skipper butterfly *Astraptes fulgerator*. *Proceedings of the National Academy of Sciences of the USA* 101: 14812–14817. <https://doi.org/10.1073/pnas.0406166101>
- Hohmann H, La Roche F, Ortega G, Barquín J (1993) *Bienen, Wespen und Ameisen der Kanarischen Inseln*. König V, Übersee-Museum, Bremen, 1–31.
- Hollister JW (2022) elevatr: Access Elevation Data from Various APIs. R package version 0.4.2. <https://CRAN.R-project.org/package=elevatr/>
- Huang J-P, Hill JG, Ortego J (2020) Paraphyletic species no more – genomic data resolve a Pleistocene radiation and validate morphological species of the *Melanophus scudderi* complex (Insecta: Orthoptera). *Systematic Entomology* 45(3): 594–605. <https://doi.org/10.1111/syen.12415>
- iNaturalist.com (2023) Abejas de Canarias. <https://www.inaturalist.org/projects/abejas-de-canarias> [accessed July 2023]
- IUCN Standards and Petitions Committee (2022) Guidelines for Using the IUCN Red List Categories and Criteria. Version 15.1. Prepared by the Standards and Petitions Committee. <https://www.iucnredlist.org/documents/RedListGuidelines.pdf> [accessed July 2023]
- Jacobi B, Suárez D (2018) First records of *Philanthus triangulum* (Fabricius, 1775) for Fuerteventura (Spain) and further data on the distribution and phenology of *Colletes perezii* Morice, 1904 recently recorded on the island (Hymenoptera, Aculeata). *Ampulex* (10): 20–23.
- Jacobi B, Peña Tejera G, Marquina Reyes D, Rae S, Checa López JE (2013) Present distribution of *Philanthus triangulum* (Hymenoptera, Crabronidae) on the Canary Islands. *bembiX* 37: 5–14.

- Jacobi B, Flügel H-J, Beckert J (2021) Nachweise der Zwergwollbiene *Pseudoanthidium nanum* (Mocsáry, 1881) in Nordrhein-Westfalen. Elektronische Aufsätze der Biologischen Station Westliches Ruhrgebiet 44: 1–6.
- Jaiswara R, Sreebin S, Monaal, Robillard T (2022) A new species of *Indigryllus* (Orthoptera, Gryllidae, Eneopterinae, Xenogryllini) from Kerala, India, with first data on acoustics and natural habitat. Zootaxa 5205(6): 532–546. <https://doi.org/10.11646/zootaxa.5205.6.2>
- Karger DN, Conrad O, Böhner J, Kawohl T, Kreft H, Soria-Auza RW, Zimmermann NE, Linder HP, Kessler M (2017) Climatologies at high resolution for the earth's land surface areas. Scientific Data 4(1): 170122. <https://doi.org/10.1038/sdata.2017.122>
- Kasperek M, Ebmer AW (2023) The wool carder bee *Pseudoanthidium alpinum* (Morawitz, 1873): identity of the enigmatic type species of the genus *Pseudoanthidium* (Hymenoptera: Megachilidae: Anthidiini). Osmia 11: 39–50. <https://doi.org/10.47446/OSMIA11.7>
- Katoh K, Standley DM (2013) MAFFT multiple sequence alignment software v.7: improvements in performance and usability. Molecular Biology and Evolution 30: 772–780. <https://doi.org/10.1093/molbev/mst010>
- Kearse M, Moir R, Wilson A, Stones-Havas S, Cheung M, Sturrock S, Buxton S, Cooper A, Markowitz S, Duran C, Thierer T, Ashton B, Meintjes P, Drummond A (2012) Geneious Basic: an integrated and extendable desktop software platform for the organization and analysis of sequence data. Bioinformatics 28: 1647–1649. <https://doi.org/10.1093/bioinformatics/bts199>
- Kratochwil A (2020) Revision of the *Andrena wollastoni* group (Hymenoptera, Anthophila, Andrenidae) from the Madeira Archipelago and the Canary Islands: Upgrading of three former subspecies and a description of three new subspecies. Linzer Biologische Beiträge 52(1): 161–244.
- Kratochwil A, Schwabe A (2018) Wild bees (Anthophila) of Macaronesia—biogeographical and evolutionary aspects. Berichte der Reinhold-Tüxen-Gesellschaft 30: 149–162.
- Kratochwil A, Schwabe A (2020) Flower-visiting behaviour and habitats of the taxa of the *Andrena wollastoni* group (Hymenoptera, Anthophila, Micrandrena) on the Canary Islands compared to the Madeira Archipelago. Linzer Biologische Beiträge 52(1): 309–326.
- Kuhlmann M (2000) Katalog der paläarktischen Arten der Bienengattung *Colletes* Latr., mit Lectotypenfestlegungen, neuer Synonymie und der Beschreibung von zwei neuen Arten (Hymenoptera: Apidae: Colletinae). Linzer Biologische Beiträge 32: 155–193.
- Kunkel G (1976) Biogeography and ecology in the Canary Islands. Monographiae Biologicae 30: 1–511. https://doi.org/10.1007/978-94-010-1566-0_1
- Le Breton TD, Zimmer HC, Gallagher RV, Cox M, Allen S, Auld TD (2019) Using IUCN criteria to perform rapid assessments of at-risk taxa. Biodiversity and Conservation 28: 863–883. <https://doi.org/10.1007/s10531-019-01697-9>
- Leclercq N, Marshall L, Caruso G, Schiel K, Weekers T, Carvalheiro LG, Dathe HH, Kuhlmann M, Michez D, Potts SG, Rasmont, P, Roberts SPM, Smagghe G, Vandamme P, Vereecken NJ (2022) European bee diversity: Taxonomic and phylogenetic patterns. Journal of Biogeography 50(7): 1244–1256. <https://doi.org/10.1111/jbi.14614>
- Litman J, Fateryga AV, Griswold T, Aubert M, Proshchalykin M, Le Divellec R, Burrows S, Praz C (2021) Paraphyly and low levels of genetic divergence in morphologically distinct taxa: revision of the *Pseudoanthidium scapulare* complex of carder bees (Apoidea: Megachilidae):

- Anthidiini). *Zoological Journal of the Linnean Society* 195(4): 1287–1337. <https://doi.org/10.1093/zoolinlean/zlab062>
- Liu J, Slik F, Zheng S, Lindenmayer DB (2022) Undescribed species have higher extinction risk than known species. *Conservation Letters* 15: e12876. <https://doi.org/10.1111/conl.12876>
- Lugo D, Peña G, De la Rúa P, Ruiz C (2022) Presence of exotic species of the wild bee genus *Hylaeus* (Hymenoptera: Colletidae) in the Canary Islands revealed by molecular and citizen science. *Journal of Apicultural Research* 61(4): 460–468. <https://doi.org/10.1080/00218839.2022.2053034>
- Mace GM, Collar NJ, Gaston KJ, Hilton-Taylor C, Akçakaya HR, Leader-Williams N, Milner-Gulland EJ, Stuart SN (2008) Quantification of extinction risk: IUCN's system for classifying threatened species. *Conservation Biology* 22(6): 1424–1442. <https://doi.org/10.1111/j.1523-1739.2008.01044.x>
- Machado A (1976) Introduction to a faunal study of the Canary Islands' Laurisilva with special reference to the ground-beetles. In: Kunkel G (Ed.) *Biogeography and ecology in the Canary Islands*. Dr. W. Junk, The Hague, The Netherlands, 347–411. https://doi.org/10.1007/978-94-010-1566-0_13
- Maddison WP, Maddison DR (2023) Mesquite: a modular system for evolutionary analysis. Version 3.81. <http://www.mesquiteproject.org>
- Martín-Cejas RR, Ramírez Sánchez PP (2010) Ecological footprint analysis of road transport related to tourism activity: The case for Lanzarote Island. *Tourism Management* 31: 98–103. <https://doi.org/10.1016/j.tourman.2009.01.007>
- Martín-Cejas RR (2015) The environmental impact caused by road access to Timanfaya Natural Park on Lanzarote Island. *Transportation Research Part D: Transport and Environment* 41: 457–466. <https://doi.org/10.1016/j.trd.2015.09.027>
- Masson Rosa R, Caracanhas Cavallari D, Brincalpe Salvador R (2022) iNaturalist as a tool in the study of tropical molluscs *PLoS ONE* 17(5): e0268048. <https://doi.org/10.1371/journal.pone.0268048>
- McKinney ML (1999) High rates of extinction and threat in poorly studied taxa. *Conservation Biology* 13: 1273–1281. <https://doi.org/10.1046/j.1523-1739.1999.97393.x>
- Michener CD (2007) *The Bees of the World*. 2nd edn. The Johns Hopkins University Press, Baltimore, Maryland and London, [xvi +] 953 pp.
- Michez D, Rasmont P, Terzo M, Vereecken NJ (2019) *Hymenoptera of Europe volume 1 - Bees of Europe*. NAP Editions, Paris, France.
- Moat J (2020) rCAT: Conservation Assessment Tools. R package version 0.1.6. <https://CRAN.R-project.org/package=rCAT>
- Monasterio León Y, Ruiz Carreira C, Escobés Jiménez R, Almunia J, Wiemers M, Vujic A, Macadam C, Raser J, Hochkirch A (2023) *Canarian Islands endemic pollinators of the Laurel Forest zone - Conservation plan 2023–2028*. Publication prepared for the European Commission within the framework of the contract No 07.0202/2020/839411/SER/ENV.0.
- Müller A, Kuhlmann M (2008) Pollen hosts of western palaeartic bees of the genus *Colletes* (Hymenoptera: Colletidae): the Asteraceae paradox. *Biological Journal of the Linnean Society* 95(4): 719–733. <https://doi.org/10.1111/j.1095-8312.2008.01113.x>

- Müller A, Mauss V (2016) Palaearctic *Hoplitis* bees of the subgenera *Formicapis* and *Tkalcua* (Megachilidae, Osmiini): biology, taxonomy and key to species. *Zootaxa* 4127(1): 105–120. <https://doi.org/10.11646/zootaxa.4127.1.5>
- Müller A (2022) Palaearctic Osmiine Bees, ETH Zürich. <http://blogs.ethz.ch/osmiini> [Accessed on October 11, 2023]
- Nieto A, Roberts SPM, Kemp J, Rasmont P, Kuhlmann M, García Criado M, Biesmeijer JC, Bogusch P, Dathe HH, de la Rúa P, de Meulemeester T, Dehon M, Dewulf A, Ortiz-Sánchez FJ, Lhomme P, Pauly A, Potts SG, Praz CJ, Window J, Michez D (2014) European Red List of Bees. In IUCN Global Species Programme.
- Nogales M, Rodríguez-Luengo JL, Marrero P (2006) Ecological effects and distribution of invasive non-native mammals on the Canary Islands. *Mammal Review* 36(1): 49–65. <https://doi.org/10.1111/j.1365-2907.2006.00077.x>
- Pauly A (2016) Le genre *Lasioglossum*, sous-genre *Evyllaes* Robertson, 1902, de la Région Paléarctique. *Atlas Hymenoptera*. <http://www.atlashymenoptera.net/page.aspx?ID=95>
- Oneal E, Knowles LL (2013) Ecological selection as the cause and sexual differentiation as the consequence of species divergence? *Proceedings of the Royal Society B, Biological Sciences* 280: 20122236. <https://doi.org/10.1098/rspb.2012.2236>
- Ortiz-Sanchez J, La Roche F, Fuhrmann M (2016) Primera cita del género *Xylocopa* Latreille, 1802 en las Islas Canarias (Hymenoptera, Apidae). *Boletín de la Sociedad Entomológica Aragonesa (S.E.A.)* 58: 206.
- Pauly A (2017) The genus *Nomioides* Schenck, 1867. <http://www.atlashymenoptera.net/page.aspx?ID=96>
- Pérez AJ, Marcías-Hernández NE (2012) Presencia de *Bombus (Megabombus) ruderatus* en Canarias. *Revista de la Academia Canaria de Ciencias: Folia Canariensis Academiae Scientiarum* 24(1): 103–114.
- Pesenko YA, Pauly A (2005) Monograph of the bees of the subfamily Nomioiinae (Hymenoptera: Halictidae) of Africa (excluding Madagascar). *Annales de la société entomologique de France (n.s.)* 41(2): 129–236. <https://doi.org/10.1080/00379271.2005.10697443>
- QGIS Development Team (2023) QGIS Geographic Information System. Open Source Geospatial Foundation Project. <http://qgis.osgeo.org>
- R Core Team (2022) R: A language and environment for statistical computing. R Foundation for Statistical Computing, Vienna, Austria. <https://www.R-project.org/>
- Ramón Arévalo J, Tejedor M, Jiménez C, Reyes-Betancourt J, Díaz FJ (2016) Plant species composition and richness in abandoned agricultural terraces vs. natural soils on Lanzarote (Canary Islands). *Journal of Arid Environments* 124: 165–171. <https://doi.org/10.1016/j.jaridenv.2015.08.012>
- Reyes-Betancourt J, Wildpret de la Torre W, León Arencibia M (2001) The vegetation of Lanzarote (Canary Islands). *Phytocoenologia* 31(2): 185–248. <https://doi.org/10.1127/phyto/31/2001/185>
- Rijsdijk KF, Hengl T, Norder SJ, Otto R, Emerson BC, Ávila SP, López H, van Loon E, Tjørve E, Fernández-Palacios JM (2014) Quantifying surface-area changes of volcanic islands driven by Pleistocene sea-level cycles: Biogeographical implications for the Macaronesian archipelagos. *Journal of Biogeography* 41: 1242–1254. <https://doi.org/10.1111/jbi.12336>

- Rodríguez JP, Keith DA, Rodríguez-Clark KM, Murray NJ, Nicholson E, Regan TJ, Miller RM, Barrow EG, Bland LM, Boe K, Brooks TM, Oliveira-Miranda MA, Spalding M, Wit P (2015) A practical guide to the application of the IUCN Red List of Ecosystems criteria. *Philosophical Transactions of the Royal Society B, Biological Sciences* 370(1662): 20140003. <https://doi.org/10.1098/rstb.2014.0003>
- RStudio Team (2020) RStudio: Integrated Development for R. RStudio, PBC, Boston, MA. <http://www.rstudio.com/>
- Ruiz C, Suárez D, Naranjo M, De la Rúa P (2020) First record of the carpenter bee *Xylocopa pubescens* (Hymenoptera, Apidae) in the Canary Islands confirmed by DNA barcoding. *Journal of Hymenoptera Research* 80: 169–175. <https://doi.org/10.3897/jhr.80.59649>
- Schoener TW (1968) The Anolis lizards of Bimini: resource partitioning in a complex fauna. *Ecology* 49: 704–726. <https://doi.org/10.2307/1935534>
- Sedivy C, Praz CJ, Müller A, Widmer A, Dorn S (2008) Patterns of host-plant choice in bees of the genus *Chelostoma*: the constraint hypothesis of host-range evolution in bees. *Evolution* 62(10): 2487–2507. <https://doi.org/10.1111/j.1558-5646.2008.00465.x>
- Shebl AM, Alqarni AS, Engel MS (2016) First record of the bee genus *Melitta* from the Arabian Peninsula (Hymenoptera: Apoidea: Melittidae). *Zoology in the Middle East* 62(4): 352–357. <https://doi.org/10.1080/09397140.2016.1250713>
- Smit J (2007) New wasps and bees for the fauna of the Canary Islands (Hymenoptera, Aculeata). *Linzer biologische Beiträge* 39(1): 651–656.
- Strudwick T, Jacobi B (2018) The American Resin bee *Megachile (Chelostomoides) otomita* Cresson, 1878 established on Tenerife, Canary Islands (Spain) (Hymenoptera, Anthophila). *Ampulex* 10: 41–45.
- Suárez D, Hernández-Teixidor D, Pérez AJ, Ferrera-León E, Arechavaleta JJ, Oromi P (2017) New chorological data on arthropod biodiversity in the Canary Islands (Spain). *Boletim de la Sociedad Entomológica Aragonesa (S.E.A.)* 60: 349–351.
- Tkalčů B (1993) Neue Taxa der Bienen von den Kanarischen Inseln. Mit Bemerkungen zu einigen bereits bekannten Arten. *Veröffentlichungen aus dem Überseemuseum Bremen. Reihe A Naturwissenschaften* 12: 791–858.
- Tkalčů B (2001a) Nouvelle espèce d'*Osmia* de l'île de La Palma (Iles Canaries). *Bulletin de la Société entomologique de Mulhouse* 57(3): 29–31.
- Tkalčů B (2001b) Une nouvelle espèce du genre *Dioxys* des Iles Canaries. *Bulletin de la Société entomologique de Mulhouse* 57(3): 49–50.
- Trifinopoulos J, Nguyen L-T, von Haeseler A, Quang Minh B (2016) W-IQ-TREE: a fast online phylogenetic tool for maximum likelihood analysis. *Nucleic Acids Research* 44(W1): W232–W235. <https://doi.org/10.1093/nar/gkw256>
- Warncke K (1968b) Zur Kenntnis der Bienengattung *Andrena* F. auf den Kanarischen Inseln. *Notulae Entomologicae* 48: 63–80.
- Warren DL, Glor RE, Turelli M (2008) Environmental niche equivalency versus conservatism: quantitative approaches to niche evolution. *Evolution* 62: 2868–2883. <https://doi.org/10.1111/j.1558-5646.2008.00482.x>
- Wheeler WM (1927) The ants of the Canary Islands. *Proceedings of the American Academy of Arts and Sciences* 62(3): 93–120. <https://doi.org/10.2307/25130107>

- Wickham H (2016) ggplot2: Elegant Graphics for Data Analysis. Springer-Verlag New York, USA, 260 pp. <https://doi.org/10.1007/978-3-319-24277-4>
- Wood TJ, Ghisbain G, Rasmont P, Kleijn D, Raemakers I, Praz CJ, Killewald M, Gibbs J, Bobiwash K, Boustani M, Martinet B, Michez D (2021) Global patterns in bumble bee pollen collection show phylogenetic conservation of diet. *Journal of Animal Ecology* 90(10): 2421–2430. <https://doi.org/10.1111/1365-2656.13553>
- Zhang YM, Sasan K, O'Kennon RJ, Kranz AJ (2022) Discovery through iNaturalist: a new species and new records of oak gall wasps (Hymenoptera: Cynipidae: Cynipini) from Texas, USA. *Zootaxa* 5168(1): 063–074. <https://doi.org/10.11646/zootaxa.5168.1.5>

Supplementary material 1

Information on *Pseudoanthidium* specimens used for the barcoding

Author: Jessica R. Litman

Data type: csv

Explanation note: List of specimens and associated metadata used for the Maximum likelihood-based tree based on analysis of a 658 base pair fragment of COI sequenced from selected *Pseudoanthidium* species in the *P. scapulare* complex.

Copyright notice: This dataset is made available under the Open Database License (<http://opendatacommons.org/licenses/odbl/1.0/>). The Open Database License (ODbL) is a license agreement intended to allow users to freely share, modify, and use this Dataset while maintaining this same freedom for others, provided that the original source and author(s) are credited.

Link: <https://doi.org/10.3897/jhr.96.111550.suppl1>

Supplementary material 2

Distribution data of each *Pseudoanthidium* species in the Canary Islands

Author: Nicolas J. Vereecken

Data type: csv

Explanation note: Distribution data including all occurrence records available to us and relevant to both *P. (P.) canariense* and *P. (P.) jacobii* Vereecken & Litman spec. nov. in the Canary Islands.

Copyright notice: This dataset is made available under the Open Database License (<http://opendatacommons.org/licenses/odbl/1.0/>). The Open Database License (ODbL) is a license agreement intended to allow users to freely share, modify, and use this Dataset while maintaining this same freedom for others, provided that the original source and author(s) are credited.

Link: <https://doi.org/10.3897/jhr.96.111550.suppl2>

Phylogenetic affinities of the non-cyclostome subfamilies Amicrocentrinae and Dirrhopinae (Hymenoptera, Braconidae) confirmed by ultraconserved element data

Jovana M. Jasso-Martínez¹, Seán G. Brady¹, Robert R. Kula²

1 Department of Entomology, Smithsonian Institution, National Museum of Natural History, 10th St. & Constitution Ave. NW, Washington, DC 20560, USA **2** Systematic Entomology Laboratory, Beltsville Agricultural Research Center, Agricultural Research Service, U.S. Department of Agriculture, c/o Department of Entomology, Smithsonian Institution, National Museum of Natural History, Washington, D.C., USA

Corresponding author: Jovana M. Jasso-Martínez (jovana.jasso@gmail.com)

Academic editor: Jose Fernandez-Triana | Received 10 August 2023 | Accepted 9 September 2023 | Published 22 November 2023

<https://zoobank.org/322DF6BE-78EF-4C6C-BE95-6B8669B5E10B>

Citation: Jasso-Martínez JM, Brady SG, Kula RR (2023) Phylogenetic affinities of the non-cyclostome subfamilies Amicrocentrinae and Dirrhopinae (Hymenoptera, Braconidae) confirmed by ultraconserved element data. Journal of Hymenoptera Research 96: 1017–1030. <https://doi.org/10.3897/jhr.96.111012>

Abstract

The subfamilies Amicrocentrinae and Dirrhopinae (Hymenoptera, Braconidae) are two small, monogeneric braconid subfamilies whose species exclusively attack lepidopteran larvae. The phylogenetic placement of Amicrocentrinae as a member of the helconoid complex of subfamilies has been supported by morphological and nuclear Sanger sequence data. The subfamilial status of Dirrhopinae on the other hand has been subject to debate, although it has been suggested as closely related to the microgastroid complex based on morphology only. Here we generated for the first time genomic ultraconserved element data for members of the above subfamilies (*Amicrocentrum seyrigi* van Achterberg and *Dirrhope americana* Muesebeck) to assess their phylogenetic affinities using exhaustive taxon sampling that includes all but one of the currently valid braconid subfamilies. Our results strongly confirm the placement of both taxa within the non-cyclostome helconoid and microgastroid complexes, respectively.

Keywords

Amicrocentrinae, Braconidae, Dirrhopinae, non-cyclostomes, ultraconserved elements

Introduction

The parasitoid wasp family Braconidae is an extremely species-rich group within the order Hymenoptera, currently having more than 21,000 described species (Yu et al. 2016). Braconids mainly attack larval stages of other holometabolous insects with only some exceptions, including a few species within the subfamilies Braconinae, Doryctinae and Mesostoinae that are secondarily phytophagous (Infante et al. 1995; Dangerfield and Austin 1998; Ranjith et al. 2016; Zaldívar Riverón et al. 2014). The members of this family are divided into two major monophyletic groups (Dowton et al. 2002; Sharanowski et al. 2011, 2021; Jasso-Martínez et al. 2022a, 2022b), the cyclostomes and the non-cyclostomes, with the respective groups originally proposed based on the presence or absence of an ovoid cavity between the clypeus and mandibles with the labrum visible and concave in cyclostomes (Sharkey 1993; Wharton 1993). Some groups within the cyclostome clade, remarkably Alysiniinae and Opiinae, have secondarily lost the cyclostome condition, although this is also observed in some members of other subfamilies such as Rogadinae and Telengaiinae.

As for other megadiverse groups, the phylogenetic affinities of various taxa within Braconidae have been debated extensively due to the lack of morphological synapomorphies, limited taxon sampling and limited molecular information (Quicke and van Achterberg 1990; Dowton et al. 2002; Pitz et al. 2005). In recent past, a consensus has emerged regarding subfamily-level relationships within the family (Zaldívar-Riverón et al. 2006; Sharanowski et al. 2011, 2021; Jasso-Martínez et al. 2022a, 2022b). Recently, the family Braconidae was proposed to comprise 41 subfamilies (Apozyginae, 25 non-cyclostome and 15 cyclostome *s.l.* subfamilies) based on ultraconserved element (UCE) and mitogenome sequence data (Jasso-Martínez et al. 2022a, 2022b). However, the subfamilies Amicrocentrinae, Dirrhopinae and Xiphozelinae were not included in the above study due to a lack of either available specimens or sufficient sequence data.

The subfamily Amicrocentrinae was established by van Achterberg (1979) and contains five species, two of which have been reared from stem-boring Lepidoptera larvae (van Achterberg 1979). Its single genus, *Amicrocentrum* Schulz, was placed previously in the non-cyclostome subfamily Macrocentrinae; however, *Amicrocentrum* lacks synapomorphic features of Macrocentrinae such as trochantellus with spines (van Achterberg 1979) (Fig. 1). A molecular phylogeny supported the subfamily status of *Amicrocentrum*, recovering it as more closely related to the subfamily Charmontinae than Macrocentrinae within the helconoid complex in the braconid non-cyclostome clade (Sharanowski et al. 2011).

The placement within Braconidae of the rare, lepidopteran parasitoid genus *Dirrhope* Foerster has changed through time, with it suggested as a member of Microgastrinae (Muesebeck 1935; Tobias 1967; Marsh 1979), Miracinae (Tobias 1986; Belokobylskij 1989) or the previously recognized subfamily Adeliinae (Telenga 1955; Capek 1970), the latter currently regarded as a tribe within Cheloninae (Dowton and Austin 1998; Kittel et al. 2016). However, *Dirrhope* shows autapomorphic features



Figure 1. Lateral habitus of *Amicrocentrum seyrigi*.

such as the spiracles of the first metasomal tergum posterior to the middle of the tergum (Fig. 2A) that led to its recognition as a subfamily (van Achterberg 1984) that currently contains five species (van Achterberg 1984; Belokobylskij 1989; Whitfield and Wagner 1991; Belokobylskij et al. 2003). The placement of Dirrhopinae as closely related to the microgastroid complex of subfamilies has been recovered based on morphological data (van Achterberg 1984; Quicke and van Achterberg 1990; Wharton et al. 1992; Whitfield and Mason 1994; Belokobylskij et al. 2003), but it has never been included in a molecular-based study.

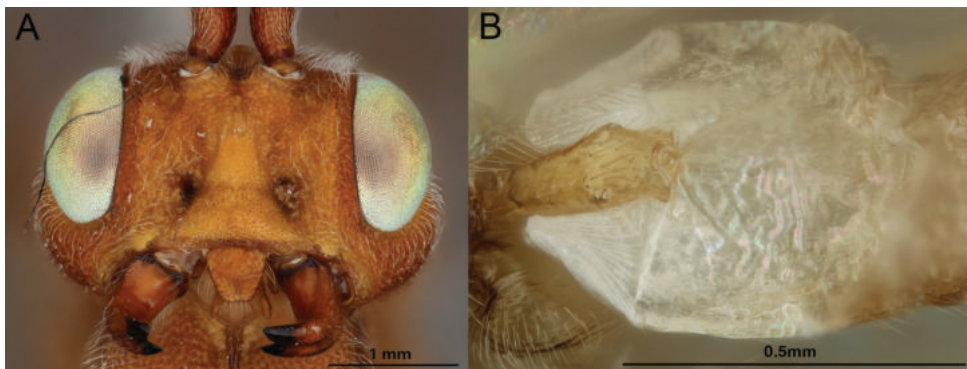


Figure 2. **A** Head of *Amicrocentrum seyrigi* showing two-segmented palpi **B** *Dirrhope americana* metasomal terga 1–3 showing the location of spiracles on the first metasomal tergum.

In this study we included representatives of Amicrocentrinae and Dirrhopinae for the first time in a phylogenomic dataset that includes all currently extant valid braconid subfamilies except Xiphozelinae. Based on genomic-scale data obtained from UCEs, we evaluated both their proposed subfamilial status and their phylogenetic affinities within Braconidae. Additionally, we assessed previously proposed morphological apomorphic features for these taxa in relation to their recovered phylogenetic relationships.

Methods

Taxon sampling

Our taxon sampling comprises a total of 401 terminal taxa, including outgroups. Our braconid ingroup includes 233 species that belong to the cyclostome *s.l.* group, 156 species of the non-cyclostome group (including *Amicrocentrum seyrigi* and *Dirrhope americana*) and *Apozyx penyai* Mason (Apozyginae). All braconid taxa used in this study, except *A. seyrigi* and *D. americana*, are part of the dataset that was included in a recently published phylogenetic study of Braconidae (table S1 in Jasso-Martínez et al. 2022a). As outgroup, we included 10 species belonging to nine subfamilies of Ichneumonidae, representing all major lineages within the family. Both Braconidae and Ichneumonidae are the only two extant families of the superfamily Ichneumonoidea. In a recent study that used UCEs as the data source for phylogenetic reconstruction (Blaimer et al. 2023), the superfamily Ichneumonoidea was recovered as sister to all remaining Apocrita, which includes the superfamily Gasteruptionidae; thus, we used *Gasteruption floridanum* Bradley to root our trees as was done by Jasso-Martínez et al (2022a) for a dataset that included most of the taxa in the present study. Specimens of *A. seyrigi* and *D. americana* (Table 1) are deposited in the Hymenoptera collection of the National Museum of Natural History (NMNH), Smithsonian Institution, Washington, D.C.

Terminology for external morphology, including wing venation, follows Sharkey and Wharton (1997).

Table 1. Locality and SRA information of *Amicrocentrum seyrigi* and *Dirrhope americana*.

Specimen voucher	Subfamily	Genus	Species	Label information	SRA accession number
USNMMENT1322780	Amicrocentrinae	<i>Amicrocentrum</i>	<i>seyrigi</i>	MADAGASCAR: Antsokay. Latitude: 23°25.40'S, longitude: 43°44.51'E. Collection year: 2012. Collectors: M. Irwin, Rin'ha.	SAMN37185746
USNMMENT1322781	Dirrhopinae	<i>Dirrhope</i>	<i>americana</i>	USA: Virginia, Fauquier Co. Granruth Grove. Latitude: 38°49'9.60"N, longitude: 77°54'35.60"W. Collection year: 2014. Collector: Kula, R., et al.	SAMN37185747

UCE data and matrices

Genomic DNA extraction of *A. seyrigi* and *D. americana* was performed using a leg and whole specimen, respectively, with the Quiagen DNeasy Blood and Tissue kit (Quiagen Inc., Valencia, California, U.S.A.). DNA quantitation was measured with Qubit 2.0 fluorometer (Life Technologies Inc. Carlsbad, CA). Total DNA of both samples (*A. seyrigi*: 41 ng; *D. americana* 16 ng) was used as input for shearing and library preparation. DNA was sheared for 45 seconds in a Qsonica Q800R sonicator (Qsonica LLC, Newton, CT). Genomic libraries were prepared using the Kapa Hyper Prep Kit (Roche) and the custom Tru-Seq-style dual-indexing adapter (Glenn et al. 2016). We included both libraries in a pool that was enriched with the Hymenoptera bait set 2.5Kv2 (Branstetter et al. 2017), which targets 2,590 UCE loci. Sequencing was conducted on an Illumina HiSeq 2500 instrument (2×150 rapid run; Illumina Inc. San Diego, CA).

Raw reads were cleaned and trimmed using Illuminaprocessor v 2.0.7 (Faircloth, 2013), a wrapper around Trimmomatic (Del Fabbro et al. 2013; Bolger et al. 2014) in the phyluce pipeline v 1.7.0 (Faircloth 2016). *Amicrocentrum seyrigi* and *D. americana* cleaned reads assembly was performed in spades v 3.14.0 (Prjibelski et al. 2020). We merged both newly generated and previously published assemblies for UCE loci extraction in phyluce version 1.7.0 (Faircloth 2016). Extracted UCE loci were aligned with MAFFT v 7 (Kato and Standley 2013), and the resulting alignments were filtered with Gblocks version 0.91b (Castresana 2000) using reduced stringency settings for b1–b4: 0.5, 0.5, 12 and 7, respectively. We prepared two matrices containing loci recovered for at least 25% and 50% of the taxa included. Raw data are available in the Sequence Read Archive (SRA) database under the BioProject PRJNA1010366. SRA accession numbers are provided in Table 1.

Phylogenetic reconstruction

Both aligned matrices were partitioned using the Sliding-Window Site Characteristics Entropy (SWSC-EN) algorithm (Tagliacollo and Lanfear 2018) to define partitions within each UCE locus accounting for rate heterogeneity. We selected the best-fit partitioning scheme and substitution model with ModelFinder (Kalyaanamoorthy et al. 2017) in IQ-TREE v2 (Minh et al. 2020) according to the Bayesian information criterion. Finally, we conducted Maximum Likelihood (ML) analyses using IQ-TREE v2 (Minh et al. 2020) with 10,000 bootstrap (BTP) replicates.

Results

UCE data

We obtained a total of 2,526 UCE loci in a complete dataset. We recovered 1,161 UCE loci with a mean length of 762.25 bp for the included species of *A. seyrigi*, whereas for *D. americana* we obtained 828 UCE loci with a mean length of 442.22 bp. A total of 1,578 and 917 UCE loci were retained for the 25% and 50% matrix, resulting in matrices with lengths of 342,464 and 170,549 bp, respectively.



Figure 3. Lateral habitus of *Dirrhope americana*.

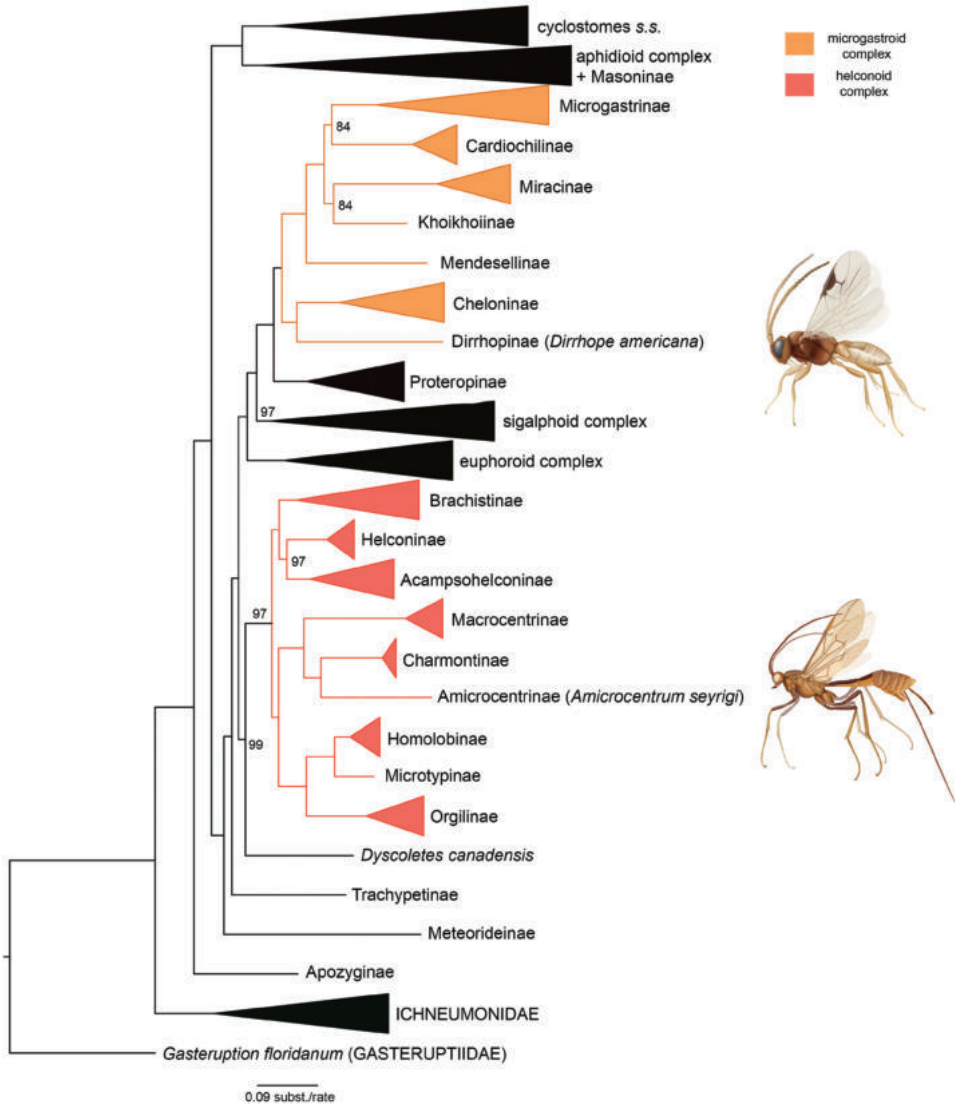


Figure 4. Maximum likelihood phylogram resulting from the 50% complete matrix. Amicrocentrinae was recovered as sister to Charmontinae within the non-cyclostome helconoid complex (red). Dirrhopinae was recovered as sister to Cheloninae in the microgastroid complex (orange). Remaining Braconidae and outgroup taxa are in black. Numbers near nodes are BTP values that were under 100.

Phylogenetic inference

The ML phylograms derived from the two different datasets analyzed (50% and 25%; Fig. 4, Suppl. materials 1, 2, respectively) were highly similar and strongly supported, recovering as monophyletic the three main clades of the braconoid complex, *i.e.* cyclostomes *s.s.*, aphidioid subfamilies, Masoninae and non-cyclostomes. Similarly, the

phylogenetic relationships among the four non-cyclostome complexes were identical, with the sigalphoid and microgastroid complexes recovered as sister taxa, followed by the euphoroid complex and the helconoid complex as sister to all of them (Fig. 4, Suppl. materials 1, 2).

Within the helconoid complex both topologies recovered Amicrocentrinae as sister to Charmontinae with high support (BTP=100), with both subfamilies being sister to Macrocentrinae. These three subfamilies together were recovered as sister to a clade comprised by the subfamilies Homolobinae, Microtypinae and Orgilinae, followed by a clade containing the subfamilies Brachistinae, Helconinae and Acampsohelconinae (Fig. 4, Suppl. materials 1, 2). Finally, in both topologies Dirrhopinae was recovered as sister to Cheloninae (BTP = 100) within the microgastroid complex and both were sister to all remaining microgastroid subfamilies, *i.e.*, Micrograstinae, Cardiochilinae, Miracinae, Khoikhoinae and Mendesellinae (Fig. 4, Suppl. materials 1, 2).

The only topological difference at the subfamily level between both datasets analyzed was the placement of the cyclostome subfamily Pambolinae, which was recovered in a clade containing “Old World” Doryctinae with weak support (BTP = 60) or as sister to the Avgiini with moderate support (BTP = 86) in the 25% (Suppl. material 2) and 50% datasets (Suppl. material 1), respectively.

Discussion

In its current status, the non-cyclostome helconoid complex contains eight subfamilies, Acampsohelconinae, Brachistinae, Charmontinae, Helconinae, Homolobinae, Macrocentrinae, Microtypinae and Orgilinae (Sharanowski et al. 2011; Jasso-Martínez et al. 2022a, 2022b). Amicrocentrinae, together with other subfamilies that are now placed within different non-cyclostome complexes, has been also treated as a member of this complex (Wharton 1993). However, Amicrocentrinae was not included in the most recent phylogenetic hypothesis of Braconidae based on genomic-scale data; thus, the authors did not include it in the helconoid complex (Jasso-Martínez et al. 2022a).

Amicrocentrum, the only genus of Amicrocentrinae, was previously considered a member of Macrocentrinae; however, species of *Amicrocentrum* lack spines on the hind trochantellus (Fig. 1), which is considered an apomorphy for Macrocentrinae, and lack prepectal and hypostomal carinae, which are also features of Macrocentrinae. Further, in macrocentrines the maxillary palpi are 5–6 segmented, the labial palpi 4 segmented, and forewing vein 2RS is basad vein m-cu; in species of *Amicrocentrum* the palpi are two segmented (Fig. 2A) (van Achterberg 1979: fig. 23) and 2RS is distad m-cu (Fig. 1). A new subfamily was proposed for species of *Amicrocentrum* given those differences with respect to Macrocentrinae and the large number of morphological apomorphies shared among amicrocentrines (van Achterberg 1979). The only molecular study that has included a member of Amicrocentrinae recovered it as sister to Charmontinae with strong support, with both being sister to a clade containing Xiphozelinae and Macrocentrinae (Sharanowski et al. 2011). These four subfamilies plus Homolobinae,

Microtypinae and Orgilinae comprise a subcomplex within the helconoid complex, named 'macrocentroid' (Sharanowski et al. 2011). The macrocentroid subcomplex is biologically characterized as parasitoids of immature stages of Lepidoptera rather than Coleoptera as is the case with the other members of the helconoid complex, *i.e.*, Helconinae and Brachistinae (Sharanowski et al. 2011).

In this study, we confirm with strong support the phylogenetic placement of Amicrocentrinae as sister to Charmontinae, with both being sister to Macrocentrinae within the helconoid complex based on genomic UCE data, as was previously proposed based on nuclear Sanger sequence data (Sharanowski et al. 2011). Among the shared morphological features of Amicrocentrinae and Charmontinae are a well-developed ctenidia of the lower valve egg canal (Rahman et al. 1998), and a long ovipositor with a pre-apical swelling of the rachis of olistheter mechanism (Quicke et al. 1995).

Some lineages of the braconid non-cyclostome group such as Cardiochilinae and Miracinae have been treated as members of Microgastrinae (Nixon 1965). After their establishment as separate subfamilies, and the description of other closely related subfamilies, the name 'microgastroid' group or complex was adopted to refer to those subfamilies collectively. The microgastroid subfamilies in general comprise species with a small metasoma relative to the length of wings and the rest of the body (Quicke 2015). However, among the members of the microgastroid complex (and other braconids), members of *Dirrhope* show the autapomorphy of having the spiracles of the first metasomal tergum posterior to the middle of the tergum (Fig. 2B); thus, it was elevated to subfamily status by van Achterberg (1984).

The limits of the microgastroid complex have remained relatively stable since the publication of a phylogenetic hypothesis based on morphology, together with the recognition of the subfamilies Khoikhoiinae and Mendesellinae (Mason 1983; Whitfield and Mason 1994). The monophyly of this assemblage of subfamilies has been recovered using different sources of data, including molecular (Whitfield 1997a; Belshaw et al. 1998; Dowton et al. 1998; Banks and Whitfield 2006; Murphy et al. 2008; Sharanowski et al. 2011; Jasso-Martínez et al. 2022a, 2022b) and combined molecular and morphological (Dowton et al. 2002). However, none of the phylogenetic hypotheses of this complex based on molecular data included *Dirrhope*, and thus, its subfamily-level status based on morphology was never tested using additional sources of evidence.

Our genomic-scale data recovered Dirrhopinae as sister to Cheloninae within the microgastroid complex of subfamilies with strong support. *Dirrhope* species resemble members of the chelonine tribe Adeliini in body shape; however, in addition to the spiracle synapomorphy for dirrhopines, they have forewing vein RS distinctly curved anteriorly (Fig. 3), while RS is relatively straight in chelonines. Further, tergum 1 articulates with tergum 2 in dirrhopines, while the first and second terga are fused in chelonines (Shaw 1997; Whitfield 1997b). As in previous morphology-based studies (Quicke and van Achterberg 1990; Whitfield and Mason 1994), our UCE data recovered the Dirrhopinae + Cheloninae clade as sister to the remaining microgastroid subfamilies. Thus, based on molecular phylogenetic analysis, we confirm the placement of Dirrhopinae as a member of the non-cyclostome microgastroid complex.

Acknowledgments

We thank the staff from the Smithsonian Institution Laboratories of Analytical Biology (SI-LAB) at the Smithsonian National Museum of Natural History for their general support. Thanks to Jeffrey Sosa-Calvo for his help and advice with lab work; Taina Litwak for the illustrations included in Figs 1, 3, 4); Rebekah Rogers for her advice for imaging specimens and to the reviewers that helped improve the first submitted version of this manuscript. This study was supported by the National Science Foundation (DEB-1555905 and DEB-1754242 to SGB). JMJM was supported by a Peter Buck Postdoctoral Fellowship (Smithsonian Institution). Mention of trade names or commercial products in this publication is solely for the purpose of providing specific information and does not imply recommendation or endorsement by the USDA. USDA is an equal opportunity provider and employer.

References

- Banks JC, Whitfield JB (2006) Dissecting the ancient rapid radiation of microgastrine wasp genera using additional nuclear genes. *Molecular Phylogenetics and Evolution* 4: 690–703. <https://doi.org/10.1016/j.ympev.2006.06.001>
- Belokobylskij SA (1989) Eastern Palaearctic braconid species of the genera *Dirrhope* and *Mirax* (Hymenoptera, Braconidae, Miracinae). *Vestnik Zoologii* 4: 34–46.
- Belokobylskij SA, Iqbal M, Austin AD (2003) First record of the subfamily Dirrhopinae (Hymenoptera: Braconidae) from the Australian region, with a discussion of relationships and biology. *Australian Journal of Entomology* 42: 260–265. <https://doi.org/10.1046/j.1440-6055.2003.00362.x>
- Belshaw R, Fitton M, Herniou E, Gimeno C, Quicke DLJ (1998) A phylogenetic reconstruction of the Ichneumonoidea (Hymenoptera) based on the D2 variable region of 28S ribosomal RNA. *Systematic Entomology* 23: 109–123. <https://doi.org/10.1046/j.1365-3113.1998.00046.x>
- Blaimer BB, Santos BF, Cruaud A, Gates MW, Kula RR, Mikó I, Rasplus JY, Smith DR, Talamas EJ, Brady SG, Buffington ML (2023) Key innovations and the diversification of Hymenoptera. *Nature Communications* 14: 1212. <https://doi.org/10.1038/s41467-023-36868-4>
- Bolger AM, Lohse M, Usadel B (2014) Trimmomatic: a flexible trimmer for Illumina sequence data. *Bioinformatics* 30: 2114–2120. <https://doi.org/10.1093/bioinformatics/btu170>
- Branstetter MG, Longino JT, Ward PS, Faircloth BC (2017) Enriching the ant tree of life: enhanced UCE bait set for genome-scale phylogenetics of ants and other Hymenoptera. *Methods in Ecology and Evolution* 8: 768–776. <https://doi.org/10.1111/2041-210X.12742>
- Capek M (1970) A new classification of the Braconidae (Hymenoptera) based on the cephalic structure of the final instar larvae and biological evidence. *The Canadian Entomologist* 102: 846–875. <https://doi.org/10.4039/Ent102846-7>
- Castresana J (2000) Selection of conserved blocks from multiple alignments for their use in phylogenetic analysis. *Molecular Biology and Evolution* 17: 540–552. <https://doi.org/10.1093/oxfordjournals.molbev.a026334>

- Dangerfield PC, Austin AD (1998) Biology of the *Mesostoa kerri* Austin and Wharton (Insecta: Hymenoptera: Braconidae: Mesostoinae), an endemic Australian wasp that causes stem galls on *Banksia marginata*. *Australian Journal of Botany* 46: 559–569. <https://doi.org/10.1071/BT97042>
- Del Fabbro C, Scalabrin S, Morgante M, Giorgi FM (2013) An extensive evaluation of read trimming effects on Illumina NGS data analysis. *PLoS ONE* 8: e85024. <https://doi.org/10.1371/journal.pone.0085024>
- Dowton M, Austin AD (1998) Phylogenetic relationships among the microgastroid wasps (Hymenoptera: Braconidae): combined analysis of 16S and 28S rDNA genes and morphological data. *Molecular Phylogenetics and Evolution* 10: 354–366. <https://doi.org/10.1006/mpev.1998.0533>
- Dowton M, Belshaw R, Austin AD, Quicke DLJ (2002) Simultaneous molecular and morphological analysis of braconid relationships (Insecta: Hymenoptera: Braconidae) indicates independent mt-tRNA gene inversions within a single wasp family. *Journal of Molecular Evolution* 54: 210–226. <https://doi.org/10.1007/s00239-001-0003-3>
- Faircloth BC (2013) Illumiprocessor: A Trimmomatic Wrapper for Parallel Adapter and Quality Trimming. <https://doi.org/10.6079/J9ILL>
- Faircloth BC (2016) PHYLUCE is a software package for the analysis of conserved genomic loci. *Bioinformatics* 32(7): 86–788. <https://doi.org/10.1093/bioinformatics/btv646>
- Glenn TC, Nilsen RA, Kieran TJ, Sanders JG, Bayona-Vásquez N, Finger JW, Pierson TW, Bentley KE, Hoffberg SL, Louha S, García-De Leon FJ, del Río Portilla MA, Reed KD, Anderson JL, Meece JK, Aggrey SE, Rekaya R, Alabady M, Belanger M, Winker K, Faircloth BC (2016) Adapterama I: universal stubs and primers for thousands of dual-indexed Illumina libraries (iTru and iNext). *PeerJ* 7: e7755. <https://doi.org/10.7717/peerj.7755>
- Infante F, Hanson P, Wharton R (1995) Phytophagy in the genus *Monitoriella* (Hymenoptera: Braconidae) with description of new species. *Annals of the Entomological Society of America* 88: 406–415. <https://doi.org/10.1093/aesa/88.4.406>
- Jasso-Martínez JM, Santos BF, Zaldívar-Riverón A, Fernández-Triana JL, Sharanowski BJ, Richter R, Dettman JR, Blaimer BB, Brady SG, Kula RR (2022a) Phylogenomics of braconid wasps (Hymenoptera, Braconidae) sheds light on classification and the evolution of parasitoid life history traits. *Molecular Phylogenetics and Evolution* 173: 107452. <https://doi.org/10.1016/j.ympev.2022.107452>
- Jasso-Martínez JM, Quicke DLJ, Belokobylskij SA, Santos BF, Fernández-Triana JL, Kula RR, Zaldívar-Riverón A (2022b) Mitochondrial phylogenomics and mitogenome organization in the parasitoid wasp family Braconidae (Hymenoptera: Ichneumonoidea). *BMC Ecology and Evolution* 22: 46. <https://doi.org/10.1186/s12862-022-01983-1>
- Kalyaanamoorthy S, Min BQ, Wong TK, von Haeseler A, Jermini LS (2017) ModelFinder: fast model selection for accurate phylogenetic estimates. *Nature Methods* 14: 587–589. <https://doi.org/10.1038/nmeth.4285>
- Katoh K, Standley DM (2013) MAFFT multiple sequence alignment software version 7: improvements in performance and usability. *Molecular Biology and Evolution* 30: 772–780. <https://doi.org/10.1093/molbev/mst010>

- Kittel RN, Austin AD, Klopstein S (2016) Molecular and morphological phylogenetics of chelonine parasitoid wasps (Hymenoptera: Braconidae), with a critical assessment of divergence time estimations. *Molecular Phylogenetics and Evolution* 101: 224–241. <https://doi.org/10.1016/j.ympev.2016.05.016>
- Marsh PM (1979) Family Braconidae. In: Krombein KV, Hurd PD, Smith DR, Burks BD (Eds) *Catalog of the Hymenoptera in America North of Mexico*. Smithsonian Institution Press (Washington, D.C.), 144–313.
- Mason WRM (1983) A new South African subfamily related to Cardiochilinae (Hymenoptera: Braconidae). *Contributions of the American Entomological Institute* 2: 49–62.
- Minh BQ, Schmidt HA, Chernomor O, Schrempf D, Woodhams MD, von Haeseler A, Lanfear R (2020) IQ-TREE 2: new models and efficient methods for phylogenetic inference in the genomic era. *Molecular Biology and Evolution* 37: 1530–1534. <https://doi.org/10.1093/molbev/msaa015>
- Muesebeck CFW (1935) On two little known genera of Braconidae (Hymenoptera). *Proceedings of the Entomological Society of Washington* 37: 173–177.
- Murphy N, Banks J, Whitfield JB, Austin A (2008) Phylogeny of the parasitic microgasteroid subfamilies (Hymenoptera: Braconidae) based on sequence data from seven genes, with an improved time estimate of the origin of the lineage. *Molecular Phylogenetics and Evolution* 47: 378–395. <https://doi.org/10.1016/j.ympev.2008.01.022>
- Nixon GEJ (1965) A reclassification of the tribe Microgasterini (Hymenoptera: Braconidae). *Bulletin of the British Museum (Natural History) Entomology* 2: 284. <https://doi.org/10.5962/p.144036>
- Pitz KM, Dowling APG, Sharanowski BJ, Boring CA, Seltmann KC, Sharkey MJ (2007) Phylogenetic relationships among the Braconidae (Hymenoptera: Ichneumonoidea): A reassessment of Shi et al. (2005). *Molecular Phylogenetics and Evolution* 43: 338–343. <https://doi.org/10.1016/j.ympev.2006.11.010>
- Prjibelski A, Antipov D, Meleshko D, Lapidus A, Korobeynikov A (2020) Using SPAdes de novo assembler. *Current Protocols in Bioinformatics* 70: e102. <https://doi.org/10.1002/cpbi.102>
- Quick DLJ (2015) *The braconid and ichneumonid parasitoid wasps: biology, systematics, evolution and ecology*. John Wiley & Sons (Chichester): 1–537. <https://doi.org/10.1002/9781118907085>
- Quicke DLJ, van Achterberg C (1990) Phylogeny of the subfamilies of the family Braconidae (Hymenoptera). *Zoologische Verhandelingen* 258: 1–95. <https://doi.org/10.1111/j.1096-0031.1992.tb00068.x>
- Quicke DLJ, Fitton MG, Harris J (1995) Ovipositor steering mechanisms in braconid wasps. *Journal of Hymenoptera Research* 4: 110–120.
- Rahman MH, Fitton MG, Quicke DLJ (1998) Ovipositor internal microsculpture in the Braconidae (Insecta, Hymenoptera). *Zoologica Scripta* 27: 319–331. <https://doi.org/10.1111/j.1463-6409.1998.tb00464.x>
- Ranjith AP, Quicke DLJ, Saleem UKA, Butcher BA, Zaldívar-Riverón A, Nasser M (2016) Entomophytophagy (‘Sequential predatory, then phytophagous behaviour’) in an Indian braconid ‘parasitoid’ wasp (Hymenoptera): specialized larval morphology, biology and description of a new species. *PLoS ONE* 11: e0156997. <https://doi.org/10.1371/journal.pone.0156997>

- Sharanowski BJ, Dowling AP, Sharkey MJ (2011) Molecular phylogenetics of Braconidae (Hymenoptera: Ichneumonoidea), based on multiple nuclear genes, and implications for classification. *Systematic Entomology* 36: 549–572. <https://doi.org/10.1111/j.1365-3113.2011.00580.x>
- Sharanowski BJ, Ridenbaugh RD, Piekarski PK, Broad GR, Burke GR, Deans AR, Lemmon AR, Moriarty Lemmon EC, Diehl GJ, Whitfield JB, Hines HM (2021) Phylogenomics of Ichneumonoidea (Hymenoptera) and implications for evolution of mode of parasitism and viral endogenization. *Molecular Phylogenetics and Evolution* 156: 107023. <https://doi.org/10.1016/j.ympev.2020.107023>
- Sharkey MJ (1993) Family Braconidae. In: Goulet H, Huber JT (Eds) *Hymenoptera of the World: An Identification Guide to Families*. Research Branch Agriculture Canada Publication, Ottawa, 362–395.
- Sharkey MJ, Wharton RA (1997) Morphology and Terminology. In: Wharton RA, Marsh PM, Sharkey MJ (Eds) *Manual of the New World Genera of the Family Braconidae (Hymenoptera)*. Special Publication of The International Society of Hymenopterists, Washington, D.C., 19–37.
- Shaw SR (1997) Subfamily Cheloninae. In: Wharton RA, Marsh PM, Sharkey MJ (Eds) *Manual of the New World Genera of the Family Braconidae (Hymenoptera)*. Special Publication of The International Society of Hymenopterists, Washington, D.C., 193–201.
- Tagliacollo VA, Lanfear R (2018) Estimating improved partitioning schemes for ultraconserved elements. *Molecular Biology and Evolution* 35: 1798–1811. <https://doi.org/10.1093/molbev/msy069>
- Telenga NA (1955) Fauna of the U.S.S.R. Hymenoptera. Braconidae: Microgastrinae and Agathidinae. *Izvestiya Rossiiskoi Akademii Nauk. Seruya Geograficheskaya* 5: 4. [In Russian]
- Tobias VI (1967) A review of the classification, phylogeny and evolution of the family Braconidae (Hym.). *Entomological Review* 46: 387–399.
- Tobias VI (1986) Keys to the insects of the European part of the USSR. III. Hymenoptera. *Akademia Nauk Leningrad* 4: 1–501. [In Russian]
- van Achterberg C (1979) A revision of the species of Amicrocentrinae, a new subfamily (Hymenoptera, Braconidae), with a description of the final larval instar of *Amicrocentrum curvinervis* by J.R.T. Short. *Tijdschrift voor Entomologie* 122: 1–28.
- van Achterberg C (1984) Essay on the phylogeny of Braconidae (Hymenoptera: Ichneumonoidea). *Entomologisk Tidskrift* 105: 41–58.
- Wharton RA (1993) Bionomics of the Braconidae. *Annual Review of Entomology* 38: 121–143. <https://doi.org/10.1146/annurev.en.38.010193.001005>
- Wharton RA, Shaw SR, Sharkey MJ, Wahl DB, Woolley JB, Whitfield JB, Marsh PM, Johnson W (1992) Phylogeny of the subfamilies of the family Braconidae (Hymenoptera: Ichneumonoidea): a reassessment. *Cladistics* 8: 199–235. <https://doi.org/10.1111/j.1096-0031.1992.tb00068.x>
- Whitfield JB (1997a) Molecular and morphological data suggest a common origin for the polydnaviruses among braconid wasps. *Naturwissenschaften* 34: 502–507. <https://doi.org/10.1007/s001140050434>
- Whitfield JB (1997b) Subfamily Dirrhopinae. In: Wharton RA, Marsh PM, Sharkey MJ (Eds) *Manual of the New World Genera of the Family Braconidae (Hymenoptera)*. Special Publication of The International Society of Hymenopterists, Washington, D.C., 203–204.

Whitfield JB, Wagner DL (1991) Annotated key to the genera of Braconidae (Hymenoptera) attacking leaf-mining Lepidoptera in the Holarctic Region. *Journal of Natural History* 25: 733–754. <https://doi.org/10.1080/00222939100770481>

Whitfield JB, Mason WRM (1994) Mendesellinae, a new subfamily of braconid wasps (Hymenoptera: Braconidae) with a review of relationships within the microgastroid assemblage. *Systematic Entomology* 19: 61–76. <https://doi.org/10.1111/j.1365-3113.1994.tb00579.x>

Yu DS, van Achterberg C, Horstmann K (2016) *Taxapad 2016, Ichneumonoidea 2015*. Database on flash-drive, Ottawa.

Zaldívar-Riverón A, Mori M, Quicke DLJ (2006) Systematics of the cyclostome subfamilies of braconid parasitic wasps (Hymenoptera: Ichneumonoidea): a simultaneous molecular and morphological Bayesian approach. *Molecular Phylogenetics and Evolution* 38: 130–145. <https://doi.org/10.1016/j.ympev.2005.08.006>

Zaldívar-Riverón A, Martínez JJ, Belokobylskij SA, Pedraza-Lara CS, Shaw SR, Hanson PE, Varela-Hernández F (2014) Systematics and evolution of gall formation in the plant-associated genera of the wasp subfamily Doryctinae (Hymenoptera: Braconidae). *Systematic Entomology* 39: 633–659. <https://doi.org/10.1111/syen.12078>

Supplementary material 1

Maximum likelihood tree resulting from the 50% complete matrix without collapsed clades and with full names of the terminal taxa

Authors: Jovana M. Jasso-Martínez, Seán G. Brady, Robert R. Kula

Data type: jpg

Copyright notice: This dataset is made available under the Open Database License (<http://opendatacommons.org/licenses/odbl/1.0/>). The Open Database License (ODbL) is a license agreement intended to allow users to freely share, modify, and use this Dataset while maintaining this same freedom for others, provided that the original source and author(s) are credited.

Link: <https://doi.org/10.3897/jhr.96.111012.suppl1>

Supplementary material 2

Maximum likelihood tree resulting from the 25% complete matrix

Authors: Jovana M. Jasso-Martínez, Seán G. Brady, Robert R. Kula

Data type: jpg

Copyright notice: This dataset is made available under the Open Database License (<http://opendatacommons.org/licenses/odbl/1.0/>). The Open Database License (ODbL) is a license agreement intended to allow users to freely share, modify, and use this Dataset while maintaining this same freedom for others, provided that the original source and author(s) are credited.

Link: <https://doi.org/10.3897/jhr.96.111012.suppl2>

A new species of social wasp from Madagascar with an inverted nest architecture (Hymenoptera, Vespidae)

Ozren Polašek^{1,2,3}, Len de Beer⁴

1 Croatian Science Foundation, Zagreb, Croatia **2** University of Split, School of Medicine, Split, Croatia
3 Algebra University College, Zagreb, Croatia **4** Eden Reforestation Projects, Antananarivo, Madagascar

Corresponding author: Ozren Polašek (opolasek@gmail.com)

Academic editor: Volker Lohrmann | Received 12 March 2023 | Accepted 27 October 2023 | Published 29 November 2023

<https://zoobank.org/88FF9B1F-D65E-4F08-B7ED-7A5D40530176>

Citation: Polašek O, de Beer L (2023) A new species of social wasp from Madagascar with an inverted nest architecture (Hymenoptera, Vespidae). *Journal of Hymenoptera Research* 96: 1031–1044. <https://doi.org/10.3897/jhr.96.103379>

Abstract

Ropalidia jemmae **sp. nov.** is described from the protected Ankafobe evergreen forest in central Madagascar. This species is characterized by a variable black and green body colour pattern and a unique nest architecture within the genus *Ropalidia*. The nests of this species have an inverted cell opening orientation that exposes the cell bottoms outwardly, mimics the tree bark, and provides excellent visual nest concealment.

Keywords

Nest, new species, protected areas, social wasp, Vespidae

Introduction

Social insects occasionally have very welcome features that supplement the taxonomic work. In addition to their morphology, some species have unique nest architecture. This reflects their life cycle, and adaptive mechanisms that can contribute to speciation (Invernizzi and Ruxton 2019). Numerous evolutionary effects can be reflected in the nest architecture and nesting behaviour (Jeanne 1975), which prevents catastrophic brood loss (Furuichi and Kasuya 2015). Interestingly, the nesting architecture in vespid wasps is considered to have evolved predominantly in response to another group of social insects, the ants (Richards 1971; Jeanne 1975). Stalked nests, the outer

envelope or adding the pulp to larva cocoon tops were developed to repel or reduce invertebrate access to the brood (Jeanne 1975; Furuichi and Kasuya 2015). In contrast to adaptations protecting against invertebrate predators, visually masking or concealing nests in the envelopes or tree hollows are believed to have evolved due to vertebrate nest predation, primarily driven by visual cues (Jeanne 1975).

Among social wasps, the most diverse nest architecture was reported in the genus *Ropalidia* (Kojima 1982; Spradbery and Kojima 1989; Wenzel 1998). Members of the former subgenus *Icarielia*, present in Asia and Australia, build enveloped nests with complex structures (Kojima 1982). On the other hand, most species in this genus build gymnodomous stelocytтарous nests, characterized by the stalked nest without any envelope (Jeanne 1975; Wenzel 1998). Most African mainland species build simple discoid nests (Polašek et al. in press), while Malagasy *Ropalidia* exhibit much greater nest architecture diversity (Vesey-Fitzgerald 1950; Blommers 2012).

All 43 Malagasy *Ropalidia* species are endemic (Carpenter and Madl 2009; Blommers 2012). Despite substantial obstacles in their separation due to the lack of a taxonomic revision, some species were shown to have unique nest architecture, which provides a valuable supplement to species determination (Blommers 2012). Notably, some Malagasy species build visually concealed nests directly on the tree trunks (Vesey-Fitzgerald 1950), a feature described in only one African mainland species (Polašek et al. 2022). In addition, *R. cocoscola* Blommers was reported to build entirely concealed nests within the tree trunk cavities, while *R. merina* Blommers (previously considered as *R. formosa* de Saussure) and *R. favulorum* Blommers create large nesting colonies of hundreds of nests that provide an additional layer of security (Wenzel 1987; Blommers 2012).

The aim of this study was to identify and describe a taxon that was recently observed in a protected area of the Ankafoobe forest. The Tampoketsa de Ankafoobe, including the Ambohitantely forest, is one of the last and the largest remaining fragmented forests on the highlands of Madagascar, a mosaic of forest and grassland. Ambohitantely forest consists of about around 80 sections of the subhumid, high plateau evergreen forest at an altitude between 1,300 and 1,650 metres. With about 1800 hectares of surface area, it harbours many endemic and critically endangered species of insects (Wesener et al. 2010; Wiorek et al. 2021; Moravec and Trzna 2022), frogs and mammals (Stephenson et al. 1994; Barata et al. 2022), requiring careful management, protection and restoration efforts.

Materials and methods

This study was based on the field observation of the wasps on a nest in the Ankafoobe forest in October and November 2022. The initial observation prompted a wider-scale search for the corresponding specimen in the accessible entomological collections. In total, 18 collections were examined, including the American Museum of Natural History, New York, US [AMNH], Centre for Biodiversity Genomics,

Guelph, Ontario, Canada [CBCG], Centrum für Naturkunde, Zoological Museum, Universität Hamburg, Germany [CeNaK], Entomological Collection, ETH Zurich, Switzerland [ETH], Hungarian Natural History Museum, Budapest, Hungary [HNHM], Museo di Storia Naturale di Venezia, Italy [MSNV], Muséum d'Histoire Naturelle, Geneva, Switzerland [MHNG], Museum für Naturkunde, Berlin, Germany [MFNB], National Museum of Natural History, Naturalis, Leiden, the Netherlands [NNM], Natural History Museum London, UK [NHM], National Museum Kenya, Nairobi, Kenya [NMK], National Museums Scotland, Edinburgh, Scotland [NMS], Oberösterreichisches Landesmuseum, Linz, Austria [OLM], Royal Museum for Central Africa, Tervuren, Belgium [RMCA], Swedish Museum of Natural History, Stockholm, Sweden [NHRS], Statens Naturhistoriske Museum, Copenhagen, Denmark [SNM], Zoologisches Forschungsmuseum Alexander Koenig, Bonn, Germany [ZFMK] and Zoologische Staatssammlung München, Munich, Germany [ZSM].

All specimens were examined under a Leica S9i stereomicroscope and photographed with an integrated camera. Images were stacked using Helicon Focus version 6.8.0 (Kharkiv, Ukraine). All terga and sterna were denoted as T or S, while the flagellomeres were denoted as AF1–AF10.

Results

Taxonomy

Ropalidia jemmae Polášek & de Beer, sp. nov.

<https://zoobank.org/13ADD49A-3E0A-45B6-9889-22AB94EB40D4>

Figs 1–5, holotype labels Fig. 6

Material. Holotype: “Ankafobe/Ambohitantely”, 1 ♀. **Paratypes:** the same location as the holotype, 2 ♀♀. The nest from the same series also has an additional label “5. 52/ (RP)”, [nest A] (all in MSNV).

Observation data. Ankafobe [-18.10492, 47.187227], 27 Oct 2022 and 10 Nov 2022, 2 ♀♀ and a nest [nest B], obs. Len de Beer [<https://www.inaturalist.org/observations/141686572>, <https://www.inaturalist.org/observations/140282514>].

Diagnosis. This species is characterized by the combination of the following characters: T1 shape streamlined, propodeal excavation impunctate, black basal colour and variably expressed whitish-green markings on the head and mesosoma, green markings only on coxa II, widened posterior yellow-green bands on T1 and T2, and overall longer pilosity. **Wing length:** 7.9 [7.8–8.0] mm.

Description. Female. Colour. Basal body colour black (Figs 1, 2). Head black, with green line in apical fourth of clypeus (Fig. 3). Interantennal area and inner orbits with faint green markings, mandible with basal green spot (Fig. 3). Gena and tempora suffused brown-green (Fig. 1). Antennal scape, pedicel and AF1 green ventrally,

flagellum dorsally black, remaining flagellomeres ventrally orange (Fig. 1). Pronotum suffused green, with stronger green hue close to carina; inferior angle darker; mesonotum without green markings (Fig. 2). Suffused green spot high on mesopleuron, posterior third of tegula green (Figs 1, 2). Scutellum with two green spots; metanotum with two green spots that have stronger margins than those on scutellum (Fig. 4). Propodeum black (Fig. 4). Coxa I and III black, coxa II with lateral green quadrant (very faint in one specimen). Femora black with elongated or circular green spot near distal margin on femora II and III. Tibia with two shades of green; tarsi green, distally light brown (Figs 1, 2). Wings translucent, with some yellowing anteriorly; nervature yellow to brown, stigma yellowish and translucent, apical spot faintly developed in anterior third of marginal cell (Fig. 1). T1 with posterior yellow band that occupies about half of the total surface, thin connecting green suffused area and a dorsal remaining black diamond-shaped area (one paratype has mainly black T1, with thin remaining green band). T2 with posterior widened band, characterized by two larger attached areas and two remaining spots in basal colour near posterior margin, located close to T2/S2 suture (Fig. 1; band substantially reduced in one paratype, shown in Fig. 5). This pattern extends on S2 as short and smaller yellow-green spot, integrated with posterior band (very reduced in one specimen). Remaining terga and sterna in basal colour or somewhat brownish.

Head. Head frontally 1.2× as wide as high; clypeus 1.15× as wide as long (Fig. 3). Clypeal base elongated, lateral margins parallel, juxtamandibular lobe moderately developed, apex pointy and projecting (Fig. 3). Clypeus surface with basal sculpture and evenly spaced and well-defined small punctures, obscured by pubescence; punctures on apex coarser and converting into poorly defined craters (Fig. 3). Frons with dense, moderately sized and comparatively shallow punctures, vertex behind ocelli with diminishing punctures, area close to occipital carina impunctate and shiny. Gena and tempora with equally sized, but shallower punctures. Gena posteriorly 0.6–0.8× as wide as eye, mainly parallel to posterior eye margin; occipital carina complete, reaches mandible. Clypeus and frons covered by dense and straight silvery-yellowish pubescence and yellowish protruding setae, about equally long as forward ocellus diameter (Fig. 3). Compound eyes setose (Fig. 3). Ocellar triangle equidistant; distance between lateral ocelli about 0.6× of ocelli-eye distance. Scape equally long as AF1, AF1 equally long as AF2+3+4, AF2 about 1.4–1.5× as long as wide.

Mesosoma. Mesosoma about 1.8× as long as wide in dorsal view, mesonotum 1.2× as long as wide (Fig. 2). Head wider than pronotal carina width (Fig. 2). Pronotal carina developed as translucent rim, twice wider dorsally than laterally; entire pronotum covered by shallow and very dense punctures separated from each other by their diameter; inferior pronotal corner with increasingly larger punctures (Fig. 1). Mesonotum punctures less dense and shallow, somewhat denser close to scutellum. Mesopleuron densely punctate. Metapleuron shiny, with an occasional very weak punctum that can only be visualized in specimen rotation. Scutellum densely punctate, with shallower punctures than those on mesonotum. Median scutellar carina developed and thin, reaches about half of scutellar length. Metanotum dorsally punctate, with shiny

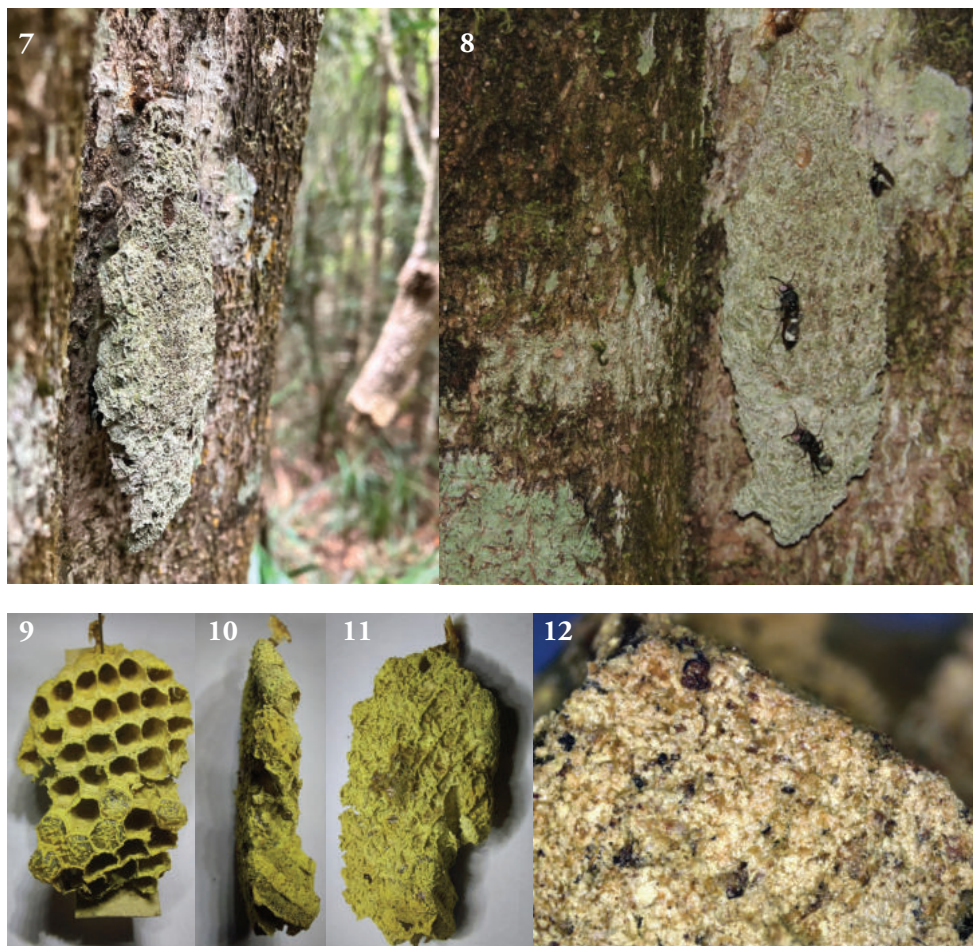
impunctate posterior triangle with small projecting area towards propodeum. Propodeal excavation shallow, without strong carina; upper half with cuticular surface, lower half with minute striae; entire propodeal excavation completely impunctate (Fig. 4). Entire mesosoma covered by silvery-yellowish pubescence and some protruding setae; setae



Figures 1–6. *R. jemmae* sp. nov., female, habitus **1** lateral view **2** dorsal view **3** head in frontal view **4** propodeal excavation **5** distal margin of T2 **6** label of the holotype.

on dorsal side of pronotum silvery, those on mesonotum yellowish. Propodeal excavation covered by longer silvery setae.

Metasoma. T1 pyriform and elongated, with developed dorsal part, but not globular in shape; posterior sulcus very weak (Figs 1, 2). T1 shallowly punctate, punctures poorly defined. T2 shiny, with shallow, dense and small punctures, covered by silvery pubescence and longer silvery-yellowish protruding setae that extend well over lamella (Fig. 5). T2 somewhat shorter than S2, visible in dorsally oblique lamella (Fig. 4). Remaining metasomal segments with weakly developed punctures and pubescence longer than that on T2 and S2.



Figures 7–12. *R. jemmae* sp. nov. nest **7** nest B, in situ, lateral view **8** with wasps **9** nest A, cell openings **10** lateral view **11** outer view (notably, the spot in the middle is the glue that connected the nest to the underlying cardboard) **12** greater magnification, showing a brittle paper structure.

Males are unknown (two more pre-hatching larvae were recovered from the cocoons of nest A, macerated and examined, but both were females). Notably, at least one male was observed on nest B (Fig. 8), with entirely yellow clypeus. However, in the absence of the specimen, the male remains undescribed.

Similar species. Several Malagasy species have a similar morphology and a general colour pattern. In order to provide sufficient support to separating *R. jemmae* sp. nov. from previously described species, a partial key is provided here. The key is designed to separate the four similar species from others (key couplet 1). The key couplet 2 can be treated as 25b in the previous key to Malagasy species (Giordani Soika 1991).

Nest. The nest is the single most interesting feature of this species, with unique architecture in the entire genus *Ropalidia*. Instead of the cell openings oriented outwardly, the nests of *R. jemmae* sp. nov. are inverted, with the cell openings oriented towards the nesting surface and the cell bottoms oriented outwardly (Fig. 7). The loosely built cell bottoms thus correspond to the rugged texture of the tree bark or the lichen and provide excellent concealment of the nest (Fig. 8). In addition, the nest is built with greenish-grey material, mostly homogenous, without streaks of different colours integrated into the cell walls, which are common in some other species.

The first examined nest, nest A, has a total of 43 cells, arranged in the 7*9 cells maximum. The nest is somewhat elongated, with six enclosed cells (Fig. 9). The paper structure is brittle, visible in several collapsed cells (Fig. 9). Approximately 50%–75% of the cell length overlap between the cell rows (Fig. 10). The stalk of the same nest is also inverted, suggesting attachment on the cell openings side (Fig. 10). The outer (bottom-exposed) side of the cells has a very textured surface with numerous arches, which do not reflect the cell wall structure but are located much more densely, providing a heavily textured outer surface (Fig. 11). The greater magnification shows no elongated fibres, but only clumps of heavily masticated and mostly rounded chips (Fig. 12).

The second, nest B, was only observed *in situ* (Figs 7, 8). The nest was on the tree trunk, 1.3 m above the ground. The nest colour and shape resemble the nearby greyish-green lichen patch (Fig. 7).

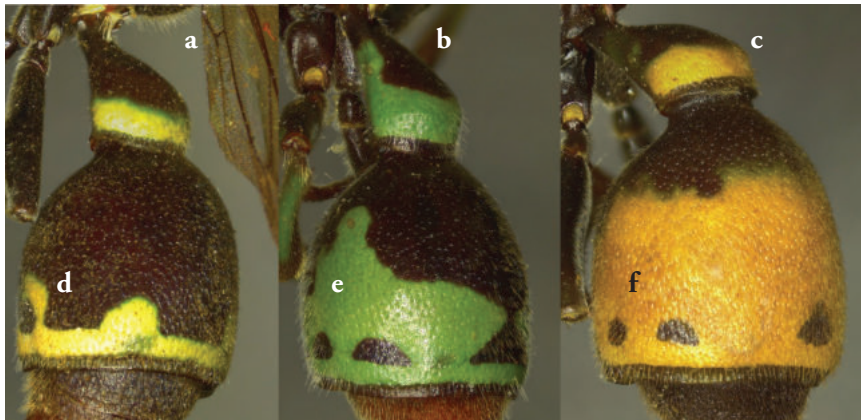
In comparison, the nests of *R. ranavali* are elongated with a pointy tip, suspended from similarly coloured branches (<https://www.inaturalist.org/observations/63188743>, <https://www.inaturalist.org/observations/9173358>). The nests of *R. venustula* and *R. scottiana* are unknown.

Etymology. The name is given after Jemma de Beer, who participated in the nest B discovery.

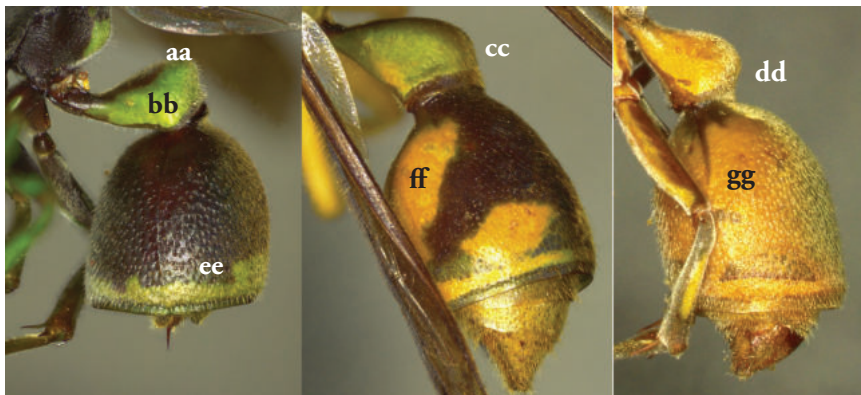
Distribution. All the examined specimens and observations originated from a narrow area (of no more than 16 km of distance) in central Madagascar near Ankafobe, at the edge of the Ambohitantely forest.

Partial key to species

- 1 T1 streamlined and posteriorly rounded, with poorly defined punctures (**a–c**). Basal body colour black(ish)-olivaceous, T2 with obligate posterior green or yellow band on T1 and T2, with additional four attached spots on T2 that can be small in size (**d**), intermediate and merged (**e**) or occupy most of T2 surface (**f**). Femora II and III black, sometimes with distal green or yellow spot. Mesonotum black. Wing length 7.5–10.3 mm **2**



- T1 differently shaped, dorsally developed (**aa**) and distally punctate (**bb**), more angulate (**cc**) or with stronger posterior sulcus (**dd**). Basal body colour variable; if there are green or yellow markings on T2 then those are either just a posterior band (**ee**), bilateral green-yellow spot near base (**ff**) or entire T2 surface green or yellow (**gg**). Femora II and III variably coloured (if T2 has wider posterior band, then femora are green). Mesonotum variably coloured (if T2 has wider posterior band, then mesonotum always with a pair of green longitudinal lines) **other species**, according to the Giordani Soika (1991) key



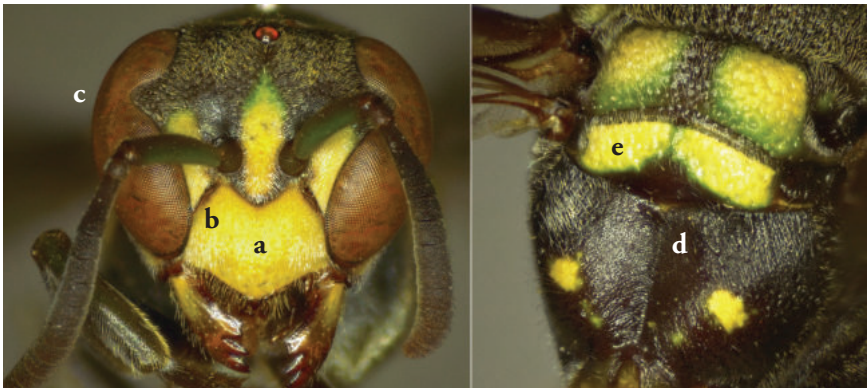
- 2 Head and mesosoma with numerous green or yellow markings (a). Pronotal carina twice broader dorsally than laterally, commonly with a fine translucent rim (b). Base of clypeus with poorly defined punctures (c). Femora II and III black with distal yellow or green spot (d) 3



- Clypeus, interantennal area, pronotum, scutellum, mesopleuron and metanotum commonly black, at most with olivaceous suffused greenish colouration (aa). Pronotal carina equally wide dorsally and laterally, without translucent rim (bb). Base of clypeus with large and well-defined punctures (cc). Femora II and III at most with a very faint suffused olivaceous spot, commonly entirely black (dd) 4



- 3 Face with numerous yellow markings, clypeus entirely yellow (a). Clypeus wider apically, pentagonal (b). Eyes aetose (c). Propodeal excavation shiny, with more developed striae, present in upper half (d); markings on body yellow-green (e). AF2 as long as wide..... *R. scottiana* (de Saussure)



- Face mostly black, with lesser amount of greenish-white markings (**aa**). Clypeus elongated, with parallel sides (**bb**). Eyes covered by numerous straight setae (**cc**). Propodeal excavation shiny, upper half without punctures or striae (**dd**); markings greenish-white (**ee**). AF2 about 1.4–1.5× as long as wide.....
.....*R. jemmae* sp. nov.



- 4 T2 with broad posterior yellow band (**a**). Distal margin of T2 towards lamella evenly rounded and straight; lamella with linear digitations, impunctate (**b**).
.....*R. ranavali* (de Saussure)



- T2 with thin posterior whitish-yellow band with integrated spots (**aa**). Distal margin of T2 towards lamella serrated, with translucent rim; lamella coarsely punctate (**bb**)..... *R. venustula* (de Saussure)



Discussion

The new *Ropalidia* species exhibits an interesting case of an inverted nest, which can be considered an evolutionary reversal. Instead of favouring economically and structurally stronger ancestral nest type, with regular cell size and shared adjacent walls, this species evolved a trade-off by favouring visual concealment. Such architecture requires more founder and worker effort than ancestral nests, which might directly contribute to the low abundance and scarcity of collected or observed specimens. This kind of concealing of the nest is unique in *Ropalidia*, but a similar example of visual concealment is known from the Neotropical species of *Mischocyttarus* (Milani et al. 2021; O'Donnell 2021), suggesting that visual predation of social wasps nests is a common evolutionary pressure across continents.

The biology of *R. jemmae* sp. nov. remains unknown, but this is similar to almost all Malagasy *Ropalidia*, with only a handful of documented field observations (Vesey-Fitzgekald 1950; Wenzel 1987; Blommers 2012). Lastly, the declining habitat undoubtedly presents another negative factor towards species abundance, suggesting the need to reverse this trend, propelled by the restoration of the native forests.

The green cuticular colour in Malagasy Vespidae is a strong indicator of the selective pressure exerted on the nests and the adult wasps. Interestingly, the same feature is known not only for numerous *Ropalidia* species, but also for several *Belonogaster* species (Hensen and Blommers 1987), and at least one eumenid species (Giordani Soika

1941). This pattern of local camouflage can be viewed as both colour matching (fitting the background colour) and disruptive colouring (the pattern of green and black areas on the body that cause visual confusion and break the expected body contour). It seems that the adaptive radiation in Madagascar has taken more concealed pathway in vespid wasps, as opposed to bright black-and-yellow species present in temperate regions or brown- red-black predominant colour in tropical regions.

The conservation efforts in Malagasy forests are of utmost importance in maintaining their biodiversity. The restoration efforts, while present in the area, are hampered by cultural practices, exploitation of the forests, and invasive species. Additional effort is warranted, in order to retain the known and unknown biodiversity of this irreplaceable area. The mosaic of forest and grassland called the Tampoketsa d' Ankazobe, which is the only proven habitat for *Ropalidia jemmae* sp. nov., has the disadvantage of proximity to Madagascar's capital city and has been subject to years of exploitation for wood in an area, where the use of fire regularly during the dry period, has almost totally decimated what was once a diverse mix of trees and grass.

Protective and restorative efforts focused on the remaining fragments of evergreen forests in the Tampoketsa, namely Ankafoibe and Ambohitantely are of paramount importance in retaining their utterly unique elements of biodiversity that are not found anywhere else, including in some cases not even anywhere else in Madagascar. Several NGOs are undertaking restorative reforestation under challenging conditions.

Acknowledgements

A very special thanks goes to all researchers and museum curators, who assisted in creation of this paper (in alphabetical order): Frederique Bakker (NNM), Gavin Broad and Andrew Polaszek (NHM), James M Carpenter (AMNH), Michael Greeff and Rod Eastwood (ETH), Allison Brown and Gergin Blagoev (CBCG), Martin Husemann and Thure Dalsgaard (CeNaK), Bernard Landry (MHNG), Laban Njoroge (NMK), Michael Ohl and Lukas Kirschey (MFNB), Ralph S. Peters (ZFMK), Lars Vilhelmsen (SNM), Martin Schwarz (OLM), Vladimir Blagoderov (NMS), Olga and Stefan Schmidt (ZSM), Marco Uliana (MSNV), Didier van den Spiegel and Stéphane Hanot (RMCA), Hege Vårdal (NHRS) and Zoltan Vas (HNHM).

References

- Barata I, Razafindraibe J, Ravelojaona R, Ralovarisoa E, Mullin K, Hudson M, Dawson J (2022) First population estimates of two Critically Endangered frogs from an isolated forest plateau in Madagascar. *Oryx* 56(6): 897–903. <https://doi.org/10.1017/S0030605321001034>
- Blommers LH (2012) Taxonomy and natural history of 18 *Ropalidia* species (Hymenoptera, Vespidae) of Madagascar. *Tijdschrift voor Entomologie* 155(2–3): 133–192. <https://doi.org/10.1163/22119434-00002010>

- Carpenter JM, Madl M (2009) A Catalogue of the Vespidae of the Malagasy Subregion (Insecta, Hymenoptera). Linzer Biologische Beiträge 41(2): 1871–1935.
- Furuichi S, Kasuya E (2015) Construction of nest defensive structure according to offspring value and its effect on predator's attack decision in paper wasps. *Ethology* 121(6): 609–616. <https://doi.org/10.1111/eth.12374>
- Giordani Soika A (1941) Studi sui vespidi solitari (Hymenoptera). *Bulletin of the Venetian Society of Natural History and of the Civic Museum of Natural History* 2(3): 130–278.
- Giordani Soika A (1991) Vespoidei raccolti da L. A. NILSSON nel Madagascar con una tabella per determinazione delle *Ropalidia* del Madagascar (Hymenoptera Vespoidea). *Lavori Società Veneziana di Scienze Naturali* 16: 79–90.
- Hensen RV, Blommers LM (1987) Review of the Malagasy species of *Belonogaster* Saussure (Hymenoptera, Vespidae). *Tijdschrift voor Entomologie* 130: 11–31.
- Invernizzi E, Ruxton GD (2019) Deconstructing collective building in social insects: Implications for ecological adaptation and evolution. *Insectes Sociaux* 66(4): 507–518. <https://doi.org/10.1007/s00040-019-00719-7>
- Jeanne RL (1975) The adaptiveness of social wasp nest architecture. *The Quarterly Review of Biology* 50(3): 267–287. <https://www.jstor.org/stable/2822255>
- Kojima JI (1982) Nest architecture of three *Ropalidia* species (Hymenoptera: Vespidae) on Leyte Island, the Philippines. *Biotropica* 14(4): 272–280. <https://doi.org/10.2307/2388085>
- Milani LR, de Queiroz RAB, de Souza MM, Aparecido MC, Prezoto F (2021) Camouflaged nests of *Mischocyttarus mirificus* (Hymenoptera, Vespidae). *Neotropical Entomology* 50(6): 912–922. <https://doi.org/10.1007/s13744-021-00910-1>
- Moravec JI, Trzna M (2022) New or rare Madagascar tiger beetles—25. *Pogonostoma (Microstenocera) borisbubeniki* sp. nov., compared to *P. (M.) andreevae* Moravec, 2007 and a revised key to the species-group (Coleoptera: Cicindelidae). *Zootaxa* 5155(2): 245–260. <https://doi.org/10.11646/zootaxa.5155.2.4>
- O'Donnell S (2021) *Mischocyttarus*. In: Starr C (Ed.) *Encyclopedia of Social Insects*. Springer, Cham, 593–598. https://doi.org/10.1007/978-3-030-28102-1_78
- Polašek O, Bellingan T, van Noort S (2022) A new species of paper wasp from the genus *Ropalidia* Guérin-Méneville from South Africa (Hymenoptera, Vespidae). *Journal of Hymenoptera Research* 90: 213–222. <https://doi.org/10.3897/jhr.90.81581>
- Polašek O, Onah I, Kehinde T, Rojo V, van Noort S, Carpenter J (in press) Revision of the mainland African species of the Old World social wasp genus *Ropalidia* GUÉRIN-MÉNEVILLE 1831 (Hymenoptera; Vespidae). *Zootaxa*.
- Richards OW (1971) The biology of the social wasps (Hymenoptera, Vespidae). *Biological Reviews of the Cambridge Philosophical Society* 46(4): 483–528. <https://doi.org/10.1111/j.1469-185X.1971.tb01054.x>
- Spradbery JP, Kojima JI (1989) Nest descriptions and colony populations of eleven species of *Ropalidia* (Hymenoptera, Vespidae) in New Guinea. *Japanese Journal of Entomology* 57(3): 632–653. <https://pascal-francis.inist.fr/vibad/index.php?action=getRecordDetail&idt=6731623>
- Stephenson PJ, Randriamahazo H, Rakotoarison N, Racey PA (1994) Conservation of mammalian species diversity in Ambohitantely special reserve, Madagascar. *Biological Conservation* 69(2): 213–218. [https://doi.org/10.1016/0006-3207\(94\)90062-0](https://doi.org/10.1016/0006-3207(94)90062-0)

- Vesey-Fitzgekald D (1950) Notes on the genus *Ropalidia* (Hymenoptera: Vespidae) from Madagascar. Proceedings of the Royal Entomological Society of London, Series A, General Entomology 25(7–9): 81–86. <https://doi.org/10.1111/j.1365-3032.1950.tb00098.x>
- Wenzel JW (1987) *Ropalidia formosa*, a nearly solitary paper wasp from Madagascar (Hymenoptera: Vespidae). Journal of the Kansas Entomological Society 60(4): 549–556. <https://www.jstor.org/stable/25084944>
- Wenzel JW (1998) A generic key to the nests of hornets, yellowjackets, and paper wasps worldwide (Vespidae, Vespinae, Polistinae). American Museum Novitates; no. 3224. <https://digitallibrary.amnh.org/handle/2246/3502>
- Wesener T, Bupalova I, Sierwald P (2010) Madagascar's living giants: discovery of five new species of endemic giant pill-millipedes from Madagascar (Diplopoda: Sphaerotheriida: Arthrosphaeridae: *Zoosphaerium*). African Invertebrates 51(1): 133–161. <https://doi.org/10.5733/afn.051.0102>
- Wiorek M, Malik K, Lees D, Przybyłowicz Ł (2021) Malagasy Polka Dot Moths (Noctuoidea: Erebidae: Arctiinae: Syntomini) of Ambohitantely—endemism in the most important relict of Central Plateau rainforest in Madagascar. PeerJ 9: e11688. <https://doi.org/10.7717/peerj.11688>

***Ooencyrtus mirus* (Hymenoptera, Encyrtidae), discovered in Europe parasitizing eggs of *Halyomorpha halys* (Hemiptera, Pentatomidae)**

Lucian Fusu¹, Stefanos S. Andreadis²

1 Research Group in Invertebrate Diversity and Phylogenetics, Faculty of Biology, “Al. I. Cuza” University, Bd. Carol I, Nr. 11, 700506 Iași, Romania **2** Hellenic Agricultural Organization “Dimitra”, Institute of Plant Breeding and Genetic Resources, PO Box 60458, 57001 Thermi, Greece

Corresponding author: Stefanos S. Andreadis (sandreadis@elgo.gr)

Academic editor: Petr Janšta | Received 18 July 2023 | Accepted 22 November 2023 | Published 13 December 2023

<https://zoobank.org/380C2721-9DB1-4155-9538-CBE8DB091327>

Citation: Fusu L, Andreadis SS (2023) *Ooencyrtus mirus* (Hymenoptera, Encyrtidae), discovered in Europe parasitizing eggs of *Halyomorpha halys* (Hemiptera, Pentatomidae). Journal of Hymenoptera Research 96: 1045–1060. <https://doi.org/10.3897/jhr.96.109739>

Abstract

Ooencyrtus mirus Triapitsyn & Power (Hymenoptera, Encyrtidae) is recorded for the first time in Europe. It was found parasitising eggs of the invasive true bug *Halyomorpha halys* Stål (Hemiptera, Pentatomidae). This parasitoid is part of the *Ooencyrtus telenomicida* species complex where accurate species identification requires molecular data. Using morphology, the identification of the *Ooencyrtus* species parasitising brown marmorated stink bug eggs in Greece is ambiguous, but the sequences of the standard DNA barcode region (*COI*) and *ITS2* place them in *O. mirus*.

Keywords

brown marmorated stink bug, DNA barcoding, egg mass, new record, parasitoid

Introduction

The brown marmorated stink bug, *Halyomorpha halys* (Hemiptera, Pentatomidae), is native to eastern Asia but it was accidentally introduced into the United States in 1996 in Pennsylvania, and several years later in Europe, in 2004 in Switzerland (Hoebeke and Carter 2003; Leskey et al. 2012; Haye et al. 2014; Xu et al. 2014). It was primarily considered as an urban and household pest (Wermelinger et al. 2008; Inkley 2012), however,

H. halys is highly polyphagous, and causes severe damage to a wide range of economically important plants (Lee et al. 2013; Leskey and Nielsen 2018; Andreadis et al. 2022).

In the native range of *H. halys* (north-eastern Asia), substantial control is provided by numerous natural enemies including parasitoids, predators, and entomopathogens (Lee et al. 2013). In China, the egg parasitoid *Trissolcus japonicus* (Ashmead) (Hymenoptera, Scelionidae) has been identified as the most specialized and efficient agent for classical biological control of *H. halys* populations, while *Trissolcus mitsukurii* (Ashmead) (Hymenoptera, Scelionidae) is the main parasitoid in Japan (Yang et al. 2009; Qiu 2010; Lee et al. 2013; Zhang et al. 2017). Adventive populations of *T. japonicus* and *T. mitsukurii* that followed their host have been reported worldwide (Talamas et al. 2015; Sabbatini Peverieri et al. 2018; Stahl et al. 2019a; Abram et al. 2019; Bout et al. 2021; Dieckhoff et al. 2021; Rot et al. 2021). In the newly invaded areas, mainly the eggs and more rarely the nymphs and adults of *H. halys* are attacked by various predators and a complex of egg parasitoids belonging to the genera *Trissolcus* Ashmead, *Telenomus* Haliday, *Gryon* Haliday (Hymenoptera, Scelionidae), *Anastatus* Motschulsky (Hymenoptera, Eupelmidae) and *Ooencyrtus* Ashmead (Hymenoptera, Encyrtidae) (Abram et al. 2017; Biddinger et al. 2017; Morrison et al. 2017; Costi et al. 2019; Tillman et al. 2020). However, parasitism caused by native egg parasitoids is generally not high enough to effectively reduce the population density of *H. halys* (Dieckhoff et al. 2017; Costi et al. 2019; Stahl et al. 2019b). In Greece, *H. halys* eggs were found to be parasitised by *Anastatus bifasciatus* (Geoffroy) (Hymenoptera, Eupelmidae) and by the species identified here as *Ooencyrtus mirus* Triapitsyn & Power (Hymenoptera, Encyrtidae) (Andreadis et al. 2021, as *O. telenomicida*). The parasitism rate under natural conditions was assessed in Andreadis et al. (2021), while in this study we discuss its identity.

Methods

Host colony maintenance

To obtain large numbers of natural host eggs, captive *H. halys* were reared on green bean (*Phaseolus vulgaris*) pods and green bean plants in a mesh cage (30 × 30 × 30 cm) with vinyl window and zip closure (Raising Butterflies, UT, USA) and maintained at 26 °C, 60% RH under a 16:8 h light dark photoperiod. This colony was initiated in 2019 from mixed-sex adults collected from homes and fields in the area of central Macedonia, Northern Greece. Egg masses were removed carefully every other day, placed in Petri dishes (60 mm diameter), and labelled by date to monitor the age of host eggs. Moistened cottonwool was placed in the dishes to increase humidity.

Parasitoid colony

Ooencyrtus mirus (Chalcidoidea: Encyrtidae) adults were obtained in the summers of 2020 and 2021 from parasitized *H. halys* eggs collected from the underside of apricot

tree leaves and of green bean plant leaves, respectively, in Thermi, Thessaloniki, Northern Greece (40°32'17"N, 23°00'04"E and 40°32'12"N, 23°00'01"E, respectively). A colony of *O. mirus* was established for multiple generations at the Institute of Plant Breeding and Genetic Resources, Laboratory of Entomology at 26 °C, 60% RH and under a 16:8 h L:D photoperiod. The colony reported here is not exactly the same as in Andreadis et al. (2021) because it additionally has the specimens from the 2021 collecting event. Parasitoids were reared in the laboratory using fresh *H. halys* egg masses that were placed in the lid of a plastic Petri dish (3.5 cm in diameter) at the bottom of 460 ml round clear plastic cups (9 cm diameter × 7 cm high). Cups were closed with a plastic lid fitted with a 250-mesh net for air circulation. Pure honey drops *ad libitum* and a cotton wick saturated in honey water were placed on the bottom of a small plastic Petri dish (3.5 cm in diameter). Moistened cottonwool was placed inside the plastic cups to increase humidity. Two egg masses were left in the parasitoid rearing cups for 24 h, after which they were removed and transferred to new cups. Adult wasps that emerged from these cups were returned to the parasitoid rearing cups.

Sex ratio (proportion of males) of *O. mirus* was measured on 1- and 3-days old eggs of *H. halys*. Freshly emerged male and female parasitoids from the colony were placed together in single pairs for 48 h to ensure mating. After this period, each female was offered 10 *H. halys* eggs, on the lid of a plastic Petri dish (3.5 cm in diameter) inside the plastic cups. After 24 h, the parent parasitoids were removed and the parasitized eggs were reared at 26 °C, 60% RH under a photoperiod of 16:8 h L:D until adult emergence for a total period of 30 days, to ensure all adults are accounted for. Emergent wasps were counted and identified by sex. Only replicates in which parasitoid attack by *O. mirus* occurred on at least one egg were included in the data analysis.

Morphological characterisation

For this study specimens were sampled at two different moments from the laboratory colony, in February 2021 and January 2022. Live parasitoids were killed in 80% ethanol and kept at -20 °C until preparation. For examination, specimens were chemically dried using hexamethyldisilazane (HMDS) (Heraty and Hawks 1998), mounted on rectangular cards or point mounted on black points for photography. Images were taken as described in Fusu et al. (2018). The use of diffuse light is paramount not only for imaging but also for the correct interpretation of colour and sculpture when comparing and identifying specimens (Gibson and Fusu 2016). Imaged specimens, except for the DNA vouchers, were labelled with a unique number "Fusu PHOTO 2023-NN" to ensure their future recognition.

Identification of the specimens was done by comparing them with specimens from the same rearing event as the neotype of *O. telenomicida* (Vassiliev) (see Triapitsyn et al. 2020), specimens of *O. telenomicida* from Italy from the same locality (Tuscany) and host but not the same rearing event as in Roversi et al. (2018), and specimens from the same lab grown colony that served for the description of *O. mirus* (Triapitsyn et al. 2020). All the above specimens, the DNA barcoded specimens, and specimens

in ethanol are deposited in the Lucian Fusu Collection at the “Alexandru Ioan Cuza” University, Iasi, Romania. Further specimens of *O. mirus* from Greece are stored in ethanol at the Institute of Plant Breeding and Genetic Resources, Thermi, Greece. We additionally used for identification the keys published by Ferrière and Voegelé (1961), Triapitsyn (1989), Huang and Noyes (1994), Hayat and Mehrnejad (2016) and Samra et al. (2018).

Gastral tergites are abbreviated as Gt1 to Gt3.

Molecular methods

DNA was individually extracted from four whole specimens using a non-destructive method as described in Cruaud et al. (2019). After extraction the exoskeleton was mounted as described above. Two molecular markers (*COI* and *ITS2*), used before for the delimitation of *Ooencyrtus* species (Samra et al. 2018; Triapitsyn et al. 2020, 2021) were amplified by PCR. For *COI* we used the standard primer pair for the animal DNA barcode, LCO1490/HCO2198 (Folmer et al. 1994) while the *ITS2* region was amplified with the primers ITS2-F and ITS2-R2 (Yara 2006). Standard 25 µl PCRs were performed as described in Triapitsyn et al. (2020), the sequences were assembled as in Fusu and Polaszek (2017) and deposited on GenBank under the accession numbers OQ870212–OQ870215 (*COI*) and OQ877248–OQ877251 (*ITS2*).

To our sequences we added those of *Ooencyrtus mevalbelus* Guerrieri & Samra, *Ooencyrtus pistaciae* Hayat & Mehrnejad, and *Ooencyrtus zoeae* Guerrieri & Samra (from Samra et al. 2018). For *O. telenomicida* we included sequences from the type locality, from the East Mediterranean populations (*sensu* Triapitsyn et al. 2020), and from the Italian populations (from Roversi et al. 2018). Sequences of *Ooencyrtus pit-yocampae* (Mercet) from Samra et al. (2015, 2018) were used as outgroup. The *COI* sequences were trivial to align while the *ITS2* sequences were aligned using MAFFT v.7.475 with the E-INS-i algorithm (Kato and Standley 2013).

Separate phylogenetic analyses were performed for the two genes because the goal was to check congruence between mitochondrial and nuclear gene trees. The *ITS2* sequences were analysed in an unpartitioned analysis while the *COI* sequences were partitioned by codon position. The best partitioning scheme and substitution models were selected during the phylogenetic reconstruction using IQTree v.1.6.12 (Nguyen et al. 2015; Kalyanamoothy et al. 2017); support was assessed based on 1,000 bootstrap pseudoreplicates. Phylogenetic analyses were also conducted in Mr-Bayes V.3.2.7 (Ronquist et al. 2012) as described in Dascălu et al. (2022). Distances were calculated in MEGA X v.10.0.5 (Kumar et al. 2018) using the *p* distance and the Kimura 2 parameters model to facilitate comparison with Triapitsyn et al. (2020) and Samra et al. (2018).

The nuclear and mitochondrial sequences were not concatenated for a partitioned phylogenetic analysis because most of the published sequences for the two genes cannot be correlated. This analysis was performed by Triapitsyn et al. (2020) by concatenating one randomly selected exemplar sequence for each gene and species.

Results

Sex ratio

In the investigated Greek population of *O. mirus*, a strongly female-biased eclosion sex ratio (proportion of males 0.39 ± 0.05) is observed (Independent Student's t-test, $p = 0.004$).

Morphology

Using Ferrière and Voegelé (1961) and Trjapitzin (1989) the specimens from Greece are identified as *O. telenomicida*. However, in the more recent key of Huang and Noyes (1994) they will not run smoothly to this species because of conflicting character states in the first couplet: hind coxa is brown (though not exactly concolorous with mesoscutum it is not yellow either) in combination with a basally orange gaster (Fig. 1C, E). If the colour of the hind coxa is disregarded, it will run to *O. telenomicida* but again the colour of the scutellum will not fit because it is not bright metallic green.

In Hayat and Mehrnejad (2016) they will run to *O. telenomicida*, but again the hind coxa is not yellow, F1 is not shorter than F2, while F2 to F5 are not more than 2× as long as broad (they are less than 2× as long as broad and F1 is of the same length as F2). In the key provided by Samra et al. (2018) they will not run to *O. telenomicida*, again because of the dark hind coxa.

Following the designation of a neotype for *O. telenomicida* by Triapitsyn et al. (2020) the hind coxa is brown in this species in all specimens from the type locality situated in East Romania and in most specimens from Ukraine and European Russia (Triapitsyn et al. 2020). A dark hind coxa would hence agree with the specimens from Greece. However, when comparing them (Table 1), they differ in the colour of the head and mesosoma which in topotypical *O. telenomicida* have a bluish-green luster (Triapitsyn et al. 2020, figs 10A, 14), while these are almost completely black in the Greek specimens (Fig. 1). On the other hand, the dark and mostly non-metallic colour of the head and mesosomal dorsum is characteristic for the Mediterranean *O. telenomicida* and *O. mirus*.

The extent of the yellow coloration on the base of the gaster varies in the Greek *Ooencyrtus*, from only the basal half of Gt1 to Gt1–Gt3 being yellow (basal half of the gaster up to the cercal plates). The least yellow specimens are thus similar in this respect to typical *O. telenomicida*, while the more yellow ones to *O. mirus* and the Mediterranean *O. telenomicida* (Table 1). Also, in the Greek population the anterior surface of the mid coxa can be variably extensively brown.

One must take into consideration when comparing *Ooencyrtus* specimens that the yellow colour of the legs and base of the gaster is influenced by the treatment received by the specimen. Air dried specimens that have the gaster strongly collapsed will exhibit a darker base of the gaster compared to uncollapsed specimens in alcohol or specimens dried with hexamethyldisilazane. Specimens that had their DNA extracted through lysis, will have the basal tergites of the gaster and the legs of a pale brown colour instead

Table 1. Colour characteristics of *O. telenomicida* and *O. mirus*.

Body part	<i>O. telenomicida</i> (type locality)	<i>O. telenomicida</i> (Mediterranean)	<i>O. mirus</i> (type locality)	<i>O. mirus</i> (Greece)
Frontovortex	Dark with comparatively strong greenish-blue lustre	Black with weak bronze-green reflections	Black with weak bronze-green reflections	Black with weak bronze-green reflections
Mesoscutum	Dark with comparatively strong greenish-blue lustre	Black with bronze-green reflections	Black with weak bronze-green reflections	Black with weak bronze-green reflections
Scutellum	Dark with comparatively strong greenish-blue lustre apically	Black with weak bronze-green reflections apically	Black with weak bronze-green reflections apically	Black with weak bronze-green reflections apically
Base of gaster	From only base of Gt1 yellow to Gt1 and Gt2 yellow	Gt1–Gt3 yellow	Gt1–Gt3 yellow	From only base of Gt1 yellow to Gt1–Gt3 completely yellow
Hind coxa	Brown	Yellow	Yellow	Brown

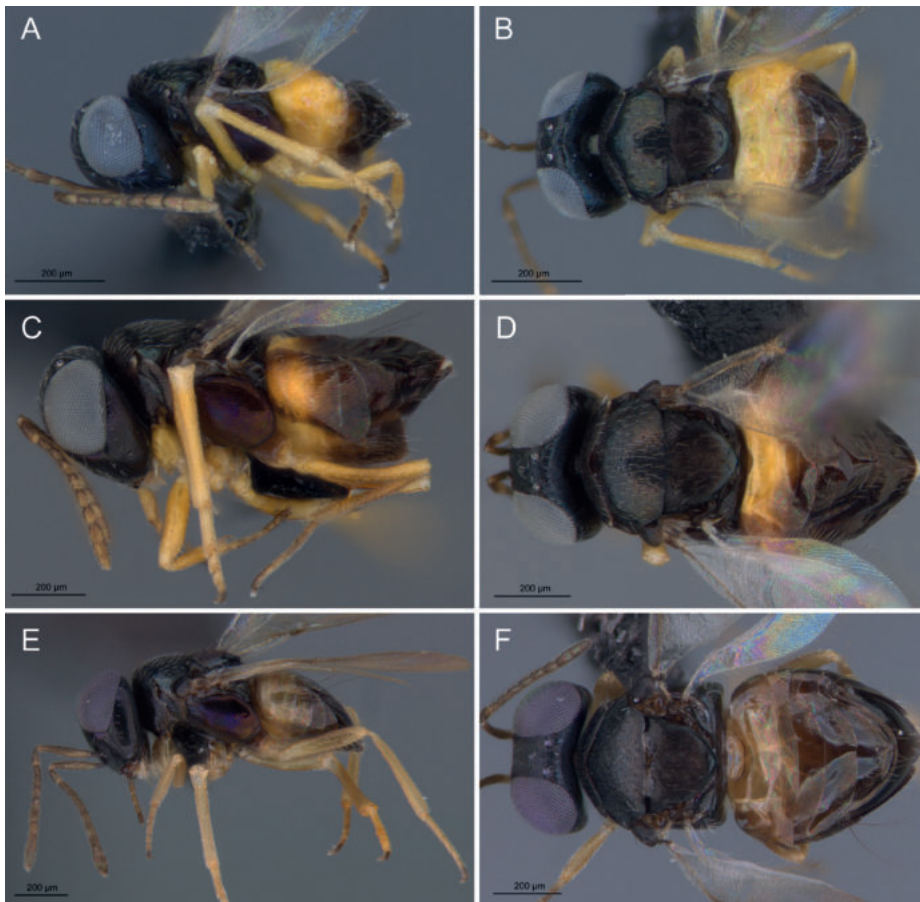


Figure 1. *Ooencyrtus mirus*, lateral and dorsal habitus **A, B** *O. mirus* from Pakistan, specimen 2023-02 **C, D** *O. mirus* from Greece, specimen 2023-03 **E** *O. mirus* from Greece, specimen OoGr04 **F** *O. mirus* from Greece, specimen OoGr03.

of a saturated yellow colour (cf. Fig. 1C with Fig. 1E). This is presumably because the yellow colour is in part generated by the internal tissues seen through the thin cuticle; removing the tissues during DNA extraction changes the colour. The metallic colour of the dark body parts is not affected by the DNA extraction process, unless the specimens are examined in transmitted light instead of, or combined with, reflected light.

Molecular markers

The divergence calculated using either the p-distance or the K2P distance was very similar, hence we discuss further only the p-distance. On both molecular markers the specimens from Greece are most similar to *O. mirus*. On the *COI* sequences the divergence between the Pakistani (type locality) and Greek *Ooencyrtus* is 1.3%, while on *ITS2* it is 0.7%. The closest species to *O. mirus* in terms of genetic divergence is *O. pistaciae* with 6.2% on *COI* and 4.5% on *ITS2* when compared to the sequences of *O. mirus* of Pakistani origin. On both ML phylogenetic trees (Figs 2, 3) the specimens from Greece and Pakistan are grouped together with 100% bootstrap. The species is

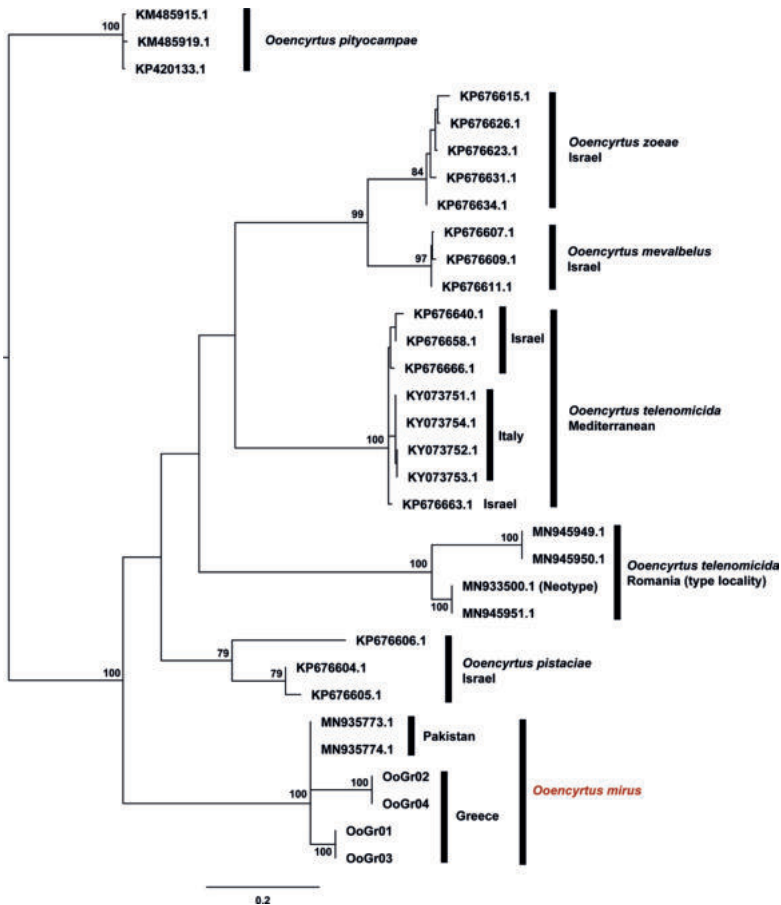


Figure 2. ML tree of the *Ooencyrtus telenomicida* species complex inferred from the analysis of *COI* sequences.

an antenna with elongated antennomeres, all funiculars being longer than broad and the clava about as long as the three preceding funiculars combined, the mandible with one to two teeth and a broad truncation, and the gaster with at least the first tergite yellow to brown, lighter than the following tergites. Hayat et al. (2014) additionally characterised the group as having all coxae and most of the femora dark brown, however, in *O. telenomicida* (Mediterranean populations) all legs including coxae are yellow (Samra et al. 2018), while in *O. telenomicida* from the type locality the legs are similarly light coloured, only the hind coxa being darkened (Triapitsyn et al. 2020). *Ooencyrtus mirus* likewise has all legs completely yellow including coxae (Pakistan population) (Triapitsyn et al. 2020) or the hind coxa is partly brown (Greek population).

The group includes *O. telenomicida* (the first described species), *Ooencyrtus acastus* described by Trjapitzin from the Russian Far East as part of the group (Trjapitzin 1967) and *Ooencyrtus gonoceri* described by Viggiani from Italy (Viggiani 1971), both stated as being very close to *O. telenomicida* by Huang and Noyes (1994); *Ooencyrtus brunneipes* described by Noyes (1978) from England as close to *O. telenomicida*; *Ooencyrtus nigerrimus* and *Ooencyrtus fecundus* described by Ferrière and Voegelé (1961) from Morocco and included in the group by Trjapitzin (1967); *O. exallus* described from Zimbabwe by Prinsloo (1987) and *Ooencyrtus seronis* Hayat from Saudi Arabia, included in the first definition of the group by Hayat et al. (2014); *O. zoeae* and *O. mevalbelus* described from Israel as very close to *O. telenomicida* (Samra et al. 2018); and finally *O. mirus* described from specimens reared in quarantine in USA and originating in Pakistan (Triapitsyn et al. 2020).

Ooencyrtus acestes Trjapitzin, though originally included in the group by Trjapitzin (1967) was not mentioned by subsequent authors, probably because it has a uniformly dark gaster. Hayat and Mehrnejad (2016) broaden the sense of the *O. telenomicida* group to also include species with a uniformly dark gaster and exclude the colour of the legs from the definition. Thus, they include more species such as *O. pistaciae* that has a uniformly dark brown gaster. Judging from the genetic closeness of this species to *O. mirus*, broadening the concept of the species group is phylogenetically justified.

Within this species group we define a subset of morphologically very close species that we name “*O. telenomicida* species complex”. These species are characterized by the sculpture of the scutellum consisting of elongate cells, cells more obviously elongate mesally and especially on sides (Ferrière and Voegelé 1961, fig. IG; Hayat and Mehrnejad 2016, fig. 38; Hunag and Noyes 1994, fig. 309) in combination with the presence of conspicuous white setae on the mesoscutum and a bare band behind parastigma, between the linea calva and basal fold (Ferrière and Voegelé 1961, fig. IIA; Hayat and Mehrnejad 2016, fig. 37; Hunag and Noyes 1994, fig. 309). In the west Palaearctic the complex contains *O. telenomicida*, *O. brunneipes*, *O. mevalbelus*, *O. zoeae* and *O. mirus*.

The species within this complex differ only in the colour of the legs, the intensity and hue of the metallic shine on head and thorax (Samra et al. 2018) and propodeum size (Noyes 1978). However, the genetic divergence between species on *COI* is very high, ranging from 5 to 9% (Samra et al. 2018; Triapitsyn et al. 2020) being above the largest intraspecific distance of 4.8% recorded in Chalcidoidea (Al Khatib et al. 2014;

Viciriuc et al. 2021). The presence of very divergent *COI* sequences is not necessarily an indication of specific status because this could have been generated by mitochondrial capture from another more distantly related species (e.g. Dascălu et al. 2022), or by geographic isolation (e.g. Fusu 2017: 536) in combination with extreme philopatry of females. It could also be an artefact generated by the preferential amplification of NUMTS in selected populations (Cruaud et al. 2017). However mitochondrial capture and NUMTS can be excluded because of the similar divergence seen on a nuclear marker (*ITS2*), while geographic isolation is an unlikely explanation in this case because the species are fully winged and presumably good dispersers. Crossing experiments by Samra et al. (2018) showed that even less divergent *Ooencyrtus* species (5% on *COI*) are reproductively isolated, while Pollmann et al. (2023) found that in *Lariophagus* Crawford (Hymenoptera, Pteromalidae) there is strong to complete reproductive isolation above 7.2%.

In the case of *O. mirus* the divergence between the specimens from Pakistan and those from Greece is very small on both genes (1.3 and 0.7% on *COI* and *ITS2*, respectively). To put this into perspective, the smallest interspecific K2P distance on *COI* in the *Ooencyrtus telenomicida* species group is 5% (between *O. mevalbelus* and *O. zoeae*) (Samra et al. 2018) while 4.6% is the *p*-distance between the most divergent sequences from the type locality of *O. telenomicida*. On *ITS2* the divergence is less clearcut interspecific or intraspecific because *O. mevalbelus* and *O. zoeae* differ by 0.4%, while the next smallest interspecific *p*-distance of 3.4% is between *O. telenomicida* (Mediterranean) and *O. pistaciae*.

When comparing *O. mirus* with *O. telenomicida*, Triapitsyn et al. (2020) used the colour of the legs and the extent of yellow colour on the base of the gaster: in *O. mirus* the legs, including coxae and at least the proximal half of the gaster are yellow while in *O. telenomicida* (in the narrow sense as defined by their neotype designation) the hind coxa is brown and the gaster has a much narrower yellow basal band, never extending to the cercal plates. According to these colour characteristics, the specimens from Greece are *O. telenomicida*, as published already by Andreadis et al. (2021). However, the colour of the head and mesosoma are very similar between the specimens of *O. mirus* irrespective of their origin (Fig. 1). The frontovertex, scutellum and mesoscutum have only a faint dark green, bronze and copper luster, visible under certain angles of light. In this, the species differs from *O. telenomicida* which has a much stronger metallic shine on the frontovertex, mesoscutum and especially the apex of scutellum. Furthermore, the metallic colour is blue-green in *O. telenomicida* instead of bronze-green (Triapitsyn et al. 2020, figs 10A, 12A, 14). The blue colour is present both in the type locality according to the neotype (Triapitsyn et al. 2020, figs 10A, 14) and in Ukraine, the original type locality (Triapitsyn et al. 2020, fig. 12A). A violet to blue scutellum is also mentioned by Ferrière and Voegelé (1961) who examined specimens from Morocco, Spain, and Turkey but also from the south of European Russia.

In conclusion, because of the high genetic similarity, we include the Greek *Ooencyrtus* in *O. mirus* even though the colour of the hind coxa disagrees and the gaster is

as yellow as in typical *O. mirus* only in few specimens. The colour differences could be due to the geographic distance and to the thelytokous parthenogenetic reproduction of the Pakistan population used to describe the species. It is infected with a strain of *Wolbachia* and thelytoky appears to be irreversible: even if males are produced after curing the infection, the females are not receptive to their courtship behaviour (Power et al. 2022). The newly discovered Greek population has both males and females.

Acknowledgments

We are grateful to Giuseppino Sabbatini Peverieri (Research Centre for Plant Protection and Certification, Florence) and Serguei V. Triapitsyn (Department of Entomology, University of California, Riverside) for sending the *Ooencyrtus* specimens from laboratory colonies used as comparative material. Acknowledgement is given to infrastructure support from the Operational Program Competitiveness 2014–2020, Axis 1, under POC/448/1/1 Research infrastructure projects for public R&D institutions/ Sections F 2018, through the Research Center with Integrated Techniques for Atmospheric Aerosol Investigation in Romania (RECENT AIR) project, under grant agreement MySMIS no. 127324. This research has been partially co-financed by the European and Greek national funds through the Operational Program Competitiveness, Entrepreneurship and Innovation, under the call RESEARCH – CREATE – INNOVATE (MIS-5072510, KIWIPO).

References

- Abram PK, Hoelmer KA, Acebes-Doria A, Andrews H, Beers EH, Bergh JC, Bessin R, Biddinger D, Botch P, Buffington ML, Cornelius ML, Costi E, Delfosse ES, Dieckhoff C, Dobson R, Donais Z, Grieshop M, Hamilton G, Haye T, Hedstrom C, Herlihy MV, Hoddle MS, Hooks CRR, Jentsch P, Joshi NK, Kuhar TP, Lara J, Lee JC, Legrand A, Leskey TC, Lowenstein D, Maistrello L, Mathews CR, Milnes JM, Morrison III WR, Nielsen AL, Ogburn EC, Pickett CH, Poley K, Pote J, Radl J, Shrewsbury PM, Talamas E, Tavella L, Walgenbach JF, Waterworth R, Weber DC, Welty C, Wiman NG (2017) Indigenous arthropod natural enemies of the invasive brown marmorated stink bug in North America and Europe. *Journal of Pest Science* 90: 1009–1020. <https://doi.org/10.1007/s10340-017-0891-7>
- Abram PK, Talamas EJ, Acheampong S, Mason PG, Garipey TD (2019) First detection of the samurai wasp, *Trisolcus japonicus* (Ashmead) (Hymenoptera, Scelionidae) in Canada. *Journal of Hymenoptera Research* 68: 29–36. <https://doi.org/10.3897/jhr.68.32203>
- Al Khatib F, Fusu L, Cruaud A, Gibson G, Borowiec N, Rasplus JY, Ris N, Delvare G (2014) An integrative approach to species discrimination in the *Eupelmus urozonus* complex (Hymenoptera, Eupelmidae), with the description of 11 new species from the Western Palearctic. *Systematic Entomology* 39(4): 806–862. <https://doi.org/10.1111/syen.12089>

- Andreadis SS, Gogolashvili NE, Fifis GT, Navrozidis EI, Thomidis T (2021) First report of native parasitoids of *Halyomorpha halys* (Hemiptera: Pentatomidae) in Greece. *Insects* 12(11): e984. <https://doi.org/10.3390/insects12110984>
- Andreadis SS, Moysiadis T, Gogolashvili NE, Koutsogeorgiou EI, Fifis GT, Tsaliki E (2022) Quality degradation of industrial hemp due to infestation by *Halyomorpha halys* (Hemiptera: Pentatomidae). *International Journal of Pest Management*. <https://doi.org/10.1080/09670874.2022.2089769>
- Biddinger DJ, Surci a A, Joshi NK (2017) A native predator utilising the invasive brown marmorated stink bug, *Halyomorpha halys* (Hemiptera: Pentatomidae) as a food source. *Bio-control Science and Technology* 27: 903–907. <https://doi.org/10.1080/09583157.2017.1354247>
- Costi E, Haye T, Maistrello L (2019) Surveying native egg parasitoids and predators of the invasive *Halyomorpha halys* in Northern Italy. *Journal of Applied Entomology* 143: 299–307. <https://doi.org/10.1111/jen.12590>
- Cruaud A, Nidelet S, Arnal P, Weber A, Fusu L, Gumovsky A, Huber J, Polaszek A, Rasplus J-Y (2019) Optimised DNA extraction and library preparation for minute arthropods: application to target enrichment in chalcid wasps used for biocontrol. *Molecular Ecology Resources* 19: 702–710. <https://doi.org/10.1111/1755-0998.13006>
- Cruaud P, Rasplus JY, Rodriguez LJ, Cruaud A (2017) High-throughput sequencing of multiple amplicons for barcoding and integrative taxonomy. *Scientific Reports* 7: e41948. <https://doi.org/10.1038/srep41948>
- Dasc alu MM, Caba FG, Fusu L (2022) DNA barcoding in Dorcadionini (Coleoptera, Cerambycidae) uncovers mitochondrial-morphological discordance and the hybridogenic origin of several subspecies. *Organisms Diversity & Evolution* 22: 205–229. [online first 23 November 2021] <https://doi.org/10.1007/s13127-021-00531-x>
- Dieckhoff C, Tatman KM, Hoelmer KA (2017) Natural biological control of *Halyomorpha halys* by native egg parasitoids: A multi-year survey in northern Delaware. *Journal of Pest Science* 90: 1143–1158. <https://doi.org/10.1007/s10340-017-0868-6>
- Dieckhoff C, Wenz S, Renninger M, Reib ig A, Rauleder H, Zebitz CPW, Reetz J, Zimmermann O (2021) Add Germany to the list – adventive population of *Trissolcus japonicus* (Ashmead) (Hymenoptera: Scelionidae) emerges in Germany. *Insects* 12(5): e414. <https://doi.org/10.3390/insects12050414>
- Ferri re C, Voegel  J (1961) Les *Ooencyrtus* parasites des oeufs des punaises des cereals au Maroc. *Cahiers de la Recherche Agronomique* 14: 27–36.
- Folmer O, Black M, Hoeh W, Lutz R, Vriienhoek R (1994) DNA primers for amplification of mitochondrial cytochrome c oxidase subunit I from diverse metazoan invertebrates. *Molecular Marine Biology and Biotechnology* 3: 294–299. https://www.mbari.org/wp-content/uploads/2016/01/Folmer_94MMBB.pdf
- Fusu L (2017) An integrative taxonomic study of European *Eupelmus* (*Macroneura*) (Hymenoptera, Chalcidoidea, Eupelmidae), with a molecular and cytogenetic analysis of *Eupelmus* (*Macroneura*) *vesicularis*: several species hiding under one name for 240 years. *Zoological Journal of the Linnean Society* 181: 519–603. <https://doi.org/10.1093/zoolinnean/zlw021>

- Fusu L, Askew RR, Ribes A (2018) Rediscovery of *Calymmochilus russoi* Gibson, 1995 (Hymenoptera, Chalcidoidea, Eupelmidae), and revision of European *Calymmochilus* Masi, 1919. *Zootaxa* 4504(4): 501–523. <https://doi.org/10.11646/zootaxa.4504.4.4>
- Fusu L, Polaszek A (2017) Description, DNA barcoding and phylogenetic placement of a remarkable new species of *Eopelma* (Hymenoptera: Eupelmidae) from Borneo. *Zootaxa* 4263(3): 557–566. <https://doi.org/10.11646/zootaxa.4263.3.7>
- Gibson GAP, Fusu L (2016) Revision of the Palearctic species of *Eupelmus* (*Eupelmus*) Dalman (Hymenoptera: Chalcidoidea: Eupelmidae). *Zootaxa* 4081(1): 1–331. <https://doi.org/10.11646/zootaxa.4081.1.1>
- Hayat M, Ahmad Z, Khan FR (2014) Encyrtidae (Hymenoptera: Chalcidoidea) from the Kingdom of Saudi Arabia. *Zootaxa* 3793(1): 1–59. <https://doi.org/10.11646/zootaxa.3793.1.1>
- Hayat M, Mehrnejad MR (2016) *Ooencyrtus* (Hymenoptera: Encyrtidae), egg parasitoids of the pistachio green stink bugs (Hemiptera: Pentatomidae) in Iran. *Zootaxa* 4117(2): 198–210. <https://doi.org/10.11646/zootaxa.4117.2.4>
- Haye T, Abdallah S, Garipey T, Wyniger D (2014) Phenology, life table analysis and temperature requirements of the invasive brown marmorated stink bug, *Halyomorpha halys*, in Europe. *Journal of Pest Science* 87: 407–418. <https://doi.org/10.1007/s10340-014-0560-z>
- Heraty J, Hawks D (1998) Hexamethyldisilazane: A chemical alternative for drying insects. *Entomological News* 109: 369–374. <https://ia800200.us.archive.org/13/items/biostor-76640/biostor-76640.pdf>
- Hoebeker ER, Carter ME (2003) *Halyomorpha halys* (Stål) (Heteroptera: Pentatomidae): A polyphagous plant pest from Asia newly detected in North America. *Proceedings of the Entomological Society of Washington* 105: 225–237. <https://doi.org/10.1016/j.biocontrol.2005.08.003>
- Huang DW, Noyes JS (1994) A revision of the Indo-Pacific species of *Ooencyrtus* (Hymenoptera: Encyrtidae), parasitoids of the immature stages of economically important insect species (mainly Hemiptera and Lepidoptera). *Bulletin of The Natural History Museum (Entomology Series)* 63(1): 1–136. <https://biostor.org/reference/113515>
- Inkley DB (2012) Characteristics of home invasion by the brown marmorated stink bug (Hemiptera: Pentatomidae). *Journal of Entomological Science* 47: 125–130. <https://doi.org/10.18474/0749-8004-47.2.125>
- Kalyaanamoorthy S, Minh BQ, Wong TKF, von Haeseler A, Jermiin LS (2017) ModelFinder: fast model selection for accurate phylogenetic estimates. *Nature Methods* 14: 587–589. <https://doi.org/10.1038/nmeth.4285>
- Katoh K, Standley DM (2013) MAFFT multiple sequence alignment software version 7: improvements in performance and usability. *Molecular Biology and Evolution* 30: 772–780. <https://doi.org/10.1093/molbev/mst010>
- Kumar S, Stecher G, Li M, Niyaz C, Tamura K (2018) MEGA X: Molecular Evolutionary Genetics Analysis across Computing Platforms. *Molecular Biology and Evolution* 35(6): 1547–1549. <https://doi.org/10.1093/molbev/msy096>
- Lanfear R, Frandsen PB, Wright AM, Senfeld T, Calcott B (2017) PartitionFinder 2: new methods for selecting partitioned models of evolution for molecular and morphological phylogenetic analyses. *Molecular Biology and Evolution* 34(3): 772–773. <https://doi.org/10.1093/molbev/msw260>

- Lee DH, Short BD, Joseph SV, Bergh JC, Leskey TC (2013) Review of the biology, ecology, and management of *Halyomorpha halys* (Hemiptera: Pentatomidae) in China, Japan, and the Republic of Korea. *Environmental Entomology* 42(4): 627–641. <https://doi.org/10.1603/EN13006>
- Leskey TC, Nielsen AL (2018) Impact of the invasive brown marmorated stink bug in North America and Europe: history, biology, ecology, and management. *Annual Review of Entomology* 63: 599–618. <https://doi.org/10.1146/annurev-ento-020117-043226>
- Leskey TC, Hamilton GC, Nielsen AL, Polk DF, Rodriguez-Saona C, Bergh JC, Herbert DA, Kuhar TP, Pfeiffer D, Dively GP, Hooks CRR, Raupp MJ, Shrewsbury PM, Krawczyk G, Shearer PW, Whalen J, Koplinka-Loehr C, Myers E, Inkley D, Hoelmer KA, Lee D-H, Wright SE (2012) Pest status of the brown marmorated stink bug, *Halyomorpha halys* in the USA. *Outlooks on Pest Management* 23: 218–226. <https://doi.org/10.1564/23oct07>
- Morrison WR III, Bryant AN, Poling B, Quinn NF, Leskey TC (2017) Predation of *Halyomorpha halys* (Hemiptera: Pentatomidae) from web-building spiders associated with anthropogenic dwellings. *Journal of Insect Behavior* 30: 70–85. <https://doi.org/10.1007/s10905-017-9599-z>
- Nguyen LT, Schmidt HA, Von Haeseler A, Minh BQ (2015) IQ-TREE: a fast and effective stochastic algorithm for estimating maximum-likelihood phylogenies. *Molecular Biology and Evolution* 32(1): 268–274. <https://doi.org/10.1093/molbev/msu300>
- Noyes JS (1978) New chalcids recorded from Great Britain and notes on some Walker species (Hym., Encyrtidae, Eulophidae). *Entomologist's Monthly Magazine* 113(1352–1355): 9–13.
- Pollmann M, Kuhn D, König C, Homolka I, Paschke S, Reinisch R, Schmidt A, Schwabe N, Weber J, Gottlieb Y, Steidle JLM (2023) New species based on the biological species concept within the complex of *Lariophagus distinguendus* (Hymenoptera, Chalcidoidea, Pteromalidae), a parasitoid of household pests. *Ecology and Evolution* 13: e10524. <https://doi.org/10.1002/ece3.10524>
- Power NR, Rugman-Jones PF, Stouthamer R, Ganjisaffar F, Perring TM (2022) High temperature mortality of *Wolbachia* impacts the sex ratio of the parasitoid *Ooencyrtus mirus* (Hymenoptera: Encyrtidae). *Peer Journal* 10: e13912. <https://doi.org/10.7717/peerj.13912>
- Prinsloo GL (1987) A revision of the genus *Ooencyrtus* Ashmead (Hymenoptera: Encyrtidae) in sub-saharan Africa. *Entomology Memoir, Department of Agriculture and Water Supply, Republic of South Africa* 67: 1–46.
- Qiu L-F (2010) Natural enemy species of *Halyomorpha halys* and control effects of the parasitoids species in Beijing. *Northern Horticulture* 9: 181–183.
- Ronquist F, Teslenko M, van der Mark P, Ayres DL, Darling A, Höhna S, Larget B, Liu L, Suchard MA, Huelsenbeck JP (2012) MrBayes 3.2: efficient Bayesian phylogenetic inference and model choice across a large model space. *Systematic Biology* 61(3): 539–542. <https://doi.org/10.1093/sysbio/sys029>
- Rot M, Maistrello L, Costi E, Bernardinelli I, Malossini G, Benvenuto L, Trdan S (2021) Native and non-native egg parasitoids associated with brown marmorated stink bug (*Halyomorpha halys* [Stål, 1855]; Hemiptera: Pentatomidae) in Western Slovenia. *Insects* 12: e505. <https://doi.org/10.3390/insects12060505>

- Roversi PF, Maltese M, Simoni S, Cascone P, Binazzi F, Strangi A, Sabbatini Peverieri G, Guerrieri E (2018) *Graphosoma lineatum* (Hemiptera: Pentatomidae): a suitable host for mass rearing *Ooencyrtus telenomicida* (Hymenoptera: Encyrtidae). *International Journal of Pest Management* 64(4): 294–302. <https://doi.org/10.1080/09670874.2017.1403059>
- Sabbatini Peverieri G, Talamas E, Bon MC, Marianelli L, Bernardinelli I, Malossini G, Benvenuto L, Roversi PF, Hoelmer K (2018) Two Asian egg parasitoids of *Halyomorpha halys* (Stål) (Hemiptera, Pentatomidae) emerge in northern Italy: *Trissolcus mitsukurii* (Ashmead) and *Trissolcus japonicus* (Ashmead) (Hymenoptera, Scelionidae). *Journal of Hymenoptera Research* 67: 37–53. <https://doi.org/10.3897/jhr.67.30883>
- Samra S, Cascone P, Noyes J, Ghanim M, Protasov A, Guerrieri E, Mendel Z (2018) Diversity of *Ooencyrtus* spp. (Hymenoptera: Encyrtidae) parasitizing the eggs of *Stenozygum coloratum* (Klug) (Hemiptera: Pentatomidae) with description of two new species. *PLoS ONE* 13(11): e0205245. <https://doi.org/10.1371/journal.pone.0205245>
- Samra S, Ghanim M, Protasov A, Branco M, Mendel Z (2015) Genetic diversity and host alternation of the egg parasitoid *Ooencyrtus pityocampae* between the pine processionary moth and the caper bug. *PLoS ONE* 10(4): e0122788. <https://doi.org/10.1371/journal.pone.0122788>
- Stahl J, Tortorici F, Pontini M, Bon M-C, Hoelmer K, Marazzi C, Tavella L, Haye T (2019a) First discovery of adventive populations of *Trissolcus japonicus* in Europe. *Journal of Pest Science* 92: 371–379. <https://doi.org/10.1007/s10340-018-1061-2>
- Stahl JM, Babendreier D, Marazzi C, Caruso S, Costi E, Maistrello L, Haye T (2019b) Can *Anastatus bifasciatus* be used for augmentative biological control of the brown marmorated stink bug in fruit orchards? *Insects* 10(4): e108. <https://doi.org/10.3390/insects10040108>
- Talamas EJ, Herlihy MV, Dieckhoff C, Hoelmer KA, Buffington M, Bon M-C, Weber DC (2015) *Trissolcus japonicus* (Ashmead) (Hymenoptera, Scelionidae) emerges in North America. *Journal of Hymenoptera Research* 43: 119–128. <https://doi.org/10.3897/JHR.43.4661>
- Tillman G, Toews M, Blaauw B, Sial A, Cottrell T, Talamas E, Buntin D, Joseph S, Balusu R, Fadamiro H, Lahiri S, Patel D (2020) Parasitism and predation of sentinel eggs of the invasive brown marmorated stink bug, *Halyomorpha halys* (Stål) (Hemiptera: Pentatomidae), in the southeastern US. *Biological Control* 145: e104247. <https://doi.org/10.1016/j.biocontrol.2020.104247>
- Triapitsyn SV, Andreason SA, Power N, Ganjisaffar F, Fusu L, Dominguez C, Perring TM (2020) Two new species of *Ooencyrtus* (Hymenoptera, Encyrtidae), egg parasitoids of the bagrada bug *Bagrada hilaris* (Hemiptera, Pentatomidae), with taxonomic notes on *Ooencyrtus telenomicida*. *Journal of Hymenoptera Research* 76: 57–98. <https://doi.org/10.3897/jhr.76.48004>
- Triapitsyn SV, Rugman-Jones PF, Perring TM (2021) Re-collection and identity of *Ooencyrtus californicus* (Hymenoptera: Encyrtidae), and its new synonym, *Ooencyrtus lucidus*. *Zootaxa* 4966(1): 97–100. <https://doi.org/10.11646/zootaxa.4966.1.11>
- Trjapitzin VA (1967) Encyrtids (Hymenoptera, Encyrtidae) of the Primorye Territory. *Trudy Zoologicheskogo Instituta* 41: 173–221.
- Trjapitzin VA (1989) Parasitic Hymenoptera of the Fam. Encyrtidae of Palaearctics. *Opredeliteli po Faune SSSR* 158. Nauka, Leningrad, 489 pp. [An English translation by J. Noyes] <https://doi.org/10.5281/zenodo.7470212>

- Viciriuc I-M, Thaon M, Moriya S, Warot S, Zhang J, Aebi A, Ris N, Fusu L, Borowiec N (2021) Contribution of integrative taxonomy to tracking interspecific hybridisations between the biological control agent *Torymus sinensis* and its related taxa. *Systematic Entomology* 46(4): 839–855. <https://doi.org/10.1111/syen.12493>
- Viggiani G (1971) Ricerche sugli Hymenoptera Chalcidoidea. XXXI. Descrizioni di *Ooencyrtus gonoceri* n.sp., parassita oofago del coreide *Gonocerus acuteangulatus* (Goeze), con notizie biologiche. *Bollettino del Laboratorio di Entomologia Agraria 'Filippo Silvestri'*, Portici 29: 315–325.
- Wermelinger B, Wyniger D, Forster B (2008) First records of an invasive bug in Europe: *Halyomorpha halys* (Stål) (Heteroptera: Pentatomidae), a new pest on woody ornamentals and fruit trees? *Bulletin de la Société Entomologique Suisse* 81: 1–8. <https://doi.org/10.5169/seals-402954>
- Xu J, Fonseca DM, Hamilton GC, Hoelmer KA, Nielsen AL (2014) Tracing the origin of US brown marmorated stink bugs, *Halyomorpha halys*. *Biological Invasions* 16: 153–166. <https://doi.org/10.1007/s10530-013-0510-3>
- Yang Z-Q, Yao Y-X, Qiu L-F, Li Z-X (2009) A new species of *Trissolcus* (Hymenoptera: Scelionidae) parasitizing eggs of *Halyomorpha halys* (Heteroptera: Pentatomidae) in China with comments on its biology. *Annals of the Entomological Society of America* 102: 39–47. <https://doi.org/10.1603/008.102.0104>
- Yara K (2006) Identification of *Torymus sinensis* and *T. beneficus* (Hymenoptera: Torymidae), introduced and indigenous parasitoids of the chestnut gall wasp *Dryocosmus kuriphilus* (Hymenoptera: Cynipidae), using the ribosomal *ITS2* region. *Biological Control* 36(1): 15–21. <https://doi.org/10.1016/j.biocontrol.2005.08.003>
- Zhang J, Zhang F, Garipey T, Mason P, Gillespie D, Talamas E, Haye T (2017) Seasonal parasitism and host specificity of *Trissolcus japonicus* in northern China. *Journal of Pest Science* 90: 1127–1141. <https://doi.org/10.1007/s10340-017-0863-y>

Limited phylogeographic structure in a flightless, Appalachian chalcidoid wasp, *Dipara trilineata* (Yoshimoto) (Hymenoptera, Diparidae), with reassessment of the male of the species

Michael S. Caterino¹, Nathan C. Arey²

1 Department of Plant and Environmental Sciences, Clemson University, Clemson, SC 29634, USA **2** Department of Entomology and Plant Pathology, University of Tennessee, Knoxville, TN 37996, USA

Corresponding author: Michael S. Caterino (mcateri@clemson.edu)

Academic editor: Ankita Gupta | Received 1 November 2023 | Accepted 7 December 2023 | Published 19 December 2023

<https://zoobank.org/792C4DBB-2F49-4724-8928-201BBE945797>

Citation: Caterino MS, Arey NC (2023) Limited phylogeographic structure in a flightless, Appalachian chalcidoid wasp, *Dipara trilineata* (Yoshimoto) (Hymenoptera, Diparidae), with reassessment of the male of the species. Journal of Hymenoptera Research 96: 1061–1072. <https://doi.org/10.3897/jhr.96.115001>

Abstract

Dipara trilineata (Diparidae) is a widespread eastern North American parasitoid with apterous females and winged males. Despite its seemingly limited dispersal capabilities, phylogeographic analysis over southern Appalachia reveals little structure, with only limited population level isolation. DNA barcoding surveys also definitively associate the male of the species, which had previously been misattributed, and a description of the correctly associated male is provided.

Keywords

aptery, megabarcoding, parasitoid, phylogeography

Introduction

Dipara Walker, 1833 is a member of the Diparidae, a globally distributed family of about 130 species of Chalcidoidea (Desjardins 2007), recently elevated to family status from a subfamily of Pteromalidae (Burks et al. 2022). Among North American Chalcidoidea, *Dipara* are unusual with females that are flightless and ant-like in morphology. There is little literature on *Dipara* biology. For several years, Diparinae were thought solely to

parasitize soil dwelling Curculionidae (Coleoptera) based on the first documented host record in 1988 (Bouček 1988). However, several species have been successfully reared from mantid egg cases and tsetse fly puparia (Desjardins 2007). The host range of Diparidae needs further research to gain a better picture of parasitoid-host relationships. There are presently three native species of the genus *Dipara* known from North America (Desjardins 2007), *D. canadensis* Hedqvist, 1969, *D. nigriceps* (Ashmead, 1904), and *D. trilineata* (Yoshimoto, 1977). The European *D. petiolata* Walker, 1833, has also apparently been introduced to the region (Garrido Torres and Nieves-Aldrey 1999; Wiśniowski and Jirak-Leszczynska 2021), though we aren't aware of specific records.

Dipara trilineata is the most common species of *Dipara* in the eastern United States. Described from Kentucky, there are also published records from Missouri, North Carolina, Florida, Arkansas, Texas, Oklahoma, Tennessee, and the District of Columbia (several of these under the now synonymous *Trimicrops bilineatus* Yoshimoto 1977 (Yoshimoto 1977; Bouček 1993; Desjardins 2007), and online photographic records from Louisiana and Quebec (based on identifiable photographic vouchers on BugGuide.net). This is a remarkably broad range for a species whose females are wingless and flightless. Finding the species to be abundant in leaf litter samples from the higher elevations of the southern Appalachian mountains, which function as a series of sky islands for many inhabitants (Browne and Ferree 2007; Hedin et al. 2015; Caterino and Recuero 2023), it seemed likely that *D. trilineata* would exhibit considerable genetic structure, and potentially cryptic species over its range. Using mitochondrial, barcode-region sequences from numerous southern Appalachian populations, we examine this hypothesis here.

We also address a mistaken attribution of males to this species. We have associated three male specimens from multiple populations unambiguously with females of *Dipara trilineata* through DNA barcodes, and find them to differ significantly from males originally described by Yoshimoto (1977). We rectify this error, and provide a new description of male morphology.

Methods

New data for this paper include 69 *Dipara trilineata* COI sequences, generated as part of an 'all-arthropods' metabarcoding study on the fauna of leaf litter in the high Appalachians, plus a small selection of other Chalcidoidea outgroups for rooting. Specimens of *D. trilineata* were identified using keys in Yoshimoto (1977). Descriptions of all described Diparidae with flightless females occurring in North America were carefully compared to our specimens. Significant character conflicts are found for all but *D. trilineata* (and its well-justified synonym *D. bilineatus* (Yoshimoto)), and the type and other known localities for these names correspond closely to the species as we treat it here. In preliminary analyses we included selected 'Diparidae' specimens from the Barcoding of Life Database (BoLD). However, finding that none of these affected the monophyly or polarity of the *D. trilineata* topology, we conducted most analyses without these.

Sequenced specimens came from our own recent collections (sampling map shown in Fig. 1), where we sifted leaf litter at sites ranging in elevation from 1300–2000 m

(~4500–6600 ft). The highest elevation sites (> 1500 m) were dominated by a canopy of red spruce (*Picea rubens*) and Fraser fir (*Abies fraseri*), with a litter layer composed mainly of their shed foliage. Lower localities were associated with more typical southeastern deciduous forest, with litters of oak, maple, birch, and *Rhododendron*. Litter samples were Berlese extracted until dry, and all specimens were collected into and preserved in 100% ethanol until extraction.

Prior to extraction, each specimen was imaged (images available at https://www.flickr.com/search/?user_id=183480085%40N02&desc&text=Dipara&view_all=1). Abdomens were subsequently punctured for digestion, and moved to a 96-well plate. Tissues were digested with lysis buffer and proteinase K (Omega BioTek, Norcross, GA), the liquid fraction then removed to a new plate and extracted using Omega BioTek's MagBind HDQ Blood and Tissue kit, eluting with 150 μ L elution buffer. Voucher specimens were retained, labelled, assigned unique identifiers, and deposited in the Clemson University Arthropod Collection.

The data set includes sequences produced by Illumina and Nanopore methods. In both cases, mini- (421 bp) barcodes were amplified from the mitochondrial COI gene using the primers BF2-BR2 (GCHCCHGAYATRGCHT'TYCC & TCDGGRT-GNCCRAARAAYCA; Elbrecht and Leese 2017), corresponding to the downstream two-thirds of the standard barcoding region. Each PCR reaction was tagged with a unique combination of 9 bp indexes (Meier et al. 2016). All PCRs were conducted in 12.5 μ L volumes (5.6 μ L water, 1.25 μ L Taq buffer, 1.25 μ L dNTP mix [2.5 mM each], 0.4 μ L MgCl [50 mM], 1.5 μ L each primer, 0.05 μ L Platinum Taq polymerase, 1 μ L DNA template, with a 95 °C initial denaturation for 5 minutes, followed by 35 cycles of 94 °C (30 sec), 50 °C (30 sec), 72 °C (30 sec), and a 5 minute 72 °C final extension on an Eppendorf Gradient Mastercycler.

PCR products were combined and purified using Omega Bio-Tek's Mag-Bind Total Pure NGS Kit, in a ratio of 0.7:1 (enriching for fragments >300 bp). Illumina adapters and sequencing primers were ligated to PCR products using New England BioLab's Blunt/TA Ligase Master Mix. Resulting libraries were purified using Mag-Bind Total Pure NGS, quantified using a Qubit fluorometer, and sequenced on an Illumina MiSeq using a v.3 2 \times 300 paired-end kit. For Nanopore MinION sequencing, libraries were prepared using the ligation sequencing kit LSK-112 (Oxford Nanopore Technologies, Oxford, UK), and loaded onto a v10.4 flowcell.

Illumina reads were processed with bbtools software package (<https://jgi.doe.gov/data-and-tools/bbtools/>; v38.87; Bushnell et al. 2017), trimming adapters, removing PhiX control reads, merging paired-end reads, filtering reads for the correct size, removing reads with quality score < 30, clustering sequences by similarity allowing 5 mismatches (~1%), and generating a final matrix in FASTA format. Nanopore reads were basecalled using the 'super-accurate' algorithm of Guppy (v6.1.2) running on Clemson's Palmetto cluster, then demultiplexed using ONTbarcode v0.1.9 (Srivathsan et al. 2021), with minimum coverage set at 5. FASTA files from all sequencing runs were combined and aligned with the online version of Mafft v7 (Katoh et al. 2017) using the auto strategy. All barcode sequences have been deposited in GenBank, with accession #s listed in Suppl. material 1.

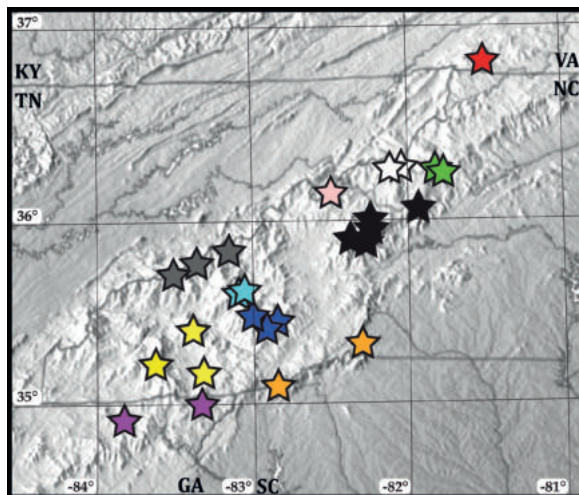


Figure 1. Map of all localities represented by COI sequences in the present study. Colors refer to those in trees in Figs 2, 3.

We produced a phylogeny using W-IQ-Tree (Nguyen et al. 2015; Trifinopoulos et al. 2016) under maximum likelihood criteria, applying a GTR+gamma model, with empirical base frequencies. Branch support was estimated using 10000 replicates of ultrafast bootstrapping (Minh et al. 2013). To assess relationships among haplotypes under a population genetic framework, a TCS haplotype network (Clement et al. 2000) was constructed using Popart (Leigh and Bryant 2015).

Results

Phylogenetic analyses that included a broader selection of Diparidae (not shown) from BOLD invariably resolved southern Appalachian *D. trilineata* as monophyletic, with no other available sequences very closely related. Sequences unidentified beyond ‘Diparidae’ from Thailand and Western Australia appeared more closely related to *D. trilineata* than did sequences of the Palaearctic *Dipara petiolata* or what appears (from a voucher photo in the BOLD database) to represent *D. canadensis* (from Virginia, USA).

Within *D. trilineata*, 69 individuals resolved into 35 distinct haplotypes. Divergences among them were remarkably low, with most less than 2% (uncorrected). The largest divergences were between a single individual from Brasstown Bald, Georgia (BBld.A.048) and most other sequences, at 4–6%. Comparisons to a couple other more divergent and well supported lineages (those from the Black Mts. in North Carolina and those from White-top Mt. in southwestern Virginia) were intermediate, ranging from 2–3.6%. Phylogenetic resolution was low and mostly weakly resolved (see Fig. 2). The deeply divergent individual from Brasstown Bald in northeastern Georgia was resolved as the sister to all other populations, although it differs in no obvious morphological characteristics. Among the latter, a single individual from a lower elevation locality in south-central North Carolina (Green

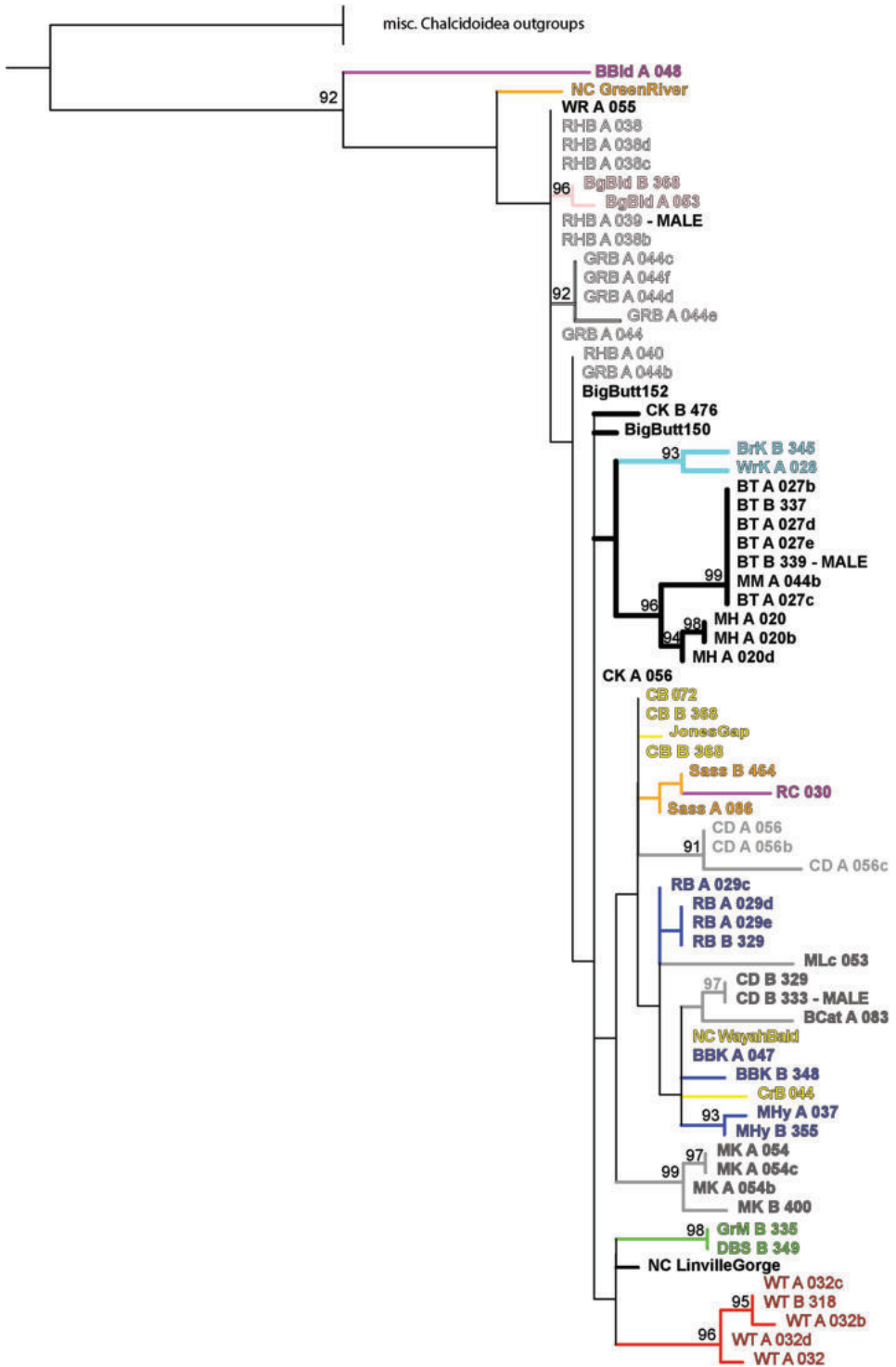


Figure 2. Maximum likelihood phylogeny of *Dipara trilineata* individuals, with locality abbreviations as in Suppl. material 1, and colors of OTUs keyed to localities shown in Fig. 1.

much more slender, every flagellomere tapered basally and distally, and verticillate, with few very long setae borne in whorls (Fig. 4E). Yoshimoto also figures the wings in his Figure 8 (1977: p. 1050), showing the hind wing to be broadly rounded apically, while our *D. trilineata* has much narrower, apically subacute hind wings (Fig. 4F). Those are the only characters illustrated by Yoshimoto, but it is apparent that the described "allotype" male from the type locality represents a distinct species. The male he attributed to *Dipara pedunculata* (with antennae figured in Yoshimoto's Fig. 27; 1977: p. 1053), now considered a synonym of *D. canadensis*, matches our *D. trilineata* males much better than it does *D. canadensis* (the male antenna of which is shown in his fig. 26: (1977: p. 1053). Heydon and Bouček (1992), when synonymizing *D. pedunculata* with *D. canadensis*, previously noted some inconsistencies between Yoshimoto's (1977) description and female holotype. We suggest that the male presumed to represent Yoshimoto's *D. pedunculata* was a misidentified *D. trilineata*. *Dipara pedunculata* was described from Kentucky, well within the range of *D. trilineata*, so the two valid species must be sympatric there, and the original series of *D. pedunculata* a mix of *D. canadensis* and *D. trilineata*.

Comparing our confirmed males of *D. trilineata* directly to Yoshimoto's (1977) description of *D. pedunculata*, we note several other points of difference, and provide a brief re-description here (with slightly updated terminology).

Male (Fig. 4C–F): Head, mesosoma, and metasoma fuscous; legs (except mesocoxa), petiole, and bases of antennae yellowish, the antennae gradually darker from 3rd flagellar segment distad, mesocoxa also darker toward base; head almost hemispherical, very shallowly depressed above toruli, smooth and shining above, finely transversely reticulate below toruli, with scattered setae throughout; eyes prominent, eye height slightly more than half lateral head height, coarsely faceted; ocellar triangle wide, individual ocelli oval; clypeus outlined by disconnected series of punctures, convex, apical margin evenly rounded; mandibles tridentate; antennae inserted in front of middle of eye, slightly above middle of frons, toruli approximately equally separated from each other as from inner edge of eye; scape cylindrical, slightly curved, almost as long as pedicel and flagellomeres 2 and 3 combined; pedicel short, expanded to slightly wider than scape at apex, flagellomeres narrow basally and apically ('pedunculate'), but bulbous in basal half, tapered apically, with few (~6) long setae (about 1.5 times as long as flagellomere) inserted in an uneven series around bulbous base; entire antenna nearly as long as rest of body; neck transversely reticulate, bounded posteriorly by evenly curved, weakly impressed collar; notauli subcrenately impressed, curving to meet along finely and deeply impressed mesoscutum-scutellar suture, the mesoscutum polygonally microsculptured between; frenal groove of scutellum only weakly indicated, but frenum smoother than polygonally microsculptured scutellum; propodeum with coarsely raised reticulate microsculpture; anterior insertion of petiole slightly narrower than posterior insertion, petiole about 3 times as long as maximum width, with weak longitudinal carinae; 1st gastral segment nearly half entire gastral length, 2nd–5th gastral segments subequal in length; forewing widening only slightly beneath costal cell, widening more abruptly beyond, anterior margin bent slightly forward at this point; submarginal vein bearing two conspicuous dorsal setae; marginal vein more densely setose, the setae directed distad at about 45°, their maximum length about ¼ maximum wing width; postmarginal vein

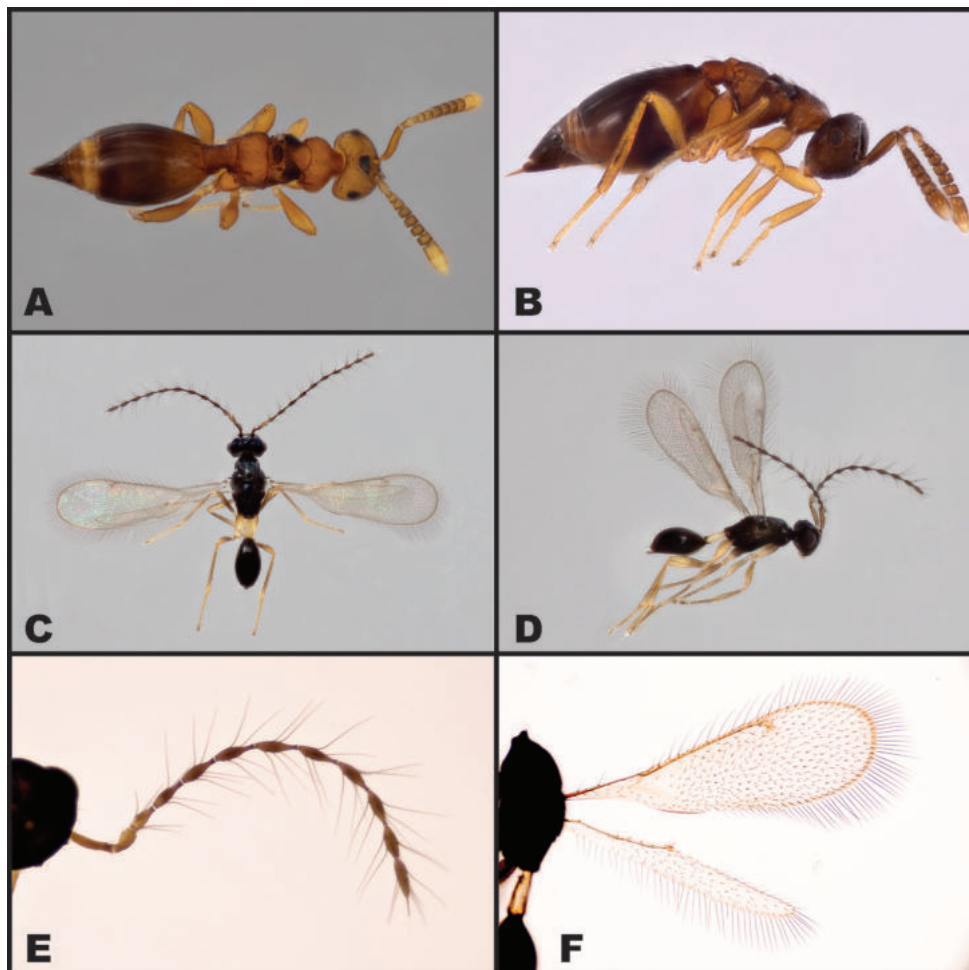


Figure 4. Female (A, B) and male (C–F) *Dipara trilineata* (Yoshimoto).

weak, fading evenly beyond short stigmal vein, stigma slightly expanded, uncus poorly developed; wing with sublinate series of short setae in basal cell, bare briefly within specular area, densely and evenly setose beyond; setae of apical and posteroapical margins of wing long, nearly half maximum wing width; hind wing about three-fourths length of forewing, posterior margin rounded, widened slightly beyond midpoint, narrowed to subacute apex, setae along posterior margin longer than width of hindwing membrane.

Material examined (males): North Carolina, Yancey County, Mt. Mitchell State Park, Big Tom near summit (35.7799, -82.2596), 7-Sep-2021 (CUAC000135520); North Carolina, Swain County, Great Smoky Mountains National Park, Clingmans Dome (35.5589, -83.4983), 14-Sep-2021 (CUAC000157203); North Carolina, Mitchell County, Roan High Bluff (36.0931, -82.1453), 15-Aug-2018 (CUAC000002974).

Other taxonomic remarks: No recent authors have addressed the mismatch in gender of *Dipara trilineatus* (sic). Walker's (1833) genus name would be feminine, appearing to be based on a Greek adverb used as a singular noun (S. Chatzimanolis, pers. comm.),

and virtually all usage from Walker's onward has used feminine species names. It is unfortunate that when synonymizing *Trimicrops* Keiffer with *Dipara* Walker, Desjardins (2007) did not properly amend 'trilineatus' to the singular feminine ending, but we do that here.

Discussion

Dipara trilineata is a remarkably widespread species for one having such seemingly limited dispersal capabilities. Our collections, along with reliable records from other sources reveal the species to cover much of the eastern US, extending from central Texas into southeastern Canada. As to state records, the species was previously unreported for Mississippi, Indiana, Georgia, South Carolina, Virginia, and West Virginia (Fig. 5).

Even more surprising is the relatively limited degree of population structuring, at least over the range we sampled. Some geographic clustering is evident, and a number of populations exhibit haplotype monophyly, but the overall patterns exhibit only loose correspondence with geography. One potential confounding factor is the relatively high haplotype diversity, as would be expected for a species with large population sizes. This could slow coalescence and limit phylogenetic resolution even if populations are largely isolated. But based on available data, there are no indications that *D. trilineata* represents a cryptic species complex, despite its flightlessness. If additional individuals from the more divergent lineages (BBld.A.048 or NC_GreenRiver) showed comparable genetic difference, more systematic morphological comparisons may reveal subtle differences not yet apparent.

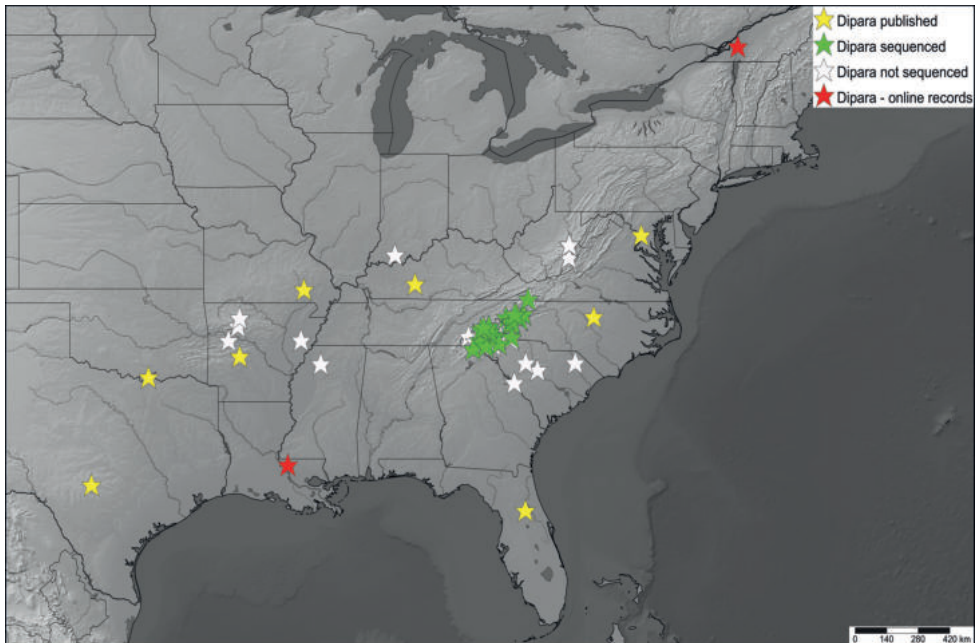


Figure 5. Total known distribution of *Dipara trilineata*, based on a combination of published, online, and newly contributed records.

The lack of phylogeographic structuring may provide some indirect hints as to host breadth. Even though individual *Dipara* females may not themselves be capable of long-distance dispersal, it is worth suggesting the potential for dispersal in the larval stage by a more mobile, flying or ballooning host, which would serve to reduce effective isolation (as has been shown for Dryinidae parasitoids of leafhoppers; Mita et al. 2012). Host records for *Dipara* to date include only non-mobile stages, eggs, larvae, and pupae (Desjardins 2007). But these already cover a considerable range, and more mobile hosts should not be ruled out.

As to potential host identities for *Dipara trilineata*, its general abundance over a wide range argues against any close host specificity. There are few other arthropod species in eastern US leaf litter that have so wide a distribution, occurring in such a wide range of microhabitats, although perhaps some of the spider species do (Recuero et al. 2023). Previous suggestions of weevil associations would not seem likely, at least not as a primary host, as weevils are poorly represented in our highest elevation samples. There are intriguing possibilities to better understand host/parasitoid relationships through metabarcoding approaches, such as detecting the DNA of a parasitoid as co-amplifying with that of its host (Miller et al. 2021), and the *Dipara* system would be a promising one to explore such potential.

Acknowledgments

This study was funded by the U.S. National Science Foundation (Award DEB-1916263 to MSC) and the Clemson University Experiment Station (SC-1700596 to MSC). We also acknowledge the support of the John and Suzanne Morse Endowment for Arthropod Biodiversity. For permissions and assistance with field work we are grateful to the North Carolina State Parks, Great Smoky Mountains National Park, Blue Ridge Parkway National Park, Monica Martin, Frank Etzler, Ernesto Recuero, Curt Harden, Patricia Wooden, Adam Haberski, Roy Kucuk, Laura Vásquez-Vélez, Laary Cushman, Paul Marek, Michael Ferro, and Will Kuhn. Mary Atieh, Caroline Dukes, Caroline McCluskey, Grace Holliday, Grace Arnold, Hannah Skinner, Alejandra Carranza, and Anthony Villanueva provided valuable assistance in the lab. We thank Fernando Farache and Mircea-Dan Mitroiu for comments that improved the manuscript, and Stylianos Chatzimanolis for providing insight into the nomenclature. This paper represents Technical Contribution No. 7248 of the Clemson University Experiment Station.

References

- Bouček Z (1988) Australasian Chalcidoidea (Hymenoptera): A biosystematic revision of genera of fourteen families, with a reclassification of species. CAB International, Wallingford, 832 pp.
- Bouček Z (1993) New taxa of North American Pteromalidae and Tetracampidae (Hymenoptera), with notes. *Journal of Natural History* 27: 1239–1313. <https://doi.org/10.1080/00222939300770741>

- Browne RA, Ferree PM (2007) Genetic structure of southern Appalachian “Sky Island” populations of the southern red-backed vole (*Myodes gapperi*). *Journal of Mammalogy* 88: 759–768. <https://doi.org/10.1644/06-MAMM-A-049R1.1>
- BugGuide.net (2023) BugGuide.net. <https://bugguide.net/node/view/517354/bgpape> [accessed 5 December 2023]
- Burks R, Mitroiu MD, Fusu L, Heraty JM, Janšta P, Heydon S, Papilloud NDS, Peters RS, Tselikh EV, Woolley JB, van Noort S, Baur H, Cruaud A, Darling C, Haas M, Hanson P, Krogmann L, Rasplus JY (2022) From hell’s heart I stab at thee! A determined approach towards a monophyletic Pteromalidae and reclassification of Chalcidoidea (Hymenoptera). *Journal of Hymenoptera Research* 94: 13–88. <https://doi.org/10.3897/jhr.94.94263>
- Bushnell B, Rood J, Singer E (2017) BBMerge – Accurate paired shotgun read merging via overlap. *PLoS ONE* 12(10): e0185056. <https://doi.org/10.1371/journal.pone.0185056>
- Caterino MS, Recuero E (2023) Shedding Light on dark taxa in high Appalachian leaf litter – assessing patterns of endemism using large scale, voucher-based barcoding. *Insect Conservation and Diversity*. [online early] <https://doi.org/10.1111/icad.12697>
- Clement M, Posada D, Crandall KA (2000) TCS: a computer program to estimate gene genealogies. *Molecular Ecology* 9: 1657–1659. <https://doi.org/10.1046/j.1365-294x.2000.01020.x>
- Desjardins CA (2007) Phylogenetics and classification of the world genera of Diparinae (Hymenoptera: Pteromalidae). *Zootaxa* 1647: 1–88. <https://doi.org/10.11646/zootaxa.1647.1.1>
- Elbrecht V, Leese F (2017) Validation and development of COI metabarcoding primers for freshwater macroinvertebrate bioassessment. *Frontiers in Environmental Science* 5: 1–11. <https://doi.org/10.3389/fenvs.2017.00011>
- Garrido Torres AM, Nieves-Aldrey JL (1999) Pteromálidos de la comunidad de Madrid: faunística y catálogo (Hymenoptera, Chalcidoidea, Pteromalidae). *Graellsia* 55: 9–147. <https://doi.org/10.3989/graellsia.1999.v55.i0.322>
- Hedin M, Carlson D, Coyle F (2015) Sky island diversification meets the multispecies coalescent – divergence in the spruce-fir moss spider (*Microhexura montivaga*, Araneae, Mygalomorphae) on the highest peaks of southern Appalachia. *Molecular Ecology* 24: 3467–3484. <https://doi.org/10.1111/mec.13248>
- Heydon S, Bouček Z (1992) Taxonomic changes in Nearctic Pteromalidae, with the description of some new taxa (Hymenoptera: Chalcidoidea). *Proceedings of the Entomological Society of Washington* 94: 471–489.
- Katoh K, Rozewicki J, Yamada KD (2017) MAFFT online service: multiple sequence alignment, interactive sequence choice and visualization. *Briefings in Bioinformatics* bbx108: 1–7. <https://doi.org/10.1093/bib/bbx108>
- Leigh JW, Bryant D (2015) POPART: Full-feature software for haplotype network construction. *Methods in Ecology and Evolution* 6: 1110–1116. <https://doi.org/10.1111/2041-210X.12410>
- Meier R, Wong W, Srivathsan A, Foo M (2016) \$1 DNA barcodes for reconstructing complex phenomes and finding rare species in specimen-rich samples. *Cladistics* 32: 100–110. <https://doi.org/10.1111/cla.12115>
- Miller KE, Polaszek A, Evans DM (2021) A dearth of data: fitting parasitoids into ecological networks. *Trends in Parasitology* 37: 863–874. <https://doi.org/10.1016/j.pt.2021.04.012>

- Minh BQ, Nguyen MAT, Von Haeseler A (2013) Ultrafast approximation for phylogenetic bootstrap. *Molecular Biology and Evolution* 30: 1188–1195. <https://doi.org/10.1093/molbev/mst024>
- Mita T, Matsumoto Y, Sanada-Morimura S, Matsumur M (2012) Passive long-distance Migration of apterous dryinid wasps parasitizing rice planthoppers. In: Stevens LE (Ed.) *Global Advances in Biogeography*. Intech, London, 49–60. <https://doi.org/10.5772/35885>
- Nguyen LT, Schmidt HA, Von Haeseler A, Minh BQ (2015) IQ-TREE: A fast and effective stochastic algorithm for estimating maximum-likelihood phylogenies. *Molecular Biology and Evolution* 32: 268–274. <https://doi.org/10.1093/molbev/msu300>
- Recuero E, Etzler F, Caterino MS (2023) Most soil and litter arthropods are unidentifiable based on current DNA barcode reference libraries. *Current Zoology*. [online early] <https://doi.org/10.1093/cz/zoad051>
- Srivathsan A, Lee L, Katoh K, Hartop E, Kutty SN, Wong J, Yeo D, Meier R (2021) ONTbar-coder and MinION barcodes aid biodiversity discovery and identification by everyone, for everyone. *BMC Biology* 19: 1–21. <https://doi.org/10.1186/s12915-021-01141-x>
- Trifinopoulos J, Nguyen LT, von Haeseler A, Minh BQ (2016) W-IQ-TREE: a fast online phylogenetic tool for maximum likelihood analysis. *Nucleic Acids Research* 44: W232–W235. <https://doi.org/10.1093/nar/gkw256>
- Walker F (1833) *Monographia chalcidum*. *The Entomological Magazine* 1: 367–384.
- Wiśniowski B, Jirak-Leszczyńska A (2021) Additions to the list of pteromalid wasps (Hymenoptera: Chalcidoidea, Pteromalidae) of Ojców National Park in Poland with records of seven species new to the Polish fauna. *Annals of the Upper Silesian Museum in Bytom Entomology* 30: 1–14.
- Yoshimoto CM (1977) Revision of the Diparinae (Pteromalidae: Chalcidoidea) from America North of Mexico. *The Canadian Entomologist* 109: 1035–1056. <https://doi.org/10.4039/Ent1091035-8>

Supplementary material I

Excel spreadsheet with specimen level data for all records of *Dipara trilineata* reported here

Authors: Michael S. Caterino, Nathan C. Arey

Data type: xlsx

Explanation note: Fields include source of record, project morphospecies code (searchable on Flickr), sex, Caterino lab DNA extraction number, GenBank accession number (where sequenced successfully), verbal locality description, decimal latitude/longitude, date collected, and unique CUAC voucher code.

Copyright notice: This dataset is made available under the Open Database License (<http://opendatacommons.org/licenses/odbl/1.0/>). The Open Database License (ODbL) is a license agreement intended to allow users to freely share, modify, and use this Dataset while maintaining this same freedom for others, provided that the original source and author(s) are credited.

Link: <https://doi.org/10.3897/jhr.96.115001.suppl1>